Beyond 2010
Use of habitat suitability models in the re-assessment of the 2010 Biodiversity Target for plant species

Aletrari, Elina

Awarding institution:
King's College London

KING'S COLLEGE LONDON, SCHOOL OF SOCIAL SCIENCE AND PUBLIC POLICY,
DEPARTMENT OF GEOGRAPHY

Beyond 2010:
Use of habitat suitability models in the re-assessment of the 2010 Biodiversity Target for plant species

Ph.D Thesis

ELINA ALETRARI

King's College London
Supervisor: Dr Mark Mulligan

Natural History Museum London
Supervisor: Dr Neil Brummitt

APRIL 2016

COPYRIGHT

ACKNOWLEDGMENTS

First and foremost, I would like to express my deepest gratitude and warm appreciation to my supervisors, Mark Mulligan and Neil Brummitt for their extraordinary guidance and generosity; both have been true mentors. I am thankful to Mark for patiently guiding me through what was for me the unknown territory of spatial analysis and programming, and for always being available despite his many commitments. I thank Neil for giving me the opportunity to work with him and for so generously sharing his invaluable botanical and fieldwork knowledge.

I would like to acknowledge the Natural History Museum, London for enabling this study through providing the Sampled Red List Index data for pteridophytes and the much-necessary fieldwork funding. I am indebted to the Royal Botanic Gardens, Kew for providing the Sampled Red List Index data for angiosperms, and to Steve Bachman for introducing me to the Sampled Red List Index project and the world of natural history collections. I also thank Harald Schneider for helping me understand pteridophytes and Michael Kessler for sharing his team's field data in order to validate my work.

Thank you to Mindy Syfert who has broadened my knowledge on GIS techniques, joined me in Costa Rica for fieldwork adventures and shared her Species Distribution Models. Most importantly, I thank her for always being there when I needed her scientific advice. I would also like to thank Sarah Stow for her encouragement during this thesis' writing process.

This PhD thesis would not have been possible without the financial (as this was a self-funded project) and emotional support of my husband and family. I cannot thank them enough for everything they have done for me these past four years. My parents supported me in all my pursuits and have sacrificed many things for me through the years. I owe becoming a scientist to my father, to whom I am immensely grateful, as I am to my mother for teaching me everything I know about life. Special thanks to Chris, Stelios, Christos and Lara for their continued support and understanding. Finally but not least I would like to thank my husband, the love of my life, for his infinite support, encouragement, patience and for believing in me and my work.

TABLE OF CONTENTS

TABLE OF FIGURES

TABLE OF TABLES

ABSTRACT

Human activities are placing unprecedented pressure on natural ecosystems, threatening to push many species into extinction. In response to this, a call for a reduction in the current rate of biodiversity loss by 2010 was made and global biodiversity indicators were adopted to monitor progress. Perhaps the best known of these are the Red List Indices, which are based on temporal changes in extinction risk of species assessed for the International Union for Conservation of Nature (IUCN) Red List. In the case of plants, conservation assessments for globally-representative samples of species have been carried out mainly utilising comprehensive worldwide herbarium resources, and have shown that more than 1 in 5 plant species is threatened with extinction under IUCN Red List Criteria. The aim of this thesis was to provide the scientific bases for an automated procedure to re-assess plant species pan-tropically on a 5-year time frame in order to calculate the change in the IUCN Sampled Red List Index (SRLI) for Plants as a measure of global trends in plants extinction risk.

This study has focused first on improving the method used for calculating species ranges using the available IUCN SRLI for Plants data and to develop a new measure of species range, the Extent of Suitable Habitat (ESH). The results show that this new calculation method is effective at reflecting a closer reality of plant distributions on the ground, and that such a simple method can be used to predict the current distribution of species globally. The species ESHs were then assessed through time against the degree of human impact using data from a global monitoring system for deforestation and from a future land use change scenario applied by the Co$ting Nature tool. On the basis that land cover change can be used as a proxy for local extinction risk and that a species' ESH can be re-calculated to factor in the impact of land cover change (habitat loss), this thesis showed that a species' ESH could be used for re-assessing the conservation status of plant species under IUCN Criterion B sub-criterion b(iii). This way, more dynamic, comparable and spatially-detailed Red List Index updates could be provided. To test the ESH range calculation this method was also compared with a widely accepted species distribution modelling approach and validated using new species occurrence points. Additionally, ESH derived species richness maps were produced for conservation prioritisation, validated using fieldwork data from previous studies and compared with existing species richness maps for plants.

CHAPTER 1

1.1 RATIONALE

The continuing increase in human population, in conjunction with rising per-capita consumption rates, is placing unprecedented pressure on natural ecosystems, threatening to push many species into extinction. In response to this, in 2002 the UN Convention on Biological Diversity (CBD) called for 'a significant reduction in the current rate of loss of biological diversity' by 2010 (UNEP, 2002), but this target was not met (Butchart *et al.*, 2010). However, conservation of biodiversity and its associated ecosystem services underpins many of the Millennium Development Goals (UNEP, 2005; Sachs *et al.*, 2009) and failure to meet the 2010 Target has galvanised stronger action towards a suite of new 2020 Targets (UNEP, 2010). This includes a series of global biodiversity indicators adopted in 2006 to monitor progress (UNEP, 2006).The the Red List Indices (RLI) which are based on temporal changes in conservation status of the International Union for Conservation of Nature (IUCN) Red List species (Butchart *et al.*, 2005), have been perhaps the most widely adopted and successful.

Due to the number of species in larger taxonomic groups and the lack of information for many species, the IUCN Sampled Red List Index (SRLI) was developed (Baillie *et al.*, 2008) in order to monitor over time the conservation status of a representative sample of the world's known biodiversity. The Natural History Museum, London (NHM), together with the Royal Botanic Gardens, Kew (RBG Kew) have taken the lead in developing the IUCN Sampled Red List Index (SRLI) for different plant groups (Nic Lughadha *et al.*, 2005; Baillie *et al.*, 2008; Brummitt *et al.*, 2008) and have together generated conservation assessments for globally-representative samples of species based on their comprehensive worldwide herbarium resources, together with previously-digitised online specimen resources, coupled with in-house GIS analysis (Willis *et al.*, 2003; Rivers *et al.*, 2010). These species were assessed for the SRLI for plants in 2010 and showed that more than 1 in 5 plant species is threatened with extinction (Brummitt & Bachman, 2010; Brummitt *et al.*, 2015b). They now need to be re-assessed on a 5-year time frame to calculate the change in the Index and so monitor global trends in conservation status.

With a sample of c.7000+ plant species spanning the globe, the re-assessment process needs to be simplified and automated as much as possible; for example, by making use of existing remote-sensing resources to highlight species at increasing risk of extinction (Brummitt *et al.*, 2015a), such as through rapid habitat (land cover) modification or climate change. In order to ensure confidence in the SRLI for Plants, it is essential that such re-assessments detect near real-time changes on the ground and reflect actual levels of threat to the relevant taxonomic groups. Georeferenced specimen data now exist in considerable quantity, and the SRLI project has synthesized high-quality, representative datasets from targeted databasing and online sources. Large, moderate and high spatial resolution and high temporal resolution datasets of land cover change have also now been made available (Mulligan, 2009; Reymondin *et al.*, 2012; Hansen *et al.*, 2013), against which known ranges of both threatened and non-threatened

species can be assessed for degree of fragmentation, number of subpopulations, and continuing decline in range and/or extent or quality of habitat; key measures for a revised IUCN species conservation assessment (IUCN, 2012a). Having undertaken this analysis the results will form the basis of species conservation status re-assessments, and the importance of land cover versus climate change for biodiversity conservation can be assessed. The application of automated global re-assessment methods would represent a major step forward in the acceleration of reliable, specimen-based, species conservation assessments. Only by coupling the best available global habitat change data with the best available measures of species distribution can measurable targets be routinely monitored and regional conservation policy thus informed.

Criterion B (geographic range) was used to categorise more than half of species assessed for the SRLI for Plants (Brummitt & Bachman, 2010; Brummitt *et al*., 2015a; Brummitt *et al*., 2015b). As is specified in the IUCN guidelines (IUCN, 2014), specific measures of species' range size and occupancy (Extent of Occurrence (EOO) and Area of Occupancy (AOO)) (Gaston, 1994) which have quantified thresholds for threatened Red List Categories under Criterion B, were used in carrying out conservation assessments. However, these measures are static (Brummitt *et al*., 2015b) and do not incorporate habitat (land cover information) making the detection of decline in range over time difficult. Therefore, a habitat suitability metric such as the Extent of Suitable Habitat (ESH) would be more appropriate in an automated re-assessment process which will calculate species ranges every five years and detect decline in extent and quality of the species' suitable habitat using remote-sensing data.

The species selected for this study will be taken from the set of plant species chosen for the Sampled Red List Index project, for which baseline conservation assessments will already exist. The sample contains 7000 species from 5 major taxonomic groups; bryophytes, pteridophytes, gymnosperms, monocots and legumes. Pteridophytes, the second largest plant group (Smith *et al.*, 2005; Paton *et al.*, 2008) after angiosperms, would be the most appropriate study group for their geographical and ecological diversity and due to the strong relationship between their range size and suitable habitat availability (Tryon, 1986; Tuomisto *et al.*, 2003; Jones *et al.*, 2006).

This study will contribute to the next stage (Phase II) of the SRLI project. Results from this work will provide a case study with which to further evaluate the correspondence between baseline herbarium-based conservation assessments and field-based threat status, abundance and population structure in a taxonomically and ecologically diverse sample of species (Brummitt *et al.*, 2015a). It will provide a novel methodology for accelerating the production of reliable species conservation assessments which will be conducted every 5 years. Therefore, results from this study will underpin the first contribution to establishing trends in the status of plant species worldwide, as is currently possible for better known groups such as mammals, birds and amphibians.

1.2 AIM and OBJECTIVES

1.2.1 Aim

The aim of this joint King's College London – Natural History Museum PhD is to provide the scientific basis for an automated procedure to assess and re-assess species' conservation status pan-tropically, using species' occurrence data for forest pteridophytes as a test case and incorporating near-real time remotely-sensed land cover information, spatial analysis and a future land use change scenario applied by the Co$ting Nature tool. This approach is validated in-country by ground-truthing in a recognised biodiversity hotspot and also by fieldwork data available from previous studies. The results from this approach will be used to calculate extinction likelihoods for pan-tropical plant conservation. This type of information is fundamental to the reassessment of the 2010 targets at least every five years from 2010.

1.2.2 Objectives

Scientific questions

The project will address the following questions:

1. Can the widely-used method (EOO) for calculating species distributions, be improved by incorporating habitat?

2. What are the impacts of current anthropogenic land cover change on fragmenting species ranges by degrading suitable habitat?

3. Are these impacts different across the biogeographical regions and how are they affecting global patterns of species richness for the SRLI forest pteridophyte species?

4. How will likely future land use scenarios affect the conservation status of the SRLI forest pteridophyte species?

Specific Objectives

In order to achieve the project aim, the following objectives need to be met:

1. Analyse the available specimen data for IUCN SRLI forest pteridophyte species and improve the method for calculating species ranges within it to better account for the impact of habitat on species distributions.

2. Generate global maps of the SRLI forest pteridophyte species richness and endemism using the improved method for calculating species ranges incorporating habitat.

3. Apply the improved method for calculating species ranges to the major SRLI plant groups (pteridophytes and angiosperms) in Africa and use the species' ranges to generate species richness and endemism richness maps for those groups.

4. Compare the the new improved method for calculating species ranges with the established species distribution modelling (SDM) approach.

5. Validate the results of the spatial analysis using new occurrence data from the Global Biodiversity Information Facility (GBIF) database, by conducting fieldwork in a recognised biodiversity hotspot and also with fieldwork data available from previous studies.

6. Assess plant species ranges against the degree of current human impact using global deforestation data.

7. Apply a future land use scenario using the Co$ting Nature Land Use change model (QUICKLUC 2.0) to investigate any change on the species ranges in the future.

8. Document the necessary methodology for an operational system which will assess and re-assess plant species' conservation status pan-tropically.

1.3 OVERVIEW of THESIS

This thesis contains eight chapters. An overview of what can be found in each chapter is given below:

CHAPTER 1

This chapter provides an introduction to the research problem and describes the specific research aims and objectives. A general layout of the thesis is also given. Chapter 1 also offers a general introduction to the study. The problem of biodiversity and habitat loss is explained and the global measures that were put in place to address this biodiversity decline are covered. Specifically, the International Union for Conservation of Nature (IUCN) Sampled Red List Index and the newly-developed rapid conservation assessment method for plants are described. Finally the key concepts used throughout the thesis (Extent of Occurrence (EOO), Area of Occupancy (AOO), Extent of Suitable Habitat (ESH), Species Distribution Model (SDM)) are introduced.

CHAPTER 2

This chapter describes the IUCN standardised method for calculating species' geographical range, and introduces a new metric as applied to pteridophytes, the Extent of Suitable Habitat (ESH), in order to improve it. Different variables and remote sensing-derived datasets are tested in order to establish the most appropriate method for the ESH calculation for SRLI forest pteridophyte species. The final ESH calculation method is standardised through building a GIS script and the results are validated by new species occurrence point data from the Global Biodiversity Information Facility (GBIF) online database and by fieldwork conducted in Costa Rica.

CHAPTER 3

In this chapter, global species richness and endemism richness maps for the SRLI forest pteridophyte species are generated using the improved (ESH) method for calculating species ranges. The chapter's aim is (1) to produce the first global maps of species richness and endemism for SRLI forest pteridophytes and (2) to determine whether the species ESHs can be used in producing meaningful biodiversity maps. These maps are produced using the ESHs of the SRLI pteridophyte forest species calculated in Chapter 2. In order to determine if the ESH-derived species richness map reflect the reality found on the ground, the map is validated using fieldwork data collected in Costa Rica (for this study) and additional fieldwork data from a previous study (Kessler *et al*., 2011). Furthermore, the global patterns of the ESH-derived species richness and endemism are compared with those of existing well-known maps of species richness and endemism and analysed together with environmental variables in order to understand the determinants of those patterns.

CHAPTER 4

This chapter presents the comparison of the ESH method for calculating species' ranges (Chapter 2) with an established species distribution modelling approach. Both a Species Distribution Model (SDM) and an ESH are generated for each SRLI forest pteridophyte species endemic to the Neotropics (Central and South America), using identical sets of occurrence point data, in order for the two methods to be comparable. The two sets of species' geographical ranges (ESHs and SDMs) and the subsequent species richness maps (ESH and SDM-derived maps) are compared using multiple metrics. Furthermore, the species richness maps are validated using two independently-derived fieldwork datasets.

CHAPTER 5

Chapter 5 focuses on Africa. The aim of this chapter is (1) to apply the ESH calculation method to a different SRLI plant group, the angiosperms and (2) to use the ESH-derived maps of species richness and endemism to identify areas for future botanical expeditions for the SRLI for Plants. Species ESHs are calculated (based on Chapter 2) for the major SRLI plant groups (angiosperms and pteridophytes) and species richness and endemism richness maps are generated (based on Chapter 3) and compared. These maps are then combined together and

with deforestation data, to produce an integrated map of biodiversity and threat for the SRLI major plant groups and used to prioritise areas for fieldwork.

CHAPTER 6

Chapter 6 assesses the forest pteridophyte species ESH-derived ranges against the degree of human impact through time. For each species, an ESH is calculated five times: the species' estimated original ESH (before human impact); the ESH in 2005; the ESH in 2012; the ESH in 2032 and the ESH in 2062 (future scenario). The species' original ESHs and ESHs for 2005 are calculated (following the method set out in Chapter 2), using as land cover dataset, an original forest dataset and GlobCover (2005), respectively. The species' ESHs for 2012 are produced by deducting from the species' ESHs2005 any suitable habitat that, according to forest loss data (Global Forest Change dataset (GFC)), was removed between the years 2005 and 2012. Similarly, the species' ESHs for 2032 and 2062 are calculated based on forest loss data (2012 – 2062) generated using a land use change future scenario in Co$ting Nature. Furthermore, in order to estimate the uncertainty in using the selected land cover change monitoring system (GFC), the ESHs (2012) of endemic species to the Neotropics are calculated twice using two different monitoring systems of land cover change (GFC & Terra-i) and compared. Finally, the methodology, which will be the basis of an automated system for updating the species' assessments, is presented using example species.

CHAPTER 7

Chapter 7 brings together the main conclusions from each of the research chapters. It explains how the objectives of this study have been met through detailed investigation and analysis, and identifies areas of further research.

Figure 1 presents a schematic diagram showing how the empirical chapters (Chapter 2 – 6) are linked to the objectives of this study.

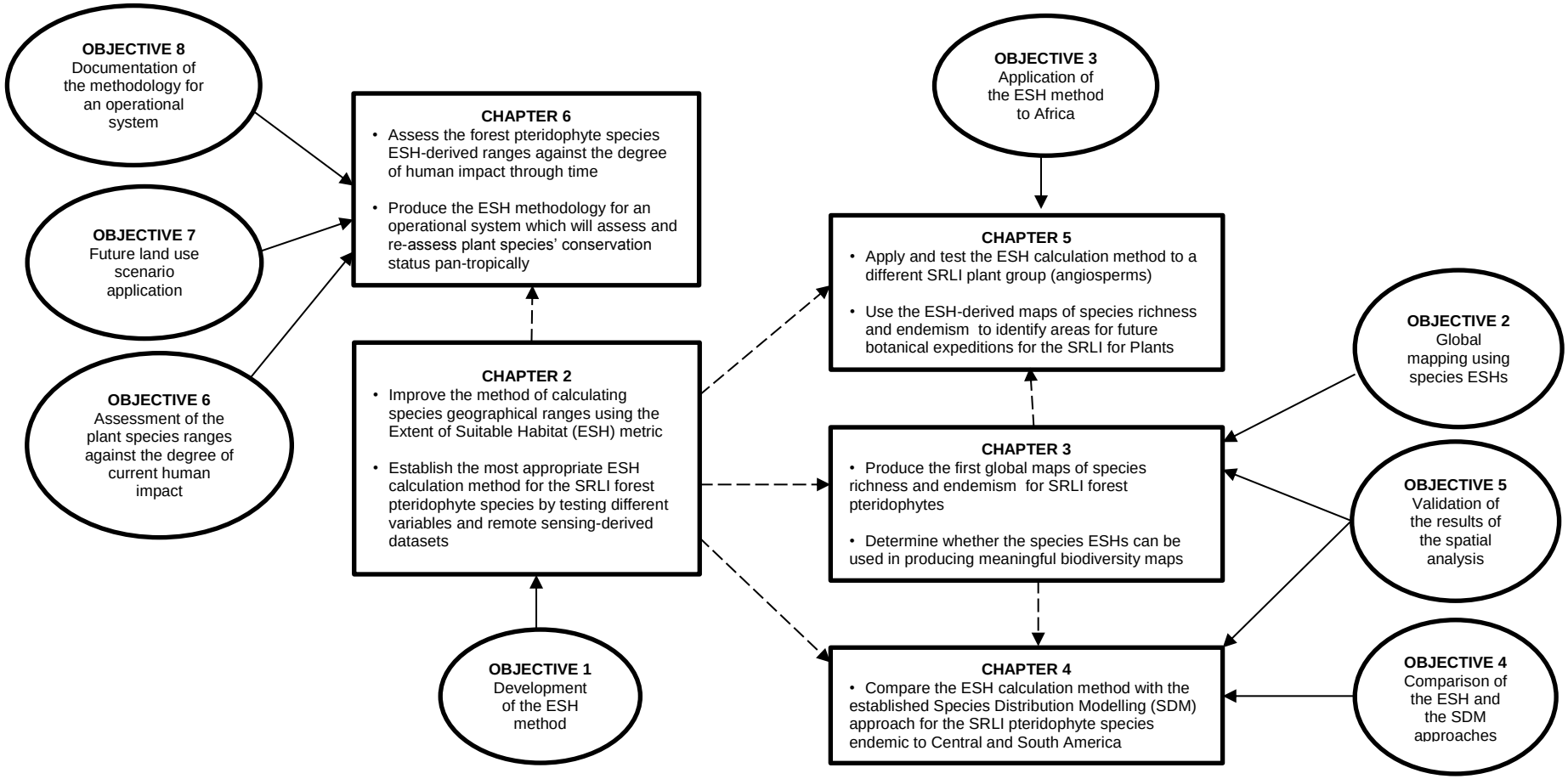

Figure 1. Schematic diagram of the empirical chapters (2 – 6) of this study (boxes) together with the objectives of this study (ovals). Solid-line arrows represent the link between chapters and objectives. Dashed-line arrows represent associations between chapters (common methods).

1.4 GENERAL INTRODUCTION

1.4.1 Biodiversity & Habitat Loss

Biological diversity or 'biodiversity', 'means the variability among living organisms from all sources including, *inter alia*, terrestrial, marine and other aquatic ecosystems and the ecological complexes of which they are part; this includes diversity within species, between species and of ecosystems' (CBD, 2005, p.5). Biodiversity therefore includes species diversity, genetic diversity and ecosystem diversity; however, it is most frequently measured using only species diversity (Gaston, 2000). According to Gaston (2000, p.220), species diversity or species richness is 'the number of species observed or estimated to occur in an area'. It is estimated that the planet's total species richness is between 5 million and 30 million species (May *et al.*, 1995) with approximately 1.75 million known species (Groombridge & Jenkins, 2002). Hence, only a small proportion of the total richness has been currently described, with an average of 15 000 species described per year (Stork, 1993), of which c. 2000 are plant species (Brummitt & Bachman, 2010). This species richness is unequally distributed over the surface of the planet with species richness peaking in the tropics (Gaston, 2000) and with biodiversity hotspots covering just 1.4% of the land surface but harboring 44% of vascular plants and 35% of vertebrate diversity (Myers *et al.*, 2000).

Humans have always been dependent on natural ecosystems and their biodiversity as ecosystem services including natural food and fibre products are essential for human well-being (Millennium Ecosystem Assessment, 2005). However, the continuing increase in human population, in conjunction with rising per-capita consumption rates, is placing unprecedented pressure on biodiversity and natural ecosystems. This pressure is pushing many species into extinction; some even argue that the Earth is undergoing a sixth great mass extinction of life (May *et al.*, 1995; Barnosky *et al.*, 2011; Dirzo *et al.*, 2014; Ceballos *et al.*, 2015), with the extinction rate being many times higher than the average estimated background rate (0.1 to 1 species extinction per million species per year) in the past (Groombridge & Jenkins, 2002; Pimm *et al.*, 2014; Ceballos *et al.*, 2015). The International Union for the Conservation of Nature (IUCN) is the global body responsible for evaluating the conservation status of species, adding more threatened species to every iteration of the IUCN Red List. According to the IUCN Red List, 41% of amphibians, 25% of mammals and 13% of birds are threatened with extinction (IUCN, 2012b). In the case of plants, 20% of the c. 380 000 species (Paton *et al.*, 2008) that are known to exist on the planet are threatened with extinction (Brummitt & Bachman, 2010; Brummitt *et al.*, 2015b). In addition, most threatened plant species are found in the tropics (Neotropics:23%, Afrotropics:22%, Australasia: 21%) and the most threatened plant group is the gymnosperms (40%) followed by the monocots (18%) (Brummitt & Bachman, 2010; Brummitt *et al.*, 2015b).

While the previous great mass extinctions were caused by natural threats, the main cause of the current species extinction is human activities. According to Brummitt & Bachman (2010), 81% of the threats to plant species derive from human impact threats (e.g. arable farming,

livestock and logging activities). Habitat loss and land use change were identified as the main causes of biodiversity loss (Groombridge, 1992; Dirzo & Raven, 2003; Gaston *et al.*, 2003a; Mace, 2005; Brummitt & Bachman, 2010; Brummitt *et al.*, 2015b). Several studies have also identified other causes of biodiversity loss, ranking climate change (McLaughlin *et al.*, 2002; Thomas *et al.*, 2004), invasive alien species (Pimentel, 2001; Gaston *et al.*, 2003b; Baillie *et al.*, 2004), overexploitation (Hutchings & Reynolds, 2004) and pollution (Baillie *et al.*, 2004) as the most important factors after habitat destruction.

Species conservation assessments for the IUCN Red List have confirmed that the biggest threat to species is indeed habitat loss (Baillie *et al.*, 2004; Brummitt & Bachman, 2010; Brummitt *et al.*, 2015b). A habitat is here defined as the area where an organism lives (Odum, 1971) and specifically the 'resources and conditions present in an area that produce occupancy, including survival and reproduction, by an organism' (Hall *et al.*, 1997). Habitats are often classified based on vegetation composition (Morrison *et al.*, 2006), with forest being one of the most vital major terrestrial habitats. Forests hold over 80% of the global terrestrial biodiversity (FAO, 2010) with tropical forests harboring more species than any other ecosystem (Myers *et al.*, 2000; Pimm *et al.*, 2001; Mace, 2005). This high level of biodiversity is threatened by high deforestation rates with many known species already extinct. In 2010, the Earth's total forest area had decreased by 15% (from 46% – pre-human impact forest cover – to 31%); forest is defined as areas with minimum 5m tree height, 10% crown cover and 5000 m² forest area size (FAO, 2010) (Figure 2). According to the Food and Agriculture Organisation of the United Nations (FAO) (2010), South America has the highest percentage of remaining forest cover, followed by Europe, Central America and North America.

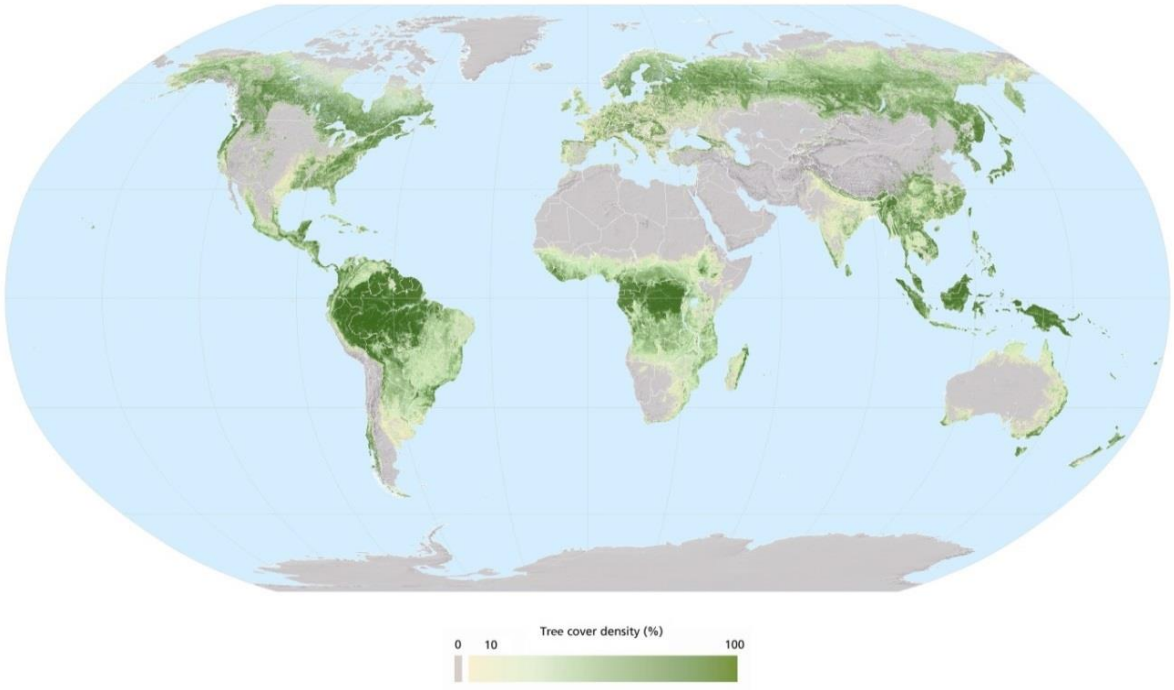

Figure 2. The World's forests. Tree cover density calculated using tree cover data derived from MODIS VCF 250 meter pixels for the year 2005 (FAO, 2010).

Deforestation is the 'removal of tree cover below the threshold value that defines a forest and converting the land to another use' (Achard, 2009). Before the 19th century, deforestation mainly occurred in forests of the temperate region, but that changed in the 20th century when the main focus was forests in tropical regions (Williams, 2002). In 1997, the World Resources Institute estimated that approximately 20% of the Earth's original forest cover remained undisturbed (Bryant *et al.*, 1997). Despite the fact that the deforestation rate has decreased due to global conservation efforts over the last two decades, 13 million hectares of forest were still deforested per year between 2000 and 2010 (FAO, 2010). The degree of deforestation differs across the world since it is driven by several factors (economic; policy and institutional; technological; cultural; and demographic) (Geist & Lambin, 2001) and has different causes (expansion of agricultural and pasture land, wood extraction, mining and infrastructure extension) (Contreras-Hermosilla, 2000; Geist & Lambin, 2002; Laurance *et al.*, 2012). Studies have revealed that the most important proximate cause of deforestation is to use the land for agriculture (Geist & Lambin, 2002; FAO, 2010; Hosonuma *et al.*, 2012; Laurance *et al.*, 2012). Between 2000 and 2010, South America and Africa were the regions with the highest deforestation rates, losing 4 million hectares and 3.4 million hectares per year, respectively (FAO, 2010) (see Chapter 6, section 6.1 for more details on deforestation).

While conservationists recognise the severity of the problem of biodiversity loss, it is impossible for the survival of all threatened species to be secured. Due to limited funds and lack of time, conservationists have been using the biodiversity hotspots approach to prioritise global conservation efforts (Mittermeier *et al.*, 1998; Myers *et al.*, 2000; Brummitt & Nic Lughadha, 2003; Lamoreux *et al.*, 2006). These areas, the majority of which are in the tropics, are only a small portion of the Earth's land cover. In this way, conservation strategies target areas with high species richness and endemism – species that are not found elsewhere – but also areas with high levels of threat; according to Myers *et al*. (2000) biodiversity hotspots have already lost 88% of their primary vegetation. While this is the most popular approach, there are a range of other conservation prioritisation schemes that are either proactive or reactive in nature (Brooks *et al.*, 2006).

1.4.2 The IUCN Sampled Red List Index

In response to continuing biodiversity loss, in 1992 the Convention on Biological Diversity (CBD) was adopted with signatories from 193 parties (national governments). This international treaty has three objectives: (1) to conserve biodiversity, (2) to use biodiversity in a sustainable way and (3) to share the benefits of biodiversity fairly and equally (CBD, 2005). In 2002, the sixth Conference of the Parties (COP) to the CBD (COP VI) agreed on a Strategic plan with the aim 'to achieve by 2010, a significant reduction in the current rate of loss of biological diversity at the global, regional and national level as a contribution to poverty alleviation and to the benefit of all life on Earth' (UNEP, 2002). In order to monitor progress towards the 2010 Biodiversity Targets, a series of biodiversity indicators were adopted (UNEP, 2006) and a Biodiversity Indicators Partnership (BIP) subsequently established to assist in monitoring this progress. Despite much

effort, by 2010, it was clear that the Biodiversity target had not been met − no significant reduction in the rate of loss of biodiversity had been achieved (Butchart *et al.*, 2010). Since the conservation of biodiversity and its associated ecosystem services also underpins many of the Millennium Development Goals (UNEP, 2005; Sachs *et al.*, 2009), the failure to meet the 2010 Target catalysed the adoption of a set of 20 new Targets for 2020 (UNEP, 2010). These Targets were set during the tenth Conference of the Parties to the CBD (COP X) in Nagoya where an updated Strategic Plan, which included these 20 Aichi Biodiversity Targets, was adopted for the period from 2011 to 2020.

The biodiversity indicators that were adopted in 2006, together with additional indicators developed through the BIP, are the main metrics by which the CBD will monitor progress towards the goals of the Strategic Plan and the Aichi Biodiversity Targets. The Red List Indices (RLI), which measure the Aichi Target 12 (preventing extinction), have been the most widely and successfully adopted. The RLI are based on the IUCN Red List for threatened species and measure temporal changes in conservation status from repeated conservation assessments of IUCN Red List species (Butchart *et al.*, 2005). The IUCN Red List includes assessments of the conservation status of species for the world's major groups of plants and animals, against the IUCN Red List Criteria (Appendix A1) and classifies them into nine categories (Not Evaluated, Data Deficient, Least Concern, Near Threatened, Vulnerable, Endangered, Critically Endangered, Extinct in the Wild and Extinct) (Figure 3) (see Appendix A2 for description of categories). Quantitative thresholds for any of the five Criteria are applied to the threatened categories of Critically Endangered, Endangered and Vulnerable (IUCN, 2012a).

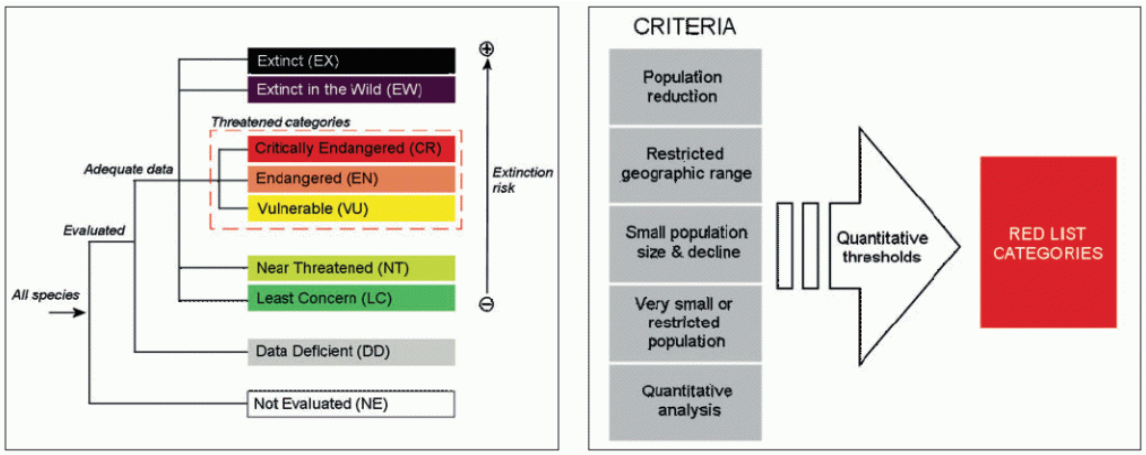

Figure 3. IUCN Red list Categories and Criteria (Vie *et al.*, 2008, p. 4).

By re-assessing these species at regular intervals, changes in the conservation status of species are detected and used to monitor overall trends in extinction risk. However, due to the number of species in larger taxonomic groups and the lack of information for many species, the assessment of all known species is not feasible. Hence, out of the 1.75 million known species (Groombridge & Jenkins, 2002) only a small percentage has been assessed, mostly species from comparatively small and well-known groups such as birds, mammals and amphibians. To address this problem, the IUCN Sampled Red List Index (SRLI) was developed (Baillie *et al.*,

2008) in order to monitor over time the conservation status of a representative sample of the world's known biodiversity. The NHM, together with the RBG Kew, has taken the lead in developing the IUCN Sampled Red List Index (SRLI) for different plant groups (Nic Lughadha *et al.*, 2005; Baillie *et al.*, 2008; Brummitt *et al.*, 2008). The SRLI has been adopted since 2006, together with other indicators, as a formal CBD indicator measuring whether or not a significant reduction in the current rate of loss of biodiversity has been achieved.

Five major plant groups are included in the SRLI for Plants: bryophytes, pteridophytes, gymnosperms, monocots and lastly legumes. The well-studied legume family was selected as a proxy for dicotyledonous plant families due to the lack of an available global checklist for all dicots at the time the sample was taken. A sample of 1500 species, the minimum sample size to ensure credible taxonomic and geographical breath suggested by Baillie *et al.* (2008) from conducting simulation modelling of the complete assessment of bird species, has been taken for each major taxonomic group with the exception of gymnosperms (which has fewer than 1500 species worldwide), for which all species are included (c.1000 spp). In order to calculate the SRLI with 95% confidence, 900 out of 1500 species of each group needed to be data sufficient. Almost 7000 species, out of 380,000 known plant species (Paton *et al.*, 2008), have so far been assessed for the SRLI for Plants and by 2010 showed that more than 1 in 5 plant species are threatened with extinction (Brummitt & Bachman, 2010; Brummitt *et al.*, 2015b).

1.4.3 IUCN Red List assessments for SRLI plant species

Due to the lack of documentation on population sizes or dynamics of plant species, conservation assessments for the SRLI plant species have predominantly been generated based on the known geographical distribution of the species, utilising Criterion B. For the conservation assessments, comprehensive herbarium specimen data were used, together with previously-digitised online specimen resources coupled with in-house GIS analysis (Willis *et al.*, 2003; Brummitt *et al.*, 2008; Rivers *et al.*, 2010). Firstly, for each species all available herbarium specimens (dried plant samples mounted on a sheet) were gathered and digitised. These specimens were georeferenced (assigned with a spatial coordinate) based on the locality information on the specimen label and using maps, gazetteers and online tools such as Google Earth. They were then combined with additional digitised specimens retrieved from freely-accessible online databases (e.g. TROPICOS, GBIF), thereby gathering all available specimens for each species. The target was to georeference at least 15 specimens per species as 15 is the minimum number of specimens that are needed to detect a threatened species (Rivers *et al.*, 2011), although in practice many species had fewer available specimens than this. The georeferenced specimens were incorporated into GIS software and preliminary assessments based on the IUCN Criteria and Categories were conducted using the Conservation Assessment Tool (CAT) (Bachman *et al.*, 2011). The CAT tool estimates the Extent of Occurrence (EOO), the Area of Occupancy (AOO), the number of subpopulations, the number of locations and measures of fragmentation, all of which are parameters used to assess the conservation status of that species against Criterion B (geographic range) of the IUCN Red List

(Willis *et al.*, 2003). Building on the data from the preliminary assessments, full 'desktop' conservation assessments were conducted for potentially threatened species by adding further information from literature, more detailed GIS analysis fieldwork data and expert knowledge to satisfy additionally two out of the three sub-criteria of Criterion B (Appendix A1). The full assessments including the IUCN Red List rating were published on the SRLI for Plants Scratchpad website (http://threatenedplants.myspecies.info/) in order for experts to provide feedback on them before being submitted to the IUCN Red List Authorities, evaluated and published on the IUCN Red List.

1.4.4 Species geographical range metrics

As mentioned above, threatened species are categorised based on five quantitative criteria (Appendix A1), any one of which needs to be met in order for a species to be classed as threatened (IUCN, 2012a). According to Gaston and Fuller (2009), 47% of threatened species in the IUCN Red List were categorised based on the size of their geographic range (IUCN Criterion B), due to lack of population information. Criterion B is - in the majority of cases - the most appropriate for specimen-based assessments since the geographic range metrics can be calculated using the locality information found on the specimen label (Willis *et al.*, 2003). These geographic range metrics are the Extent of Occurrence (EOO) and the Area of Occupancy (AOO), both of which are calculated in a preliminary conservation assessment and their values compared with the quantitative thresholds for threatened Categories under Criterion B.

According to IUCN (2012a), EOO is defined as 'the area contained within the shortest continuous imaginary boundary which can be drawn to encompass all the known, inferred or projected sites of present occurrence of a taxon, excluding cases of vagrancy'. The EOO metric was firstly introduced by Gaston (1991) to capture 'the overall geographic spread of the localities at which a species occurs'. Due to the relationship between the species geographic range and extinction risk, the IUCN has been using the EOO as a measure of the degree of risk spread across the species' population. Assessors have estimated the EOO using various methods which calculate the outermost boundary of the species' distribution. The main methods are (1) the minimum convex polygon (MCP), (2) the a-hull (Delauney triangulation of the occurrence points minus connecting lines longer than a certain multiple of the average line length) and (3) the interpolated threshold of abundance (Gaston & Fuller, 2009). Expert's maps, which were based on marginal occurrences, have been also used to calculate the species' EOOs of relatively small and well-known taxonomic groups such as birds and mammals. However, these maps are not available for the species of larger groups such as plants (Brummitt *et al.*, 2015a). Joppa *et al.* (2015) assessed the impact on extinction risk categories of applying different methods for calculating the EOO of approximately 22,000 species. It was shown that different methods can give different estimates of EOO and it was suggested to use the MCP method to ensure consistency across the conservation assessments. Their suggestion

was in agreement with the IUCN's Standards and Petitions Subcommittee's recommendation to strictly use the MCP method to estimate EOO (IUCN, 2014).

The EOO includes all discontinuities in the species' occurrences (i.e. areas with unsuitable habitat). For this reason, by using the EOO as a measure of range size, the geographic range is overestimated (Burgman & Fox, 2003; Shaw *et al*., 2003; Orme *et al*., 2006; Jetz *et al*., 2008), since species do not occur throughout the whole range of their EOO. Thus, the IUCN uses the AOO metric together with the EOO. The AOO is defined as 'the area within its EOO which is occupied by a taxon, excluding cases of vagrancy' (IUCN, 2012a) and is calculated by summing the area of occupied grid cells, the size of which is set appropriately for each species. Thus, the AOO is better correlated with population size than the EOO is (Gaston & Fuller, 2009). The calculation of AOO is strongly dependent on the spatial resolution and the cell size of the data used to calculate species distribution maps (Willis *et al*., 2003; Rondinini *et al*., 2006) and affected by sampling intensity (Brummitt *et al*., 2015b).

The species geographic range has been also estimated using predictive distribution models (Rondinini *et al*., 2006). Such models are the Species Distribution Models (SDMs) which have been used to predict areas that have suitable environmental conditions for a species (Franklin, 2009) (see Chapter 4, section 4.1 for more details on SDMs). Others have used habitat suitability models to predict the species' preferred habitats/combinations of environmental conditions (i.e. the Extent of Suitable Habitat (ESH)) (see Chapter 2, section 2.1 for more details on ESHs). Although, these metrics are widely used, they are not incorporated in the IUCN species conservation assessments.

Since all geographic range metrics are calculated using data acquired from herbarium specimens, the assessments are dependent on the accuracy of these data. Herbarium specimens could have a detailed label with precise locality information; however, there are many specimens with only limited or without any locality information, making their georeferencing difficult. The quality of georeferencing is important when using specimen data since any georeferencing errors could lead to the miscalculation of the geographic range metrics on which the conservation assessment is based (Brummitt *et al.*, 2008). Additionally, taxonomic inaccuracies and incorrect determination of specimens are reflected in the specimen data for each species (Williams *et al.*, 2002) and therefore could also influence the calculation of these metrics. Lastly, geographic sampling bias is reflected in the natural history collections since specimens tend to be collected in areas with easy access (Reddy & Dávalos, 2003; Willis *et al.*, 2003; Kadmon *et al.*, 2004) and for taxa in areas of high interest at the time of the expedition (Nelson *et al.*, 1990; Dennis & Thomas, 2000). Although museum collections are valuable in providing a historical coverage of the species range (Boakes *et al.*, 2010), it is recognised that often they may not cover the whole spatial range of the species (Haila & Margules, 1996). There is also geographic bias in the holdings of individual institutions and in what is available digitally (Boakes *et al.*, 2010; Jetz *et al.*, 2012). Hence, the biases in the spatial coverage of the available specimens for each species could also affect the accuracy of the calculated species range.

CHAPTER 2

IMPROVING THE METHOD OF CALCULATING SPECIES GEOGRAPHICAL RANGES

2.1 INTRODUCTION

According to Gaston and Fuller (2009), 47% of threatened species in the IUCN Red List – at the time – were categorised based on the size of their geographic range (IUCN Criterion B). Where detailed distribution maps for species do not exist, as is the case for most plant species, these can be created from historical specimens held in natural history collections. Criterion B is the most appropriate for specimen-based assessments in the majority of cases since the geographic range metrics can be calculated using the locality information found on the specimen label, and GIS scripts to automate these calculations exist (Willis *et al.*, 2003). Specifically, Criterion B was used to categorise more than half (59%) of species assessed for the SRLI for Plants (Brummitt & Bachman, 2010; Brummitt *et al.*, 2015a; Brummitt *et al.*, 2015b) (Figure 4). Specific measures of species' range size and occupancy are used in carrying out conservation assessments under IUCN Criterion B and although these have precise definitions in the IUCN Red List Categories and Criteria, there is still debate over the most effective representation of the EOO and AOO of a species (Gaston, 1991; Gaston, 1994; Gaston & Fuller, 2009; Joppa *et al.*, 2015).

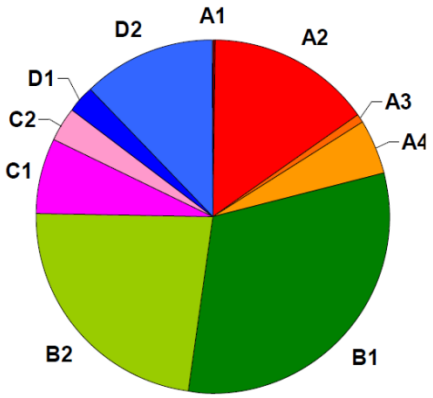

Figure 4. Frequency of criteria used in the IUCN SRLI plant conservation assessments (Brummitt *et al.*, 2015a) (See Appendix A1 for Definitions of criteria).

The SRLI for Plants team has used point distribution maps from georeferenced specimen data for SRLI plant species to create minimum convex polygons to measure the range size of each species, under the IUCN definition of EOO. The minimum convex polygon approach is now recommended by IUCN (IUCN, 2014) since its universal adoption will ensure consistency across the IUCN Red List assessments of all taxonomic groups (Joppa *et al.*, 2015). The minimum convex polygon can be thought of as the area inside an elastic band stretched around

all points (Bachman *et al.*, 2011). Each convex polygon includes all occurrence points and is the smallest polygon in which no internal angle exceeds 180 degrees (Figure 5). Hence, the species ranges were calculated with consistency in contrast with the species range maps manually constructed by experts.

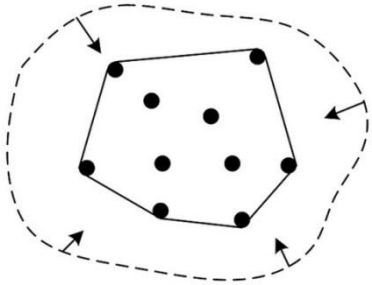

Figure 5. Illustration of a minimum convex polygon of a set of points (Bachman *et al*., 2011, p. 121).

While the EOO is the simplest way to calculate a species range size when using presence-only data, its accuracy has been extensively criticised. Gaston (1991) introduced the EOO measure and described it as the 'area between the outer-most limits to a species occurrence', including areas where the species may not actually occur, since it assumes that the species distribution is homogenous (Rondinini *et al.*, 2006). These non-suitable areas were included by Gaston in order to have a clear distinction between EOO and AOO (the area within the EOO that is known to be occupied by the species). Furthermore, discontinuities in habitat or occupancy were included in the EOO since it represents the full geographical extent of the species' localities and can be used to estimate the chance of extinction of all populations of a species by a single threat (Gaston & Fuller, 2009). The effect, however, of using the EOO as a measure of range size is to overestimate the species geographical range (Burgman & Fox, 2003; Shaw *et al.*, 2003; Orme *et al.*, 2006; Jetz *et al.*, 2008), since species do not occur throughout the whole range of their EOO. When using the species EOO for conservation planning, this metric could be misleading since often protected areas within the species EOO are thought to protect that particular species, whereas in reality the species may not occur in those areas (Loiselle *et al.*, 2003; Rondinini *et al.*, 2005; Rondinini *et al.*, 2006; Pimm *et al.*, 2014). IUCN therefore uses EOO together with AOO (grid cells within the EOO where the species is actually known to occur), and both these measures have quantified thresholds for threatened Red List Categories under Criterion B. However, the calculation of AOO is also problematic since it is strongly dependent on the spatial resolution and the cell size of the data used to calculate species distribution maps (Willis *et al.*, 2003; Rondinini *et al.*, 2006) and affected by sampling intensity (Brummitt *et al.*, 2015b).

A solution to this problem is to use deductive habitat suitability models to calculate species ranges (da Fonseca *et al.*, 2000). Species Distribution Models (SDMs) have been used to predict areas that have suitable environmental conditions for a species (Franklin, 2009) and have been suggested to be incorporated in species conservation assessments (Sérgio *et al.*, 2007; Pena *et al.*, 2014; Syfert *et al.*, 2014). However, accurate SDMs are time-consuming to

produce and require detailed knowledge of the ecology of the species being investigated (Franklin, 2009) and hence cannot easily be used in IUCN species conservation assessments. Thus, a new measure of species range that can reduce the commission errors (false positives) associated with the EOO (Beresford *et al.*, 2011a; Beresford *et al.*, 2011b; Buchanan *et al.*, 2011; Rondinini *et al.*, 2011), has been introduced. This new measure, the Extent of Suitable Habitat (ESH), is described as the 'maximum potential extent of the AOO' (Beresford *et al*., 2011a, p.100) and is calculated from the species EOO by reducing it according to the habitat preference of the species. It therefore selects the areas that provide appropriate conditions for the species without assuming that the species occupancy is homogenous across its range, as the EOO does. The ESH metric has already been used to calculate the geographical distribution of IUCN mammal (Rondinini *et al.*, 2005; Boitani *et al.*, 2008; Catullo *et al.*, 2008; Rondinini *et al.*, 2011; Visconti *et al.*, 2011; Visconti *et al.*, 2015) and bird species (Jetz *et al.*, 2007; Beresford *et al.*, 2011a; Buchanan *et al.*, 2011).

2.2 METHODS

To improve the method of calculating the ranges for SRLI pteridophyte species (the first objective of this project), the ESH metric was adopted; making this the first time that ESH has been calculated globally for plant species. The ESH maps for SRLI forest pteridophyte species were produced based on information of the appropriate ecology of each species (altitude range and water balance range preference) and land cover information, both within the convex hull defining the species' EOO. Due to the fact that the species' EOO were calculated using the species' occurrence points, an investigation into the geographical bias in the SRLI dataset was conducted. In order to select the appropriate habitat preference for each species, three different land cover datasets (GLCC, GLC2000, GlobCover) were used and the results were compared to select the most suitable dataset for use with plant species. Additionally, the species ESHs were used to produce species richness and endemism richness maps, one for each land cover dataset. This was followed by a comparison of the three species richness maps and final selection of the most appropriate method. Furthermore, the ESH method was finalised by including species water availability range preference after comparing water balance and water deficit data and selecting the most appropriate one. Lastly, species ESHs were validated using independent occurrence point data from the Global Biodiversity Information Facility (GBIF) online database.

2.2.1 Gathering and investigating the bias in the IUCN Sampled Red List Index data

As mentioned in the General introduction (Chapter 1), the sample of species for the SRLI for Plants was chosen at random. The sample contains 1500 species from each of the 4 major taxonomic groups (bryophytes, pteridophytes, monocots and legumes), plus all species of gymnosperms (approx. 1000 species), a total of c.7000 species. The species selected for the work described here were taken from this set of plant species and for which baseline conservation assessments already exist. The pteridophytes, the second largest plant group after

angiosperms (Smith *et al.*, 2005; Paton *et al.*, 2008), were selected as the most appropriate case study group due to their wide geographical and ecological diversity. Pteridophytes were also selected for this study due to the strong relationship between their range size with the suitable habitat availability (Tryon, 1986; Tuomisto *et al.*, 2003; Jones *et al.*, 2006). The Natural History Museum gave permission to use the SRLI pteridophyte data and also access to the specimen collections. In addition, at the Natural History Museum, there is taxonomic expertise for reliable identification of material from the field and world-leading research on pteridophyte systematics.

As it is important to investigate the response of plant species to the degree of human impact and land cover change, the forest pteridophyte species were selected as the most appropriate group for detailed study given our focus on impacts of deforestation. The forest species were selected from the SRLI pteridophyte MS Access database based on their habitat classification as recorded by the IUCN habitats authority file, in which forest type habitats are under Category 1 (Appendix A3). The IUCN forest habitat type covers both temperate and tropical forests, 'includes primary and secondary forest habitats and forest edges/margins' (IUCN, 2007) and has nine subcategories (Appendix A4). Out of the 1500 SLRI pteridophytes, 635 species were identified as species associated with forest habitats (Figure 6).

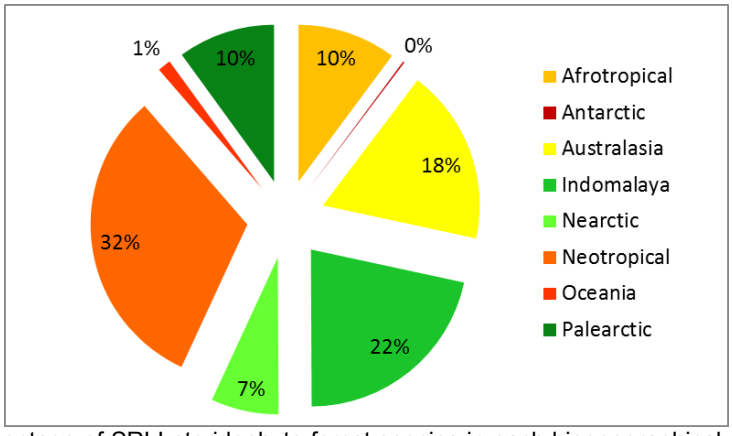

Figure 6. The percentage of SRLI pteridophyte forest species in each biogeographical realms of the world (Species that occur in more than one biogeographical realm are not included in this figure).

The SRLI pteridophyte forest species have a total of 116 000 records (specimens) globally. The source of these records is herbarium specimens found in RBG, Kew and the NHM, and GBIF. All records have been georeferenced from the specimen locality information, or recorded digitally in the field, by the digitizers of the SRLI team and a point distribution map produced for each species (Figure 7).

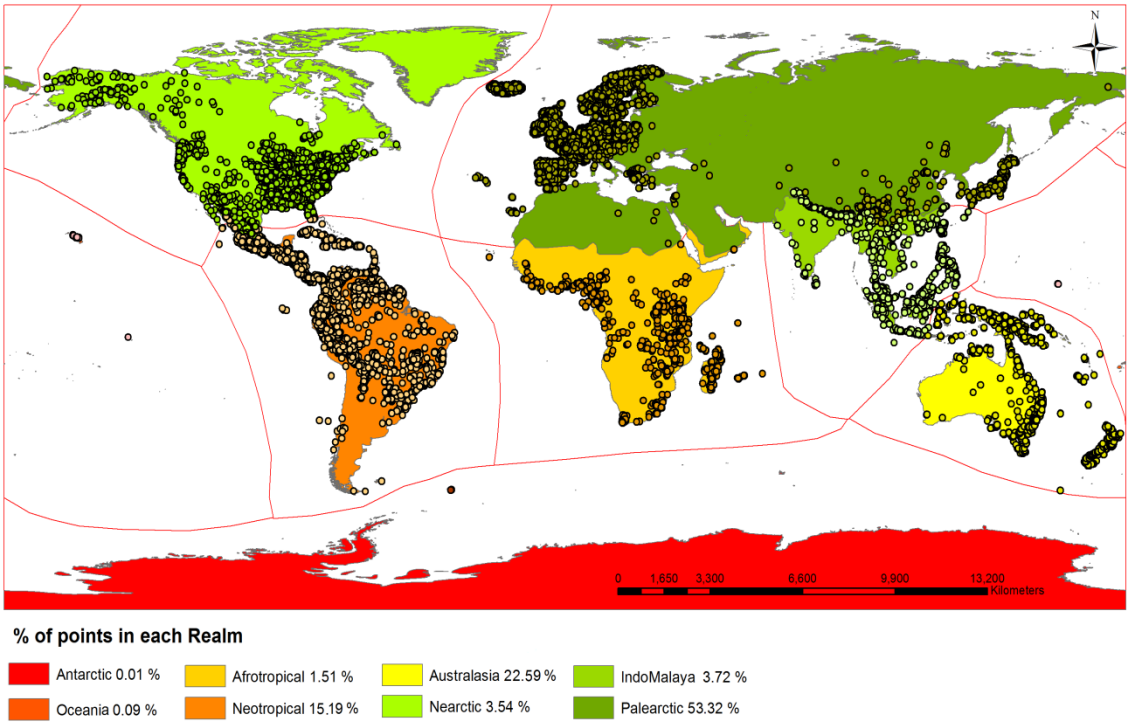

Figure 7. Number of records (% of total) of SRLI pteridophyte forest species in each biogeographical realms of the world (following Olson *et al.* (2001)).

Different analyses were conducted to investigate the bias within the selected SRLI species sample (forest pteridophytes). This subsample (SRLI forest pteridophytes) was compared with the SRLI sample (1500 randomly selected pteridophyte species) as well as with a global pteridophyte checklist, a database of all known pteridophyte species with information on their distribution. The percentage of species in each biogeographical realm (Neotropical, Afrotropical, Indomalaya, Nearctic, Palaearctic, Austalasia, Oceania and Antarctic (Olson *et al*. 2001)) of the three datasets was compared.

The differences found between SRLI forest pteridophyte species and the full SRLI dataset and global pteridophyte checklist were investigated by determining whether the species occurrence data (SRLI point data) are representative of the distribution of those species, as represented by pteridophyte checklists. A comparison was conducted of the number of SRLI forest pteridophyte species in each biogeographical realm when calculated based on the species occurrence points (SRLI point data derived from herbarium specimens) and on the distribution information found in the global pteridophyte checklist. There is a distinct difference between the two since, for example, one species could occur in two realms according to the checklist but have been collected in only one of them.

Sampling effort, the number and frequency of specimen collections (occurrence points) within different regions was also investigated. In order to investigate such geographical sampling bias, the number of occurrence points in each biogeographical realm was calculated taking into consideration the area of suitable habitat in each realm. Furthermore, the density of all occurrence points was calculated in order to identify such sampling effort bias. Additionally, the

occurrence points of the SRLI forest pteridophyte species were analysed together with the available information on the distribution of the species taken from the global pteridophyte checklist. The aim of this analysis was to find any countries in which SRLI forest pteridophyte species are listed but for which there are no occurrence data.

2.2.2 Refining the species geographical range

2.2.2.1 Calculating the Extent of Occurrence

The EOO is defined as the smallest minimum convex polygon that includes all occurrence points of a species. Hence, the EOO assumes that any given species will not be found outside its margins, which is probably not true. It was decided at the outset that this study will not address the issue of false absence (additional records that should be found outside the EOO boundary but by definition cannot be) due to the strict IUCN guidelines to use the objective and comparable EOO metric for species conservation assessments (IUCN, 2014). Therefore the EOO metric was used as the basis for calculating the species geographical range.

The point distribution maps for SRLI forest pteridophyte species were imported into ArcGIS 9.3 (ESRI, 2009) and were projected to a cylindrical equal area projection with a World Geodetic System 1984 (WGS84) datum. Using the ArcGIS extension Hawth's tools (Beyer, 2007) a minimum convex polygon (MCP) was calculated for each species (Figure 8). The MCP requires a minimum of 3 georeferenced localities, therefore the EOO was not calculated for 148 species which had fewer than 3 unique localities.

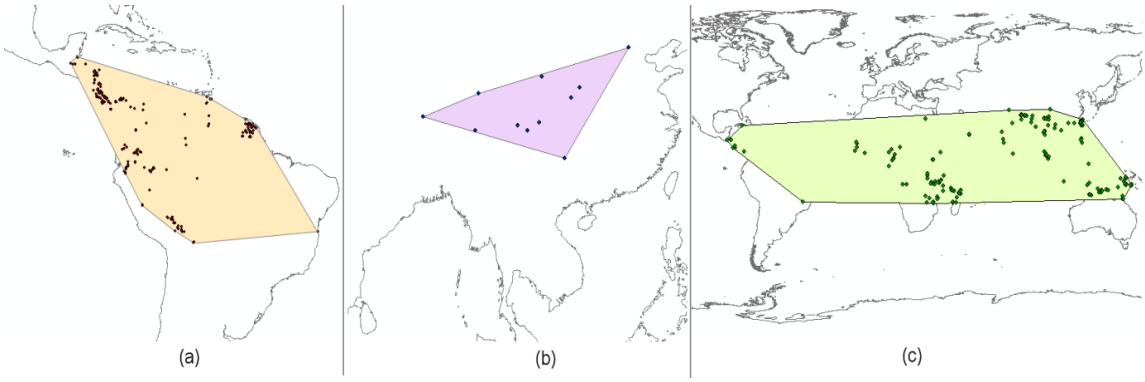

Figure 8. Extent of occurrence of (a) *Polybotrya caudata*, (b) *Notholaena borealisinensis* and (c) *Adiantum philippense.*

2.2.2.2 Calculating the Extent of Suitable Habitat

ESHs for pteridophyte species were calculated within the minimum convex polygon (EOO) by removing grid cells with values outside of the known ecological/environmental preferences for each species (details in sections 3.2.2.2.2 and 3.2.2.2.3). Previous studies have applied this deductive approach with two variables: elevation and land cover (Rondinini *et al.*, 2005; Boitani *et al.*, 2008; Beresford *et al.*, 2011a; Buchanan *et al.*, 2011; Rondinini *et al.*, 2011). In this study,

water availability was also included in the calculation of the species' ESHs due to the known strong relationship between pteridophytes and the availability of water (Page, 2002; Bickford & Laffan, 2006; Kessler *et al.*, 2011).

2.2.2.2.1 Ecological/environmental variables

ALTITUDE

Altitude has been used in calculating species distribution since altitude can restrict species ranges (Harris & Pimm, 2008; Oke & Thompson, 2015). A relationship has been found between species range size and altitude which was explained by the decrease of land area with the increase of altitude and by the topographical complexity in high altitudes, the geographic isolation of which can instigate speciation and thus the occurrence of narrow-ranged species (Stevens, 1992; Rahbek, 1995). Some pteridophyte species have wide altitudinal ranges whereas others have a more distinct altitudinal preference (Mehltreter, 1996; Kessler, 2002b). Information about plant species altitudinal ranges is typically available in Floras and herbarium collections. In this study, species altitude preferences were determined from four sources: (1) the herbarium specimen labels (notes taken by the specimen collector), (2) the IUCN Red List assessments carried out for the pteridophyte species in the SRLI project (from a literature search undertaken by the assessor), (3) extended search of the scientific literature and (4) extracting altitude values of the georeferenced point data from remotely sensed elevation data (Shuttle Radar Topography Mission (SRTM), version 4 (Jarvis *et al.*, 2008)). The SRTM dataset has approximately a 1km spatial resolution and is in a geographic coordinate system with a WGS84 datum. Version 4 of the SRTM dataset is an improved version of the National Aeronautics and Space Administration's (NASA) and United States Geological Survey's (USGS) original dataset which included data voids over water bodies, snow covered areas and high altitude areas. This improved version by the Consultative Group for International Agricultural Research (CGIAR) has solved this specific problem by filling the no data holes using interpolation techniques (Jarvis *et al*., 2008). The minimum and maximum values from any of these above sources were assigned to each species and used to calculate the species altitudinal range.

LAND COVER

Models that are just based on bioclimatic variables may over predict a species distribution since they do not include the human impact factor influencing these 'bioclimatic' suitable areas (Araújo, 2003) and are thus representative of potential ranges. While some studies show the importance of including land cover in species distribution models (Pearson *et al.*, 2004; Thuiller *et al.*, 2004; Venier *et al.*, 2004; Luoto *et al.*, 2007; Stanton *et al.*, 2012) others show that land cover does not improve the accuracy of their models (Cardillo *et al.*, 1999; Maes *et al.*, 2003). Nevertheless, since habitat loss is considered the greatest threat to species (Groombridge, 1992; Baillie *et al.*, 2004; Brummitt & Bachman, 2010; Brummitt *et al.*, 2015b), land cover

change should be taken into consideration when calculating a species distribution especially if the species is being monitored over time (Harris & Pimm, 2008; Pimm *et al.*, 2014).

Three different global land cover datasets are publically available: Global Land Cover Classification (GLCC) (USGS-NASA, 2000), Global Land Cover map 2000 (GLC2000) (European Commission, 2003) and GlobCover (IONIA, 2009) all of which will be tested in order to select the most suitable dataset for the species' ESH calculation. Details on the three different classification datasets can be viewed in Table 1. These datasets were produced from different sensors, classification techniques, classification schemes and forest definitions. A description of the classes of each dataset can be found in Appendix A5 – A7. GlobCover is the highest resolution (300m) and the most recent of the available global land cover maps. There are, however, two available GlobCover versions with the same resolution and include the same detailed land cover classes. The first version, Globcover version 2.2, was released in 2008 and represents a global land cover map for 2005 (Globcover 2005) (Bicheron *et al.*, 2008), whereas the second version, GlobCover version 2.3 was released in 2011 and represents a global land cover map for 2009 (Globcover 2009) (Bontemps *et al.*, 2011). Globcover 2009, the most recent version, was used for the comparison with the other land cover datasets. Although GlobCover has a 300m resolution, its data were aggregated here to a 1km resolution using the resampling tool in in ArcGIS version 9.3 (ESRI, 2009), in order to be comparable with the other datasets. The GLC2000 and the GlobCover layers have been previously used in calculating the ESH for bird (Jetz *et al.*, 2007; Beresford *et al.*, 2011a; Buchanan *et al.*, 2011) and mammal (Catullo *et al.*, 2008; Rondinini *et al.*, 2011) species, respectively, whereas the GLCC global ecosystem map has been used in investigating the fragmentation of habitat types (Riitters *et al.*, 2000; Willis *et al.*, 2003) and in calculating the ESH for mammal species (Rondinini *et al.*, 2005; Boitani *et al.*, 2008).

Table 1. Comparison between the GLCC global ecosystems, GLC2000 and GlobCover global databases (adapted from Bai, 2010).

	GLCC Global ecosystems	**GLC2000**	**GlobCover**
Type	Ecosystems map	Land Cover map	Land Cover map
Sensor	AVHRR	SPOT 4 Vegetation	MERIS
Spatial Resolution	1 km	950 m	300 m
Data Collection time	1992 – 1993	1999 – 2000	2004 – 2005 / 2008 – 2009
Classification technique	Continental unsupervised classification & post-classification refinement	Regional unsupervised classification	Generally unsupervised classification
Classification scheme	IGBP/Olson ecosystem classification	FAO LCCS	FAO LCCS
Validation	no validation for v.2.0	Statistical sampling / confidence building method	Statistical sampling / independent validation by experts
Global Accuracy		68.6±5%	67.1% / 70.7%

Classes	94	22	23
Produced by	USGS/JRC	JRC	ESA
Version used	v2.0	v1.1	V2.2 / V2.3
Product Reports	Loveland *et al*. (2000)	Mayaux *et al*. (2006)	Bicheron *et al*. (2008) / Bontemps *et al*. (2011)

Each dataset's categories were matched to the IUCN habitats classification scheme (IUCN, 2007), with a focus on forest classes. Habitat information was taken from the assigned habitat category in the Red List assessment for each species, which was one of nine forest subcategories. These subcategories were matched to the GLCC, GLC2000, and GlobCover datasets (Table 2) and the appropriate classes assigned to each species. In addition, class values of the georeferenced point data of the species were extracted using the classification datasets and were added to the assigned classes of each species.

Table 2. Assigned classification classes for each IUCN habitat category (See Appendix A5 – A7 for classes' description).

IUCN habitat category	GLCC classes	GLC2000 classes	GlobCover classes
Subtropical/Tropical Moist Montane Forest	28, 29	1, 4	40 , 50, 60, 90, 100
Subtropical/Tropical Moist Lowland Forest	5, 6, 19, 24, 26, 33, 34, 48, 54, 90	1, 2, 3, 4, 6	40, 50, 60, 100
Temperate Forest	3, 4, 5, 21, 22, 24, 26, 54, 27, 29, 77, 78	1, 2, 3, 4, 5, 6	50, 60, 70, 90, 100
Subtropical/Tropical Dry Forest	29, 32	2, 3, 5, 6	40, 50, 60, 100
Boreal Forest	21 , 61	4, 5, 6,	70, 90, 100,
Subantarctic Forest	54	6	100

WATER AVAILABILITY

Water availability variables are important in constraining plant geographical ranges (Woodward & Williams, 1987; Stephenson, 1990; Stephenson, 1998; Stephenson, 2000). Studies focusing on pteridophyte distribution have shown the strong correlation between pteridophytes and the availability of water (Page, 2002; Bickford & Laffan, 2006; Kreft *et al.*, 2010; Kessler *et al.*, 2011). This strong influence by water availability is explained by the dependence of the gametophyte phase of the pteridophytes life cycle and, specifically, of the dispersal of the male gametes, on water availability (Page, 2002). This relationship is reflected in the global pteridophyte species richness pattern since according to Kreft *et al.* (2010) water availability is one of the main drivers of pteridophyte species richness which peaks in areas with high potential evapotranspiration and precipitation and degree of topographic complexity. When investigating the global distribution of terrestrial vegetation, two water availability variables are widely used, water balance and water deficit; both of which represent the species' tolerance to drought. Both datasets will be tested in order to select the most appropriate dataset for calculating the species' ESHs.

Water balance is calculated as precipitation minus actual evapotranspiration (AET). The water balance data (Mulligan, 2011) were calculated with fog input data from the FIESTA fog delivery model (Mulligan & Burke, 2005) and are cumulative at 1km resolution. The model used precipitation data from the WorldClim database and the Moderate Resolution Imaging Spectroradiometer (MODIS) actual evapotranspiration data. It was important to include fog as this is a significant extra input of water in some tropical montane environments (Mulligan, 2010). Since pteridophyte distributions are limited by the length and severity of the dry season of each year (Moran, 2004), the annual water balance data (annual minimum or annual average) were not used in the analysis. Instead, the minimum value of each pixel for all 12 maps (one map for each month, representing a climatological water balance from 1950 – 2000) was calculated and a global water balance map (at 1km resolution) was produced with these minimum pixel values. Water deficit is calculated as potential evapotranspiration (PET) minus AET (Stephenson, 1998). PET and AET data (at 1km resolution) were obtained from the CGIAR-CSI database (CGIAR-CSI, 2008) which were calculated from WorldClim climate data. The maximum monthly water deficit (equivalent to minimum water balance) was used instead of the mean annual water deficit. Maximum water deficit was produced by selecting the maximum value of each pixel for all 12 maps (one map for each month) and calculating a water deficit map with these maximum pixel values.

There is no specific information on water availability requirements of species in the IUCN assessments. Assigning a range of water availability values to each species based on literature is difficult, as many species are poorly known ecologically and often all the information that exists is a taxonomic description plus the broad outline of their distribution. Hence, water balance values and water deficit values (both at 1km resolution) were extracted using the georeferenced point data for each species in order to (1) assign the equivalent minimum and maximum value of each water availability variable to each species and (2) identify any clusters of species with similar water availability requirements and assign a generic range of water availability values to each cluster (instead of a specific range to each species).

2.2.2.2.2 ESH calculation using two variables

The species ESHs were first calculated using two variables, altitude and land cover. Once the data were prepared, a GIS analysis was performed in order to calculate the ESH for each species. Due to the number of species, a GIS script was built, in ArcGIS version 9.3 (ESRI, 2009) for batched automated processing. The steps of the model were designed in the Model Builder application creating a graphic flow chart model. The flow chart was then automatically converted into a Python language script and the code was implemented to apply the model to each species by iterating them and applying the functions to them.

Three models were made for each species, each with a different land cover dataset: altitude + GLCC, attitude + GLC200, altitude + GlobCover. For each species, the EOO (minimum convex

polygons) was used to mask the SRTM elevation data and then the SRTM output map was used to mask the land cover data. The SRTM output map was then reclassified (to 0-1) based on the altitude range of each species whereas the land cover output map was reclassified according to the land cover classes assigned to each species (Figure 9).

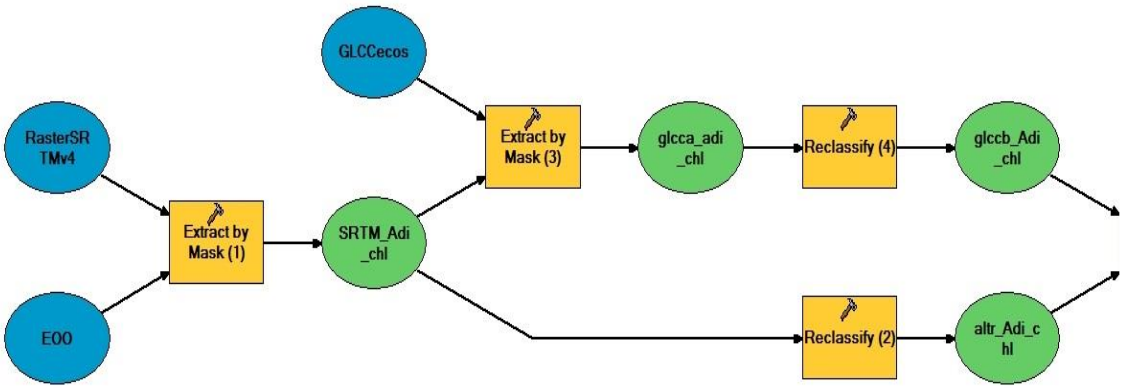

Figure 9. Part 1 of the ArcGIS model for calculating a species ESH (this example uses altitude + GLCC land cover dataset). Yellow boxes represent spatial functions (tools) and blue and green ellipses represent input and output data, respectively.

These steps were followed by selecting the land cover data that were within the altitude range of the species and reclassifying the output map to values 1 and 0, representing presence and absence. The reclassified output map was further projected to a cylindrical equal area projection with a WGS84 datum to calculate the area of the ESH (Figure 10).

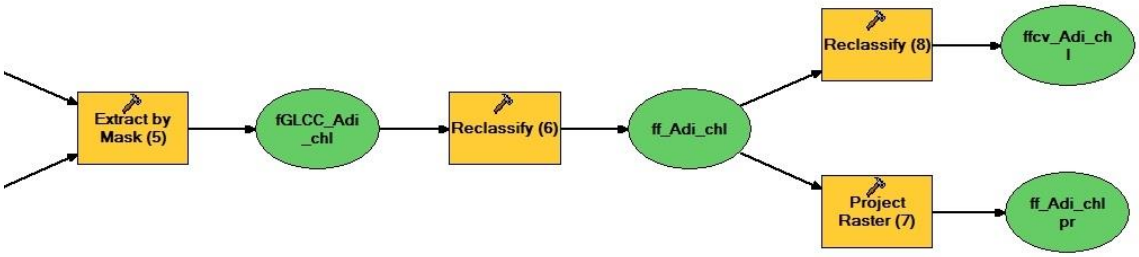

Figure 10. Part 2 of the ArcGIS model for calculating a species ESH (this example uses altitude + GLCC land cover dataset). Yellow boxes represent spatial functions (tools) and blue and green ellipses represent input and output data, respectively.

2.2.2.2.2.1 Selecting the best land cover classification database

A comparison was made between the original EOO and the three ESHs derived from altitudinal range and the different land cover datasets for each species using scatter plots, frequency distribution plots and boxplots. Additonally, species richness and endemism (or range size rarity) maps were generated using the ESHs from each run and the similarity of the three maps were

evaluated by randomly selecting specimen points from SRLI pteridophyte species and plotting these points against the equivalent species richness values for each pixel.

Each species richness map, using the ESHs derived from different land cover datasets, was produced by stacking the species' ESHs and therefore summing the presence of the species. A sampled species richness map was also produced by stacking the original species' EOOs in order for this to be compared with the ESH-derived species richness map.

Each ESH-derived map of endemism richness, using the different land cover datasets, was produced by calculating the C-value for each species. The C-value of a species is the inverse of the number of occupied grid cells (range size) (Usher, 1986) (Equation 1). Thus, since the range size (ESH) of each species differs when using different habitat/land cover classification dataset, the c-value of the species also differed.

$$\mathrm{Ci} = \frac{1}{\mathrm{Gi}} \qquad \textbf{(Equation 1)}$$

Where *Ci* is the species C-value and *Gi* is the global range of the species (total number of occupied cells globally).

The C-values were then summed for all species occurring in a cell (Equation 2) resulting in a total cumulative C-value for the global map (Barthlott *et al.*, 2001; Kier & Barthlott, 2001).

$$\mathrm{C} = \sum_{\mathrm{i}=1}^{\mathrm{n}} \mathrm{Ci} \qquad \textbf{(Equation 2)}$$

Ranges that were narrow (width < 30 km) and long (length > 1500 km) are likely to be biologically unrealistic and such ranges for 6 species were excluded from analysis

The habitat/land cover classification datasets were compared using the three species richness maps and identifying any differences in their predictions globally and per biogeographical realm. The datasets were also compared using the species' ratio of ESH size to EOO size in each case. The one-way analysis of variance by ranked Kruskal-Wallis non parametric test was also used to determine if there were statistically significant differences between the ESH/EOO ratio of each dataset. Furthermore, the mean ESH size and the mean ESH/EOO ratio in each IUCN Red List Category were compared in each case. Based on these comparisons and on the properties and characteristics of each habitat/land cover classification dataset, the most suitable dataset was selected and was used for the next steps.

2.2.2.2.2.2 Comparison of ESHs and EOOs for trans-continental species

It was then investigated whether the ESH across continents overestimated area compared to when the ESH was calculated based on each continental EOO. Since all available specimens are used to calculate the EOO for each species, the EOOs of species having a distribution across more than one continent include (a) marine areas and (b) terrestrial areas that would not

have been included if the distribution was calculated separately for each continent. Marine areas were dealt with by deleting water bodies during the ESH calculation since the equivalent land cover class was never assigned to each species. To investigate whether the ESH is overestimated by not calculating EOOs per continent, those species with wide distributions had their EOOs re-calculated separately for each continent (Figure 11, right panel). Thirty-seven species with trans-continental distribution were identified; however, the re-calculation of the EOO was only possible for eleven species since the rest of the trans-continental species did not have at least three points in each continent.

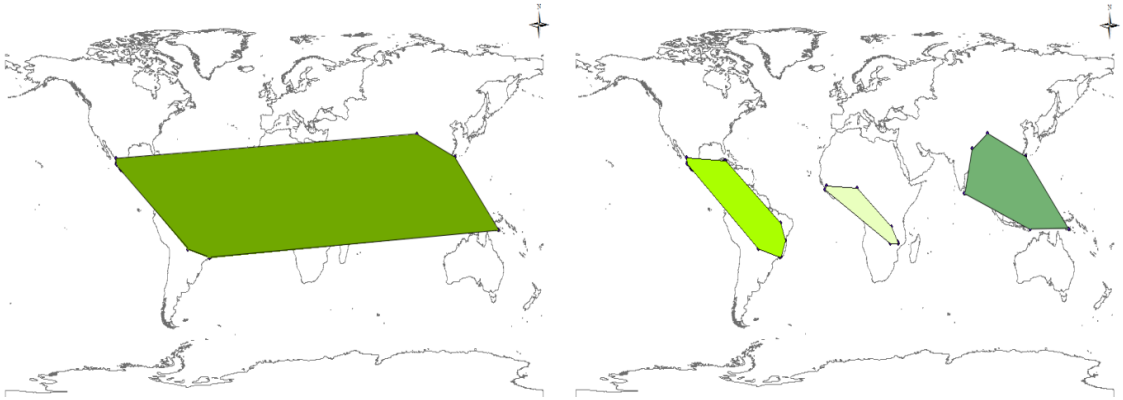

Figure 11. Illustration of the global EOO of *Adiantum lunulatum* (left) and of its component continental EOOs (right).

The separate continental EOOs of these eleven species were used to calculate the species continental ESHs as described in section 2.2.2.2. Their total area was compared with the area of the ESHs that were produced using complete global EOOs (Figure 11, left panel).

2.2.2.2.3 ESH calculation using three variables

A third variable was added to the ESH model. Species' ESHs were recalculated to include a water availability variable. The two models (with and without water availability) were compared with each other based on each species ESH area and the species' ESH size to EOO size ratio. Furthermore, using the one-way analysis of variance by ranked Kruskal-Wallis non-parametric test, it was investigated whether there are statistically significant differences between the ESH/EOO ratio of the biogeographical realms in each case (with and without water availability). The flow chart of the new analytical script (the Python code is given in Appendix A8) which includes the water availability variable is shown in Figure 12.

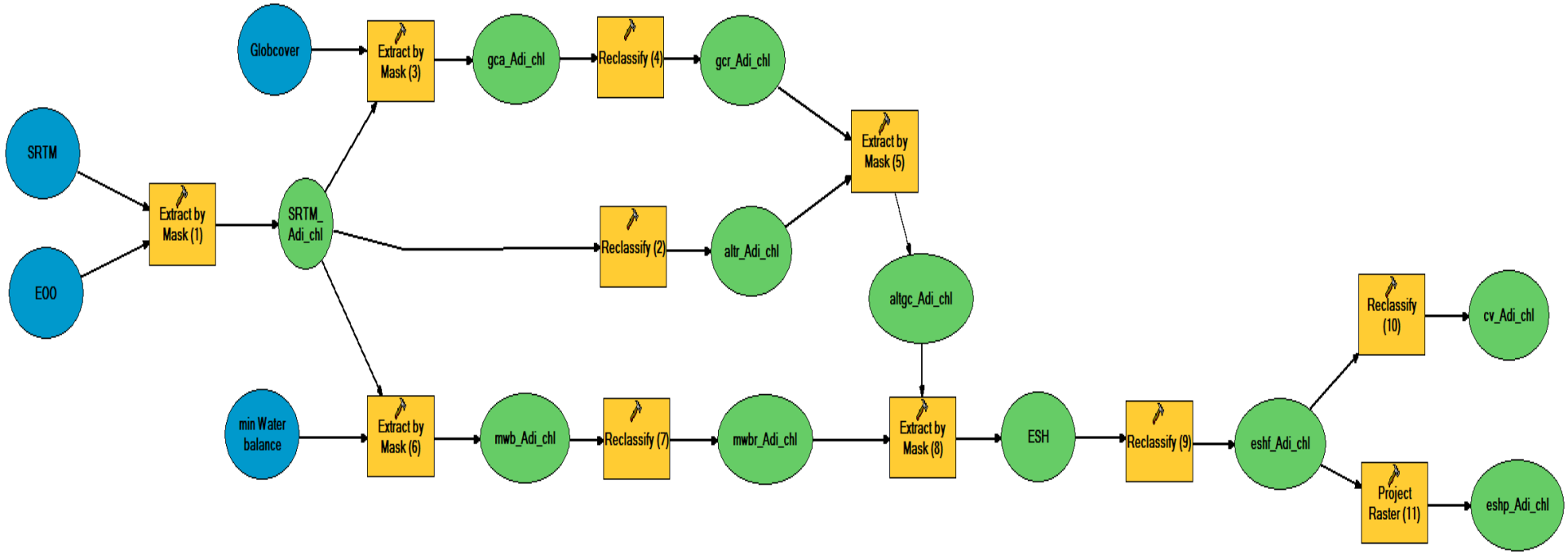

Figure 12. ArcGIS model for producing species' ESHs from four input components. Yellow boxes represent spatial functions (tools) and blue and green ellipses represent input and output data, respectively (the water balance dataset is used in this example; the model for water deficit is otherwise identical).

As in the previous version of the analytical script (section 2.2.2.2.2), in this version the species EOO was used to mask the altitude raster data which was then used to mask the land cover raster data (GlobCover in this version). However, instead of using the SRTM version 4 elevation data, in this version a new combined altitude dataset was used, due to the fact that the SRTM dataset does not cover areas north of 60°20' and therefore another elevation dataset with the same resolution and projection, GTOPO30 (USGS-EROS, 1996), was used for those areas. A mosaic elevation dataset combining these two datasets (SRTM+GTOPO30) was created and reclassified based on the altitude range of each species. The GlobCover output map was also reclassified according to the GlobCover classes assigned to each species. These steps were followed by selecting the GlobCover data that were within the altitude range of the species, resulting in the altitude-GlobCover output map.

The combined elevation output map was also used to mask the water availability data and the water availability output map was reclassified based on the range of water availability values assigned to each species. The next step was to select the water availability data that were found within the altitude-Globcover output map. The final ESH output map for each species was reclassified to values 1 (species presence) and 0 (species absence). The reclassified output map was projected to a cylindrical equal area projection with a WGS84 datum to calculate the area of each ESH in m^2

2.2.2.2.3.1 Selecting the most suitable water availability dataset for the analytical script

Box plots were used to identify any obvious clusters of water availability values in either case, for water balance or water deficit variables. Since no meaningful clusters were identified, the minimum and maximum value for either water balance or water deficit was assigned to each species. Once these data were prepared, water balance was added to the calculation of the ESH for each species, and the same also for water deficit. The two versions were compared using scatter plots, frequency distribution plots and boxplots. Additonally, stacked species richness maps were generated for each water availability dataset and the similarity of the two maps was evaluated by randomly selecting specimen points for SRLI pteridophyte species and plotting the number of these points against the equivalent species richness values. Based on the comparison with species richness but also on the comparison of the species' ESH/EOO ratio in each case, the most suitable water availability database was selected and used for producing the final maps of ESH for each species.

Whereas the altitudinal range for each species was calculated based on four sources of data, the species water availability range was based only on the georeferenced point data of each species. To test if broad water availability ranges are more appropriate for groups of species (instead of assigning a specific range to each species based on the minimum and maximum values of the extracted values), an unsupervised clustering method, the Parameter Free Clustering (PFClust) (Mavridis *et al.*, 2013), was used to identify species clusters and their respective ranges of water availability values. The PFClust algorithm, which until now has been

used with gene expression data, is able to automatically cluster a dataset without having any information on how to group the data. Hence, it agglomerates data into a number of meaningful clusters that share common characteristics without requiring any parameters (e.g. number of clusters) or information on how to group the data specified by the user. The method starts by estimating twenty thresholds produced by a randomisation process and using the similarity distribution between the cluster members (the species in this case). Each threshold is then used to cluster the data and the best threshold is selected based on the Silhouette width and the Dunn Index (cluster validity measures). This step is repeated four times to ensure that the clusters created by each threshold match. If the results do not agree, the algorithm replaces the least successful of the four runs with a fresh attempt and repeats this step (Figure 13).

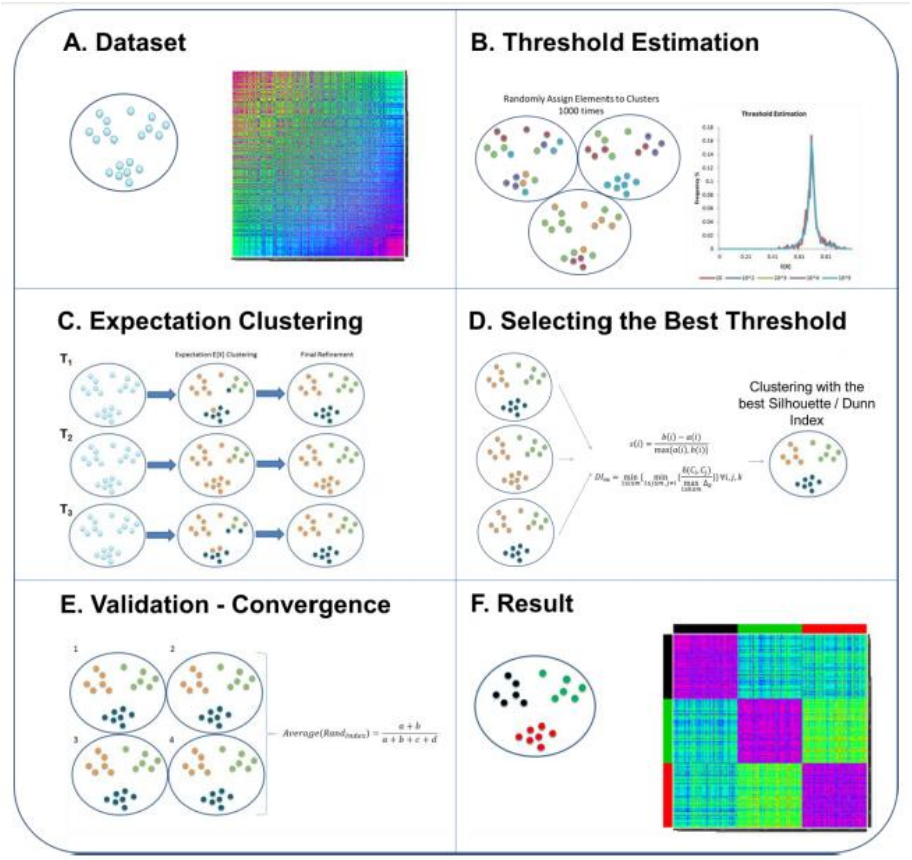

Figure 13. Graphical representation of the PFClust algorithm (Mavridis et al., 2013, p.3.).

Since it was decided to select the water balance variable and not the water deficit variable for the final ESH calculation method (see Results section 2.3.2.2.1), the water balance (minimum monthly) values for each species extracted using the georeferenced point data were used in the clustering analysis. The PFClust clustering analysis requires the minimum value, the maximum value, the median value and the standard deviation of a sample, all of which were extracted from the points of each species. These values were used in the algorithm to estimate the best thresholds and select the most meaningful clusters of the dataset. All species were included in the analysis and were placed in one of the resulting clusters. Each cluster is represented by a minimum value and a maximum value of water balance and this range was assigned to each species for that cluster. The species ESHs were recalculated using the clustered water balance

ranges and compared with the ESHs calculated using just the minimum and maximum water balance values of each species.

2.2.3 Validating the species Extent of Suitable Habitat

The ESH for each species was validated using independent occurrence point data from the Global Biodiversity Information Facility (GBIF) online database. These occurrence point data were not used in the species' ESHs calculation. Since the ESHs were calculated using the GlobCover 2005 land cover database (see Results, section 2.3.2.1.1), all new point records that had been collected before 2005 were excluded from the analysis since they may no longer exist where land cover has changed. 257 species (out of 487) had new point data on GBIF and just 115 species had new point data that were collected after 2005. These species covered a wide taxonomic (73 out of 102 genera) and geographic range (representing all biogeographical realms except the Antarctic). Also, these species occurred in all land cover classes covered by all investigated species (487 sp.) and covered the whole altitudinal (0 – 6000 m) and water balance (-1800 – 5200 mm/month) range of all investigated species. A mean of 29±80 occurrence points for each species was available to evaluate the species' ESHs. A circular buffer (1km radius) was applied to each point to capture any georeferencing errors. The proportion of new point records that are contained in any cell of the ESHs, and therefore validated the ESHs, was calculated for each of these 115 species. In addition, the proportion of the new point records that validated the species ESHs was plotted against the equivalent ESH/EOO ratios. This analysis was based on Rondinini *et al.* (2011) who argued that when the proportion of new point records that are contained within the species' ESH is higher than the equivalent ESH/EOO ratio, the ESH is better in predicting the species geographical range than the EOO.

Furthermore, to test whether the species' ESHs were capturing the new point records (GBIF data) better than they capture random points, a permutation test was conducted following Maiorano *et al.* (2007). For each species, 1000 sets of random points were generated within their EOOs. The number of random points for each species was identical to the number of new point records (GBIF data) that were used to evaluate the species' ESH. For each set, the proportion of the random points that validated the species' ESH was calculated and the mean value was compared with the proportion of the new point records (GBIF data) that validated the species' ESH. The ESH model performance was considered as better than expected by chance if the percentage of validation calculated for the GBIF points was in the top 5% of the validations obtained from the 1000 random sets.

The ESHs were also validated through validating the ESH-derived species richness maps using independent field data collected during fieldwork in Costa Rica (see Chapter 3, Section 3.2.2.2 for more details). Species richness numbers from fourteen different species richness plots (5m x 5m) at altitudes from 647 m to 3368 m were compared with the ESH-derived species richness values. Although the field data do not cover the whole altitudinal range of the SRLI forest

species occurring in Costa Rica (0 – 3500 m), they were used to compare the ESH-derived species richness of the two cases within the altitudes covered by the species richness plots.

2.3 RESULTS

2.3.1 Investigation into the bias in the SRLI data

To investigate the bias in the species selected from the SRLI species dataset (635 forest species), a comparison of the percentage of species of the ESH sample (SRLI forest pteridophyte species), of the SRLI sample (1500 pteridophyte species randomly selected) and of the global pteridophyte checklist (all recorded pteridophyte species) found in each biogeographical realm was carried out. As shown in Figure 14, the three datasets had similar distributions of species numbers across biogeographical realms. The highest proportion of species in all datasets was found in the Neotropics, with the SRLI forest pteridophyte dataset having the highest percentage (ESH: 32%, SRLI: 28%, Checklist: 27%). The second highest percentage of species from the checklist, meanwhile, was found in the Palearctic realm, while for the complete SRLI sample this was found in the Indomalayan realm, followed by the Palearctic realm. Surprisingly, the percentage of SRLI forest pteridophyte species in the Palearctic realm was very low (10%) compared with the other two datasets (SRLI: 20%, Checklist: 22%).

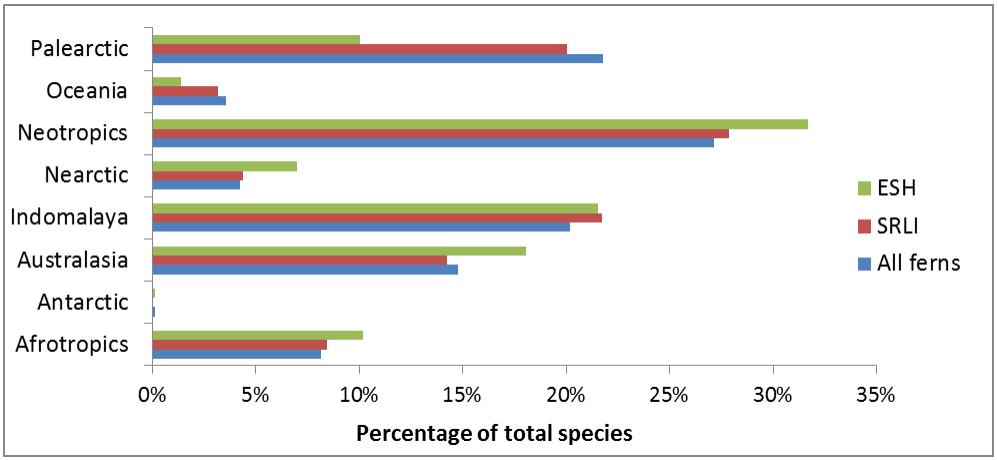

Figure 14. Comparison of the ESH sample (SRLI forest pteridophyte species), SRLI sample and All ferns (all pteridophyte species from a global checklist) using the percentage of total species in each realm.

The results of the analysis to investigate the differences found between the SRLI forest pteridophyte species dataset and the full SRLI sample and global checklist datasets is shown in Figure 15. The number of SRLI forest pteridophyte species in each biogeographical realm was compared when calculated based on the species occurrence points (ESH species specimens) and when based on the distribution information recorded in the global pteridophyte checklist (ESH species checklist). The two datasets showed the same pattern; however, there were more records for SRLI forest pteridophytes from the global checklist than from specimen occurrence

points in the Palearctic, Oceanic, Afrotropical, Neotropical and Indomalayan realms. The biggest difference was seen in the Palearctic biogeographical realm with 94 records of SRLI forest pteridophyte species from the global checklist and 66 from specimen occurrences.

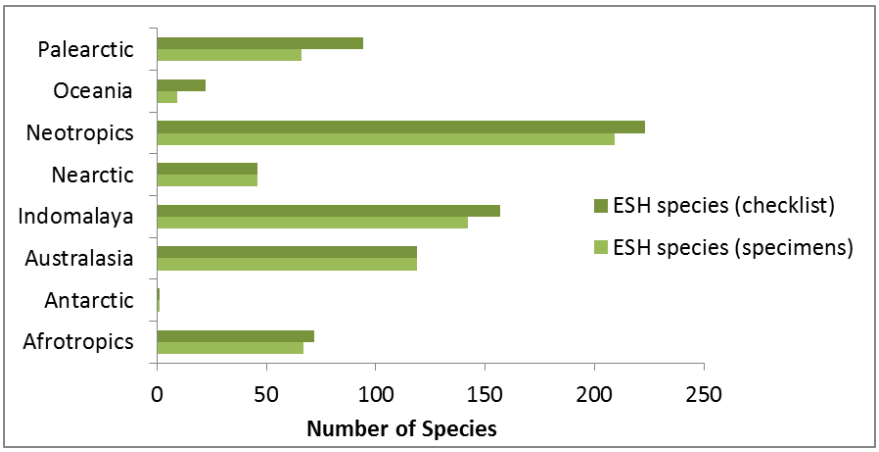

Figure 15. A comparison of the number of ESH species in each biogeographical realm when calculated based on the species occurrence points (specimens) and on the distribution information found in the global pteridophyte checklist (checklist).

A separate investigation was conducted to investigate sampling effort in the occurrence points of the SRLI forest pteridophyte species (i.e. the number and density of species occurrence points used to calculate the species' ESHs). A higher number of occurrence points per area of suitable habitat is shown in Oceania (37 points / 10000 Km²) and the Australasian (29 points / 10000 Km²) and Antarctic (27 points / 10000 Km²) biogeographical realms, followed by the Palearctic biogeographical realm with 18 points per 10000 Km². Among tropical biogeographical realms, the Neotropics have a higher number of points per area of suitable habitat (9 points / 10000 Km²) than do the Indomalayan realm (5 points / 10000 Km²) and the Afrotropics (1 point / 10000 Km²) (Figure 16).

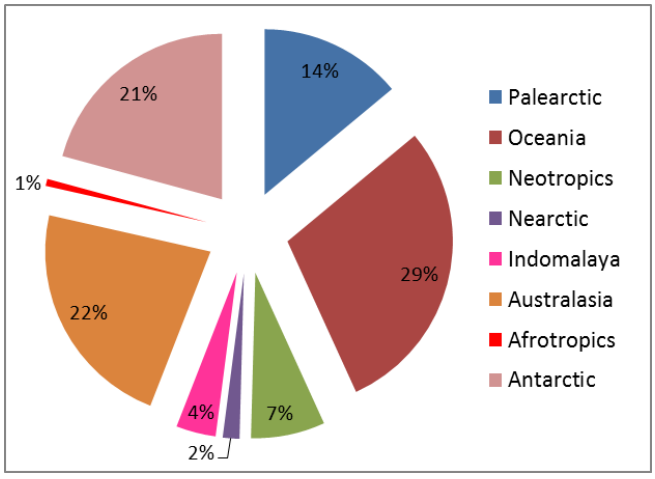

Figure 16. Percentage of the number of occurrence points for SRLI forest pteridophyte species per area of suitable habitat for each biogeographical realm.

The density of specimen occurrence points for SRLI forest pteridophyte species is shown in Figure 17. The highest density of points occurs in the Palearctic biogeographical realm, and specifically in the UK and France. The second highest density of points occurs in New Zealand, and hence in the Australasia realm. In both cases this is caused by a high number of points for only a few species. The high density of points in the UK and France is due to specimens of *Equisetum palustre*, whereas in New Zealand the high density of points is mainly due to specimens of *Blechnum discolor*. The biogeographical realm with the third highest density of points is the Neotropical realm, with Central America the highest area within the Neotropics: in this case, high point density is caused by a high number of occurrence points for several species. These points covered the whole geographical range of the species and therefore did not influence the species' ESHs, since once the EOOs are calculated any points within it are not relevant.

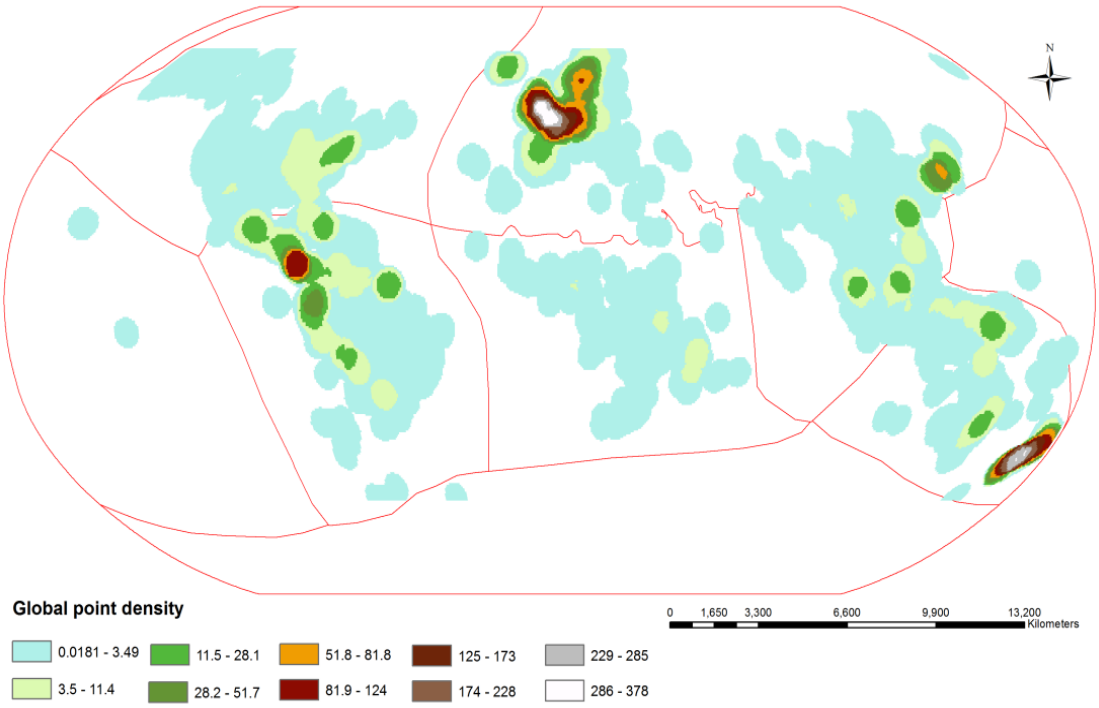

Figure 17. Global density of specimen occurrence points for SRLI forest pteridophyte species.

An analysis was also conducted to determine whether or not specimen occurrence points for SRLI forest pteridophyte species cover all countries where each species is known to occur. Figure 18 presents, by biogeographical realm, the number of countries (and their suitable habitat area) without specimen occurrence data but where SRLI forest pteridophyte species do occur according to the global pteridophyte checklist. The Palearctic and the Afrotropical biogeographical realms have the highest number of countries (and the biggest area of suitable habitat) lacking representative herbarium specimens of species from these realms.

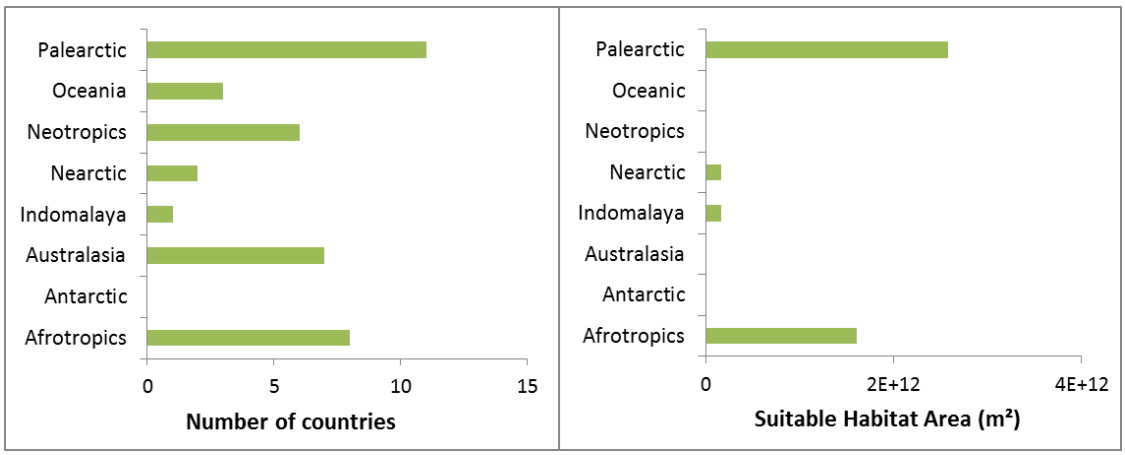

Figure 18. The number of countries in which SRLI forest pteridophyte species are known to occur but for which there are no occurrence data (left) and the total area of suitable habitat in those countries (right), in each biogeographical realm.

2.3.2 Calculation of species' Extent of Suitable Habitat

2.3.2.1 ESH calculation using two variables

The ESH was calculated for each of the 487 forest species for which there were sufficient specimen data using two variables, the altitudinal range and habitat preference, and implementing the GIS analytical script (Figures 9 & 10) described in section 2.2.2.2 (Methods section). An example of the ESH procedure is shown in Figure 19.

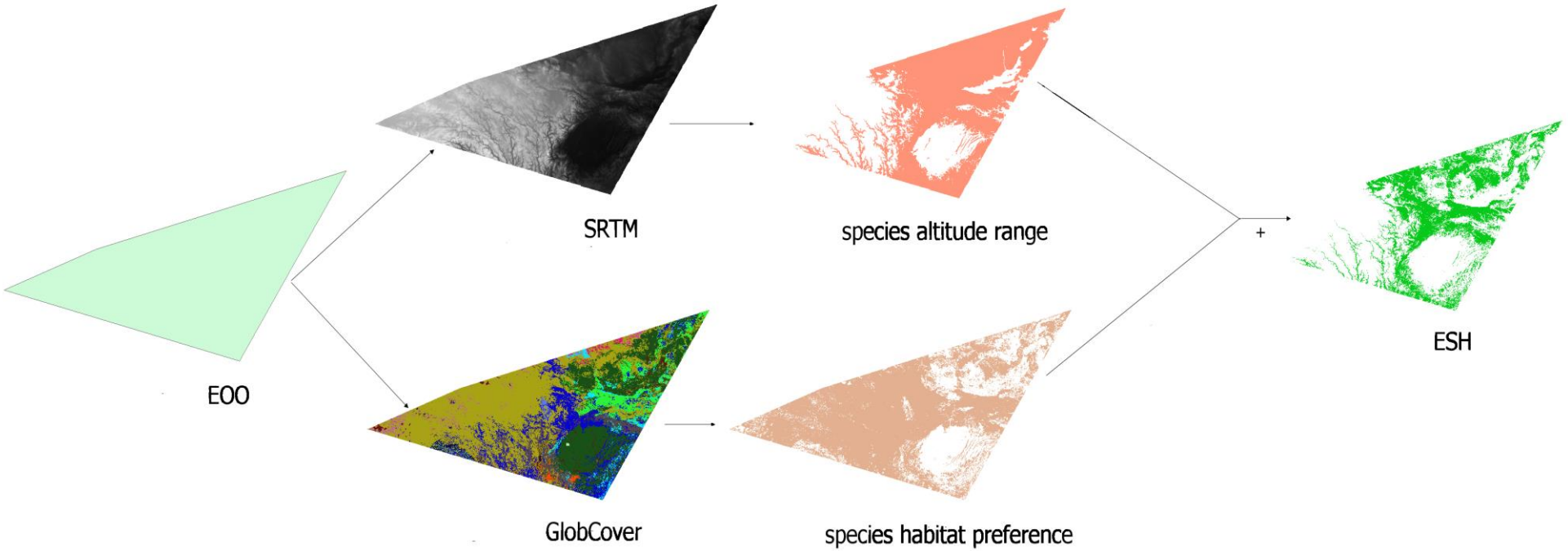

Figure 19. Schematic diagram to illustrate calculation of a species ESH (*Notholaena borealisinensis* in this example) using the species original EOO, altitudinal range and habitat preference.

2.3.2.1.1 Selecting the best land cover classification database

As expected, there was a strong positive relationship ($r^2 > 0.9$, $p<0.001$) between the area of the original EOO and the ESH of each species for all three land cover datasets (Figure 20).

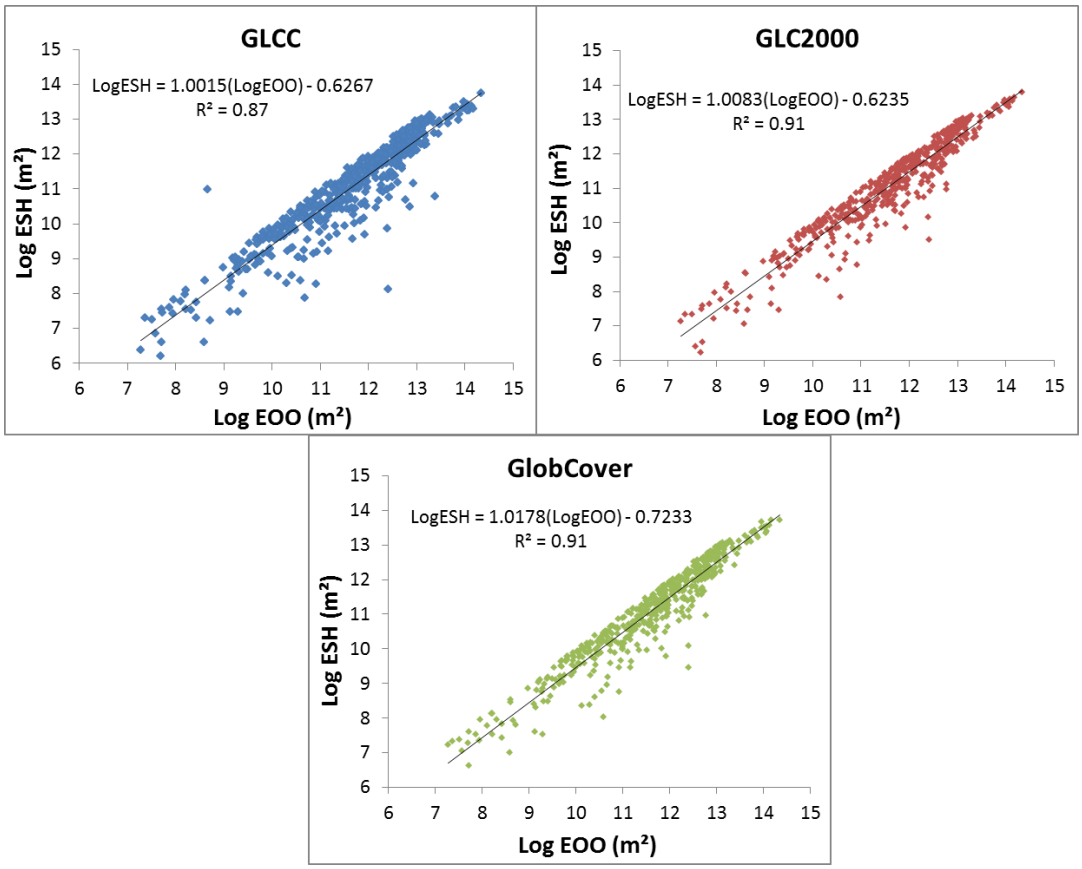

Figure 20. Relationship between the Extent of Occurrence (EOO) and the Extent of Suitable Habitat (ESH) of 487 species using 3 different land cover databases (GLCC, GLC2000, GlobCover).

The geographical range of a species is an important factor contributing to its extinction risk under land use (and/or climatic) change. Due to this and to the fact that the EOO is strongly positively correlated with the ESH, it was expected that the average ESH size would differ between the IUCN threat categories as the EOO does. There is indeed a relationship between the IUCN Red List Categories and the size of the ESH (Figure 21) with the average ESH being larger for species in the Least Concern category and smaller in the Critically Endangered category.

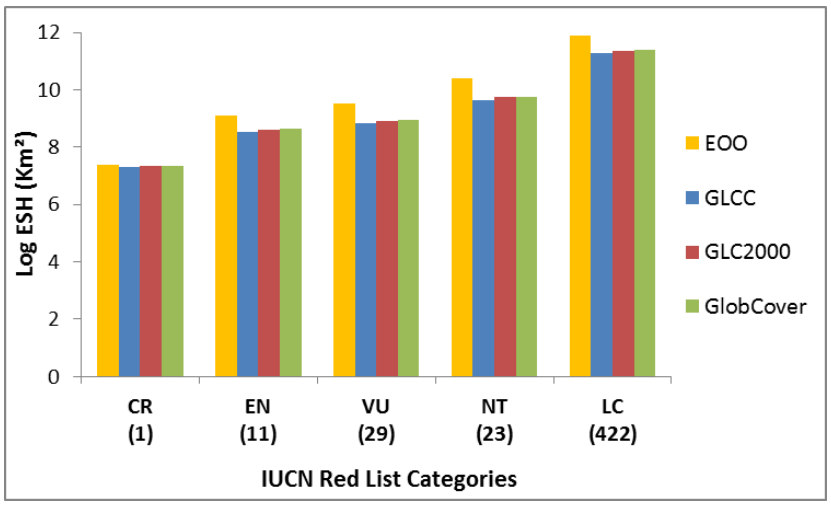

Figure 21. Mean EOO and ESH (calculated with GLCC, GLC2000 and GlobCover) (log) by IUCN Red List Category. Categories: CR: Critically Endangered, EN: Endangered, VU: Vulnerable, NT: Near Threatened, LC: Least Concern. Numbers in brackets represent number of species in each category.

The species ESH was significantly smaller than the original EOO for each land cover dataset. This reduction of the species range when using the ESH metric is shown in Figure 22. There was a mean reduction in area from EOO to ESH of 69.7±0.2%, 64.3±0.2% and 62.1±0.2% using the GLCC, GLC2000 and GlobCover land cover datasets, respectively.

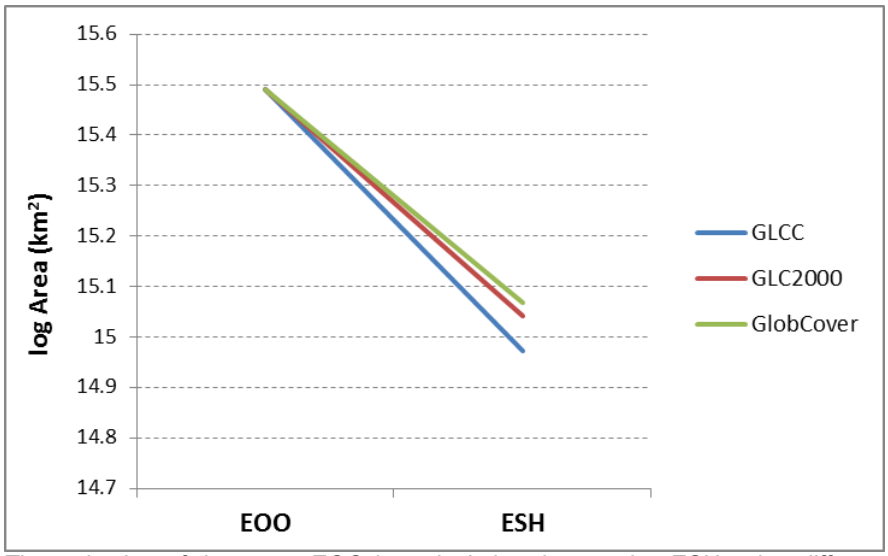

Figure 22. The reduction of the mean EOO by calculating the species ESH using different land cover databases.

In calculating the ESH, the resulting range was reduced by at least 50% for approximately 400 species with all three land cover datasets compared with the area of the EOO. Furthermore, the area of the ESH for more than half of the species studied covered less than 30% of the EOO of that species (Figure 23) showing that the EOO metric consistently produces larger estimates of species range size than does the ESH. For many species (GLCC:33%, GLC2000:29%, GlobCover:30%) the ESH covers only 10% of the EOO.

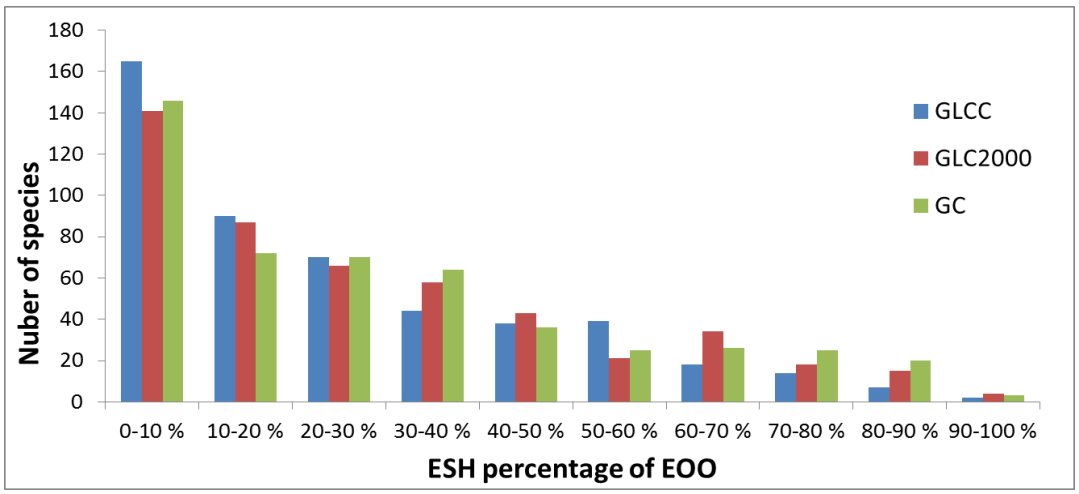

Figure 23. The Extent of Suitable Habitat (ESH) as a percentage of the Extent of Occurrence (EOO) calculated with three different land cover datasets (GLCC, GLC2000, GlobCover) and the number of species in each percentage group.

No relationship was found between the size of the EOO and of the ESH area as a percentage of the EOO (Figure 24). Wide-spread species with large EOOs (e.g. *Anemia hirsuta*) had broadly the same ESH/EOO ratio as highly localised species with small EOOs (e.g. *Asplenium underwoodii*). The species with the largest EOOs have the smallest ESH/EOO ratio.

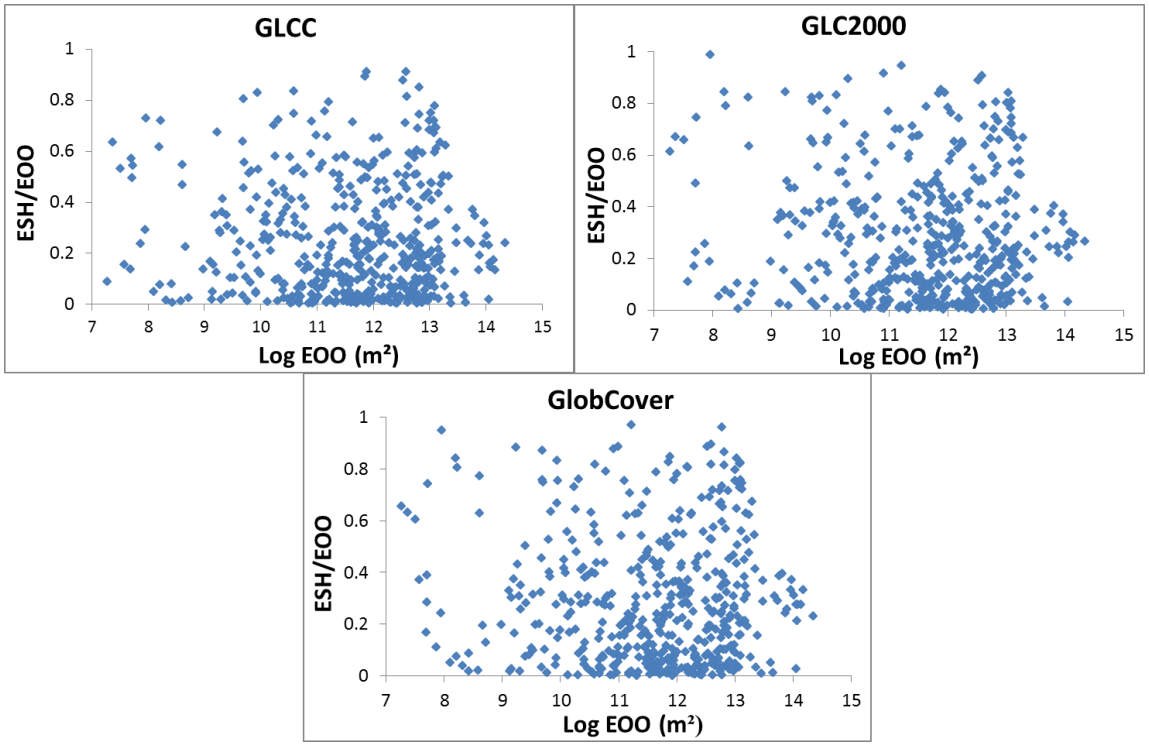

Figure 24. Relationship between the ESH/EOO ratio and the size of the species EOO using 3 different land cover databases (GLCC, GLC2000, GlobCover).

Figure 25 shows the ESHs of an example species, *Asplenium acutiusculum,* in Southeast Asia, produced using the GLCC, GLC2000 and GlobCover datasets and with 24%, 25% and 26% ESH/EOO ratio respectively. The three different ESHs for each species, produced using

different land cover datasets had only small discrepancies due to the relatively small differences in the land cover classes of each database. The similarity between the three ESH versions is also reflected on the ESH/EOO ratio of each case (Kruskal-Wallis χ^2=7.3, d.f.=2, p> 0.05) (Figure 26).

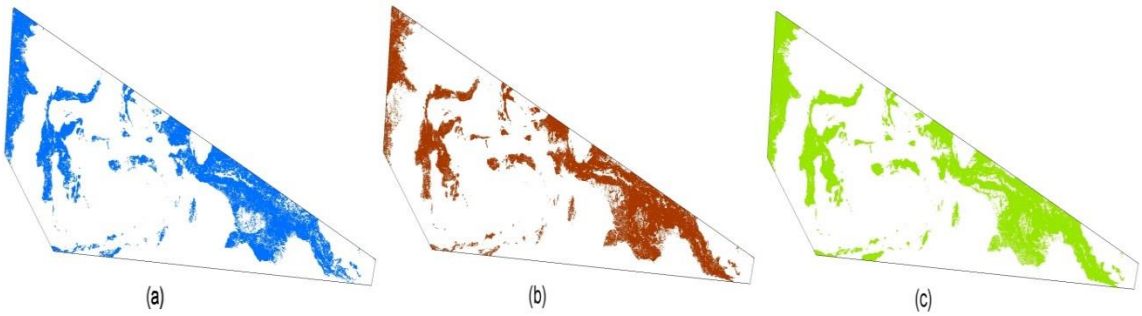

Figure 25. The ESH of *Asplenium acutiusculum* produced by using the (a) GLCC database, (b) GLC2000 database and (c) GlobCover database.

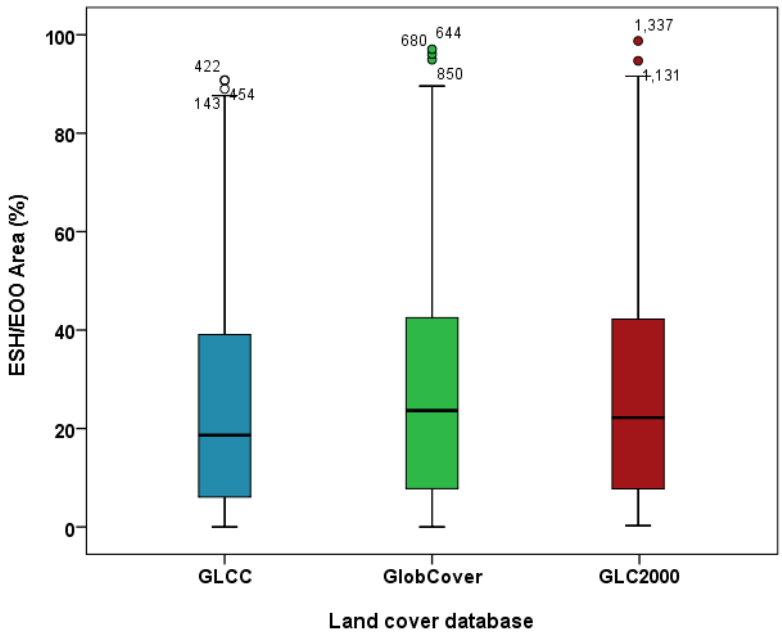

Figure 26. Boxplots representing the SRLI forest pteridophyte species ESH/EOO ratio when using different land cover databases.

Since the selection of the most suitable land cover database could not be based entirely on the extent of reduction in area of the EOO, the species richness and endemism richness maps which were generated with the ESHs from each land cover dataset were also used. As shown in Figure 27 and Figure 28, the three sets of maps from the three land cover datasets are very alike, identifying the same areas of high species richness and high endemism in each biogeographical realm and predicting similar maximum value of global species richness GlobCover = 90 species, GLC2000 = 88 species and GLCC = 85 species) and endemism (GlobCover = 0.5003, GLC2000 = 0.5003 and GLCC = 0.5004).

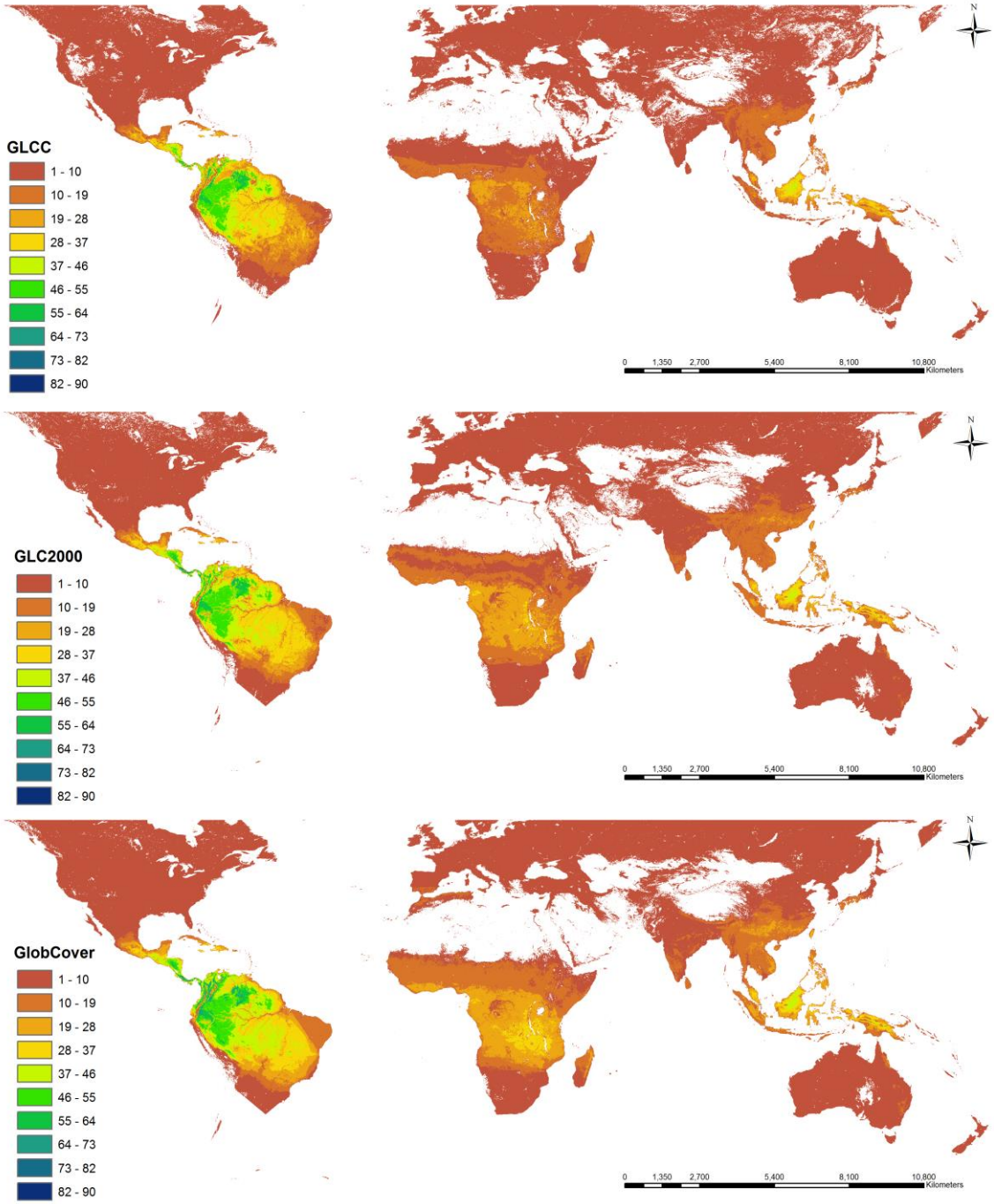

Figure 27. Pteridophyte species richness maps produced using different land cover databases (a) GLCC, (b) GLC2000 and (c) GlobCover.

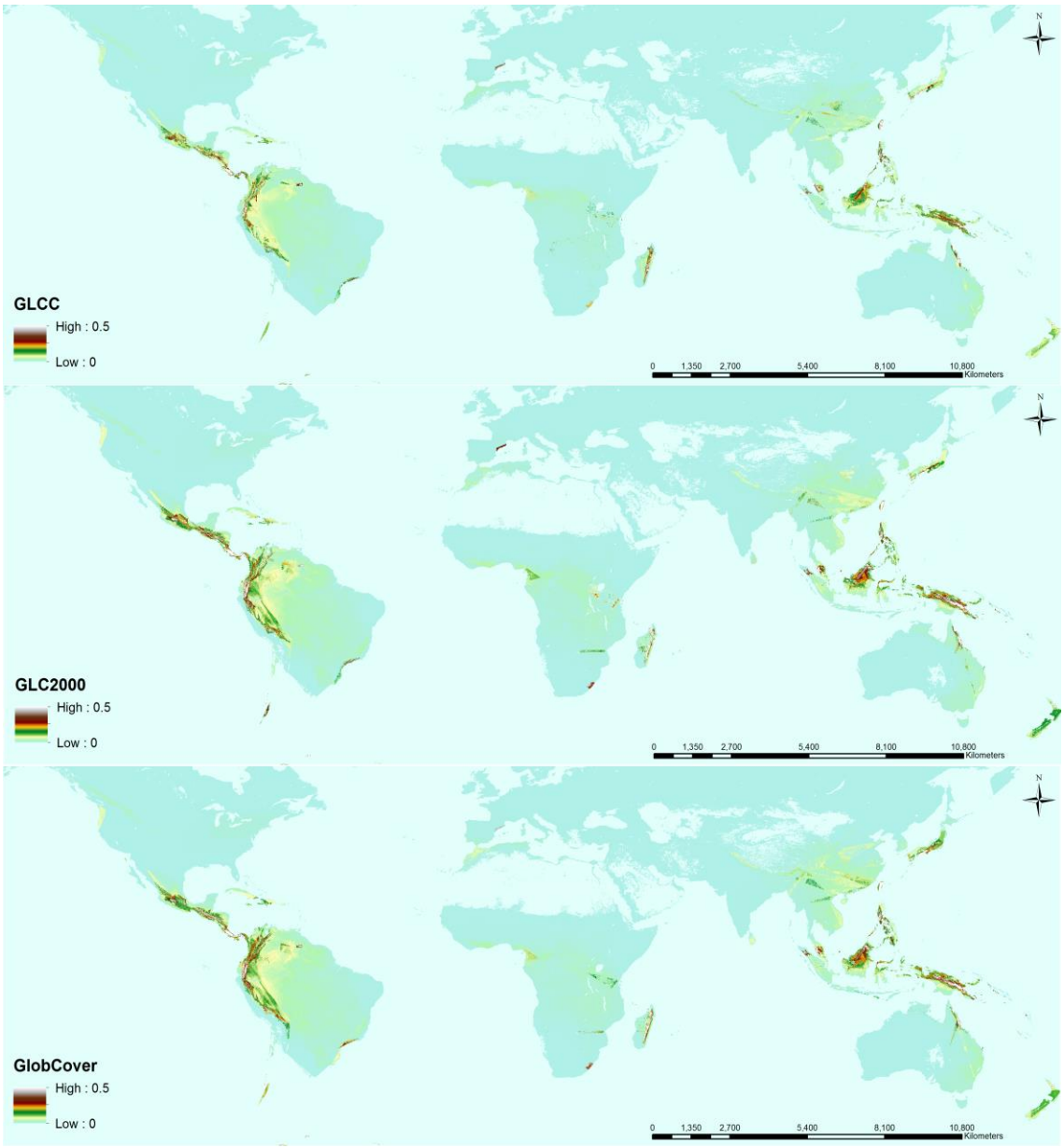

Figure 28. Pteridophyte endemism richness maps produced using different land cover databases (a) GLCC, (b) GLC2000 and (c) GlobCover.

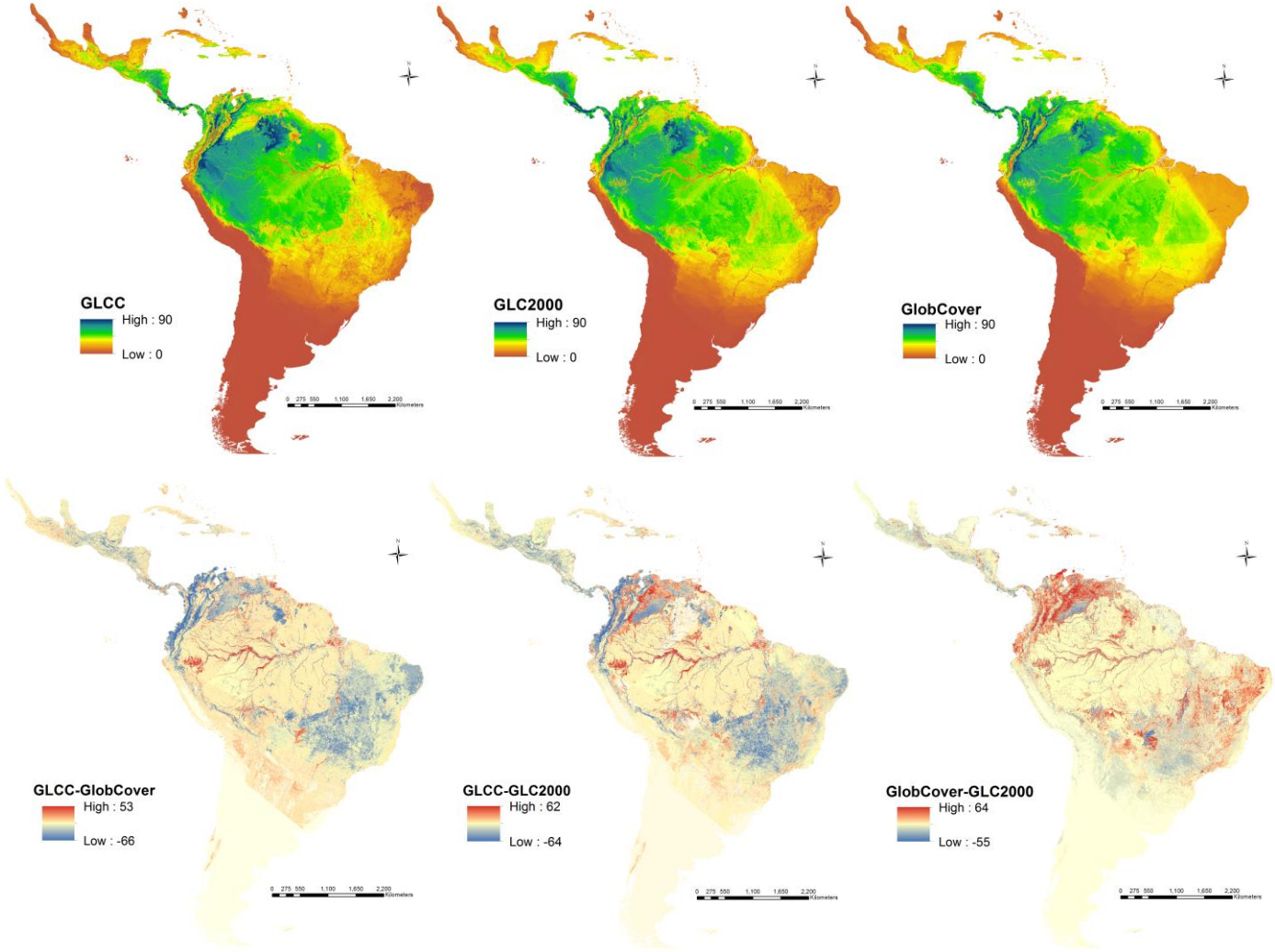

Figure 29. Pteridophyte species richness maps for South and Central America produced using different land cover databases (a) GLCC, (b) GLC2000 and (c) GlobCover (top) and difference maps between the three species richness maps (bottom).

The species richness maps of the three runs were compared spatially showing that the GLC2000 and GlobCover derived maps were the most similar (Figure 29). This matches the results of the comparison of the three land cover datasets by randomly selecting specimen occurrence points for SRLI pteridophyte species and plotting the points against the equivalent species richness values (Figure 30).

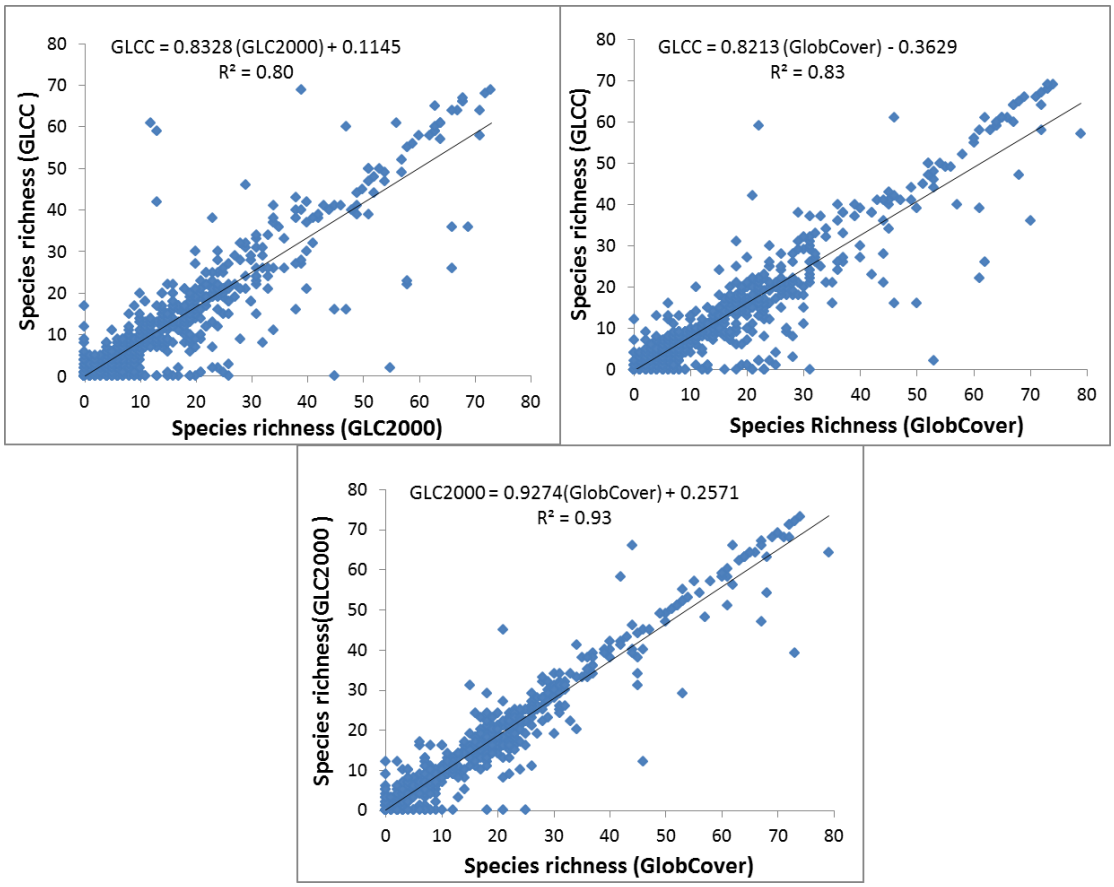

Figure 30. Comparison of the GLCC, GLC2000 and GlobCover databases from plotting the equivalent species richness values of randomly selected specimen occurrence points for SRLI species.

Due to the fact that the GlobCover data were collected more recently and at higher spatial resolution and considering that there are otherwise no substantial differences between the two databases the GlobCover (2009) dataset was selected (details in the Discussion section 2.4.2) as the most suitable land cover dataset for calculating the species ESHs and was used in the next steps of the study. When calculating the species ESHs with the two GlobCover versions (2005 and 2009), there was a mean reduction in area from EOO to ESH of 62.1±0.2% and 62.5±0.2% using GlobCover 2005 and Globcover 2009 respectively. Moreover, the species richness map generated using the two GlobCover versions predicted similar global species richness, with 90 species as the maximum species richness when using GlobCover 2009 and 91 when using GlobCover 2005. Despite the similarities, it was decided to calculate the species ESHs using GlobCover 2005 since it is the most appropriate one for this study which will investigate next, the habitat loss of species' ESH between 2005 – present, and into the future

(details in the Discussion section 2.4.2). Table 3 compares the characteristics of the three different classification datasets against the selection criteria.

Table 3. A comparison of the characteristics of the classification datasets GLCC, GLC2000 and GlobCover against the selection criteria.

CRITERIA	GLCC	GLC2000	GlobCover 2005/2009
Date collection time	1992-1993	1999-2000	2004-2005/2008-2009
Spatial resolution	1km	900m	300m
Consistancy with Global Forest Change (GFC) data	no	no	yes
Consistancy with Terra-i data	no	no	yes
Updated in regular intervals	no	no	yes
Derived entirely from remote sensing data	no	yes	yes
Data voids	yes	no	no
Validation	no	yes	yes
Validation according to the recommendations of the Committee on Earth Observing Satellites Land Product Validation subgroup	n/a	no	yes
Accuracy	n/a	68.6±5%	67.1% / 70.7%
Mean reduction from EOO to ESH	69.70%	64.30%	62.1%/62.5%

2.3.2.1.2 Comparison of ESHs and EOOs for trans-continental species

The re-calculation of range size using the ESH only within each continent for eleven widespread species showed that the summed area of each continental ESH is significantly smaller than the ESH area calculated using the global EOO of the species. There was a reduction using each of the three land cover data sets (GLCC, GLC2000, GlobCover), as seen in Figure 31, showing that such a reduction is not related to the respective selection of the land cover categories but rather to the overall reduction of the global EOO area.

Out of a sample of 487 species, 37 species have a trans-continental distribution, but calculation of the continental EOO was feasible for only eleven species since the rest of the species identified did not have at least three unique localities from each continent. These eleven species are common species with wide distributions and a large number of recorded localities and therefore were not considered to be threatened. The conservation status of none of these species would have changed with EOO calculated as the sum of each continental distribution, since their EOO would in this case still be greater in area than the threshold of the lowest threatened Red List Category under Criterion B [Vulnerable, 20,000 km^2]. Based on this and considering that the ESH calculation will identify the suitable habitat within the EOO area, there is no obvious advantage in calculating the EOO of wide-spread species separately within each continent from the point of view of their IUCN conservation status.

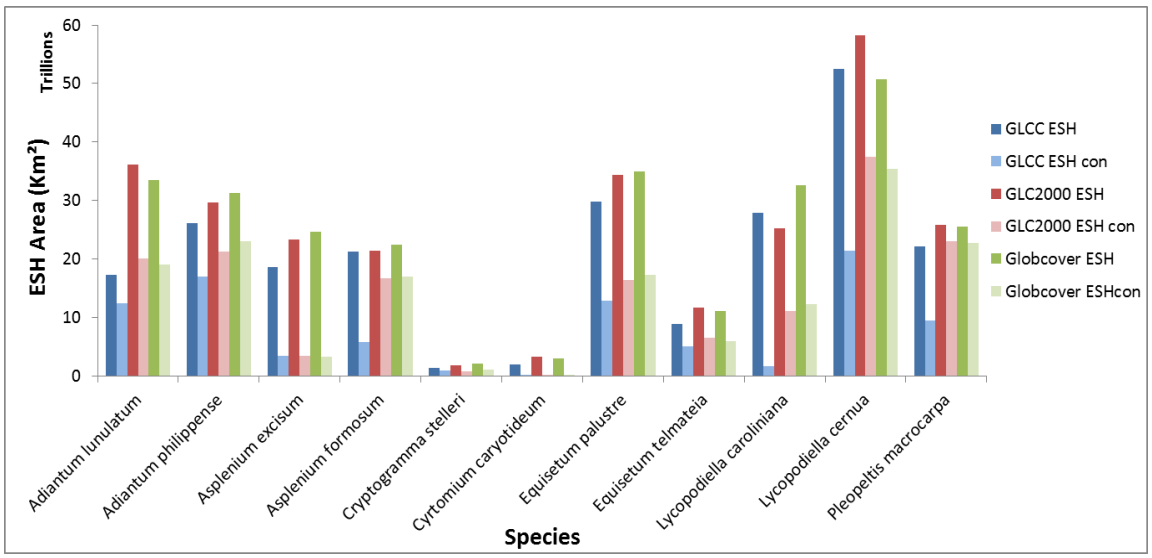

Figure 31. Comparison of the ESH area calculated using Global EOOs (dark colour) and Continental EOOs (light colour) of 11 trans-continental species.

2.3.2.2 ESH calculation using three variables

The ESH calculation procedure when using 3 variables is shown in Figure 32.

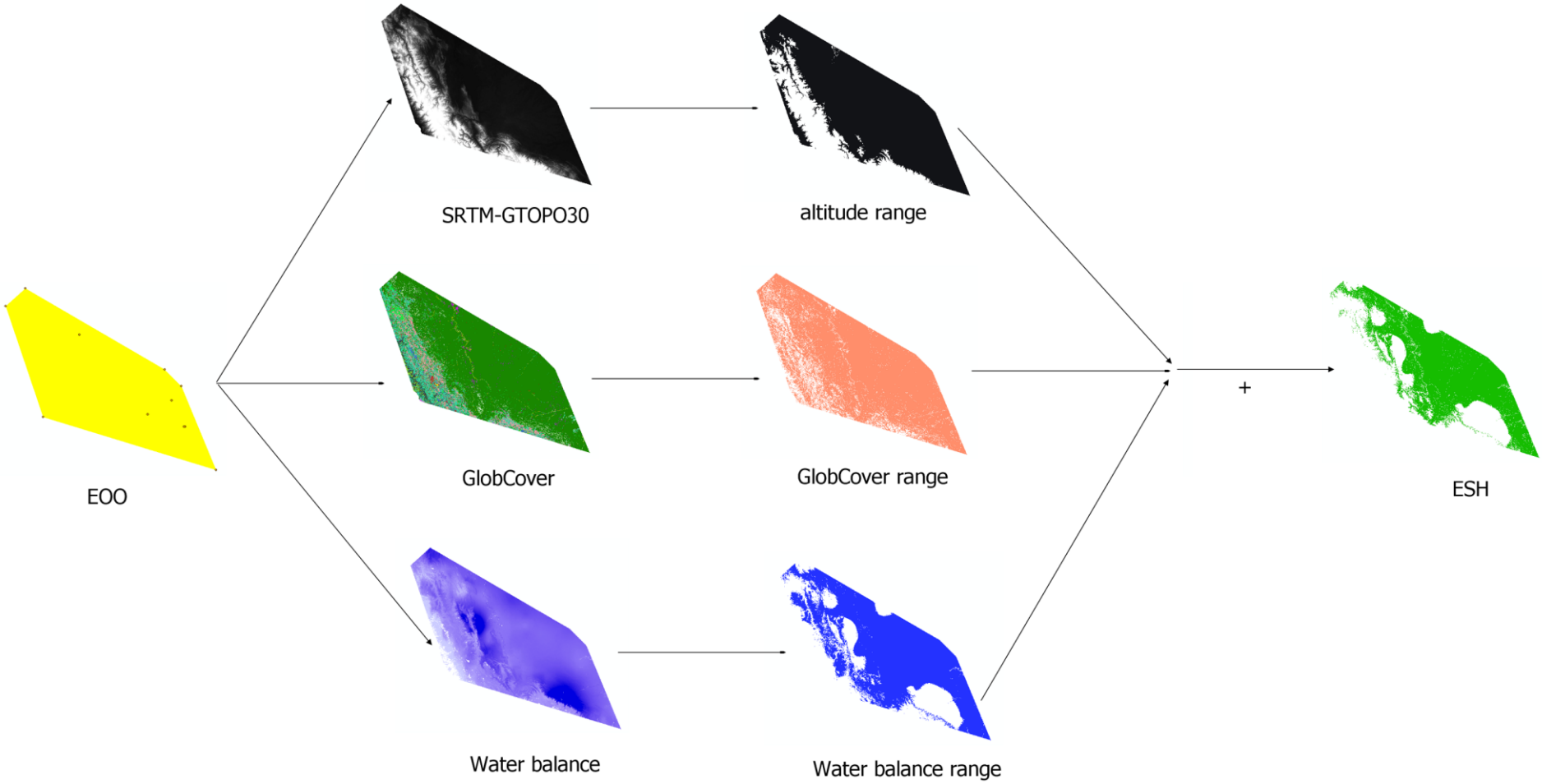

Figure 32. Schematic diagram of the calculation of ESH (for the species *Adiantum poeppigianum*)

2.3.2.2.1 Selecting the best water availability dataset for the ESH calculation

In order to add water availability preference for each species to the ESH model, the minimum water balance values and the maximum water deficit values were extracted with georeferenced point data for SRLI forest pteridophyte species in order to identify any clusters of species formed based on the water availability data. Figure 33 shows the maximum deficit values and the minimum water balance values of the forest pteridophyte species for the case study area, Costa Rica. No obvious clusters were identified regionally (for Costa Rica) nor globally.

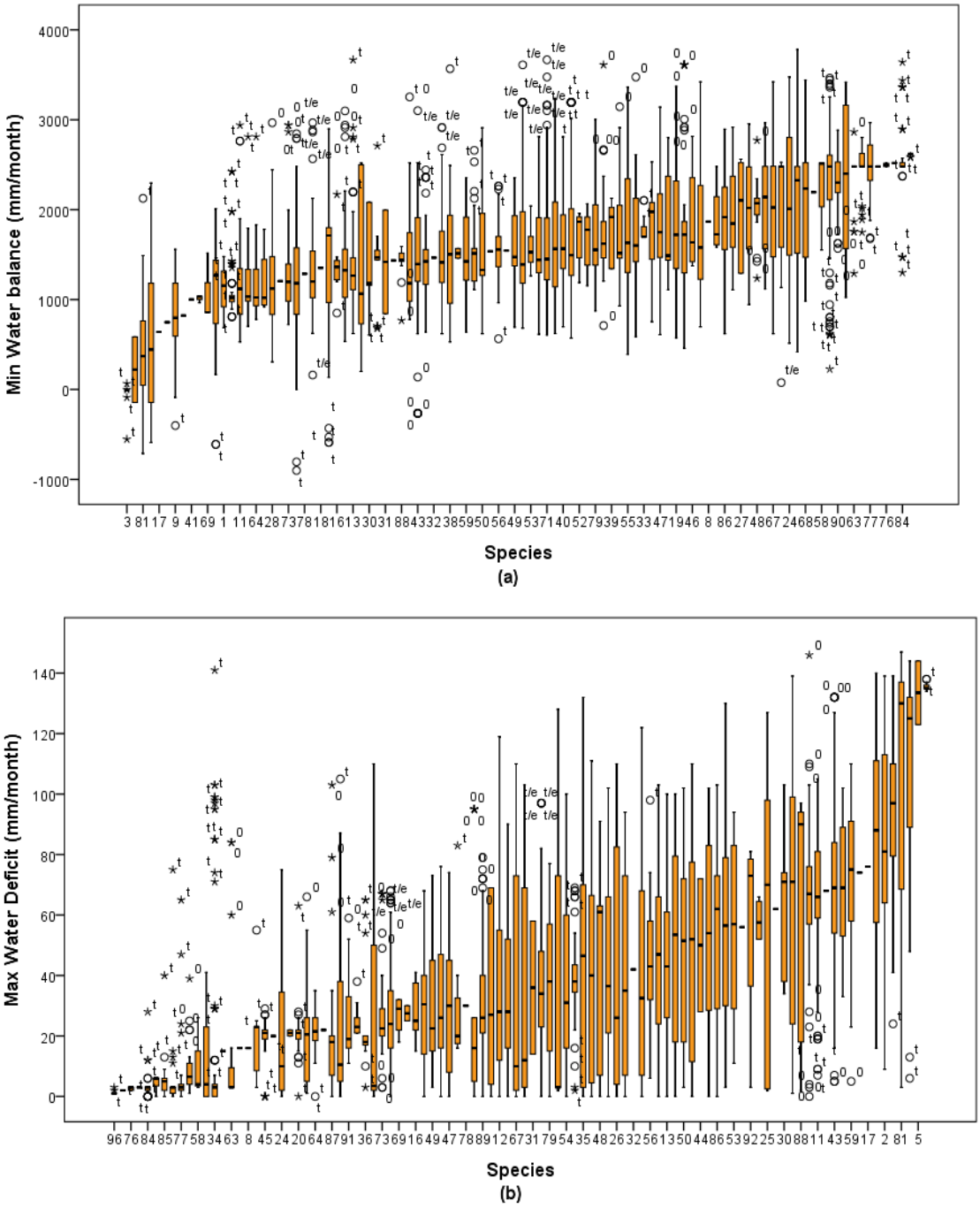

Figure 33. Boxplots of the (a) maximum water deficit values and (b) minimum water balance values of Costa Rican SRLI forest pteridophyte species.

Based on the analysis of the minimum water balance and the maximum water deficit values, species that occur in the same IUCN habitat categories (e.g. temperate forest) or share the same life form (e.g. epiphytes) had a similar water availability preference, as did species in other groups (Figure 34). As expected, epiphytic pteridophyte species are less drought-tolerant than terrestrial peteridophyte species are. However, the difference was not as great as expected. Unsurprisingly, the Subtropical/Tropical Dry forest species had a greater tolerance to low water availability relative to species from the other three forest types. Both water availability datasets (water balance and water deficit) identified the same trend.

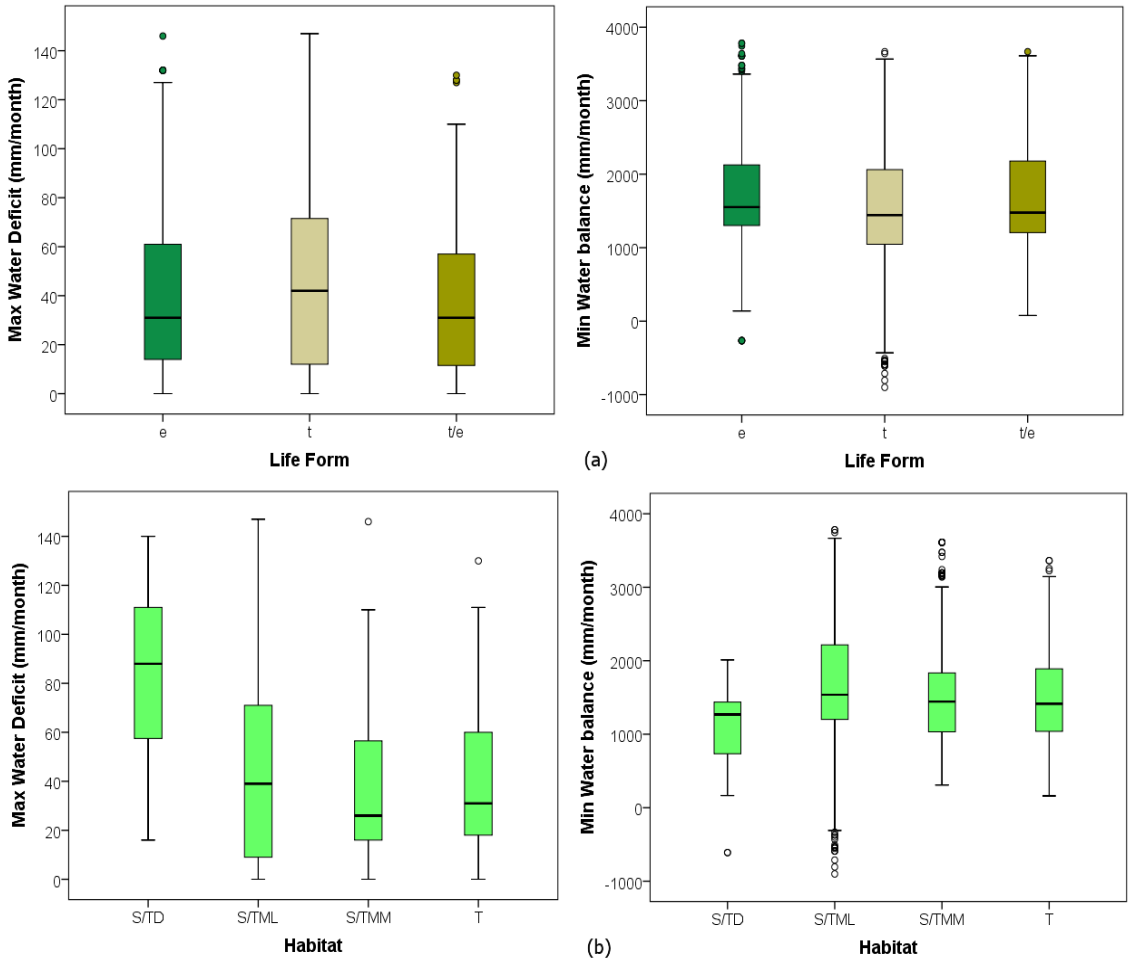

Figure 34. Boxplots of the maximum water deficit (left hand side) and minimum water balance (right hand side) values for SRLI forest pteridophyte species in each (a) life form type (t= terrestrial, e=epiphytic, t/e=both terrestrial and epiphytic) and (b) IUCN habitat category (S/TD=Subtropical/Tropical Dry forest, S/TML= Subtropical/Tropical Moist Lowland forest, S/TMM= Subtropical/Tropical Moist Montane forest, T=Temperate forest).

Since none of the analyses using the two different water availability datasets revealed an easy way to group the species based on their water availability preference, the minimum and maximum value of water balance was assigned to each species and used in the ESH calculation. The two datasets (water balance and water deficit) resulted in a similar mean reduction in area from EOO to ESH with 71.4±0.2% and 69.9±0.2% reduction when using water balance and water deficit respectively, compared with 62.1±0.2% when using altitude and land cover only. In addition, there was a strong positive relationship (linear regression: $r^2 > 0.9$,

p<0.001) between the species ESHs from the two datasets (Figure 35a). For both datasets, the resulting species range was reduced by at least 50% compared with the size of the original EOO size for approximately 70% of the species (350 species) (Figure 35b).

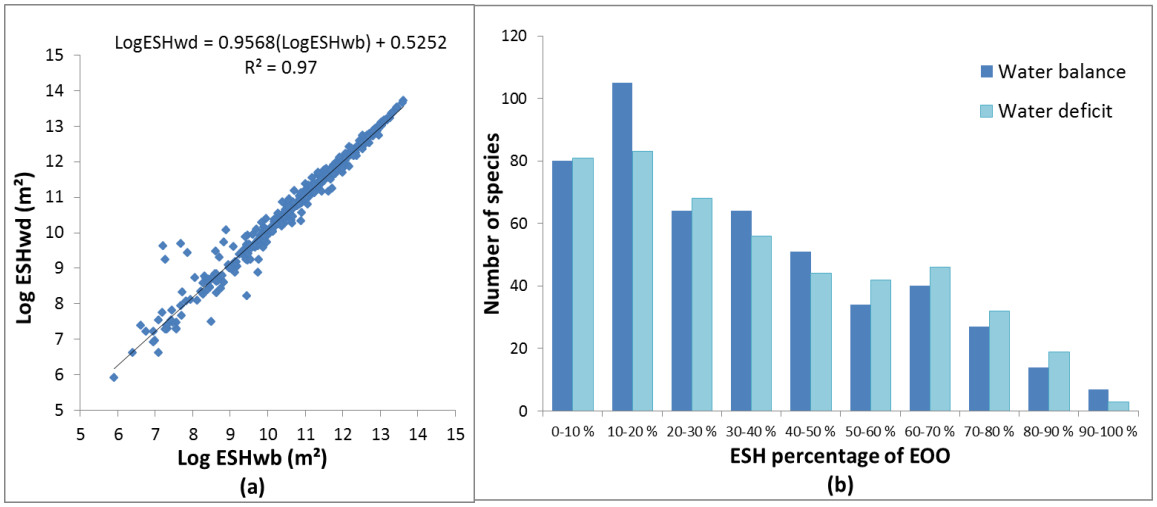

Figure 35.(a) The relationship between species' ESHs using two different water availability datasets (Water balance = wb, Water deficit=wd), and (b) the ESHs as a percentage of EOO calculated with two different water availability datasets and the number of species in each percentage group.

When comparing the two datasets by randomly selecting specimen occurrence points for SRLI forest pteridophyte species and plotting the points against the equivalent species richness values, the richness maps are very similar (r^2=0.94) (Figure 36). Both species richness maps derived from the two different water availability datasets predicted a maximum species richness value of 90 species.

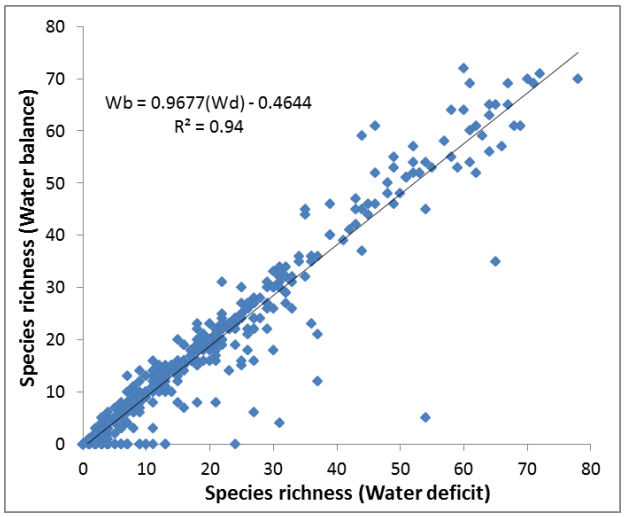

Figure 36. Comparison of water availability preference from the water deficit dataset by randomly selecting specimen occurrence points for forest SRLI pteridophyte species and plotting the equivalent species richness values for the water balance dataset.

The two datasets, water balance and water deficit, are correlated (bivariate correlation: r = -0.679, n=10000, p < 0.05) and produced very similar results, there was therefore no indication as to which dataset is more appropriate for calculating the ESH for SRLI forest pteridophyte species. However, the water balance variable was selected for the final ESH calculation method since it includes fog inputs and the reduction in evapotranspiration associated with cloud frequency in the wet environments that characterise tropical mountains, the ideal habitat for pteridophytes.

To test if broad water balance ranges for groups of species are more appropriate than assigning the minimum and maximum value to each species, the PFClust unsupervised clustering method was used to classify the species into clusters based on their water balance preference. A visual representation of the results is shown in Figure 37.

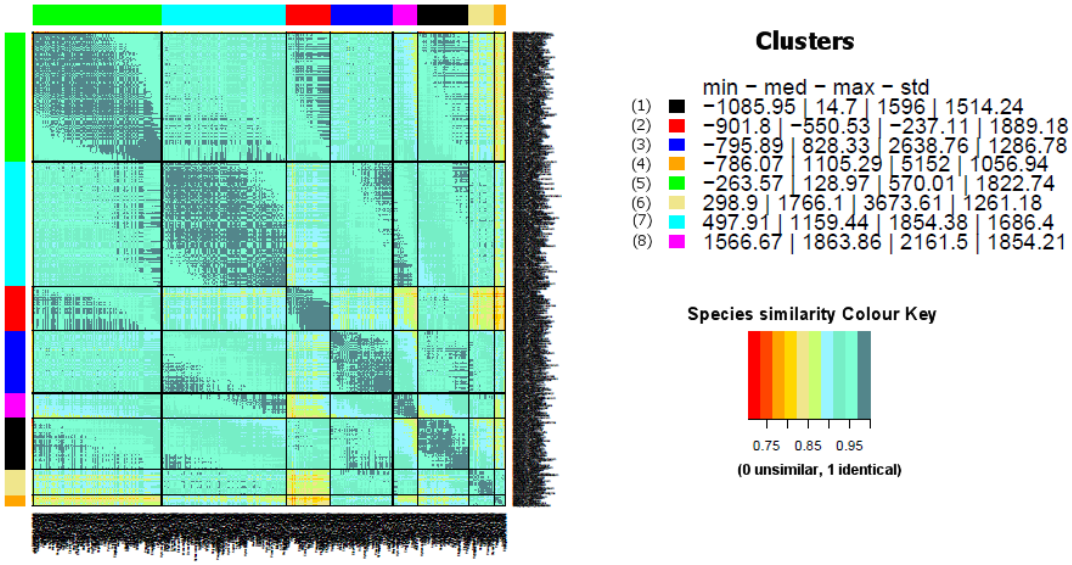

Figure 37. Heat map of the Pfclust clusters (left) and the range of values in each water balance cluster (right). The clusters are sorted based on their minimum value

The cluster analysis resulted in 8 clusters of species. Figure 38 shows that while the clusters were formed based on the species' water availability preference, they do not differentiate as expected based on the life form of the species nor based on their habitat type preference. No distinct pattern was identified among the clusters (e.g. higher number of epiphytes in a cluster with high minimum water balance). Further, the species spatial distribution in each cluster did not show any meaningful pattern with species in each cluster covering any parts of the world.

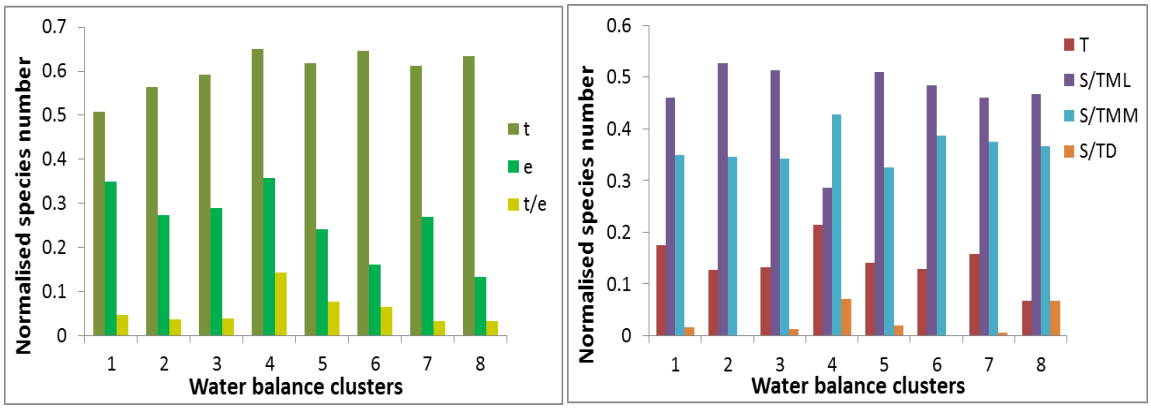

Figure 38. Number (normalised) of terrestrial (t), epiphytic (e) and both terrestrial and epiphytic (t/e) species in each water balance cluster (left hand side) and number of species (scaled) in each IUCN Habitat class (S/TD=Subtropical/Tropical Dry forest, S/TML= Subtropical/Tropical Moist Lowland forest, S/TMM= Subtropical/Tropical Moist Montane forest, T=Temperate forest) for each water balance cluster (right hand side). The range of values in each water balance cluster is presented in Figure 37.

When calculating the species' ESHs using the clustered water balance values, the new resultant ESH had a bigger mean reduction in area from the original EOO (73.7±0.2%) compared with the one that used the minimum and maximum water balance values (extracted from the specimen occurrence points for forest SRLI pteridophyte species) for each species (71.4±0.2%). Furthermore, there was a strong positive relationship (linear regression: $r^2 > 0.9$, $p<0.001$) between the ESHs (using the clustered water balance values and using the species minimum and maximum water balance values) (Figure 39). Lastly, the species richness maps generated by the two sets of ESHs were alike ($r^2=0.89$) (Figure 39) and predicted a similar maximum value of species richness (water balance = 90 species, water balance using clusters = 89 species).

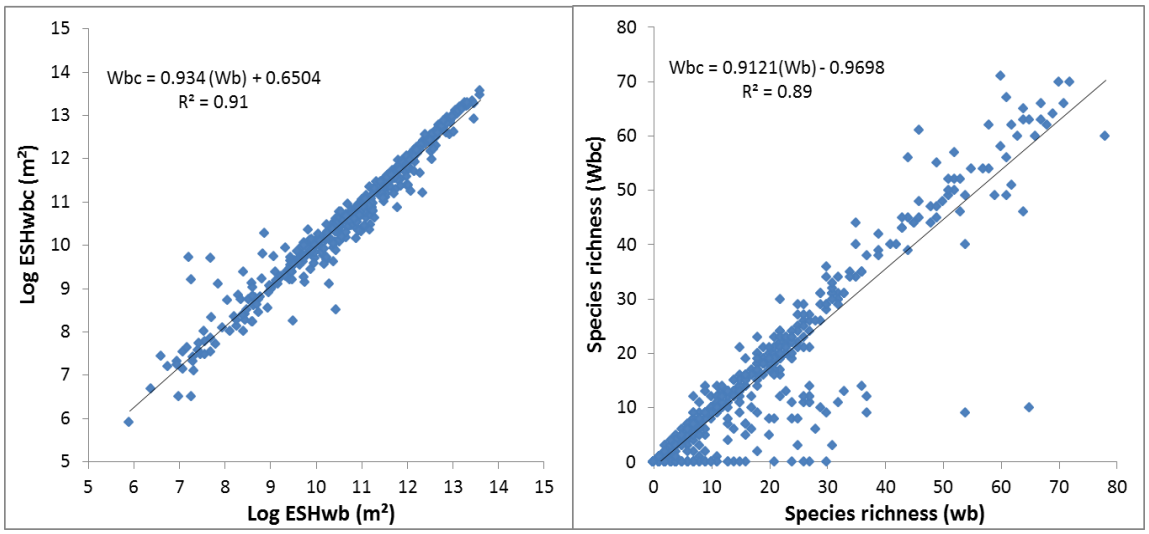

Figure 39. Relationship between the species ESHs generated using the clustered water balance ranges (wbc) and the species minimum and maximum water balance values (wb) (left hand side) and the comparison of both shown by randomly selecting specimen occurrence points of SRLI forest pteridophyte species against the equivalent species richness values (right hand side).

Based on the similarity of the two runs, it was decided not to use the clustering method in assigning water balance values to the species, thus avoiding an extra step in the procedure and keeping the simplest minimum-maximum value approach.

2.3.2.2.2 Comparison of the 2-variable and 3-variable ESH models

On average, the ESH covered 30.1±0.2% of the species EOO when using water balance data in addition to elevation and land cover criteria, 7% less than when the ESH was calculated without the water balance data (37.1±0.2%) (Figure 40a). As expected, there was still a strong positive relationship (r^2=0.9, p<0.001) between the EOO and the ESH even after adding the range of water availability values for each species to the calculation method (Figure 40b).

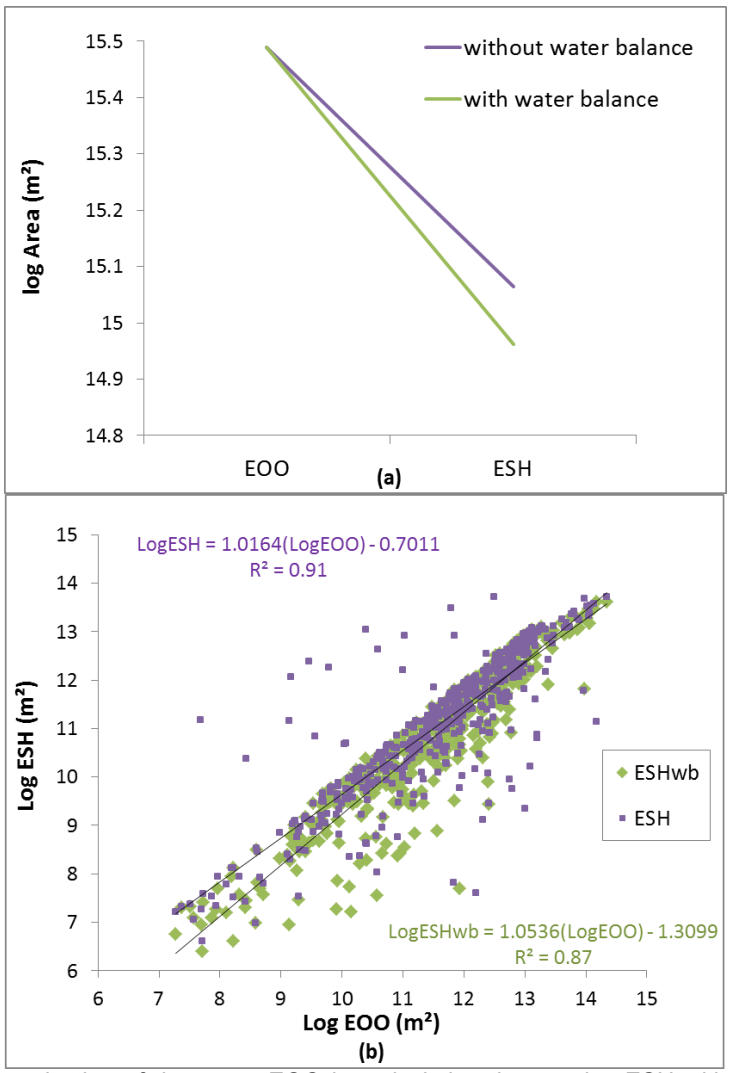

Figure 40. (a) The reduction of the mean EOO by calculating the species ESH with and without water balance data and (b) the relationship between the Extent of Occurrence (EOO) and the Extent of Suitable Habitat (ESH) calculated with (ESHwb) and without (ESH) water balance data.

A greater number of species had their EOOs reduced by 70–90% when the ESH for that species was calculated with water balance data than without it. Furthermore, the resulting ESH was reduced by at least 50% compared with the area of the original EOO, for 392 species when

the ESH was calculated incorporating water balance values, 40 species more than when calculated without water balance values (Figure 41).

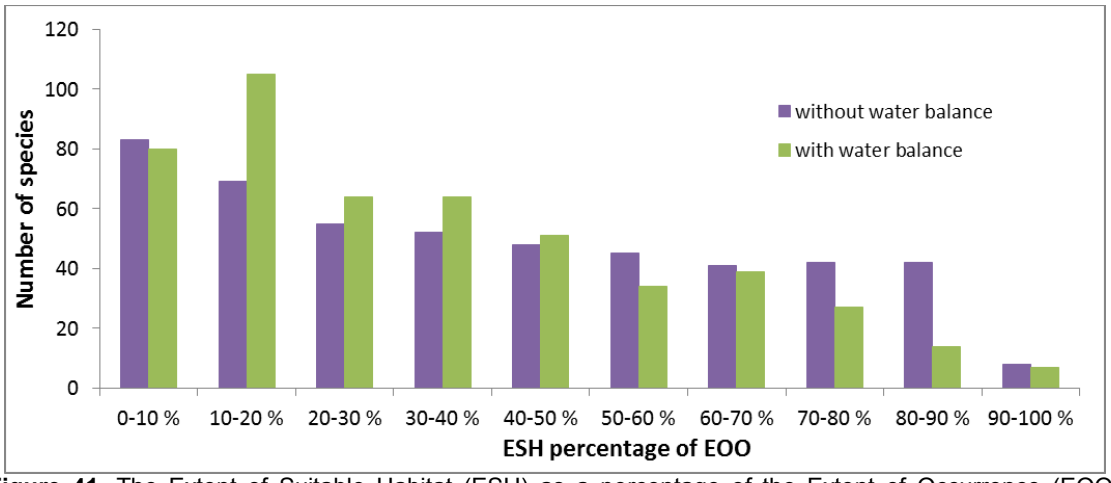

Figure 41. The Extent of Suitable Habitat (ESH) as a percentage of the Extent of Occurrence (EOO) calculated with and without water balance data.

The ratio of EOO to ESH calculated with or without water balance values differ significantly between each biogeographical realm (with water balance: Kruskal-Wallis χ^2= 29.1, d.f.=6, p<0.0001 / without water balance: Kruskal-Wallis χ^2= 24.3, d.f.=6, p<0.0001) (Figure 42). Among the tropical biogeographical realms, the highest median and mean ESH/EOO ratio (a smaller reduction from EOO to ESH) was found in the Neotropics and the lowest median and mean (a bigger reduction from EOO to ESH) in the Indomalayan region.

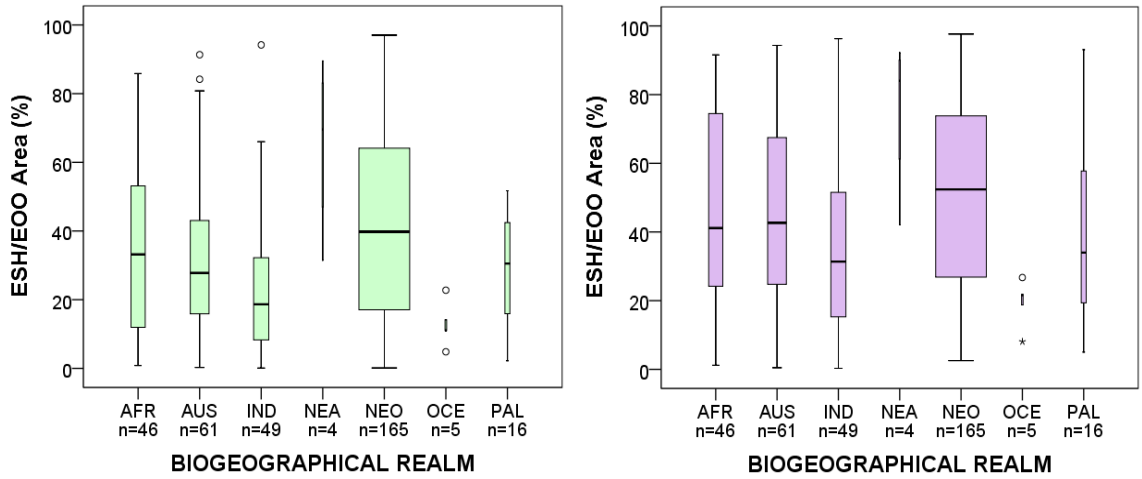

Figure 42. Boxplots representing the ESH/EOO ratio (when calculated with (left hand side) and without (right hand side) water balance) by biogeographical realms (AFR=Afrotropical, AUS=Australasia, IND=Indomalaya, NEA=Nearctic, NEO=Neotropical, OCE=Oceania, PAL=Palearctic). Species that occur in more than one biogeographical realm are not included in this figure. Box widths indicate species number.

The size of the ESHs (both with and without water balance values) differed significantly between the IUCN threat categories as the EOO does (EOO: Kruskal-Wallis χ^2=25.6, d.f.=4, p<0.0001, ESH with water balance: Kruskal-Wallis χ^2=21.4 , d.f.=4, p<0.0001, ESH without water balance:

Kruskal-Wallis χ^2=22.1 , d.f.=4, p<0.0001). There is a relationship between the IUCN Red List Categories and the size of the new ESH (Figure 43), with the average ESH being larger in the Least Concern category and smaller in the Critically Endangered category. While there was a difference in the species' ESH/EOO ratio between the IUCN Red List Categories, this difference was not statistically significant (Kruskal-Wallis χ^2= 52.2, d.f.=4, p>0.05). However, there was a bigger mean reduction from EOO to ESH in the threatened categories (CR, EN, V) (76.4%) than the non- threatened ones (NT, LC) (63.5%).

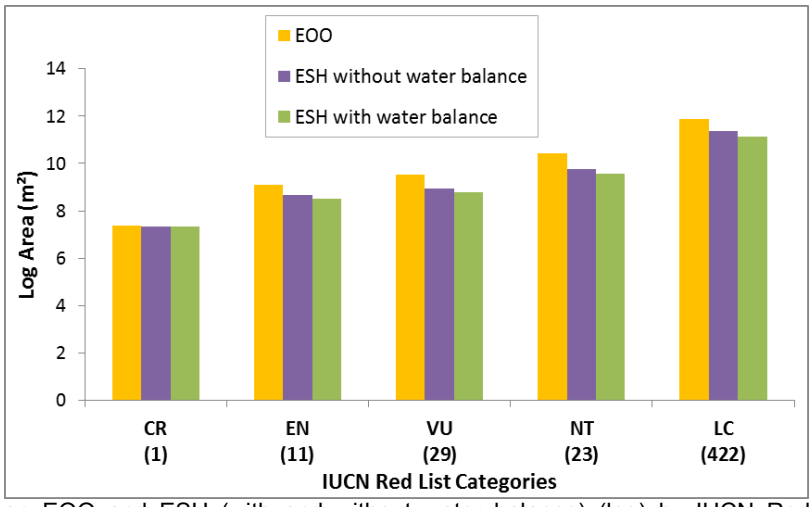

Figure 43. Mean EOO and ESH (with and without water balance) (log) by IUCN Red List Category. Categories: CR: Critically Endangered, EN: Endangered, VU: Vulnerable, NT: Near Threatened, LC: Least Concern. Numbers in brackets represent number of species in each category.

2.3.3 Validating the species Extent of Suitable Habitat

The ESHs of 115 species (25% of the species) were evaluated using independent specimen occurrence records from the GBIF online data portal which were not used in the species' ESHs calculation. The ESH of 78 species (Figure 44a) was validated by every new occurrence found (100% validation) and the ESH was validated by 50% or fewer of new occurrence records for only 15 species. No additional occurrence records were found for 9 species. In addition, despite the fact that there was a high number of new occurrence records for 2 species, just 30% of these records validated the respective ESHs for these species. Figure 44b shows the percentage of new occurrence records collected since 2005 that validate the ESH for species with an ESH/EOO ratio smaller than 50% (less than half of the original EOO). The proportion of occurrence records validating the ESH model for these species was the same as for all species together, with 49 species out of 81 validated by every new record. This is also obvious by the fact that 90% of the species had higher proportion of new point records that validated the species' ESH than the equivalent ESH/EOO ratio with a mean difference of 59±19% (Figure 44c).

When comparing the proportion of GBIF occurrence points that validated the species' ESH with the proportion of random points that also validated the species' ESH, it was found that the

species' ESHs were broadly capturing the GBIF occurrence points better than the random points (Figure 44d). For 73% of the species, the proportion of the GBIF occurrence that validated the species ESH was higher than the equivalent proportion of random points. The opposite was found in only 9% of the species. The proportion of the two set of points (GBIF and random) were identical in 18% of the species. The majority of the species' ESHs provided statistically significantly better fit to the GBIF points than to the random points. For 62% of the species' ESHs considered for evaluation, the percentage of GBIF points that validated the species' ESHs was significantly higher than the equivalent percentage of the random points at the α=0.05 level.

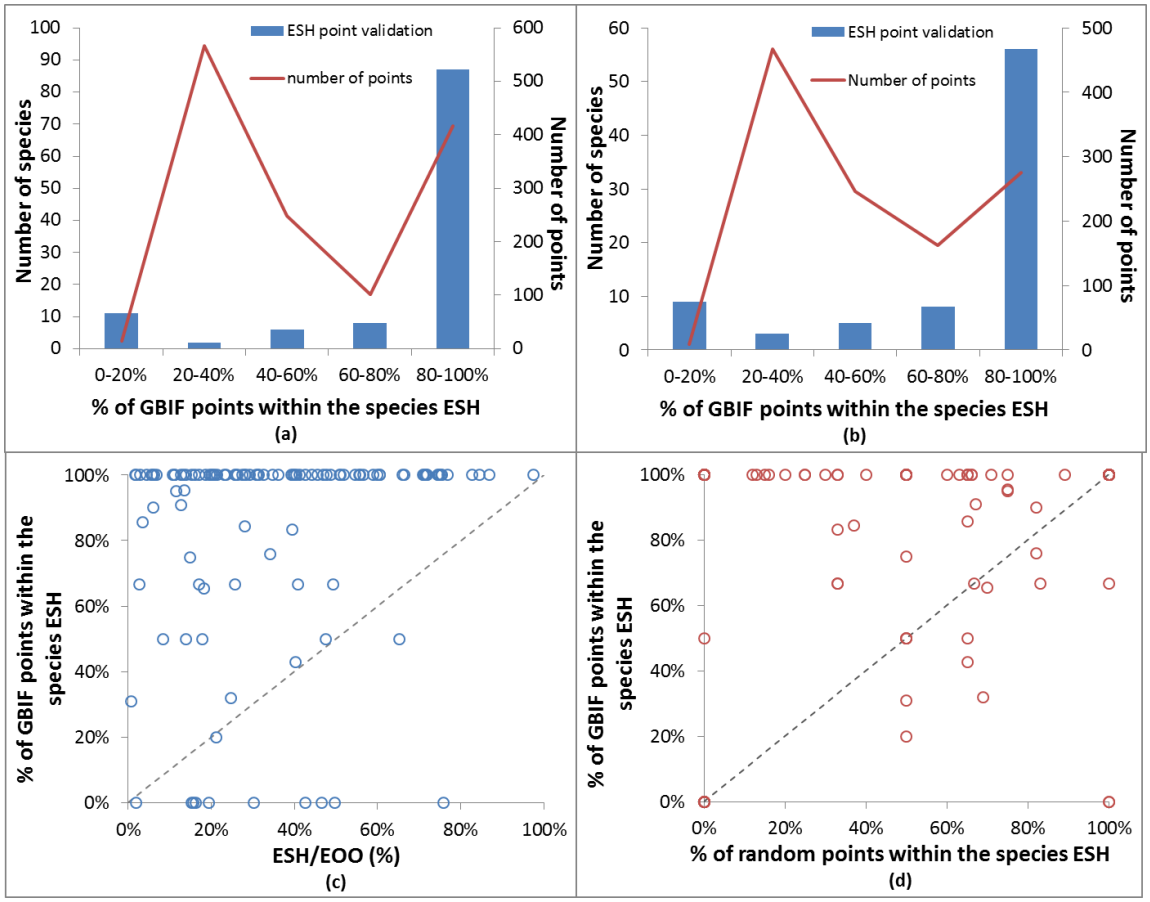

Figure 44. Percentage of GBIF occurrence records collected after 2005 validating the species ESH for (a) all species (115 species) and (b) species with ESH/EOO ratio smaller than 50% (81 species); Percentage of GBIF occurrence records collected after 2005 validating the species ESH against (c) the species' ESH/EOO ratio and (d) the percentage of random points validating the species ESH.

Data collected during fieldwork in Costa Rica were used for the ground-truthing validation of the predictions of the species maps derived from ESH calculated with and without water balance. As shown in Figure 45, the mid-elevation peak in species richness from the map of stacked species' ESHs calculated with water balance broadly agrees with the mid-elevation peak in pteridophyte species found from fieldwork data, although the species richness derived from stacked ESHs calculated without water balance data does not.

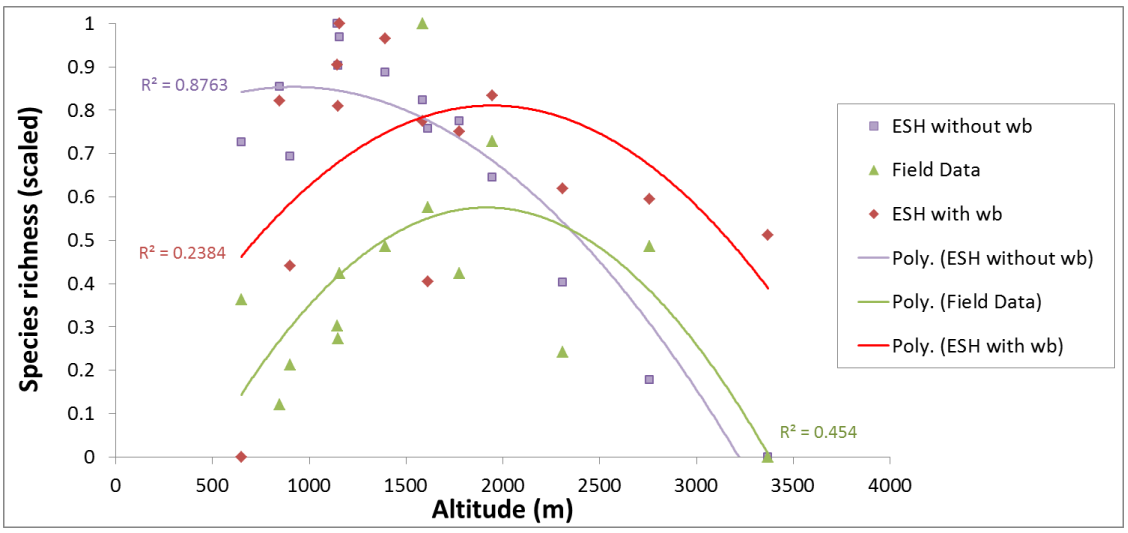

Figure 45. Normalised species richness along an elevation gradient from field data collected in Costa Rica and from ESH derived species richness maps calculated with and without water balance values (wb=water balance).

2.4 DISCUSSION

2.4.1 Investigating the bias in the SRLI data

The SRLI for plants contains 1500 pteridophyte species, which is 6% of the estimated pteridophyte species numbers (13 000 pteridophytes (Paton *et al*., 2008)), a much higher representation than the one of angiosperms (3000 species out of 352 000 species (Paton *et al.*, 2008)). Baillie *et al*. (2008) showed for mammals, amphibians and birds that the random selection of species for the SRLI index does not create any geographical bias if the sample size is greater than 1500 species. This is also true of pteridophytes: a comparison of the pteridophyte species percentage of the SRLI sample and the pteridophytes checklist (all recorded pteridophyte species) in each biogeographical realm showed that the two datasets have similar species representation in each realm. Interestingly, when the species representation in each realm of the SRLI and checklist datasets was compared with the one of the ESH dataset (forest SRLI pteridophytes) the differences were not as great as expected even though it contains just 635 species. The greatest difference was seen in the Palearctic realm with the ESH dataset having 50% fewer species than the other two datasets resulting in bigger species representation in other realms (e.g. Neotropics) of the ESH dataset. Further analysis showed that 28 ESH species, known to occur in the Palearctic realm, did not have any Palearctic records in the ESH dataset. This shows that the large gap in the Palearctic realm is not a result of selection of species in the ESH sample but, rather of the available herbarium specimens not representing the whole range of these species and therefore creating geographical bias at smaller scales (e.g. country level). Specifically, it reflects the small number of available Chinese herbarium specimens. This is evidenced by the fact that 69 SRLI forest species should occur in China based on the pteridophyte checklist but only 44 of them appear to occur there based on the herbarium specimens. This is not a surprise since museum

collections are valuable in providing a historical coverage of the species range (Boakes *et al.*, 2010) but often do not cover the whole spatial range of the species (Haila & Margules, 1996).

Based on the above comparison, it appears that the pool of species in the ESH sample does not create any obvious geographical bias. The case is different with the occurrence points (from herbarium specimens) of the ESH species, creating geographical bias mainly at smaller scales. Here, it was found that the density and number of the occurrence points were different in each biogeographical realm. Twenty-five countries mainly in the Palearctic and Afrotropics, known to have ESH species presence and suitable habitat, were not covered by any occurrence points. In these cases, the species are not represented by occurrence points which cover their whole known range and therefore, the calculated species' EOOs and ESHs will also not cover their whole known range. Geographical sampling bias in the natural history collections is a recognised issue that heavily affects species distribution and biodiversity maps, which are produced with occurrence data and therefore it has been the focus of many studies (Walther & Martin, 2001; Phillips *et al.*, 2009; Boakes *et al.*, 2010; Jetz *et al.*, 2012; Syfert *et al.*, 2013; Yang *et al.*, 2013). Specimens are not collected randomly but rather in areas with easy access (Reddy & Dávalos, 2003; Willis *et al.*, 2003; Kadmon *et al.*, 2004) and for taxa in areas of high interest at the time of the expedition (Nelson *et al.*, 1990; Dennis & Thomas, 2000). Furthermore, there is also geographic bias in the holdings of individual institutions and in what is available digitally (Boakes *et al.*, 2010; Jetz *et al.*, 2012).

2.4.2 Building the most appropriate ESH method

The ESH method was built based on a combination of deductive and inductive modeling approaches. Previous studies have applied a purely deductive approach to calculate species' ESHs using mainly two environmental variables (Rondinini *et al.*, 2005; Boitani *et al.*, 2008; Beresford *et al.*, 2011a; Buchanan *et al.*, 2011; Rondinini *et al.*, 2011). Here, however, an inductive approach was added to understand the species' habitat requirements using the available occurrence records. This way, the maximum amount of information was extracted from the available data. The altitudinal range of the species was calculated using expert knowledge, information on herbarium specimens but also information that was extracted from remote sensing data with the species' occurrence points. The species' water availability and land cover preferences that were used in the ESH calculation, were based exclusively on information that was extracted using the species' occurrence points. A similar approach was also seen in Corsi *et al.* (1999) who calculated the suitable habitat of Italian wolves following the suggestion of Stoms *et al.* (1992).

The ESH calculation method was carefully created by selecting the most appropriate variables for the group being investigated (a sample of forest pteridophyte species worldwide) in order to select the most suitable conditions for each species from the best available GIS datasets. While it was recognised that the best dataset for deriving species altitudinal ranges was the high resolution SRTM-GTOPO30 database, such an obvious selection was not clear for the land cover and water availability databases. The available global land cover datasets were compared

in order to select the most suitable one. For each species, the three different ESHs produced using each land cover datasets had only small discrepancies due to the relatively small differences in the land cover classes of each dataset. In addition, the ESH for each species was always significantly less extensive than was the EOO using each land cover dataset. However, the mean reduction in area from EOO to ESH was greatest when using the GLCC land cover dataset (GLCC=69.7%, GLC2000=64.3%, GlobCover=62.5%). However, the selection of the most suitable land cover dataset cannot be based entirely on the reduction in area of the EOO, since there is no reason to suppose that the greater the reduction in area, the more realistic and accurate the species' ESHs produced. Hence, for each land cover dataset, the ESHs were used to generate the species richness and endemism richness maps. These showed that indeed the differences between the species' ESHs were reflected in the different species richness and endemism richness maps. The three sets of maps were all very similar, identifying the same areas of high species richness and high endemism (Figure 27 & Figure 28).

Due to the similarities between the three sets of species' ESHs, and also between the species richness and endemism richness maps, the decision to select the best land cover dataset was based on the properties and characteristics of each dataset. The three land cover datasets agree substantially (Bai, 2010); however, since the three datasets were generated from different remotely-sensed data and were processed with different classification techniques, there are also differences between them (Table 1&3).

The greatest difference between the three datasets is that, while the GLC2000 and GlobCover are land cover maps derived entirely from remote sensing data, the GLCC map is an ecosystem map that applies the Global Ecosystem Framework proposed by Olson (1994). When comparing areas in the three species richness maps, the map that incorporated the GLCC data appears more detailed (Figure 29). This is due to the fact that the GLCC database includes 94 classes whereas the GLC2000 and GlobCover databases include only 22 and 23 classes, respectively. The 94 classes of the GLCC ecosystem classification include details on seasonality, climate and vegetation structure. Hence, compared with the other two datasets, the GLCC database is not solely based on remote sensing of land cover. But since species respond to climate as well as land cover it is probably a more realistic estimate of the likely ESH than would occur from land cover alone. The climate data in the GLCC maps (Loveland *et al.*, 2000) is, however, very simplistic when compared with the gridded datasets commonly used in species distribution modelling (e.g. Maxent).

The GLCC data were obtained by the Advanced Very High Resolution Radiometer (AVHRR) sensor in 1992/1993, making this database the oldest compared with the GLC2000 and GlobCover datasets (from 1999/2000 and 2004/2006, respectively). Furthermore, the GLCC dataset is missing data from various locations, especially for small oceanic islands. These data voids proved to be a problem when calculating the ESH for species endemic to those areas. No similar problem was encountered when using the other two datasets. Despite the above limitations, the GLCC dataset has been used in studies that have investigated habitat quality

and fragmentation (Riitters *et al.*, 2000; Willis *et al.*, 2003; Rondinini *et al.*, 2005) since at the time of these studies no other global land cover dataset was available. Recent studies, similar to this work, have either used the GLC2000 database or the GlobCover database (Beresford *et al.*, 2011a; Buchanan *et al.*, 2011; Rondinini *et al.*, 2011). For the above reasons and due to the fact that the specific version of the dataset (v.2.0) was never validated, it was decided that the GLCC database is not the most suitable dataset for calculating ESHs of plant species for this study.

When comparing the three datasets, the species richness maps derived from the GLC2000 and GlobCover datasets are shown to be the most similar (Figure 30). This result is consistent with the findings of Kaptué Tchuenté *et al.* (2011) who showed that between four land cover maps of Africa (GLC2000, GlobCover, MODIS LC-I and ECOCLIMAP-II) GLC2000 and GlobCover were the most similar. The GLC2000 and GlobCover databases have approximately the same number of classes but differ in the spatial resolution of the remotely-sensed data and the time period when the data were obtained. GlobCover (v2.2) data were collected between 2008 and 2009 with a 300 m spatial resolution whereas GLC2000 data were collected between 1999 and 2000 with a 950 m spatial resolution. While both datasets were created using the same classification technique and scheme, GlobCover could be easily repeated and updated at regular intervals due to its automated classification algorithms (Bicheron *et al.*, 2008; Bontemps *et al.*, 2011), and be used in long-running projects such as the SRLI project. Both datasets were validated and a global accuracy of 68.6±5%.and 70.7% was reported for GLC2000 (Mayaux *et al.*, 2006) and GlobCover (Bontemps *et al*., 2011) respectively. However, only GlobCover's validation was conducted according to the recommendations of the Committee on Earth Observing Satellites Land Product Validation subgroup (Strahler *et al.*, 2006) including an independent validation by international land cover experts. Based on the above, GlobCover appears to be more suitable than GLC2000 for the purpose of this study. Since the GlobCover data were collected more recently and at higher spatial resolution and considering that there are otherwise no substantial differences between the results produced by the two datasets, the GlobCover database was selected as the most suitable dataset for calculating the plant species ESHs in this thesis.

There are, however, two available GlobCover versions (v.2.2 & v2.3). Both versions are based on fine resolution MERIS data, have the same resolution (300m), include the same detailed land cover classes and are more recent than the other available land cover datasets. Globcover 2005 (v.2.2) was created using data collected between December 2004 and June 2006. Globcover 2009 (V.2.3) was created using data collected between January 2009 and December 2009, and GlobCover 2005 as a reference system. Globcover 2009 was used for the comparison with the other land cover datasets; however, GlobCover 2005 was also tested in the ESH calculation method. When calculating the species' ESHs with the two GlobCover versions, the total area of the species ESHs did not change significantly (0.4% difference in mean reduction in area from EOO to ESH) since the average land cover change over a period of 4 years was small. While the most obvious choice was to use the most recent database, it was

decided to calculate the species ESHs using Globcover 2005 since, in the next stage of this study, deforestation data will be used to investigate the habitat loss of species' ESH between 2005 – present, and into the future, hence a 2005 baseline is more appropriate than a 2009 one.

The next step was to select the most appropriate water availability dataset. Two highly correlated variables, maximum water deficit and minimum water balance, both of which represent species' tolerance to drought, were tested and compared. Both water availability datasets identified the same pattern when comparing their values for species in each IUCN habitat category and life form type (Figure 34). In addition, there was a strong positive relationship between the species ESHs of the two water availability datasets (Figure 35), which was reflected in their respective species richness maps. The two datasets produced very similar results, including mean reduction in area from EOO to ESH (water balance = 70.4%, water deficit = 69.9%), and therefore gave no indication as to which dataset is more appropriate for calculating the ESH for pteridophyte species. However, it was decided that the water balance variable should be selected for the ESH method since it incorporates fog inputs and reduced evapotranspiration as a function of cloud cover. Hence, water balance is taken as better representing the climatic conditions that the species are exposed to.

Unlike the altitudinal range for each species, which was calculated based on four sources, species' water availability values were just based on the georeferenced point data for each species. The hypothesis, that broad water availability ranges for groups of species are more appropriate than assigning a specific range to each species based on the minimum and maximum values, was tested by classifying the species into clusters based on their water balance preference. The different clusters were not as meaningful as expected; there was no differentiation between clusters based on the species life form, habitat type preference or geographical location. For example, it was expected that clusters with high water availability range (e.g. cluster 8) would include a large number of epiphytic species or that the species that appear in temperate forests would be included in clusters with low water availability range (e.g. cluster 2). While, no such pattern was identified among the clusters, the degree of similarity of the two ESH sets (with and without using the clustering method) was very high. This shows that the PFClust method could be used with biogeographical data in addition to the already tested gene expression data. The biggest advantage of this method is that the user does not need to specify any requirements, such as the number of clusters, which is important when working on global scale and therefore not enough information is available for all species. Moreover, unlike with other clustering methods, the PFClust method includes the range of the values of the variable (in this case water availability) for each cluster. However, based on the similarity of the analyses with and without clustered values, it was decided not to use the clustering method in assigning water balance values to the species, avoiding this way an extra step in the procedure and keeping the simplest minimum-maximum value approach. It is important that the new ESH calculation method should be simple and quick in order to be easily used by anyone when assessing the species conservation status every five years.

Although adding a third variable to the ESH model increases its complexity and adds an extra step to the process, water availability preference was added to the ESH model as a third variable, due to the known strong correlation between pteridophyte distributions and the availability of water (Stephenson, 1990; Stephenson, 2000; Page, 2002; Bickford & Laffan, 2006; Kessler *et al.*, 2011). It was therefore assumed that a species does not occur in areas of a suitable land cover class when water availability is not suitable. The two models (with and without water availability) were compared in order to investigate whether the third variable improved the ESH method. On average, the ESH covered 7% less than when the ESH was calculated without the water balance data. This reduction was expected since the species' suitable habitat will decrease when all three conditions are met (altitude range, assigned land cover classes, water balance range). Data collected during fieldwork in Costa Rica were used for the ground-truthing validation of the predictions of the ESH-derived stacked species richness maps (generated using water balance and without). The results support the decision of including water balance in the ESH calculation since without water balance the peak in ESH-derived species richness does not follow the species richness pattern evident from the field data. On the contrary, the mid-elevation peak of the ESH-derived species richness map calculated with water balance broadly agrees with the pteridophyte species richness-altitude relationship found from fieldwork data (Figure 45).

2.4.3 EOO/ESH comparison

As mentioned in the Introduction (section 2.1), the EOO metric tends to overestimate species' geographic range (Burgman & Fox, 2003; Shaw *et al.*, 2003; Orme *et al.*, 2006; Jetz *et al.*, 2008) due to the fact that it may include extensive areas that are not environmentally suitable or accessible to the species. To overcome this limitation, the ESH metric (which is ultimately derived from the EOO) was introduced, and habitat suitability models have now been used in several studies (Rondinini *et al.*, 2005; Jetz *et al.*, 2007; Boitani *et al.*, 2008; Buchanan *et al.*, 2008; Catullo *et al.*, 2008; Beresford *et al.*, 2011a; Rondinini *et al.*, 2011; Visconti *et al.*, 2011). Unsurprisingly, there was still a strong positive relationship (r^2=0.9, $p<0.001$) between the EOO and the ESH, since the species EOO was used in the ESH calculation. In calculating the ESH, the resulting range of approximately 400 species (out of 487 species) was reduced by at least 50% compared with the area of the EOO. On average, the ESH covered 30.1±0.2% of the species EOO, a relatively small percentage taking into consideration that the approach of this study was conservative (including all habitat types and the broader altitude/water balance ranges associated with each species). Assuming that the species' ESHs are accurate, the small average percentage of suitable habitat within the species EOO shows that the EOO metric generally overestimates species actual range size. Thus, the ESH metric could be used to reduce potential errors of commission in the EOO.

The mean reduction in area from EOO to ESH (69.9±0.2%) was greater than the mean reduction in the studies of Rondinini *et al.* (2011) (45.2±21.5%), Buchanan *et al.* (2011) (48.2±0.4%) and Jetz *et al*. (2007) (21.5±3.5%), and similar to the study of Beresford *et al.*

(2011a) (73.3±2.2%). The difference in the mean reduction in area can be explained by the habitat specificity of the investigated group in each study. Thus, a big mean reduction in area from EOO to ESH was expected in the case of forest pteridophytes since they are habitat specific to wet forests. The study of Beresford *et al*. (2011a) was focused just on threatened birds of Africa which can explain the bigger mean reduction of EOO to ESH when compared with the results of Buchanan *et al*. (2011) and Jetz *et al*. (2007) who investigated forest bird species on a global scale.

It was expected that species with large EOOs would have a smaller ESH/EOO ratio than would species with small EOOs since it was assumed that large EOOs will include a larger percentage of unsuitable habitat than small EOOs do. Surprisingly, however, no relationship was found between the size of the EOO and of the ESH area as a percentage of the EOO. Widespread species with large EOOs (e.g. *Anemia hirsuta*) had the same ESH/EOO ratio as highly-localised species with small EOOs (e.g. *Asplenium underwoodii*). Hence, this could mean that significant commission errors are found even in small EOOs where they are clearly more important in determining changes in IUCN threat category. It is important to mention that the species with the largest EOOs have the smallest ESH/EOO ratio. These widespread species have a trans-continental distribution; thus, when their ESHs were calculated, a large percentage of their range (covering marine areas) was excluded.

There was a statistically significant difference in the species' ESH/EOO ratio between biogeographical realms (Kruskal-Wallis $\chi^2= 29.1$, d.f.=6, $p<0.0001$). The difference in the amount of reduction in EOO between realms could be explained by the different extents of habitat fragmentation and conversion and the amount of continuous suitable habitat (forest land for forest pteridophytes) in each realm. Deforestation has occurred in different regions through time (firstly in temperate regions and then in tropical regions) (Williams, 2002) and, since 2000, South America and Africa have been the regions with the highest deforestation rate (FAO, 2010) historically. According to FAO (2010), South America has the highest percentage of remaining forest cover, followed by Europe, Central America and North America. Unsurprisingly, the highest mean proportion of suitable habitat within the EOO was found in the Nearctic, Palearctic and Neotropical realms. Species in Oceania had the smallest mean proportion of suitable habitat, a result that agrees with the results shown in Rondinini *et al.* (2011). This can be explained by the fact that the EOO of the oceanic species includes a large area of sea that is automatically excluded in the ESH calculation as it is clearly unsuitable habitat. Asia has the smallest percentage of remaining forest cover (FAO, 2010), which explains why the lowest mean proportion of suitable habitat within the EOO in tropical realms was found in Australasia and Indomalaya, followed by the Afrotropics.

The area of the EOO is generally the basis of a Red List Conservation assessment for a plant species when being assessed under Criterion B (as most plant species are), since geographical range is an important factor contributing to the extinction risk of a species under land use (and/or climatic) change. As expected, the size of the new ESHs differed significantly between

the IUCN Red List categories, as does the EOO showing that Criterion B was the only criterion used in the IUCN categorisation of these species. There is indeed a relationship between the IUCN Red List Categories and the size of the new ESH, with the average ESH decreasing from the Least Concern category to the Critically Endangered category. Furthermore, as other studies reported (Jetz *et al.*, 2008; Beresford *et al.*, 2011a; Rondinini *et al.*, 2011), the percentage of ESH in EOO also differed between the IUCN Red List categories although this difference was not statistically significant. However, it was found that there was a greater mean reduction from EOO to ESH in the threatened categories (76.4%) than the non-threatened ones (63.5%) agreeing with the results of Jetz *et al*. (2008). The greater overestimation of the range of threatened species shows the importance of incorporating habitat in calculating the geographical range of threatened species.

While it has been shown that the ESH metric reduces commission errors in the species EOO, the precision of this new species distribution prediction was previously unknown for plants. This was tested by validating the species ESHs using newly-available occurrence point data that were collected after 2005. It is important to note that such occurrence point data were available for only 25% of the investigated species; however, these species covered a wide taxonomic and geographic range, representing the distribution patterns of all investigated species. For 70% of the species, 100% of their new points validated their ESH (points-ESH overlay) (Figure 44a). The ESH of 1% of the species (10 sp.) could not be validated by any points due to the low number of new point data (1 – 2 points) for these particular species. Although there was a high number of new points for 2 species, just 30% of these points were within the equivalent ESHs. These two species (*Equisetum palustre* and *Thelypteris palustris*) are widespread species with large distributions; however, their newly-available points covered mainly northern Europe. Since the closer the ESH is to the EOO the higher the chances are for new points to validate the species ESH, the ESH for species with an ESH/EOO ratio smaller than 50% was validated separately using new occurrence points collected since 2005 (Methods section 2.2.3). While it was expected that a smaller percentage of these points would have validated the ESHs for these species, validation of these species showed similar results as the validation of all of the species, with the ESH of 62% of these species being validated by all their new points (Figure 44b). This was also shown by the higher proportion of new point records which validated the species' ESH than the equivalent ESH/EOO ratio for 90 % of the species (Figure 44c). According to Rondinini *et al.* (2011) this indicates that the species' ESHs are better in predicting the species geographical range than the EOOs.

When investigating whether the species' ESHs and GBIF occurrence points agree more than expected by chance, it was found that the species' ESHs were broadly capturing the GBIF occurrence points better than the random points (Figure 44d). For 73% of the species, the proportion of the GBIF occurrence points that validated the species ESH was higher than the equivalent proportion of random points. The two set of points (GBIF and random) generated identical results in 18% of the species. The proportion of random points that validated the species' ESHs was higher than the equivalent of the GBIF points in only 9% of the species. The

only case that 100% of random points validated the species' ESH when none of the GBIF data did was in the case of *Vittaria owariensis*, the ESH of which was validated by only one point.

Furthermore, the ground-truthing validation of the predictions of the stacked ESH-derived species richness map in Costa Rica showed that the mid-elevation peak observed in the ESH-derived species richness data broadly agrees with the relationship of pteridophyte species diversity with altitude found from fieldwork data (Figure 45). These results together with the results of the ESH validation using new occurrence data show that the ESH metric is effective at reflecting the reality of plant distributions on the ground. Therefore, the ESH metric is indeed reducing commission errors relative to the EOO since on average, the ESH covered 30.1±0.2% of the species EOO.

2.4.4 Using the ESH metric

This study has shown that the ESH metric can be used in calculating species' geographical range, since it effectively reduces the EOO area without compromising the accuracy of species' predicted distributions. Despite the fact that it is a simple and practical method, there are limitations associated with this metric similar to those of other predictive metrics for species distributions:

1. Since the ESH is calculated within the area that the species can occur as defined by the convex hull of the EOO, it is still assumed that the species does not exist outside of the margins of the EOO. The EOO is calculated using presence-only point data, generally from georeferenced herbarium specimens in the case of plant species, the number of which could be limited for species in areas that are under-sampled. Hence, in that case the EOO would not have included areas in which the species potentially occurs but where localities have never been recorded. As shown with the bias investigation of the SRLI data, species occurrence data are geographically biased mainly at smaller scales. Although museum collections are valuable in providing a historical coverage of the species range (Boakes et al., 2010), it is recognised that often they do not cover the whole species range spatially (Haila & Margules, 1996). In addition, the precision of the EOO and other similar species distribution prediction metrics is dependent on the accuracy of the recorded species data and of the georeferenced points (Elith *et al.*, 2002; Burgman & Fox, 2003; Brummitt *et al.*, 2008). Limited information on the locality of the herbarium specimen could result in an inaccurately georeferenced species occurrence point, which may affect the species final EOO. Lastly, taxonomic inaccuracies and incorrect determination of specimens are reflected in the occurrence data (Williams *et al.*, 2002) and could also influence the calculation of the EOO metric. As mentioned in section 2.2.2.1, despite these potential errors of omission, the EOO metric was used as the base for calculating the species ESH due to the strict IUCN guidelines for using the EOO metric in Red List species conservation assessments (IUCN, 2014). While for conservation planning the reduction of commission errors should have a priority over the reduction of the omission errors (Loiselle *et al.*, 2003; Rondinini *et al.*, 2006), it is recognised that this issue should be addressed in the

future. Applying a suitable buffer zone around the EOO, before calculating the ESH, could be a solution.

2. According to Gaston & Fuller (2009), habitat suitability models still overestimate species' distributions even after reducing commission errors relative to the EOO. The reason for this is that they do not take into consideration abiotic (e.g. meso- and microclimatic) and biotic factors (e.g. competitive species interactions, species tolerance to land cover change) that could further limit a species range (Davis *et al.*, 1998; Morrison *et al.*, 2006). Hence, the actual ESH could still exceed the bounds of the AOO of the species.

3. The accuracy and the realism of habitat suitability models are influenced by the scale (Scott *et al.*, 2002) and the resolution (Rondinini *et al.*, 2006) of the data on environmental variables used. As shown in this study, using different land cover maps in the ESH calculation could change the final result. Depending on the focus of each study, high resolution land cover maps should be used to better detect small patches of habitats in an area than is possible with coarse scale maps. Like with the different land cover maps, different water availability datasets could also change the final result of habitat suitability models. When calculating the extent of suitable habitat of plant species, a high resolution water availability map should be used that will better represent the climatic conditions that species are exposed to. However, it is recognised that often even high resolution maps do not match the scale at which the species interacts with the environment and the fact that many species are separated from their climatic environment by structural organisms such as trees that create their own microclimate in which species exist.

4. Despite the conservative approach of this study (including all habitat types and the broader altitude/water balance range associated with each species), it is recognised that the species ESH is dependent upon the selection of the categories/value ranges for each variable that are assigned to the species. A different species ESH will be produced if a different combination of land cover categories is assigned to the species. Thus, the assignment of land cover categories to a species is a crucial step in the procedure. Ideally, the selection of land cover categories assigned to each species should be made by experts on the individual species. However, this was not feasible due to the large number of SRLI species and the lack of expertise for most taxa. The selection of species' water availability and altitudinal ranges was less complicated since the minimum and maximum value was used in each case. However, this method is dependent on the accuracy of the georeferenced occurrence points for the species, since the values for each variable were extracted using the species' georeferenced point data.

Nevertheless, this study has shown that the ESH metric can reduce commission errors relative to the EOO, a result which agrees with other similar studies (Rondinini *et al.*, 2005; Jetz *et al.*, 2008; Beresford *et al.*, 2011a; Beresford *et al.*, 2011b; Buchanan *et al.*, 2011; Rondinini *et al.*, 2011). The average ESH covered 30.1±0.2% of the species EOO, despite the conservative approach of this study. Since conservation efforts are based on the species geographical range

size, this approximately 70% mean reduction of the EOO could mean that current range sizes are overestimated. When the EOO metric is used in conservation assessments without the appropriate thresholds the degree of threat may be underestimated.

Additionally, while the species EOO does not change over time unless a new species locality is found (Brummitt *et al.*, 2015a), the ESH can be re-calculated based on land cover change observations. In this study the species' ESHs represented the species geographical range in 2005, since GlobCover 2005 was the land cover classification used. The species' ESHs can be recalculated using GlobCover 2009 or any other recent land cover dataset to represent their ranges in 2009 or at whatever time. Moreover, deforestation data between 2005 and the present can be used in calculating the species ESH and therefore subtracting the suitable habitat that was lost between that period and the most recent species ESH. Thus, an updated and strictly comparable ESH will show the change to the species distribution due to land cover change, and could therefore be used for re-assessing the conservation status of plant species under IUCN Criterion B (geographic range).

Currently, when applying Criterion B and assessing the Red List status of a species, there are only quantified thresholds for EOO (Criterion B1) and AOO (Criterion B2). Replacing these two metrics with the ESH metric would be unrealistic since that would mean all species previously assessed under Criterion B would need to be re-assessed. In addition, since these metrics may also be used under Criterion A (population size), their replacement will also affect the thresholds determining threatened categories under Criterion A. Assessments under Criterion B also require two out of three subcriteria to be fulfilled, and a standardised, comparable and objective ESH metric could be incorporated within sub-criterion b(iii): 'Continuing decline observed, inferred or projected in area, extent and/or quality of habitat' (IUCN, 2012a), since a stable relationship between the ESH size and the degree of IUCN threat was found (Figure 43). Specifically, the average size of suitable habitat decreases with increasing category of threat and therefore the ESH metric could be used to create quantified ESH thresholds for threatened Red List Categories under sub-criterion b(iii) as was also suggested by Rondinini *et al*. (2011) and Brummitt *et al.* (2015a). The degree of habitat loss observed in already assessed species could be quantified and the ESH thresholds determined as representing an appropriate amount of suitable habitat for setting thresholds for each threatened category.

2.5 CONCLUSIONS

This chapter has presented the first attempt to use a standardised ESH metric in calculating the geographical range of plant species globally. It has shown that the ESH is an improved measure of calculating the species range since it reduces commission errors relative to the widely-used EOO metric and only incorporates areas with appropriate conditions for the species. While the ESH calculation method is simple and practical, it should be used carefully by selecting the most appropriate variables for each taxonomic group and by choosing the most suitable

available remote sensing datasets. High spatial resolution datasets should be used when calculating the species ESH in order to better detect the areas with suitable habitat for the species. The validation of the species ESHs showed that this new calculation method is effective at reflecting the reality of plant distributions on the ground, demonstrating that such a simple method can be used to predict the distribution of species globally.

Furthermore, since the ESH was derived from remotely sensed data, it can be re-calculated based on land cover change observations, in contrast with the EOO which changes only slightly over time. Thus, the ESH could be used for re-assessing the conservation status of plant species under IUCN Criterion B (geographic range) sub-criterion b(iii) (decline in habitat quality), since it was also found that the average amount of suitable habitat decreases with increasing category of threat. By re-calculating the species' ESH from increasingly available remotely-sensed land cover data, and so re-assessing the conservation status of species on a 5-year time frame, the change in the SRLI for Plants could be calculated and the global trends in plant conservation status monitored. In this way, more dynamic, comparable, repeatable and spatially-detailed Red List Index updates could be provided.

CHAPTER 3

MAPPING GLOBAL PTERIDOPHYTE SPECIES RICHNESS & ENDEMISM

3.1 INTRODUCTION

3.1.1 The use of global biodiversity patterns in conservation strategies

Interest in biogeography can be traced back to ancient times, with Aristotle being one of the first scientists to pose questions about the biogeographical patterns of the distribution of species. In the past, the need to understand biogeographical patterns was driven principally by curiosity. However, during the past few decades, the knowledge of these patterns has become increasingly important in attempts to reduce the rate of biodiversity loss.

Human activities are placing unprecedented pressure on biodiversity and natural ecosystems. This pressure is pushing many species into extinction with the extinction rate now many times (1000 - 10 000) higher than the average estimated background rate (0.1 to 1 species extinctions per million species per year) in the past (Groombridge & Jenkins, 2002; Pimm *et al.*, 2014; Ceballos *et al.*, 2015). Protected areas are successfully used as a tool for conserving species and ecosystems in conservation strategies (Bruner *et al.*, 2001; Chape *et al.*, 2005). Aichi Target 11, one of the targets outlined in the Strategic Plan for Biodiversity 2011 – 2020 adopted at the 10th Conference of the Parties to the Convention on Biological Diversity, calls for at least 17% of terrestrial land to be protected by 2020 (UNEP, 2010). Bertzky *et al.* (2012) reported that 13% of the terrestrial areas are already protected, although it has been shown earlier that global hotspots are not well represented in those areas (Rodrigues *et al.*, 2004). Biodiversity hotspots, areas with high diversity (containing at least 1500 endemic plant species) and level of threat (70% loss of their original habitat) (Myers et *al.*, 2000), need to be identified and established as protected areas in order to meet Aichi target 11.

Given the limited funding available for nature conservation, it is clear that it is impossible to conserve all biodiversity in every part of the world. Species richness and endemism have been used as measures of biodiversity in order to prioritise areas for conservation efforts (Brooks *et al.*, 2006; Wilson *et al.*, 2006). Studies have used species richness and endemism separately as indicators of biodiversity (Mittermeier *et al.*, 1998; Myers *et al.*, 2000; Brummitt & Nic Lughadha, 2003; Stattersfield *et al.*, 2005; Lamoreux *et al.*, 2006; Pimm *et al.*, 2014) or combined the two measures into one index (Kier & Barthlott, 2001; Linder, 2001; Kier *et al.*, 2009). All global studies have identified the hottest hotspots of species richness and endemism within tropical regions with the Tropical Andes, Mesoamerica, Sundaland, Madagascar and the Caribbean islands always making it in the top list. Naturally, conservation efforts have focused on the global hottest hotspots; however, Kier *et al.* (2005) argued that the hottest species richness hotspots of each biogeographical realm should be included in conservation strategies.

3.1.2 Species – Area relationship

When investigating which part of the world has the richest biodiversity, the area of each region must be taken into account. Forests cover 31% of the world's surface and hold over 80% of global terrestrial biodiversity (FAO, 2010). However, they are not equally distributed globally with the largest forest cover found in South America (tropical forests) followed by Europe (Russian temperate forests). The forests richest in species are the tropical forests, both lowland rainforests and montane cloud forests (Myers *et al.*, 2000; Pimm *et al.*, 2001; Mace, 2005). Within tropical regions, the distribution of forest is also uneven. According to FAO (2010), the Americas has $891x10^4$ km² of tropical forest, Africa has $344x10^4$ km² and Asia has $356x10^4$ km², the largest areas being those in the Amazon basin, the Congo basin and South East Asia in each continent respectively. This distribution can be explained by the different past and present climatic patterns and events (e.g. Pleistocene climatic oscillations) (Emanuel *et al.*, 1985) and the level of human impact in each region (Hansen *et al.*, 2013).

It has long been well known that the relationship of the number of species to the area in which those species are found is not linear (Williams, 1943) and, therefore, that it is not realistic to simply divide maximum species richness by area to obtain a comparative measure of species richness per unit area. (Connor & McCoy, 1979). The relationship is better described by a power function (Dengler, 2009). The most closely described equation of the species-area relationship was given by Rosenzweig (1995) ($S=cA^z$, where S is species richness, A is Area and c and z are constants). Brummitt and Nic Lughadha (2003) stressed the importance of using the species-area power function relationship when comparing species richness of different areas and when selecting biodiversity hotspots. Although this equation has been used in global biodiversity studies (Kier *et al.*, 2005; Pimm *et al.*, 2006; Wilson *et al.*, 2006), it has been argued that it should be used with caution, since it is dependent on the species richness sampling methodology (Dengler, 2009), habitat heterogeneity of the investigated area (Smith, 2010) and biogeographical regions (Guilhaumon *et al.*, 2008). For this reason, the z constant varies between taxonomic groups and habitat types (MacArthur & Wilson, 1967) with values between 0.1 and 0.5 (Lomolino, 2000).

3.1.3 Pteridophyte species richness and patterns

Pteridophytes, are a suitable group for biogeographical studies due to their number –they are the second largest group of vascular plants (Smith *et al.*, 2005) – and also due to their wide geographical distribution mainly explained by their ability to disperse over long distances (Nathan, 2006). Pteridophytes have approximately 13 000 species globally (Paton *et al.*, 2008) and according to Tryon (1986) and Tryon & Tryon (2012) there are more species in the Neotropics and Indomalaya than the Afrotropics. This spatial variation in species richness is explained by different determinants that vary across the regions (Kessler, 2010; Kreft *et al.*, 2010; Kessler *et al.*, 2011).

Species richness of pteridophytes is higher in the tropics than in temperate areas (Smith, 1972; Tryon, 1986; Kessler, 2010; Kreft *et al.*, 2010; Kessler *et al.*, 2011; Tryon & Tryon, 2012), a pattern known as the latitudinal diversity gradient, and which is similar for flowering plants and many other taxonomic groups (Willig & Lyons, 1998; Willig *et al.*, 2003; Kreft & Jetz, 2007; Buckley & Jetz, 2008). There are many hypotheses on the causes of this gradient with historical (historical perturbation hypothesis), ecological, evolutionary (evolutionary speed hypothesis), climatic (climatic stability hypothesis, climate harshness hypothesis, ambient energy hypothesis), geographical (geographic area hypothesis) and geometrical (mid-domain effect) explanations, as well as hypotheses based on combinations of these factors (Willig *et al.*, 2003). Among the tropical areas, the Neotropics and Indomalaya have the highest pteridophyte species richness, between 3000 and 4500 species each (Tryon, 1986). The Afrotropics are relatively poor in pteridophyte species (630 species in mainland Africa and 560 species in the islands (Tryon, 1986)) something which can be explained by their warmer and drier climate conditions compared to the other tropical realms, their smaller cover of tropical moist forests in the region (Moran *et al.*, 1995) and the great extinction of species that occurred during Pleistocene climatic oscillations (Kornas, 1993).

Many studies have found a strong correlation between gradients in plant species richness and climatic gradients either on local or global scales (Francis & Currie, 2003; Hawkins *et al.*, 2003; Field *et al.*, 2005; Barthlott *et al.*, 2007; Kreft & Jetz, 2007). Pteridophytes however, are more closely correlated with climatic conditions than other vascular plants since they are dependent on abiotic conditions for fertilization and not biotic pollinators (Barrington, 1993) and also due to the fact that are less adaptable to environmental conditions (Kessler *et al.*, 2011). Water-energy variables have been found to have a direct effect on pteridophyte species richness with temperature being the main determinant of pteridophyte species richness in high altitudes and water availability at low and mid-altitudes (Bhattarai *et al.*, 2004; Kluge *et al.*, 2006). Studies focusing on pteridophyte distributions have shown strong correlations between pteridophyte species richness and the availability of water (Page, 2002; Bickford & Laffan, 2006; Kreft *et al.*, 2010; Kessler *et al.*, 2011). This strong influence of water availability is explained by the dependence of the gametophyte phase of the pteridophyte life cycle, and specifically of the dispersal of the male gametes, on water availability on leaf surfaces (Page, 2002). This relationship is reflected in the global pteridophyte species richness patterns, since water availability is one of the main drivers of pteridophyte species richness which peaks in areas with high potential evapotranspiration and precipitation such as humid tropical forests (Kreft *et al*., 2010).

Pteridophyte species richness is also determined by topographic diversity (Moran *et al.* (1995); Kreft *et al.*, 2010), making montane tropical forests their ideal habitat. For example, the complex Andes mountain range contains five times more species than does the more uniform Amazon basin (Moran *et al.*, 1995; Tryon & Tryon, 2012). The species richness-altitude relationship of pteridophytes is described by a hump-shaped distribution with species richness peaking at mid-elevation, the range of which varies across regions (Kessler, 2000; Hemp, 2002; Bhattarai *et al.*,

2004; Kluge *et al.*, 2006; Watkins *et al.*, 2006; Kessler *et al.*, 2011). This species richness-altitude pattern has also been found in the majority of other taxonomic groups (Rahbek, 1995; Rahbek, 2005) although other patterns has also been described (e.g. monotonically decreasing species richness with altitude) (McCain, 2009). This mid-elevation peak in species richness in pteridophytes cannot be explained by species-area relationships alone (the larger the area the more able it is to support a larger number of species) (Rahbek, 1995; Rosenzweig & Ziv, 1999) since the amount of available area decreases with altitude. However, it has been suggested that plant species richness can be explained by the mid-domain effect (Bachman *et al.*, 2004; Kluge *et al.*, 2006) which is due to the overlapping of different sized species ranges at mid-altitudes (Colwell & Hurtt, 1994). Other studies have explained the mid-altitude species richness peak through drawing a strong association between pteridophytes and water availability. Kluge et al (2006) showed that high species richness reflects the high humidity and medium temperatures at mid-altitudes, while others have also found that it reflects high humidity (Hemp, 2002; Page, 2002; Kessler *et al.*, 2011) including fog (Rahbek, 1995; Hamilton *et al.*, 2012) at those altitudes.

3.1.4 Pteridophyte species endemism

A species is defined as endemic if its distribution is restricted to one geographic region (Primack, 2006). Range rarity is a form of endemism (Rabinowitz, 1981). A species however, could be endemic without necessarily be rare or even have a small range (Kruckeberg & Rabinowitz, 1985). For example species can be endemic to a continent but are not true rarities as their distribution covers a huge geographic region. The term narrow endemics refers to a species that occurs only in a small fraction of a regional floristic province and is therefore rare (Mason, 1946). Examples of narrow endemics are species in isolated oceanic islands and species in topographically complex areas. Narrow endemics differ from widespread endemics in terms of habitat, adaptation to new environments, dispersal ability and genetic variability (Rabinowitz, 1981; Kruckeberg & Rabinowitz, 1985). Rabinowitz (1981) described a rarity model which was built based on three characteristics: habitat specificity, local popularion density and species range. The focus of conservation efforts is often “restricted” endemics, which according to Rabinowitz (1981) are species with very narrow geographical distributions and narrow habitat specificity. These “classic rarities” are more prone to extinction (Kruckeberg & Rabinowitz, 1985; Pimm *et al.*, 1995; Kani, 2011).

Areas of high endemism are used to prioritise areas for conservation (Stattersfield *et al.*, 2005; Lamoreux *et al.*, 2006). While several studies have identified hotspots for endemism on a global scale for different taxonomic groups (Myers et al., 2000; Brummitt & Nic Lughadha, 2003; Kier et al., 2005; Stattersfield et al., 2005; Lamoreux et al., 2006; Kier et al., 2009), no similar study has been conducted just for pteridophytes. Pteridophytes, one of the oldest plant groups (Knoll, 1998), have lower endemism levels than other vascular plant groups due to their long-distance dispersal ability (Smith, 1972). However, field-based assessments and regional studies have shown that the level of endemism of pteridophyte species is higher in tropical islands and tropical montane areas (Tryon, 1970; Smith, 1972; Tryon, 1986; Kessler, 2000; Moran, 2004;

Kessler, 2010), as it also is for all vascular plants. This is explained by the isolation (geographical or due to past climatic events) (Hengeveld, 1990) and eco-climatic stability of these areas (Jetz *et al.*, 2004), which has resulted in speciation and survival of narrow ranged-species. When pteridophyte species endemism was evaluated along an altitudinal gradient, it was found to peak at higher altitudes compared with species richness, although the general pattern was similar. Endemism was found low in the lowlands but also at very high altitudes (Tryon, 1972; Kessler, 2000; Kluge *et al.*, 2006).

3.2 METHODS

The second objective of this project was to generate global species richness and endemism richness maps for SRLI forest pteridophyte species using the improved Extent of Suitable Habitat (ESH) method for calculating species ranges (see Chapter 2, section 2.2.2.2). This chapter had two aims: (1) to produce the first global maps of species richness and endemism for SRLI forest pteridophytes and (2) to determine whether the species' ESHs can be used in producing meaningful biodiversity maps. These maps were produced using the ESHs of the SRLI pteridophyte forest species calculated in Chapter 2. The species' ESHs were stacked to generate the first global map of species richness derived from ESH measures for SRLI forest pteridophytes and used to calculate the first global map of endemism richness for SRLI forest pteridophytes. In order to determine if the ESH-derived species richness map reflects the reality found on the ground, the map was validated using fieldwork data collected in Costa Rica (for this study) and additional fieldwork data from a previous study (Kessler *et al.*, 2011). Furthermore, the global patterns of the ESH-derived species richness and endemism were compared with those of existing well-known maps of species richness and endemism and analysed together with environmental variables in order to understand the determinants of those patterns.

3.2.1 Generating species richness and endemism richness maps using the species' ESHs

Species richness patterns have been mainly predicted using the direct macroecological modelling approach (calculated with surveyed data, environmental predictors and statistical models) (Jetz & Rahbek, 2002; Luoto *et al.*, 2004; Gotelli *et al.*, 2009). However, recent studies have predicted species richness patterns by summing geographical range maps of individual species (Cumming, 2000; Loiselle *et al.*, 2003; Rondinini *et al.*, 2005; Catullo *et al.*, 2008; Parviainen *et al.*, 2009; Buchanan *et al.*, 2011; Mateo *et al.*, 2012), mainly derived from Species Distribution Models (SDMs).

Here, a global species richness map was produced using habitat suitability models: the ESH of each SRLI forest pteridophyte species. This set of species was taken from the random sample

of species for the SRLI for Plants, which includes 1500 species from each of 4 major taxonomic groups (bryophytes, pteridophytes, monocots and legumes), plus all species of gymnosperms (approx. 1000 species), a total of c.7000 species. The forest pteridophyte sample contains 487 species (details in Chapter 2, section 2.2.1).

The ESH of each forest pteridophyte species was calculated based on information appropriate to the ecology for that species, as well as land cover and environmental information, within the convex hull defining the species' EOO (Chapter 2, section 2.2.2.2). The species richness map (1km resolution) was generated by stacking the species ESHs and thereby summing the presence of the species. As the species' ESHs were calculated using a global land cover map for 2005 (Globcover v.2.2) (Bicheron *et al.*, 2008), the ESH-derived species richness map reflects the patterns for this year (2005).

Information on endemic plant species (i.e. percentage of species confined to an area) can be found in Floras and taxonomic literature. Some studies such as Myers *et al.* (2000) and Mittermeier *et al.* (1998) have used that information in order to define areas with high levels of endemism (areas containing at least 1500 endemic plant species). Other studies (Barthlott *et al.*, 2001; Kier & Barthlott, 2001; Linder, 2001; Kier *et al.*, 2009) have used species geographical ranges to calculate range-size rarity, a continuous measure of endemism. Here, endemism is treated as a form of range rarity following Kier and Barthlott (2001). The range size-rarity of each SRLI forest pteridophyte species was calculated using the C-value. The C-value of a species is the inverse of the number of occupied grid cells, in this case from the species ESH (Equation 1.) (Usher, 1986).

$$\mathrm{Ci} = \frac{1}{\mathrm{Gi}} \qquad \textbf{(Equation 1)}$$

Where *Ci* is the species C-value and *Gi* is the species global range (total number of occupied grid cells globally).

The C-value of all species occurring in a cell were then summed (Equation 2), resulting in a combined C-value per grid cell for the global map of endemism richness as it is a function of both species richness and endemism.

$$\mathrm{C} = \sum_{\mathrm{i}=1}^{\mathrm{n}} \mathrm{Ci} \qquad \textbf{(Equation 2)}$$

Ranges that were narrow (width < 30 km) and long ranges (length > 1500 km) are likely to be biologically unrealistic and such ranges for 6 species were excluded from analysis. These species had only 3 occurrence points and thus the removal of the point that caused the unrealistic shape was not an option since the calculation of the species EOO requires at least 3 points.

A species richness map and an endemism richness map were also produced using the original EOOs of the SRLI forest pteridophyte species in order to be compared with the ESH-derived maps of species richness and endemism richness.

3.2.2 Validating the ESH-derived maps of species richness

Since the species richness map for SRLI forest pteridophytes was produced using the species' ESHs calculated from the species' occurrence points, the map was validated using new species occurrence points from additional localities. Specifically, the ESH-derived species richness map was validated using independent field data collected in Costa Rica for this study and from a previous study which was conducted on a global scale. Endemism data were not available for the validation of the ESH-derived endemism richness map.

3.2.2.1 Fieldwork data from the study by Kessler et al. (2011)

The ESH-derived species richness map was validated using fieldwork data from the study by Kessler *et al.* (2011). These data were collected from twenty elevational transects in natural forest habitats globally (Figure 46), in which multiple 20 x 20 m² pteridophyte species richness plots were sampled. The transects covered areas from 0m elevation to the nearest highest point inside a 50 km radius. Details on the 20 study sites can be found in the Appendix (A9). The species richness of those plots was compared with the ESH-derived species richness value of the equivalent 1km resolution pixel. The comparison was done globally and by biogeographical realm by plotting the pteridophyte species diversity against altitude.

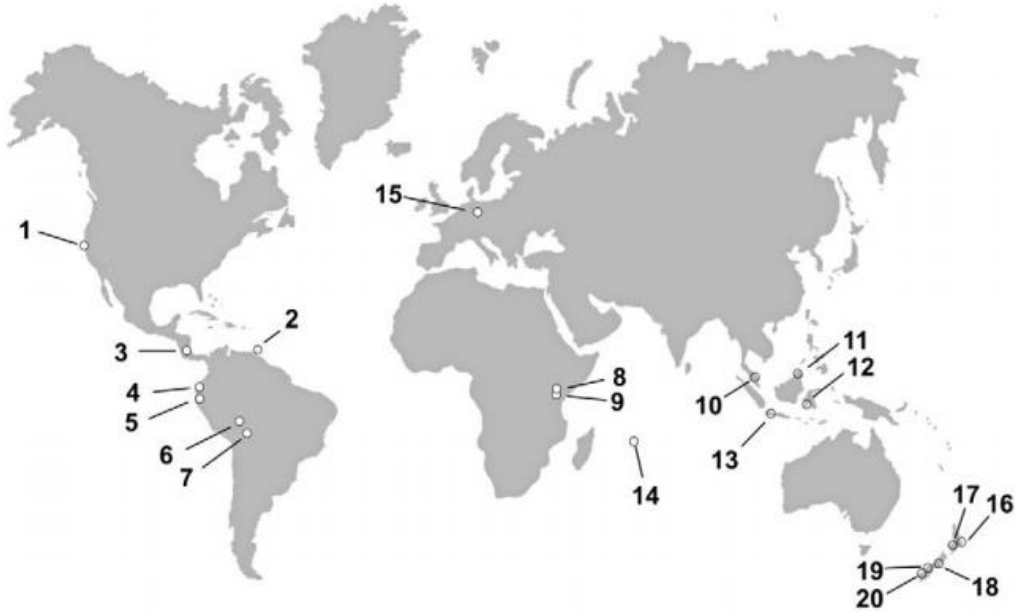

Figure 46. Location of the 20 study transects of Kessler *et al.* (2011) study (Kessler *et al*., 2011, p.871).

3.2.2.2 Fieldwork in Costa Rica: Case study area

3.2.2.2.1 Selection of a case study region

Costa Rica, a recognised biodiversity hotspot, has been chosen as the case study area for elements of this project. It contains 4.75% of the world's known biodiversity despite the fact that it represents just 0.03% of the world's surface (Obando-Acuña, 2007). According to Groombridge and Jenkins (1994), Costa Rica is one of the 20 countries with the highest species diversity worldwide, as shown by the fact that there are more than 95 000 identified species from the country. It is also a relatively well-sampled and protected country by tropical standards with 169 well-protected areas covering 26% of the country (SINAC, 2009). Costa Rica has an estimated total of 11 451 plant species with 234.8 plant species per 1000 km (Obando-Acuña, 2007). Moreover, 10% of the total number of plant species are endemic, occurring mainly in the Talamanca region, the Isla de Coco, the Osa peninsula and the Central Cordillera Volcanica Region (Obando-Acuña, 2002). The wide range of altitude and the different environmental conditions between the Antlantic and the Pacific sides of the country (either side of the continental divide) are mainly responsible for Costa Rica's high biodiversity (Sánchez-Azofeifa *et al.*, 2001).

Costa Rica was also chosen for its good representation of extensive tropical montane cloud forests, forests with frequent exposure to fog (Mulligan, 2010), which is an ideal habitat for high fern species diversity (Figure 47). According to UNEP-WCMC (1997) Costa Rica contains 14 sites of cloud forest out of the 120 sites in Central America. There are 38 SRLI pteridophyte species that occur in Costa Rica above 500 m altitude, with a total of 700 recorded specimens (points).

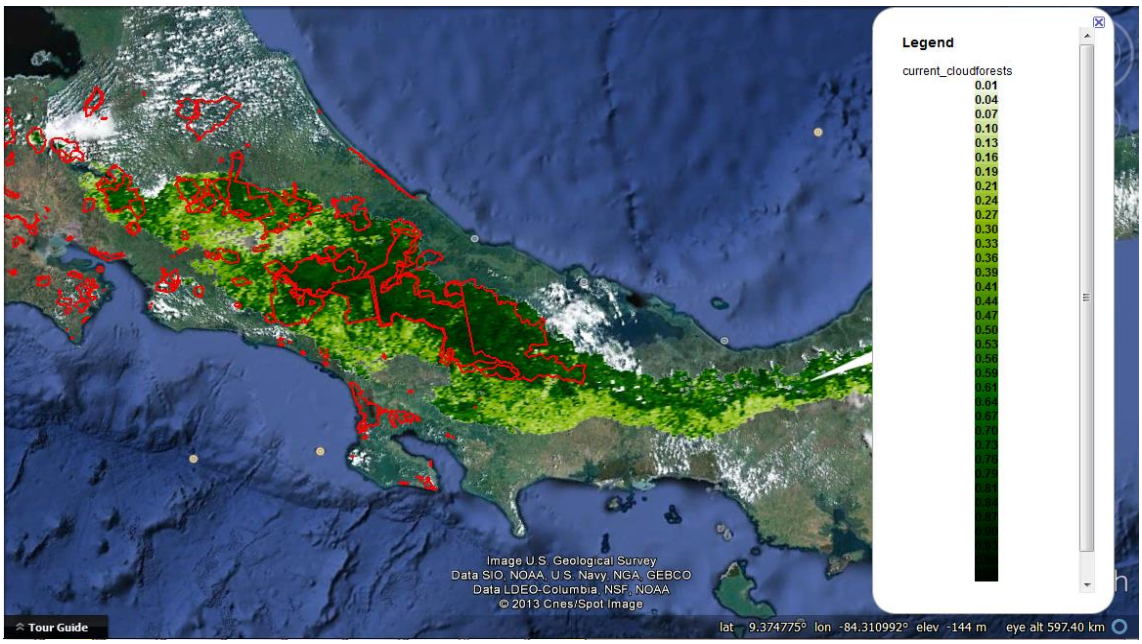

Figure 47. Current Tropical Montane Cloud Forest fraction cover (%) in Costa Rica (data source: Mulligan & Burke, 2005) and the country's protected areas (red line) (data source: IUCN & UNEP. 2010). Background map data: Google.

Lastly, Costa Rica was also selected due to the fact that its landscape is a mosaic of pristine forests, secondary forests and areas that were deforested and transformed into pastures and farmland between the 1940s and the 1980s (FAO, 1993). Between 1940 and 1984, Costa Rica's primary forest cover was reduced by 50% (Sader & Joyce, 1988) with a deforestation rate of 3.2 % per year between 1973 and 1980 (FAO, 1990). Forests were mainly converted into pasture for cattle production. Since the 1980s, however, the government has made big efforts to reforest deforested areas and preserve existing forest areas (Sánchez-Azofeifa, 2001), resulting in 26% of the total land area being designated as protected. Despite these successful efforts, deforestation continues to occur in unprotected areas and, according to Sánchez-Azofeifa et al. (1999), the deforestation rate outside the protected areas was 2.8% between 1986 and 1991 and 3.2% between 1991 and 1996. The country's mosaic landscape is ideal for sampling along a human impact gradient and understanding what the impacts of anthropogenic land use change on species ranges are.

3.2.2.2.2 Fieldwork details

Fieldwork was conducted between 19th February 2013 and 13th March 2013 and it was a joint expedition between the Natural History Museum London, led by NHM co-supervisor Dr. Neil Brummitt, and the Instituto Nacional de Biodiversidad (INBio) a non-governmental organisation in Costa Rica.

The aims of the fieldwork were:

1. to investigate how effective herbarium-based conservation assessments are at reflecting the reality of both ranges of and threats to pteridophyte plant species in the field

2. to validate on the ground the species richness map that was generated for SRLI pteridophytes species.

3. to improve the SRLI pteridophytes species database by collecting specimen vouchers in various areas of Costa Rica

In each site, voucher specimens for pteridophyte species were collected, pressed and preserved in ethanol while in the field. Between each trip, the specimens were dried in the INBio facilities and identified to genus and, where possible, species level. Where enough material was available, each specimen had at least one duplicate in order for the first set of vouchers to be left in the INBio herbarium and the remaining to be sent to the Natural History Museum in London. When the vouchers arrived in London, they were frozen (quarantined), identified to species level, mounted and deposited in the Cryptogamic herbarium.

3.2.2.2.3 Fieldwork data

Data collected during fieldwork in Costa Rica were used for validation of the species distribution predictions in Costa Rica. Pteridophyte species were collected in a total of fourteen species richness plots along the country covering a large altitudinal range (647 m to 3368 m) (Figure 48). The size of each plot was 5 x 5 m², in agreement with the minimum quadrat size for herbs and small bushes (4m x 4m) suggested by (Cain & Castro, 1960). Species richness was compared with predicted species richness of the ESH map in the same way as with the data of Kessler *et al*. 2011.

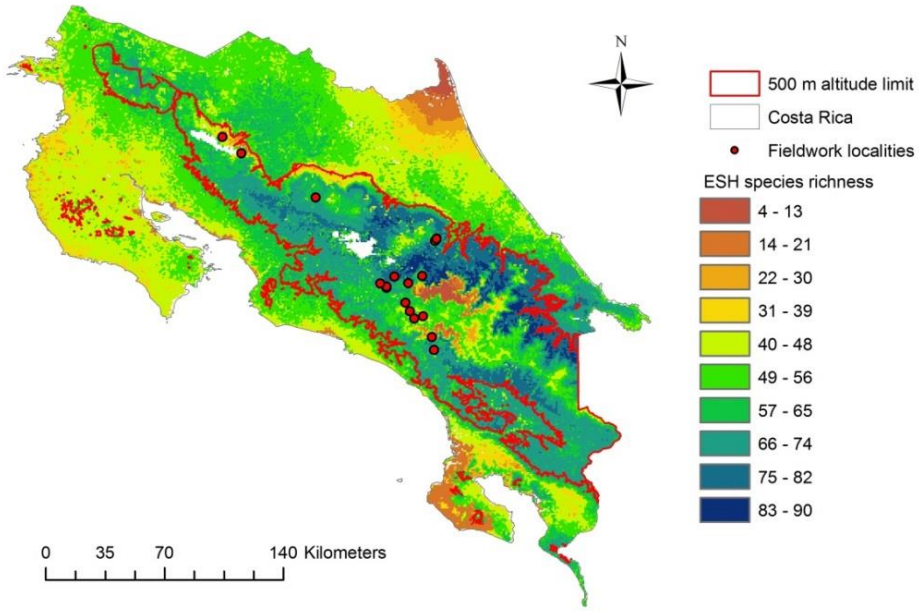

Figure 48. Locations of species richness plots sampled during fieldwork conducted as part of this study.

The areas where sampling was undertaken were located using the occurrence point data for SRLI forest pteridophytes together with environmental variables, human pressure and road accessibility. The aim was to choose sites across the country with different environmental conditions and different levels of human impact. The environmental variables used to select the sampling sites were minimum temperature and annual precipitation, which were obtained from the WorldClim database (Hijmans *et al.*, 2005), and mean topographic exposure, based on topographic exposure (topex) analysis of 90m Shuttle Radar Topography Mission (SRTM) data, which was obtained from the Water World policy support system (www.policysupport.org/waterworld) (Mulligan & Burke, 2005). All three variables had a 1km spatial resolution. Since the fieldwork expedition was focused on cloud forest areas of Costa Rica, data that occurred in areas with altitudes below 500 m were masked out using the SRTM elevation data (version 4) (Jarvis *et al.*, 2008). The raster maps of these environmental variables were classified into 3 classes (high, medium, low) and combined, resulting in 27 classes, each one with a different combination of environmental variables. Additionally, human pressure data (combination of relative population density, relative fire frequency, relative grazing intensity, relative agricultural intensity, relative dam density and relative infrastructural density) obtained from the Co$ting Nature tool (version 2) (Mulligan, 2015b), a web-based policy support system for mapping conservation priority, were also classified into 3 classes, adding 3 classes to each combination of environmental variables and generating a total of 79 classes. In order to ensure accessibility of the selected sampling sites, a road layer (Defense Mapping Agency, 1992) was used to select all classes (62) that are located between 200 m and 1000 m away from the road.

Sampling areas were prioritised using the SRLI pteridophyte occurrence points. Occurrence points for SRLI forest pteridophyte species that fall inside the pixels for each of these separate classes (125 occurrence points) were used to produce a frequency distribution chart in order to identify the classes where SRLI pteridophyte species occur more frequently. The occurrence points covered only 21 classes. As illustrated in Figure 49, SRLI points occur more frequently in classes 1112, 1233, 2222 and 3333, which correspond to the following 4 combinations of environmental variables: high environmental conditions (3333: high minimum temperature, high annual precipitation, high topographic exposure and high human pressure); medium environmental conditions (2222: medium minimum temperature, medium annual precipitation, medium topographic exposure and medium human pressure); low environmental conditions (1112: low minimum temperature, low annual precipitation, low topographic exposure and medium human pressure); and mixed environmental conditions (1233:low minimum temperature, medium annual precipitation, high topographic exposure and high human pressure) (Figure 50). The pixels of these classes were then imported into Google Earth in order to study the specific areas using available high resolution satellite images before going to the field.

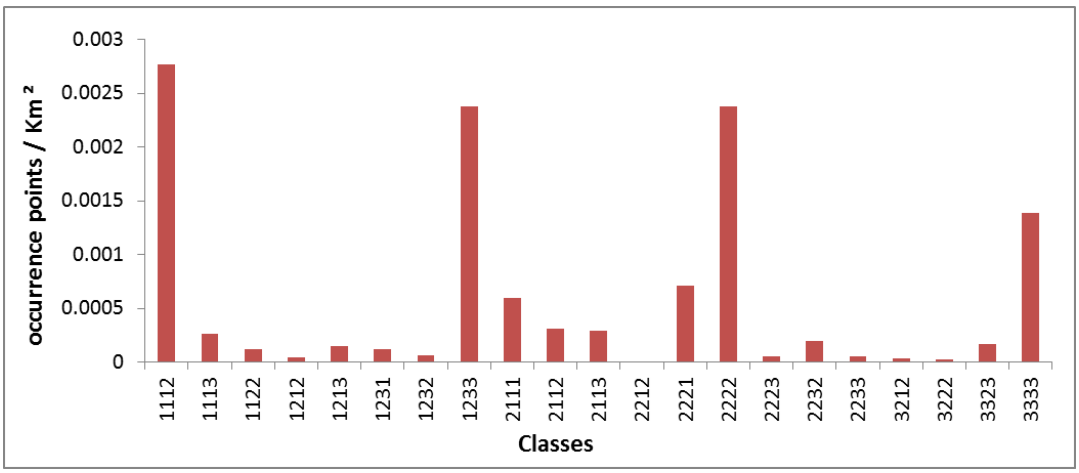

Figure 49. Frequency distribution chart of number of specimens per Km² in each class. Class number: first digit represents temperature, second digit represents precipitation, third digit represents topographic exposure and the fourth digit represents human pressure with 1=low, 2=medium, 3=high.

While sampling along all environmental classes would have been ideal, it was recognised from early stages that this was not feasible. By using the SRLI points, the species preference was examined and areas with suitable environmental conditions were prioritised. This way the probability of finding these species in the field was increased. This approach was selected to maximise the amount of data collected since fieldwork time was limited. However while this approach ensures high degree of representativeness, it suffers from bias as the sample was not random and may not truly represent the area's species richness patterns.

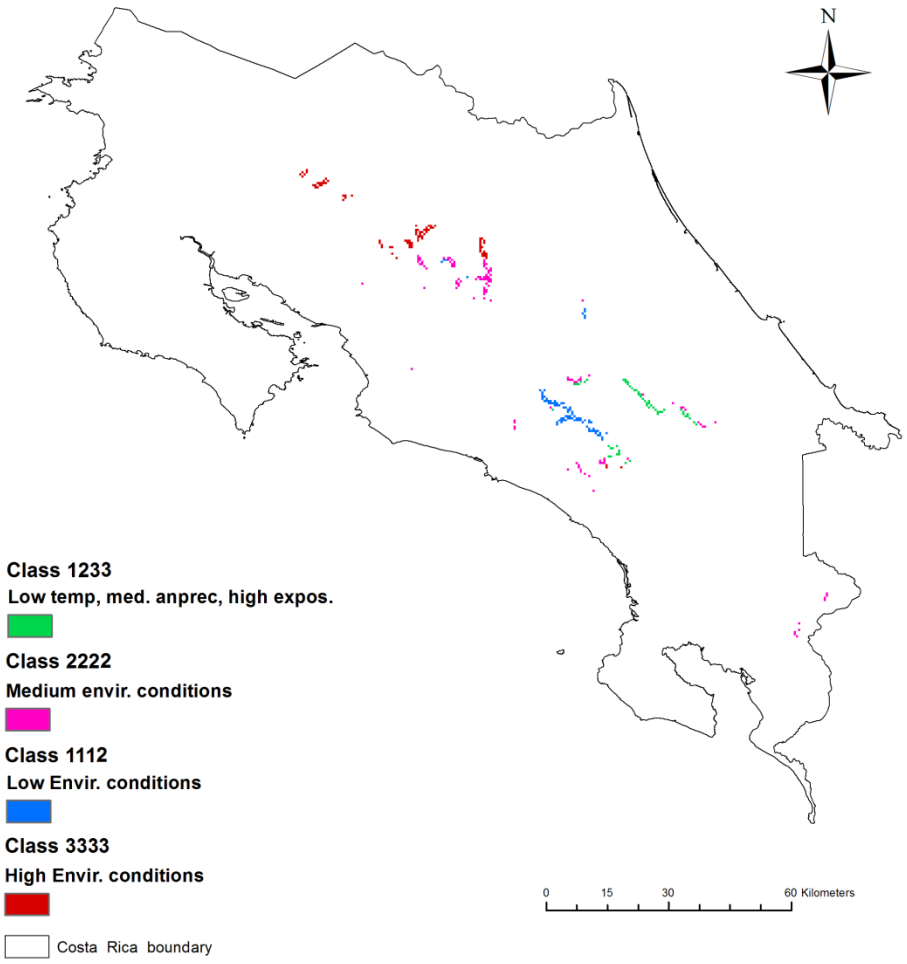

Figure 50. Final sampling areas for fieldwork in Costa Rica: four combinations of environmental conditions including 3 levels of human pressure (low, medium, high).

3.2.3 Improving the species richness map

The validation (section 3.2.2) of the ESH-derived species richness map using independent field data from Kessler *et al*. (2011), showed an overestimation of the ESH-derived species richness in the lowlands. Therefore, an attempt was made to improve this problem in order to better reflect the reality found on the ground. To deal with the overestimate of the ESH-derived species richness observed in the lowlands, the species' ESHs were recalculated, according to the method described in Chapter 2 (section 2.2.2.2), using the 5 – 95 percentiles of the altitudinal range for each species (instead of the whole range), taking into account the frequency distribution within the species' altitudinal range and excluding the extreme (outlying) altitude values. This was based on the assumption that there were outlying altitude values in the species' altitudinal ranges (used during the calculation of the species' ESHs) leading to a larger than in reality extent of many species' ESHs in the lowlands. The new ESHs were used to produce a new species richness map which was tested using the fieldwork data from the Kessler *et al.* (2011) study and the fieldwork data from Costa Rica and compared with the original ESH-derived species richness map.

3.2.4 Interpreting the species richness and endemism patterns

In order to compare different areas in the ESH-derived maps of species richness and endemism, a classification of global biogeographical realms was used: Neotropical, Afrotropical, Indomalaya, Nearctic, Palaearctic, Austalasia, Oceania and Antarctic (Olson *et al*. 2001) (Figure 51).

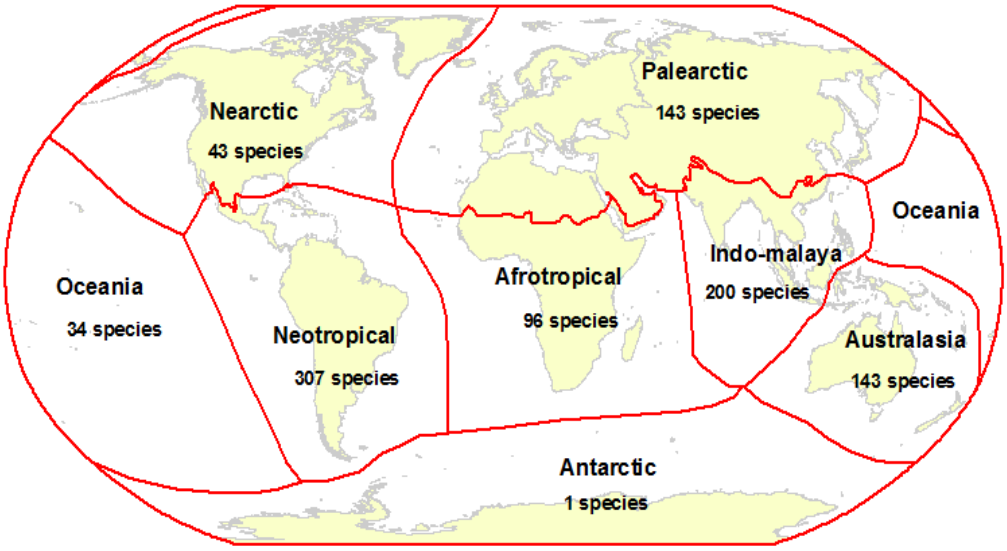

Figure 51 The number of SRLI pteridophyte forest species in each biogeographical realms of the world (following Olson *et al.* (2001)).

The ESH-derived maps of species richness and endemism were then compared with previous studies of global patterns of species richness and endemism (Mittermeier *et al.*, 1998; Myers *et al.*, 2000; Brummitt & Nic Lughadha, 2003; Kier *et al.*, 2005; Barthlott *et al.*, 2007; Kreft & Jetz, 2007; Kier *et al.*, 2009; Kreft *et al.*, 2010; Kessler *et al.*, 2011). The ESH-derived species richness map was compared with the results of Kreft *et al.* (2010) specifically, a study that estimated the global species richness of pteridophytes using a spatial prediction model based on environmental variables (Figure 52). Estimated species numbers were predicted mainly from information derived from checklists and Floras and used together with abiotic predictor variables (land cover classes, altitudinal range, water availability, mean annual temperature and potential evapotranspiration) in a multivariate Generalised Linear Model to produce a global pteridophyte species richness map (Kreft *et al*. 2010). The ESH patterns of species richness and endemism were also compared with pteridophyte species richness and endemism levels reported in field-based assessments in different parts of the world (e.g. Tyron, 1986).

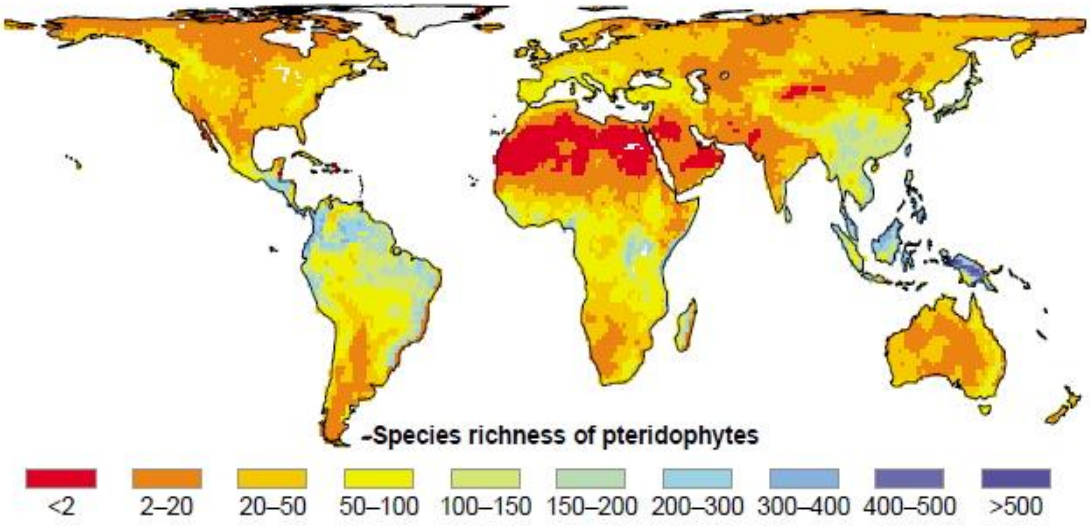

Figure 52. Global pteridophyte species richness map of *Kreft et al*. (2010) study (Kreft *et al*., 2010, p. 416).

The maximum value of species richness in each biogeographical realm was calculated by clipping the ESH-derived species richness map to each biogeographical realm. However, comparing maximum species richness between biogeographical realms without taking account of the effects of area would not be realistic as shown in Brummitt & Nic Lughadha (2003). As mentioned in the Introduction (section 3.1), it is widely accepted that the species-area relationship is described by a power function (Equation 3).

$$S = cA^z \qquad \textbf{(Equation 3)}$$

Where S is species richness, A is area and c and z are constants (Rosenzweig, 1995).

Hence, it was important to rescale the ESH-derived species richness by A^z for each realm. Due to the fact that Kier *et al.* (2005), calculated the z values for vascular plants within each major biome of the world, the ESH-derived species richness was rescaled for each biome instead in order to use these z-values. The WWF biome map (WWF, 2015), which is based on the maps of Olson *et al.* (2001), was used to extract the maximum ESH-derived species richness of each biome. The WWF data identifies 16 major biomes, global scale biogeographical regions shaped by climate and distinguished from one another by a unique collection of ecosystems and species assemblages that have evolved there (Hoekstra *et al.*, 2005)

Instead of simply calculating the area of each biome, the total area of suitable habitat for forest pteridophytes in each biome was used. This was calculated by selecting all GlobCover classes (Bicheron *et al.*, 2008) in which each of the SRLI forest pteridophyte species occurs, based on the species occurrence data. Following Brummitt and Nic Lughadha (2003), the constant c was calculated for each biome according to the equation $c=S/A^z$ and using the maximum ESH-derived species richness of each biome, area of suitable habitat of each biome and the appropriate z value from Kier *et al*. (2005). The maximum ESH-derived species richness for

each biome was used in the equation, treating it as the species richness of a point within the biome; the same way as using the maximum species richness of an area which was estimated based on fieldwork. This maximum ESH-derived species richness was rescaled using a standardised unit of area (100 km²) for each biome. The biogeographical realms were then compared using the rescaled ESH-derived species richness for the forest biomes.

An alternative way to compare the species richness of the biogeographical realms is to use the average species richness value per suitable area of each biogeographical realm. In contrast to the previous approach (S-A relationship) which treated the maximum species richness of an area as a point, this approach assumes that species exist throughout their ESHs and therefore a species richness value represents an area and not a point. The average species richness value per suitable area of each biogeographical realm was calculated, following Mulligan (2015a), by summing the species richness values of all pixels (excluding 0 values) covering the realm and dividing the sum by the number of pixels. As the pixel size of the ESH-derived map was 1km², the calculated number represented species richness per 1km².

A direct comparison of the species richness in tropical biogeographical realms and of the sampling effort was also conducted. This was done by plotting the number of occurrence points per area of suitable habitat against the maximum species richness in each tropical biogeographical realm.

3.2.4.1 Understanding the drivers of the species richness and endemism patterns

The drivers of patterns of ESH-derived species richness along latitudinal, longitudinal and altitudinal gradients were investigated by randomly selecting specimen occurrence points for SRLI forest pteridophyte species and plotting the equivalent species richness values together with each variable. A mosaic altitude dataset, a combination of Shuttle Radar Topography Mission (SRTM) data (version 4, 1km resolution) (Jarvis *et al.*, 2008) and GTOPO30 data (1km resolution) (USGS-EROS, 1996) was used in the analysis. The data were reclassified into 500m bands and species richness was sampled within those bands. In addition, species richness patterns were evaluated along a moisture gradient. This analysis was conducted within latitudinal (tropical and temperate regions) and altitudinal (500m) bands in order to distinguish the effects of latitude and altitude, respectively, from those of water balance. Water balance data (Mulligan, 2011), calculated with the FIESTA fog delivery model (Mulligan & Burke, 2005), were used in this analysis. Instead of using the annual water balance data (annual minimum or annual average), the minimum monthly water balance data (minimum value of each pixel for all 12 months) was used. Similar analyses were performed to evaluate the ESH-derived endemism - altitude and ESH-derived endemism - water balance relationships by geographical realm. Spearman's rank non-parametric correlation analysis was used to measure the strength of the association between the variables and species richness/endemism.

3.3 RESULTS

3.3.1 ESH-derived pteridophyte species richness and endemism richness maps

The species richness map, derived from stacking the ESHs of the SRLI forest pteridophyte species, is presented in Figure 53.

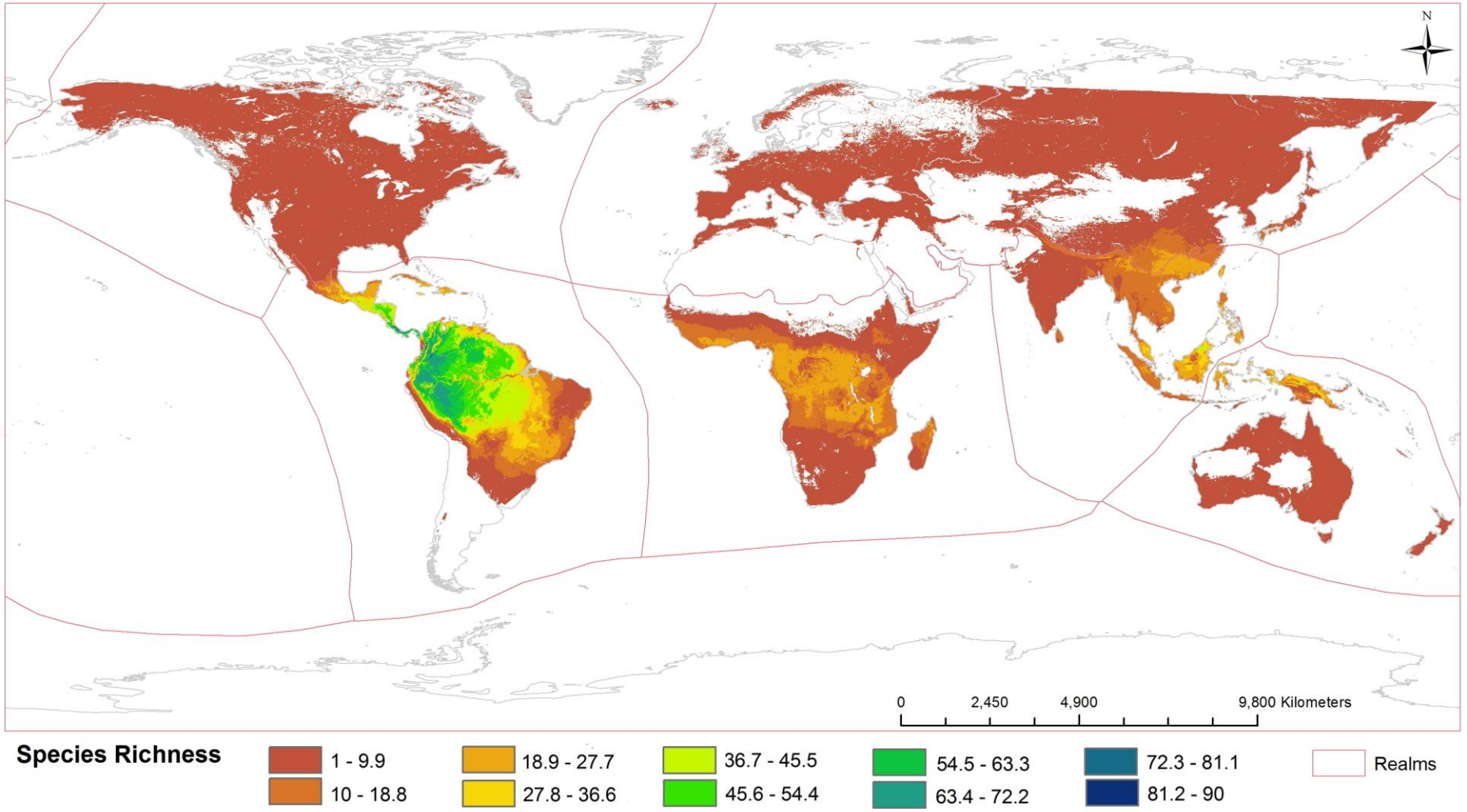

Figure 53. The species richness map for SRLI forest pteridophytes produced from stacked species ESHs (calculated using SRLI specimen data, species' altitudinal ranges, species' habitat preference and species' water balance values). Data are classified in ten equal intervals. White colour represents 0 value of species richness.

The species richness map generated by stacking the original species' EOOs (Figure 54a), appears more continuous than the ESH-derived species richness map (Figure 53). Both ESH-derived (Figure 53) and the EOO-derived (Figure 54a) species richness maps predict higher species richness in the tropics than the rest of the world, with the highest values in the Neotropics. However, the ESH-derived species richness map (Figure 53) predicts lower maximum species richness compared with the predictions of the EOO-derived species richness map (Figure 54a). While the ESH-derived map predicted a value of 90 (species) as the maximum number of species globally (mean value per Km²: 9.1±13.2 species), the EOO-derived map predicted a maximum global value of 92 species (mean value per Km²: 10.7±13.3 species). The mean absolute difference per pixel between the two maps was 3.7±5.7 species (Figure 54b). Areas of the Neotropics with greater differences between the two maps were Mesoamerica, part of the Andes, the Cerrado and Caatinga areas of Brazil and the Amazon basin. In the Afrotropics the greatest differences were identified in the East African Plateau and Anaggar, Muchinga and Mitumba Mountains. Other areas with large differences included South-west China, the island of Borneo and New Guinea.

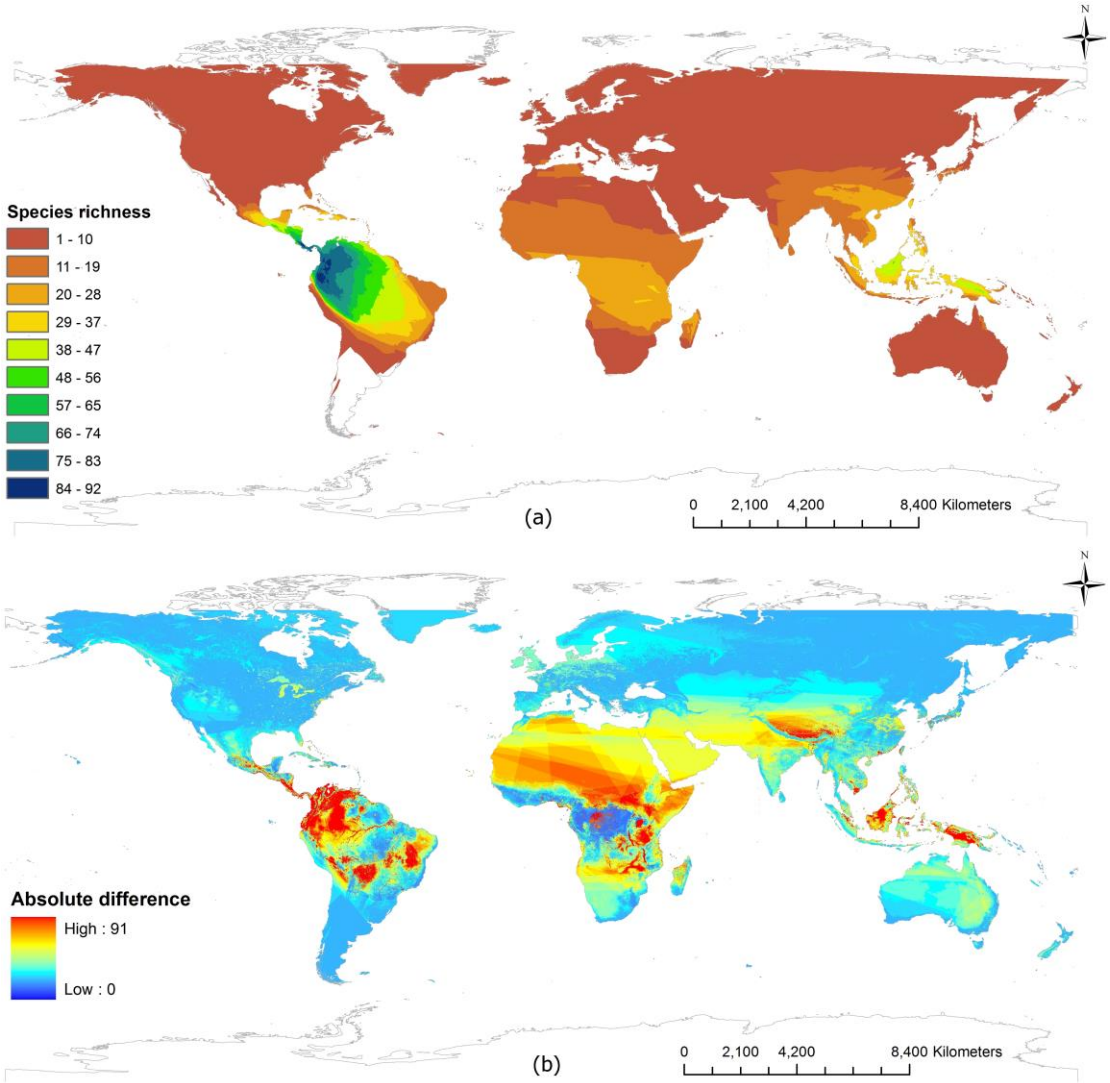

Figure 54. (a) Pteridophyte species richness map produced by stacking the species' original EOOs (Data classified in ten equal intervals) and (b) absolute difference map between the EOO- and the ESH-derived species richness maps. Positive values mean ESH is lower than EOO. The ESH-derived species richness map is shown in Figure 53.

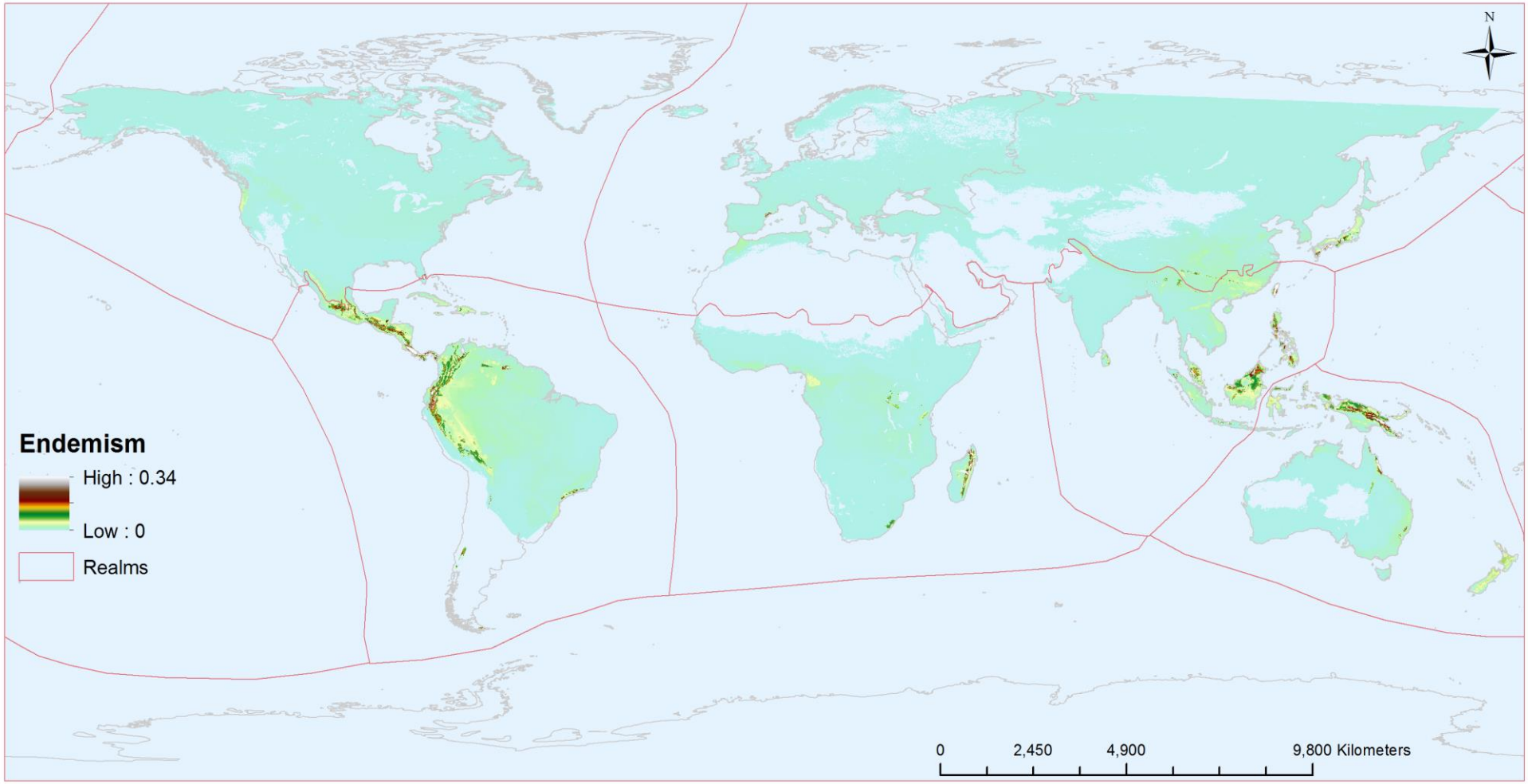

Figure 55. The global map of SRLI forest pteridophyte species endemism calculated by using the species ESHs that were produced using SRLI data, species altitude ranges, species habitat preference and species water balance preference.

The two maps of endemism, calculated using the original species' EOOs (Figure 56) and the species' ESHs (Figure 55), respectively, highlighted the same areas as hotspots of endemism and predicted the highest values mainly in areas of the tropical region. Therefore, a difference map is not presented here since the differences were small. However, the ESH-derived endemism richness map predicted a higher global maximum value of endemism (0.34) compared to the predictions of the EOO derived endemism richness map (0.05). The area with the highest value of endemism in both maps and the greatest absolute difference between the maps was in the montane region of Costa Rica and Panama (Talamanca mountain range). As with the two species richness maps, the endemic areas in the EOO-derived endemism richness map appear more continuous than the ESH-derived species richness map.

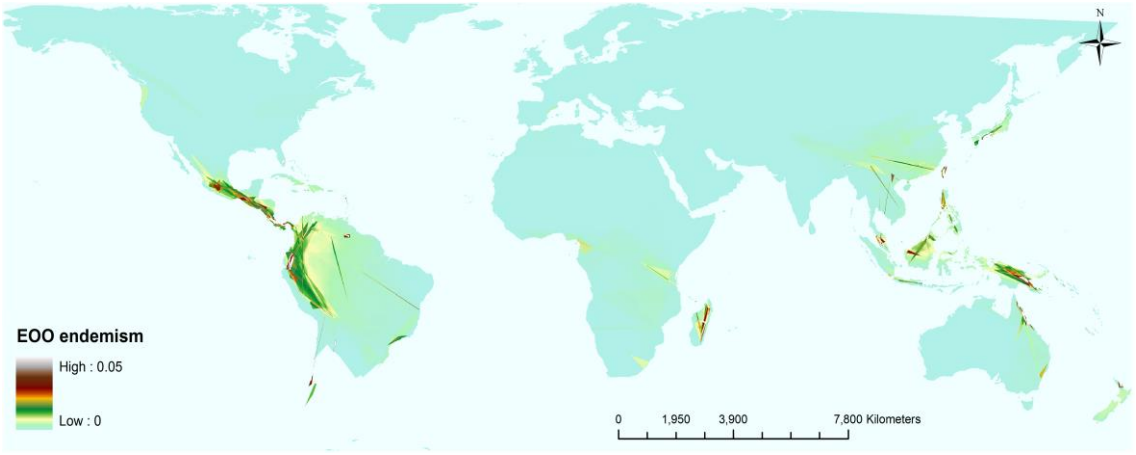

Figure 56. Pteridophyte endemism richness map produced using the species' original EOOs.

3.3.2 Validation of the pteridophyte species richness map

The ESH-derived species richness map was firstly validated using fieldwork data from the study of Kessler *et al.* (2011) (Figure 57). The data from 20 study sites from across the globe revealed a mid-altitude (1500 – 2500m) peak of species richness and a hump-shaped relationship between species richness and altitude. This pattern did not agree with the one from the ESH-derived map in which species richness, of the same pixels as the field data, peaks at lower altitudes (0 – 500m). Based on this finding, the ESH-derived species richness map appears to be overestimating species richness in the lowlands. This overestimation of ESH-derived species richness in the lowlands was also found when comparing the two datasets by biogeographical realm (Figure 58). In all realms, the ESH-derived map predicted much higher species richness in the lowlands compared with the Kessler *et al*. (2011) field data, although in the Afrotropics the difference was smaller. While the Kessler *et al.* (2011) field data showed a mid-altitude peak in the Neotropics and the Afrotropics, there was a positive relationship between species richness and altitude in Indomalaya and tropical Australasia. The ESH-derived species richness map predicted a negative relationship with higher values in lower altitudes. No specific pattern was found between altitude and the EOO-derived species richness since the EOO-derived map predicted high and low species richness at all altitudes.

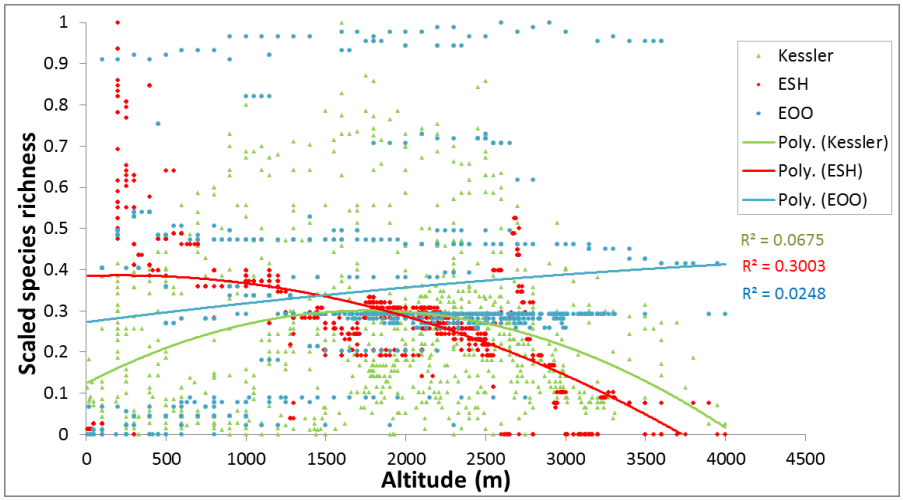

Figure 57. Scaled global species richness (0 – 1) along an elevation gradient using field data from Kessler *et al*. (2011), from the EOO-derived species richness map and from the ESH-derived species richness map. Goodness of fit of polynomial regression (R^2) is reported.

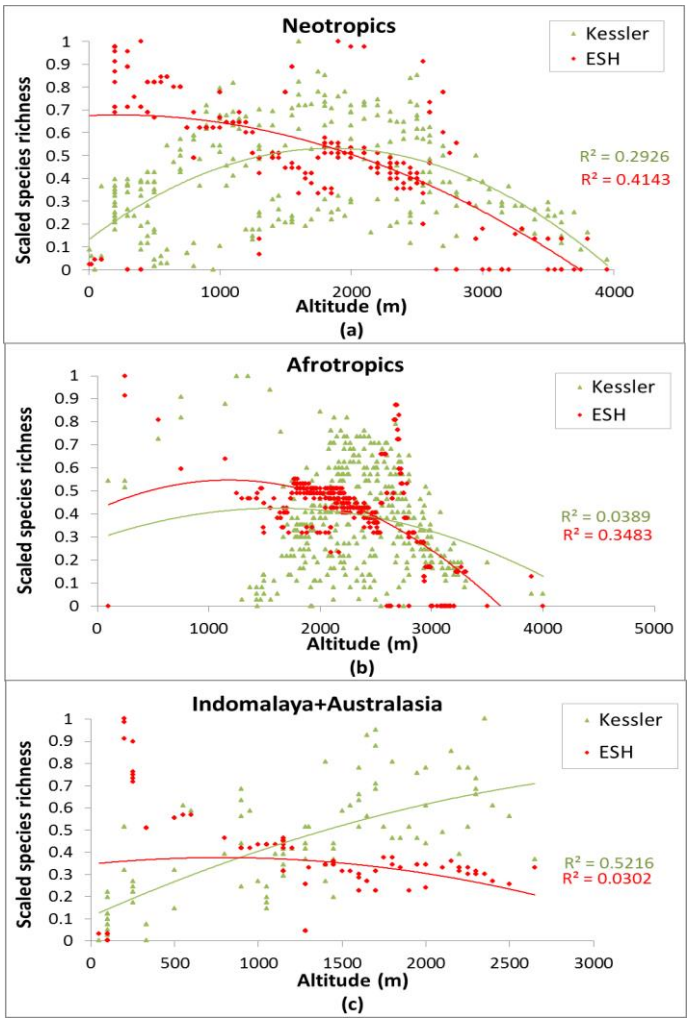

Figure 58. Scaled species richness (0 – 1) along an elevation gradient using field data from Kessler et al. (2011) and from the ESH-derived species richness map. Results are presented by tropical biogeographical realm (a) Neotropics, (b) Afrotropics and (c) Indomalya and tropical Australasia (points occurring in temperate Australia were excluded from the analysis). Goodness of fit of polynomial regression (R^2) is reported.

As shown in Figure 59, the EOO-derived species richness map predicted high species values at all altitudes in study areas in Costa Rica. Furthermore, the mid-altitude peak in species richness from the ESH-derived map agrees with the mid-altitude peak in pteridophyte species found from fieldwork data, although the decline in richness in lower (below 1000m) and higher (above 3000m) altitudes is less pronounced. The overestimation of ESH-derived species richness at lower altitudes, found in comparison with the fieldwork data of Kessler *et al.* (2011), was not seen here.

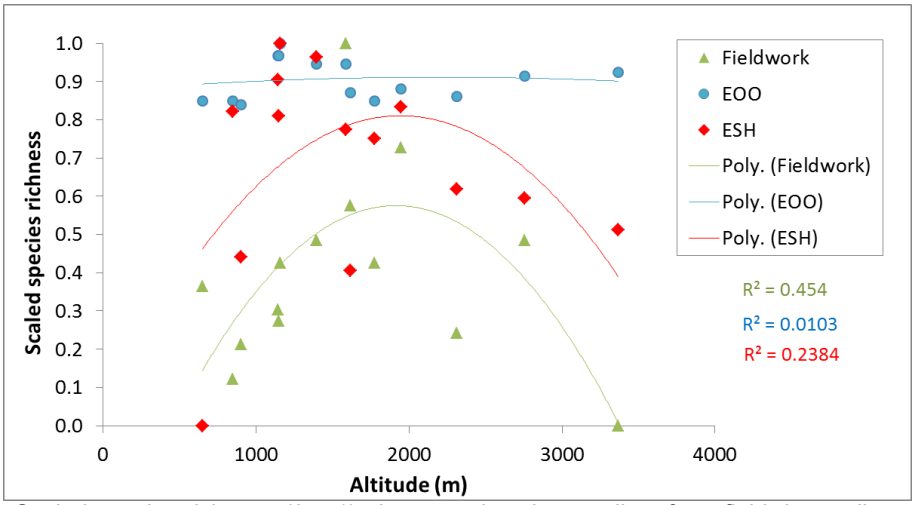

Figure 59. Scaled species richness (0 – 1) along an elevation gradient from field data collected in Costa Rica, from EOO-derived species richness map and from ESH-derived species richness map. Goodness of fit of polynomial regression (R^2) is reported.

Improving the species richness map by using restricted altitudinal ranges

The species richness map produced with the species ESHs calculated using the 5 – 95 percentiles of the altitudinal range instead of the whole range is presented in Figure 60a. The predicted maximum species richness value of the map produced using 5 – 95 percentiles of the species altitudinal range was 83 species, 7 species fewer than the value predicted by the ESH map using full altitudinal ranges for species. The mean value per Km^2 was 8.3±12.6 species for the new ESH map (5 – 95 percentiles of altitudinal range) which is lower than the equivalent value of the original ESH map (mean value per Km^2: 9.1±13.2 species). By excluding the extreme outlying altitude values in each species range calculation, species richness was reduced mainly in the montane areas, with the biggest differences seen in tropical Andes, Mount Kilimanjaro, the Mitumba mountains, the Talamanca mountain range and the Guiana highlands. It appears that this approach did not improve the overestimation problem since the only lowland areas with big differences between the two maps were the areas along the Amazon river and the Atlantic coast of Venezuela, Guyana and Suriname (0 – 50m altitude) (Figure 60b).

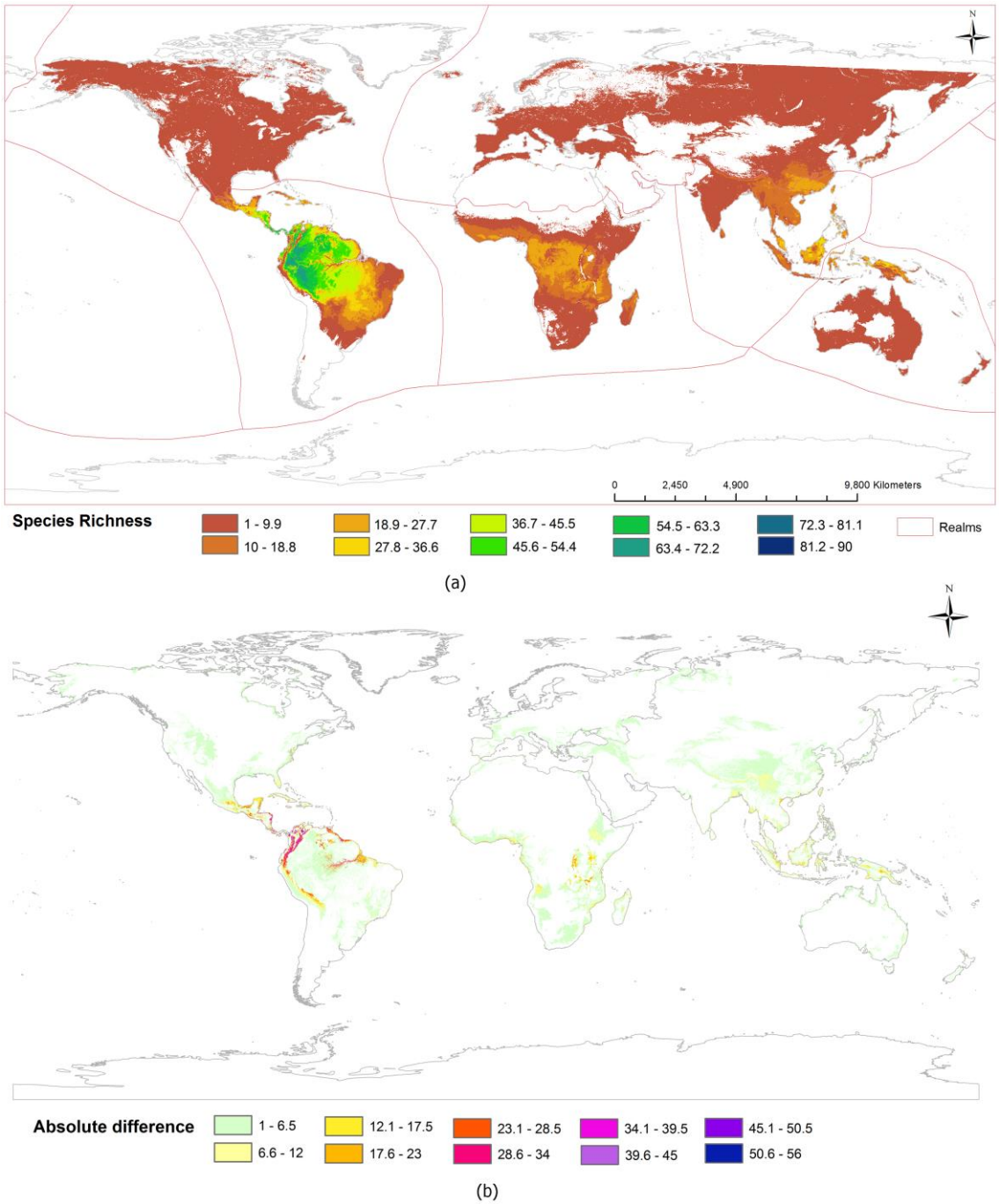

Figure 60. (a) Pteridophyte species richness map produced by stacking the species' ESHs which were calculated using the 5 – 95 percentiles of the species' altitudinal range. Data classified in ten equal classes based on original ESH map (Figure 53) and (b) absolute difference between the original ESH map (Figure 53) and the new ESH map (Figure 60a). Positive values represent a reduction in species. Data classified in ten equal intervals.

Figure 61 shows that the species richness pattern of the map derived from ESHs with species distributions restricted to between 5 and 95 percentiles of their altitudinal ranges does not match the mid-altitude peak seen in the Kessler *et al.* (2011) fieldwork data. Instead, species richness peaks in the lowlands (0 – 500m), in a similar way to the original ESH-derived map. Interestingly, a decrease in species richness was found at mid-altitude (1500 – 2500m), driven principally by the South Kilimanjaro Mountain study area of Kessler et al. (2011). Species richness at the study area of North Kilimanjaro Mountain (the second species richness peak at

2700 – 3000m altitudes) had the same pattern as for the original ESH-derived species richness map.

While a hump-shaped relationship between species richness and altitude was found between the original ESH-derived species richness map and the data collected for this study during fieldwork in Costa Rica, this was no longer the case with the new ESH-derived species richness map using 5 and 95 percentiles of the species' altitudinal range (Figure 62). The new ESH-derived species richness map predicted lower species richness at high and mid altitudes (1200 – 3500m) than did the ESH-derived map based on full altitudinal range for species, but similar species richness in the lower altitudes (600 – 1200m). In both cases, the original ESH-derived map reflected better the reality of species richness on the ground than the new ESH-derived map with restricted altitudinal species ranges.

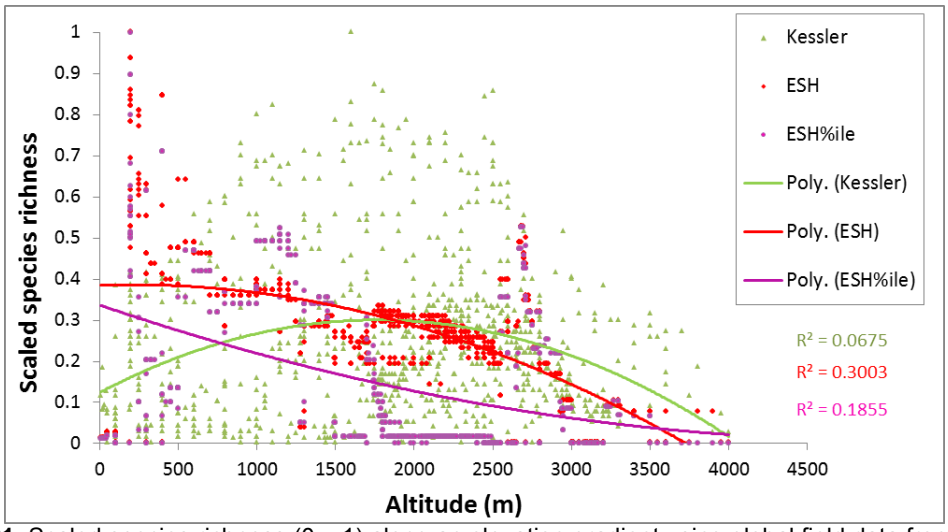

Figure 61. Scaled species richness (0 – 1) along an elevation gradient using global field data from Kessler *et al.* (2011) compared with the original ESH-derived species richness map (ESH) and the ESH-derived map calculated using the 5 **–** 95 percentiles of the species' altitudinal range (ESH%ile). Goodness of fit of polynomial regression (R^2) is reported.

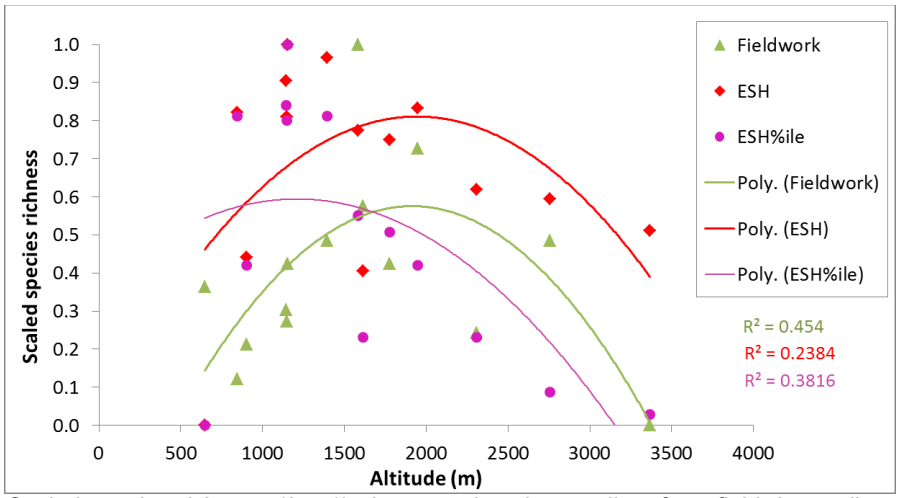

Figure 62. Scaled species richness (0 – 1) along an elevation gradient from field data collected in Costa Rica, from the original ESH-derived species richness map (ESH) and from the ESH-derived map calculated using the 5 **–** 95 percentiles of the species' altitudinal range (ESH%ile). Goodness of fit of polynomial regression (R^2) is reported.

3.3.3 Interpretation of the pteridophyte species richness and endemism patterns

3.3.3.1 Pteridophyte species richness map

The map of pteridophyte species richness, calculated by stacking the ESHs of the SRLI forest pteridophyte species, is presented in Figure 63 focusing on the tropical biogeographical realms (Neotropics, Afrotropics, Indomalaya and tropical Australasia).

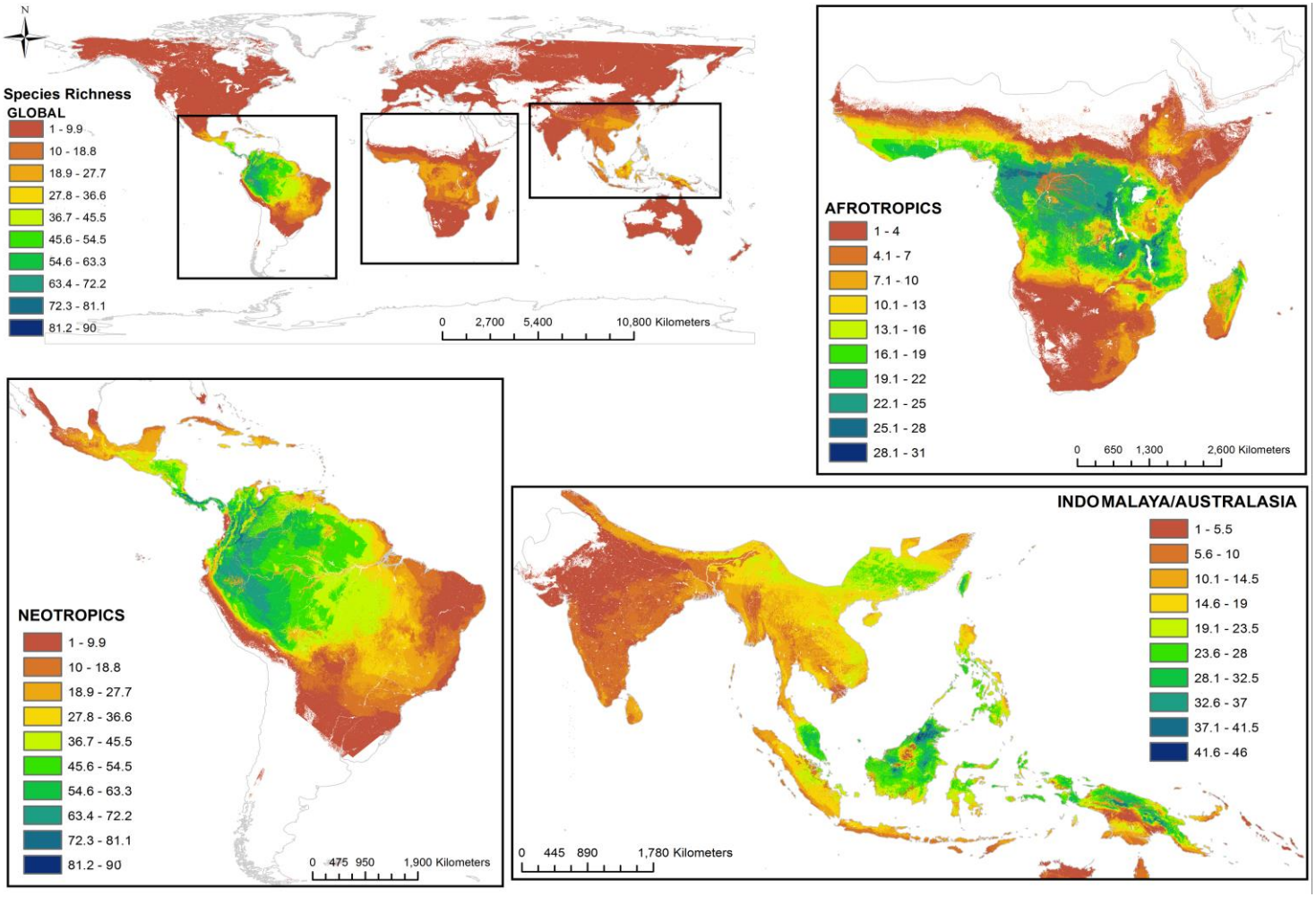

Figure 63. The ESH-derived map of forest pteridophyte species richness for (a) the world (b) the Neotropical biogeographical realm (c) the Indomalayan/Australasian biogeographical realms (d) the Afrotropical biogeographical realm. The Indomalayan and Australasian realms are combined in the same map excluding the Australian continent. There is a different scale and legend in each map. Data are classified in ten equal intervals.

In the ESH-derived map in Figure 63 there is no information on species richness in areas known to be unsuitable for forest pteridophyte species (e.g. deserts, water bodies, polar regions) or in areas covered by small numbers of species occurrence points in the analysis (in the southern part of South America, or the northern part of Europe). Regarding the tropical biogeographical realms, the Neotropics appear to be more species rich (maximum species richness: 90, mean species richness per km²: 31.8±19.7) than the Indomalayan realm (and the tropical part of Australasia) (maximum species richness: 46, mean species richness per km²: 13.3±7.8) and the Afrotropics (maximum species richness: 31, mean species richness per km²: 11.1±7.9). In the Neotropics, species richness as derived from ESHs was higher in Mesoamerica, the northern tropical Andes and the Amazon basin. The highest species richness values in the Indomalayan realm occurred in Borneo and peninsular Malaysia, whereas in the tropical part of the Australasian realm high species richness was estimated in New Guinea. The most species rich areas in the Afrotropics were the Mitumba Mountains in eastern Congo and the Muchinga Mountains in North-east Zambia. The Palearctic biogeographical realm appeared to have low species richness (maximum species richness: 27, mean species richness per km²: 2.8±3.3) compared with the tropical areas. However, areas in China, Japan and the Mediterranean basin had higher species richness than the rest of the Palearctic areas. Although the Nearctic biogeographical realm appeared to be as species rich as the Afrotropics (maximum species richness: 31), this high richness is due to two small areas in the southern part of the realm (the Southern part of Mexico and the Florida peninsula). The rest of the realm had relatively low species richness (0 – 9 species). This is shown by the big difference between their mean species richness per Km² (Nearctic: 3.1±2.1, Afrotropical: 11.1±7.9).

Additionally to the calculation of the mean species richness value per km² of each biogeographical realm, another method was used for the comparison of the biogeographical realms which also takes the effect of different sized suitable habitat areas of each realm into account. The ESH-derived maximum species richness was recalculated for each biome based on the power-function species-area relationship (Table 4). The results showed that amongst the tropical biogeographical realms, the Neotropical realm is the richer one (3.85 species per 100 Km² in the richest forest biome) followed by the Indomalayan realm (3.63 species per 100 km² in the richest forest biome) and then the Afrotropics (1.2 species per 100 km² in the richest forest biome), agreeing with the results of the comparison of absolute maximum species richness values (Neotropics:90, Indomalaya:45, Afrotropics:31) and of the mean species richness values per Km² (Neotropics: 31.8±19.7, Indomalaya: 13.3±7.8, Afrotropics: 11.1±7.9). In this analysis, the Palearctic (2.48 species per 100 Km² in the richest forest biome) and the Nearctic (2.26 species per 100 km² in the richest forest biome) biogeographical realms have richer forest biomes than do the Afrotropics (1.2 species per 100 km² in the richest forest biome). This is partly due to the fact that the richest forest biomes in the Palearctic and Nearctic realms border with the neighbouring tropical zones (with Indomalaya and with the Neotropics, respectively). Nonetheless, the Afrotropics do seem to be genuinely depauperate in species of pteridophytes. It is important to note that, in the case of the tropical biogeographical realms, the richest forest biome for pteridophyte species in each biogeographical realm was not always the expected

one. The richest forest biome in the Afrotropics is the Tropical & Subtropical Dry Broadleaf Forests, not the Tropical & Subtropical Moist Broadleaf Forests. Similarly, the Temperate Conifer Forests biome was the richest in both the Neotropics and Indomalaya, rather than the Tropical & Subtropical Moist Broadleaf Forests.

Table 4. Area of suitable habitat, maximum ESH-derived species richness and scaled species richness (Species per 100 Km²) per forest biomes within each biogeographical realm. Scaled species richness was calculated using the species-area relationship power function ($S=c*A^z$, where c and z are constants). Z values were taken from Kier *et al*. (2005).

	AFROTROPICS	**Area of suitable habitat (Km²)**	**z-value**	**Species**	**c-value**	**Scaled species /100 Km²**
1	Tropical & Subtropical Dry Broadleaf Forests	186589170	0.21	26	0.112	1.253
2	Tropical & Subtropical Moist Broadleaf Forests	3420754740	0.24	29	0.028	0.451
3	Mediterranean Forests, Woodlands & Scrub	93508020	0.20	5	0.032	0.320
	AUSTRALASIA	**Area of suitable habitat (Km²)**	**z-value**	**Species**	**c-value**	**Scaled species /100 Km**
1	Tropical & Subtropical Moist Broadleaf Forests	1097498160	0.24	44	0.057	0.899
2	Tropical & Subtropical Dry Broadleaf Forests	82862190	0.21	15	0.076	0.858
3	Temperate Broadleaf & Mixed Forests	697558230	0.17	11	0.107	0.755
	INDOMALAYA	**Area of suitable habitat (Km²)**	**z-value**	**Species**	**c-value**	**Scaled species /100 Km**
1	Temperate Conifer Forests	52756110	0.14	23	0.725	3.636
2	Temperate Broadleaf & Mixed Forests	155315070	0.17	23	0.288	2.038
3	Tropical & Subtropical Coniferous Forests	94003740	0.19	25	0.206	1.832
4	Tropical & Subtropical Dry Broadleaf Forests	1475854020	0.21	25	0.070	0.781
5	Tropical & Subtropical Moist Broadleaf Forests	5214952530	0.26	46	0.023	0.453
	NEARCTIC	**Area of suitable habitat (Km²)**	**z-value**	**Species**	**c-value**	**Scaled species /100 Km**
1	Tropical & Subtropical Moist Broadleaf Forests	4079160	0.24	29	0.143	2.269
2	Tropical & Subtropical Coniferous Forests	258453990	0.19	30	0.204	1.815
3	Temperate Conifer Forests	2228139090	0.14	12	0.224	1.123
4	Tropical & Subtropical Dry Broadleaf Forests	63298260	0.21	18	0.097	1.089
5	Temperate Broadleaf & Mixed Forests	2720929320	0.17	10	0.077	0.545
6	Mediterranean Forests, Woodlands & Scrub	114239970	0.20	2	0.012	0.123
	NEOTROPICS	**Area of suitable habitat (Km²)**	**z-value**	**Species**	**c-value**	**Scaled species /100 Km**
1	Temperate Conifer Forests	333720	0.14	12	0.769	3.854
2	Tropical & Subtropical Coniferous Forests	349577370	0.19	66	0.423	3.769
3	Tropical & Subtropical Dry Broadleaf Forests	1100410920	0.21	83	0.246	2.756
4	Tropical & Subtropical Moist Broadleaf Forests	9065240550	0.32	90	0.006	0.256
5	Temperate Broadleaf & Mixed Forests	333072000	0.17	1	0.011	0.078
6	Mediterranean Forests, Woodlands & Scrub	105665310	0.20	1	0.006	0.062
	OCEANIA	**Area of suitable habitat (Km²)**	**z-value**	**Species**	**c-value**	**Scaled species /100 Km**
1	Tropical & Subtropical Dry Broadleaf Forests	342630	0.21	5	0.081	0.905
2	Tropical & Subtropical Moist Broadleaf Forests	806760	0.32	10	0.014	0.562
	PALEARCTIC	**Area of suitable habitat (Km²)**	**z-value**	**Species**	**c-value**	**Scaled species /100 Km**
1	Tropical & Subtropical Coniferous Forests	1300050	0.19	15	0.278	2.480
2	Temperate Conifer Forests	1538496990	0.14	24	0.472	2.366
3	Temperate Broadleaf & Mixed Forests	8235861300	0.17	23	0.147	1.038
4	Tropical & Subtropical Moist Broadleaf Forests	507683700	0.26	27	0.024	0.487
5	Mediterranean Forests, Woodlands & Scrub	1698587820	0.20	12	0.043	0.430

Figure 64 shows that estimated species richness derived from the map of stacked species ESHs increases with the number of occurrence points (sampling effort) per area of suitable habitat in tropical biogeographical realms. The Neotropical biogeographical realm has higher species richness and sampling effort and the Afrotropical biogeographical realm has the lowest species richness and sampling effort of the three tropical realms.

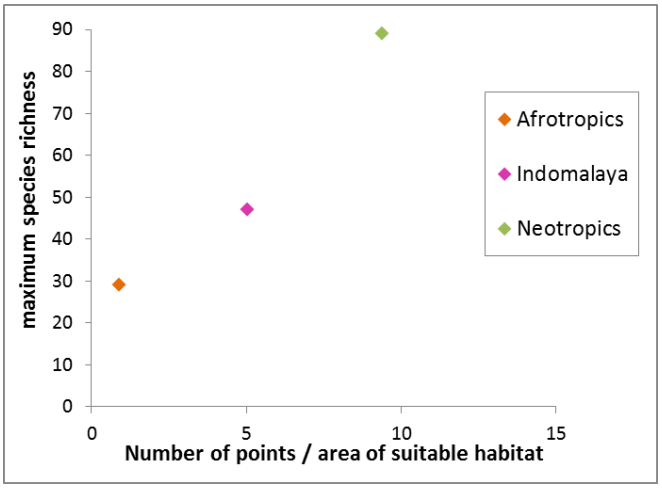

Figure 64. Number of specimen occurrence points per area of suitable habitat plotted against maximum estimated species richness for each tropical biogeographical realm.

3.3.3.2 Determinants of global forest pteridophyte species richness

As shown in Figure 65, species richness of forest pteridophytes shows a strong continental pattern; unsurprisingly there is no diversity of forest species over marine areas and lower species diversity in coastal zones than in the interior of continents. The noticeable peaks represent the three tropical biogeographical realms, with the Neotropical region having the highest species richness.

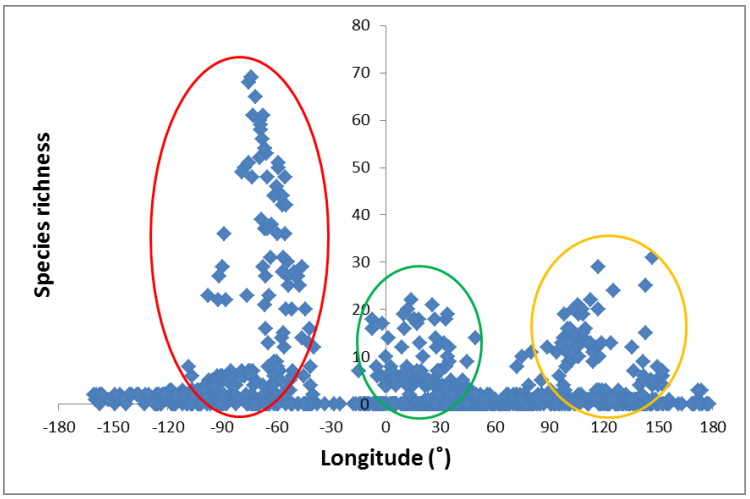

Figure 65. Species richness across longitude using randomly selected points for SRLI forest pteridophytes and plotting the equivalent species richness values against longitude. Red circle: Neotropical realm; Green circle: Afrotropical realm; Yellow circle: Indomalayan realm.

Furthermore, species richness is higher in the tropics than in temperate areas for pteridophytes. Specifically, there is a negative relationship of decreasing species richness with increasing latitude (Figure 66). A moderate correlation was shown between global species richness of randomly selected specimen occurrence points and latitude (bivariate correlation, northern hemisphere: $r = -0.41$, $n=1000$, $p < 0.001$; southern hemisphere: $r = -0.50$, $n=1000$, $p < 0.001$). However, a stronger correlation was shown between the two variables in the tropical region (-23.5˚ to 23.5˚) (bivariate correlation, northern hemisphere: $r = -0.48$, $n=1000$, $p < 0.001$; southern hemisphere: $r = -0.602$, $n=1000$, $p < 0.001$).

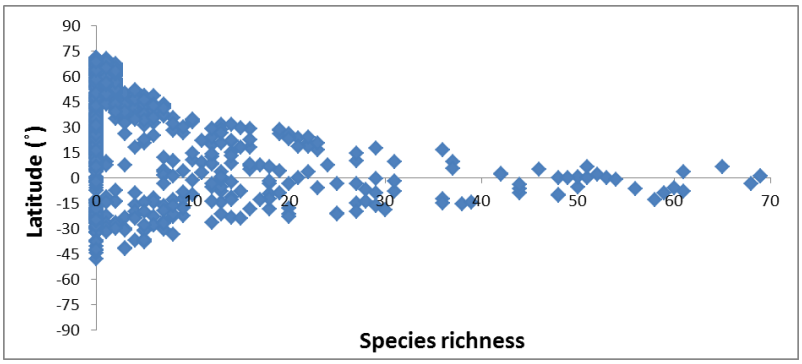

Figure 66. Species richness across latitudes using randomly selected points for SRLI forest pteridophytes (n=1000) and plotting the equivalent species richness values against latitude.

Species richness was moderately correlated with altitude globally (bivariate correlation: $r = -0.31$, $n=1000$, $p < 0.001$). A mid-altitude peak in species richness was found (1000 – 2000m) with higher species richness in lower (0 – 1000m) than higher altitudes (3000 – 6000m) (Figure 67).

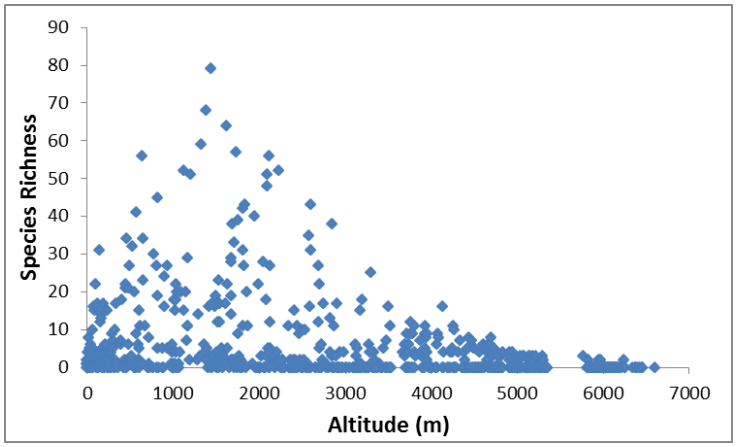

Figure 67. The relationship between species richness and altitude for SRLI forest pteridophyte species produced using randomly selected points per 500m altitudinal bands and plotting the equivalent species richness values against altitude.

Species richness was more strongly correlated with water balance (bivariate correlation: r = -0.41, n=1000, p < 0.001) than with altitude. Species richness was only moderately correlated with water balance globally but strongly correlated within the tropics (-23.5˚ to 23.5˚) (bivariate correlation: r = -0.71, n=1000, p < 0.001). The ESH-derived species richness-water balance relationship showed a humped shape that peaked at positive medium water balance values (500 – 1500 mm/per month) (Figure 68). While species richness in the tropical zones (-23.5˚ to 23.5˚) peaked at water balance values between 500 and 1500 mm/per month, it peaked between -500 and 500 mm/per month in temperate zones (23.5˚ to 66.5˚ and -66.5˚ to -23.5˚). A stronger hump-shaped species richness-water balance relationship was found in the tropical zone (linear regression R^2=0.5) than in the temperate zone of the southern hemisphere (linear regression R^2=0.3).

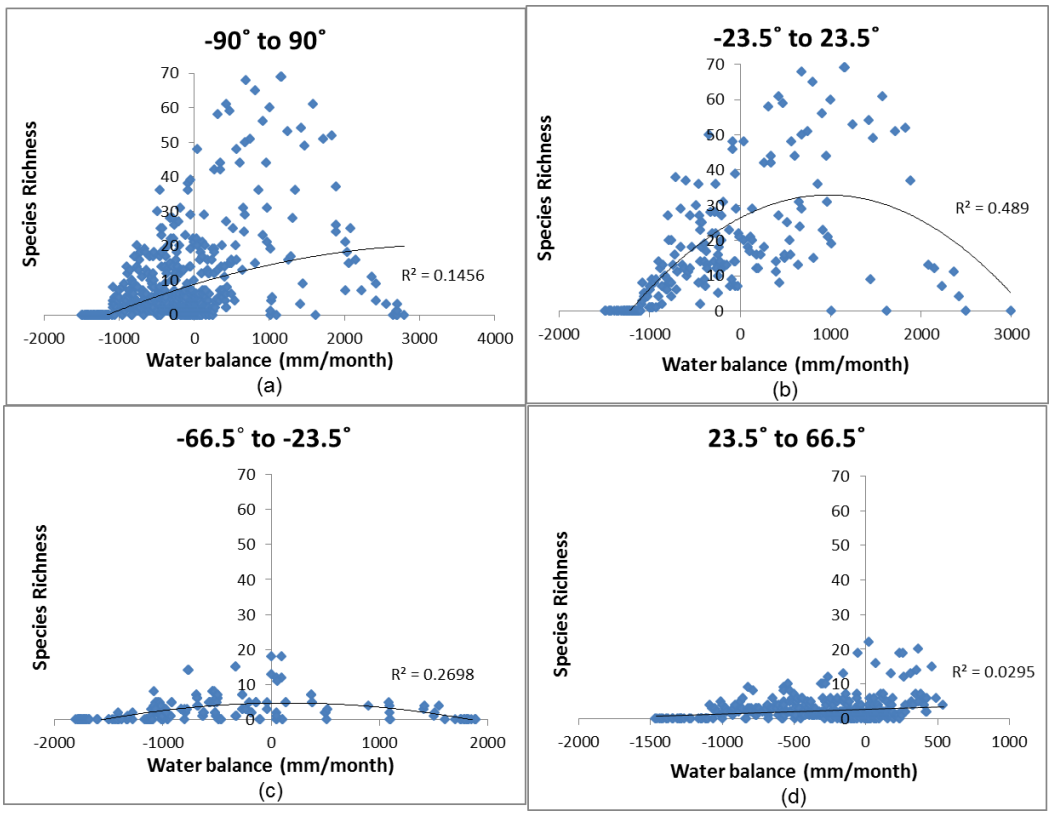

Figure 68. The relationship between species richness and water balance for SRLI forest pteridophyte species (a) globally (-90 ˚ to 90˚), (b) in the Tropics (-23.5˚ to 23.5˚), in (c) the Southern (-66.5 ˚ to -23.5 ˚) and (d) the Northern (23.5 ˚ to 66.5 ˚) hemispheres. Species richness was plotted against values for water balance at 1,000 randomly-selected pteridophyte occurrence points .Goodness of fit of regression (R^2) is reported.

Figure 69 shows the species richness-water balance relationship at intervals of 500m altitude. Species richness peaked at water balance values between 0 and 1000 mm/month at altitudes below 2500m but peaked at drier conditions (-100 – 500mm/month) at altitudes above 2500m. A moderate to strong correlation between species richness and water balance was found at all altitudinal intervals. Species richness was more strongly correlated with water balance at lower

altitudes (0 – 500m, bivariate correlation: r = 0.49, n=1000, p < 0.001) (Figure 69a) and higher altitudes (>2500m, bivariate correlation: r = 0.49 - 0.57, n=1000, p < 0.001) (Figures 69f-h) than at intermediate altitudes.

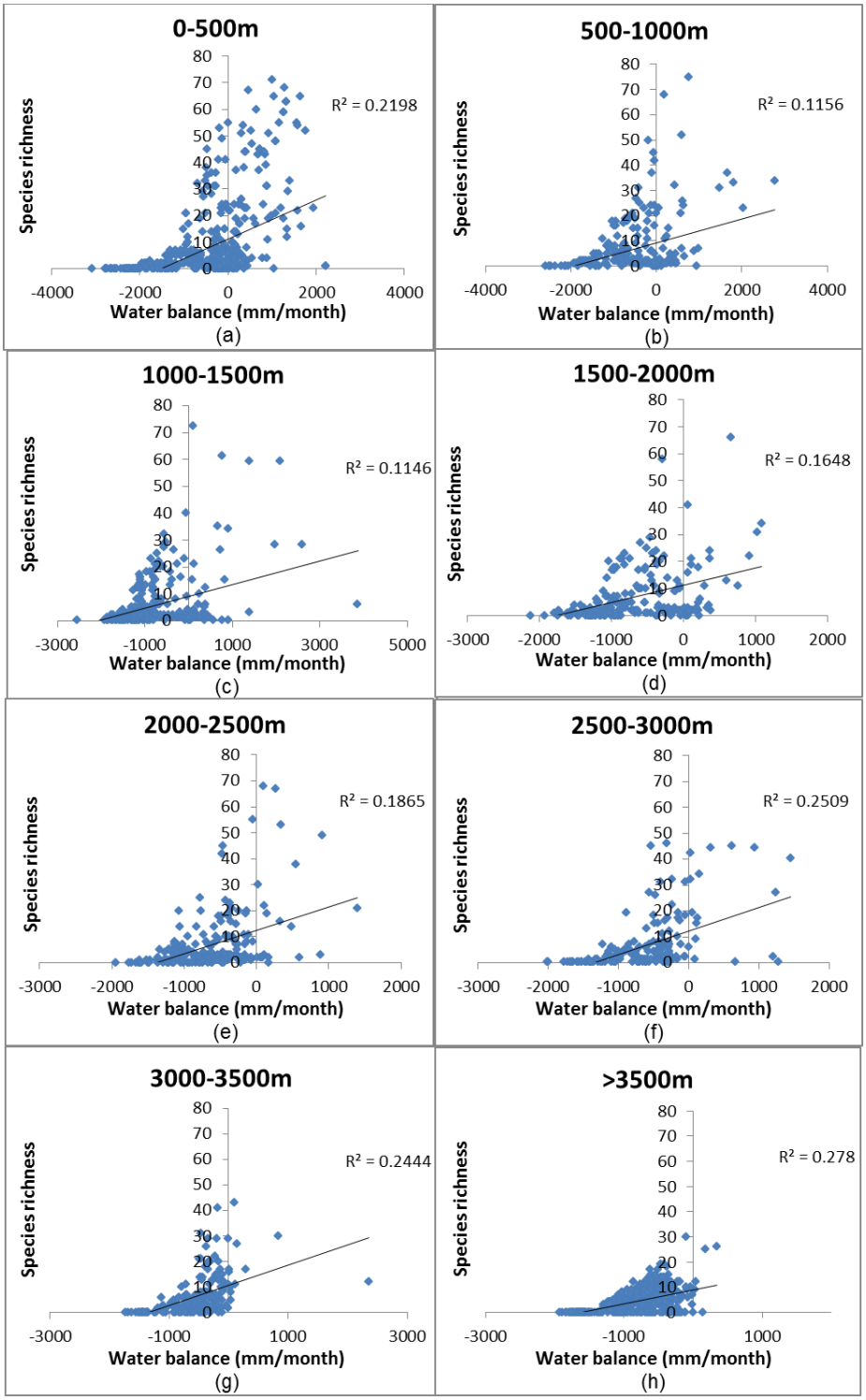

Figure 69. The relationship between species richness and water balance at intervals of 500m altitude. For each interval, species richness was plotted against water balance values for 500 randomly-selected pteridophyte occurrence points. Goodness of fit of linear regression (R^2) is reported.

3.3.2.3 Pteridophyte map of endemism richness

The map of endemism richness for pteridophytes, calculated using the ESHs of the SRLI forest pteridophyte species, is presented in Figure 70, focusing on the tropical biogeographical realms (the Neotropics, Afrotropics, Indomalaya and tropical Australasia).

High levels of endemism were found in tropical islands (Madagascar, the Caribbean islands and the islands in the Indo-Pacific area) and in montane areas (Tropical Andes). The region with the highest maximum value of endemism appeared to be Mesoamerica (0.34) in the Neotropics followed by the island of Borneo (0.14) in Indomalaya. Other areas of high endemism in the ESH-derived map are the Brazilian Atlantic Forest in the Neotropics, the Malay Peninsula and Taiwan in Indomalaya, the Great Dividing Range in Australia and the Cameroon Highlands and Mitumba Mountains in the Afrotropics. While the majority of areas of endemism are found in tropical regions, three important areas were identified outside the tropics: Japan, New Zealand and the north east Iberian Peninsula.

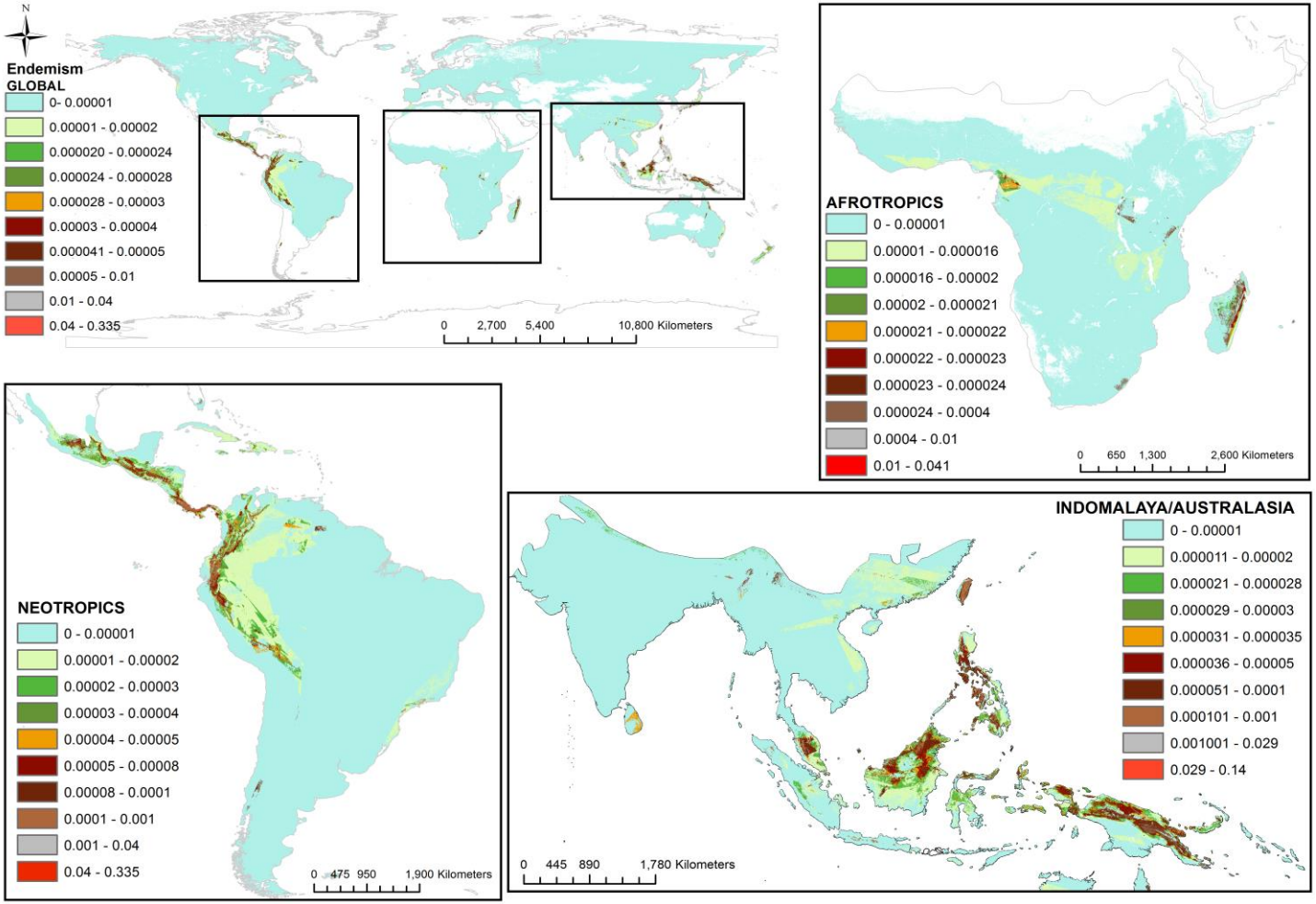

Figure 70. The ESH-derived map of endemism richness for SRLI forest pteridophyte species for (a) the world (b) the Neotropical biogeographical realm (c) the Indomalayan/Australasian biogeographical realms and (d) the Afrotropical biogeographical realm. The Indomalayan and Australasian realms are combined into the same map excluding the temperate Australian continent. Scales and legends differ for each map. Data are classified into ten intervals based on Jenks' natural breaks.

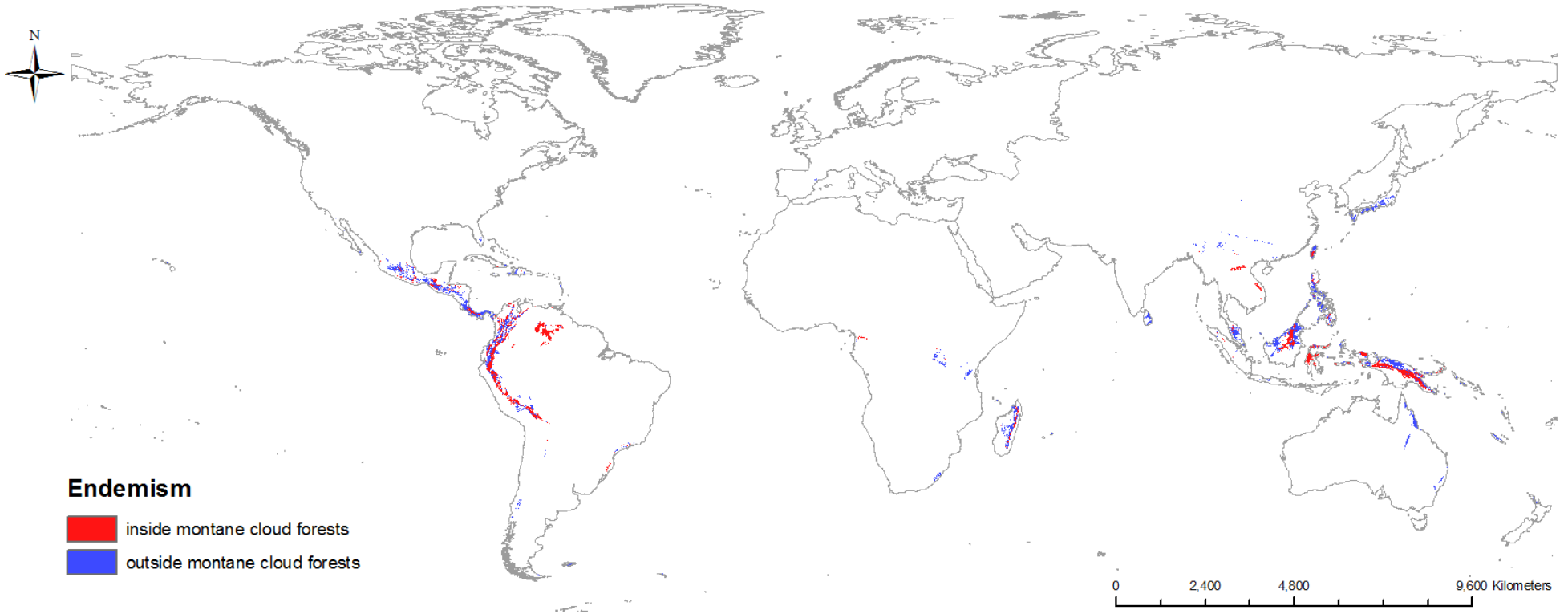

Figure 71. Areas with high ESH-derived endemism of SRLI forest pteridophyte species within Tropical Montane Cloud Forests (Tropical Montane Cloud Forest data source: Mulligan, 2010).

The endemic areas have the same spatial pattern as the tropical montane cloud forest areas (Figure 71) with high levels of endemism (0.01 – 0.34) always within those forests. A moderate correlation (bivariate correlation: r = 0.34, n=1000 per biogeographical realm, p < 0.001) was found between degree of endemism and altitude. Interestingly, the pattern of the relationship resembles that between species richness and altitude, with a mid-altitude peak at 1000 – 2000m (Figure 72).

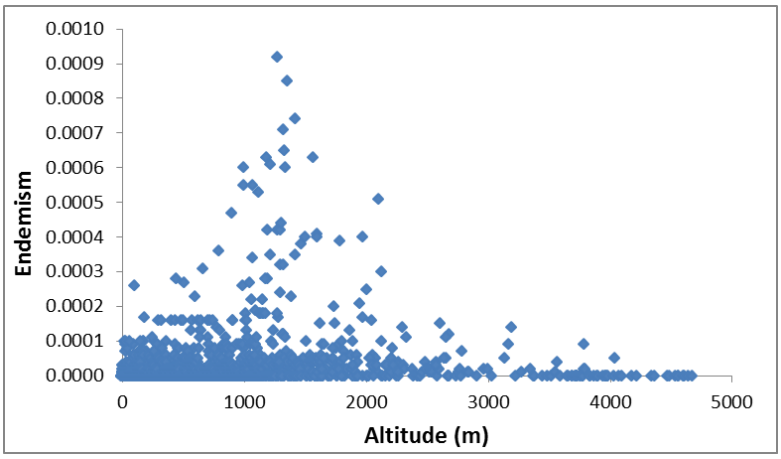

Figure 72. Endemism – Altitude relationship of SRLI forest pteridophyte species. The graph was produced using 1000 random points in each tropical biogeographical realm (Neotropics, Afrotropics, Indomalaya and tropical Australasia) at intervals of 500m altitude.

The correlation between endemism and water balance was also moderate (bivariate correlation: r = 0.37, n=1000 per biogeographical realm, p < 0.001). While global species richness peaked at positive medium water balance values (500 – 1500 mm/per month), endemism appeared to peak at lower water balance values (0 – 1000 mm/per month) (Figure 73). This is strongly influenced by high endemism at these water balance values in the Afrotropics.

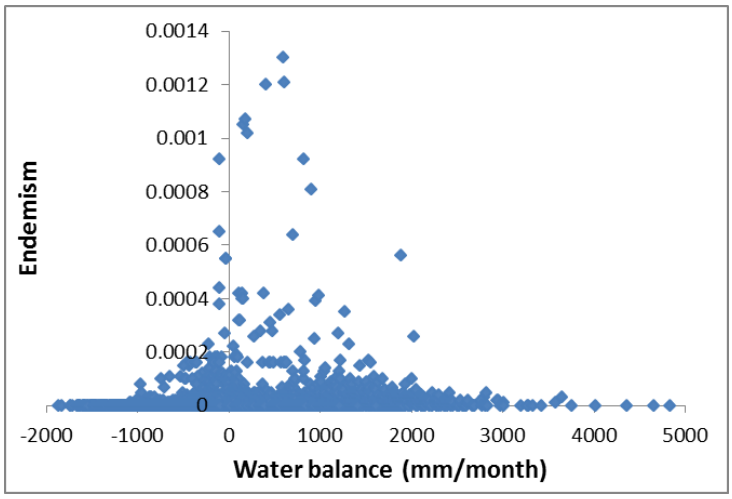

Figure 73. Endemism – water balance relationship of SRLI forest pteridophyte species. The graph was produced using 1000 random points in each tropical biogeographical realm (Neotropics, Afrotropics, Indomalaya and tropical Australasia) at intervals of 500m altitude.

.

3.4 DISCUSSION

3.4.1 Using SRLI species' ESHs on producing biodiversity maps

Until now, biodiversity maps were produced using macroecological models (Jetz & Rahbek, 2002; Luoto *et al.*, 2004; Gotelli *et al.*, 2009) or Species Distribution Models (Cumming, 2000; Parviainen *et al.*, 2009; Mateo *et al.*, 2012). While these maps are used as a tool for conservation planning, both these methods are time consuming and require detailed information on the ecology of the taxonomic group being investigated. With conservation targets of international organisations and conventions not being met in time (Butchart *et al.*, 2010; Hirsch, 2010; Juffe-Bignoli *et al.*, 2014), time-effective methods are needed to produce biodiversity maps in order to rapidly prioritise areas for conservation. Given the practical and relatively easy method of producing species ESHs (see more details in Chapter 2), using species occurrence data and high resolution environmental and land cover data, the ESH-derived biodiversity maps could be ideal for such use. In this chapter, the maps of species richness and endemism were produced using the ESHs of the SRLI forest pteridophyte species; the first attempt, to the author's best knowledge, to produce global biodiversity maps by stacking the ESHs and therefore summing the presence of pteridophyte species. Due to the fact that the species' ESHs were calculated using a global land cover map representing habitat for 2005 (Globcover v.2.2) (Bicheron *et al.*, 2008), the ESH-derived maps reflect the biodiversity patterns of forest pteridophytes for the year 2005.

The comparison between the ESH and EOO-derived biodiversity maps demonstrated once again (see Chapter 2) the advantage of using the species' ESH over the species' original EOO, a widely-used geographical range metric. While the two sets of maps broadly agreed on the species richness and endemism richness patterns, the EOO-derived maps appeared to be homogeneous across large regions in contrast to the ESH-derived maps which appeared to better reflect the habitat heterogeneity on the ground. This is explained by the differences in size and homogeneity of a species' range between the EOO and ESH. When using the ESH metric a species' range is smaller and less homogeneous than when using the EOO metric; this is because the species ESH includes only the suitable habitat for that species within its EOO. Since the species ESHs incorporate habitat, the equivalent biodiversity maps also include the habitat suitability component. For this reason someone could argue that the EOO-derived biodiversity maps present the potential species richness and endemism richness of the group whereas the ESH-derived biodiversity maps present its realised species richness and endemism richness. While the two species richness maps (ESH- and EOO-derived) predicted similar maximum species richness values globally, the ESH-derived map of endemism richness predicted six times higher values of endemism globally than did the EOO-derived map. Since species' range rarity is calculated with the c-value (the inverse of the number of the range size), it was expected that species endemism richness would be substantially bigger when calculated using the ESH metric than when using the EOO metric.

Independent field data (Kessler *et al*. (2011) and field data collected for this study) showed that the ESH-derived species richness map is indeed better at reflecting the reality on the ground than the EOO-derived map, which predicted higher species richness values at all altitudes. In addition, the species richness data collected during fieldwork in Costa Rica showed a mid-altitude peak in species richness (Figure 59); this is a pattern agreeing with the predictions of the ESH-derived species richness map and is consistent with the results of previous field-based studies in Costa Rica (Kluge *et al.*, 2006; Watkins *et al.*, 2006). However, due to the limitations of this dataset (sampling localities restricted to Costa Rica and a lack of data in areas with altitude less than 647m due to lack of natural vegetation at lower altitudes) the ESH-derived species richness map was also validated using global field data from Kessler *et al*. (2011). For Kessler *et al*. (2011) study sites, the ESH-derived species richness - altitude pattern did not agree with the hump-shaped mid-altitude peak in species richness of Kessler *et al*. (2011) since the ESH-derived species richness peaked at the study sites with low altitudes (0 – 500m) (Figure 57). However, when using random points across the ESH-derived species richness map (Figure 67), the ESH-derived species richness peaked at mid-altitudes with lower values in the lowlands, but not as low as in a hump-shaped pattern. This shows that the overestimation of species richness in the lowlands is not as high as the validation with the data from Kessler *et al.* (2011) indicates. Differences between the two datasets were expected due to different spatial scales between field studies and modelling (40m² vs 1km²) and to the fact that the data from Kessler *et al*. (2011) does not cover all parts of the world evenly (i.e. geographical sampling bias). Specifically, the high values of ESH-derived species richness in the lowlands in both the Afrotropics and the Neotropics are linked to only two study sites of Kessler *et al*. (2011), Reunion and Bolivia (Carrasco), respectively. Nevertheless, it was obvious that species richness in the lowlands from the ESH-derived map was an overestimation since the high values in the lowlands relative to higher altitudes also do not agree with the results of previous studies that have investigated pteridophyte species richness along altitudinal gradients (Kornas, 1993; Mehltreter, 1996; Kessler, 2000; Bhattarai *et al.*, 2004; Kluge *et al.*, 2006; Watkins *et al.*, 2006), nor with different field-based assessments (Tryon & Conant, 1975; Moran *et al.*, 1995; Tryon & Tryon, 2012).

An explanation of the overestimation of the species richness in the lowlands was sought through the species ESHs used to calculate the species richness map. Looking at the ESHs, the species ranges are more extensive in the lowlands than in montane areas. This could be explained by the small percentage (27%) of the world's land surface which is covered by mountains (FAO, 2010). Since land area decreases with elevation, there is more suitable habitat for a species that typically occurs in the lowlands than for one that occurs in the montane areas (Rahbek, 1995). Thus, when calculating a species ESH that occurs in the lowlands, a relatively large area is selected as suitable habitat even if the species does not occur in all of it. This is more obvious in cases where the species original EOO covers a large continuous lowland area such as in the Amazon basin where climate and altitude tend to be similar over very large areas. The reason for this is that habitat suitability models, like the ESH one, can overestimate species distribution since they do not take into consideration abiotic (e.g. meso- and micro-climatic

variables) and biotic factors (e.g. competitive species interactions, species tolerance to land cover change) that could limit a species' range (Davis *et al.*, 1998; Austin, 2002; Morrison *et al.*, 2006; Gaston & Fuller, 2009).

Another explanation of the overestimation of species richness in the lowlands could be due to a possible overestimation of the species' altitudinal range used when calculating the species' ESHs. The source of the species altitude ranges, used in the ESH calculation, was either the literature / herbarium specimens (altitude range provided by the species expert or collector) or the altitude values extracted using the species' occurrence points and remotely sensed elevation data. The ESH of 80% of the species that had their altitude range calculated based on literature/herbarium specimens, included the lowlands (0 – 500m), regardless of the species maximum altitude. It could be that experts have overestimated species' altitude ranges by always including the lowlands (0 – 500m) even if the species have never been recorded at these altitudes or that the information on old herbarium specimens (pre-twentieth century) is inaccurate (Bachman *et al.*, 2004). Furthermore, due to the fact that species occurrence points were used in calculating the species altitude ranges, large expanses of lowland areas could have been included in a species' ESH because of just one or two points. These few points could have been georeferenced incorrectly or they may have been the exception of the species' range. The occurrence points were checked for obvious georeferencing mistakes. However, due to the number of occurrence records, it was impossible to verify the accuracy of each of them before using them in the ESH calculation. An attempt was made to deal with these issues. The species' ESHs were recalculated using the 5 – 95 percentiles of the altitudinal range (instead of the whole range), taking into consideration the altitudinal frequency distribution within the species range and excluding the extreme (outlying) altitude values. The results showed that this approach failed to address the issue, instead decreasing species richness mainly in the highlands and in some cases in mid-elevation areas, showing that the overestimation of lowland species richness was not a result of such outliers. Also, since the resulting species richness-altitude pattern did not match the equivalent ones found with field data, the new 'trimmed' ESH-derived map was not used but instead the original ESH map was retained.

Based on the investigation into the bias in the SRLI data (Chapter 2, section 2.3.1), it appears that the pool of species in the ESH sample does not create any obvious geographical bias and, therefore, did not influence the pattern of the ESH-derived species richness map. Gaps in species coverage, specifically in the Palearctic realm, is not a result of selection of species in the ESH sample but, rather of the available herbarium specimens not representing the whole range of these species and therefore creating geographical bias at smaller scales (e.g. country level). Twenty-five countries mainly in the Palearctic and Afrotropical realm, known to have ESH species present and suitable habitat, were not covered by any occurrence points. This shows that museum collections often do not cover the whole spatial range of the species (Haila & Margules, 1996). Therefore, the ESH-derived species richness map could have been affected by this geographical sampling bias in the natural history collections.

3.4.2 The SRLI forest pteridophyte species richness map

Unsurprisingly, the ESH-derived species richness map predicted higher species richness for the SRLI forest pteridophytes in the tropics than in temperate areas, agreeing with the typical pattern known as the latitudinal diversity gradient (Smith, 1972; Tryon, 1986; Kessler, 2010; Kreft *et al.*, 2010; Kessler *et al.*, 2011; Tryon & Tryon, 2012). This pattern of higher species richness with decreasing latitude is similar to the richness pattern for flowering plants (Kreft & Jetz, 2007) but appeared to have a steeper gradient, as has also been shown by Kreft *et al.* (2010). In addition, Kreft *et al.* (2010) found that pteridophyte species richness peaks in humid tropical mountain regions, which is also the case in the ESH-derived species richness map. As expected, ESH-derived species richness was significantly correlated with water balance as other studies have also found (Page, 2002; Bickford & Laffan, 2006; Kreft *et al.*, 2010; Kessler *et al.*, 2011) and particularly strongly correlated in tropical regions. Species richness peaked at water balance values between 500 and 1500 mm per month; however, it peaked at lower water balance values (-500 – 500 mm/month) in relatively dry environments such as high altitudes (>2500m) and northern temperate areas. Water balance was significantly correlated with species richness at all altitudes, with a stronger correlation at lower altitudes (0 – 500m) and higher altitudes (>2500m). This strong correlation at high altitudes was not a surprise since it has been documented that, at high altitudes, the main determinant of pteridophyte species richness is temperature (Bhattarai *et al.*, 2004; Kluge *et al.*, 2006). Temperature is correlated with water balance at high altitudes since it determines the strength of the negative water balance where rainfall is low or zero (Jarvis & Mulligan, 2011).

Species richness also peaked in topographically complex areas with the highest values in the Andes and the Talamanca Mountain range. Furthermore, species richness was moderately correlated with altitude, with a mid-altitude peak in species richness as found in previous global and regional studies (Kessler, 2000; Hemp, 2002; Bhattarai *et al.*, 2004; Kluge *et al.*, 2006; Watkins *et al.*, 2006; Kessler *et al.*, 2011). However, the ESH-derived species richness - altitude relationship did not follow a similar hump-shaped distribution to that described in those studies. The decline of species richness at higher altitudes (>3000) was more pronounced than at lower altitudes (0 – 1000m), with a species richness of zero above the pteridophyte upper altitudinal limit (4800m) (Thapa, 2002; Bhattarai *et al.*, 2004). As mentioned in the previous section (3.4.1) compared with independent field data and the literature, the ESH-derived species richness map overestimated species richness at lower altitudes (0 – 1000m).

The ESH-derived species richness map predicted reasonable species richness patterns for pteridophytes, with no information on species richness in areas known to be unsuitable for forest pteridophyte species (e.g. deserts, water bodies). As expected, the tropical biogeographical realms (Neotropics, Indomalaya, Afrotropics and tropical Australasia) were richer in species than the rest of the realms (Palearctic, Nearctic, temperate Australasia, Oceania), due to the latitudinal diversity gradient. In the temperate biogeographical realms, though, areas known to have relatively high species richness were also the richest in these realms. These areas were Southern Mexico, China, Japan, and small areas in the

Mediterranean, all of which had the highest species richness values within temperate regions in the map of Kreft *et al.* (2010).

Although China is the richest area in pteridophyte species among temperate biogeographical realms, its species richness was expected to be higher. Even the southernmost part of the country that is in the Indomalayan realm did not appear to be as rich as described in checklists. According to López-Pujol *et al.* (2006), 20% of the world's pteridophyte species occur in China. This high species richness is thought to be due to the country's geographical, climatological and topographic diversity and especially to the fact that its southern part is in the tropical zone. In addition, Kreft *et al.* (2010) predicted high species richness in China similar to tropical biogeographical realms whereas Barthlott *et al.* (2007) identified China as one of the areas richest in vascular plant species. On the contrary, China appears to have much lower species richness values in our ESH derived map, compared with areas in the tropical realms, reflecting the geographical bias in the species occurrence points. The investigation into the bias in the ESH dataset (Chapter 2, section 2.3.1) showed that there are relatively small numbers of available Chinese herbarium specimens, which do not cover the whole range of species in China but also do not represent all species occurring in China. The low number of localities is not likely due to sampling bias, since China has been the focus of many botanical studies, but is likely the result of the difficulty of accessing the relevant collected data. Data gathered by Chinese institutions are not available in global databases such as the Global Biodiversity Information Facility (GBIF) from which much of the data for SRLI species was sourced. Furthermore, there are taxonomic issues with Chinese species delimitation due to the "narrow species concept" of many Chinese botanists (Nooteboom, 1992), who have the tendency to describe Chinese species under different names from the same species found outside China.

While the Mediterranean basin is a recognised biodiversity hotspot (Myers *et al.*, 2000; Brummitt & Nic Lughadha, 2003; Shi *et al.*, 2005) and holds 10% of the world's vascular plants (Medail & Quezel, 1997), its climate (hot and dry summers and cool and humid winters) is considered a limiting condition for growth of pteridophytes (Kreft *et al.*, 2010). However, there are areas in southern Europe that have been identified by Kreft *et al*. (2010) and the ESH species richness map as areas with relatively high species richness. One of those areas is the Iberian Peninsula, which according to Pausas and Sáez (2000), is the richest in pteridophyte species in the South Mediterranean region. This shows that pteridophytes can adapt to drought (Hietz, 2010) and do not exclusively occur in humid areas.

Looking at the tropical biogeographical realms, the ESH-derived species richness map predicted lower species richness in the Afrotropics than the Neotropics and Indomalaya. This was shown not only with the absolute maximum species richness values of each biogeographical realm but also when the effect of differing area size was taken into account. This agrees with the assessment of Tryon (1986), field data of Kessler *et al.* (2011) and the species richness map by Kreft *et al.* (2010), all of which calculated medium levels of species richness in the Afrotropics. Richards (1973) also reported lower plant species richness in the

Afrotropics than in the tropical areas of the Americas and Asia. This relatively poor pteridophyte species richness in the Afrotropics was explained by warmer and drier climate conditions compared to the other tropical realms, the limited extent of warm and humid tropical mountains (Moran *et al.*, 1995) but also by the great extinction of species that occurred during the Pleistocene climatic oscillations (Hamilton, 1976; Kornas, 1993). As expected, pteridophyte species richness was higher in areas with tropical moist forests and topographical complexity. Species richness in East Africa was influenced by smaller-ranged species (those with a smaller mean ESH), whereas species richness in West Africa was influenced by wide-ranged species (those with a bigger mean ESH) including those that also occur in the Neotropics. The most species-rich areas were predicted to be in the Mount Cameroon area of West Africa, the Mitumba Mountains in Eastern Congo and Muchinga Mountains in North-east Zambia (also known as the Zambezi-Congo watershed area), areas known to be rich in plant species (Linder, 2001; Barthlott *et al.*, 2005; Barthlott *et al.*, 2007; Kreft & Jetz, 2007; Kreft *et al.*, 2010). Higher species richness was predicted in the eastern mountains (Muchinga and Mitumba Mountains) than the western mountains (Mount Cameroon), a result that agrees with Schelpe (1983). Moreover, as expected, pteridophyte species richness in Madagascar is higher in the eastern part of the island where according to Mayaux *et al.* (2000), dense humid forest occurs. Therefore, despite the known taxonomic issues with African species, (taxa (e.g. *Asplenium*) which are taxonomically challenging and include many species under the same species name (Schneider, 2013)) and the low percentage of SRLI occurrence points (1%) in the realm, the ESH-derived map predicted the anticipated species richness patterns for pteridophytes. The proportion of SRLI occurrence points in the Afrotropical realm (1 point / 10000 km²) appears small compared with the other realms, however, one can argue that the relatively low percentage is linked to the small number of species in the realm and not to sampling bias.

Areas in the Neotropical and Indomalaya areas appeared to have higher species richness than the rest of the realms, a finding that also agrees with the pteridophyte species richness map by Kreft *et al.* (2010). Specifically, Mesoamerica and the tropical Andes are identified as the most species rich areas. This finding was not a surprise since previous studies (Mittermeier *et al.*, 1998; Myers *et al.*, 2000; Brummitt & Nic Lughadha, 2003; Barthlott *et al.*, 2007; Kreft & Jetz, 2007) have identified both areas as the most diverse hotspots. In addition, the ESH derived species richness map predicted high species richness in the Guiana Highlands in Venezuela, an area also identified as rich in pteridophyte species by Kreft *et al*. (2010). However, the species richness predictions of two areas in the ESH-derived species richness map did not agree with the ones of Kreft *et al*. (2010): the Brazilian Atlantic forest and the Amazon basin. Firstly, the Brazilian Atlantic forest, a recognised hotspot, appeared to have low species richness in the ESH-derived map. Despite the heavy deforestation in the area (Paciencia & Prado, 2005), higher species richness similar to that of Kreft *et al.* (2010) was expected to be predicted there. This could be explained by the small number of SRLI forest species covering the Brazilian Atlantic forest due to the lack of occurrence points in the area; thus underestimating the species richness there. Further, the lowlands of the Amazon basin were predicted by the ESH-derived species richness map as areas with high species richness; based on previous studies this is not

true. Pteridophyte species richness in the Amazon basin has been recorded as poor with only 600 species, 5 times less than the species in the tropical Andes (Moran, 2004). The overestimation of species richness in this area could be explained by the overall overestimation of species richness in the lowlands of the ESH-derived species richness map due to the nature of the species' ESHs calculation method (see section 3.4.1).

Overall, the ESH-derived species richness pattern in Indomalaya and tropical Australasia matched the equivalent areas of the map of Kreft *et al* (2010). Unsurprisingly, New Guinea, Borneo, the Philippines, Sulawesi, Taiwan and Peninsular Malaysia appear to have the highest species richness in those two biogeographical realms, which agrees with field-based assessments in the region (Moran, 2004). However, these areas have lower ESH-derived species richness than expected since they appeared to be much poorer than the richest areas in the Neotropics. New Guinea and Borneo especially were expected to stand out in terms of pteridophyte richness since it has been estimated that there are 2000 pteridophyte species on each island (Parris, 1985; Johns, 1995) and these areas are always included in areas of higher plant species richness globally (Kier *et al.*, 2005; Barthlott *et al.*, 2007; Kreft & Jetz, 2007; Kreft *et al.*, 2010). In addition, areas in Thailand, Vietnam and Myanmar, identified as species-rich areas by Kreft *et al*. (2010), appeared to have low ESH-derived species richness. According to Schneider (2013), these areas are undersampled which explains the small number of occurrence points of SRLI forest pteridophytes.

According to the ESH-derived species richness map, the Neotropics appeared to have twice as many species as Indomalaya (Neotropics: 90 species, Indomalaya: 46 species). After accounting for the effect of area, a similar difference was still found (Neotropics mean species richness per km²: 31.8±19.7, Indomalaya mean species richness per km²: 13.3±7.8). However, when rescaling the maximum species richness based on the species-area power function and comparing the richest forest biomes of each realm, the gap between the Neotropics and Indomalaya was much smaller. (Neotropics: 3.85 species / 100 km², Indomalaya: 3.63 species / 100 km²). Kreft *et al*. (2010) predicted similar species richness level in the Neotropics and Indomalaya (including tropical Australasia) whereas the field-based assessment of Kessler *et al*. (2011) revealed higher species richness in the Neotropical study sites than in the Indomalayan sites. Nevertheless, there are a number of reasons for the low predicted species richness of the Indomalayan realm relative to the Neotropical realm. While the selection of species for this study does not generally create any obvious geographical bias on a global scale (see Chapter 2, section 2.3.1), the percentage of species with adequate species data in the ESH dataset was found to be 5% higher for the Neotropics and 2% higher for Indomalaya than the equivalent proportion in the pteridophyte checklist. This bigger percentage of available data for the Neotropics could have influenced the difference between the two realms. Second, geographical sampling bias in the data − that is, the number of specimens collected in each realm − could also have influenced the difference in species richness between the two realms: Walther *et al.* (1995) showed that predicted species richness increases with sampling effort, which is also the case in this study with the Neotropics having the highest species richness and also the highest

number of occurrence points. The Neotropics has a higher number of points per area of suitable habitat (9 points / 10000 km²) than Indomalaya does (5 points / 10000 km²). The Neotropical realm could have more specimens either because the Indomalayan area is under-sampled compared to the Neotropics, or because there are more digital data available for the Neotropics. Lastly, the large absolute difference in species richness between the Neotropical and the Indomalayan realm can be explained by the fact that botanists in S.E. Asia, influenced by the Dutch tradition, have a much broader species concept than is applied in the Neotropics. Botanists in the Neotropics tend to describe more species than in the Indomalayan area (Schneider, 2013), and thus, while according to checklists the Neotropics appear to be richer, this may not necessarily be true.

It is important to note that differences between the ESH species richness map and the Kreft *et al.* (2010) map could be explained by the fact that the ESH species richness map was produced using occurrence points of SRLI forest pteridophyte species whereas the Kreft *et al*. (2010) map was generated using available data (from checklists) of all pteridophyte species. Hence, the richness pattern of the ESH map could have been different if non-forest or/and non-exclusive forest pteridophyte species were included. For the same reason, field-based assessments of all pteridophyte species richness are not necessarily comparable with the ESH species richness predictions of the SRLI forest pteridophyte species. Finally, the ESH-derived species richness map was produced using the species ESHs which were calculated taking into account land cover from the year 2005. This means that areas with high species richness based on past field-based assessments may not appear as rich in the ESH-derived species richness map due to the impact of subsequent deforestation.

3.4.3 The SRLI forest pteridophyte map of endemism richness

The ESH-derived map of endemism richness for SRLI forest pteridophytes highlights the same centres of high endemism that previous global studies of mammals, amphibians, reptiles, birds and plants have identified (Mittermeier *et al.*, 1998; Myers *et al.*, 2000; Brummitt & Nic Lughadha, 2003; Kier *et al.*, 2005; Stattersfield *et al.*, 2005; Lamoreux *et al.*, 2006; Kier *et al.*, 2009). Although none of the studies have exclusively used pteridophytes in their analysis, the majority of them have primarily used vascular plant data to identify these hotspots. The ESH-derived map of endemism richness was compared with these studies, as it is believed that patterns of pteridophyte endemism should follow the general pattern of endemism for vascular plants. As expected, due to their isolation and eco-climatic stability (Hengeveld, 1990; Jetz *et al.*, 2004), tropical islands and tropical montane areas have been identified as endemic-rich areas, a result that agrees with the above-mentioned studies but also with field-based assessments of pteridophyte endemism (Tryon, 1972; Smith, 1972; Tryon, 1986; Moran, 2004).

The biogeographical realm with the highest maximum endemism value appeared to be the Neotropics with high values of endemism in the mountain ranges of Mesoamerica and the Tropical Andes. These areas are included in the top 10 biodiversity hotspots of Mittermeier *et al*

(1998), Myers *et al.* (2000) and Brummitt & Nic Lughadha (2003). The high speciation rates in mountain ranges has been explained by the combination of increasing isolation and decreasing area of suitable habitat with altitude, which results in isolated and fragmented species populations. These populations can gradually evolve into new species due to cessation of gene flow between them (Kruckeberg & Rabinowitz, 1985; Kessler, 2002a). Indeed the highest level of ESH-derived endemism was found at the Talamanca Mountains due to the large number of SRLI forest species with narrow ranges that occur in the area. This agrees with Moran (1995) who recorded high levels of endemism for pteridophytes in the Talamanca Mountains across Costa Rica and Panama and with Tryon (1972) who identified the Costa Rica Mountains as a centre of endemism for pteridophyte species.

High levels of endemism were also found in the mountain ranges of the Afrotropics. Studies have suggested that the patterns of endemism in Africa are explained by the 'refugium theory'; centres of endemism occurring in montane areas which acted as refugia to species during the climatic fluctuations of the Pleistocene (Hamilton, 1974; Kornas, 1993; Linder, 2001; Aldasoro *et al.*, 2004). The refugia provided either the only suitable (Haffer, 1969) or the most stable climatic environment (Fjeldsaå & Lovett, 1997) to the fragmented populations of the species which led to speciation and resulted in large centres of species richness and endemism. Interestingly, areas that appeared to have high species richness in the ESH-derived species richness map were the areas with the highest level of ESH-derived endemism on mainland Africa. These were the Cameroon highlands (Cameroon-Gabon area), the Usambara Mountains (Eastern Arc Mountains), the Mitumba Mountains (in the Albertine Rift) and an area in north-eastern Zambia, all of which are recognised centres of plant endemism (Exell & Wild, 1973; Rodgers & Homewood, 1982; White, 1983; Lovett & Friis, 1996; Myers *et al.*, 2000; Kier & Barthlott, 2001; Linder, 2001). The Cape Floristic Region in southern South Africa did not stand out in the ESH-derived map despite the fact that it is considered a major centre of plant endemism (Bond & Goldblatt, 1984; Cowling & Hilton-Taylor, 1997; Myers *et al.*, 2000; Kier *et al.*, 2009). Species occurring in South Africa were excluded from the SRLI project since there is a separate project for the assessment of the conservation status of the South African plants (Red List of South African Plants) (SANBI, 2015). Therefore, species from that region were not included in the ESH species sample and the calculation of the ESH-derived biodiversity maps.

Islands were expected to have high levels of endemism due to their biological isolation from the mainland (Whittaker & Fernández-Palacios, 2007). Kier et al. (2009) found higher levels of plant endemism in island regions than in mainland regions. This was not the case with the ESH-derived map of endemism richness since tropical islands had the highest levels of endemism after the mountain ranges of the Neotropical biogeographical realm. Madagascar, the Caribbean islands and islands in the Indo-Pacific area (Sundaland) all appeared to have high levels of endemism in the ESH-derived map with Mount Kinabalu in Borneo having the highest values of endemism followed by Madagascar. In both islands, high levels of pteridophyte endemism have been recorded (Parris, 1985; Aldasoro *et al.*, 2004) whereas Myers et al. (2000) and Brummitt & Nic Lughadha (2003) included them within their biodiversity hotspots (areas with at least 1500

endemic plant species). In addition, other areas with high to medium endemism values in the ESH-derived map have also been identified as areas rich in plant endemism in previous studies. These are the north east Iberian Peninsula (Pausas & Sáez, 2000), the Brazilian Atlantic Forest (Brummitt & Nic Lughadha, 2003), New Zealand (Myers *et al.*, 2000) and areas on the Great Dividing Range in Australia (Kier et al., 2009).

Endemism in the ESH-derived map was found to be moderately correlated with altitude and water availability. Interestingly, areas of endemism for pteridophytes have the same general spatial pattern as the tropical montane cloud forest areas, reflecting the clear habitat preference of the group. Since the cloud forest map (Mulligan, 2010) is derived from areas of tree cover and high cloud (fog) frequency, these are perhaps ideal environments for forest pteridophytes. Areas with the highest levels of ESH-derived endemism are all within tropical montane cloud forests. Montane cloud forests occur at altitudes between 400 and 2800m with an average rainfall of 2000mm per year (Jarvis & Mulligan, 2011), an ideal environment for speciation and survival of pteridophytes. In addition, the ESH-derived endemism peaked at mid-altitudes (1000 – 2000m), lower than previous studies have indicated (Tryon, 1972; Kessler, 2000; Kessler, 2002a). However, according to Kluge *et al*. (2006) endemism peaks in lower altitudes (1800 – 2400m) for pteridophytes in the Talamanca Mountains, the area with the highest ESH-derived endemism, than in other montane regions; which explains the peak in endemism at relatively low altitudes. This is partly driven by the levels of humidity at those altitudes (Kessler, 2010) shown also by the fact that the ESH-derived endemism peaked at positive water balance values. Endemism levels peaked at lower water balance values in the Afrotropical biogeographical realm than the other two tropical realms; reflecting the realm's warmer and drier climate conditions compared to the other tropical realms (Malhi & Wright, 2004).

3.5 CONCLUSIONS

This is the first attempt, to the author's knowledge, to produce global biodiversity (species richness and endemism) maps derived from ESH measures for SRLI forest pteridophytes. As expected, pteridophyte species richness peaked in tropical humid montane areas at mid-altitudes and with abundant water availability. Despite the fact that it has been shown that endemism and species richness hotspots do not necessarily overlap for different taxonomic groups (Orme *et al.*, 2005), the major centres of species richness are congruent with the major centres of endemism for forest pteridophyte species . This is explained by the particular habitat preference (montane humid forests) of the group.

The general patterns in the ESH-derived maps of species richness and endemism broadly agree with previous studies. The effectiveness of the stacked ESH approach shows that species' ESHs broadly reflect species distributions on the ground, at least within the boundaries of the original EOO. Differences between the ESH-derived maps and the findings of previous studies were attributed to the different pool of species and methods used in each study and to

the geographical sampling bias of the SRLI forest occurrence points used when calculating the species' ESHs. Based on the analysis of this study, two limitations of this approach were identified:

1. The selection of species in the ESH sample does not create any obvious geographical bias and therefore did not influence the ESH-derived species richness map. However, the geographical sampling bias in the natural history collections influenced the species richness pattern of the ESH-derived map by creating geographical bias, mainly at smaller scales. This problem can be improved by using all available occurrence points of a species and therefore covering the species' full known distribution, according to published checklists. In addition, fieldwork expeditions to under-sampled areas can contribute to the improvement of this issue. Lastly, different techniques (e.g. spatial filtering, background manipulation with bias files, using pseudo-absence data) that have been suggested to correct sampling bias in Species Distribution Modelling (Phillips *et al.*, 2009; Kramer-Schadt *et al.*, 2013; Syfert *et al.*, 2013) can be tested in the future.

2. A comparison of the ESH-derived species richness map with independent field data showed an overestimation of species richness in the lowlands (e.g. Amazon basin). This was linked to the method of calculating the species' ESHs. Two possible reasons for this overestimation were identified: (a) the overestimation of the species altitudinal range used in the ESH calculation and (b) the inability to capture the impact of abiotic (e.g. meso- and micro-climate) and biotic factors (e.g. species interactions) on species richness. This issue can be improved by using correctly georeferenced herbarium specimens and cross checking altitudinal ranges provided by collectors.

Despite these limitations, the ESH-derived biodiversity maps identified the expected areas in each biogeographical realm as hotspots of species richness and endemism. This is important, since the conservation of hotspots from each biogeographical realm instead of the 'hottest' hotspots of the world has been proposed (Kier *et al*., 2005). With conservation targets of international organisations and conventions not being met in time (Butchart *et al.*, 2010; Hirsch, 2010; Juffe-Bignoli *et al.*, 2014), time-effective methods are needed to produce biodiversity maps in order to rapidly prioritise areas for conservation. This study proposes the use of ESH-derived biodiversity maps due to the practical and easy method of producing species ESHs and the effectiveness of the ESH-derived maps. Furthermore, due to the fact that the species ESHs can be re-calculated based on land cover change observations, the ESH-derived biodiversity maps can provide an up to date reflection of the biodiversity patterns on the ground and therefore assist the decision-making process of conservation strategies.

CHAPTER 4

A COMPARISON OF ESH AND SDM METHODS

4.1 INTRODUCTION

The development of models that predict species' ranges based on the species-environment relationship has been the focus of many studies in ecology, biogeography and conservation biology. Species Distribution Models (SDMs) are currently the most established approach to quantify the environmental niche of species within a defined area using species observation data and environmental information (Guisan & Thuiller, 2005; Elith *et al.*, 2006; Elith & Leathwick, 2009; Franklin, 2009; Peterson, 2011). The niche concept is nicely summarised by Hutchinson (1957) as '…the hypervolume defined by the environmental dimensions within which that species can survive and reproduce'. With the rise of GIS tools and available databases of species occurrence data (e.g. GBIF) and spatial data, SDMs have been increasingly used to predict areas that have suitable environmental conditions for species (Franklin, 1998; Guisan *et al.*, 1998; Vetaas, 2002; Pearson *et al.*, 2007), as well as to forecast the potential impacts of environmental changes (e.g. climate change, land cover change) on species distributions (Thuiller, 2004; Araújo & Luoto, 2007; Thuiller *et al.*, 2008; Yates *et al.*, 2010).

SDMs (or ecological niche models) are 'empirical models relating field observations to environmental predictor variables based on statistically or theoretically derived response surfaces' (Guisan & Zimmermann, 2000). Species distribution modelling involves four key steps: (a) conceptual model formulation, (b) statistical model formulation, (c) evaluation and (d) spatial mapping of prediction (Guisan & Zimmermann, 2000; Austin, 2002; Elith & Leathwick, 2009; Franklin, 2009). The first step links ecological niche theory to statistical modelling and it includes investigating the ecological characteristics of the species, gathering and exploring the species' observation data and selecting suitable environmental predictor variables. SDMs are calculated based on species' observation data (presence-only, presence-absence or abundance data), which are often derived from natural history collections. The environmental predictor variables are selected based on reducing multicollinearity (Raxworthy *et al.*, 2003; Franklin, 2009) and on their ecological relevance to the modelled species (Austin, 2002; Hirzel & Le Lay, 2008; Elith & Leathwick, 2009). These environmental predictors can have a direct or indirect effect on the species' distribution and are ideally related to the primary environmental regimes (heat, light water and nutrients) (Guisan & Zimmermann, 2000; Guisan & Thuiller, 2005; Franklin, 2009) that determine where species are found.

The second step of species distribution modelling involves selecting the most appropriate modelling technique (algorithm) which will quantify the statistical association between the species observation data and the environmental predictor variables. A wide variety of modelling techniques have been developed that can produce different predictions (Araújo *et al.*, 2005;

Elith *et al.*, 2006; Franklin, 2009) showing that each technique is not suitable for all cases (Segurado & Araújo, 2004; Elith & Graham, 2009; Marmion *et al.*, 2009). According to Franklin (2010), modelling techniques can be divided into statistical learning methods (e.g. Generalized Additive Models (GAM) (Hastie & Tibshirani, 1986), Generalized Linear Models (GLM) (McCullagh & Nelder, 1989), Multivariate Adaptive Regression Splines (MARS) (Friedman, 1991), machine learning methods (e.g. Boosted Regression Trees (Friedman, 2001)), Maximum Entropy (MaxEnt) (Phillips *et al.*, 2006) and 'profile' methods (e.g. Bioclim (Busby, 1991), DOMAIN (Carpenter *et al.*, 1993)). Techniques can differ in their statistical assumptions, in the type (i.e. presence-only, presence-background or presence-absence) and sample size of species' observation data they require, in the type of predictor variables (quantitative, categorical or binary) they require, and in the selection method of the predictor variables (Elith *et al.*, 2006; Wisz *et al.*, 2008; Franklin, 2009).

The third modelling step includes the evaluation of the model's predictive performance, ideally using independent data. Different measures are used to evaluate the accuracy (i.e. fit) of the models and are divided into threshold-independent and threshold-dependent measures (Franklin, 2009; Liu *et al.*, 2009). Threshold-independent measures (e.g. area under the curve (AUC) and correlation calibration) are applied to continuous predictions, whereas threshold-dependent measures (e.g. kappa, sensitivity and specificity) are applied to binary maps in which continuous predictions have been converted to binary values by applying a threshold. The most commonly used measure of accuracy is the AUC metric (Hanley & McNeil, 1982) which is derived from Receiver Operating Characteristic (ROC) plots and summarizes the ability of the model to rank the proportion of sites where the species is known to occur higher than the proportion of sites where the species is known to be absent (Franklin, 2009).

The limitations of SDMs have been well documented (Franklin, 2009) and the uncertainty in their predictions has been recognised (Elith *et al.*, 2002; Barry & Elith, 2006). The source of uncertainty can be traced to the different decision steps made when building an SDM (e.g. selection of modelling technique and selection of predictor variables) and in data limitations such as small sample size, sample bias, inaccurate location of data, inappropriate spatial scale of environmental data (see details in Figure 74). Several studies have addressed issues related to model uncertainty and approaches to improve SDM predictive performance have been suggested (Engler *et al.*, 2004; Anderson *et al.*, 2006; Elith *et al.*, 2006; Wisz *et al.*, 2008; Phillips *et al.*, 2009). However, many of the suggested approaches are not always applied (Franklin, 2009).

In addition, as with all models, SDMs contain assumptions that add to the uncertainty of the predictions. It is assumed that SDMs are predicting the realised ecological niche of a species (i.e. where it currently occurs) and not its fundamental niche (where it could potentially occur). The two types of niche of a species differ owing to dispersal limitation and through biotic interactions between competing or dependent species (Malanson *et al.*, 1992; Vetaas, 2002; Soberón, 2007). This assumption is valid for SDMs that are based on large empirical field

datasets and for dynamic models that include biotic predictor variables. However, it has been argued that static SDMs that are based only on abiotic predictor variables, SDMs based on presence-only data and SDMs produced using coarse-scale predictor variables, describe the fundamental rather than the realised niche of a species (suitable habitat), as they do not capture how biotic interactions are affecting the distribution of a species (Guisan & Zimmermann, 2000; Soberon, 2005; Hirzel & Le Lay, 2008; Jiménez-Valverde *et al.*, 2008), including the effects of land cover and fragmentation. Another fundamental assumption is that the species is in equilibrium with the environment (Guisan & Zimmermann, 2000). This assumption has been criticised as it has been shown that species distributions are still influenced by historical factors (Graham *et al.*, 2010) and climate change (Pearson & Dawson, 2003).

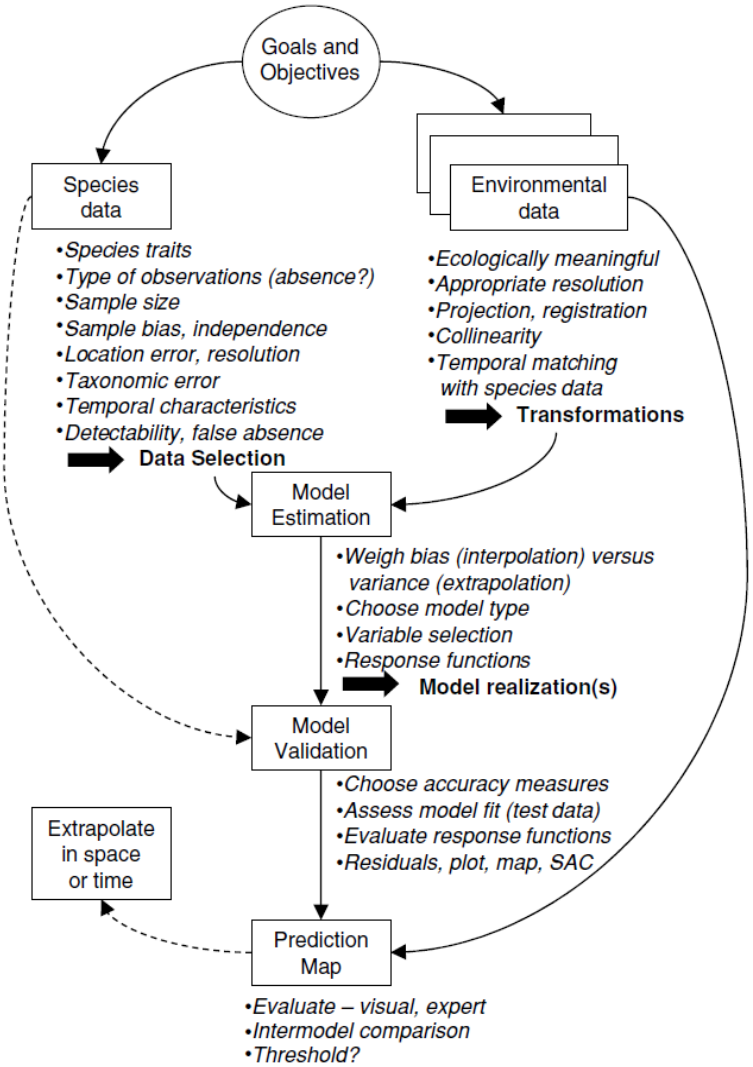

Figure 74. Sources of uncertainty in choosing data and methods when building a Species Distribution Model (Franklin, 2009, p.238).

SDMs are broadly effective in predicting species distributions, when their limitations are explicitly considered in each case, and therefore widely used (Franklin, 2009). SDMs have been used to explore biogeographical, ecological and evolutionary concepts (Leathwick & Austin,

2001; Anderson *et al.*, 2002; Austin, 2002; Guisan & Thuiller, 2005). They have also proven useful in conservation biology studies and conservation planning and for this reason it has been suggested that SDMs should be used to support conservation decision making (Guisan & Thuiller, 2005; Rodríguez *et al.*, 2007; Elith & Graham, 2009; Franklin, 2009; Peterson, 2011; Guisan *et al.*, 2013). For example, they have been used in the design of protected areas (Thorn *et al.*, 2009), in identifying biodiversity hotspots with SDM-derived species richness maps (Murray-Smith *et al.*, 2009; Parviainen *et al.*, 2009; Raes *et al.*, 2009), in providing information on rare and threatened species (Raxworthy *et al.*, 2003; Engler *et al.*, 2004; Guisan *et al.*, 2006) and in investigating the impact of climate change and land cover change on species distributions (Thuiller, 2004; Araújo & Luoto, 2007; Thuiller *et al.*, 2008; Yates *et al.*, 2010). Furthermore, SDMs have been used to estimate species geographical range sizes and it has been suggested that they should be incorporated into species conservation assessments (Sérgio *et al.*, 2007; Cardoso *et al.*, 2011; Pena *et al.*, 2014; Syfert *et al.*, 2014).

Habitat suitability models have been suggested as a solution to the overestimation of the species geographical range when calculated using the EOO metric (da Fonseca et al., 2000). For this reason, the ESH metric, that can reduce the commission errors associated with the EOO, has been used in previous studies (Rondinini *et al*., 2005; Beresford *et al*., 2011a; Beresford *et al*., 2011b; Buchanan *et al*., 2011; Rondinini *et al*., 2011), as well as in the present one, to calculate species geographical ranges. In this study, an ESH calculation method for forest pteridophyte species was built using the species' occurrence data obtained from herbarium specimens (Chapter 2). A validation of the calculated ESHs of the SRLI forest pteridophyte species was conducted using independent data and showed that the new calculation method is effective at reflecting the reality of plant distributions on the ground (Chapter 2, section 2.3.3). The species ESHs were also validated indirectly by validating the ESH-derived species richness map using independent field data (Chapter 3, section 3.3.2). However, the new ESH calculation method was not compared with any other species' distribution calculation approaches, other than the EOO approach. SDMs would be ideal for such a comparison due to their proven effectiveness in predicting species' distributions and to the fact that they have been used with species occurrence data derived from natural history collections (Anderson *et al.*, 2002; Anderson *et al.*, 2006; Wisz *et al.*, 2008; Mateo *et al.*, 2010; Newbold, 2010; Syfert *et al.*, 2013; Syfert *et al.*, 2014). Furthermore, species richness patterns can be predicted by stacking SDMs (Parviainen *et al.*, 2009; Dubuis *et al.*, 2011; Mateo *et al.*, 2012) and therefore ESH-derived and SDM-derived species richness maps could also be compared.

4.2 METHODS

The aim of this chapter was to compare the ESH method for calculating species' ranges (Chapter 2) with an established species distribution modelling approach. This has been the fourth objective of this study. Both a Species Distribution Model (SDM) and an ESH were

generated for each SRLI forest pteridophyte species that is endemic to the Neotropics (Central and South America), using identical sets of occurrence point data, in order for the two methods to be comparable. The two sets of species' geographical ranges (ESHs and SDMs) and the subsequent species richness maps (ESH and SDM-derived maps) were compared using multiple metrics. The species richness maps were validated using fieldwork data collected in Costa Rica (for this study) as well as fieldwork data from a previous study (Kessler *et al.*, 2011). A more detailed comparison was conducted focusing on Costa Rica, the case study area for this project.

4.2.1 Calculating geographical ranges using the ESH and SDM methods

The SRLI forest pteridophyte species were used to compare the SDM and ESH approaches. Due to the computational intensiveness of producing SDMs at a global scale, this study was limited to making comparisons with only SRLI forest pteridophyte species occurring in the Neotropical biogeographical realm (Central and South America). The Neotropical biogeographical realm was selected due to the known high species richness of pteridophytes in the area (Tryon, 1972; Tryon, 1986; Moran, 2004; Kreft *et al.*, 2010; Tryon & Tryon, 2012) and the high number of SRLI occurrence points for the region in order to make reasonably robust SDMs.

There are 202 forest species in the SRLI pteridophyte sample that occur in the Neotropics, 11 of which occur both in the Neotropical and Nearctic biogeographical realms and 5 of which are widespread species with trans-continental distributions. For the purpose of the ESH-SDM comparison, it was decided to use just the species that are endemic to the Neotropics, as it was complicated to include pseudo-absence data - an essential element of the SDM calculation for controlling sampling bias - for different parts of the world (Syfert *et al.*, 2013). There are 186 SRLI forest pteridophyte species that are endemic to the Neotropics with 13 640 occurrence points for them all (Figure 75). A list of the SRLI forest pteridophyte species that are endemic to the Neotropics is given in Appendix A10.

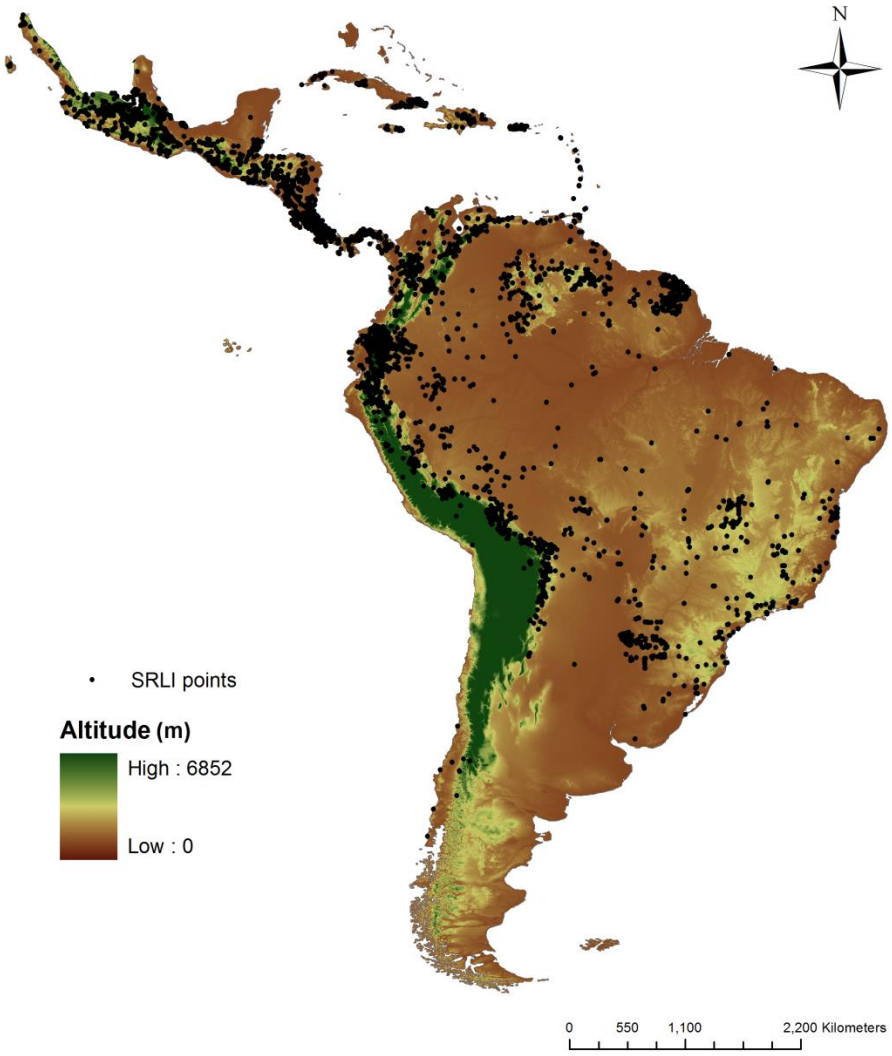

Figure 75. Altitude of the study area with the SRLI occurrence points of the 186 forest pteridophyte species, endemic to the Neotropics.

Two geographical ranges were calculated per species: using both the ESH calculation method and the SDM calculation method. The species ESHs were calculated using the ESH method presented in Chapter 2: the SRLI occurrence points of the selected pteridophyte species were used to produce the species EOO, then the ESH of each species was calculated based on information appropriate to the ecology for that species, as well as land cover and environmental information, within the convex hull defining the species' EOO (details in Chapter 2, section 2.2.2.2). Three variables were used in the calculation: altitude (SRTM v.4) (Jarvis *et al.*, 2008), land cover (GlobCover v. 2.2) (Bicheron *et al.*, 2008) and water balance (Mulligan, 2011). All variables had a 1km spatial resolution.

The species distribution models (SDMs) were produced by Mindy Syfert (Natural History Museum, London) and were created using the MaxEnt modeling technique (Version 3.3.3) (Phillips *et al.*, 2006). MaxEnt (maximum entropy) is a machine learning modelling technique which predicts species distribution based on the assumption that a probability distribution with the maximum entropy (i.e. the most spread out or closest to uniform) is the best fit for an

unknown distribution. It is widely used (Merow *et al.*, 2013) since it is among the best-performing of correlative SDM approaches using presence-only data (Elith *et al.*, 2006). Steps taken to build the SDMs follow Syfert *et al.* (2013) and Syfert *et al.* (2014). The same occurrence points used to calculate the ESH were used to build the SDMs. Ecological variables relevant to pteridophyte distributions were selected and hierarchical clustering, principal components and Pearson correlation analyses were used to reduce multicollinearity. The SDMs were built with the following variables: annual precipitation, minimum temperature of the coldest month, and the precipitation of the coldest and warmest quarters all obtained from the WorldClim database (Hijmans *et al.*, 2005), annual actual evapotranspiration (AET) (CGIAR-CSI, 2008) and water balance (Mulligan, 2011). All variables had a 1km spatial resolution. Following Phillips *et al.* (2009), to reduce the effects of the geographical sampling bias in the SRLI occurrence data, all available occurrence points of plant species were included as pseudo-absence points in the analysis based on the assumption that they have a similar sampling bias to that of the investigated species. The SDMs were evaluated using the AUC accuracy metric where an AUC value of 1 is considered to be a perfect prediction whereas a value of 0.5 or less is considered to be a prediction no better than random.

Land cover was not included as a variable in the original SDM calculation method of Syfert *et al*. (2013) as it is a dynamic non-climatic variable and is not commonly used as a variable predictor in SDMs. However, studies have shown that SDMs are better at predicting species distribution of a certain time by combining land cover together with climatic variables (Iverson & Prasad, 1998; Pearson *et al.*, 2004; Thuiller *et al.*, 2004; Stanton *et al.*, 2012). For this reason, it was decided to include land cover (GlobCover v. 2.2, Bicheron *et al*., 2008) in SDMs here, in order to make them comparable with the species ESHs. In addition, while each ESH was produced within the convex hull defining the species' EOO, each SDM spatial extent included the species' EOO plus a 200 km buffer, following VanDerWal *et al.* (2009). To make them comparable, each SDM was clipped to the species' EOO by the author of this study.

A comparison was made between the species' original EOOs and their ESHs and between the EOOs and the equivalent SDMs. To determine if there are statistically significant differences between the species' ESH/EOO and SDM/EOO ratios, the non-parametric test Mann-Whitney U was used. In addition, the species' ESH and SDM areas were compared by plotting the ESH area against the SDM area of each species. For this analysis, the species were separated firstly by the size of their EOO and secondly by their number of specimens (SRLI occurrence points), to investigate whether the similarity between the two sets is influenced by the number points and the size of the EOO used in calculating the species' ranges. An ordinal linear regression between the ESH and SDM areas was performed for each group of species. Lastly, the SDM areas that overlapped with the ESH areas were calculated using spatial tools in ArcGIS 9.3 (ESRI, 2009) for each species to further investigate the similarity between the two set of ranges.

4.2.2 Comparing the ESH and SDM species richness maps

The first species richness map (hereafter referred to as the ESH species richness map) was produced by stacking all the species' ESHs together, and therefore summing the presence of the species, whereas the second map (hereafter referred to as the SDM species richness map) was produced by stacking all the SDMs together. More details on producing the species richness maps can be found in Chapter 3, section 3.2.1.

Firstly, to test the similarity of the two maps, both maps were normalised to values between 0 and 100, and a frequency distribution graph was produced. This was followed by the calculation of a difference map to identify the biggest differences between the two maps. In addition, a map comparison method – the fuzzy numerical method – was carried out with the Map Comparison Kit (version 3.) (Visser & de Nijs, 2006). The fuzzy numerical method was developed by the Research Institute for Knowledge Systems (RIKS) based on fuzzy set theory. This theory defines a fuzzy set as "a class of objects with a continuum of grades of membership" (Zadeh, 1965). The Fuzzy Numerical statistic (Equation 1) was developed specifically for the comparison of numerical maps and it expresses "the similarity at one location which is set by the degree to which a cell in one map is similar to its counterpart in the other map" (Hagen, 2006).

$$f\ (a,b) = 1 - \frac{|a-b|}{\max(|a|,|b|)} \qquad \text{(Equation 1)}$$

Where *f(a,b)* express the similarity of two values and *a* and *b* are the values of a specific cell in each map.

The two maps were also compared with a Pearson linear correlation analysis. The analysis was conducted in order to measure the strength and direction of association that exists between the two maps. A random sample of 1000 points across the Neotropics was used in the analysis.

The species richness patterns of both maps were evaluated along an altitudinal gradient in order to explain the differences in the patterns between the two maps. In addition, due to the importance of protected areas in conservation decision-making, the two maps were compared by plotting the frequency distribution of species richness values of each map, inside and outside of protected areas. This comparison was made to examine whether the two maps were predicting higher frequency of medium and high species richness values within than outside protected areas. The World Database of Protected Areas data (IUCN & UNEP, 2015) were used for this comparison.

In order to test their accuracy, the ESH and SDM species richness maps were validated using fieldwork data from the study by Kessler *et al.* (2011). This study conducted twenty elevational transects in natural forest habitats globally, in which multiple 20 x 20 m² plots were sampled for species richness of pteridophytes (see details in Chapter 3, section 3.2.2 and Appendix, A9).

Field data from the species richness plots of six altitudinal transects located in the Neotropics were used for the validation of the ESH and SDM maps. The species richness of those plots was compared with the ESH-derived species richness value and the SDM-derived species richness value of the equivalent 1km resolution pixel.

4.2.3 CASE STUDY: Comparing ESH and SDM species richness maps of Costa Rica

The ESH-derived and the SDM-derived species richness maps were clipped to Costa Rica for a more detailed comparison. As with the Neotropical maps, the ESH-derived and SDM-derived species richness maps of Costa Rica were normalised to values between 0 and 100 and firstly compared with a difference map. Furthermore, the two maps were compared using the fuzzy numerical method with the Map Comparison Kit (version 3.) (Visser & de Nijs, 2006).

Independent field data collected during fieldwork in Costa Rica (Chapter 3, section 3.2.2.2) were used for the ground-truthing validation of the predictions of each map. Species richness numbers from fourteen different species richness plots (5m x 5m) at altitudes from 647 m to 3368 m were compared with the ESH-derived and the SDM-derived species richness values.

4.3 RESULTS

4.3.1 Comparison between ESHs and SDMs

Comparison of the area of the ESH and SDM of each species found that 79% of species had a bigger ESH than SDM. As expected, there was a strong positive relationship ($r^2 > 0.9$, $p<0.001$) between the area of the original EOOs and the ESHs of the species. In contrast, such a strong relationship was not found between the area of the original EOOs and the SDMs ($r^2 > 0.4$, $p<0.05$).

The reduction in the species range (EOO) when using the ESH and SDM metrics is shown in Figure 76. There was a greater mean reduction from EOO to SDM than from EOO to ESH, with a mean reduction in the EOO of 75.9±0.5% and 45.4±0.3% using the SDM and ESH respectively. In addition, there was a statistically significant difference in the ratio of species' EOO to the new extent between the ESH and SDM (Mann-Whitney $p<0.0001$) (Figure 77).

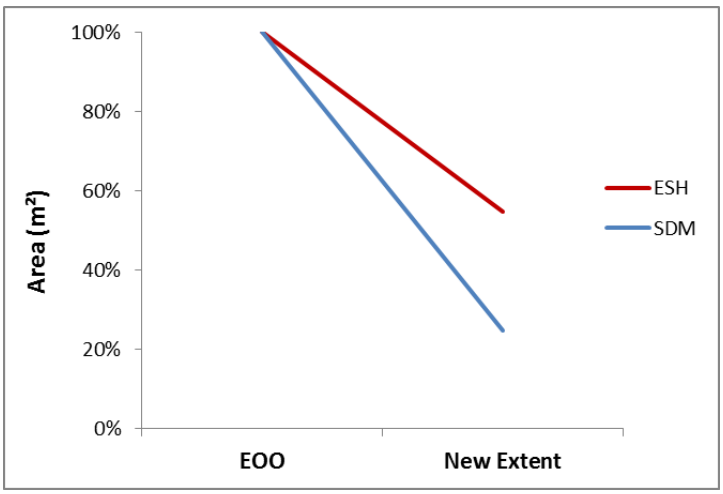

Figure 76. The reduction in the mean EOO when calculating the ESH and SDM of the SRLI forest pteridophyte species endemic to the Neotropics

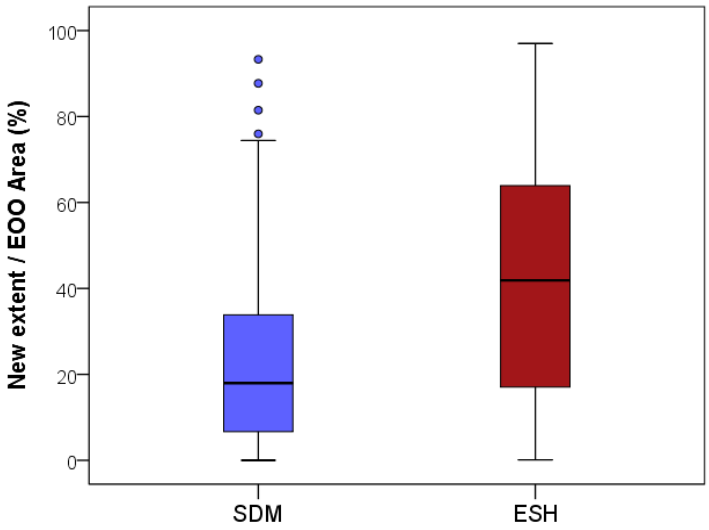

Figure 77. Boxplots representing the new extent /EOO ratio when using the ESH and SDM metrics to calculate the geographical ranges of the SRLI forest pteridophyte species which are endemic to the Neotropics.

In addition, a simple linear regression was performed to compare the size of the species' ESHs and SDMs which showed that the two sets of areas are more similar than different (r^2=0.68) (Figure 78a). The calculated areas of the two sets were most similar in species with small original EOOs (r^2=0.67) (Figure 78b), and this similarity decreased in species with medium and large EOOs (r^2=0.27-0.31) (Figure 78c & 78d). When separating the species based on number of specimens (SRLI occurrence points) and comparing their SDM and ESH area (Figure 79), the two metrics are most similar (r^2=0.93) when the species' ranges were calculated using 15 – 50 occurrence points (Figure 79b) followed by when they were calculated using 3 – 15 occurrence points (r^2=0.86) (Figure 79a). The species' SDM and ESH areas were shown to be most different in species with more than 100 occurrence points (r^2=0.33), which also had the largest EOO size (Figure 79d).

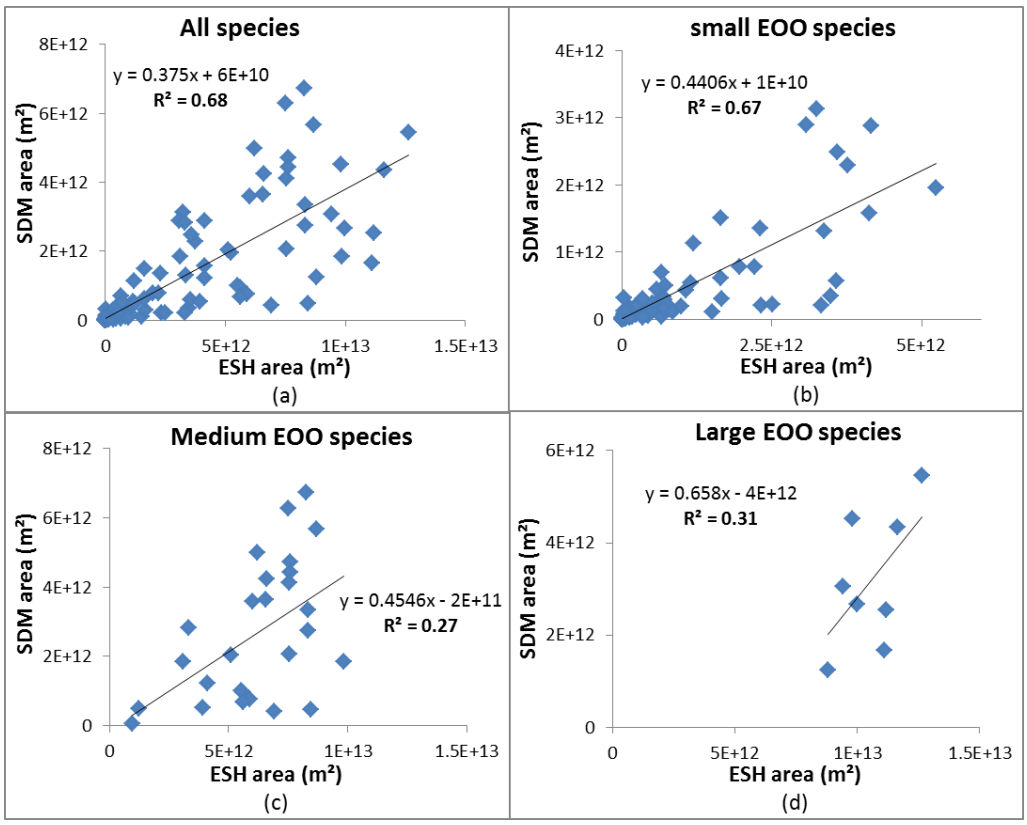

Figure 78. Comparison of the SDM area and the ESH area of (a) all SRLI pteridophyte forest species endemic to the Neotropics, (b) species in the sample with small EOO size (2.2 x 10^7 to 6.5 x 10^{12} m²), (c) species in the sample with medium EOO size (6.5 x 10^{12} to 1.3 x 10^{13} m²) and (d) species in the sample with large EOO species (1.3 x 10^{13} to 1.9 x 10^{13} m²). Goodness of fit of linear regression (R^2) is reported.

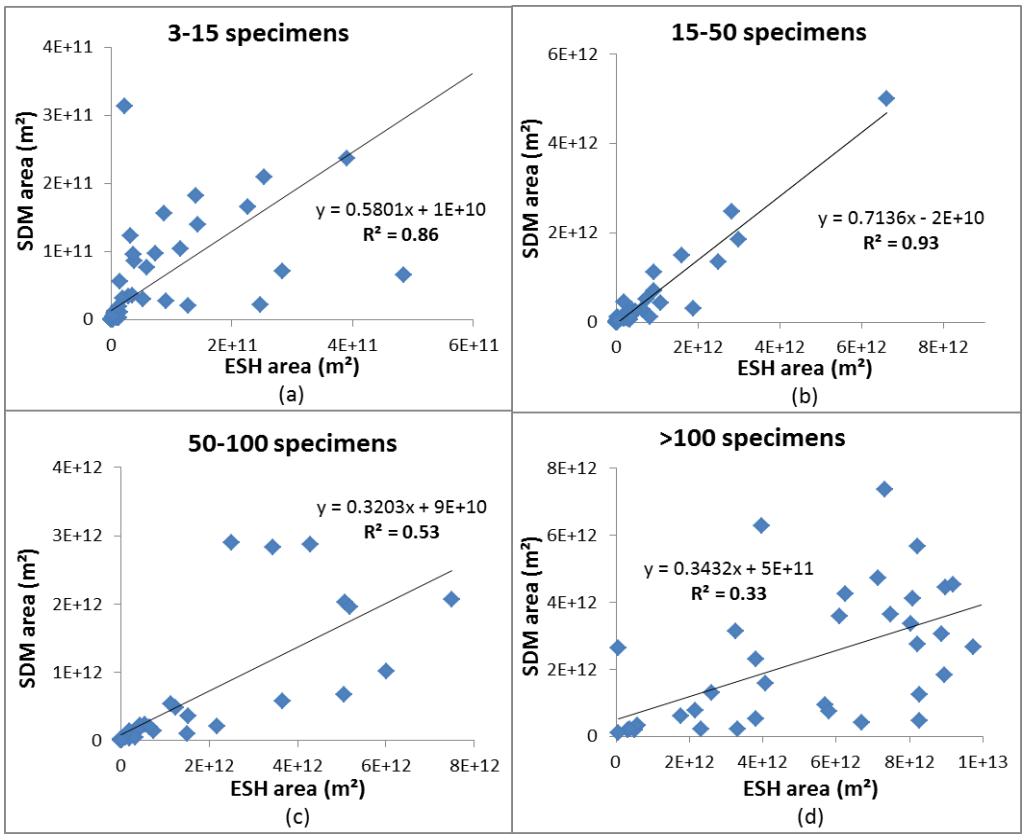

Figure 79. Comparison of the SDM and the ESH areas for species with (a) 3 – 15, (b) 15 – 50, (c) 50 – 100, (d) more than 100 SRLI occurrence points (specimens). Goodness of fit of linear regression (R^2) is reported.

The similarity between the species SDMs and ESHs was also investigated by calculating the common (overlapping) areas of the predicted SDM and ESH ranges of each species. As shown in Figure 80a, the ESH and SDM areas of more than half of the investigated species overlapped by more than 40%. Thirty species (18%) had their ESH and SDM areas overlapping by 0 – 20% whereas for twenty four species (14%) their ESH and SDM areas were overlapping by 80 – 100%. The ESH and SDM areas overlapped completely (100%) for just one species. The mean percentage of the species ESH area overlapping with the SDM area was 56±14%. Moreover, as with the comparison of the size of the ESH and SDM areas, greater similarity (overlap) was found in species with smaller original EOO (Figure 80b) and in species that had between 3 and 50 specimens (Figure 80c). However, the relationship between the ESH-SDM overlap and the two variables (EOO size and number of specimens) was not statistically significant.

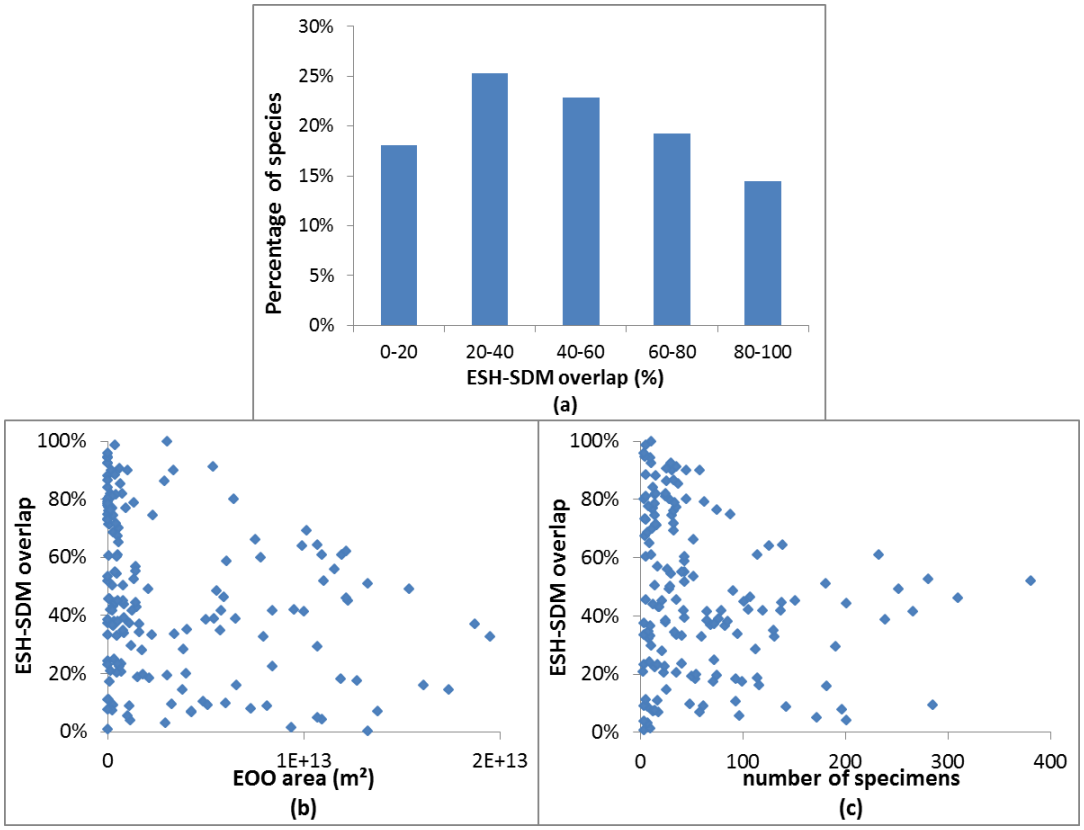

Figure 80. Percentage of the species' ESH area overlapping with the equivalent SDM against (a) percentage of species, (b) the original EOO area and (c) number of occurrence points (specimens).

4.3.2 Comparison between the ESH and SDM species richness maps

The ESH and SDM species richness maps are presented in Figure 81. The ESH species richness map predicted higher species richness across the region compared to the predictions of the SDM species richness map. While the ESH species richness map predicted a value of 71 (species) as the maximum species richness, the SDM species richness map predicted a maximum value of 41 (species). When the effect of area was taken into account (mean species richness value per suitable area (see details in Chapter 3, section 3.2.3)) the ESH species richness map had a mean value of 22.3±15.6 species per Km², 13 species more than the equivalent value of the SDM species richness map (9.3±5.4 species per Km²). In both maps, the area with the highest species richness value was the Talamanca Mountain Range in Costa Rica.

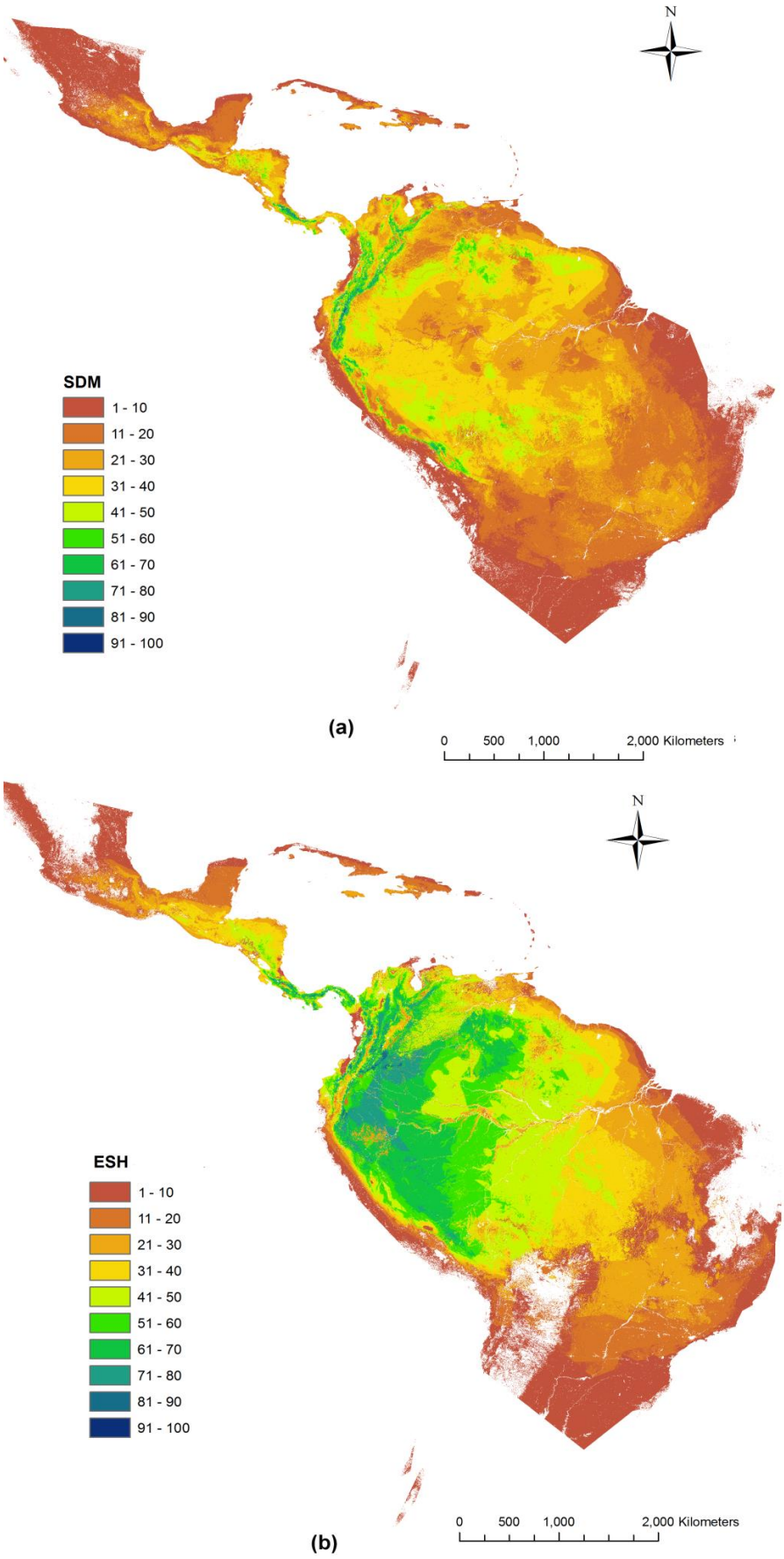

Figure 81. (a) ESH and (b) SDM species richness maps of the SRLI forest pteridophyte species endemic to the Neotropics. Data are normalised (0 – 100) and classified in ten equal intervals. White colour represents 0 value of species richness.

To investigate the similarity of the two maps, a frequency distribution map was produced of the normalised species richness maps. As shown in Figure 82, both maps have a similar trend with more pixels with low and medium species richness values and fewer pixels with high values. While the SDM species richness map has more pixels with low species richness values, the ESH species richness map has more pixels with medium and high values. This reflects the fact that the medium and high species richness values of the SDM species richness map are limited to the areas with high altitudes (Figure 81a) whereas the ESH species richness map predicts medium and high species richness values for wider areas, including the lowlands of the Amazon basin (Figure 81b).

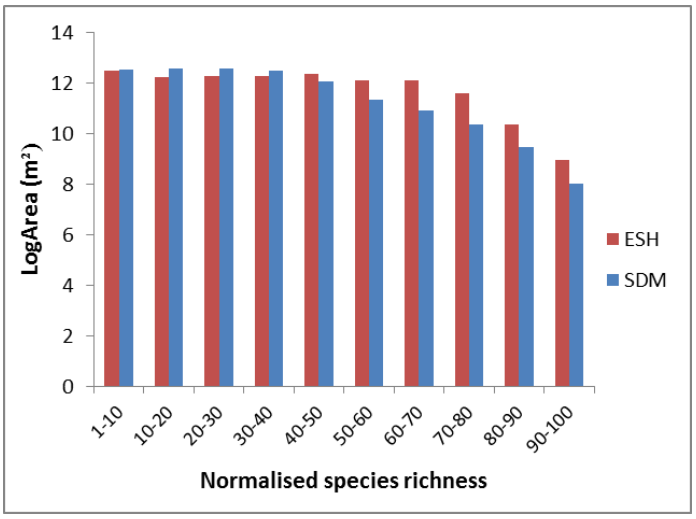

Figure 82. Frequency distribution of the ESH and SDM species richness values (normalised 0 – 100). Pixels numbers are presented as log area (m²).

The difference map of the two species richness maps (Figure 83) indicated that there were substantial differences between them even though they were derived from identical datasets. The mean absolute difference value per Km² of the two species richness maps was 18.3±8.6 species. The biggest difference was seen in the West Amazon basin area, where the ESH species richness value was higher than the SDM value, and in the highest altitudes of the Andes and Talamanca Mountain Range, where the SDM value was higher than the ESH value. The ESH species richness values were higher in low and medium altitudes whereas the SDM species richness values were higher in mountain ranges. The only exceptions to this were the arid areas of the Caatinga region of East Brazil and the Chaco Seco region of West Paraguay, which appear as non-suitable areas in the ESH species richness map (0 species) but as suitable areas in the SDM species richness map (Caatinga area: 1 – 5 species, Chaco Seco area: 4 – 9 species). When compared using the fuzzy numerical metric, the average similarity of the two maps was 0.66 (0 = fully distinct, 1= fully identical) showing that there are more areas that agree than areas that disagree (Figure 84). The fuzzy numerical map indicated that areas with the highest altitudes in the mountain ranges were the least similar between the two maps although mid altitude montane areas appeared to be the most similar. Other dissimilar areas were the surrounding areas of the Caatinga region, areas in the West Amazon and areas in the Llanos basin of Columbia.

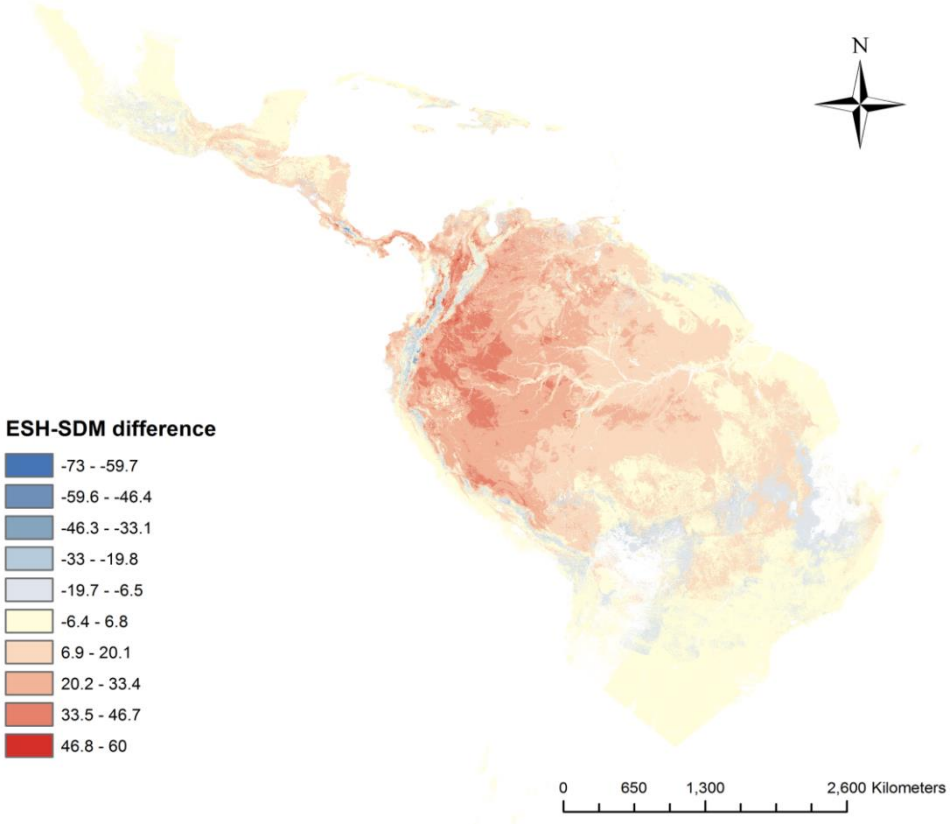

Figure 83. Difference map between the ESH species richness map (Figure 81b) and the SDM species richness map (Figure 81a) (excluding zero values of each map). Positive values mean ESH is higher than SDM and negative values that SDM is higher than ESH.

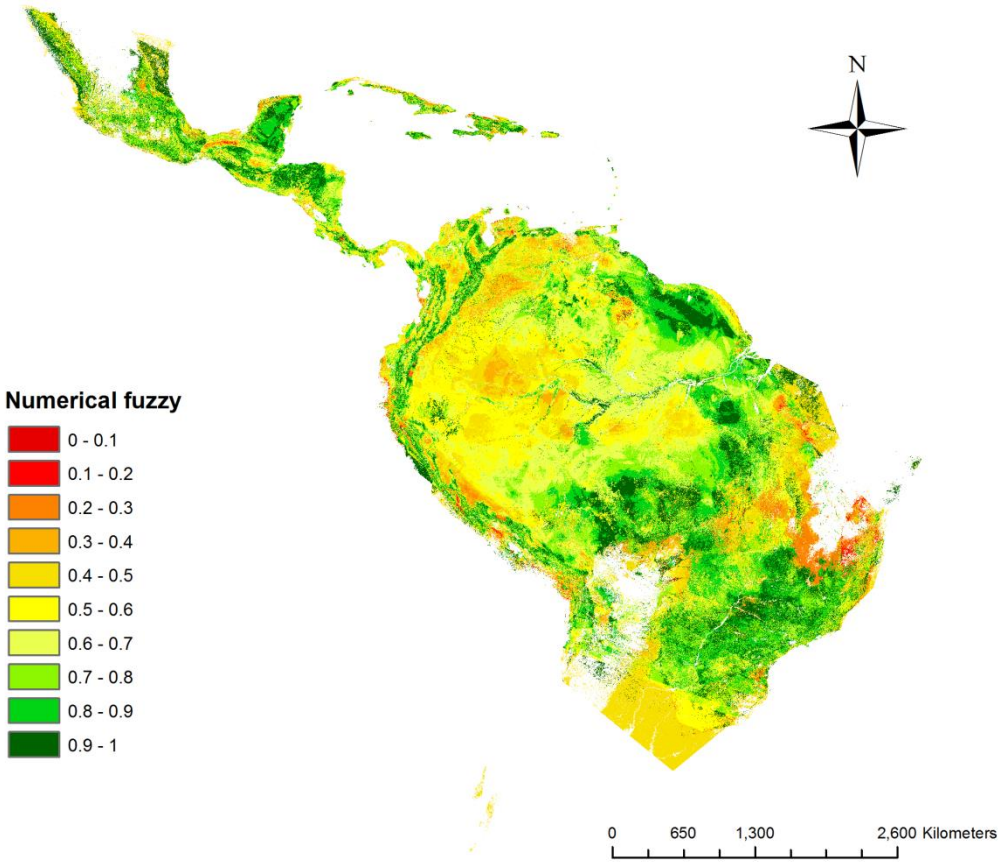

Figure 84. Similarity map of the ESH species richness map and the SDM species richness map, created using the fuzzy numerical method (0 = fully distinct, 1= fully identical). Zero values of each map were excluded in this analysis.

Figure 85 shows the comparison of the ESH and SDM species richness maps by using random points and plotting these points against the equivalent species richness. The result of the Pearson correlation analysis ($r = 0.77$, $n = 1000$, $p < 0.001$) showed that there was a strong positive correlation between the two maps, which is statistically significant.

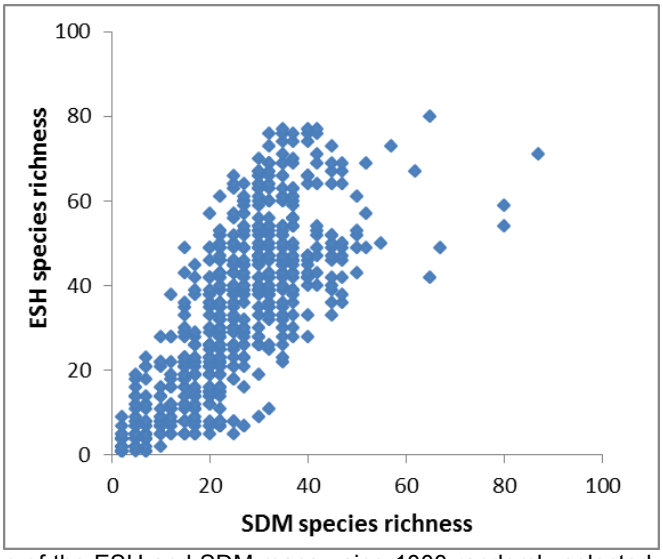

Figure 85. Comparison of the ESH and SDM maps using 1000 randomly-selected points and plotting the equivalent species richness values. Values are normalized between 0 and 100.

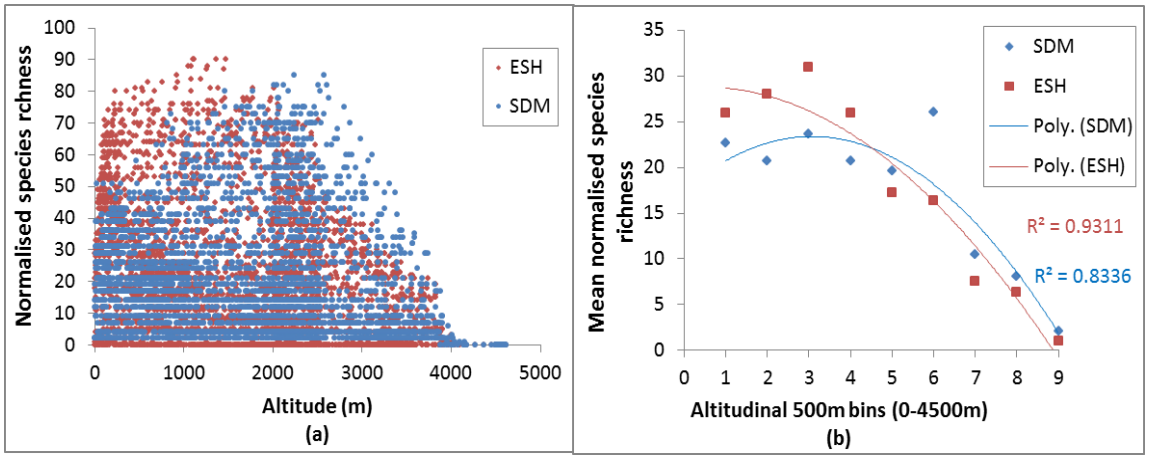

Figure 86. (a) The relationship between ESH and SDM species richness (normalized 0 – 100) and altitude for SRLI forest pteridophyte species endemic to the neotropics produced using 500 randomly-selected points per 500m altitudinal bands and plotting the equivalent species richness values against altitude. (b) Mean normalized ESH and SDM species richness in altitudinal 500m bins presented in ascending order. Goodness of fit of polynomial regression (R^2) is reported.

Species richness patterns of both species richness maps were evaluated along an altitudinal gradient (Figure 86). The ESH-derived species richness peaked at mid-altitudes (1000 – 2000m) whereas the SDM-derived species richness peaked at higher altitudes (2000 – 3000m). Relatively higher ESH-derived species richness than SDM-derived species richness was found

at the lower altitudes (0 – 2000m). The opposite pattern was found at the higher altitudes (2000 – 4000m).

The two maps were also compared by plotting their species richness frequency distribution values outside (Figure 87a) and inside (Figure 87b) protected areas. In both, outside and inside protected areas, the SDM and ESH maps had less area with high species richness values (70 – 100 species) and more area with low and medium species richness values (1 – 70 species). In addition, in the first case (outside protected areas) there was more area with low values (1 – 20 species) whereas in the second case (inside protected areas) there was more area with medium values (20 – 50 species). In the first case, while both SDM and ESH maps had more area with species richness values between 1 and 40 species, the ESH map had more area with 1 – 10 species whereas the SDM map had more area with 10 – 20 species. In the second case the SDM map had more area with 10 – 50 species whereas the ESH map had more area with 20 – 60 species. Both within and outside protected areas, the ESH map had more area with medium and high species richness values (60 – 100) than the SDM map.

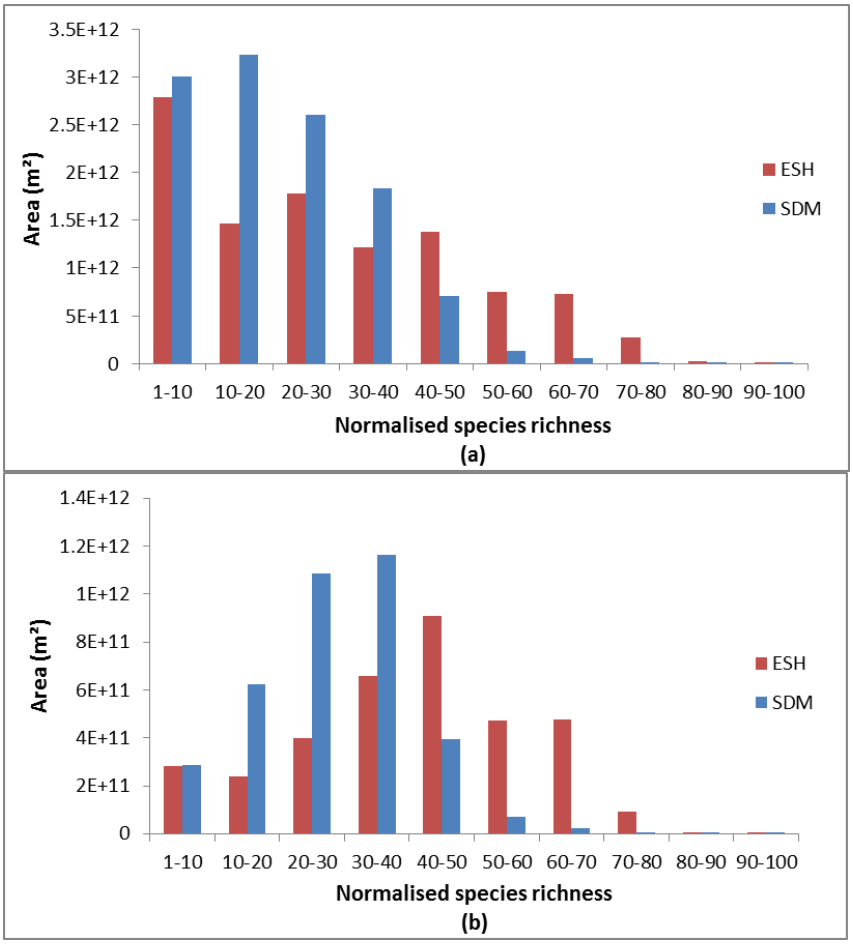

Figure 87. Frequency distribution of the ESH and SDM species richness values (normalised 0 – 100) (a) outside and (b) inside protected areas. Pixels numbers are presented as area (m²).

In order to test their accuracy, the ESH and SDM species richness maps were validated using an independent dataset, field data from the study of Kessler *et al.* (2011) (Figure 88). The field data revealed a mid-altitude (1500 – 2000m) peak of species richness and a hump-shaped

relationship between species richness and altitude. This was not the case with the patterns of the two species richness maps which appeared more similar to each other than to the field data. At the study sites from Kessler *et al*. (2011), both the SDM-derived and the ESH-derived species richness peaked between 1000 – 1700m although the SDM-derived species richness had similar high values at higher altitudes (2000 – 2500m). Based on the field data, and as seen in previous analyses, the ESH map appears to be overestimating species richness in the lowlands (0 – 1000m) whereas the SDM map appears to be overestimating species richness in the highlands (2000 – 4000m).

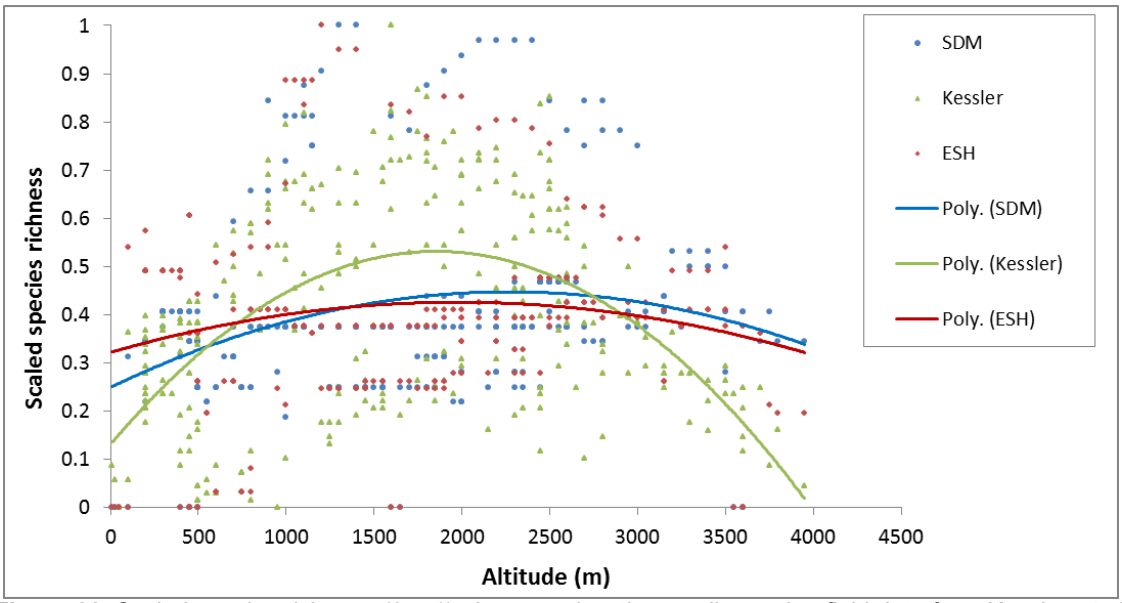

Figure 88. Scaled species richness (0 – 1) along an elevation gradient using field data from Kessler *et al*. (2011), from the SDM species richness map and from the ESH species richness map.

4.3.3 Case study: Costa Rica

The ESH and SDM species richness maps are presented in Figure 89. As with the Neotropical species richness maps, the ESH species richness map of Costa Rica had a higher maximum species richness value (71 sp.) and a higher mean value per Km² (33.3±12.7 species) than the SDM map of Costa Rica (maximum value: 41 sp., mean value per Km²: 15.6±7.4 species). Both maps predicted higher species richness in the montane areas (mid and high altitudes) and fewer species in the dry lowlands. The Talamanca Mountain range and the Central Mountain range were the areas with the highest species richness values in both maps.

The mean absolute difference value per Km² was 17.1±7.2 species. The difference map of the ESH and SDM species richness maps (Figure 90a) showed that the ESH values are higher in the lowlands whereas the SDM values are higher in the highlands. It was obvious, even by looking at the SDM species richness map (Figure 89b) that there was a great difference in species richness between the lowlands (lower species richness) and the montane areas (medium and high species richness) in the predictions of the SDM map. This was not the case with the ESH species richness map where medium species richness values were also found in areas outside the Mountain Ranges.

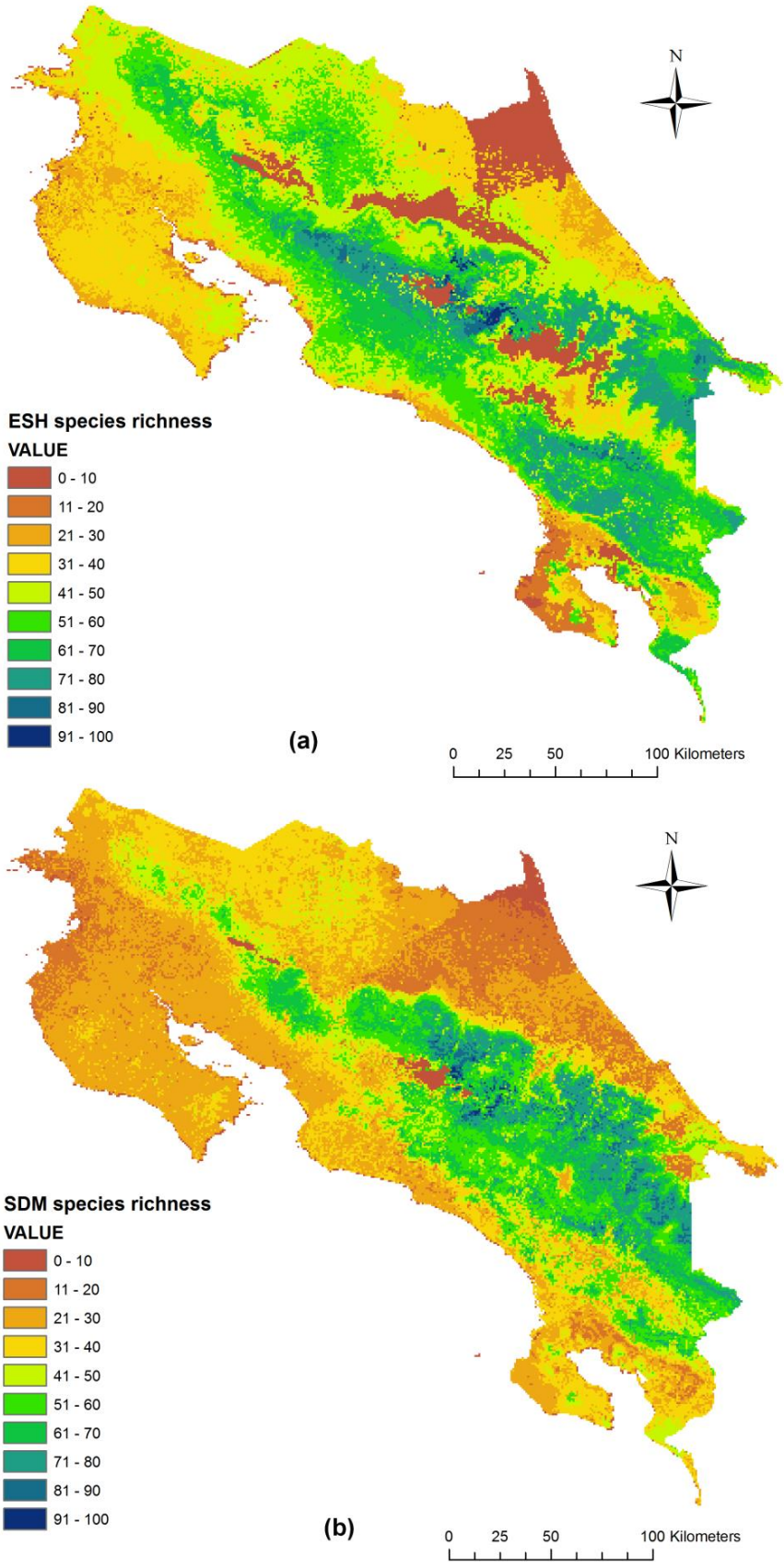

Figure 89. Species Richness maps of Costa Rica produced using the (a) ESHs and the (b) SDMs of the SRLI forest pteridophyte species endemic in the Neotropics. Data are normalised (0 – 100) and classified in ten equal intervals.

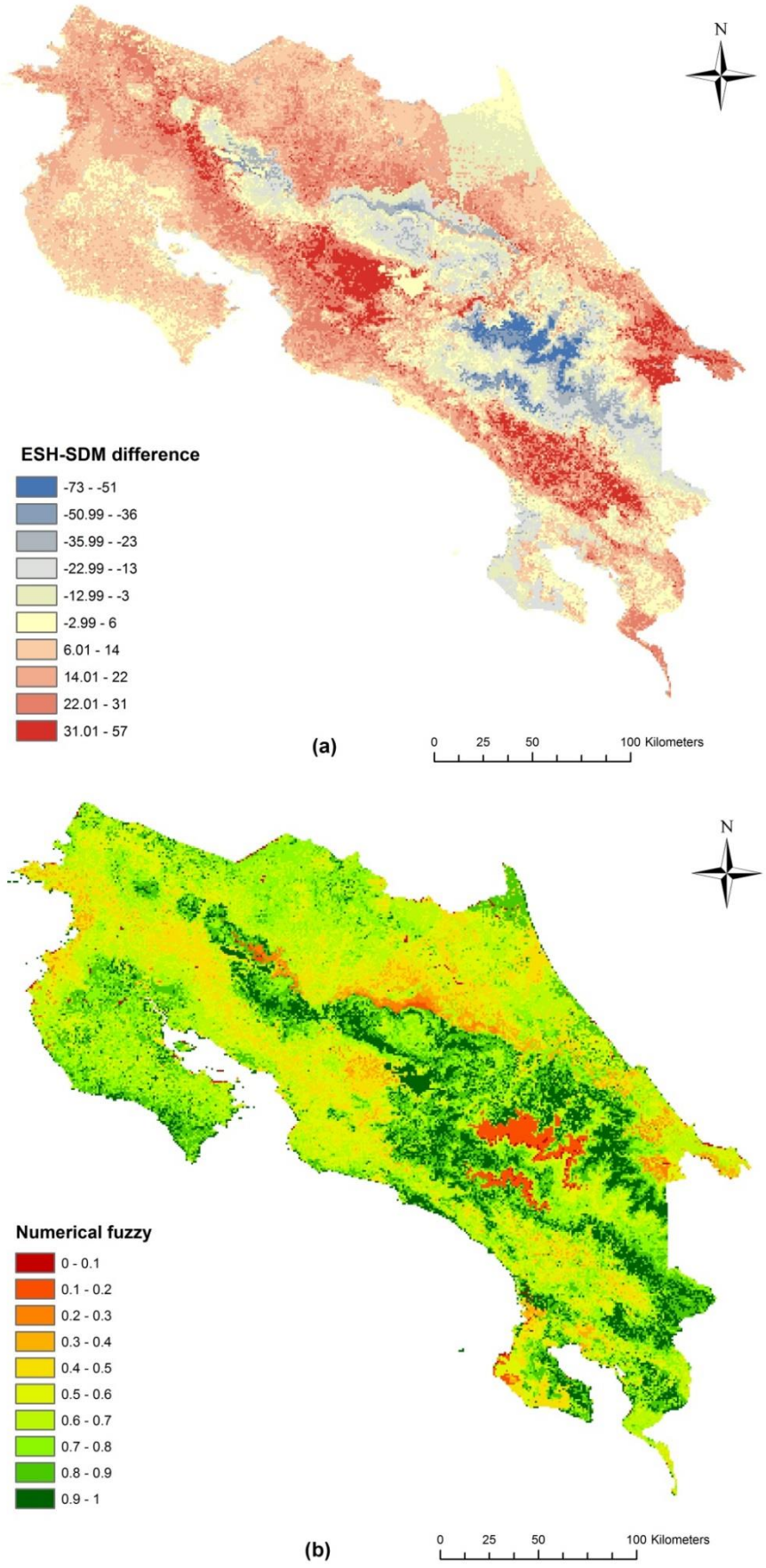

Figure 90. (a) Difference map (positive values mean ESH is higher than SDM) and (b) similarity map created using the fuzzy numerical method (0 = fully distinct, 1= fully identical), of the ESH species richness map and the SDM species richness map.

The average similarity of the two maps, according to the fuzzy numerical metric, was 0.67 (0 = fully distinct, 1= fully identical) (Figure 90b). The most similar areas between the two maps were the montane areas with mid altitudes whereas the most different areas were the ones with the highest altitudes (páramo areas). Other areas that appeared to be different based on the fuzzy numerical metric were the west part of the Osa peninsula and areas on the Atlantic side of the Talamanca mountains.

Data collected during fieldwork in Costa Rica were used for the ground-truthing validation of the predictions of the two species richness maps. As shown in Figure 91, the mid-altitude peak in species richness found from field data broadly agrees with the mid-altitude peak in species richness from the ESH and SDM maps. However, in both maps, the decline in richness at lower (less than 1500m) and higher (above 2500m) altitudes is less pronounced compared with the one found from the fieldwork data. The altitude-species richness pattern found from the ESH species richness map resembled more closely the pattern from the SDM map than the one from field data.

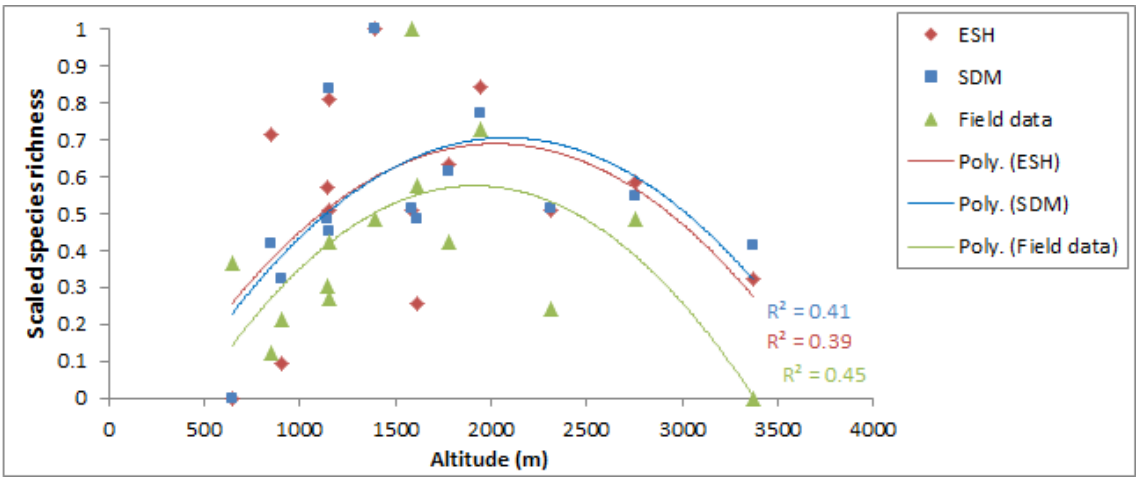

Figure 91. Scaled species richness along an elevation gradient from field data collected in Costa Rica and from the SDM and ESH species richness maps. Goodness of fit of polynomial regression (R^2) is reported.

4.4 DISCUSSION

4.4.1 Comparison of the ESH and SDM metrics

In this study, the ESH metric was used to calculate species geographical ranges by incorporating habitat and it was shown that this metric reduces commission errors associated with the EOO (Chapter 2). Here, the ESHs of the SRLI pteridophyte forest species were compared with the equivalent SDMs which were built using the same SRLI occurrence data and with an established method (Syfert *et al.*, 2013; Syfert *et al.*, 2014).

The comparison was first made with reference to the species' original EOO and it was found that there was a larger mean reduction of the EOO area when the species range was calculated with the SDM metric (75.9±0.5%) than with the ESH metric (45.4±0.3%). According to Gaston and Fuller (2009), habitat suitability models, including SDMs and ESHs have greater commission errors than omission errors. The highest mean reduction of the EOO when using the SDM metric and the high accuracy of the SDMs (mean AUC = 0.8) suggests that SDMs are more effective than the ESHs in reducing commission errors related with the EOO. However, this could not be tested as independent data from GBIF were either limited (1 – 3 points) or were not available for the investigated species (SRLI forest pteridophyte species endemic to the Neotropics). Nevertheless, SDMs were expected to have fewer commission errors and to be smaller than the ESHs due to the conservative approach of the ESH calculation method (Chapter 2, section 2.2.2.2). While ESHs included all habitat types and the broader altitude/water balance ranges associated with each species, SDMs were more specifically designed for each species as they were based on the statistical association between the species occurrence data and several predictor variables. Furthermore, the higher mean reduction of the EOO when using the SDM metric could also be explained by the fact that SDMs may better capture, through their statistical associations, many processes which have influenced the species' distribution through time. ESHs were found to overestimate the geographical range of a species (Chapter 3, section 3.4.1) at low altitudes which was partly explained by the fact that they do not take into consideration all abiotic and biotic factors that could further limit a species range (Davis *et al*., 1998; Morrison *et al*., 2006). Similarly with ESHs, SDMs do not capture biotic interactions since they were calculated without dynamic predictor variables and with presence-only data, (Guisan & Zimmermann, 2000; Soberon, 2005; Hirzel & Le Lay, 2008; Jiménez-Valverde *et al*., 2008; Gaston & Fuller, 2009). However, SDMs better capture the specific environmental space of the species since more variables are used.

Results of this study (Chapter 2, section 2.3.2.2.2 and Chapter 5, section 5.3.1) showed that the average size of suitable habitat decreases with increasing category of threat. It was then suggested that the ESH metric could be used to create quantified ESH thresholds for threatened Red List Categories under sub-criterion b(iii). It was therefore important to determine the accuracy of the calculated area size of the species' ESHs by comparing it with the area of the SDMs. The comparison of the species' ESH and SDM sizes showed that the two sets of areas are more similar than different (r^2=0.7). It was also investigated whether the two metrics were predicting identical areas within the species distribution. The mean percentage of the species ESH area overlapping with SDM area was found to be 56±14% with the ESH and SDM areas of more than half of the investigated species overlapping by more than 40%. These results from the two comparisons (size and overlapping area) show that despite the simplicity of the ESH calculation method, the ESH approach is predicting species' distributions that have a considerable level of similarity with statistically based and more sophisticated SDMs.

In both cases (size and overlapping area), ESHs were most similar to SDMs for species with small original EOOs (2.2 x 10^7 to 6.5 x 10^{12} m²) (Figures 78b & 80b). It was also found that the

ESH area is strongly correlated (r^2=0.9) with the original EOO area, showing that the larger the EOO the more suitable habitat is available for a species. This was not the case with the SDM area, which was not correlated with the EOO area (r^2=0.4). However, there was a strong relationship (r^2=0.8) between the SDM and EOO area in species with small EOOs, similar to the relationship between the ESH and EOO area. The majority of these species are either found in montane areas (e.g. *Terpsichore pichinchense* and *Ctenitis chiriquiana*) or in islands (e.g. *Asplenium hobdyi* and *Asplenium underwoodii*). The greater similarity between the ESHs and SDMs in species with small EOOs can be explained by the fact that these species are habitat specialists; for example *Terpsichore pichinchense* is only known to occur at high altitudes (>3000m) (Schneider, 2013). In their case, the species' occurrence points can effectively capture the strict ecological/habitat requirements of these species, despite their low number (3 – 50 occurrence points) (Figures 79a, 79b & 80c). Thus, adequate information on the ecological/habitat requirements is provided for both metrics (ESH and SDM) to predict accurate distributions. This agrees with previous studies that reported higher accuracy of SDMs for habitat specialist than generalist species (Segurado & Araújo, 2004; Elith *et al.*, 2006; McPherson & Jetz, 2007; Franklin, 2009; Grenouillet *et al.*, 2011). It is therefore assumed that both metrics can discriminate suitable from unsuitable habitat more easily for species with strict habitat requirements and consequently small EOOs resulting in similar predictions. However, for some species, the similarity between the ESH and SDM was low even though their EOO was small. These cases included species with small EOOs due to high levels of habitat loss within their geographical range (e.g. *Asplenium congestum* and *Ceradenia melanopus*). Thus, the low similarity between ESH and SDM reflected the different weight that each method assigned to the land cover variable.

Species with larger EOOs had lower similarity between their ESHs and SDMs. This was not a surprise as these species occur in a variety of environments (e.g. *Adiantopsis chlorophylla*) and thus their occurrence points may not have provided complete information on the species' habitat requirements, for either method. It was expected that species with medium to large EOOs with a large number of occurrence points would have relatively high similarity between their ESHs and SDMs, however. This was true for some species such as *Diplazium grandifolium* (EOO: 1.3 x 10^{13} m^2, occurrence points: 233) the ESH and SDM of which had 65% overlap and were similar in size (ESH: 6.1 x 10^{12} m^2, SDM: 5.3 x 10^{12} m^2). However, the ESHs and SDMs of other widespread species (e.g. *Elaphoglossum lingua* and *Anemia phyllitidis*) with large numbers of occurrence points were not similar. Two possible explanations were identified, the first one being the uneven distribution of the species' occurrence points (i.e. sampling bias) which can result in the habitat requirements of the species not being captured. While the effect of the geographical sampling bias in the SRLI occurrence data (identified in Chapter 2, section 2.2.1) was reduced in the SDM approach by adding pseudo-absence points (Syfert *et al*, 2013), this issue was not addressed in the ESH approach. Another explanation could be the overestimation of the ESH metric in the lowlands due to the nature of the ESH method (details in Chapter 3, section 3.4.1). This could be the case for *Elaphoglossum lingua* which has 201 occurrence points but only 10% overlap between its ESH and SDM ranges. The ESH of this species was

significantly more extensive (70%) in the lowlands than the equivalent SDM and the ESH-SDM overlap occurred mainly in montane areas.

The above comparison between SDMs and ESHs was focused on the easily-recognized uncertainty of the ESHs (details in Chapter 2) and was based on the assumption that the SDMs had higher level of accuracy. However, there were cases where both the accuracy (AUC value) of SDMs and the ESH-SDM overlap were low showing that in these cases the difference between the ESH and SDM may have been caused by the inaccuracy in the SDMs. Such cases are the species *Elaphoglossum longifolium* (SDM AUC value: 0.56, ESH-SDM overlap 5%: and *Selaginella poeppigiana* (SDM AUC value: 0.65, ESH-SDM overlap: 19%) which had fewer than 10 occurrence points. Small sample size is known to affect the accuracy of SDMs (Pearson *et al.*, 2007; Wisz *et al.*, 2008).

4.4.2 Comparison of the ESH and SDM species richness maps

The SDM and ESH approaches were not only compared using the species' ESHs and SDMs but also using the ESH- and SDM-derived species richness maps. The ESH species richness map predicted higher species richness in the Neotropical region compared to the predictions of the SDM species richness map reflecting the smaller mean reduction of the species' EOO when using the ESH metric. Interestingly, the overall similarity between the two species richness maps matched the similarity between the species' ESH and SDM sizes (r^2=0.68). The fuzzy numerical metric confirmed that the two maps were more similar than different (fuzzy numerical metric = 0.66) whereas the Pearson correlation analysis showed that there was a strong positive correlation between the two maps (r =0.77, n=1000, $p < 0.001$).

Both maps identified identical areas with the highest species richness value. These were the Talamanca Mountain Range in Costa Rica and the Andes Mountain Range in South America, both of which are known for their high levels of pteridophyte species richness (Tryon, 1986; Moran *et al.*, 1995; Tryon & Tryon, 2012) and are recognised biodiversity hotspots (Mittermeier *et al*., 1998; Myers *et al*., 2000; Brummitt & Nic Lughadha, 2003). This pattern agrees with the findings of Kreft *et al.* (2010), which showed that pteridophyte species richness reaches its highest values in tropical montane wet forests.

However, ESH-derived species richness peaked at mid-altitudes (at about 1500m) whereas the SDM-derived species richness peaked at higher altitudes (at about 2500m) (Figure 86). Previous studies showed that pteridophyte species richness peaks at mid-altitudes with maxima at about 1800m in Costa Rica (Kluge *et al.*, 2006) and at about 2000m in the Bolivian Andes (Kessler, 2000). Thus, at least for this part, the ESH pattern better agrees with the findings of these studies. In addition, at lower altitudes (0-2000m), higher ESH-derived species richness was found relative to SDM-derived species richness, with the opposite pattern at higher altitudes (2000-4000m). Based on field data from the study of Kessler *et al*. (2011) (Figure 88), the ESH map appears to be overestimating species richness in the lowlands (0-1000m)

whereas the SDM map appears to be overestimating species richness in the highlands (2000 – 4000m).

The overestimation in the lowlands of the ESH species richness map has been recognised and discussed in Chapter 3 (section 3.4.1) and therefore differences between the ESH and SDM map in the lowlands were anticipated. This is most obvious in the Amazon basin as it is a continuous area of lowlands. The overestimation of the ESH map in the lowlands explains the greater number of pixels with medium and high values in the ESH map compared with the SDM map, as the lowlands cover the largest percentage of the Neotropics. It also explains the highest frequency of medium and high ESH species richness values within the protected areas of the region. However, SDM species richness was expected to be higher within protected areas as they are selected for high conservation interest (Pressey *et al.*, 1993). Therefore, the SDM map may be underestimating species richness in lowland areas, although this is not apparent when the SDM predictions are compared with Kessler *et al*. (2011) field data. The only distinct lowland areas within which the SDM map predicts higher species richness than the ESH map are the areas of the Caatinga region of north-east Brazil and the Chaco Seco region of West Paraguay which appear as non-suitable habitat in the ESH map. These are arid areas with low water balance values (< -1500 mm/month) that were not assigned to any species during the ESH calculation as according to the SRLI specimen data none of the pteridophyte forest species occurs in those conditions. In contrast to the ESHs, SDMs have identified those areas as suitable areas for some species probably due to the greater number of environmental predictors involved in the SDM calculation.

The fuzzy numerical map indicated that areas with the highest altitudes (>3000m) were the most dissimilar between the ESH and the SDM maps. This is explained by the overestimation of species richness at those altitudes by the SDM map. Areas above 3100m are known as the páramo and are characterized by a cold and humid climate with sudden temperature fluctuations (Herrmann, 1970). Lower species richness is to be expected in these areas as their conditions are limiting for fern growth (Page, 2002; Bickford & Laffan, 2006). While the ESH map predicted low species richness for areas with altitudes between 3100 and 3500, the SDM map predicted medium species richness values at those altitudes. Although previous studies have shown that, in general, SDM species richness maps over-predict species richness compared with field data and macroecological models (Dubuis *et al.*, 2011; Mateo *et al.*, 2012), it is not clear why the SDM map here is predicting such relatively high values specifically in the páramo area. It seems, though, that the environmental predictors of many species' SDMs do not differentiate this area from the montane areas with lower altitudes.

Despite the differences identified between the SDM and ESH maps, the validation of the two maps using an independent dataset showed that the altitude-species richness pattern found in the ESH species richness map resembled more the pattern from the SDM map than the one from field data. This reflects the similarities between the two maps, their identical spatial resolution and the lack of biotic variables in the calculation of both the ESHs and SDMs which

leads to the overestimation of species richness in a geographical unit (Dubuis *et al*., 2011; Mateo *et al*., 2012).

4.4.3 CASE STUDY: Costa Rica

A more detailed comparison was conducted focusing on Costa Rica, the case study area of this project. As with the Neotropical ESH and SDM maps, the average similarity of the two maps for Costa Rica was substantial (fuzzy numerical metric =0.7). Both ESH and SDM maps predicted higher species richness in the montane areas and fewer species in the dry lowlands, similarly to the Neotropical maps. In addition, in both maps, maximum species richness was predicted at altitudes between 1500 and 2500m. This is consistent with the results of previous studies focusing on Costa Rica (Kluge *et al.*, 2006; Watkins *et al.*, 2006; Kessler *et al.*, 2011) which found that, in Costa Rica, pteridophytes' species richness peaks at mid- altitudes. The Talamanca Mountain range and the Central Mountain range are the areas with the highest values in both maps. The two Mountain ranges are designated protected areas with the Talamanca range having the largest undisturbed forest area in Central America (Powell *et al.*, 2001). They form the continental divide between the Atlantic and the Pacific Oceans and hence have a large variation in altitude (500 – 3820 m) and climatic conditions on both sides (González-Maya *et al.*, 2008). According to Obando-Acuña (2002), the montane tropical cloud forests of these ranges are the most diverse and richest in endemics of all areas of Costa Rica. It has also been reported that there are as many as 1000 pteridophyte species in the Talamanca range (Powell *et al*., 2001).

The most similar areas between the two maps were the montane areas with mid altitudes, whereas the most different areas were the ones with the highest altitudes (páramo areas). As seen in the comparison of the set of Neotropical maps, the ESH map captured lower species richness than the SDM map in the páramo area (altitude > 3100 m) of the Talamanca Mountains. The overestimation of the SDMs at these altitudes, identified in the Neotropical SDM map, is obvious here since SDMs predicted species richness in the páramo area as high as in mid-altitude areas. In contrast to the SDM map, the ESH map predicted low species richness in altitudes above 3100m, which agrees with previous studies that also found low numbers of pteridophyte species there. Barrington (2005) estimated a maximum of 80 species in the páramo areas of Costa Rica and Kappelle and Gómez-Pignataro (1992) found that just 15% of the pteritophyte species in the Chirippo National Park (Talamanca Mountains) occur above 3000m.

A great difference was found in the SDM species richness between the lowlands and the montane areas which was not the case with the ESH species richness map. The relatively high ESH species richness values outside the montane areas can be explained by the recognised overestimation of the ESHs in the lowlands. Lowland areas with high population and infrastructural density on the dry Pacific side of the country (e.g. San Isidro del General) are not known to have as high levels of species richness as the ESH map predicted. However, the

medium ESH species richness values were as expected for the areas below the Atlantic side of the Talamanca Mountains. Contrasting climatic conditions occur between the Atlantic side (wet and without a distinct rainy season) and the Pacific side (drier and with a distinct rainy season), due to the topography of the country and the oceanic weather systems of the Atlantic and Pacific Oceans. Since precipitation is an important factor determining plant distribution and diversity, the two different climate patterns are reflected in the country's vegetation (Enquist, 2002). Surprisingly, the SDM map predicted low species richness in the areas in which pre-montane moist forests occur at altitudes as low as 600m (Holdridge & Grenke, 1971). It appears that in this case, SDMs have under-estimated species richness in this region, probably because of the few SRLI occurrence points in the area and therefore little botanical information to be used in building the equivalent SDMs.

The fuzzy numerical metric identified the Osa Peninsula as an area with low similarity between the two maps. The Osa Peninsula is located in the southwest area of the country with a maximum altitude of 750 m and a hot (mean annual temperature: 25˚C) and humid (mean annual precipitation: 6000 mm) climate (Cornejo *et al*., 2012). It is well protected and known for its high plant, mammal, insect and bird diversity (Sanchez-Azofeifa *et al*., 2002). For these reasons, it was expected that both maps would predict high pteridophyte diversity in the peninsula. Unsurprisingly, both maps show high diversity (ESH map: 42 species; SDM map: 25 species) at high altitudes, but lower diversity (ESH map: 4 species; SDM map: 10 species) at lower altitudes (west side of the peninsula). This relatively low diversity at lower altitudes in the ESH map can be explained by the species altitude ranges that were used in the ESH calculation. According to these altitude ranges, most of the SRLI pteridophyte species in the Osa Peninsula do not occur in altitudes between sea level and 300 m. Thus, the altitude information of these particular species may be inaccurate.

As with the set of Neotropical maps, the ESH and SDM species richness maps for Costa Rica were validated using independent field data. The comparison was made along an altitudinal gradient and showed that the altitude-species richness pattern found from the ESH and SDM species richness maps broadly agree with the one derived from field data. The pattern reflected the overestimation of the ESH map in the lowlands and of the SDM map in the highlands as, in the specific field sites, the ESH map predicted higher species richness values than the SDM in the lowlands and lower values than the SDM in altitudes above 3000m. Higher similarity was found between the two species richness-altitude patterns of the ESH and SDM maps of Costa Rica than between the equivalent patterns of the Neotropical maps which were revealed when compared with the field data of Kessler *et al*. (2011). This can be explained by the fact that none of the field sites in Costa Rica were located at altitudes bellow 647m, where differences between the two maps were identified due to the overestimation of species richness in the lowlands in the ESH map.

4.5 CONCLUSIONS

This was the first time that the ESH calculation method, built using the SRLI pteridophyte forest data, was compared with an established species distribution calculation approach, other than the EOO approach. The ESH approach was compared with the SDM approach, which is proven to be effective in predicting species' distributions, using identical species' occurrence data. The comparison showed that the ESH metric still overestimates the species distribution even after reducing commission errors relative to the EOO, as the species' ESHs had a smaller mean reduction from EOO than the equivalent SDMs. This was explained by the conservative approach of the ESH method and by the complexity of the SDM calculation in which the statistical associations between the occurrence data and the several predictor variables better capture the unique environmental space of the species.

Differences between the ESHs and the SDMs of the SRLI forest pteridophytes were expected due to the different approaches of the two methods. The SDM approach is complex and good knowledge of the particular species-environment relationship is needed, in contrast with the more straightforward ESH approach. Despite the simplicity of the ESH method, it was found that the species' ESHs had a considerable level of similarity with the statistically-based SDMs. This shows that the ESH approach, despite its limitations, is not only a practical but also a relatively effective method in calculating species ranges. It also supports the suggestion (Chapter 2) to use the ESH metric in IUCN species conservation assessments by creating quantified ESH thresholds for threatened Red List Categories under sub-criterion b(iii).

An attempt to explain differences between SDMs and ESHs was made focusing on the uncertainty of the ESHs, assuming that the SDMs had a higher level of accuracy. It is important to note, however, that while the ESH method lacks hidden assumptions, making interpretation of results and recognition of errors easy, this was not the case for the SDM method. The degree of uncertainty in the SDM method is often related to the different decision steps in building the SDM (Barry & Elith, 2006) and therefore was not easy to identify (as SDMs were not produced by the author of this study). However, there were cases where both the accuracy of SDMs and the ESH-SDM similarity were low, showing that in some cases the difference between the ESH and SDM may have been caused by inaccuracies in the SDMs.

The similarity found between the species' ESHs and SDMs was supported by the comparison between the ESH-derived and SDM-derived species richness maps, as it was found that the two maps were more similar than different. The comparison of the predictions of the two maps with independent data revealed that the ESH and SDM maps overestimate species richness at low altitudes and high altitudes, respectively. This shows that each approach has its limitations. Nevertheless, both maps predicted identical areas with the highest level of species richness, showing that the ESH map is as effective as the SDM map in identifying centres of species richness, despite the fact that the ESH approach did not deal with the sampling bias in the occurrence points as the SDM approach did. This also supports the suggestion (Chapter 3) of

using ESHs to identify hotspots of biodiversity, as the ESH approach is more practical and easier compared to the data intensive macroecological approach and the time-consuming SDM approach.

CHAPTER 5

APPLICATION OF THE ESH METHOD TO SRLI FOREST PTERIDOPHYTES AND ANGIOSPERMS IN AFRICA AND IMPLICATIONS FOR FUTURE SRLI FIELDWORK

5.1 INTRODUCTION

As discussed in the General Introduction of this study (Chapter 1), the Natural History Museum, London (NHM), together with the Royal Botanic Gardens, Kew (RBG Kew) has taken the lead in developing the IUCN Sampled Red List Index (SRLI) for different plant groups (Nic Lughadha *et al.*, 2005; Baillie *et al.*, 2008; Brummitt *et al.*, 2008). Conservation assessments have been generated for globally-representative samples of species based on their natural history collections, together with previously-digitised online specimen resources, coupled with in-house GIS analysis (Willis *et al.*, 2003; Rivers *et al.*, 2010). These species were assessed for the SRLI for Plants in 2010 (Phase I) (Brummitt *et al*., 2010; Brummitt *et al*., 2015b) and they now need to be re-assessed on a 5-year time frame to calculate the change in the Index and so monitor global trends in conservation status (Phase II) (Brummitt *et al*., 2015a).

The current study belongs to the second phase of the SRLI project, its aim being to provide the scientific basis for an automated procedure to assess and re-assess species' conservation status through using species' occurrence data and incorporating near-real time remotely-sensed land cover information. At the same time, the SRLI team has been focusing on identifying localities in Africa for future expeditions, the aim of which are:
(1) to validate the SRLI species' geographic range calculated using occurrence points (herbarium specimens);
(2) to collect SRLI species and therefore add new occurrence points to the SRLI database; and
(3) to systematically collect population data for threatened species in order to assess them under multiple Red List Criteria and not only under Criterion B (geographic range).

Future botanical expeditions are planned together with partner institutions and conservation organisations in Africa. In order for these expeditions to be as effective as possible, areas need to be prioritised based on the likelihood of finding the targeted species. These areas should have high species richness of SRLI plant species in order to increase the probability of finding these species. In addition, areas with concentration of species with small ranges are equally important due to the fact that these species are more likely to be threatened under IUCN Red List Criteria. Finally, areas with high rates of historic deforestation and, therefore, habitat loss and habitat degradation should be avoided, since the likelihood of finding the species will be low, although such information may still be important for ground-truthing current Red List assessments if the species no longer occurs in historic localities.

The ESH metric has been suggested for use in prioritising areas for field expeditions (Brooks & Matiku, 2011). As shown in Chapter 2 of this study, the ESH is an improved measure of calculating the species' range since it reduces commission errors relative to the widely-used EOO metric and only incorporates areas with appropriate conditions for the species. The validation of the species' ESHs with independent data showed that this new calculation method is effective at reflecting the reality of plant distributions on the ground. Furthermore, the general pattern in ESH-derived maps of species richness and endemism broadly agrees with previous relevant studies showing that these maps generally reflect the reality on the ground (Chapter 3). In addition, due to the fact that the species ESHs were based on the most recent land cover remotely-sensed data, these maps can guide field expeditions. While the limitations of the ESH calculation method and the stacked ESH approach to generating biodiversity maps are recognised (details in Chapter 2 &3), these maps could be valuable in identifying areas for future expeditions for the SRLI for Plants.

The ESH calculation method was built and tested with the SRLI pteridophyte forest species (Chapter 2). This simple and practical method, which was generated by selecting the most appropriate variables for pteridophyte species, has not been tested with a different SRLI plant group. While the major SRLI plant groups (monocots, legumes, pteridophytes) belong to vascular plants, they differ distinctly. Monocots together with dicots (in this case, legumes) form angiosperms, the largest plant group with an estimated 352 000 species (Paton *et al*., 2008). Pteridophytes are the second largest group of vascular plants (Smith *et al.*, 2005) with 13 000 species globally (Paton *et al*., 2008). Pteridophytes are older than angiosperms (Rothwell, 1999) and, as it has been shown, they are the closest relatives to seed plants (angiosperms and gymnosperms) (Pryer *et al.*, 2001). However, it has been suggested that the extant pteridophyte species are a result of a more recent diversification in the Cretaceous period when the angiosperms already dominated terrestrial ecosystems, forcing pteridophytes to occupy alternative habitat spaces (Schneider *et al.*, 2004). Excluding their morphological differences, the biggest differences between angiosperms and pteridophytes are found in their reproduction. Pteridophytes reproduce by releasing spores rather than seeds and are dependent on abiotic conditions for fertilization, instead of pollinators as is in the case of most angiosperms (Page, 2002; Moran, 2004). In contrast to angiosperms, pteridophytes have two separate, independent and alternating life stages, the haploid gametophyte phase and the diploid sporophyte phase. The gametophyte phase and especially the dispersal of the male gametes are dependent on water availability, (Page, 2002). Due to their dependency on abiotic conditions for fertilization (Barrington, 1993), and because they are less adaptable to environmental conditions (Kessler *et al.*, 2011), pteridophytes are more closely correlated with climatic conditions, especially with water availability variables, than are angiosperms. The differences between the two groups help explain the dissimilarities between the groups' biogeography. Studies have shown a latitudinal gradient in species richness and high species richness in topographically complex areas in both groups (Barthlott *et al.*, 2005; Kier *et al.*, 2005; Barthlott *et al.*, 2007; Kreft & Jetz, 2007; Kreft *et al.*, 2010). Pteridophytes, however, have a wider geographical distribution and a higher ratio of island species to mainland species than angiosperms (Kreft *et al*., 2010) which is due to their

ability to disperse small wind-blown spores over long distances (Nathan, 2006). For the same reason, endemism is lower in pteridophytes than angiosperms (Aldasoro *et al.*, 2004). Furthermore, due to their dependency on the availability of water, pteridophytes have a steeper latitudinal gradient in species richness and a preference for wetter montane forests and are less diverse in arid areas, although not completely absent (Hietz, 2010), compared with angiosperms (Kreft *et al*., 2010).

The significant differences between the major SRLI plant groups show the importance of testing the ESH calculation method with angiosperms before concluding that the method can be successfully applied to all SRLI plant groups and not just pteridophytes. The ESH method should produce meaningful results for all plant groups reflecting each group's unique characteristics and should be effective at reflecting the reality of distributions on the ground for different plant groups. Only then the species' ESHs for all SRLI plant groups should be used to generate biodiversity maps of the SRLI species in order to assist the process of identifying fieldwork localities. The map of species richness could be used in prioritising areas with high SRLI species richness and the map of endemism richness could be used in identifying areas with high concentration of species with small and narrow ranges.

5.2 METHODS

The third objective of this study has been to apply the ESH calculation method (see Chapter 2, section 2.2.2.2) to the major Sampled Red List Index plant groups in Africa and to generate ESH-derived species richness and endemism richness maps for those groups. The aims of this chapter were (1) to apply and test the ESH calculation method to a different SRLI plant group, the angiosperms; and (2) to use the ESH-derived maps of species richness and endemism to identify areas for future botanical expeditions for the SRLI for Plants. Species ESHs were calculated for the major SRLI plant groups (angiosperms and pteridophytes) and species richness and endemism richness maps were generated (based on Chapter 3, section 3.2.1) and compared. These maps were then combined together and with deforestation data, to produce an integrated map of biodiversity and threat for the SRLI major plant groups and used to prioritise areas for fieldwork.

5.2.1 Study Area

The focus of this study is Africa, the largest land mass within the tropics (-23.5˚ to 23.5˚). While Africa has the largest desert area of the world, it also has the second biggest contiguous tropical moist forest, the tropical forest of the Congo basin. According to FAO (2010), Africa has 344×10^4 km² of tropical forest with lowland moist forests mainly in West and Central Africa and montane moist forests in the Eastern Arc Mountains in East Africa. In addition, important lowland moist forests exist on the Eastern side of Madagascar. The extent of forest in Africa for the year 2005, based on GlobCover land cover dataset, is shown in Figure 92.

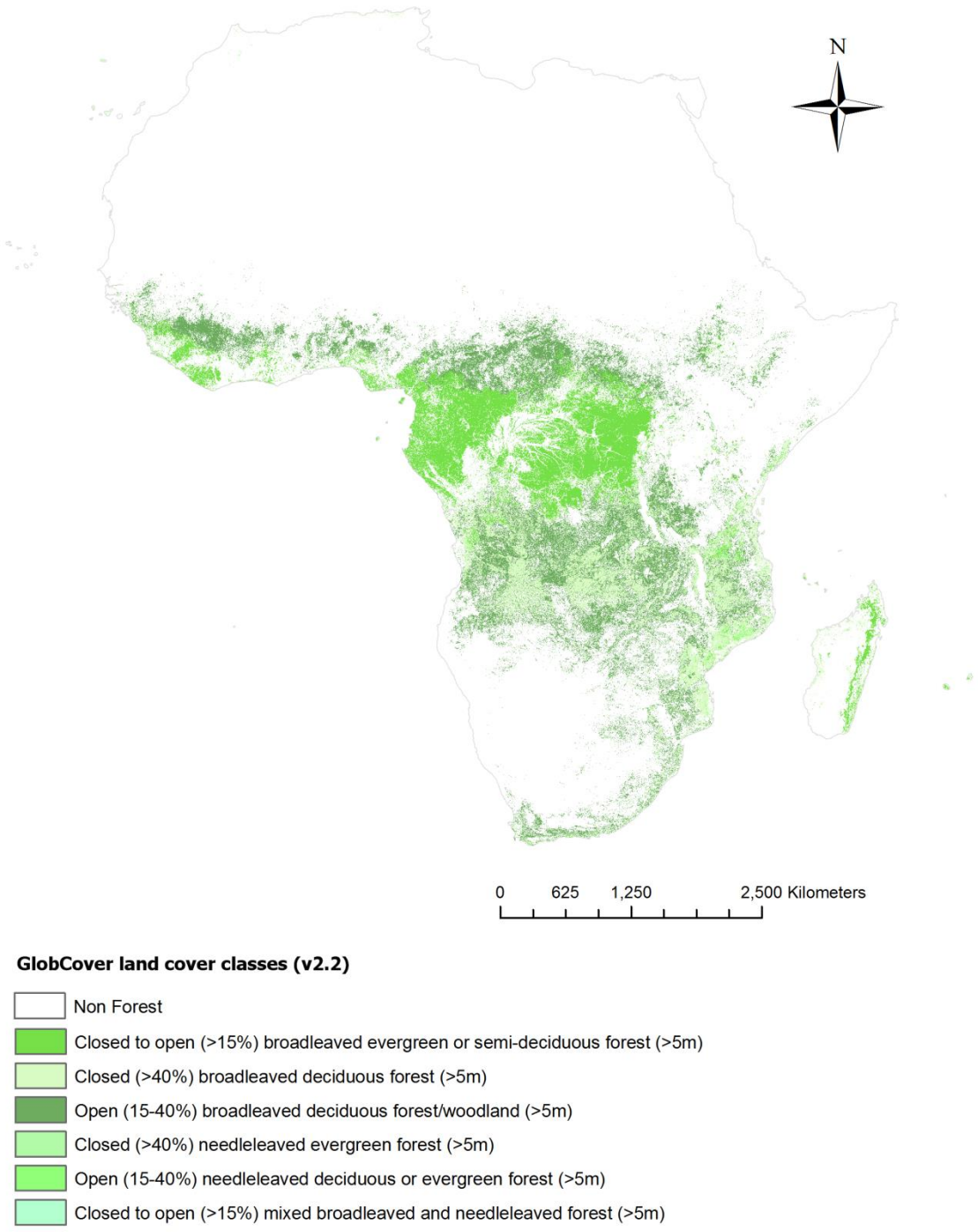

Figure 92. Forest extent of Africa based on GlobCover land cover dataset (v.2.2).

Human impact has influenced the distribution of forests in Africa during the last 4 millennia (van Gemerden *et al.*, 2003; Malhi *et al.*, 2013). While the deforestation rate in Africa has decreased since the 1980s, Africa had the second largest net loss of forest area (3.4 million hectares per annum) between 2000 and 2010 (FAO, 1993; FAO, 2001; FAO, 2010). According to Malhi *et al.* (2013) and the Global Forest Change (GFC) deforestation data (Hansen *et al.*, 2013), West Africa, the Congo basin and Madagascar are the hotspots of deforestation. It has been reported that deforestation rates were higher in dry forest areas than in the humid forests especially in areas with high population growth (Rudel, 2013). Deforestation in Africa is largely driven by

agriculture as in the other tropical regions. However, in contrast to South America and Asia, deforestation in Africa is driven more by small agricultural subsistence activities than commercial agriculture, which reflects the high levels of poverty in the continent (DeFries *et al.*, 2004; Fisher, 2010; Rudel, 2013). Another important driver of deforestation is the extraction of primary products (e.g. timber, charcoal) for domestic use (Burgess *et al.*, 2002; Hosonuma *et al.*, 2012). While the association of the drivers of deforestation with the local population in Africa can be a challenge in forming conservation strategies, protected areas have been effective in reducing habitat loss in Africa, mainly in remote and large forested areas (Joppa *et al.*, 2008; Pfeifer *et al.*, 2012; Green *et al.*, 2013). Although there has been an increase in the number of protected areas in Africa in the last 20 years, many of them are focused on non-forest areas (e.g. savannah) (Burgess *et al.*, 2004). According to Schmitt *et al.* (2009), the percentage of protection of forest cover in the Afrotropics is the second lowest (6.5%) among the other realms and did not meet the 2010 CBD target for forest conservation (10%). Moreover, only 25% of the Afrotropical forest hotspots reached the 10% protection target by 2010.

While Africa is the largest tropical continent, studies have shown that the Afrotropics are poor in plant species compared with the other tropical biogeographical realms (Neotropics and Indomalaya) (Richards, 1973; Tryon, 1986; Kreft & Jetz, 2007; Parmentier *et al.*, 2007; Kreft *et al.*, 2010; Kessler *et al.*, 2011). For this reason Africa has been labelled as the 'odd man out' by Richards (1973). This relatively low species richness and the general species richness patterns of Africa have been explained mainly by the past and present climatic patterns and events (Richards, 1973; Hamilton, 1976; Kornas, 1993; Moran, 2004), and by the level of human impact in the region (Richards, 1973).

Africa's climate is influenced by the Atlantic climatic system and the Indian Ocean Monsoon system. Despite the resulting rain, Africa has warmer and drier climate conditions compared to the other tropical continents (Malhi & Wright, 2004). These conditions together with long dry seasons can affect the species diversity of plants (Richards, 1973; Parmentier *et al.*, 2007), which is strongly correlated with climatic conditions and especially water availability and temperature (Woodward & Williams, 1987; Francis & Currie, 2003; Kreft & Jetz, 2007; Kreft *et al.*, 2010). However, many studies have suggested that the patterns of species richness, as well as endemism, can be explained by past climatic events rather than current climatic conditions (Hamilton, 1974; Hamilton, 1976; Kornas, 1993; Fjeldsaå & Lovett, 1997; Linder, 2001; Aldasoro *et al.*, 2004; Parmentier *et al.*, 2007). Despite the fact that the 'refugium theory' (Haffer, 1969) has attracted criticism by researchers with respect to its application in the Neotropics (Knapp & Mallet, 2003), this theory is still actively applied in the Afrotropics. High levels of endemism and species richness have been recorded in areas of Africa that presumably acted as refugia for species during climatic fluctuations especially during the Pleistocene. This correspondence of high biodiversity with the proposed refugia has supported the theory that fragmented populations of species were isolated in these refugia which lead to speciation and resulted in large centres of species richness and endemism. Hamilton (1976) claimed that these refugia were the only areas with permanent wet forest during the Pleistocene climatic oscillations

whereas for Fjeldsaå & Lovett (1997) these areas provided stable climatic conditions regardless of the suitability of the habitat. It has also been suggested that the great extinction of species that occurred during the cool and arid climatic episodes of the Pleistocene and the dramatic change in the vegetation during that period explains the relatively low species diversity in the Afrotropics (Hamilton, 1976; Kornas, 1993; Dupont *et al.*, 2000).

Evidence for floristic refugia (e.g. the number of palaeoendemic species, floristic composition, species richness and endemism spatial patterns) have been presented by multiple studies (Hamilton, 1974; Hamilton, 1976; Kornas, 1993; Fjeldsaå & Lovett, 1997; Linder, 2001; Aldasoro *et al.*, 2004; Parmentier *et al.*, 2007). All these studies agreed on areas of the East African coast, the Cameroon-Gabon area, small areas in West Africa (Guinea, Sierra Leone, Liberia) areas surrounding Lake Kivu, East Zambia, East Congo, the Eastern Arc Mountains and the Cape Floristic area as representing refugia. It has been shown that these areas are also centres of both species richness and endemism (Linder, 2001).

5.2.2 SRLI plant groups and data

Five plant groups are included in the SRLI for Plants: bryophytes, pteridophytes, gymnosperms, monocots (monocotyledons) and lastly legumes as a proxy for dicot (dicotyledonous) plant families (details in Chapter 1, section 1.4.3). This chapter includes the forest species of the three major SRLI plant groups – pteridophytes, monocots and legumes – and excludes bryophytes and gymnosperms due to lack of data. The SRLI bryophyte species have not been assessed yet and the equivalent data have not been gathered. Gymnosperm (Conifer and Cycad) data were not provided by the Royal Botanic Garden, Kew for use in this study.

Due to the fact that the SRLI pteridophyte species were assessed by the Natural History Museum, London and the SRLI monocot and legume species were assessed by the Royal Botanic Gardens, Kew, permission to use the SRLI data in this study was granted by both institutions. The Royal Botanic Gardens, Kew provided the angiosperm species data, the sample of which only included endemic species of Africa. Therefore, any pteridophyte species that were not endemic to Africa were excluded from analysis. In the SRLI sample, there are 174 angiosperm forest species (legumes: 89 sp., monocots: 85 sp.) and 64 forest pteridophyte species endemic to Africa with 7700 (legumes: 4900, monocots: 2800) and 3100 occurrence points respectively. The point density of the SRLI occurrence data for the angiosperms and pteridophytes is presented in figures 93 and 94. Both groups showed high density of specimens collected in Madagascar, the western part of Congo basin, Tanzania and Kenya. There was also a high density of pteridophyte collected in the Eastern Rift Mountains whereas there was an obvious cluster of angiosperms collected in eastern Zambia. The geographical bias in the species occurrence points is recognised and has been identified in Chapter 2 (section 2.3.1). When investigating the geographical bias in the SRLI forest pteridophyte data, seven countries in the Afrotropics, known to have species present and suitable habitat, were not covered by any occurrence points.

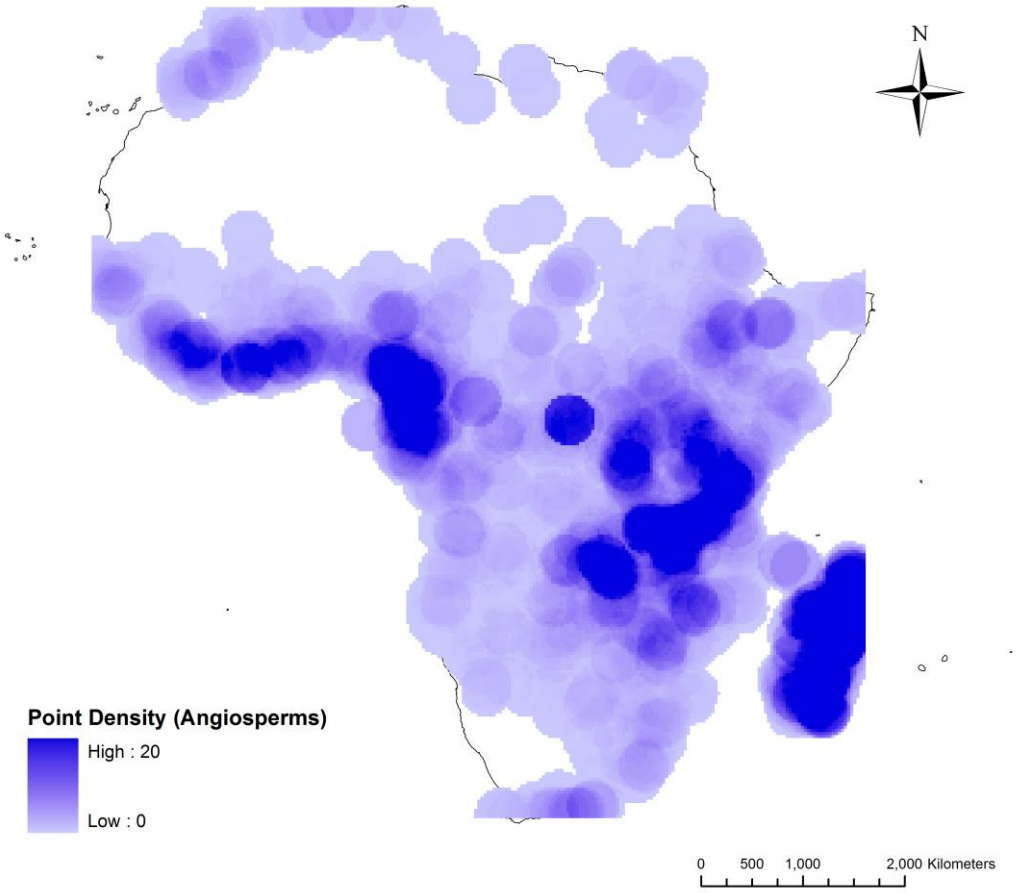

Figure 93. Density of specimen occurrence points for SRLI forest angiosperm species in Africa.

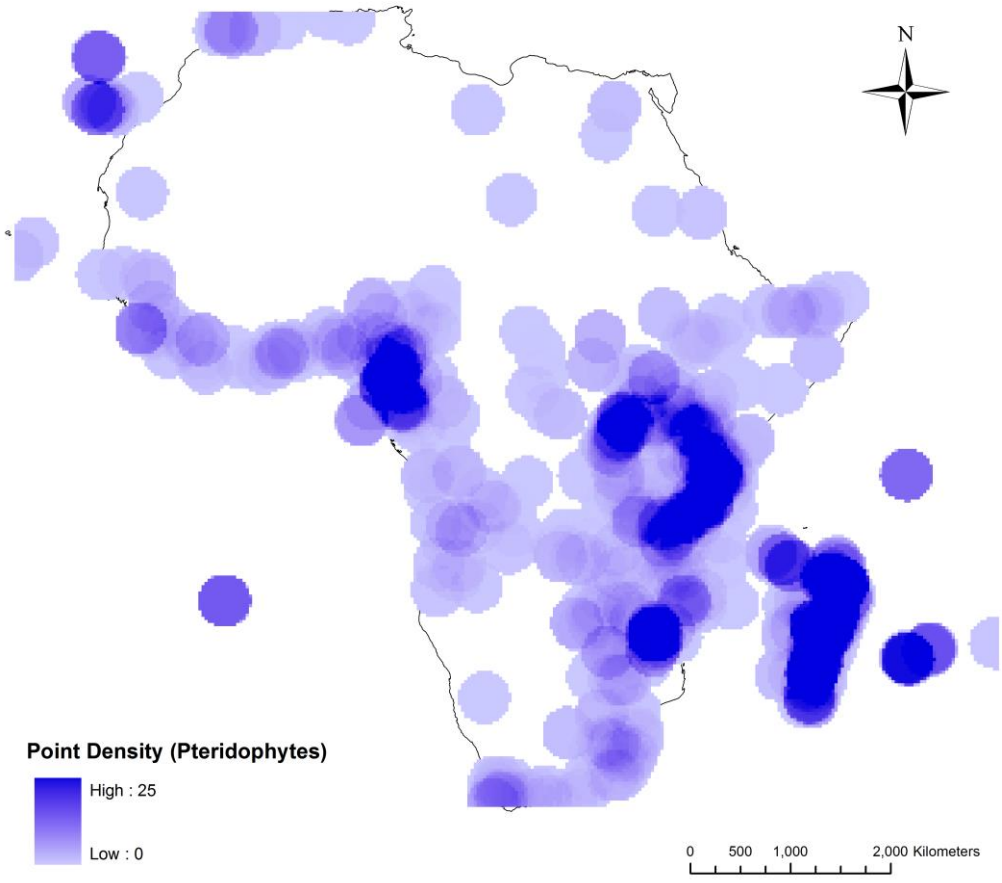

Figure 94. Density of specimen occurrence points for SRLI forest pteridophyte species in Africa.

5.2.3 Calculating ESHs for the forest species of the major SRLI plant groups

The species' geographical ranges were generated using the ESH calculation method which was built based on pteridophyte species and presented in Chapter 2. Specifically, the species' occurrence points were used to produce the species EOO for each plant group (angiosperms and pteridophytes) (details in Chapter 2, section 2.2.2.1). Thereafter, the ESH of each species was calculated based on information appropriate to the ecology of that species, as well as land cover and environmental information, within the convex hull defining the species' EOO (details in Chapter 2, section 2.2.2.2). One of the variables of the ESH calculation model is water balance; this was selected due to the strong relationship between pteridophytes and water availability. Despite the fact that water balance was selected specifically for pteridophytes, it was used in calculating the species' ESHs for both groups (pteridophytes and angiosperms), since it has been suggested that water availability is the most important factor of the distribution of forest plant species in Africa (Swaine, 1996; Holmgren *et al.*, 2004; Maharjan *et al.*, 2011) and is strongly correlated with species richness patterns in the region (Linder, 2001). Therefore, water balance (Mulligan, 2011) together with altitude (Jarvis *et al.*, 2008) and land cover (Bicheron *et al.*, 2008) was used in calculating the species' ESHs. The relationship of water balance and altitude in Africa is shown in Figure 95. Positive water balance values (local precipitation excess of actual evapotranspiration) were found in altitudes between 500m and 2500m whereas the highest negative values (<-2000mm/month) were found in altitudes below 1000m.

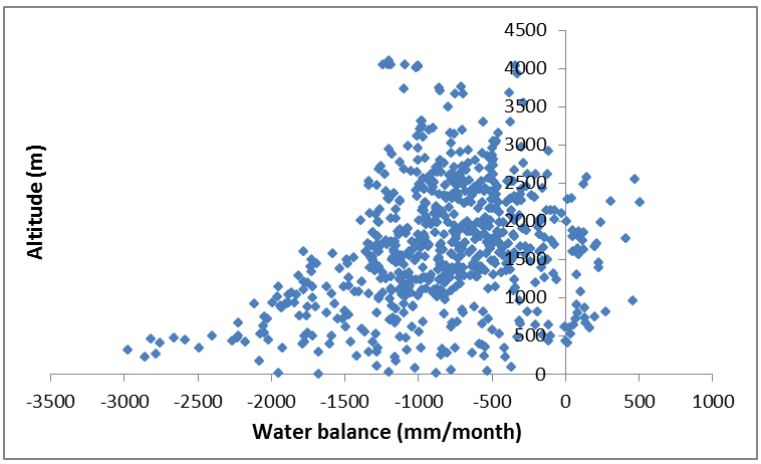

Figure 95. The relationship between water balance and altitude in Africa produced using randomly selected points per 500m altitudinal bands and plotting the equivalent water balance values against altitude.

Using the SRLI occurrence points, frequency graphs were generated to compare the frequency distribution of the three variables (land cover, altitude and water balance) between the two plant groups. In the case of altitude, the minimum and maximum altitudes of each species, taken from the assigned altitudinal ranges, were used in this analysis.

As this was the first time that the ESH calculation method was applied to angiosperms, a comparison was made between the original EOO and the ESHs of the individual species in

each group. Boxplots were used to compare the mean ESH/EOO ratio of each group and of each IUCN Red List Category in each group. To determine if there are statistically significant differences between the species' ESH/EOO ratio of each group and between the ESH/EOO ratio for each IUCN Red List Category within each group, the non-parametric Mann-Whitney U and Kruskal-Wallis tests were used respectively. The Mann-Whitney U test is suitable for comparing two groups whereas the Kruskal-Wallis test is appropriate for comparing three or more groups (McDonald, 2009). In addition, the mean size of the species' ESH and EOO in each IUCN Red List Category was compared in each plant group. Information on the IUCN Red List status of the angiosperm species was obtained from the IUCN Red List of Threatened Species website (http://www.iucnredlist.org/).

5.2.4 Generating maps of species richness and endemism richness using the species' ESHs

Maps of species richness and endemism were generated for each plant group. The species richness map of each group was generated by stacking the species' ESHs and in this way summing the presence of the species (details in Chapter 3, section 3.2.1). The map of endemism richness of each group was produced by calculating the range size-rarity (C-value) of each species and summing the C-value of all species occurring in a cell (details in Chapter 3, section 3.2.1). As the species' ESHs were calculated using a global land cover map representing habitat for 2005 (Globcover v.2.2) (Bicheron *et al.*, 2008), the ESH-derived maps reflect the patterns for that year (2005).

The patterns of species richness and endemism richness were compared between the two plant groups by generating difference maps. Moreover, the species richness patterns of both groups were evaluated along an altitudinal and moisture gradient in order to explain the differences of these patterns between the two groups. Spearman's non-parametric rank correlation analysis was used to measure the strength of the association between the variables and species richness. The predictions of the ESH-derived maps of species richness and endemism were also compared with previous studies that have investigated species richness and endemism patterns in Africa (Kornas, 1993; Lovett & Friis, 1996; Fjeldsaå & Lovett, 1997; Kier & Barthlott, 2001; Linder, 2001; Aldasoro *et al.*, 2004), and field-based estimation of species richness, in order to determine if the predicted patterns were meaningful for both plant groups.

The species richness maps of the two groups (forest angiosperms and pteridophytes) were stacked together in order to create a combined species richness map of the SRLI forest plants. This was repeated for the maps of endemism to produce a combined map of endemism richness. A species richness map was also created using the original EOOs of the species from both groups. This EOO-derived species richness map was compared with the combined ESH-derived map in order to understand the advantages of using an ESH-derived map for prioritizing fieldwork areas. An equivalent EOO-derived map of endemism richness was not created as it was found that the spatial differences between an EOO-derived map of endemism richness and an ESH-derived map of endemism richness are small (see Chapter 3, section 3.3.1).

5.2.5 Generating an integrated map of biodiversity and threat

In order to identify areas for future botanical expeditions for the SRLI for Plants, an integrated map of biodiversity and threat was calculated based on levels of species richness, endemism and threat (deforestation). This map was produced using the combined species richness map and the combined map of endemism richness of the SRLI forest plant species, together with the Global Forest Change (GFC) deforestation data (Hansen *et al.*, 2013). The GFC deforestation dataset shows changes in forest cover at 30m resolution, the result of the time-series analysis of Landsat 7 satellite images taken between 2000 and 2012. Mulligan (2014a) resampled the GFC data to 1km resolution by averaging the 30m data in each 1km pixel and calculated the percentage of each km pixel deforested over the period 2000 – 2012. In the new resampled dataset, thresholds were applied and only pixels that lost at least 50% of their forest cover were considered deforested, since it was assumed that at this level of forest loss, the remaining forest will be degraded due to fragmentation and edge effects (Laurance *et al.*, 1998; Gascon *et al.*, 2000). Pixels that lost less than 50% of their forest cover were considered as remaining forest pixels this way avoiding an overestimation of deforestation in the 1km resolution dataset by assuming that any deforestation in the pixel amounted to the pixel being completely deforested.

The three datasets (species richness map, map of endemism richness, and deforestation data), were resampled in 10km resolution and combined into one map using the RGB composite tool in SAGA-GIS software (v.2.2) (Cimmery, 2010). The tool assigns one of the three RGB (Red, Green, Blue) colour bands to each dataset before overlaying the three datasets in one image with RGB coded values. Areas with a combination of high species richness, high endemism and low deforestation density were prioritised for future expeditions for the SRLI for Plants. Furthermore, areas with high endemism levels and low recent deforestation density (between 2000 and 2012) were identified for future field trips which will focus on narrow-ranged and threatened species.

5.3 RESULTS

5.3.1 ESH calculation for the SRLI forest species in Africa

The species' ESHs were calculated for both plant groups using the species' altitudinal range, water availability preference and habitat preference. Based on the recorded altitudinal ranges of the angiosperm species, only one species had minimum altitude that was not zero (320m) (Figure 96). The majority of the pteridophyte species had a minimum altitude of zero, however; approximately 30% of the species had minimum altitude values between 100 and 1400m. The number of angiosperm species was higher (+25%) than pteridophyte species in altitudes below 1000m and lower (-15%) in altitudes over 3000m.

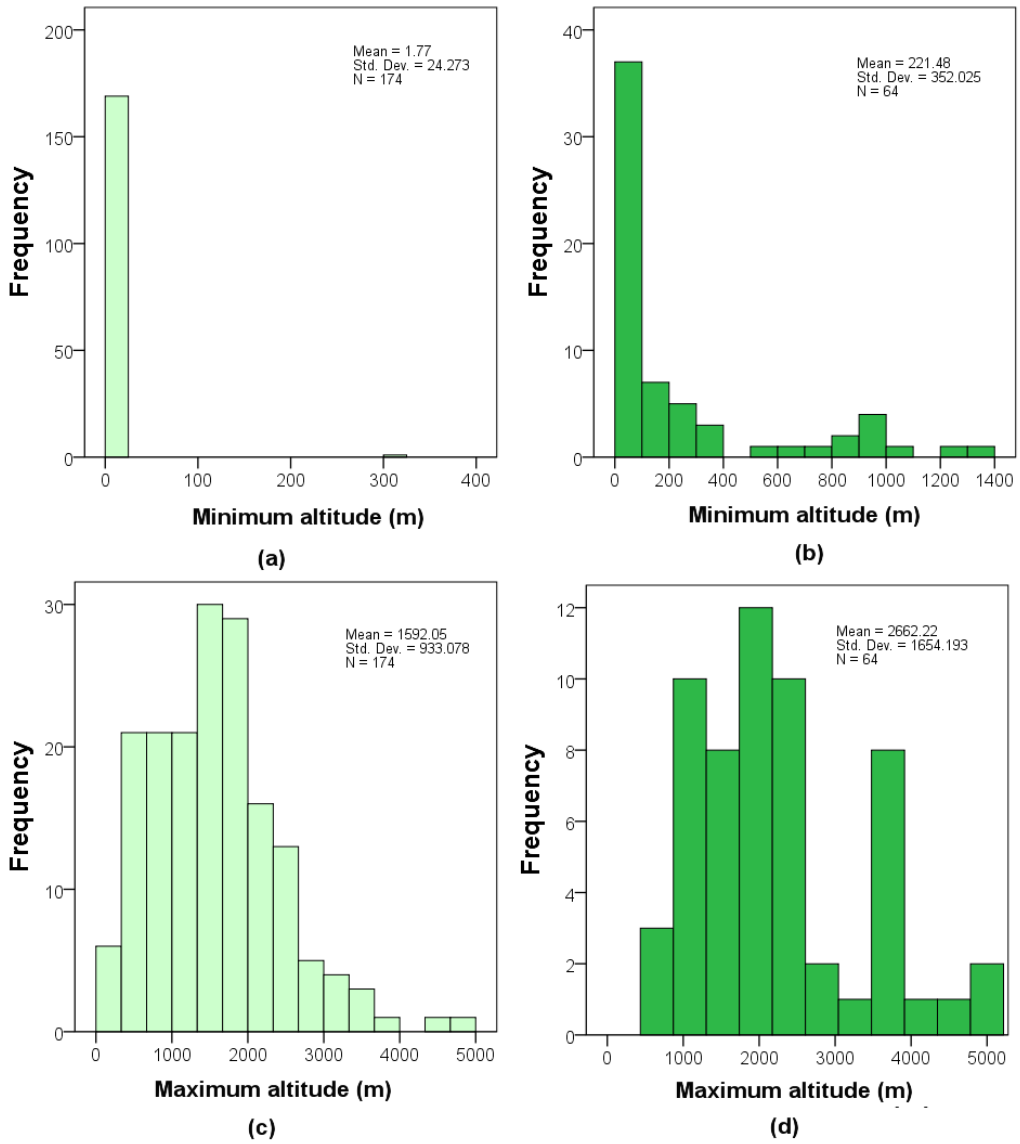

Figure 96.Frequency histograms for the minimum and maximum altitude of the SRLI forest angiosperms (a & c) and pteridophytes (b & d). Values were based on the altitudinal ranges assigned to the species during the ESH calculation.

The water availability range (water balance) for each species, used in the ESH calculation, was calculated exclusively using the species' SRLI occurrence points. Based on these points, water balance preferences of the SRLI forest angiosperms and pteridophytes are shown in Figure 97. In both groups, high and low water balance values had a lower frequency of points than medium (positive and negative) water balance values. The frequency of points for angiosperms peaked at lower water balance values (-300 – -1000 mm/month) than for pteridophytes (-500 – 100 mm/month), as might be expected.

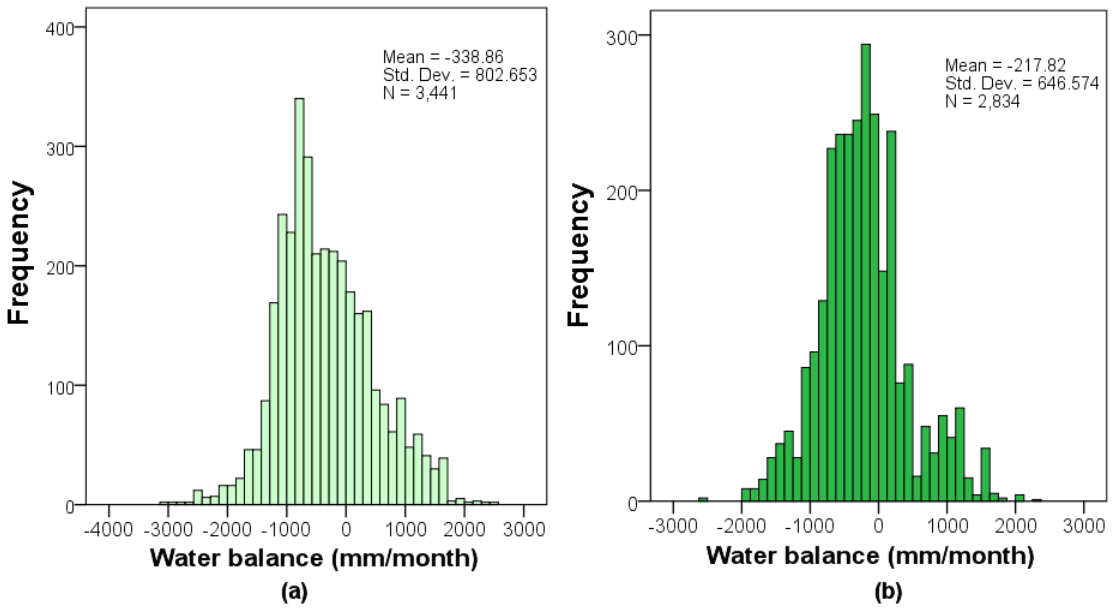

Figure 97. Frequency histogram of water balance values of the SRLI forest (a) angiosperms and (b) pteridophytes based on the SRLI occurrence points.

Although the species used in this analysis are classified by IUCN as forest species, based on their SRLI occurrence points, they occur in the majority of the GlobCover land cover classes. Based on the SRLI occurrence points, both pteridophytes and angiosperms occur more frequently in broadleaved evergreen forests (Figure 98). However, pteridophytes had a higher proportion of points (35%) in this class than angiosperms (22%). Furthermore, there was a generally lower percentage of pteridophytes than angiosperms in drier land cover classes (e.g. class 110: mosaic forest or shrubland and grassland).

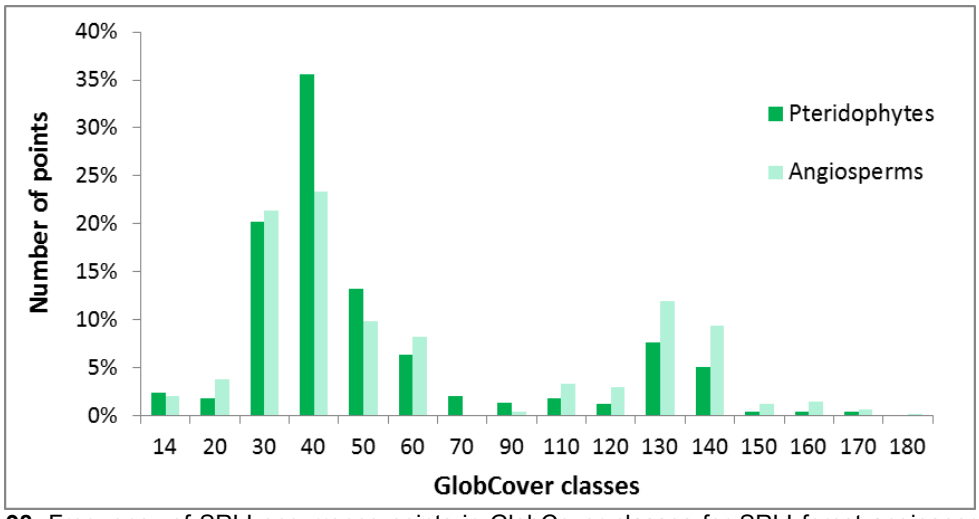

Figure 98. Frequency of SRLI occurrence points in GlobCover classes for SRLI forest angiosperms and pteridophytes. See Appendix A7 for the description of each GlobCover class.

The mean EOO size of the SRLI forest angiosperm species is 30% larger than of the SRLI forest pteridophyte species. There was a strong positive relationship ($r^2 > 0.9$, $p<0.001$) between the area of the original EOO and the ESH of each species for both plant groups. In addition, the

species' ratio of EOO to ESH differed significantly between the two plant groups (Mann-Whitney $p<0.0001$) (Figure 99). On average, the species' ESH covered 62.6±0.4% of the original EOO for the angiosperm species and 44.5±0.2% for the pteridophyte species. Therefore, there was a greater mean reduction from EOO to ESH for the pteridophyte species than the angiosperm species, reflecting their tighter habitat preferences.

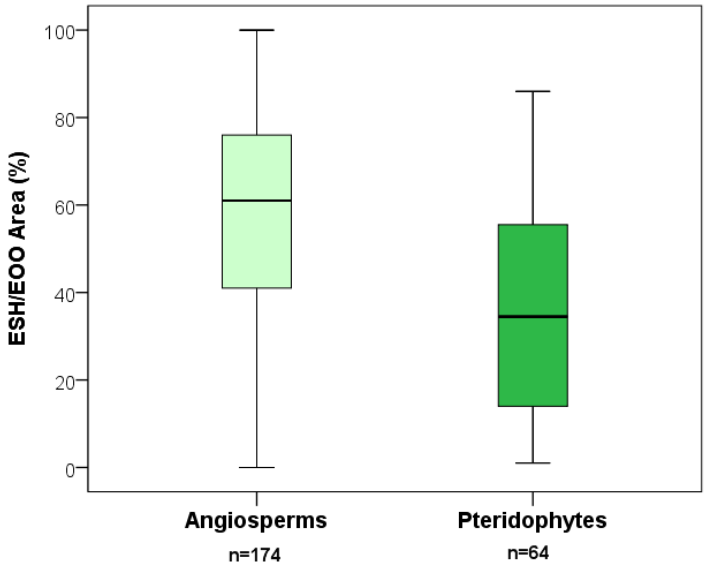

Figure 99. Boxplots representing the ESH/EOO ratio (%) for the SRLI forest angiosperm and pteridophyte species.

While the species sample was bigger for the angiosperm group (174 sp.) than the one of the pteridophyte group (64 sp.), the percentage of species in each IUCN Red List category was similar in each plant group (Figure 100). The species percentage in the Near Threatened (9%) and Vulnerable (8%) categories agreed in both groups. However, the percentage of pteridophyte species was lower (-2%) in the Endangered category and higher (+2%) in the Least Concern category than it was for angiosperm species. As expected the percentage of species in the non-threatened categories (Near Threatened and Least Concern) was higher than in the threatened categories (Critically Endangered, Endangered and Vulnerable), for both groups. The species sample of both groups did not include any Critically Endangered species.

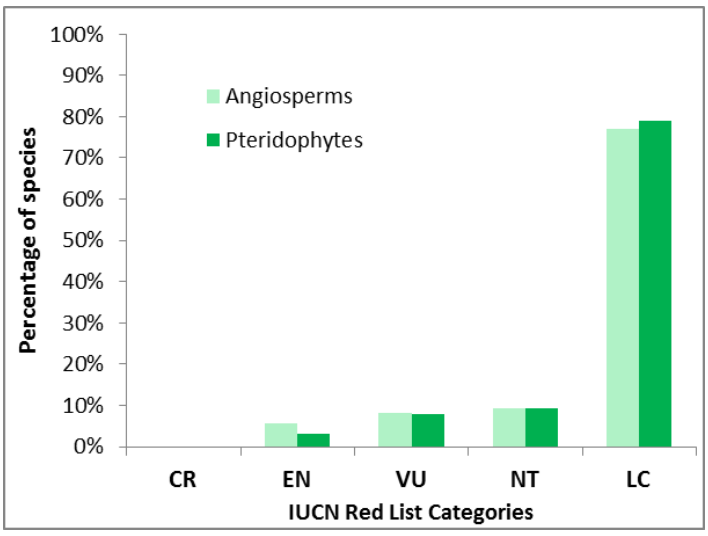

Figure 100. Percentage of SRLI forest species in the angiosperm and pteridophyte groups by IUCN Red List Category (CR: Critically Endangered, EN: Endangered, VU: Vulnerable, NT: Near Threatened, LC: Least Concern).

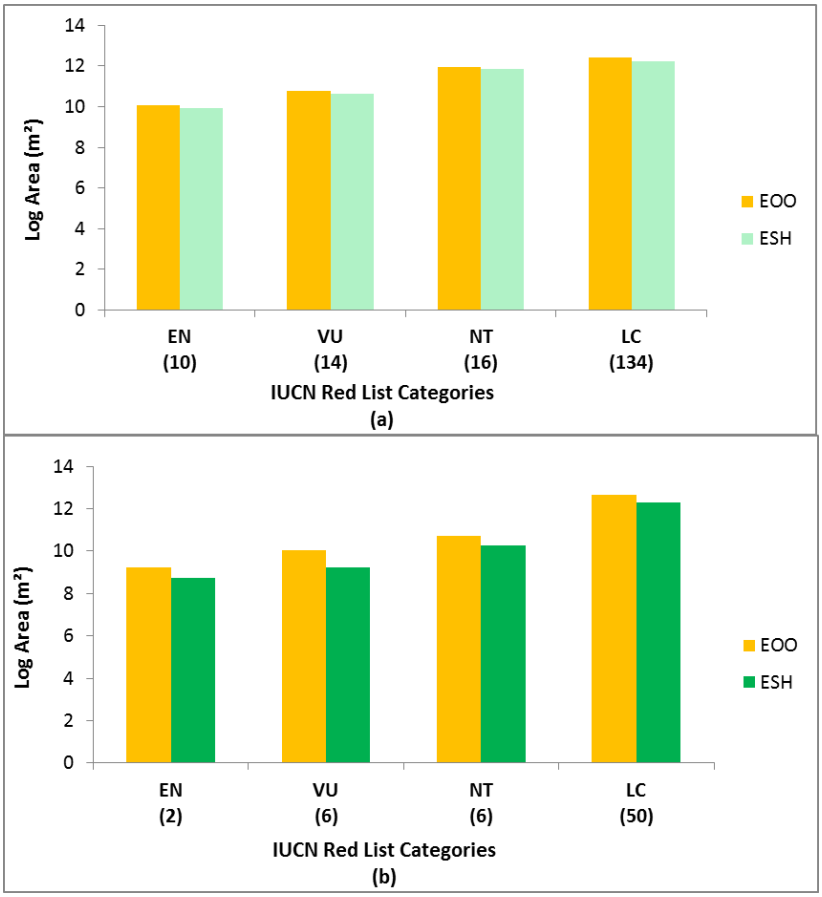

Figure 101. Mean Extent of Suitable habitat (log) of the SRLI forest (a) angiosperm and (b) pteridophyte species by IUCN Red List Category. Categories (EN: Endangered, VU: Vulnerable, NT: Near Threatened, LC: Least Concern). CR category is not shown here since the species sample of both groups did not include any CR species Numbers in brackets represent number of species in each category.

The ESH and EOO size differed significantly between the IUCN Red List categories (Angiosperms: EOO Kruskal-Wallis χ^2=61.4, d.f.=3, p<0.0001, ESH Kruskal-Wallis χ^2= 54.7,

d.f.=3, p<0.0001/ Pteridophytes: EOO Kruskal-Wallis χ^2= 22.7, d.f.=3, p<0.0001, ESH Kruskal-Wallis χ^2= 25.3, d.f.=3, p<0.0001) (Figure 101). In both plant groups, the average size of the original EOO and ESH decreased with increasing category of threat with the average EOO and ESH being larger for species in the Least Concern category and smaller in the Endangered category. The species' ratio of EOO to ESH in each plant group was also different in each IUCN Red List Category (Figure 102). However, in both cases the ESH/EOO ratio did not differ significantly between the IUCN Red List categories (Angiosperms: Kruskal-Wallis χ^2= 6.6, d.f.=3, p>0.05 / Pteridophytes: Kruskal-Wallis χ^2= 2.8, d.f.=3, p>0.05). Among the categories, the highest median and mean ESH/EOO ratio (a smaller mean reduction from EOO to ESH) was found in the Least Concern category for the case of angiosperms and the in Vulnerable category for the case of pteridophytes. The largest median and mean reduction from EOO to ESH was found in the Endangered category in both plant groups.

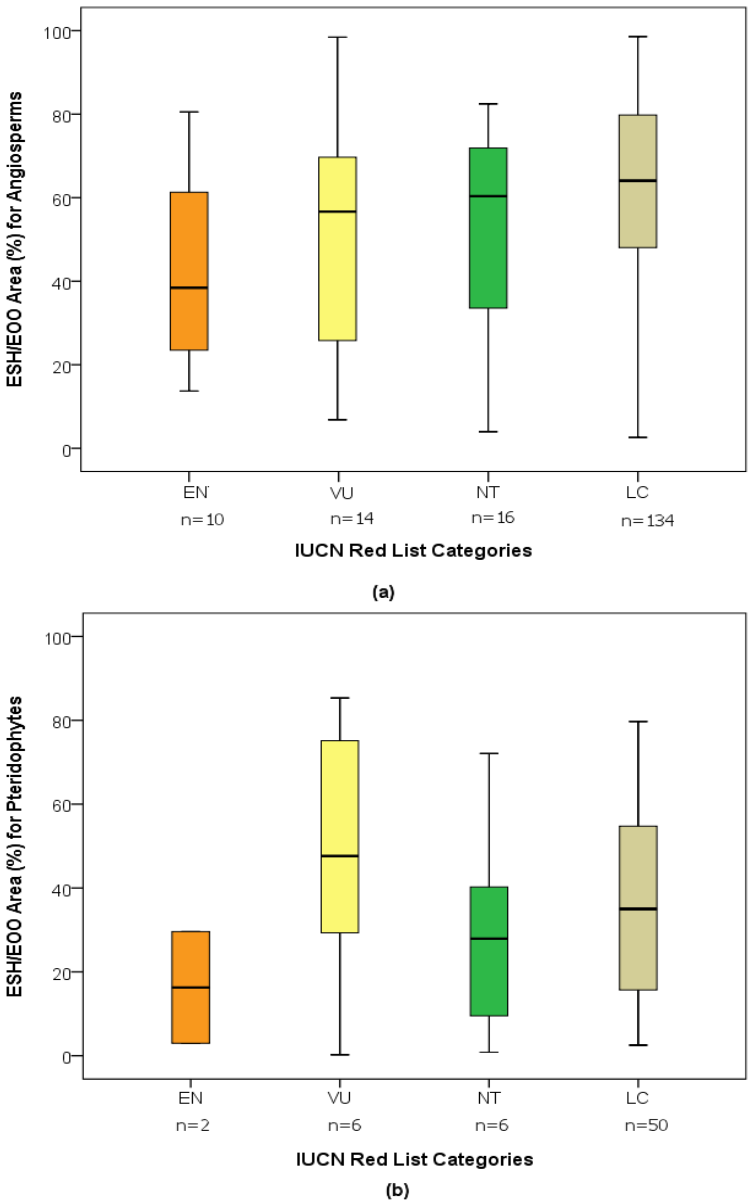

Figure 102. Boxplots representing the ESH/EOO ratio of the SRLI forest (a) angiosperm and (b) pteridophyte species by IUCN Red List Category. Categories (EN: Endangered, VU: Vulnerable, NT: Near Threatened, LC: Least Concern).

5.3.2 ESH-derived maps of species richness and endemism for the SRLI forest plant species

The species richness map derived from stacking the ESHs of the SRLI forest angiosperm species and the one from stacking the ESHs of the SRLI forest pteridophyte species are presented in Figures 103 and 104 respectively.

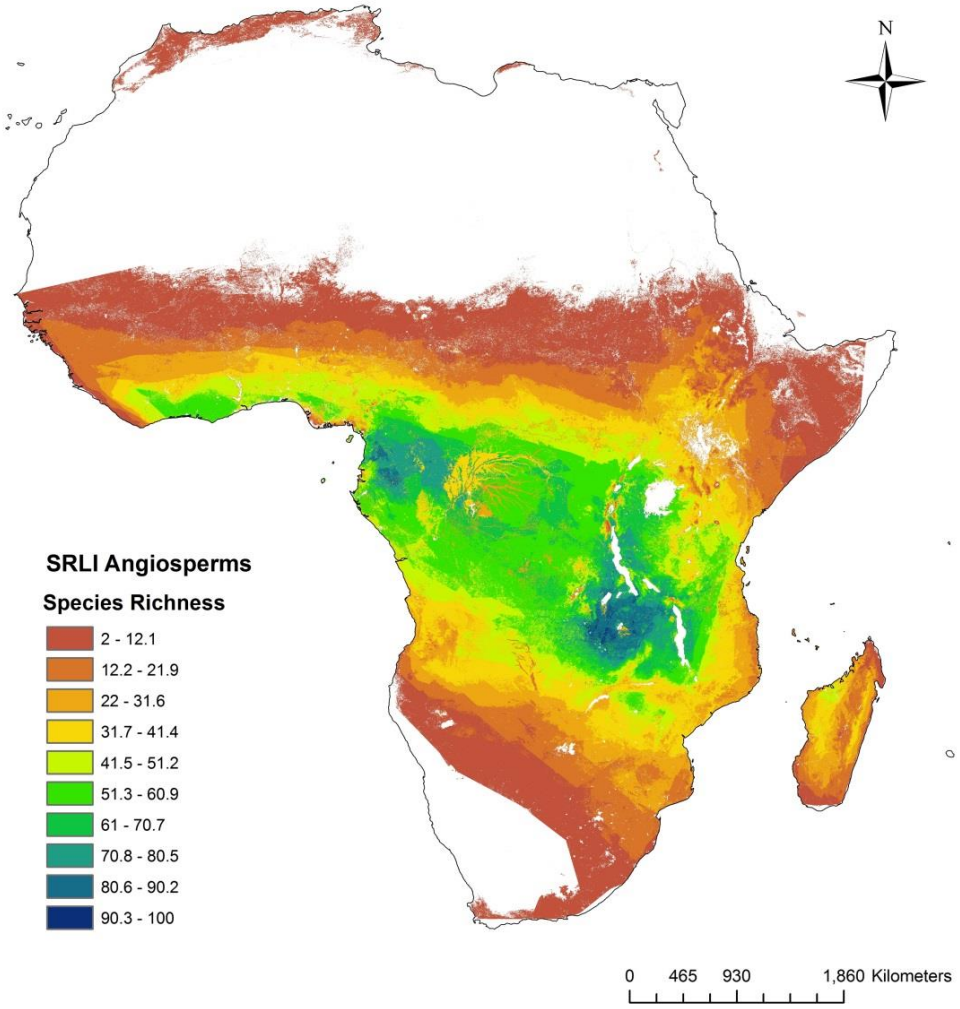

Figure 103. The species richness map of Africa for SRLI forest angiosperm species produced from stacked species ESHs (calculated using SRLI specimen data, species' altitudinal ranges, species' habitat preference and species' water balance values). Data are normalised (0 – 100) and classified in ten equal intervals. White colour represents 0 value of species richness.

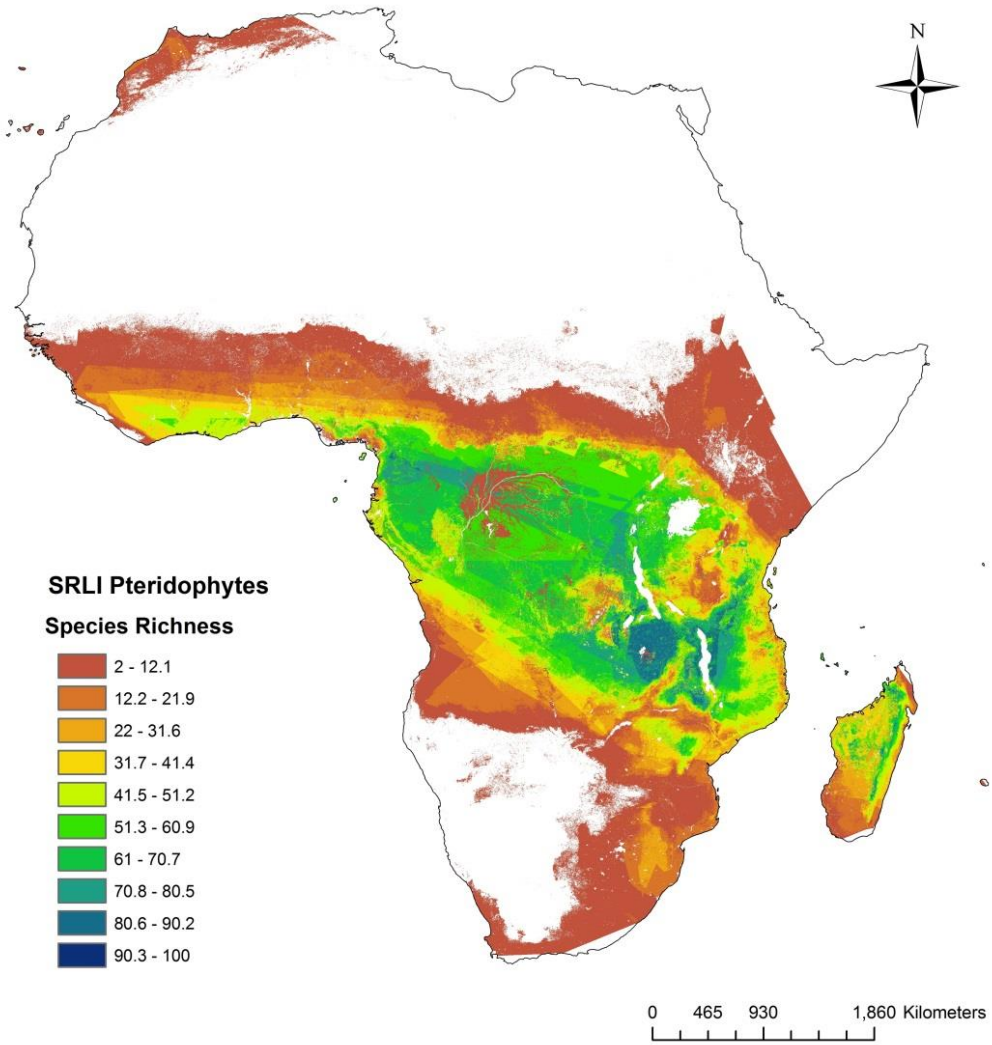

Figure 104. The species richness map of Africa for SRLI forest pteridophyte species produced from stacked species ESHs (calculated using SRLI specimen data, species' altitudinal ranges, species' habitat preference and species' water balance values). Data are normalised (0 – 100) and classified in ten equal intervals. White colour represents 0 value of species richness.

In both maps there is no information on species richness in areas known to be unsuitable for forest species (the Sahara, Namib and Kalahar deserts and water bodies) and in areas covered by small numbers of species occurrence points in the analysis (South Africa). As expected both maps predicted higher species richness in the tropical region than the rest of Africa. The ESH-derived species richness map of angiosperm species predicted a maximum value of 48 species (mean value per Km²: 12.9±9.2 species) whereas the ESH-derived species richness map of pteridophyte species predicted a maximum number of 23 species (mean value per Km²: 7.5±5.4 species), reflecting the different sample size in each group's sample. Both maps appeared to have medium to high species richness values in the Congo basin and the East African Rift area. However, in both maps, the highest species richness values were predicted in an area in East Africa covering north-east Zambia, south-east Democratic Republic of Congo and south-west Tanzania (hereby referred to as the Zambezi –Congo watershed area following Linder (2001)).

The species richness map of the angiosperm species predicted two centres of species richness; the Zambezi-Congo watershed and the western part of the Congo basin (the area covering northern Gabon, southern Cameroon, north-east Congo and Equatorial Guinea). In contrast, the pteridophyte species richness map predicted just one centre of species richness, the Zambezi-Congo watershed area. Another obvious difference is that there is species richness in the angiosperm species richness map in areas of higher latitude than there is in the pteridophyte map. Differences between the two maps were identified as shown in Figure 105. The greatest differences between the species richness maps of the two groups, with the pteridophyte species richness relatively higher, were identified in east Madagascar and in high altitudes of montane areas (e.g. the East Rift Mountains). Angiosperm species richness appeared to be relatively higher in lower altitudes such as the Niari valley in the Congo basin and the lowlands of the Central African Republic. It is also relatively higher in the areas surrounding the Ethiopian Highlands and the Eastern Arc Mountains in Tanzania.

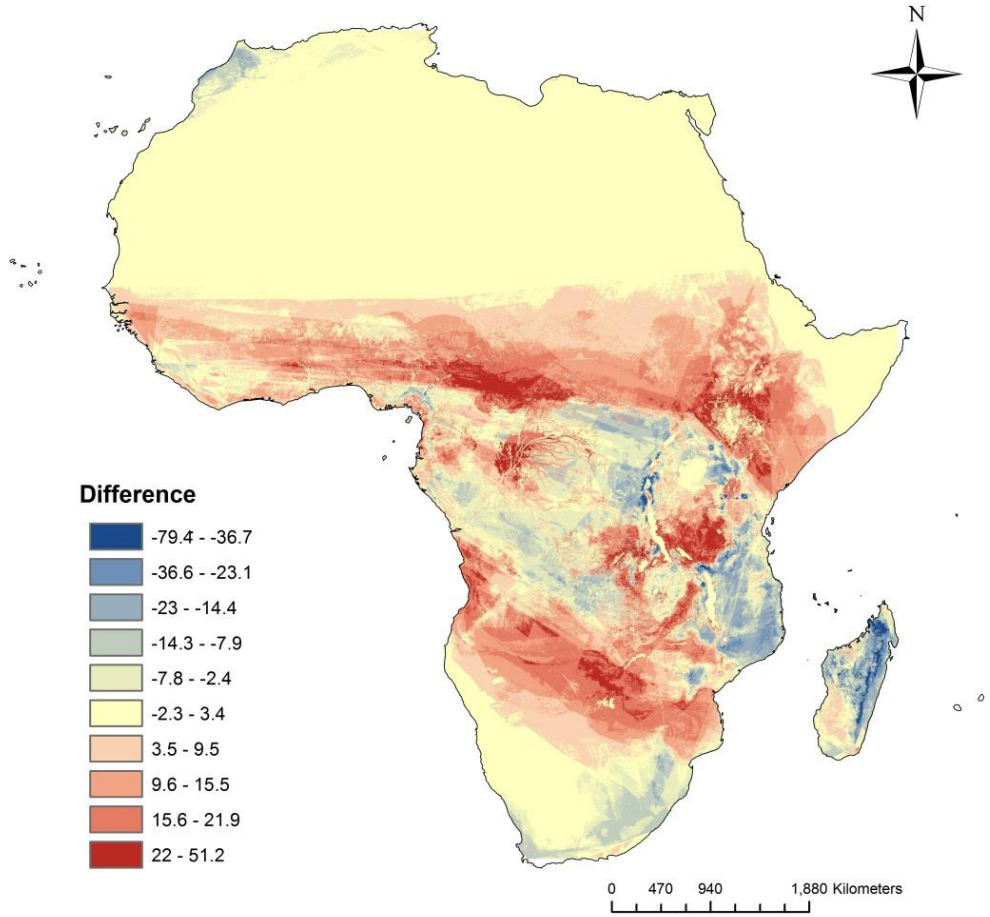

Figure 105. Difference map between the species richness of SRLI forest angiosperm species (Figure 103) and the species richness of the SRLI forest pteridophyte species (Figure 104). Positive values mean species richness of angiosperm species is higher and negative values that species richness of pteridophyte species is higher.

When species richness patterns of both groups were evaluated along an altitudinal gradient, angiosperm species richness was found to be strongly correlated to altitude (bivariate correlation: r = -0.51, n=1000, p < 0.001), whereas pteridophyte species richness was less correlated (bivariate correlation: r = -0.33, n=1000, p < 0.001). A mid-altitude peak in species richness was found (1000 – 2000m) for both groups (Figure 106). Relatively higher pteridophyte species richness values were found in altitudes over 2000m compared with angiosperm species richness values.

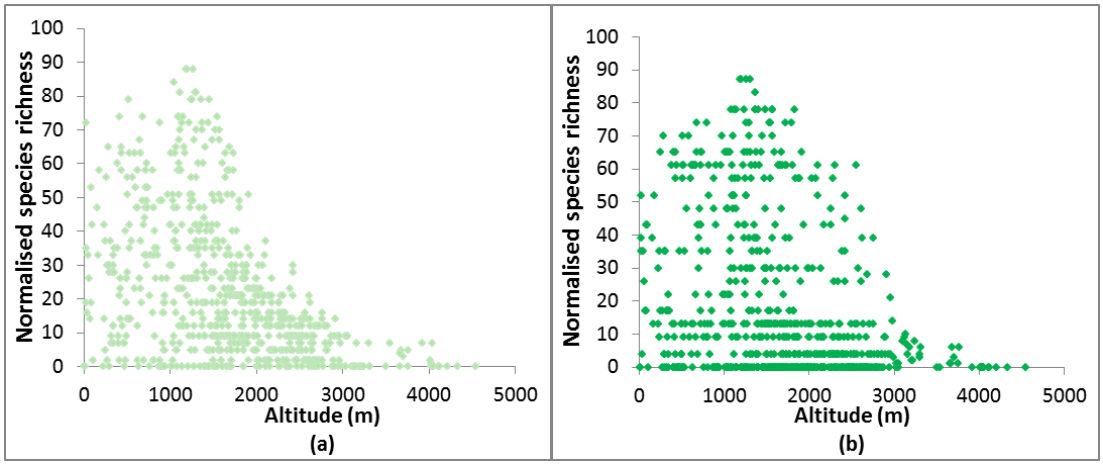

Figure 106. The relationship between species richness and altitude for SRLI forest (a) angiosperm and (b) pteridophyte species produced using randomly selected points per 500m altitudinal bands and plotting the equivalent mapped species richness values against altitude.

In contrast, water balance was strongly correlated with pteridophyte species richness (bivariate correlation: r = 0.58, n=1000, p < 0.001) and less correlated with angiosperm species richness (bivariate correlation: r = 0.41, n=1000, p < 0.001). The species richness-water balance relationship plateaued between -1000 and 0 (mm/month) values for both plant groups (Figure 107). Below 0 (precipitation = actual evapotranspiration), species richness declines as the local supply of water becomes less and less able to supply local evapotranspiration. However, higher species richness values were found for angiosperms in areas of low water balance values (-3000 – -1500 mm/month) than for pteridophytes.

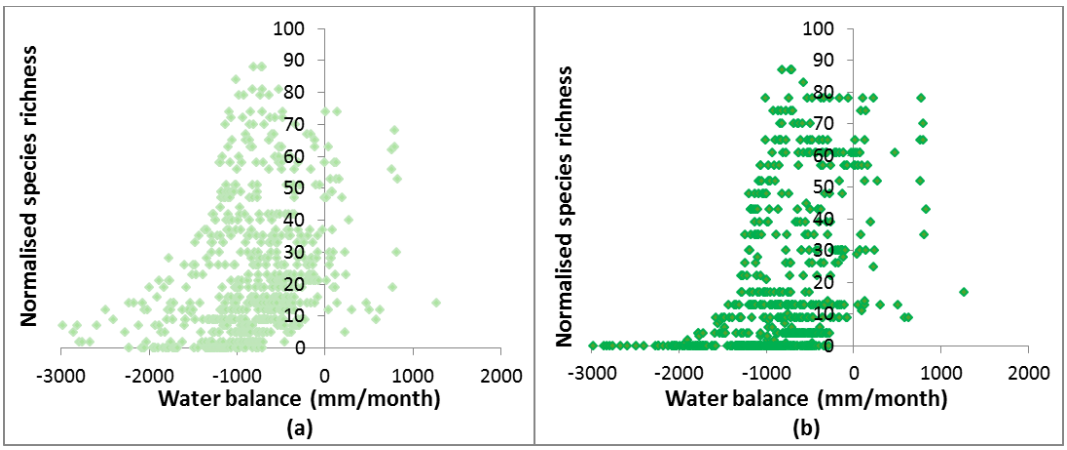

Figure 107. The relationship between species richness and water balance for SRLI forest (a) angiosperm and (b)pteridophyte species produced using randomly selected points per 500m altitudinal bands and plotting the equivalent species richness values against water balance.

The species richness maps of the two groups (angiosperms: Figure 103 and pteridophytes: Figure 104) were stacked together in order to create a combined ESH-derived species richness map for the SRLI forest species (maximum value: 71 species, mean value per Km²: 18.3±14.6 species). This combined map, which is presented in Figure 108, predicted medium to high species richness values in the Congo basin and the East African Rift area. It predicts two centres of species richness: the Zambezi-Congo watershed area, influenced by the species richness predictions for both groups; and the western part of the Congo basin, influenced by the species richness predictions for angiosperms.

The species richness map of all species (angiosperms and pteridophytes) generated using the species' original EOOs (Figure 109) predicted a higher maximum value of species richness and a higher mean value per Km² (maximum value: 80 species, mean value per Km²: 20.9±13.2 species) compared to the combined ESH-derived species richness map (Figure 108). The areas with the highest EOO-derived species richness were the western part of the Congo basin and a large area covering the montane region of East Africa and the eastern part of the Congo basin. While these two areas included the ESH-derived hotspots of species richness (the Zambezi-Congo watershed area and the western part of the Congo basin), they appeared to be homogeneous across large regions in contrast with the smaller and distinct areas with high species richness in the ESH-derived map.

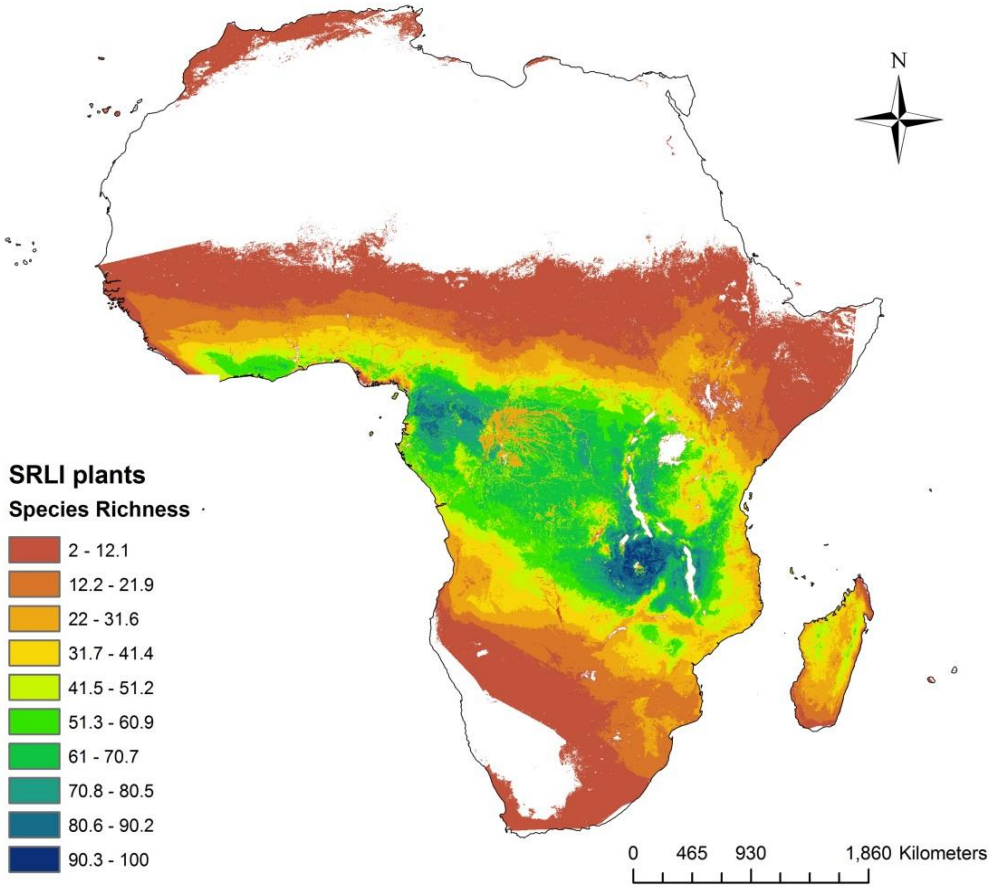

Figure 108. The species richness map of Africa for SRLI forest pteridophyte and angiosperm species produced by stacking the equivalent ESH-derived species richness maps (Figures 103 & 104). Data are normalised (0 – 100) and classified in ten equal intervals. White colour represents 0 value.

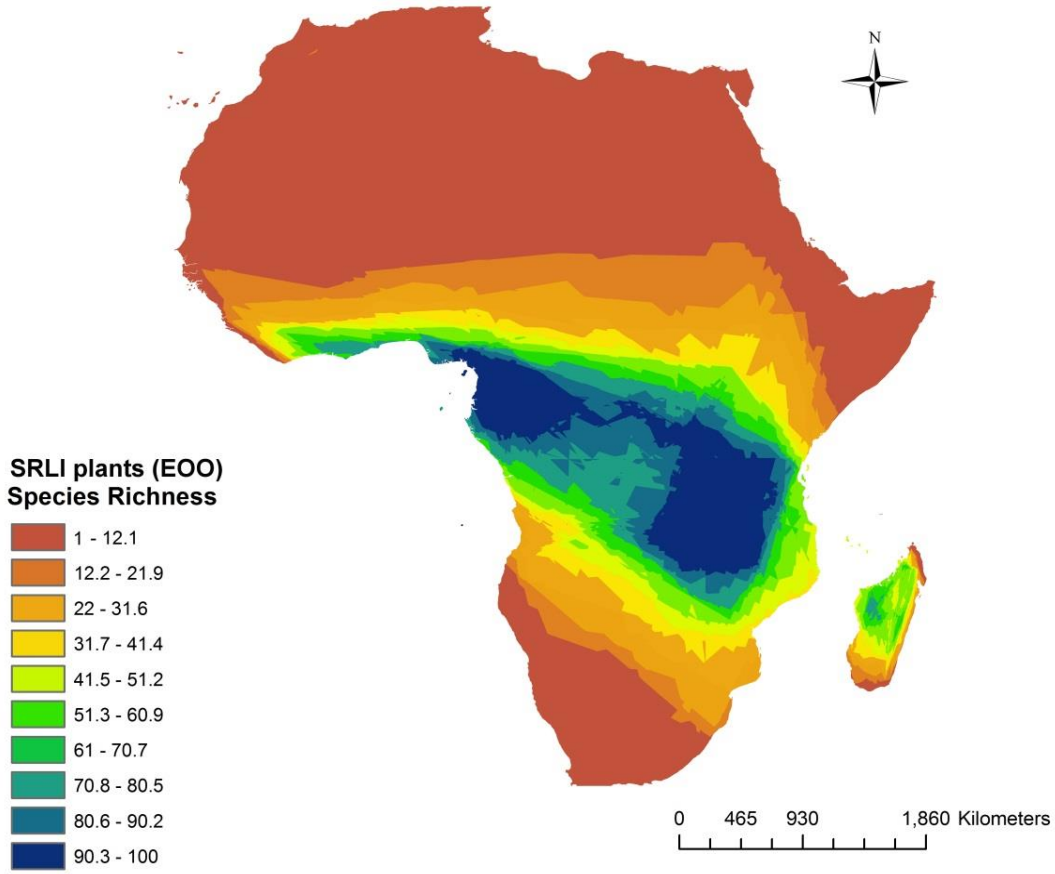

Figure 109. The species richness map of Africa for SRLI forest pteridophyte and angiosperm species produced by stacking the equivalent EOO-derived species richness maps. Data are normalised (0 – 100) and classified in ten intervals based on legend of Figure 108.

The ESH-derived maps of endemism for the SRLI forest angiosperm species and for the SRLI forest pteridophyte species are shown in Figures 110 and 111, respectively. As with the ESH-derived species richness, the maximum endemism value for the angiosperm species (0.25) was higher than that for the pteridophyte species (0.04). Both maps predicted the highest endemism values in north and east Madagascar. In addition, both maps predicted medium to high endemism values in the Comoros islands, Mount Cameroon, the Atlas Mountains in North Africa, the Eastern Arc Mountains in Tanzania and the coasts of Ghana and Côte d'Ivoire. The greatest difference between the two maps (Figure 112) was identified in Madagascar where the endemism of pteridophytes is relatively higher than the endemism of angiosperms in east Madagascar and lower in north-west Madagascar. Despite the fact that both maps identified the Zambezi-Congo watershed area as an area of endemism, the map of angiosperms predicted relatively higher values of endemism than the map of pteridophytes for part of the area. The only areas of endemism that were identified in the angiosperm map of endemism richness but not identified in the pteridophyte map were the Ethiopian Highlands and an area in the south-east part of South Africa. However, the map of pteridophyte endemism predicted relatively higher values for parts of the East African Rift Mountains and the Eastern Arc Mountains.

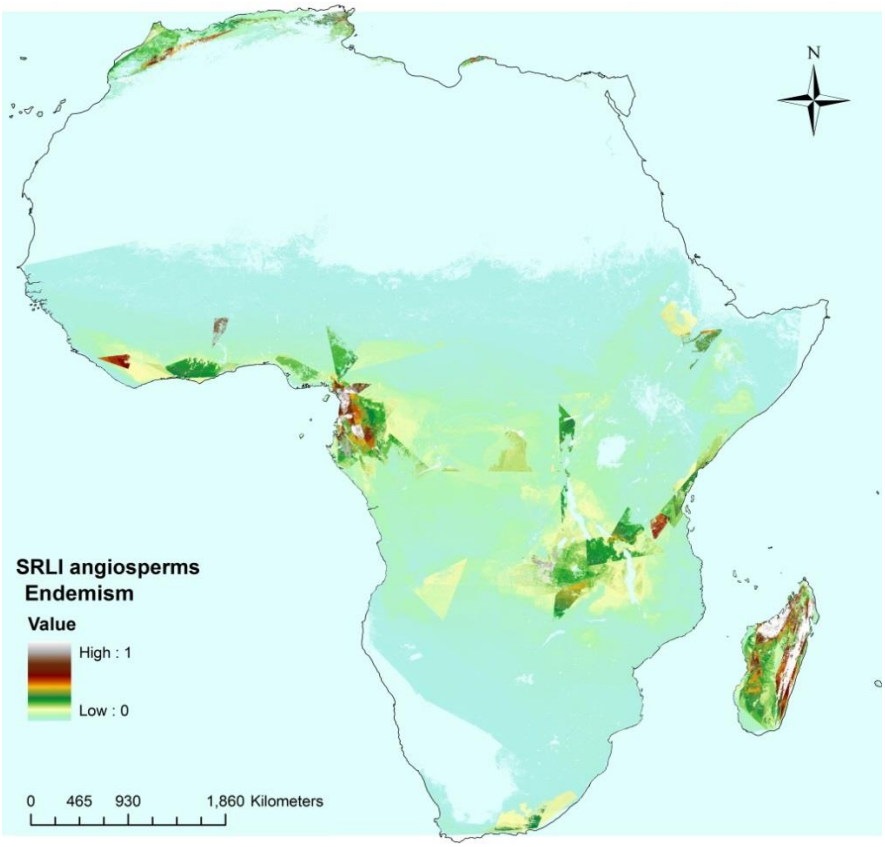

Figure 110. The endemism richness map of Africa for SRLI forest angiosperm species produced using the species ESHs (calculated using SRLI specimen data, species' altitudinal ranges, species' habitat preference and species' water balance values). Data are normalised (0 – 1).

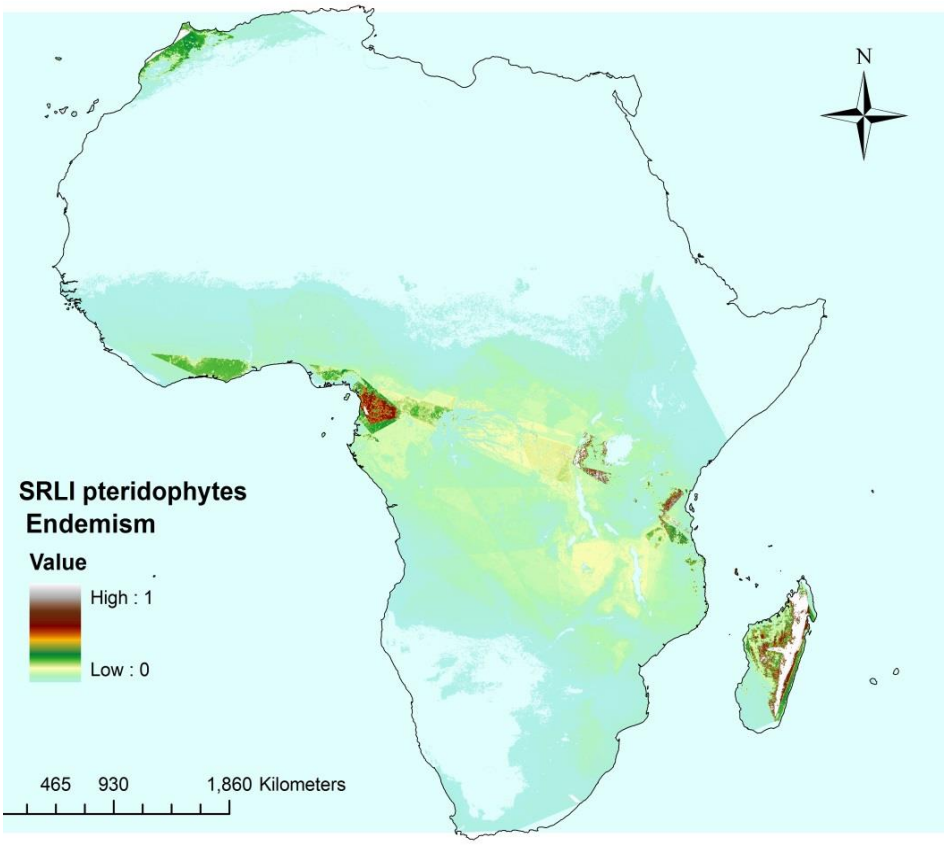

Figure 111. The endemism richness map of Africa for SRLI forest pteridophyte species produced using the species ESHs (calculated using SRLI specimen data, species' altitudinal ranges, species' habitat preference and species' water balance values). Data are normalised (0 – 1).

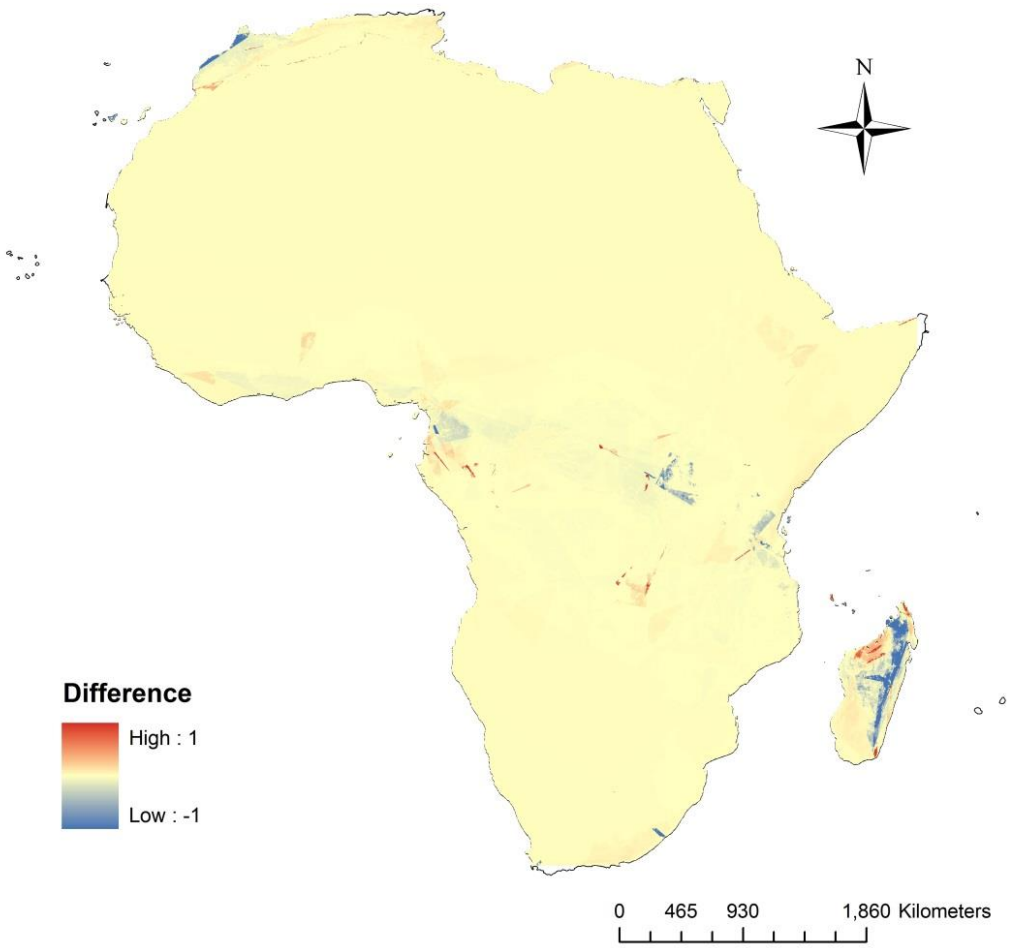

Figure 112. Difference map between the endemism of SRLI forest angiosperm species (Figure 110) and the endemism of the SRLI forest pteridophyte species (Figure 111). Positive values mean endemism of angiosperm species is higher and negative values that endemism of pteridophyte species is higher.

The endemism richness maps of the two groups (angiosperms: Figure 110 and pteridophytes: Figure 111) were stacked together in order to create a combined ESH-derived endemism richness map for the SRLI forest plants. This combined map, which is presented in Figure 113, predicted six centres of endemism; the Zambezi-Congo watershed area, the western part of the Congo basin (Mount Cameroon area), north and east Madagascar, the Atlas Mountains in North Africa, the Eastern Arc Mountains and the East Rift Mountains (Mitumba Mountains). All these areas had high levels of endemism in the endemism richness map of each plant group. Areas with medium levels of endemism were the Ethiopian Highlands and areas in West Africa (the coast of Ghana and Côte d'Ivoire), which were influenced by the predictions of the endemism richness map for angiosperms.

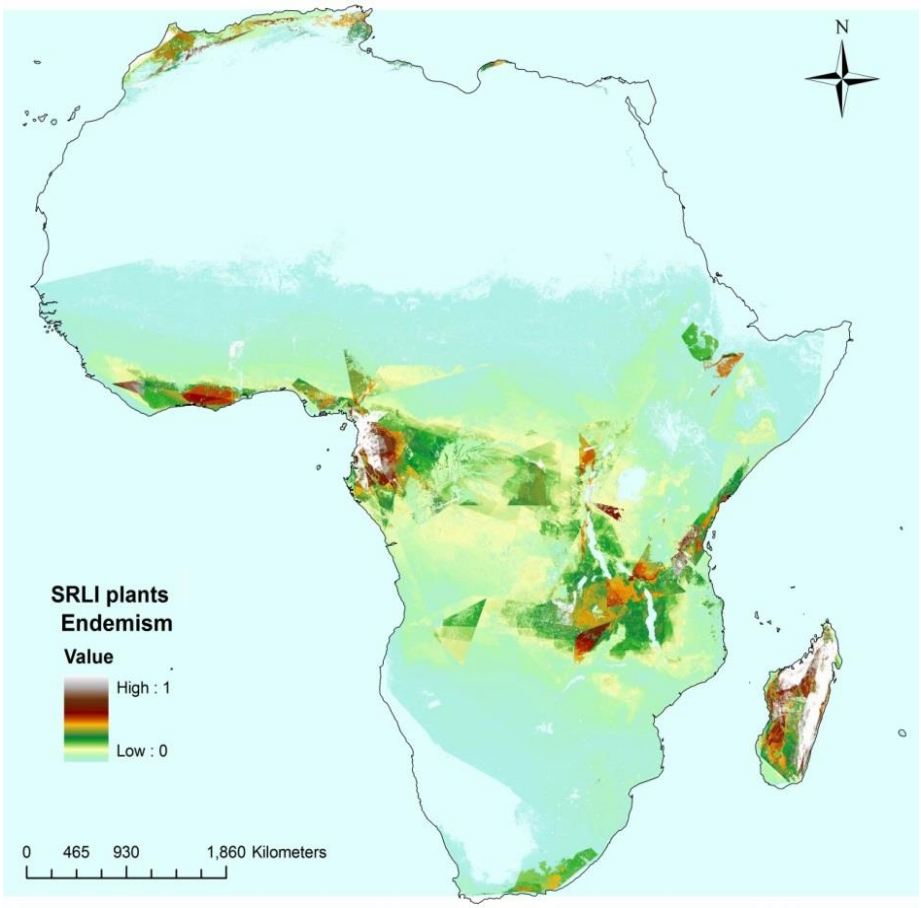

Figure 113. The endemism richness map of Africa for SRLI forest pteridophyte and angiosperm species produced by stacking the equivalent maps of endemism (Figure 110 & 111). Data are normalised (0 – 1).

5.3.3 ESH-derived integrated map of biodiversity and threat for the SRLI forest plant species

The combined species richness map, the combined map of endemism richness and deforestation data were combined into one map; this is presented with RGB coded values in Figure 114. Areas combining high species richness and high levels of endemism (yellow colour) were considered as priorities for future botanical expeditions for the SRLI for Plants. These included the Zambezi-Congo watershed area, areas in the East Rift Mountains (Mitumba Mountains) and the western part of the Congo basin (including Mount Cameroon). Furthermore, Madagascar, the Western part of Africa (Ghana and Côte d'Ivoire) and the Eastern Arc Mountains appeared to have high levels of endemism and medium levels of species richness and were also selected for fieldwork. Based on the GFC deforestation data (2000 – 2012), deforestation hotspots were the central area of Congo basin, the south-eastern part of South Africa, west Angola and West Africa (central Ghana and central Côte d'Ivoire) and Chad. Fewer deforested pixels were found in areas combining high species richness and endemism; these include the East Rift Mountains and areas in Zambia and Tanzania. The western part of the Congo basin had fewer deforested pixels than any other areas with high levels of species richness and endemism. In the case of Madagascar, deforestation occurred mainly in the south-western part of the island with lower deforestation occurring in areas with high levels of species

richness and endemism (eastern part of the island). Despite the fact that the Ethiopian Highlands, the Eastern Arc Mountains, the Atlas Mountains of North Africa and the area in the south-east part of South Africa were not identified as areas with high species richness, they were nevertheless selected due to their high levels of endemism.

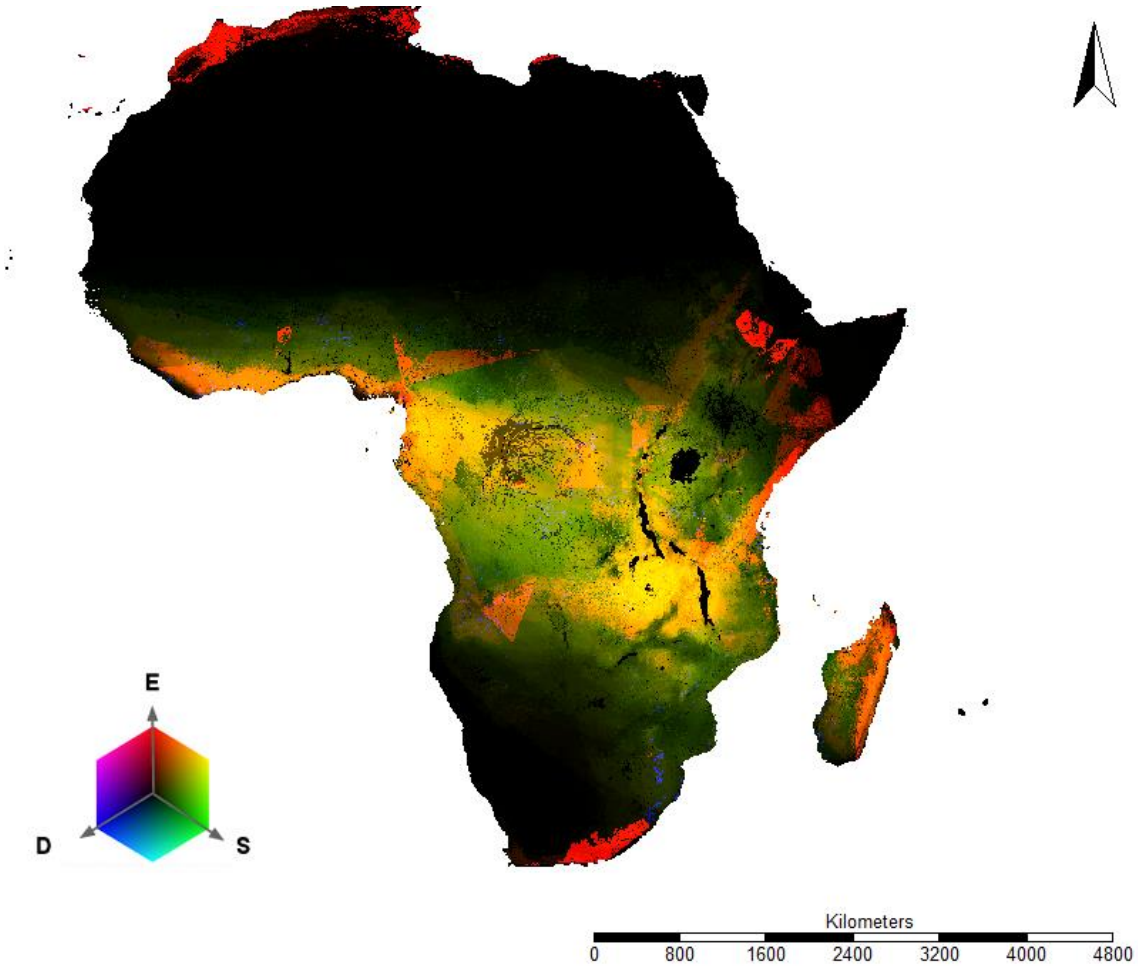

Figure 114. Map of integrated biodiversity and threat for the SRLI forest plant species produced by combining the species' maps of species richness and endemism and the GFC deforestation data (2005 – 2012). Map presented with RGB coded values. Legend: E=Endemism, R=Species Richness, D=Deforestation.

5.4 DISCUSSION

5.4.1 Applying and testing the ESH calculation method for the SRLI angiosperms

Differences between the species' ESHs of angiosperms and of pteridophytes were expected since the two groups are distinctly different. Although pteridophytes, as a group, have a larger mean range size than angiosperms (Smith, 1972; Moran, 2004; Kreft *et al.*, 2010), it was found that the mean EOO size of the SRLI forest angiosperm species was three times bigger than of the SRLI forest pteridophyte species. This was not a surprise as this analysis was conducted using species endemic to Africa, excluding the wide-ranged pantropical pteridophyte species.

The average ESH of the species in both groups was significantly smaller than the average EOO of the species, a result which is corroborated by similar studies (Jetz *et al.*, 2008; Beresford *et al.*, 2011a; Beresford *et al.*, 2011b; Buchanan *et al.*, 2011; Rondinini *et al.*, 2011). As expected, the mean ratio of EOO to ESH differed significantly between the two plant groups (angiosperms: 62.6±0.2%, pteridophytes: 44.5±0.2%), with a bigger mean reduction from EOO to ESH for the pteridophyte species than the angiosperm species. This can be explained by the stronger correlation that pteridophytes have with water availability than angiosperms have (Kreft *et al*., 2010) and by the fact that pteridophytes are less adaptable to the range of environmental conditions (Kessler et al., 2011), making them more habitat specific than angiosperms. This was obvious when analyzing altitude, water balance and land cover values of the SRLI occurrence points and considering the environmental and land cover preferences of the two groups. Pteridophyte species had a higher number of occurrences in wetter areas and areas with higher altitude than angiosperms. In addition, based on the GlobCover data, pteridophytes occurred more frequently in wet evergreen forests than angiosperms, whereas angiosperms had higher frequency in drier land cover classes (e.g. open deciduous forests, mosaic vegetation) than pteridophytes. In contrast to the pteridophytes' habitat specificity, angiosperms appeared to occur in broader environmental conditions and land cover classes, reflecting their greater ability to adapt to a wider range of ecological niches and also their known ecological dominance in the terrestrial biota (Tryon, 1972; Burger, 1981). Hence, on average, more suitable habitat was selected during the ESH calculation for angiosperms than for pteridophytes.

In the species included in this study (SRLI forest species), angiosperms had a greater percentage (14%) in threatened categories than pteridophytes (11%), agreeing with the pattern in percentage terms of all SRLI plant species in the IUCN Red List categories (Brummitt *et al*., 2010). According to the SRLI for Plants report in 2010 (Brummitt *et al*., 2010), 14% of SRLI pteridophytes, 12 % of SRLI legumes and 22% of SRLI monocots (angiosperms average: 17%) are threatened. As expected, the mean size of the ESH of both groups differed significantly between the IUCN threat categories, as does the original EOO. In both plant groups, the average size of the EOO and ESH decreased with increasing category of threat with the average EOO and ESH being greater for species in the Least Concern category and smaller in the Endangered category. These results agree with findings of this study produced using all

SRLI forest pteridophytes (see Results in Chapter 2). This stable relationship between the ESH size of the SRLI forest species in Africa and the degree of IUCN threat supports the suggestion made in Chapter 2 of this study to incorporate the ESH metric within the IUCN Criterion B sub-criterion b(iii) (decline extent/quality of habitat). The degree of habitat loss observed in already assessed species could be quantified and the ESH thresholds determined as representing an appropriate amount of suitable habitat for setting thresholds for each threatened category.

Jetz *et al*. (2008) showed that the EOO is overestimating the range of threatened species more than the non-threatened ones. This was not the case in this analysis. The species' ratio of EOO to ESH in each plant group differed between the IUCN Red List categories, although the difference was not statistically significant. In the case of angiosperms, the ESH/EOO ratio decreased (i.e. the habitat range became more restricted) with increasing category of threat, a result that agrees with Rondinini *et al*. (2011) and Beresford *et al.* (2011). For Pteridophytes, the greatest mean reduction from EOO to ESH was found in the Endangered category. However, the mean ESH/EOO ratio was not smaller in the threatened categories compared with the non-threatened. Nevertheless, the significant reduction of the EOO to ESH for both groups (Pteridophytes: 55.5%, Angiosperms: 37.4%) showed that the EOO is overestimated not only for forest pteridophyte species but also for forest angiosperms which are not as habitat specific as pteridophytes. Due to lack of data the ESHs of the angiosperm species were not validated using independent occurrence data as the ESHs of the pteridophyte species were. However, it is assumed that the ESH metric reduced commission errors relative to the EOO in the case of angiosperms as it did in the case of pteridophytes.

5.4.2 Using the ESH-derived maps of species richness and endemism to identify areas for future botanical expeditions for the SRLI for Plants.

Prior to using the ESH-derived maps of species richness and endemism to identify areas for future botanical expeditions, the patterns of these maps were interpreted in order to determine whether they were meaningful. Note that while the ESH-derived maps were compared with the results of previous studies, some differences were expected due to their different methods and species samples. Furthermore, due to the recognised bias in the SRLI data (details in Chapter 2, section 2.3.1), related anomalies were anticipated.

5.4.2.1 Interpretation of the species richness maps

The ESH-derived species richness maps of both groups (angiosperms and pteridophytes) identified the Zambezi-Congo watershed area as the centre of species richness. This area, which is mainly covered by Miombo woodlands, was identified as a centre of plant species richness by Linder (2001) and Fjeldsaå and Lovett (1997), but not by other recent biogeographical studies (Barthlott *et al*., 2005; Barthlott *et al*., 2007; Kreft & Jetz, 2007). Linder (2001) showed that this area is one of the floristic refugia of Africa while he argued that this area

has not been the focus of many studies due to the fact that it is not covered with wet forest and it is not located in a topographically complex area. One reason that the analysis here has identified this area whereas others have not is the high representation of legume species in the SRLI sample used here. The Miombo woodlands are dominated by species of the legume family (Frost, 1996), which is the only family representing dicot species in the SRLI sample and one of the two families in the angiosperm species sample. In addition, the SRLI angiosperm species sample has a low percentage of tree species which are well represented in other studies. Regional studies have shown that these woodlands have high species richness in legumes even though timber tree species are suffering from overexploitation (Malimbwi & Mugasha, 2002; Giliba *et al.*, 2011). Field-based studies showed high species richness of understory monocot species such as orchids (Goldblatt, 1977; Linder, 1983). Thus, while other studies failed to locate this centre, it was identified in the analysis here since it picked up the high species richness in the understory vegetation. While the Zambezi-Congo watershed is not as topographically complex nor as wet as other areas, high pteridophyte species richness in the area could be explained by its past (Fjeldsaå & Lovett, 1997) and current (Nicholson, 1994) stable climatic conditions with limited dry periods.

Other areas that were identified by the species richness maps of the two groups were the western area of the Congo basin (including Mount Cameroon) and topographically complex montane areas of the East African Rift. The species richness of those areas were predicted to be high in previous studies for both angiosperms and pteridophytes (Linder, 2001; Barthlott *et al*., 2005; Barthlott *et al*., 2007; Kreft & Jetz, 2007; Kreft *et al*., 2010) and have been linked to the floristic refugia of Africa (Hamilton, 1974; Hamilton, 1976; Kornas, 1993; Fjeldsaå & Lovett, 1997; Linder, 2001; Aldasoro *et al.*, 2004; Parmentier *et al.*, 2007). While species richness of angiosperms was equally high in the wet forests of the eastern and western mountains, pteridophyte species richness was higher in the eastern mountains than the western mountains, a result that agrees with Schelpe (1983).

As with the species' ESHs of the two groups, the maps of species richness differed between angiosperms and pteridophytes, reflecting the overall differences of these two plant groups. Pteridophyte species richness was relatively higher compared with angiosperms in high altitudes of montane wet areas with cloud affected forests (e.g. Eastern Rift Mountains) and was lower in the lowlands (e.g. Niari valley in the Congo basin) and in montane areas with low water balance values (e.g. the Ethiopian Highlands). In addition, information on pteridophyte species richness was lacking for dry lowland areas (e.g. Saharan areas) in contrast to that for angiosperm species richness. These differences were explained when the species richness of the two groups was evaluated along altitudinal and moisture gradients. As expected, pteridophyte species richness was strongly correlated with water balance, in line with the findings of other studies (Page, 2002; Bickford & Laffan, 2006; Kreft et al., 2010; Kessler et al., 2011). Angiosperm species richness, though, was strongly correlated with altitude, showing perhaps, its relationship with energy related variables as found in Kreft & Jetz (2007). A mid-altitude peak (1000 – 2000m) in species richness was found for both groups which is consistent

with the results of previous studies (Vetaas, 1993; Kessler, 2000; Hemp, 2002; Bhattarai *et al.*, 2004; Rahbek, 2005; Kluge *et al.*, 2006; Watkins *et al.*, 2006; Kessler *et al.*, 2011). However, relatively higher pteridophyte species richness values were found in altitudes over 2000m compared with angiosperm species richness values, whereas angiosperm species richness was relatively higher in altitudes lower than 1000m. Furthermore, the strength of the correlations of species richness of pteridophytes and angiosperms with water availability shows the important relationship of the two groups with this variable. This supports the suggestion of previous studies that water availability is an important factor of the distribution of all forest plant species in Africa (Swaine, 1996; Linder, 2001; Holmgren *et al*., 2004; Maharjan *et al*., 2011). While the species richness of both groups peaked at water balance values between -1000 and 0 mm/month, relatively higher values of species richness values were found at lower water balance values (-3000 – -1500 mm/month) for angiosperms than for pteridophytes. These patterns match the characteristics of each plant group: pteridophyte species are more habitat-specific to wet montane forests whereas angiosperms occur in a wider range of ecological niches. Note that a negative water balance indicates annual evapotranspiration in excess of local precipitation and thus reliant on inflows of subsurface and surface water from upstream. Positive values indicate a local excess of precipitation over actual evapotranspiration.

Due to the fact that the species richness map for each plant group produced meaningful patterns based on the characteristics of that plant group and identified already known centres of species richness, the two maps were combined to produce the species richness map of SRLI forest plants for Africa. In this map, areas with medium or high species richness broadly overlapped with the proposed floristic refugia of Africa. These were the Zambezi-Congo watershed area, the western part of the Congo basin (Cameroon-Gabon area), small areas in West Africa (Ghana, and Côte d'Ivoire), the East African Rift area (including the areas in Kivu) and the Eastern Arc Mountains (in Tanzania and Kenya). The only area, identified as a centre of species richness by other studies but not here, is the Cape Floristic area. The low species richness of both plant groups in that region can be explained by the lack of South African species in the SRLI sample as they were assessed in a separate regional project (Red List of South African Plants) (SANBI, 2015).

The comparison between the ESH and EOO derived species richness maps demonstrated the advantage of using the species ESH over the species' original EOO, as was also shown in Chapters 3 and 4. As expected, both maps predicted two centres of species richness identifiying the same broad areas. However, the species richness hotspots of the EOO-derived map appeared to be homogeneous across large regions in contrast to the hotspots of the ESH-derived maps which appeared smaller and more distinct. Thus, the prioritisation of specific areas for fieldwork would be difficult based on the general EOO-derived species richness pattern. In contrast, the ESH-derived map appeared to better reflect habitat heterogeneity on the ground and could be valuable in the preparation for fieldwork, as Brooks & Matiku (2011) suggested.

5.4.2.2 Interpretation of the maps of endemism

As expected, endemism levels of pteridophytes and angiosperms are high in topographically complex areas and islands due to their past and present isolation. Kier *et al*. (2009) found higher levels of plant endemism in island regions than in mainland regions globally. In both ESH-derived maps of endemism, levels of endemism were as high in the island regions as in the mainland regions (e.g. Comoros Islands, Canary Islands), with the exception of Madagascar which had higher values than areas in the mainland. Similarly, in a study focusing on Africa, Kier & Barthlott (2001) predicted the highest endemism values in East Madagascar after the Cape Floristic Region, which was not represented in the SRLI occurrence data. These predictions were not a surprise as Madagascar is one of the oldest islands in the world (Yoder & Nowak, 2006) and a designated biodiversity hotspot (Mittermeier *et al.*, 1998; Myers *et al.*, 2000; Brummitt & Nic Lughadha, 2003). Madagascar has a suite of uniquely evolved species. Based on field studies, Madagascar's level of plant endemism is 83% with pteridophyte endemism estimated at 45% of species (Goodman & Benstead, 2005) and angiosperm endemism estimated at 84% of species (Callmander *et al.*, 2011).

As Linder (2001) showed, there is an obvious overlap between the endemic and the species rich areas in mainland Africa for both plant groups. These areas were Mount Cameroon, the Eastern Arc Mountains, small areas in West Africa (Ghana and Côte d'Ivoire), areas in the East African Rift and the Zambezi-Congo watershed, all of which are recognised centres of plant endemism (Exell & Wild, 1973; Rodgers & Homewood, 1982; White, 1983; Lovett & Friis, 1996; Myers *et al*., 2000; Kier & Barthlott, 2001; Linder, 2001) and have been proposed as the floristic refugia of Africa (Hamilton, 1974; Hamilton, 1976; Kornas, 1993; Fjeldsaå & Lovett, 1997; Linder, 2001; Aldasoro et al., 2004). Unsurprisingly, levels of endemism for pteridophytes were relatively higher than angiosperms at high altitudes of montane areas (e.g. East African Rift Mountains) and lower at lower altitudes such as the Zambezi-Congo watershed. Interestingly, the Atlas Mountains in North Africa were identified as an endemic area for both plant groups. While more than 450 endemic plant species have been recorded in these Mountains (Hobohm, 2014), there is no record showing that endemism levels of pteridophytes are high in that specific area. Africa north of the Sahara is generally accepted as being part of a separate Mediterranean biogeographic region, with strong floristic links also to Macaronesia. These high levels of endemism in the Atlas Mountains were the result of two species (*Asplenium palmatum* and *Asplenium hemionitis*) which according to Bramwell and Caujapé-Castells (2011) are Macaronesian endemic species which can be found in North Africa occasionally, but not elsewhere in the continent. Therefore, the predicted high levels of endemism of pteridophyte species in North Africa is an artefact due to the lack of SRLI occurrence points of particular species in the rest of their range outside of Africa. The only areas of endemism that were identified in the angiosperm map of endemism richness but not identified in the pteridophyte map were the Ethiopian Highlands and an area in the south-east part of South Africa. Both areas are relatively drier compared with the other identified endemic areas, and were also predicted as centres of endemism for angiosperms by Kier & Barthlott (2001).

Since the maps of endemism for both groups gave meaningful patterns, they were stacked together in order to create a combined ESH-derived endemism richness map for the SRLI forest species. This combined map included the endemic areas which were common in the endemic maps of both plant groups (the Zambezi-Congo watershed area, the western part of the Congo basin, north and east Madagascar, the Atlas Mountains in North Africa, the Eastern Arc Mountains and the East African Rift Mountains) with the highest levels of endemism in the western part of Congo basin and Eastern Madagascar. It also included the Ethiopian Highlands and areas in West Africa (coast of Ghana and Côte d'Ivoire) which were influenced by the predictions of the endemism richness map for angiosperms.

5.4.2.3 Using the integrated map of biodiversity and threat to identify areas for future SRLI expeditions

The combined species richness map, the combined map of endemism richness, and deforestation data (2000-2012) were combined into one map, the integrated map of biodiversity and threat. Using this map, areas combining high species richness, high levels of endemism and low deforestation density were prioritised for future botanical expeditions for the SRLI for Plants. These areas are the Zambezi-Congo watershed area, areas in the East African Rift Mountains and the western part of the Congo basin. By selecting areas with high levels of species richness and low deforestation density, the probability of finding the SRLI plant species in the field increases. This way, areas with habitat degradation due to deforestation, where the likelihood of finding these species is low, can be avoided. In addition, the chances of finding and investigating species with small ranges which are more likely to be threatened are greater when selecting areas with high levels of endemism. Based on the selected areas, field trips have been planned to the following areas: (1) the East African Rift mountains of south -western Uganda, eastern Democratic Republic of Congo, Rwanda and Burundi; (2) the Zambezi-Congo watershed areas in the south-eastern Democratic Republic of Congo and north-western Zambia; (3) the Chimanimani mountains bordering Zimbabwe and Mozambique; and (4) the Gulf of Guinea lowlands of southern Cameroon and northern Gabon.

Since areas in Madagascar, the Western part of Africa (Ghana and Côte d'Ivoire) and the Eastern Arc Mountains appeared to have high levels of endemism and medium levels of species richness, they were also considered for future field trips. The specific areas did not appear to have high density of deforestation based on the GFC deforestation data. Based on this information, further field trips have been planned in: (1) the Eastern Arc mountains of south-eastern Kenya and eastern Tanzania; and (2) the Mount Nimba area in Côte d'Ivoire. The eastern part of Madagascar was not prioritised since it is the focus of field expeditions organised by the Royal Botanic Gardens, Kew. While the levels of species richness in the Ethiopian Highlands was relatively low, these areas were nevertheless selected due to their high levels of endemism for angiosperms making them ideal for field expeditions focusing on narrow-range species. Therefore, a trip to the Bale Mountains and southern highlands of Ethiopia, where deforestation density is low, has been scheduled.

It is important to note that the GFC deforestation data cover years between 2000 and 2012 and thus any deforestation before 2000, that was not detected by the coarser resolution of the land cover data used in the ESH calculation (GlobCover v.2.2), may still be present at some of the selected sites.

5.5 CONCLUSIONS

The ESH calculation method was built using the SRLI forest pteridophyte species (Chapter 2). In this chapter, which focuses on Africa, the ESH method was applied to a different SRLI plant group, the SRLI forest angiosperm species. The comparison between the ESHs of the two plant groups showed that the ESH method produced meaningful results as their differences reflected the overall differences of the two groups. In contrast to the habitat specificity of pteridophytes, angiosperms appeared to occur in many types of habitat, reflecting their greater ability to adapt to a wider range of ecological niches and also their known ecological dominance in the terrestrial biota. While the ESHs of the angiosperm species were not validated using independent occurrence data, it is assumed that the ESH metric reduced commission errors relative to the EOO in the case of angiosperms as it did in the case of pteridophytes. Therefore, it is believed that the ESH calculation method is effective at reflecting the reality of distributions on the ground for different plant groups. In addition, as with the pteridophyte species, a stable relationship between the size of the ESH for angiosperm species and the degree of IUCN threat was found. This supports the suggestion made in Chapter 2 of this study to incorporate the ESH metric within IUCN Criterion B sub-criterion b(iii) (decline in area, extent and/or quality of habitat).

As with the species' ESHs of the two groups, the maps of species richness and endemism differed between the two groups. Despite the recognised geographical bias in the SRLI occurrence data and the specific species sampled (SRLI forest species) (Chapter 2, section, 2.3.1) and the anticipated related anomalies (discussed in Chapter 3, section 3.4), the produced maps predicted meaningful spatial patterns in comparison with previous studies. For this reason, these maps were combined together and with deforestation data to produce an integrated map of biodiversity and threat which assisted in prioritising areas for future botanical expeditions for the SRLI for Plants. This shows that the ESH metric could be valuable in identifying areas for field expeditions as Brooks & Matiku (2011) suggested, although this will be verified by the results of the SRLI expeditions.

CHAPTER 6

PROJECTING RANGE CONTRACTION AS A RESULT OF HUMAN IMPACT

6.1 INTRODUCTION

6.1.1 Deforestation

Forests cover 31% of the world's surface (4 billion hectares) and hold over 80% of global terrestrial biodiversity (FAO, 2010). However, they are not evenly distributed globally with the largest forest areas found in South America (tropical forests) followed by northern Eurasia (Russian temperate forests) and North America (temperate forests). When comparing the forest cover of the different climate zones, the tropical zone is found to have the highest percentage of forest cover, a total of 47% (FAO, 2010). Forest distribution is also uneven within tropical regions, however; according to FAO (2010), the Neotropics have 891 million hectares of tropical forest, the Afrotropics have 344 million hectares and Indomalaya has 356 million hectares, the largest areas being those in the Amazon basin, the Congo basin and South East Asia, in each continent respectively

This distribution can partly be explained by the different past and present climatic patterns and events, with the last Ice Age ending about 10 000 years ago (Emanuel *et al.*, 1985). High climatic variability associated with repeated glaciations resulted in species extinction and forced forests to expand or shrink to areas with suitable or stable conditions (Hamilton, 1974; Hamilton, 1976; Fjeldsaå & Lovett, 1997; Williams, 2002; Graham *et al.*, 2010). Forest distribution can also be explained by past and present human impact within each region (Hansen *et al.*, 2013). Humans have been influencing the extent of forests since the prehistoric age, resulting in the reduction of the Earth's total forest area (Williams, 2000). The reduction of forests over the last 5000 years was calculated to be 1.8 billion hectares, based on estimates of the original forest cover by Williams (2002) (5.8 billion hectares) and the current total forest area of the planet (4 billion hectares) (FAO, 2010). FAO (2010) therefore reported that there was a decrease in the Earth's total forest area by 15% since the pre-human impact era. This reduction may be even higher, as according to Billington *et al.* (1996), Earth's original forest cover was 6.2 billion hectares and therefore Earth could have lost 18% of its forest cover since the pre-human impact era. It has also been estimated that approximately 20% of the Earth's original forest cover remains undisturbed (Bryant *et al.*, 1997). Periodic deforestation ('the removal of tree cover below the threshold value that defines a forest' (Achard, 2009)) has occurred over time as forests played a major role in human history by providing food, raw materials for buildings and shipbuilding, fuel and land for agriculture, farming and settlements. As human population increased, human activities had an increasing impact on forests. Until the 19th century, deforestation mainly occurred in forests of temperate region in Asia, North America and Europe. That changed in the 20th century, when the main focus was forests in tropical regions (Williams,

2002), with the deforestation peak occurring between the 1950s and the 1980s (FAO, 2012b). While FAO (2010) reported that there was a decrease in deforestation rates in the last 30 years but that the rate of loss of primary forest remains at approximately the same level as in the 1980s. Different studies have argued that deforestation rates are not decreasing in all parts of the world (Matthews, 2001; Achard *et al.*, 2002; DeFries *et al.*, 2002; Grainger, 2008; Kim *et al.*, 2015). A study that calculated forest loss based on remotely-sensed data (Hansen *et al*., 2013) revealed that there was an increase in gross forest loss of 200 000 hectares per year in the tropics between 2000 and 2012. This study also found higher annual gross rates of deforestation than reported by FAO (2010). FAO (2010) published that on average 13 million hectares of forest, mainly in the tropics, were still deforested each year between 2000 and 2010. Hansen *et al*. (2013) showed that between 2000 and 2012, 19 million hectares of forest were lost per year, 32% of which occurred in the tropics. Differences between the results of FAO (2010) and Hansen *et al*. (2013) can be attributed to their different forest definition (FAO: >10% tree cover; Hansen *et al*. (2013): > 25% tree cover) and different estimation methods.

The degree of deforestation differs across the tropics since it is driven by several factors. According to Geist & Lambin (2001), there are five groups of underlying drivers of tropical deforestation: economic; policy and institutional; technological; cultural; and demographic factors. However, in real terms the main causes of deforestation can be identified as: expansion of agricultural and pasture land; wood extraction; mining; urbanization; and infrastructure extension (Contreras-Hermosilla, 2000; Geist & Lambin, 2002; Laurance *et al.*, 2012). The most important proximate cause of deforestation is to use the land for agriculture (Geist & Lambin, 2002; FAO, 2010; Hosonuma *et al.*, 2012; Laurance *et al.*, 2012). Gibbs *et al.* (2010) demonstrated that between 1980 and 2000, approximately 80% of new agricultural land was produced from intact and undisturbed forests. It has also been reported that, between 2000 and 2010, agriculture was the proximate cause of 80% of global deforestation (Kissinger *et al.*, 2012). The conversion of forest to agricultural land is related to economic development but also to the ecological characteristics of the area (DeFries *et al.*, 2004). Deforestation in the Neotropics and Indomalaya is driven mainly by commercial agriculture, in contrast to the Afrotropics in which small-scale subsistence agriculture is more dominant than commercial agriculture (DeFries *et al.*, 2004; Fisher, 2010; Kissinger *et al.*, 2012). This reflects the high levels of poverty in the continent.

Deforestation has been concentrated in areas suitable for agricultural use. Montane areas (>1500m), which contain 23% of the global forest cover (FAO, 2010), have a lower deforestation rate than lowland areas, mainly due to poorer accessibility (Collins *et al.*, 1991). In addition, the steep mountain slopes and wet climate make montane areas less than ideal for agricultural use (with the exception of particular crops e.g. coffee plantations). However, with the expansion of road networks and the decrease in remaining lowland forest areas suitable for agricultural use, deforestation has increased in montane forests (Sader & Joyce, 1988; Armenteras *et al.*, 2011), reaching higher rates than in lowland forests during the 70s and 80s (FAO, 1993). Regardless of altitude, deforestation is not expected to occur inside legally-established protected areas

which according to FAO (2010) cover 13% of the world's forest. Nonetheless, illegal deforestation activities in protected areas still exist in different regions of the world, especially in developing tropical countries (FAO, 2001; FAO, 2010). Protected or not, remote montane forests are preferred over lowland forests for illegal deforestation due to their inaccessibility and isolation (Cavelier & Etter, 1995; Armenteras *et al.*, 2011), increasing the deforestation rate in montane areas.

The increasing demand for agricultural products from rising populations is reflected in the deforestation rates of the tropical regions. Global net deforestation occurred at a rate of 0.14% between 2005 and 2010, which is lower than the equivalent rate from 1990 to 2000 (0.20%) but higher than the deforestation rate from 2000 to 2005 (0.12%) (FAO, 2010). According to FAO (2010), South America, which is the world's most forested region, had the highest deforestation rate in the tropics, losing 4 million hectares per year between 2000 and 2010. Hansen *et al*. (2013) also found that the highest percentage of deforestation between 2000 and 2012 occurred in South America, even though there was a decrease in deforestation in Brazil due to conservation efforts. Despite significant efforts, Brazil still had the greatest forest loss in the tropical region (3 million hectares per year). FAO (2010) reported a decrease in deforestation rates of South-East Asia in which most agricultural expansion has been for tree plantations. However, Hansen *et al*. (2013) found that countries such as Indonesia, Malaysia and Cambodia showed increasing forest loss with Indonesia having the highest increase in forest loss globally (from 1 million hectares per year in 2000 to 2 million hectares per year in 2012). Further, FAO (2010) reported that Africa lost 3.4 million hectares per year between 2000 and 2010, although this estimation was based on incomplete information as not all African countries provided reliable data. While Hansen *et al.* (2013) did not report a rate of forest loss for the whole African continent, their study showed that Africa's tropical dry forests experienced high rates of loss and that its moist tropical forest had an annual increase in forest loss of 54 000 hectares between 2000 and 2012. Zambia, Angola and Tanzania were among the African countries with the greatest forest loss.

The forests richest in species are the tropical forests, both lowland rainforests and montane cloud forests (Myers *et al.*, 2000; Pimm *et al.*, 2001; Mace, 2005). Habitat loss and land use change were identified as the main causes of biodiversity loss (Groombridge, 1992; Dirzo & Raven, 2003; Gaston *et al.*, 2003a; Mace, 2005; Brummitt & Bachman, 2010; Brummitt *et al.*, 2015b). It has also been suggested that land use change will most likely affect biodiversity in the future to a greater degree than climate change (Sala *et al.*, 2000; van Vuuren *et al.*, 2006; Jetz *et al.*, 2007). Plant and animal species are vulnerable due to habitat loss and their survival is dependent on their ability to maintain stable populations in remaining fragments of forest. Deforestation is generally non-directional, occurring in a small-scale way across forested regions, and results in habitat fragmentation, leading to degraded forest patches surrounded by non-forested land cover. The interactions in the transition zone between the forest ecosystem and the adjacent surrounding non-forest ecosystem are called edge effects since the two ecosystems are separated by a sharp, artificial edge (Saunders *et al.*, 1991). Edge effects can

occur from several meters up to several kilometers from the fragment's edge. For example, Laurance *et al.* (1998) showed that tree species are affected by edge effects up to 300m from the edge, whereas Gascon *et al.* (2000) showed that the impact of these effects is obvious approximately 1 km from the transition zone. Edge effects can cause changes in the abiotic conditions of the forest patch. After its isolation, the edge of the patch is exposed to higher solar and wind penetration than experienced before deforestation, resulting in conditions of higher temperature and lower humidity (Kapos, 1989). These micro-climatic changes lead to changes in forest structure (Lovejoy *et al.*, 1986; Kapos *et al.*, 1997; Laurance *et al.*, 1998) and species composition (Laurance *et al.*, 2006), the degree of which depend on the age, physiognomy and aspect of the forest patch (Matlack, 1993; Murcia, 1995) as well as on the size and shape of the forest fragment (Laurance *et al.*, 1998). Near the edge, there is low regeneration of trees (Benitez-Malvido, 1998) and high tree mortality and damage (Ferreira & Laurance, 1997; Laurance *et al.*, 2000) and thus high litter-fall production (Sizer *et al.*, 2000). In addition, edge areas are characterized by a high abundance of pioneer and secondary tree species (Laurance *et al.*, 1998) and species of liana (Laurance, 1991; Laurance *et al.*, 2001) due to the high light availability. Thus, the impact of deforestation is not only obvious in the area where forest clearance occurred, but also in the remaining forest.

Different species are affected in different ways by forest fragmentation due to their different life history strategies and habitat requirements (Ewers & Didham, 2006) and their tolerance to the new conditions (Murcia, 1995). Studies have shown that forest fragmentation is followed in many cases by a decline in species richness (Malcolm, 1997; Gascon *et al.*, 1999; Laurance *et al.*, 2000; Ferraz *et al.*, 2003). However, other studies have shown an increase in species richness in some taxa such as frogs and small mammals (Malcolm *et al.*, 1995; Gascon & Lovejoy, 1998; Gascon *et al.*, 1999). In addition, high richness of some invertebrate species has been recorded in the edge area of forest patches (Magura, 2002; Major *et al.*, 2003). Thus, whilst the role of deforestation on populations in deforested patches is well known, the impact on species in the remaining edge habitats is less so.

In addition to the direct impact on biodiversity, deforestation also has other consequences. Several studies have shown that forest loss influences global and regional climate. Deforestation reduces evapotranspiration and thus atmospheric humidity; it also increases surface albedo. These changes may influence patterns of precipitation and result in the reduction of regional rainfall (Lean & Warrilow, 1989; Hastenrath, 1997; Spracklen *et al.*, 2012). Deforestation also releases carbon dioxide into the atmosphere since tropical forests act as a 'carbon sink' by absorbing atmospheric carbon as trees grow (Phillips *et al.*, 1998; Baker *et al.*, 2004). Hence, land cover change is contributing to greenhouse gas emissions and global warming (Fearnside, 2000). Lastly, deforestation is one of the major causes of soil degradation (Oldeman *et al.*, 1991). Vegetation removal and the consequent increase in surface temperature affect surface soil structure; this may lead to soil erosion, the decrease of infiltration and the increase of surface runoff.

6.1.2 Deforestation monitoring systems and Land use change models

Estimations about global forest cover used to be derived from national inventories which were based on inconsistent sampling methods (FAO, 1993). In the last two decades though, remote sensing data from satellite images have been used in global monitoring programmes of forest cover (e.g. FAO Forest Resources Assessment (FAO, 2010) and the TREES project (Achard *et al.*, 2002)). With the improvement in the quality and the increase of spatial resolution of remote sensing data, global and regional land cover maps have also been released. These include the global GLC2000 (European Commission, 2003) and GlobCover (IONIA, 2009) maps, the European CORINE map (Steinmeier, 2013), the AFRICOVER map (Kalensky, 1998), and several others (DeFries *et al.*, 2000; Hansen *et al.*, 2000; Mayaux *et al.*, 2000; DiMiceli *et al.*, 2010). These maps were based on different forest definitions, forest pixel thresholds, statistical sampling of satellite images and spatial resolution, preventing effective comparison of them (Mayaux *et al.*, 2005). Furthermore, while the need to convert land cover maps to time series in order to monitor land cover change in short time intervals was evident, many of the existing land cover maps were not updated frequently. Although land cover change monitoring systems were available at a national level (e.g. the Brazilian DETER system (INPE, 2008)), it was not until recently that large-scale monitoring systems have been developed. Specifically, three land cover change monitoring systems are now available: the Global Forest Change (GFC) system; the Terra-i system; and the FORMA system. GFC has provided 30m resolution data for 14 years on annual loss (2000 – 2014) based on Landsat 7 satellite data (Hansen *et al*., 2013). Terra-i (Reymondin *et al.*, 2012) and FORMA (Hammer *et al.*, 2009) are based on MODIS satellite data and are providing near-real time (16 days) data at a resolution of 250m and 500m respectively. Terra-i data have been available for Latin America since 2004, whereas FORMA has been issuing alerts just for tropical humid forests in Asia, Africa and Latin America since 2006. The aim of all three systems is to provide consistent and accurate land cover change data regularly. However, due to the differences between the three systems (e.g. spatial resolution, classification techniques, calculation algorithms, satellite sensors), the estimation of land cover change for a given area differs according to the monitoring system used (Mulligan, 2014c).

While these systems provide information about the current situation of land cover, conservation strategies are often in need of an insight into the future land cover, in order to prevent catastrophic consequences of current practices. Future drivers of deforestation have already been identified (Kissinger *et al.*, 2012). Global urbanization, meat-based diets, population growth, economic growth of developing countries, increase in demand for palm oil and wood products, and climate change, among others, will put further pressure on forests in the future. FAO (2009) estimated that with the world population reaching 9 billion by 2050, there will be an increase of 70% in the demand for food and predicted that the 50% increase in the demand of agricultural products will reduce forest cover, mainly in tropical countries.

Based on different scenario conditions, land use change models, ‘a tool to compute the change of area allocated to at least one specific land use type’ (Heistermann *et al.*, 2006), have been used to project land use change in the future, through which future forest cover loss is

estimated. These models project change in land use, the socio-economic function or purpose of land (e.g. urban living, agricultural or livestock production), rather than change in land cover, which is the observed biophysical cover of Earth (e.g. forest, water bodies, grassland). However, these two are linked since one land cover type can support many land uses, whereas one land use may be supported by many land cover types. Land use models have been developed in different disciplines and can be divided into geographical models (e.g. DINAMIC-EGO (Soares-Filho *et al.*, 2009) and QUICKLUC (Mulligan, 2015b)), economic models (e.g. IMPACT (Rosegrant *et al.*, 2001)) and integrated land use models that combine the economic and geographical land use models (e.g. GLOBIO (Havlík *et al.*, 2011)) (Heistermann *et al*., 2006). Geographical land use models are based purely on the biophysical properties and thus the land suitability of a specific area without taking into account the interaction between supply, demand and trade (Heistermann *et al*., 2006). This is in contrast to economic land use models which are based on socio-economic theories but are not explicit to specific areas (Verburg *et al.*, 2004). Limitations of land use models have been linked to their assumptions about the socio-economic and demographic changes and to their difficulties in capturing the multi-scale and complex characteristics of the land use system (Lambin *et al.*, 2000; Verburg *et al*., 2004; Heistermann *et al.*, 2006; Verburg *et al*., 2011).

Biodiversity studies have used the results from land use change models, focusing on forest cover change, in order to assess the impact of land use change on biodiversity. Such analyses have been performed on a global scale (van Vuuren *et al*., 2006; Jetz *et al*., 2007; Alkemade *et al*., 2009; Dobrovolski *et al.*, 2011; Visconti *et al.*, 2011; Visconti *et al.*, 2015) and on a regional or national scale (Soares-Filho *et al*., 2006; Alkemade *et al*., 2009; Verburg *et al*., 2011; Spangenberg *et al*., 2012; Rondinini & Visconti, 2015). Depending on the focus of the research, each study selected a different appropriate land use change model type. All global studies that assessed biodiversity change based on land use models have used the large scale Integrated Model to Assess the Global Environment (IMAGE) (Alcamo *et al.*, 1994), which contains an energy model, an agricultural model, a vegetation model and integrated land use change models. Their land use change scenarios were based on the four Milliennium Ecosystem Assessment scenarios (Millennium Ecosystem Assessment, 2005) which are incorporated within the IMAGE model.

This study has used land cover information together with information on the ecology of the pteridophyte forest species to calculate the species' ESHs (Chapter 2). The species' ESHs represented the species geographical range in 2005 since the land cover classification used was GlobCover 2005. As already mentioned, land cover change monitoring systems have been developed and thus, the species' ESHs can be re-calculated based on land cover change observations. By recalculating the species ESHs at regular intervals, the strictly comparable ESHs could show the change to the species' distribution due to habitat loss and therefore be used for re-assessing the conservation status of species under IUCN Criterion B (geographic range) sub-criterion b(iii) (decline in habitat extent, area and/or quality). Moreover, land cover change data derived from land use change models can be used to predict the species' ESH in

the future. This information could be incorporated into the rationale of the species' IUCN conservation assessment under which the reasoning behind each listing is given.

6.2 METHODS

Chapter 6 assesses the forest pteridophyte species' ESH-derived ranges against the degree of human impact through time. For each species, an ESH was calculated five times: the species' estimated original ESH (before human impact); the ESH in 2005; the ESH in 2012; the ESH in 2032 and the ESH in 2062 (future scenario). The species' original ESHs and ESHs for 2005 were calculated (following the method set out in Chapter 2) using as land cover datasets, an original forest dataset and GlobCover (2005), respectively. The species' ESHs for 2012 were produced by deducting any suitable habitat from the species' ESHs for 2005 that, according to forest loss data (Global Forest Change dataset (GFC)), was removed between the years 2005 and 2012. Similarly, the species' ESHs for 2032 and 2062 are calculated based on deforestation data (2012 – 2062) generated by applying a future land use scenario using the QUICKLUC land use change model in Co$ting Nature. Furthermore, in order to estimate the uncertainty in using forest loss data from the selected land cover change monitoring system (GFC), the ESHs (2012) of species endemic to the Neotropics are calculated twice using two different monitoring systems of land cover change (GFC & Terra-i) and compared. Finally, the methodology, that will be the basis of an automated system for updating species' assessments, is presented using example species.

6.2.1 Assessing plant species' ranges against the degree of human impact using a pan-tropical monitoring system of deforestation and a land use change model

6.2.1.1 Calculating the species' original ESHs, ESHs in 2005 and ESHs in 2012

In order to assess plant species' ranges against the degree of human impact through time, geographical ranges of the 487 SRLI forest pteridophyte species (described in Chapter 2, section 2.2) were calculated five times over the specified period. First, the species' original ranges (ESHOF), that is, before they were affected by human impact, and the species' ranges for the year 2005 (ESH2005) were calculated. Both sets were calculated with the ESH calculation method using the species' altitudinal range, water balance range and habitat preference (details in Chapter 2, section 2.2.2). The only difference in the calculation of the species' ESHOF and ESH2005 was the land cover dataset used. While the species' ESH2005s were calculated using the GlobCover 2005 land cover dataset (Bicheron *et al*., 2008), thus reflecting the species distribution in 2005, the species' ESHOFs were calculated using a land cover dataset representing the situation of the pre-human impact era.

An original forest cover dataset, which shows the extent of global forest cover before human impact, was created by UNEP-WCMC (Billington *et al.*, 1996). This map was based on various

global and regional biogeographic maps and climatic and topographic variables. Mulligan (2006) improved an updated version of this map (UNEP-WCMC, 1998) by making it compatible with the forest cover shown by GlobCover 2005 (Bicheron *et al.*, 2008). Global forest cover based on the map of Mulligan (2006) and of GlobCover (2005) is shown in Figures 115 and 116, respectively. Due to the fact that non-forest classes may be assigned to pteridophyte forest species during the calculation of their ESH (see details in Chapter 2, section 2.2.2), a combined land cover dataset (OFGC) was created (by the author of this study) using the original forest dataset of Mulligan (2006), together with GlobCover 2005. Specifically, the OFGC map was generated by including the forest pixels from the original forest dataset of Mulligan (2006) and the remaining non-forest pixels were occupied by non-forest classes based on GlobCover 2005. This map was created based on the assumptions that identical non-forest land cover classes existed in the pre-human impact period and that their extent was identical with that of the year 2005 (excluding the pixels that were converted to forest in the original forest cover map). Another assumption was that the species were occurring in those classes during that period, as the SRLI occurrence points indicated, even though the forest extent at the time was significantly larger than present. Thus, migration dynamics and evolution in the species' habitat preferences were ignored. This combined map was used for the calculation of the species' ESHOFs.

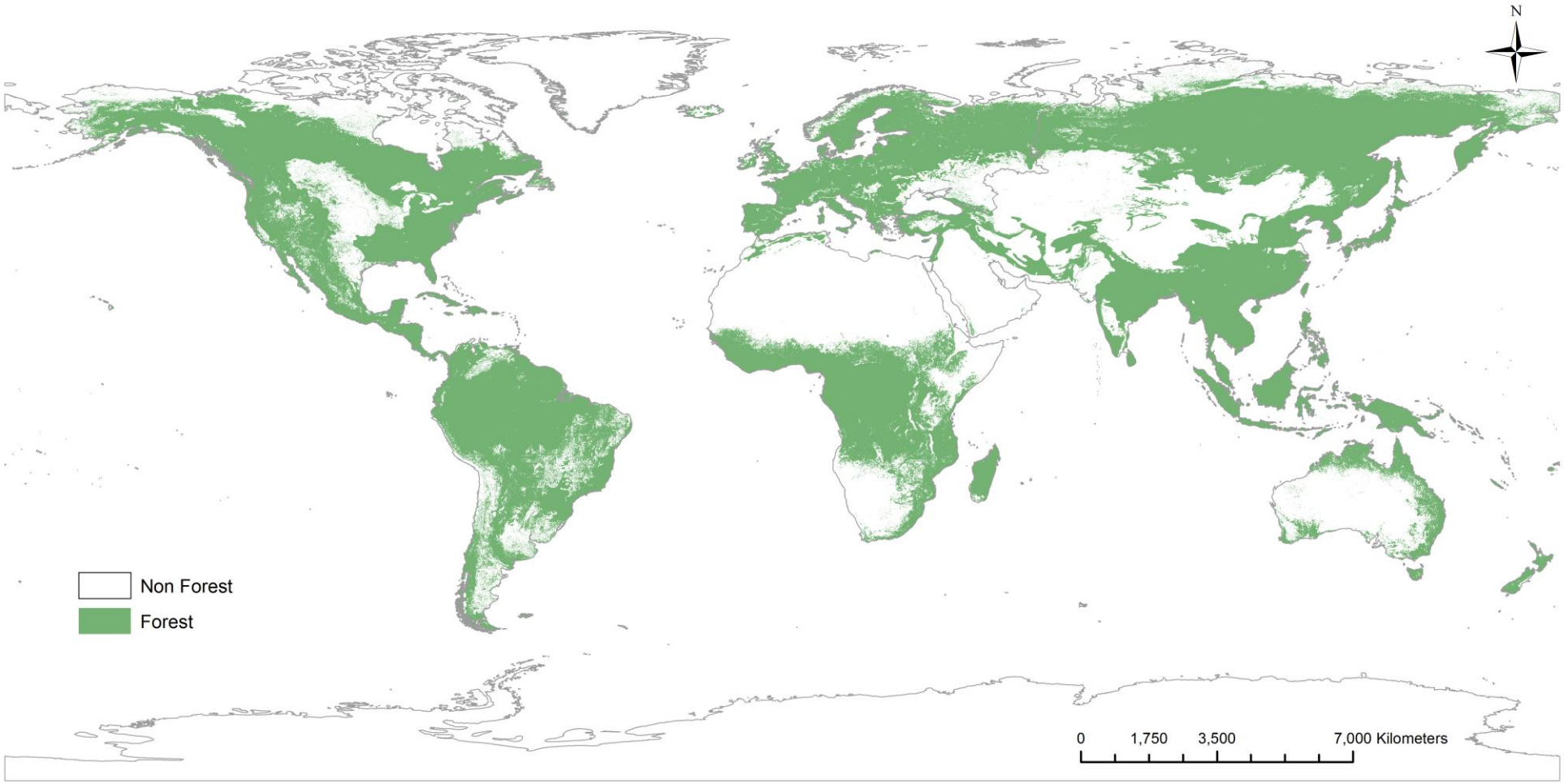

Figure 115. Global original forest cover (before human impact) calculated based on the UNEP-WCMC original forest cover and GlobCover (2005) datasets (Mulligan, 2006).

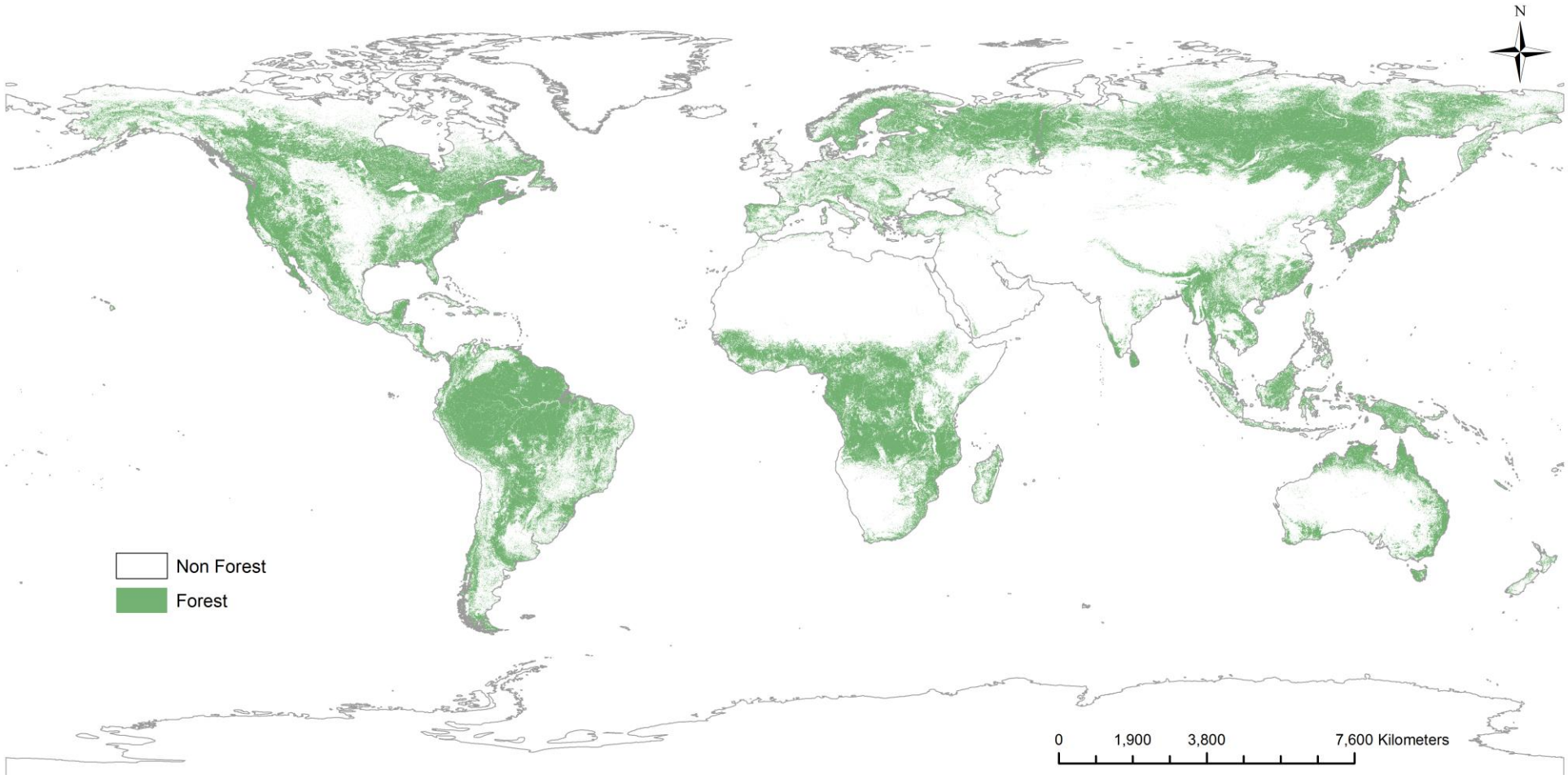

Figure 116. Global forest cover in 2005 based on the GlobCover land cover dataset (Bicheron *et al*. 2008).

The species ranges were also calculated for the year 2012 (ESH2012). The species' ESH2012s were produced by deducting from the species' ESH2005s (acting as baseline), any suitable habitat that, according to forest loss data, was removed between the years 2005 and 2012. Therefore, if a pixel was assigned as suitable habitat in a species' ESH2005 but was considered as a deforested pixel according to the forest loss data (2005 – 2012), the particular pixel was assigned as non-suitable habitat in the species' ESH2012. The forest loss data of the Global Forest Change (GFC) dataset (Hansen *et al.*, 2013) was used for this analysis. It is important to note that the GFC forest loss data represent gross forest loss and thus regrowth was ignored in this analysis.

The GFC dataset shows changes in forest cover globally at 30m resolution. The dataset was the result of the time-series analysis of satellite images from the NASA/USGS Landsat 7 (ETM+) sensor taken between 2000 and 2012. For each of the Landsat images, the tree cover per pixel was calculated using a supervised learning algorithm within the Google Earth Engine platform. Forest loss was defined as the complete loss of forest canopy within a 30m resolution pixel (Hansen *et al*., 2013). Although GFC data are available for the years 2013 and 2014, these were not included in the analysis as they were processed differently from the GFC data for 2000 to 2012, resulting in inconsistencies between the two datasets (Hansen *et al.*, 2015). Mulligan (2014a) resampled the GFC data to 1km resolution by averaging the 30m data in each 1km pixel and calculated the percentage of each 1km pixel deforested over the period 2000 – 2012 (Figure 117). In the new resampled dataset, thresholds were applied (Figure 118) and only pixels that lost at least 50% of their forest cover were considered deforested, as it was assumed that, at this level of forest loss, the remaining forest will be degraded due to fragmentation and edge effects (Laurance *et al.*, 1998; Gascon *et al.*, 2000). Pixels that lost less than 50% of their forest cover were considered as remaining forest pixels avoiding in this way an overestimation of deforestation in the 1km resolution dataset that would result from assuming that any deforestation within the pixel amounted to the pixel being completely deforested. It is also assumed that small percentages of deforestation within a pixel were more prone to detection errors. For the calculation of the species' ESH2012s, the resampled GFC data for the years 2005 to 2012 were used. Any pixels appearing to be deforested between 2005 and 2012 in the GFC dataset but were already non-forest based on GlobCover 2005 dataset, were ignored. This meant that the GlobCover (2005) and the GFC data, and therefore the species' ESH2005 and ESH2012, would now be compatible.

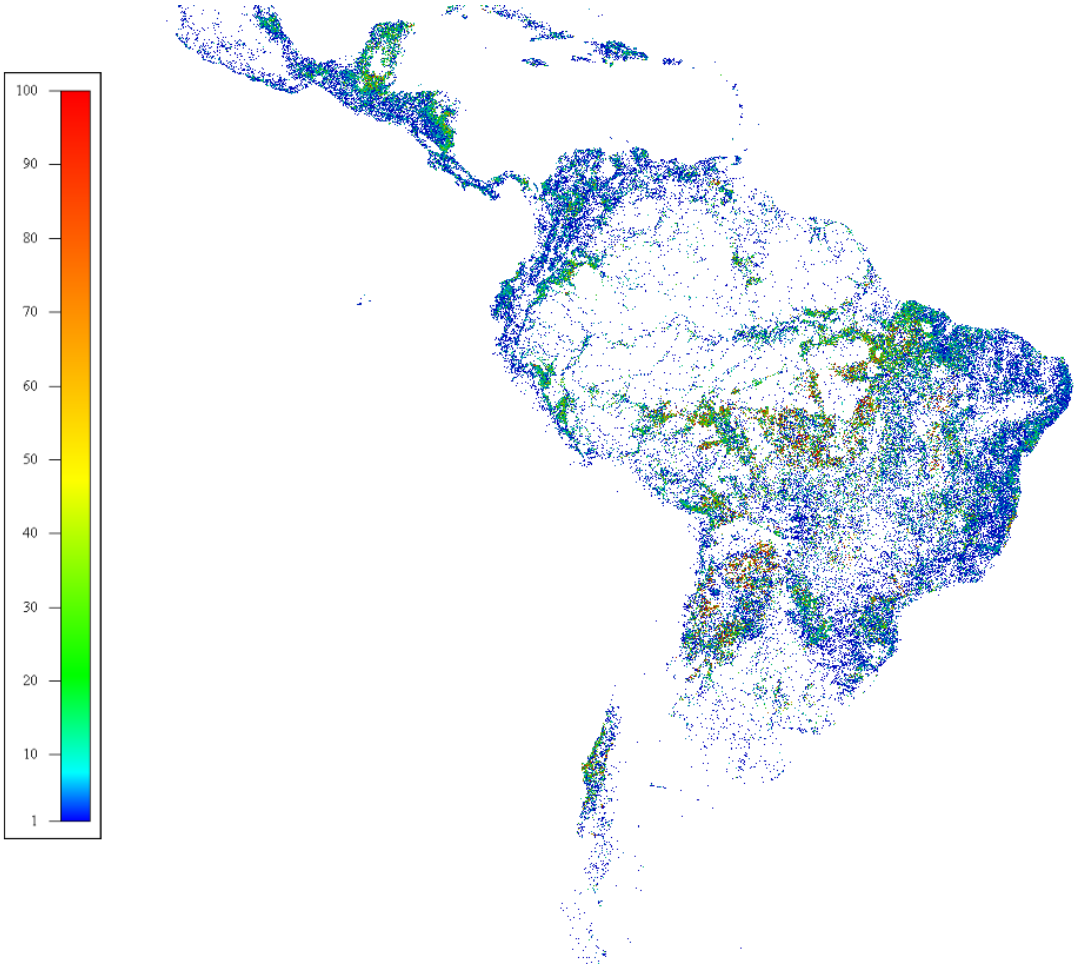

Figure 117. Deforestation data from GFC monitoring system resampled to 1km, showing the percentage of each 1km pixel deforested over the period 2000 to 2012 for Central and South America (data source: Mulligan 2014a).

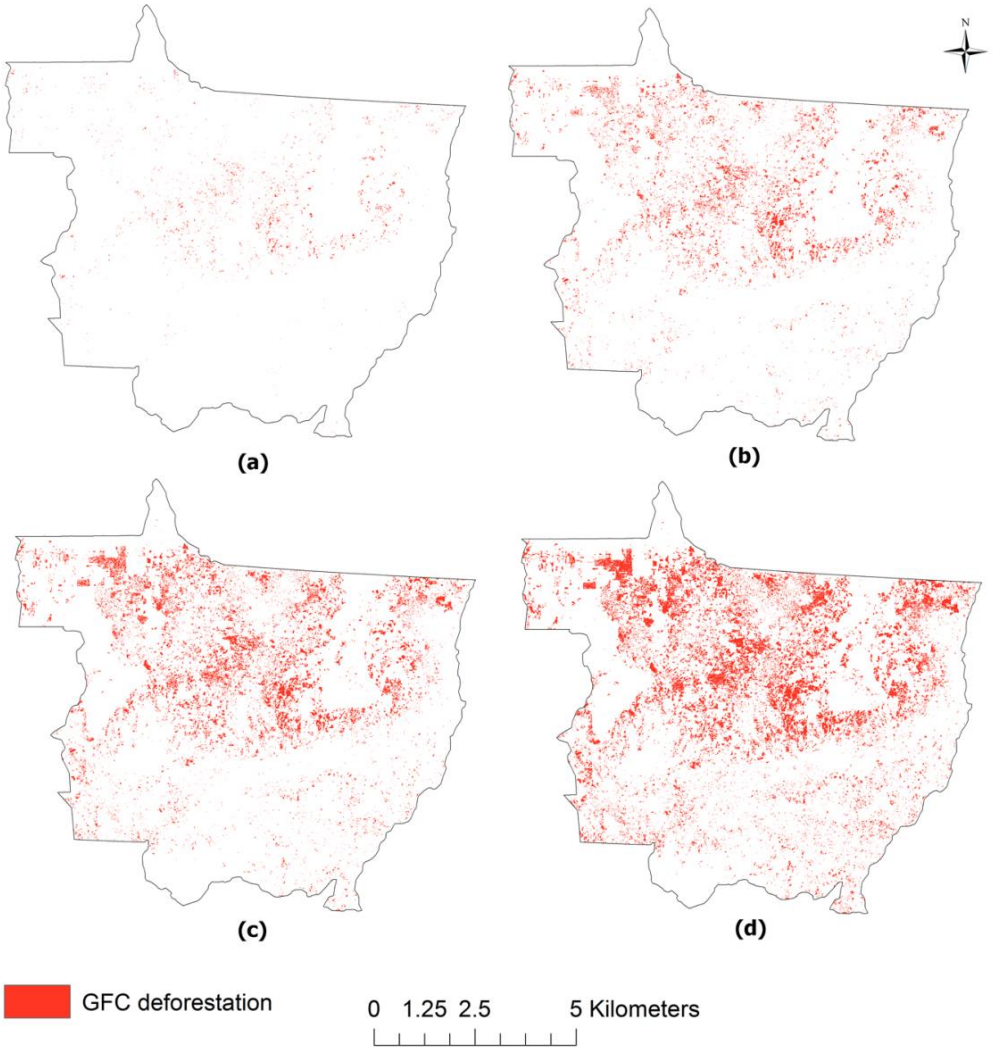

Figure 118. Resampled GFC deforestation data for the Mato Grosso state of Brazil produced by averaging the 30m data in each 1km pixel and calculating the percentage of each 1km pixel deforested over the period 2005 – 2012. Different datasets were created using (a) 100%, (b)75%, (c) 50% and (d) 25% deforestation thresholds (Data source: Mulligan, 2014).

6.2.1.2 Calculating the species' ESHs in 2032 and 2062

The species' ESHs for the year 2032 (ESH2032) and the year 2062 (ESH2062) were generated in order to investigate the degree to which human impact will affect the species' ranges in the future. The species' ESH2032s were calculated by using deforestation data for the years between 2012 and 2032 to deduct suitable habitat from the species' ESH2012s. Pixels with suitable habitat in the species' ESH2012s that according to the deforestation data were deforested between 2012 and 2032 were assigned as non-suitable habitat in the species' ESH2032s. Similarly, the species' ESH2062s were calculated by using deforestation data for the years between 2012 and 2062 to deduct suitable habitat from the species' ESH2012s.

The deforestation data for the years 2012 to 2062 were generated by applying a future land use scenario globally, using the QUICKLUC land use change model within the Co$ting Nature tool.

King's College London has developed the SimTerra database, which is a database of environmental and socio-economic data with a 1km and 1 hectare resolution, consistent projection and a near global coverage (Mulligan, 2009). SimTerra supports Co$ting Nature, a web-based policy support system for mapping conservation priority on the basis of a range of ecosystem services, biodiversity and the magnitude of current human pressure and future threat (Mulligan, 2015b). This tool can be used to generate baseline maps representative of the current conservation priority situation of an area and then apply various scenarios of climate change, land management and land cover/use change. Co$ting Nature (version 2.2) uses more than 145 input maps, mainly produced from remote sensing data, including land cover/use change data which makes the investigation of the impact of land cover/use change on biodiversity feasible. The main sources of land use data are the monitoring system for deforestation Terra-i (http://www.terra-i.org) (Reymondin *et al.*, 2012), the land use change system based on MODIS Vegetation Continuous Fields (VCF) tree cover product (http://glcf.umd.edu/data/vcf/) (DiMiceli *et al.*, 2010) and the GFC deforestation monitoring system (http://earthenginepartners.appspot.com/science-2013-global-forest) (Hansen *et al*., 2013). Co$ting Nature includes MODIS VCF data for the period 2000-2010, Terra-i data for the period 2004 – present and GFC data for the period 2000 – 2012.

A future land use scenario was built and carried out, using the QUICKLUC land use change model in Co$ting Nature, in order to calculate forest cover and therefore deforestation for the years 2012 to 2062. Co$ting Nature has an inbuilt land use change model, QUICKLUC (v.2.0), an equilibrium model that allows the development of future land use scenarios based on recent rates of deforestation which are measured per FAO regional administrative area (FAO, 2014). The deforested pixels are allocated based on Euclidean proximity to existing deforestation areas and accessibility to population centres according to the measure of urban concentration of Uchida and Nelson (2009). The model reduces tree cover in each pixel based on the user-supplied scenario rule (100% = clear-cut full pixel deforestation) whereas it replaces it according to the pixel's original tree-herb-bare cover ratio. In addition, land use type can be changed to a singe use (e.g. pasture), to the most suitable use of the area or to the most common use in the area.

The QUICKLUC model projects deforestation based on user-supplied scenario-rules. For example, the user can set a combination of cover (percentage of tree/herb/bare) for each pixel, select the deforestation monitoring system which will define the recent rates of deforestation, set the number of years of the scenario and select the type of land use that the deforested pixels will be converted to. The scenario developed here which is presented in Figure 119, was firstly tested in a small area of Mato Grosso state in Brazil before running it globally. This area was selected as it has experienced high rates of deforestation over the last decade, on which the scenario can be based, but its forest cover is still adequate in order for the scenario to be tested.

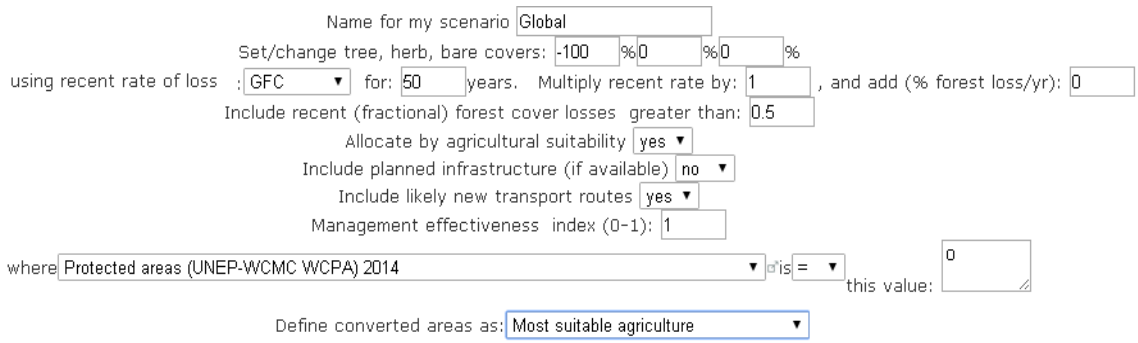

Figure 119. Rule settings of the land use change QUICKLUC (2.0) scenario which was applied in Co$ting Nature to calculate global deforestation for the years 2012 to 2062.

The scenario was run globally at 1 km resolution, for 20 years (2012 – 2032) and for 50 years (2012 – 2062), and was set for tree cover to be removed for all pixels, according to the average deforestation rates based exclusively on the GFC dataset (2000 – 2012). The decision to use the current deforestation rate was made based on the assumption that the current situation will not be improved due to additional conservation strategies, but nor will it worsen due to lack of conservation efforts in the future. The projected deforestation was allocated according to the distribution of agriculturally suitable land and potential road networks. Therefore, if a forest pixel was deforested according to the scenario, it was converted to the most suitable agricultural use based on the Global Agro-Ecological Zones (GAEZ) agricultural suitability map (v.3) (FAO, 2012a) (Figure 120).

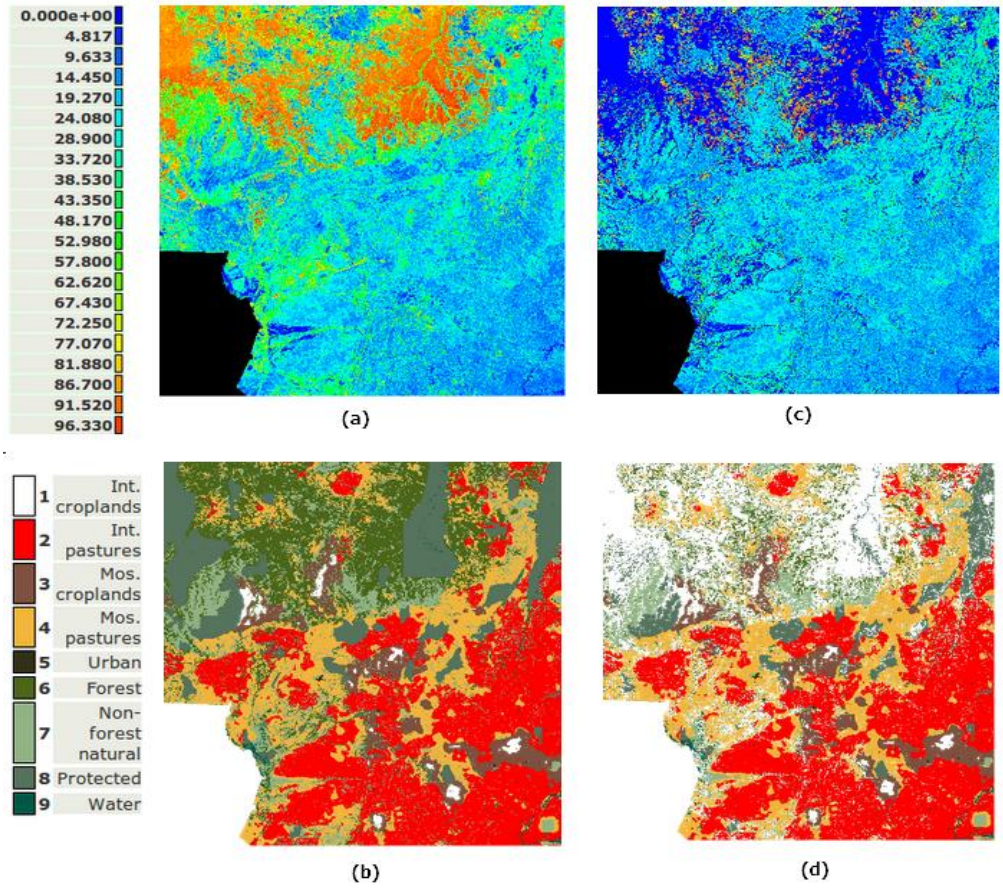

Figure 120. Current (a) Forest cover (%) and (b) land use of an area in the Mato Grosso state of Brazil and the equivalent maps (c: forest cover and d: land use) after applying a future land use scenario in Co$ting Nature (Mulligan, 2015a).

Deforestation was constrained to occur outside of protected areas, thus assuming high management effectiveness within these areas. This was based on previous studies that show that protected areas are effective in protecting biodiversity (Sánchez-Azofeifa *et al.*, 1999; Bruner *et al.*, 2001; Chape *et al.*, 2005; Joppa *et al.*, 2008; Adeney *et al.*, 2009; Joppa *et al.*, 2009; Green *et al.*, 2013), although it is recognised that their effectiveness varies from region to region (Joppa *et al.*, 2008; Joppa & Pfaff, 2010). The decision was also based on the fact that the loss of cloud forests' cover, the ideal habitat for forest pteridophyte species, is limited within protected areas according to the fractional cloud forest cover loss global data of Mulligan & Burke (2005). The cloud forest cover loss within and outside protected areas of Costa Rica is shown in Figure 121.

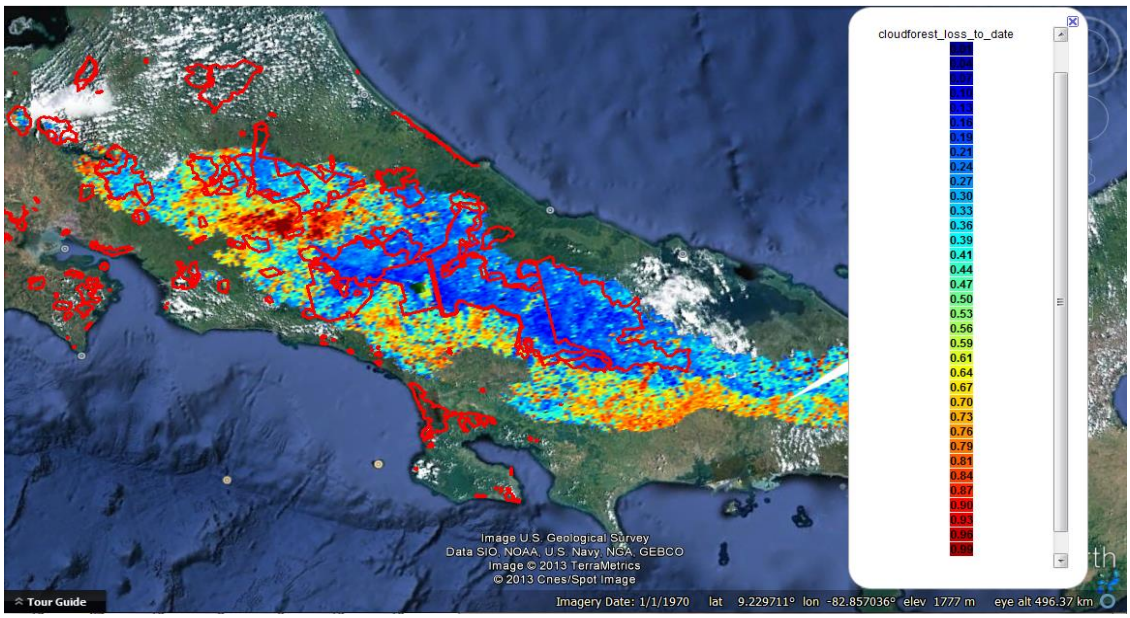

Figure 121. Fractional Cloud forest cover loss to date (%) in Costa Rica (data source: Mulligan & Burke, 2005) and the country's protected areas (red line) (data source: IUCN & UNEP. 2015). Background map data: Google.

Lastly, the option of forest degradation was included in the scenario. Forest degradation determines the fraction (%) of forest loss in the deforestation data that is necessary for the pixel to be considered deforested. For example, when forest degradation is set to 0 (capturing clear cut only), 100% of the forest must be lost in order for the pixel to be considered deforested. Here, forest degradation was set to 0.5, meaning that 50% of forest must be lost in a pixel for it to be considered as deforested and be included in the calculation of the historical deforestation rate (2000 – 2012). This is consistent with the GFC data used in the calculation of ESH2012s which were aggregated to a 1km resolution based on the rule that at least 50% of a pixel's forest cover must be lost in order for it to be considered deforested.

The five ESHs (original ESH, ESH in 2005, ESH in 2012, ESH in 2032 and ESH in 2062) of each species were compared by calculating their area and the percentage of suitable habitat loss between them. To show the trend in the loss of suitable habitat for the SRLI forest pteridophyte species over time, the mean area of suitable habitat was calculated for each point

in time (pre-human impact era, 2005, 2012, 2032 and 2062). In addition, the mean habitat loss between each point in time was calculated for species in each IUCN Red List Category as well as in each biogeographical realm in order to investigate whether the species' mean habitat loss differs between the IUCN Red List Categories and between different parts of the world. To determine whether there are statistically significant differences between the species' habitat loss for the different IUCN Red List Categories and for the biogeographical realm at each point in time, the non-parametric Kruskal-Wallis test was used. The mean size of the species' four ESHs and EOO in each IUCN Red List Category was also compared. Finally, to evaluate the relationship between the species' habitat loss, their original EOO extent and their original suitable habitat (ESHOF), the species' habitat loss (between the pre-human impact era to 2062) was plotted against the size of their EOO and their ESHOF.

6.2.1.3 Presenting the complete ESH methodology with example species

The flow chart of the complete ESH methodology, which will be the basis of an automated system for updating species' assessments, is presented in Figure 122. The equivalent analytical script (the Python code) is given in Appendix A11.

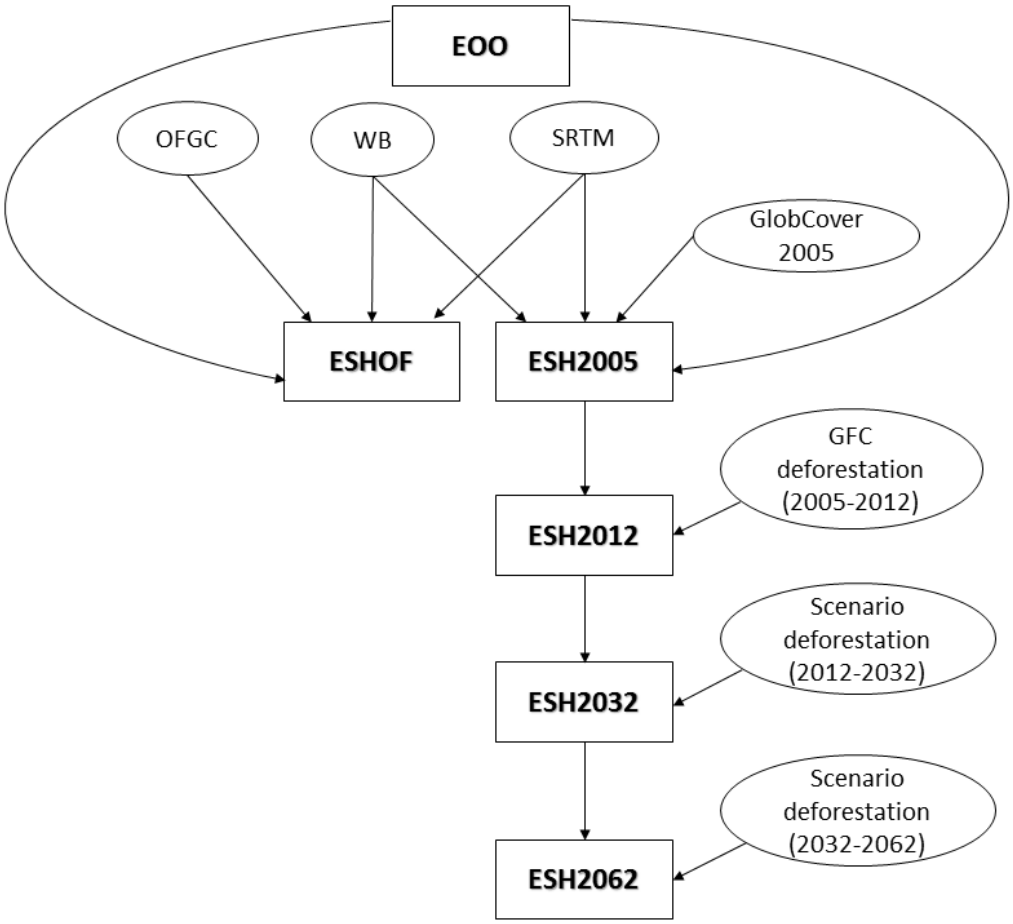

Figure 122. Flow chart of the complete ESH methodology for calculating the species' original ESH (ESHOF), ESH in 2005 (ESH2005), ESH in 2012 (ESH2012) and ESH in 2062 (ESH2062). Ellipses represent input data (OFGC: original forest cover, WB: water balance, SRTM: altitude).

Example threatened and non-threatened species (*Asplenium lamprophyllum*, *Selaginella sambasensis*, *Tectaria keckii, Ctenitis aspidioides* and *Bolbitis virens*) from different parts of the world were selected to present the ESH methodology by reporting the loss of their suitable habitat over time. Through these examples, the ESH methodology was linked to the IUCN Red List assessments (in Discussion, section 7.4).

6.2.2 Comparing the degree of human impact on species ranges when using two different monitoring systems for deforestation

In section 7.2.1.1, the GFC data were used to calculate the species' ESH2012s and thus assess the degree of human impact (2005 – 2012) on species' ranges globally. GFC data were ideal for such an analysis due to their high spatial resolution, their global coverage and their ready availability. However, using another land cover change dataset may have resulted in different ESH2012s. To test the level of uncertainty in using the selected forest loss system (GFC), the species' ESH2012s were generated two times based on the calculation method described in section 7.2.1.1. Firstly the ESH2012s were calculated with the high resolution GFC data and secondly with the deforestation data of another land cover change monitoring system, Terra-i (http://www.terra-i.org). Terra-i is a near real-time (every 16 days) monitoring system that detects land cover changes based on MODIS data. Specifically, it uses vegetation indices (the Normalized Difference Vegetation Index) from the MOD13Q1 product, precipitation data from the Tropical Rainfall Measuring Mission (TRMM) sensor and water bodies' presence data from the MOD35 product. Its model is trained to understand how vegetation dynamics behave in an area through time in relation to precipitation and predicts the vegetation response of the area to current precipitation measurements. If these predictions are different from the equivalent information from the MODIS imagery for more than 32 days, the land cover of the area is considered as 'changed'. Terra-i data are available in 250m resolution over the period 2004 – 2015 (Reymondin *et al.*, 2012).

In contrast with the GFC global data, Terra-i data are available just for Central and South America. For this reason and to be able to compare the two sets of ESH2012s created with the two monitoring systems, it was decided to run the analysis just for the SRLI forest pteridophyte species that occur in Central and South America (186 species, list of species in Appendix A10). In addition, and similarly to the GFC data, the Terra-i data were resampled by Mulligan (2014b) to 1km resolution by averaging the 250m data in each 1km pixel and calculating the percentage of each 1km pixel deforested over the period 2000 – 2012 (Figure 123).

Only pixels that lost at least 50% of their forest cover were considered deforested in both datasets (GFC & Terra-i) (details in section 7.2.1.1) and used in the comparison analysis. This threshold deforestation data for the years 2005 to 2012, resampled to 1km resolution with 50% for the GFC and Terra-i systems, are shown in Figures 124 and 125, respectively. The two sets of the species' ESH2012s were first compared by calculating the mean reduction in habitat loss from ESH2005 to ESH2012 for each set. Subsequently, the similarity of the two sets was

evaluated by plotting the species' suitable habitat loss between 2005 and 2012 when the ESH2012s were calculated using the GFC data against the equivalent habitat loss when the ESH2012s were calculated using the Terra-i data.

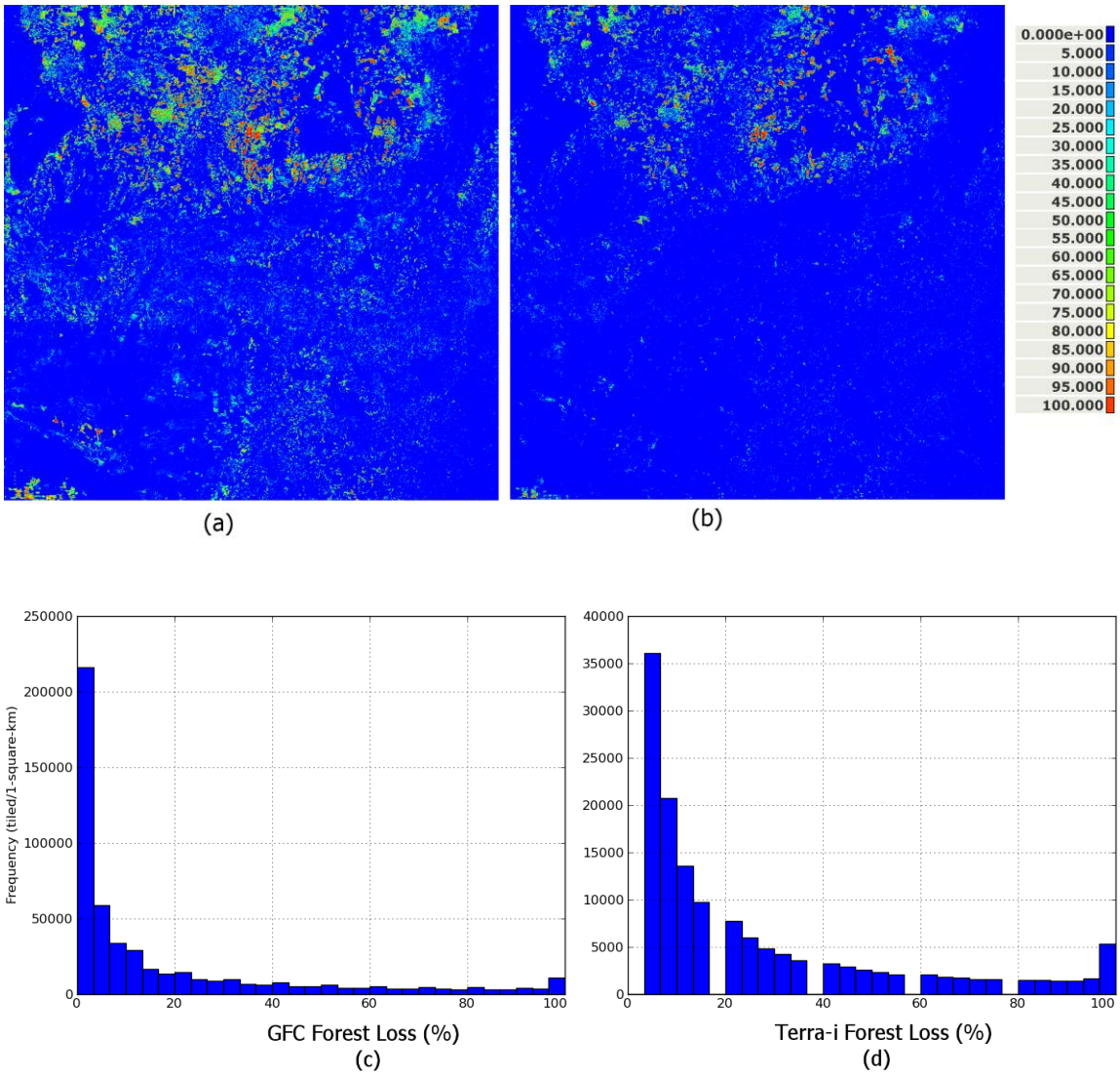

Figure 123. Deforestation data resampled to 1km from (a) GFC and (b) Terra-i monitoring systems showing the percentage of each 1km pixel deforested over the period 2000 to 2012 for an area in Mato Grosso state in Brazil (centre of 1km tile: 15S, 55W) (Data source: Mulligan 2014a; 2014b). Frequency distribution graphs of the (c) GFC and (d) Terra-i deforestation values are shown (Source: Co$ting Nature).

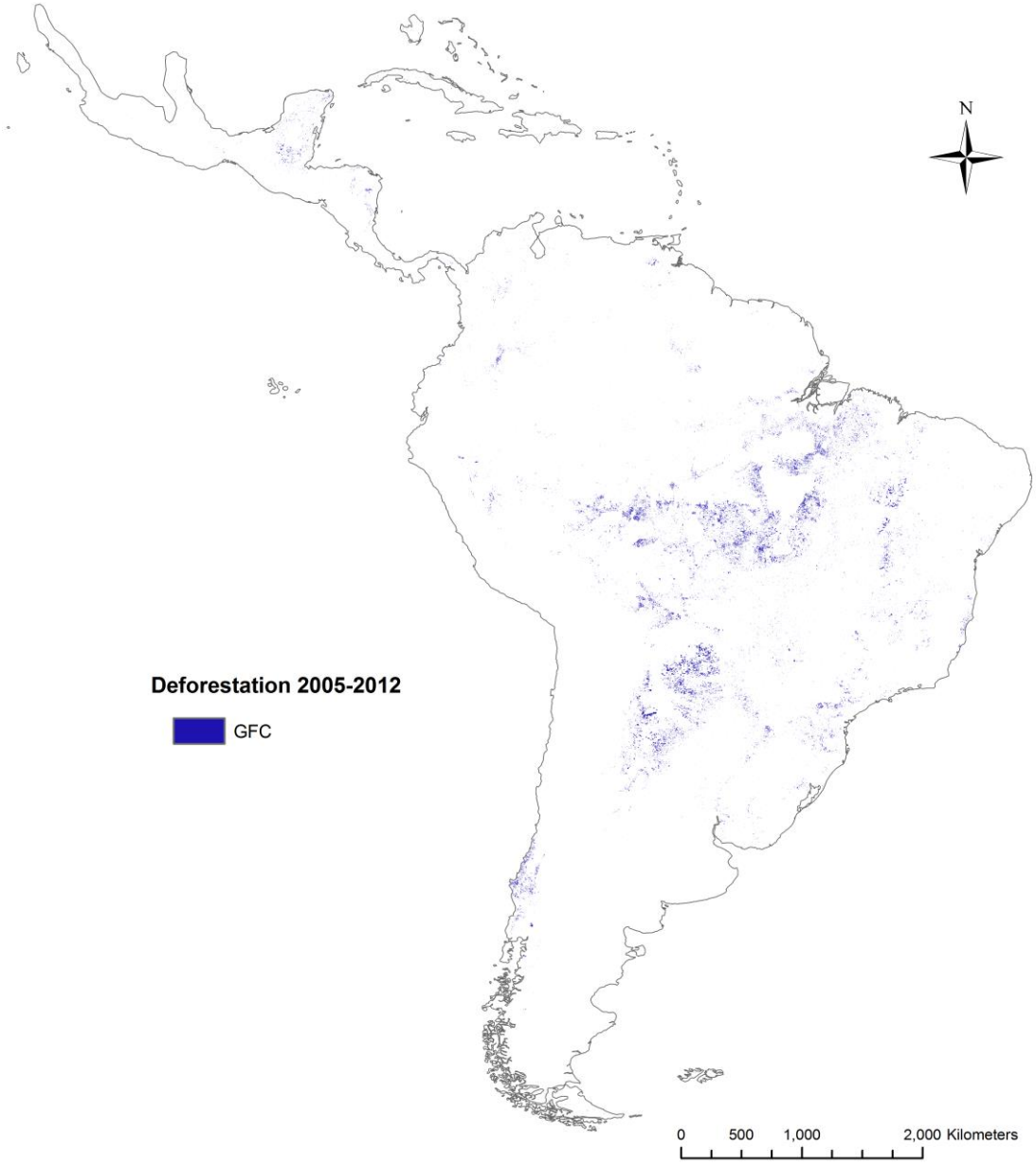

Figure 124. Deforestation over the period 2005 and 2012 in Central and South America according to the GFC deforestation monitoring system. Deforestation data were resampled by averaging the 30m data in each 1km pixel and selecting a 50% threshold for each pixel (Data source: Mulligan, 2014a).

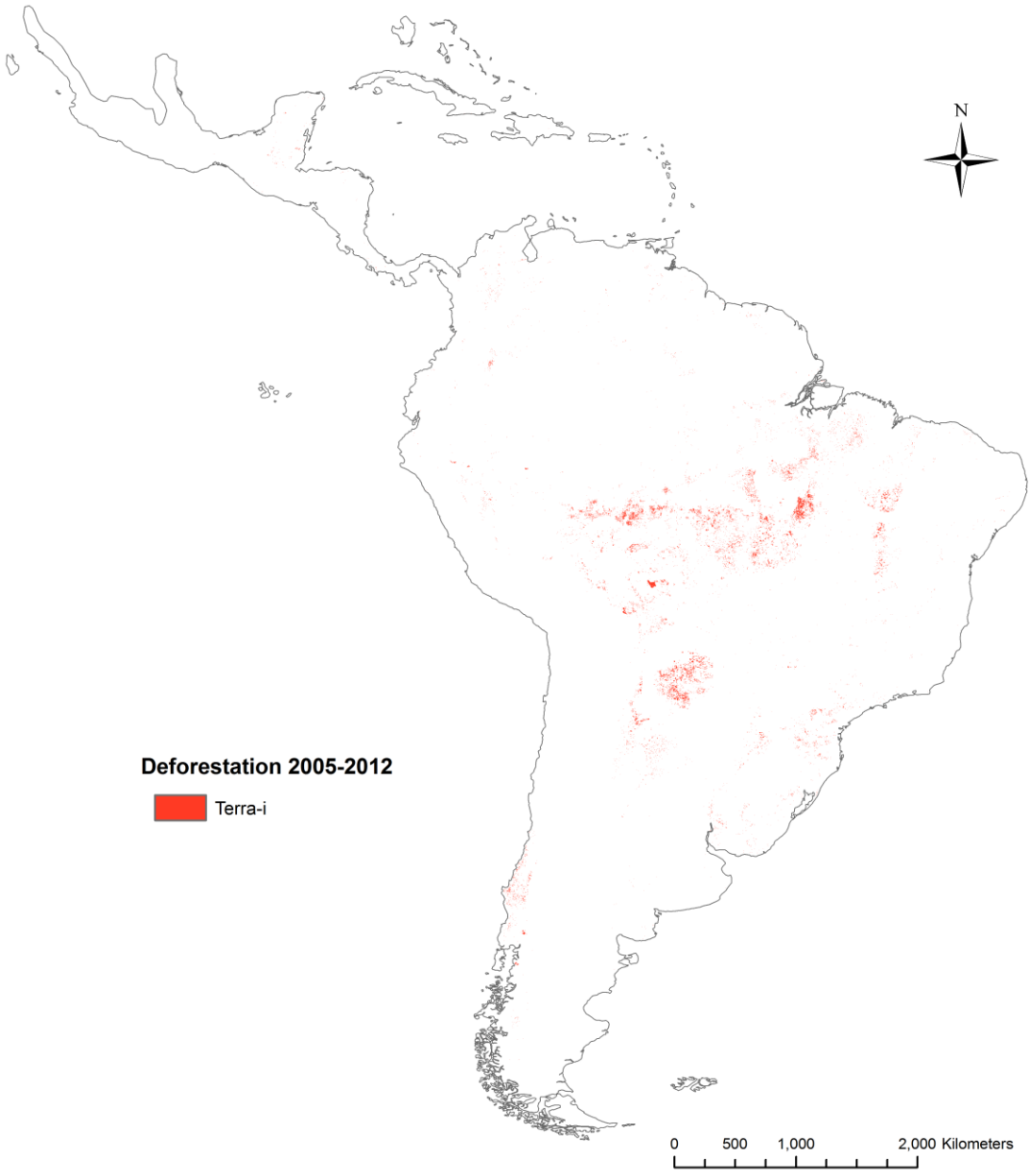

Figure 125. Deforestation over the period 2005 and 2012 in Central and South America according to the Terra-i deforestation monitoring system. Deforestation data were resampled by averaging the 250m data in each 1km pixel and selecting a 50% threshold for each pixel (Data source: Mulligan, 2014b).

6.3 RESULTS

6.3.1 Comparison of the degree of human impact on species ranges using two monitoring systems for deforestation.

Based on the deforestation data from the GFC monitoring system resampled to 1km and with a 50% deforestation threshold, 2.3 x 10^6 km² were deforested across the Neotropics between 2005 and 2012. For the same period, the resampled deforestation data from the Terra-i monitoring system showed that there were 1.3 x 10^5 km² deforested across the region, 40% less

that the GFC data revealed. There were 9.3 x 10^5 km² that both systems indicated as deforested, which accounted for 42 % of the GFC data and 70% of the Terra-i data (Figure 126).

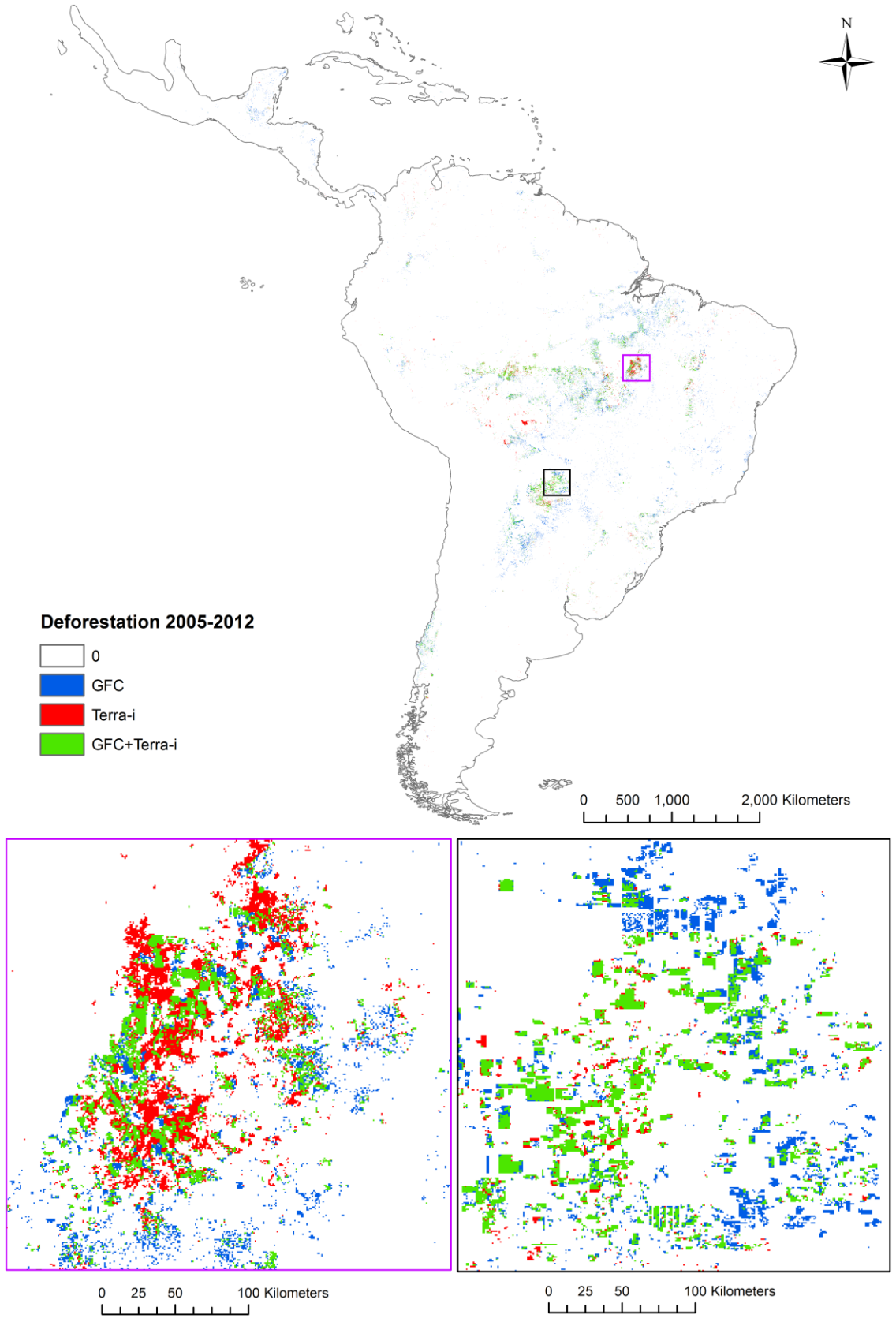

Figure 126. Deforested areas in the Neotropics between 2005 and 2012 that were estimated by both the GFC and Terra-i deforestation monitoring systems and the deforested areas that were estimated by only one of the monitoring systems.

The mean reduction in habitat extent from ESH2005 to ESH2012 when the ESH2012 was calculated using the GFC and the Terra-i deforestation data is shown in Figure 127. There was a bigger mean reduction from ESH2005 to ESH2012 when the ESH2012 was calculated with the GFC data, with a mean reduction in the ESH2005 of 0.6±0.9% and 0.4±0.8% using the GFC and Terra-i data, respectively.

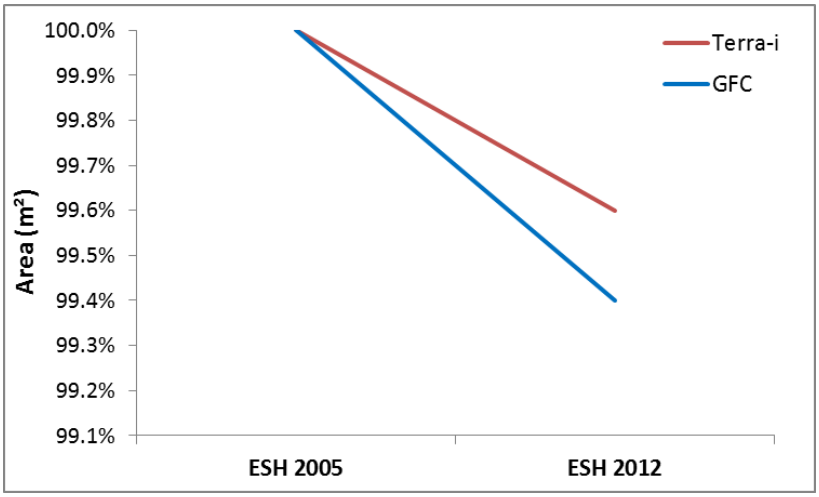

Figure 127. The mean reduction of the species' ESH in 2005 to the ESH in 2012 when using the GFC and Terra-i deforestation data.

The similarity of the two sets was also evaluated by plotting the species' suitable habitat loss between 2005 and 2012 when the ESH2012s were calculated using the GFC data against the equivalent habitat loss when the ESH2012s were calculated using the Terra-i data (Figure 128). While there are differences between the GFC and Terra-i deforestation data, there was a high similarity (r^2=0.9) between the two deforestation data sets in the amount of species' habitat loss and therefore in the species' ESH2012s. The mean difference in species' habitat loss between the two sets was 0.2±0.3% with the greatest difference of 3% in the case of *Arachniodes rigidissima.* Habitat loss for this species was 3% when the species' ESH2012 was calculated using the GFC deforestation data whereas there was no habitat loss when using the Terra-i deforestation data. In both sets, the greatest habitat loss from ESH2005 to ESH2012 was found for *Adiantum scabrum,* a Least Concern species that is endemic to Chile. All four threatened species (*Asplenium underwoodii*, *Lomariopsis wrightii*, *Elaphoglossum nanoglossum*, *Ctenitis chiriquiana*), which are endemic to the Americas, had no observed habitat loss between 2005 and 2012 according to both deforestation monitoring systems.

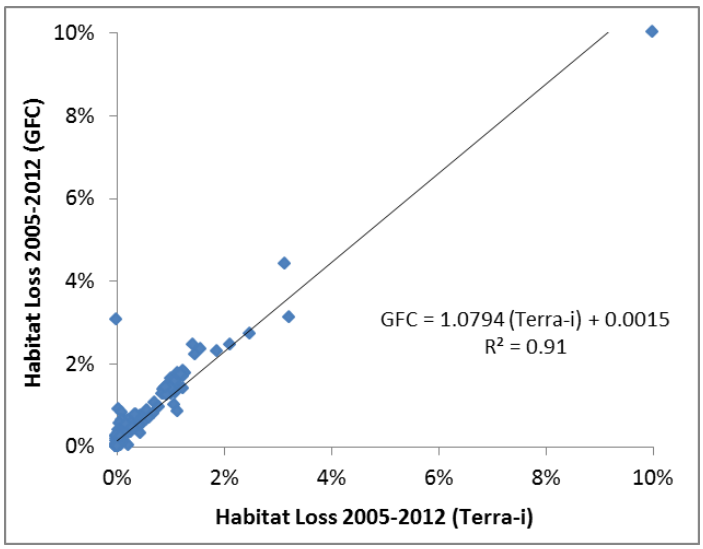

Figure 128. Comparison of the species' ESH2012s when using the GFC and Terra-i deforestation data by plotting the equivalent habitat loss of each species for the years 2005 to 2012. Goodness of fit of linear regression (R^2) is reported.

6.3.2 Assessment of species ranges against the degree of human impact using a pan-tropical monitoring system for deforestation and a land use change model.

A future land use scenario was built based on the GFC deforestation data and carried out using the inbuilt land use change model, QUICKLUC (v.2.0). The land use scenario was firstly tested in a small area (Figure 129) before it was run globally (Figure 130). The deforestation data produced by the model were used in calculating the species' ESH2032s and ESH2062s.

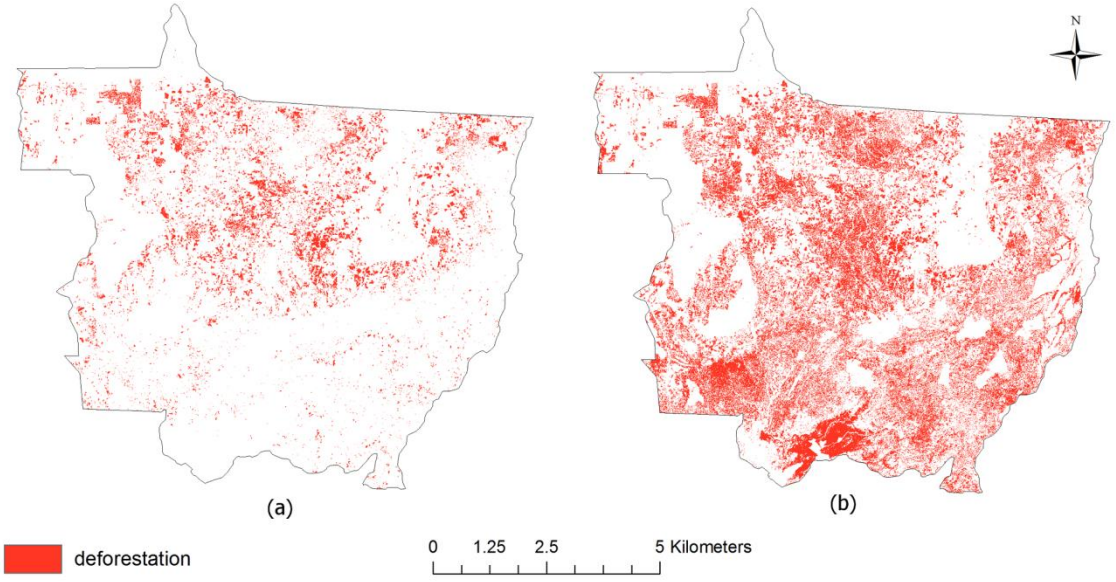

Figure 129. Deforested areas in Mato Grosso state, Brazil (a) over the years 2005 and 2012 based on the GFC deforestation data (resampled to 1km resolution with 50% deforestation threshold (Data source: Mulligan, 2014a)) and (b) over the years 2005 and 2062 based on the GFC deforestation data (2005 – 2012) and the deforestation data of a land use change model for the years 2012 to 2062.

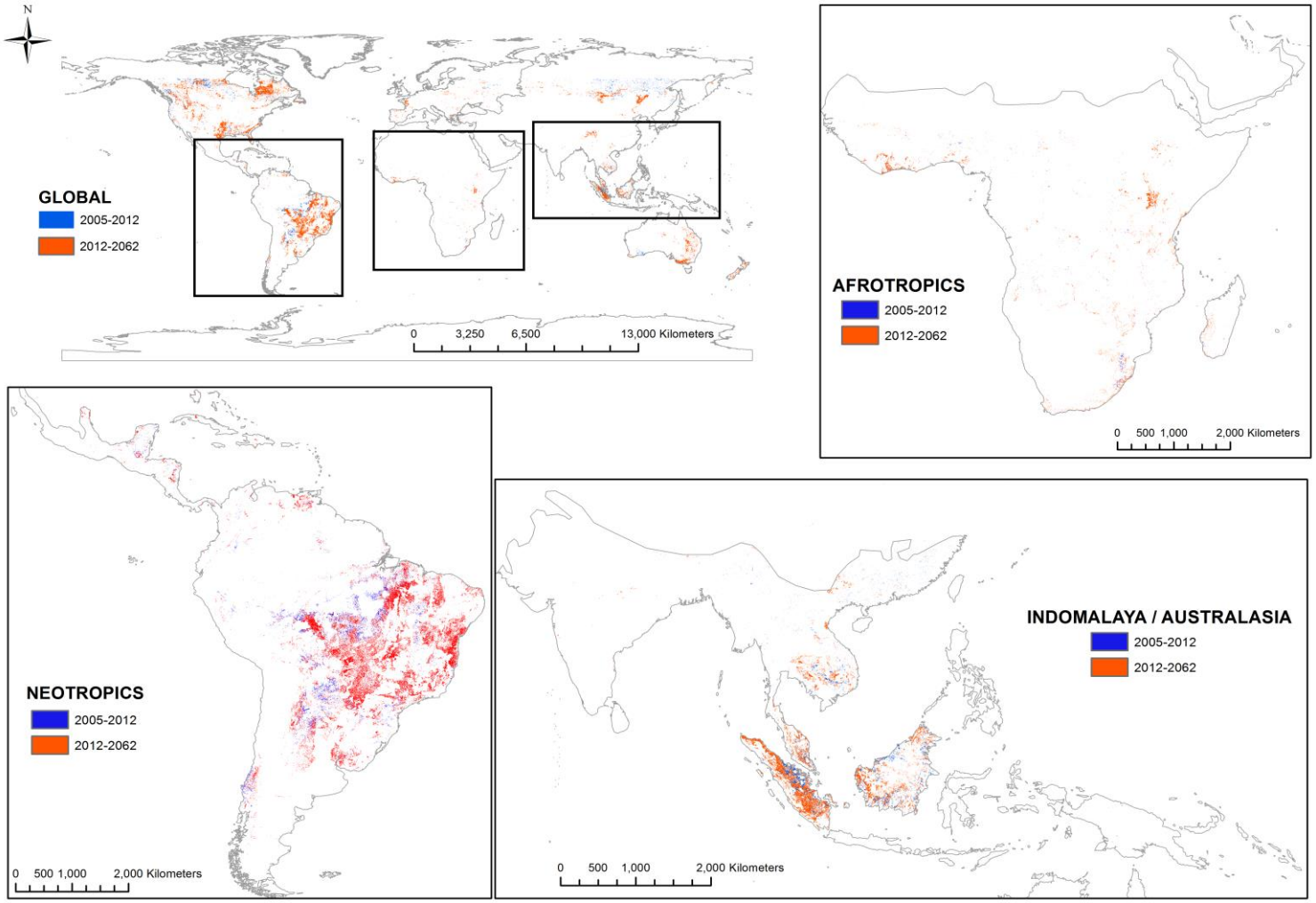

Figure 130. Areas that were deforested between 2005 and 2062 based on the GFC deforestation data (2005-2012) and a future land use scenario (2012 – 2062) for (a) the world, (b) the Neotropical biogeographical realm (c) the Indomalayan / Australasian biogeographical realms and (d) the Afrotropical biogeographical realm. The Indomalayan and Australasian realms are combined in the same map excluding the Australian continent.

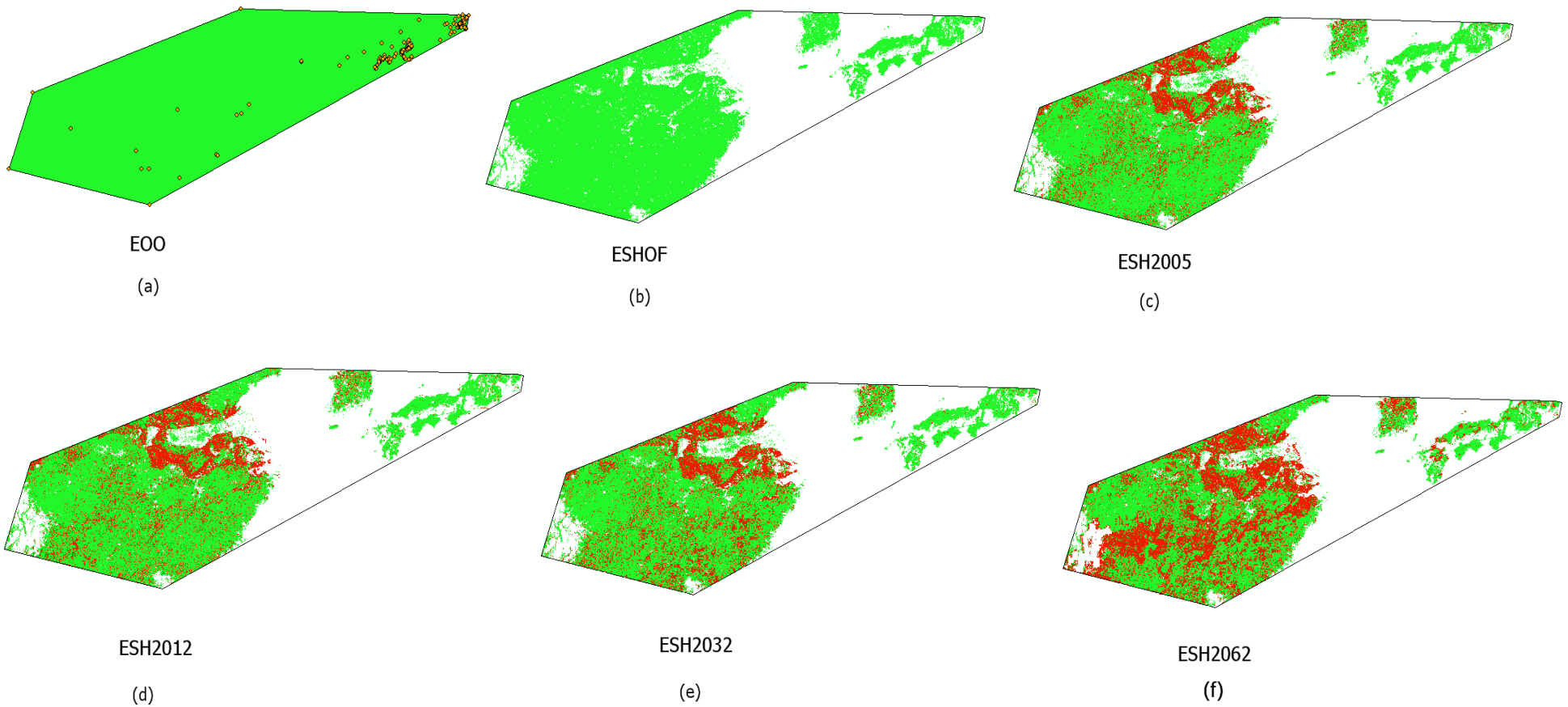

Figure 131. (a) EOO and occurrence points and (b-f) the extent of suitable habitat through time ((b) original ESH (ESHOF), (c) ESH in 2005, (d) ESH in 2012 (e) ESH in 2032 (ESH2032) and (f) ESH in 2062 (ESH2062)) of *Dryopteris erythrosora*. The green colour represents suitable habitat and the red colour represents habitat loss (deforestation).

An example of the ESHs (original ESH, ESH in 2005, ESH in 2012, ESH in 2032 and ESH in 2062) calculated for the species *Dryopteris erythrosora,* and therefore the amount of its suitable habitat through time is presented in Figure 131. Interestingly, there was a significant mean reduction in area from EOO to ESHOF of 62.7±0.2%, just 7% less than the mean reduction in area from EOO to ESH 2005 (details in Chapter 2, section 2.3.2.2). The mean area of ESHOF, ESH2005, ESH2012, ESH2032 and ESH2062 was 2.01 x 10^6 km^2, 1.88 x 10^6 km^2, 1.86 x 10^6 km^2, 1.84 x10^6 km^2 and 1.79 x10^6 km^2, respectively. In addition, the species' mean loss of habitat between the pre-human impact era and 2005 was found to be 15%, whereas the mean loss of habitat between 2005 and 2012 was 1%. The species' mean loss of habitat between 2012 and 2032 was 1% and it was 2% between 2032 and 2062 based on the future land use scenario. Interestigly, the species' mean habitat loss between 2005 and 2012 and between 2012 and 2032 was similar even though the second period is three times longer than the first one. In total, a mean loss of 19% of suitable habitat between the pre-human impact era and 2062 was found (Figure 132). Assuming that there was 100% of suitable habitat for the SRLI pteridophyte species during the pre-human impact era, these results show that, on average, 81% of suitable habitat will be available for these species by 2062. Between the pre-human impact era and 2005, only 2% of the species had 0% loss of suitable habitat whereas 50% and 37% of the species had 0% loss between 2005 and 2012, and between 2012 and 2062, respectively. While 24% of the species experienced more than 20% habitat loss between the pre-human impact era and 2005, there were fewer species that experienced such loss during the periods 2005 – 2012 (1%) and 2012 – 2062 (3%).

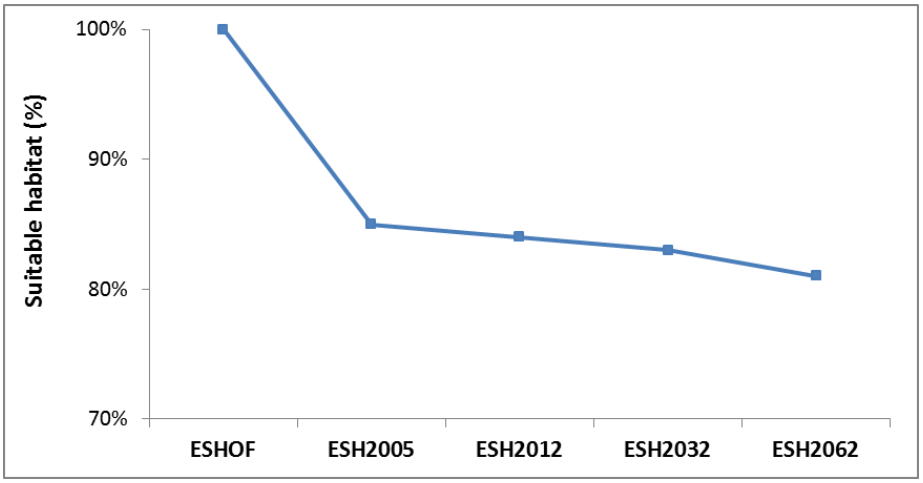

Figure 132. Mean percentage of suitable habitat for the SRLI forest pteridophyte species through four points in time (pre-human impact era, 2005, 2012, 2032 and 2062).

The mean habitat loss for forest pteridophyte species' for each of the four periods (pre-human impact era – 2005, 2005 – 2012, 2012 – 2062 and 2032 – 2062) differed between the IUCN Red List Categories (Figure 133). The difference was statistically significant for the pre-human impact era – 2005, 2012 – 2032 and 2012 – 2062 periods (pre-human impact era – 2005: Kruskal-Wallis χ^2=13.9, d.f.=4, $p<0.05$; 2012 – 2032: Kruskal-Wallis χ^2=14.2, d.f.=4, $p<0.05$; 2032 – 2062: Kruskal-Wallis χ^2=16.6, d.f.=4, $p<0.05$) but not for the period 2005 – 2012 (Kruskal-Wallis χ^2=5.1, d.f.=4, $p>0.05$). Surprisingly, the only Critically Endangered species in

the SRLI forest pteridophyte sample (*Asplenium underwoodii*) did not appear to experience any habitat loss between the pre-human impact era and 2062. The mean habitat loss of species in the Vulnerable category was the highest one among the categories for all periods (pre-human impact era – 2005: 25.6%, 2005 – 2012: 0.8%, 2012 – 2032: 1.1% and 2032 – 2062: 3.3%). The mean habitat loss for 2005– 2012 and 2012 – 2062 was higher in the non-threatened categories (Near Threatened and Least Concern) than the equivalent one in the Endangered category. However, for the period pre-human impact era – 2005, the Endangered category had higher mean habitat loss when compared with the Least Concern category and lower mean habitat loss when compared with the Near Threatened category.

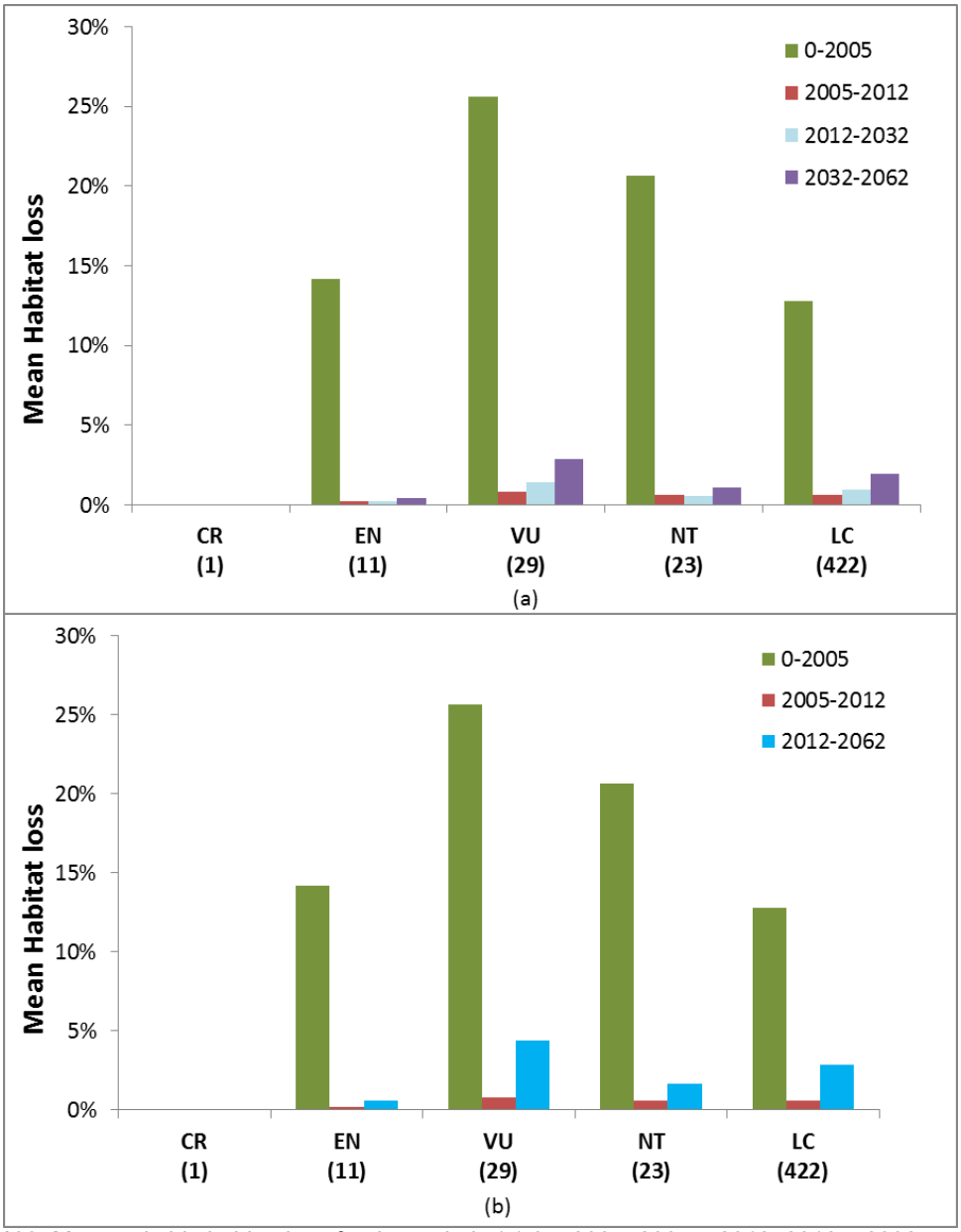

Figure 133. Mean suitable habitat loss for the periods (a) 0 – 2005, 2005 – 2012, 2012 – 2032 and 2032 – 2062 and (b) 0 – 2005, 2005 – 2012 and 2012 – 2062 for the species in each IUCN Red List Category (Critically Endangered, EN: Endangered, VU: Vulnerable, NT: Near Threatened, LC: Least Concern). Numbers in brackets represent number of species in each category. The pre-human impact era is referred to as 0 years.

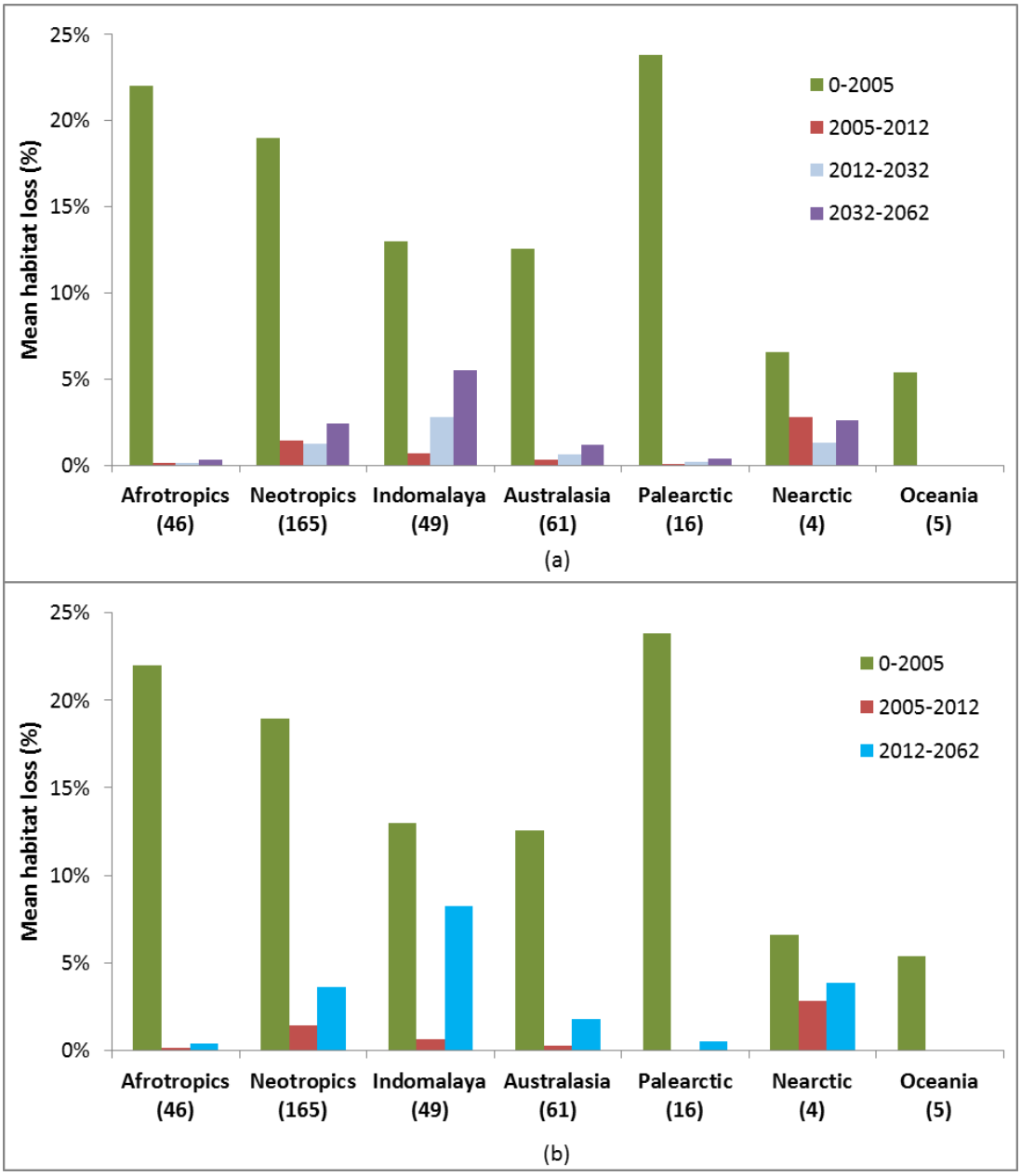

Figure 134. Mean suitable habitat loss for the periods (a) 0 – 2005, 2005 – 2012, 2012 – 2032 and 2032 – 2062 and (b) 0 – 2005, 2005 – 2012 and 2012 – 2062 for the species in each biogeographical realm. Numbers in brackets represent number of species in each biogeographical realm. The pre-human impact era is referred to as 0 years. Species that occur in more than one biogeographical realm are not included in this figure.

The species' mean habitat loss for each of the four time periods (pre-human impact era – 2005, 2005 – 2012, 2012 – 2032 and 2032 – 2062) also differed between the biogeographical realms (Figure 134), with the difference being statistically significant in every case (Kruskal-Wallis d.f.=6: pre-human impact era – 2005: χ^2=17.8, p<0.001; 2005 – 2012: χ^2=39.5, p<0.001; 2012 – 2032: χ^2=30.2, p<0.001; 2032 – 2062: χ^2=31.9, p<0.001). According to the species' ESHs, for the first period (pre-human impact era – 2005), the biogeographical realms with the largest mean habitat losses were the Palearctic and Afrotropical realms with 24% and 22% of habitat loss, respectively. The Neotropics experienced the third highest mean habitat loss (18%), followed by Indomalaya (13%) and Australasia (12%). A different pattern was found for the

second period (2005 – 2012) during which the Nearctic experienced the highest mean habitat loss (3%) followed by the Neotropics (2%) and Indomalaya (1%). Based on the land use scenario, the species' mean habitat loss between the years 2012 – 2062, was higher in Indomalaya (8%). For the same period, the Nearctic realm had a mean species' habitat loss of 4%, followed by the Neotropics (3%) and Australasia (2%). Both the Afrotropical and the Palearctic realms had relatively low mean habitat loss for species between 2005 and 2062. However, it was Oceania that had the lowest mean habitat loss in every time period.

The relationship between the species' total habitat loss (pre-human impact era – 2062) and their original EOO and the relationship between the species' total habitat loss and their ESHOF (original suitable habitat) are shown in Figures 135 and 136, respectively. It was found that on average, habitat loss was greater in species with small original EOO and small ESHOF. As also shown in Figure 133, the Critically Endangered species (with the smaller EOO) experienced 0% of habitat loss. Two species had more than 90% of total habitat loss: *Cyathea pseudonanna* and *Pellaea tripinnata*, both of which have small EOOs (< 1 x 10^{10} m^2) and were assessed as Vulnerable species. Least Concern (e.g. *Ctenitis aspidioides* and *Bolbitis virens*) and Near Threatened species (e.g. *Hymenophyllum veronicoides* and *Amauropelta firma*) with relatively small EOOs also had a significant percentage of total habitat loss (40-65%).

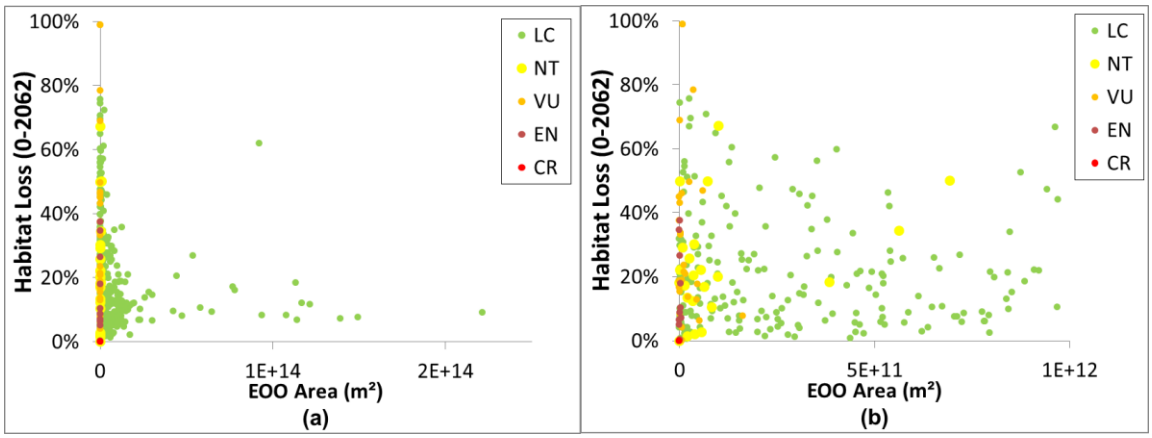

Figure 135. Relationship between the species' habitat loss over the period 0 to 2062 and their original EOO extent (a) for all species and (b) for species with small EOO area (< 1 x10^{12} m^2). The pre-human impact era is referred to as 0 years. Colour of markers (circles) represents the IUCN Red List Categories: CR: Critically Endangered, EN: Endangered, VU: Vulnerable, NT: Near Threatened, LC: Least Concern.

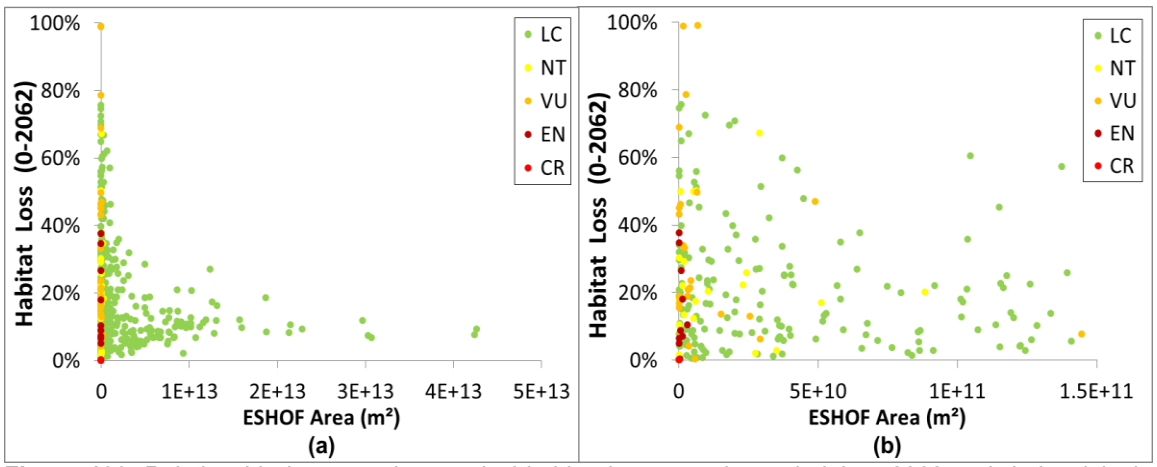

Figure 136. Relationship between the species' habitat loss over the period 0 to 2062 and their original ESH extent (ESHOF) (a) for all species and (b) for species with small ESHOF area (< 1.5 x10^{11} m^2). The pre-human impact era is referred to as 0 years. Colour of markers (circles) represents the IUCN Red List Categories: CR: Critically Endangered, EN: Endangered, VU: Vulnerable, NT: Near Threatened, LC: Least Concern.

The size of all ESHs was found to differ significantly between the IUCN threat categories (Kruskal-Wallis d.f.=4: ESHOF: χ^2=24.4 , p<0.0001; ESH2005: χ^2=21.4 , p<0.0001; ESH2012: χ^2=21.6 , p<0.0001; ESH2032: χ^2=19.2 , p<0.0001; ESH2062: χ^2=20.3 , p<0.0001), as the EOO does (EOO: Kruskal-Wallis χ^2=25.6, d.f.=4, p<0.0001). As shown in Figure 137, there is a relationship between the IUCN Red List Categories and the size of all ESHs, with the average ESH being larger in the Least Concern category and smaller in the Critically Endangered category in every case.

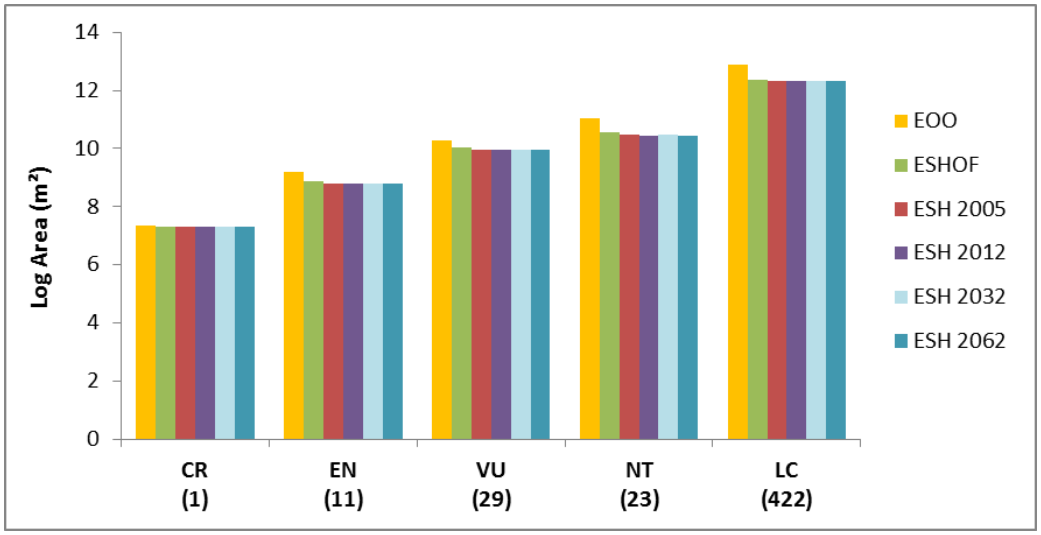

Figure 137. Mean EOO and ESH (original ESH of the pre-human impact period (ESHOF), ESH in 2005, ESH in 2012, ESH in 2032 and ESH In 2062) (log) by IUCN Red List Category: CR: Critically Endangered, EN: Endangered, VU: Vulnerable, NT: Near Threatened, LC: Least Concern. Numbers in brackets represent number of species in each category.

6.3.3 Presenting the ESH methodology with example species

The example species *Tectaria keckii* (EOO: 2.4 x10^4 km^2), *Selaginella sambasensis* (EOO: 2.5 x10^2 km^2), *Asplenium lamprophyllum* (EOO: 1.2 x10^4 km^2) and *Ctenitis aspidioides* (EOO: 2.4 x10^5 km^2) were selected to present the ESH methodology by reporting the loss of their suitable habitat over time. The EOO and four ESHs (original ESH, ESH in 2005, ESH in 2012 and ESH in 2062) of these species are illustrated in Figures 138 to 141.

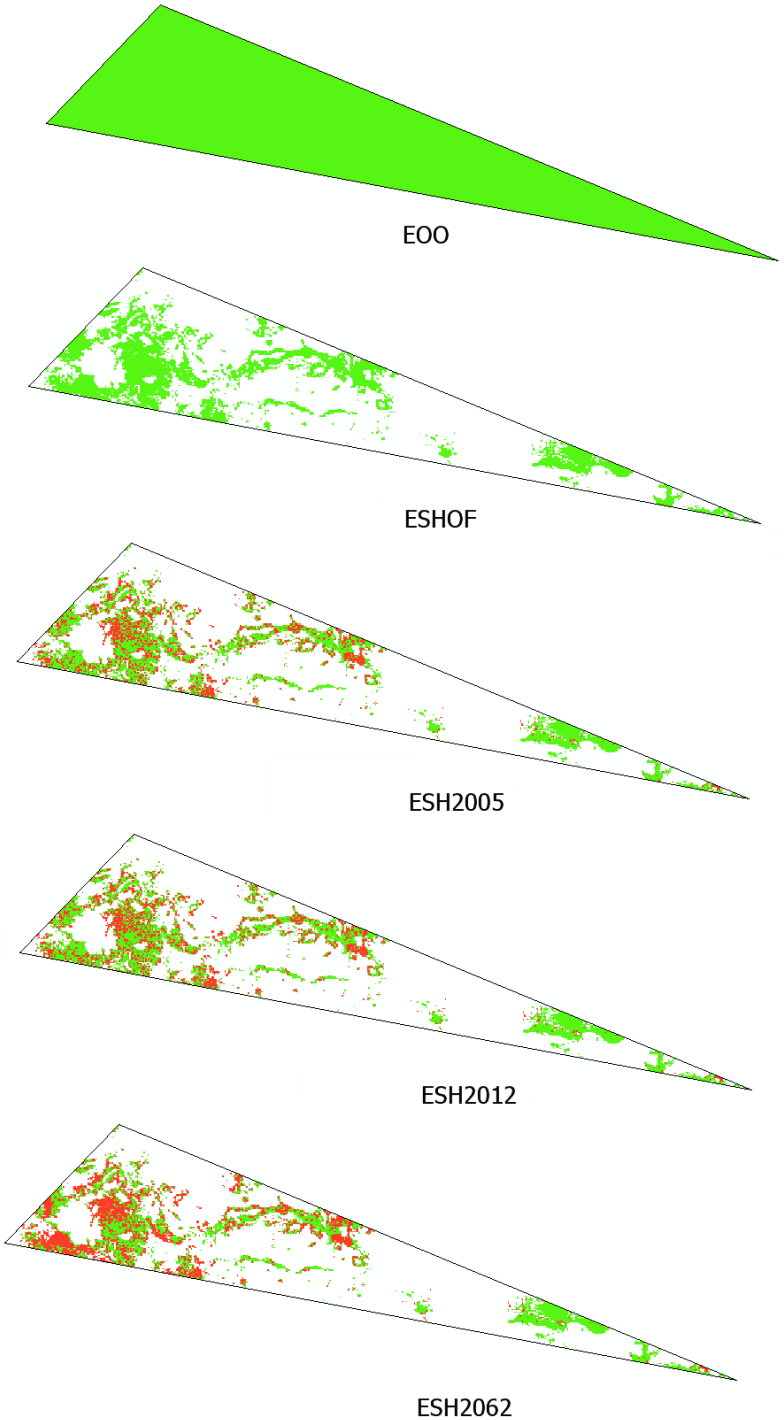

Figure 138. EOO and the extent of suitable habitat through time (original ESH (ESHOF), ESH in 2005, ESH in 2012 and ESH 2062) of *Selaginella sambasensis*. Green colour represents suitable habitat and red colour represents habitat loss (deforestation).

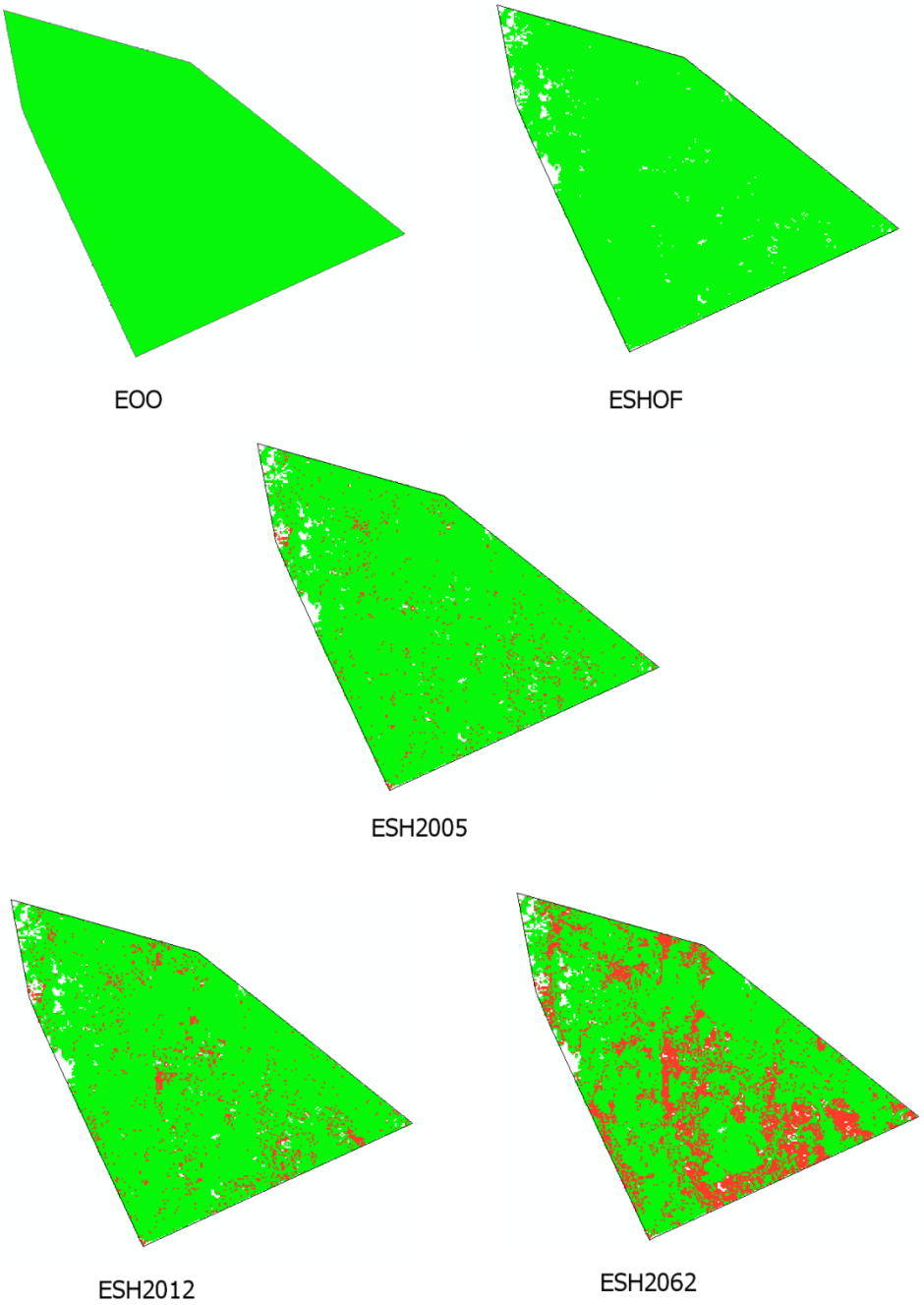

Figure 139. EOO and the extent of suitable habitat through time (original ESH (ESHOF), ESH in 2005, ESH in 2012 and ESH 2062) of *Tectaria keckii*. Green colour represents suitable habitat and red colour represents habitat loss (deforestation).

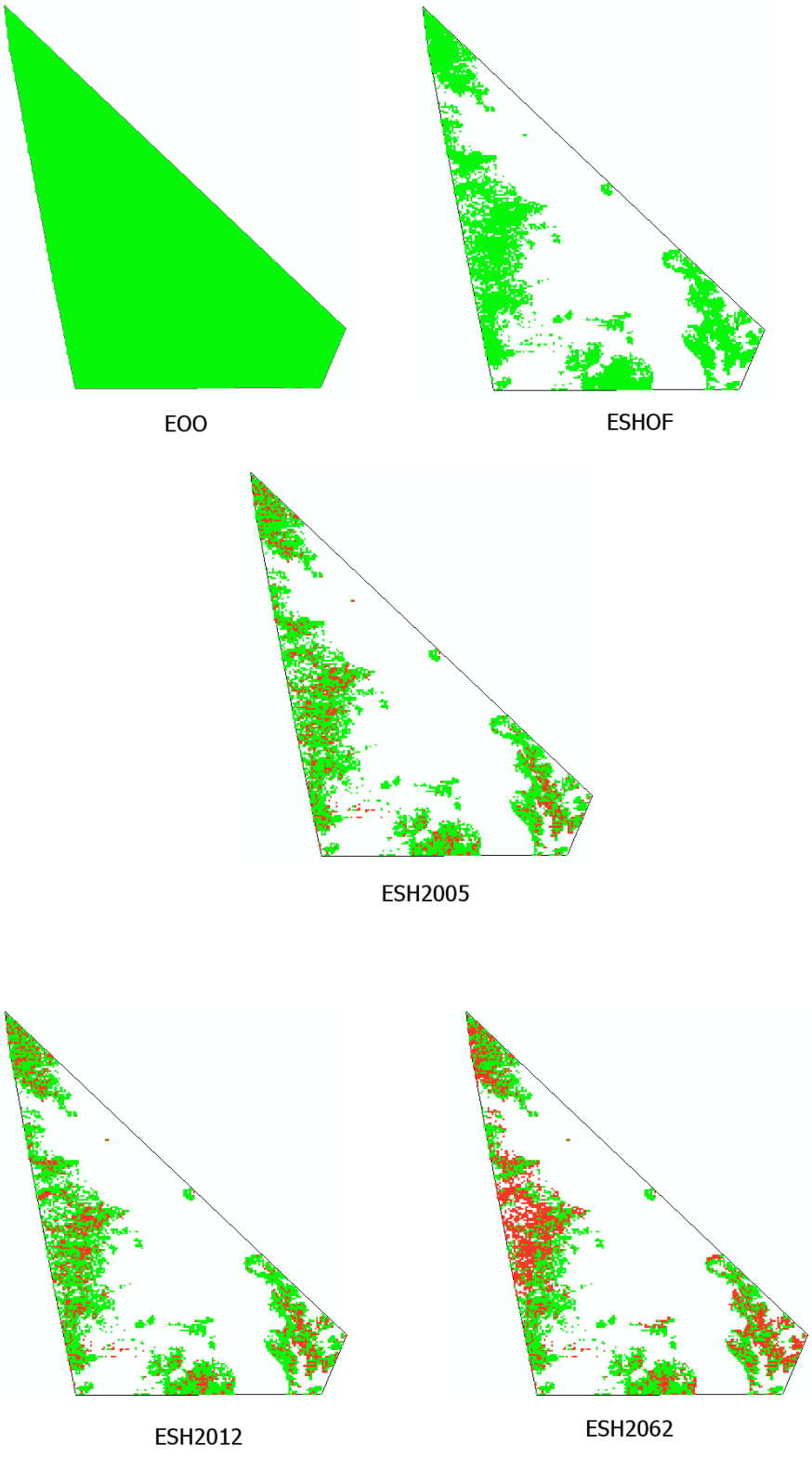

Figure 140. EOO and the extent of suitable habitat through time (original ESH (ESHOF), ESH in 2005, ESH in 2012 and ESH 2062) of *Asplenium lamprophyllum.* Green colour represents suitable habitat and red colour represents habitat loss (deforestation).

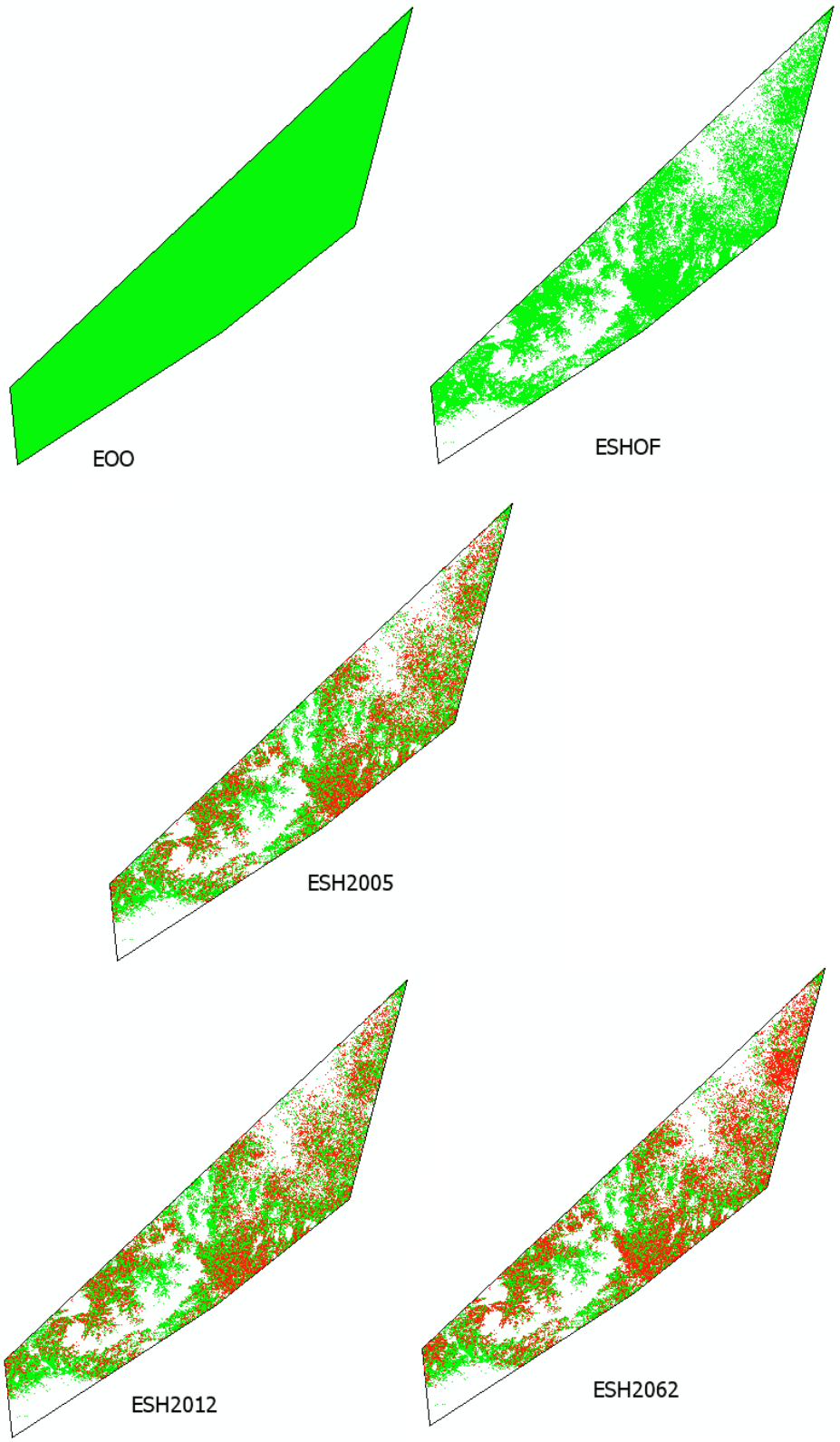

Figure 141. EOO and the extent of suitable habitat through time (original ESH (ESHOF), ESH in 2005, ESH in 2012 and ESH 2062) of *Ctenitis aspidioides*. Green colour represents suitable habitat and red colour represents habitat loss (deforestation).

The percentage of suitable habitat of the example species in each point in time is shown in Figure 142. Based on the species' ESHs, *Sellaginella sambasensis* which is a threatened (Vulnerable) species, endemic to Borneo Island, experienced 34% of habitat loss between the pre-human impact era and 2005, 2% between 2005 and 2012, 5% between 2012 and 2032 and 9% between 2032 and 2062. By 2062, *Sellaginella sambasensis* is predicted to lose a total of 50% of its original suitable habitat. The Least Concern species, *Ctenitis aspidioides* and *Asplenium lamprophyllum*, which occur in the Atlantic Forest and in New Zealand, respectively, will also lose a significant amount of suitable habitat. *Ctenitis aspidioides* and *Asplenium lamprophyllum* are predicted to lose 60% and 47% of their original suitable habitat by 2062, respectively. Finally, the Near Threatened species, *Tectaria keckii,* showed relatively low (6%) habitat loss between the pre-human impact era and 2012; however, it had the highest (19%) habitat loss between 2012 and 2062 of any Near Threatened species.

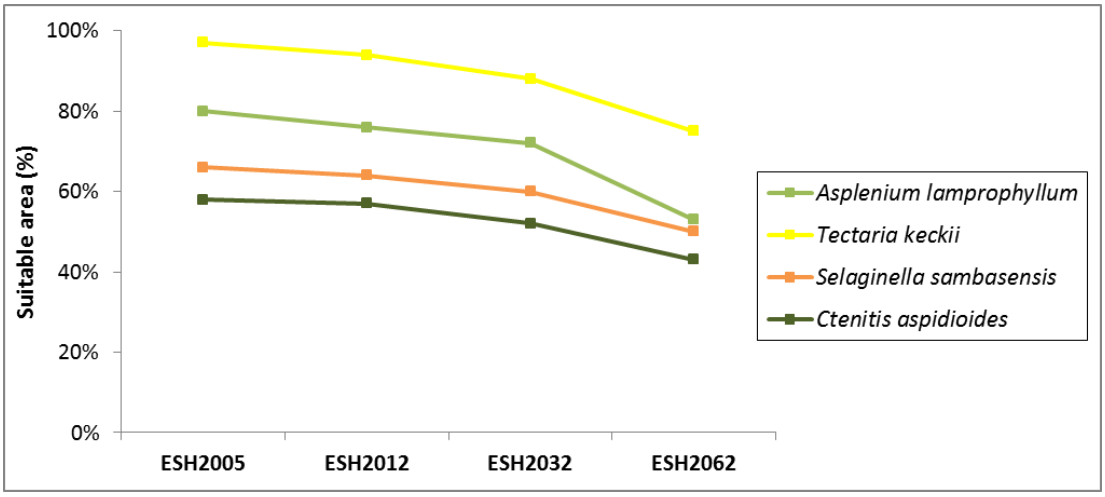

Figure 142. Mean percentage of suitable habitat for *Asplenium lamprophyllum* (Least Concern), *Tectaria keckii* (Near Threatened) *and Sellaginella sambasensis* (Vulnerable) through four points in time (pre-human impact era, 2005, 2012, 2032 and 2062).

The last example presented here is *Bolbitis virens*, a Least Concern species with an EOO area of 2.6 x10^4 km^2. Figure 143 shows the suitable habitat of *Bolbtis virens* between the pre-human impact era and 2062, during which 61% of its original suitable habitat will be lost. The suitable habitat area loss by 2062 will include the majority (6 out of 8) of the species' localities (occurrence points) and their surrounding area. These occurrence points were used to calculate the species' EOO and AOO which were then used to assess the species against the IUCN Red List Criteria in 2011.

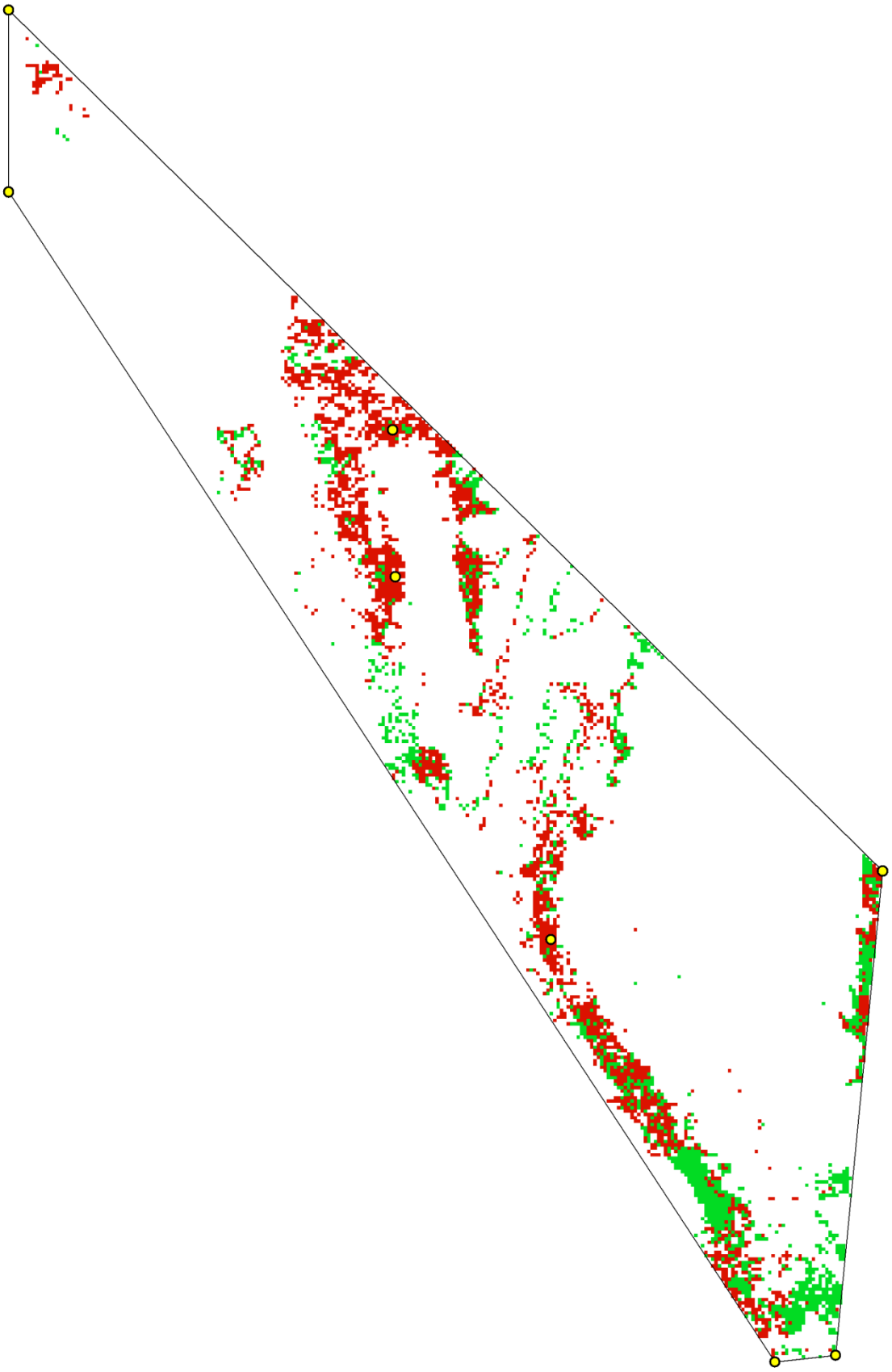

Figure 143. Occurrence points with a 2km buffer zone (yellow circles), suitable habitat (green colour) and habitat loss (red colour) between the pre-human impact period and 2062 of *Bolbitis virens*. The black line represents the extent of the species' original EOO.

6.4 DISCUSSION

6.4.1 Assessment of species ranges against the degree of human impact over time

This chapter assessed the geographical range of the SRLI forest pteridophyte species against the degree of human impact through time. The species' geographical ranges were generated for four points in time using the new ESH calculation method (Chapter 2, section 2.2.2.2) and thus the amount of suitable habitat for each species through time was predicted. The ESH of each species was calculated five times (the original ESH (before human impact); the ESH in 2005; the ESH in 2012; the ESH in 2032 and the ESH in 2062) and it was based on land cover information associated with each point in time. Ignoring any natural influences on forests, it was assumed that during the pre-human impact era 100% of suitable habitat was available for forest pteridophyte species, as then forests were not yet affected by human activities. Thus, it was not a surprise that the species' mean ESHOF was the highest in area compared with the species' mean ESHs for the human-impact era (ESH2005, ESH2012, ESH2032 and ESH2062). What was interesting, however, was that on average the ESHOF covered just 38.3±0.2% of the species original EOO. This is a relatively small percentage taking into consideration that the general ESH approach for this study was conservative (including all habitat types and the broader altitude/water balance ranges associated with each species) and that the ESHOF reflects the species' maximum suitable habitat within the EOO boundaries. This supports the view that the EOO is overestimating the species' geographical range (Burgman & Fox, 2003; Shaw *et al.*, 2003; Orme *et al.*, 2006; Jetz *et al.*, 2008), and it shows that the species original EOO does not even reflect the species' pre-human impact distribution.

The species' mean ESH reduced over the years as mean habitat loss increased. Unsurprisingly, the species' experienced the greatest habitat loss over the longest time period between the pre-human impact era and 2005 (15%). The relatively higher percentage of habitat loss in this period could be explained by the higher amount of years that exist between the pre-human impact era and 2005 compared to the other periods investigated (2005 – 2012, 2012 – 2032 and 2032-2062). However, it also reflects the higher deforestation rates that occurred during this period. Intense deforestation of temperate forests occurred in the High Middle ages (11^{th} – 13^{th} century) (Williams, 2000) and in the industrial age (18^{th} – 19^{th} century) (Richards, 1990; Williams, 2002). Also, significant clearing of tropical forests gathered pace in the 20^{th} century, with deforestation reaching a peak between 1950 and 1990 (FAO, 2012b). Moreover, the species' mean loss of suitable habitat between 2005 and 2012 was found to be 1%, a relatively high percentage for a 7-year period. This shows that, despite ongoing conservation efforts habitat loss is still occurring at an alarming rate.

The percentage of mean habitat loss found for species between the pre-human impact era and 2012 (16%) was similar to the equivalent percentage of forest loss reported by FAO in 2010 (15%). It was also similar to the percentage of forest loss found when calculating the forest cover difference between the original forest cover dataset and GlobCover 2005, excluding the

GFC deforested areas (17%). This shows that the species' habitat loss reflects the total forest loss reported for this period. An association between the total forest cover loss and the species' habitat loss was expected since the investigated species are forest species. However, it was anticipated that species' habitat loss would be lower than the total forest cover loss due to the habitat preference of the forest pteridophyte species for moist montane forests (see Chapters 3 – 5 for details). As agriculture is the most important driver of deforestation (Geist & Lambin, 2002; FAO, 2010; Hosonuma *et al.*, 2012; Laurance *et al.*, 2012), montane areas had lower historical deforestation rate than lowland areas, mainly due to their poorer accessibility and their less ideal conditions for agriculture (Collins *et al.*, 1991). Moreover, according to the deforestation data of Hansen *et al.* (2013) (resampled to 1km resolution with a 50% deforestation threshold), just 3% of the world's deforested areas occur in montane areas (>1500m) with 0.6% of the lowlands and 0.2% of montane areas deforested between 2000 and 2012. A reason for the matching percentage of species habitat loss and loss of forest cover could be the overestimation of the species distribution in the lowlands by the ESH metric (see Chapter 3, section 3.4.1) where the majority of deforestation occurs.

The species' mean habitat loss was 3% between 2012 and 2062 (2012 – 2032: 1% and 2032 – 2062: 2%) based on the future land use scenario. Other studies, all of which have used the IMAGE model, have also investigated the impact of future land use change on species ranges at a global scale. Visconti *et al.* (2011) predicted a mean habitat loss of 2.3 – 5.8% for mammal species between 2000 and 2050 whereas Jetz *et al*. (2007) estimated that between 1985 and 2050 bird species will experience a mean habitat loss of 21-26%. Both studies used the ESH metric to calculate species' geographical ranges, however, in contrast to Visconti *et al*. (2011), Jetz *et al* (2007) included climate change predictions in their model as well. van Vuuren *et al.* (2006) also combined future climate change and land use change predictions to predict a mean habitat loss of 15 – 30% for tropical vascular plants between 2000 and 2050. A comparison between the results of these studies and the results of the present study would not have been realistic since these studies have used different baseline years for their scenarios, different models and different taxonomic groups; however, of these studies it seems that the results of Visconti *et al*. (2011) are the closest to the predictions here.

The species' mean habitat loss per period investigated differed significantly across the biogeographical realms, reflecting the different drivers of deforestation for each realm through time. According to the species' ESHs, for the first period (pre-human impact era – 2005), species in the Palearctic realm experienced the largest mean habitat loss (24%). This is consistent with studies that have reported high deforestation rates and intensively-cleared forests in Europe and temperate Asia in the past. Over the last two thousand years, the natural forest cover of Europe was reduced from 80% to 34%, with forests being cleared for raw materials and replaced with agricultural land mainly due to the booms first in population and later in economy (Williams, 2002). Similarly, the temperate and subtropical forests of Asia and in particular of China, have suffered from deforestation for many centuries. China's forest cover has decreased alongside its dramatic increase in population, losing 50% of its forest cover by

the middle of the 20th century (FAO, 2012b). As already mentioned, the focus of large-scale deforestation changed from temperate to tropical forests in the 19th century, which explains the lower habitat loss for species in the tropical biogeographical realms than in the Palearctic realm over the first time period. Surprisingly, the mean habitat loss of the species in the Afrotropics was the second largest. Deforestation in Africa was low until European colonization in the 19th century when timber and other resources began to be widely exploited (Williams, 2002). According to FAO (2012b), the peak of deforestation in Africa occurred in the 1980s, but deforestation rates were not as high as in South America or Asia. While deforestation rates have declined since the 1980s, Africa had the second largest annual loss of forest between 2000 and 2005 (FAO, 2010), although as mentioned this estimation was based on incomplete information. This, together with historically high rates of deforestation in Madagascar (Green & Sussman, 1990; Mayaux *et al.*, 2000; Harper *et al.*, 2007), could partly explain the high percentage of habitat loss for Afrotropical species investigated. However, species in the Neotropics and Indomalaya were expected to have a mean habitat loss higher than the ones in the Afrotropics as the first two experienced severe deforestation in the 19th and 20th centuries (FAO, 1993; FAO, 2001; Williams, 2002; FAO, 2010; FAO, 2012b). The relatively high habitat loss of the Afrotropical species between the pre-human impact era and 2005 could be explained by a possible overestimation of Africa's original forest cover in the original forest cover dataset (UNEP-WCMC, 1998). This would have resulted in the overestimation of the species' ESHOFs and thus an unrealistic habitat loss would have been found when comparing the species' ESHOFs and ESH2005s.

Species in the Nearctic realm appeared to have the highest mean habitat loss between 2005 and 2012. This result may have been influenced by the low number of exclusively Nearctic species in the SRLI forest pteridophyte sample; however, the main reason for this result is the intensive forestry practices in the region. The timber industry of North America is most responsible for the deforestation of temperate forests in the region, the reforestation of which is slow. These forest clearings are not recorded as forest cover loss by the National Forest Services of the USA and Canada since the forests are in the process of recovering naturally, and therefore are not included in the FAO Forest Resources Assessments (FAO, 2001; FAO, 2009). This non-old-growth forest cover loss is nevertheless captured by the GFC data which were used to calculate the species ESH2012, ESH2032 and ESH2062, and is reflected in the species' habitat loss between 2005 and 2062.

Excluding the Nearctic species, the Neotropical species experienced the highest mean habitat loss between 2005 and 2012 followed by the Indomalayan species. These results were anticipated as both FAO (2010) and Hansen *et al*. (2013) reported the highest percentage of forest cover loss in the Neotropics and specifically in the tropical forests of South America, for the years 2000 to 2010 and 2000 to 2012, respectively. Deforestation rates in the Brazilian Amazon, which encompasses 60% of the Amazon forest and has been a deforestation hotspot, have been reduced since the beginning of the 21st century by targeting illegal logging using satellite images (Hansen *et al.*, 2013; INPE, 2014). However, deforestation is continuing to

shrink the Amazon forest at alarming rates with unprotected forests in Venezuela and Bolivia being cleared out (FAO, 2010). Based on the land use change model, the Indomalayan species are predicted to experience greater habitat loss than the Neotropical species between 2012 and 2062, although the percentage of mean habitat loss is significant in both sets of species. According to the GFC data, from 2005 to 2012, the deforestation rates in the Neotropics and Indomalya have decreased and increased respectively. Thus the deforested areas that were predicted by the land use change model (2012 – 2062), reflected these deforestation trends, since the land use change model based its predictions on the GFC data.

It is important to note that since the GFC data were aggregated to 1km resolution using a 50% deforestation threshold, the resampled GFC data give very low deforestation for regions with a patchy deforestation pattern (i.e. 1km pixels are less than 50% deforested), such as Africa. This may explain why the mean habitat loss of the Afrotropical species was almost as low as for the Palearctic species for the years 2005 to 2012, and consequently 2012 to 2062. Also, due to the patchy deforestation pattern in Africa, the detection of deforested areas through satellite imagery is more difficult compared to the other tropical realms with large-scale deforestation patterns (Reymondin, 2015).

6.4.2 Uncertainty in the habitat loss calculation

It was estimated that, on average, 16% of the species' suitable habitat was lost between the pre-human impact era and 2012 and that 81% of suitable habitat will be available for these species by 2062. In section 7.4.1, it was shown that reasonable results were obtained from the calculation of habitat loss through time even though the impact of climate change and the evolution in habitat preferences that might have occurred over this period were ignored. Despite these reasonable results, sources of uncertainty can be traced to the calculation of the species' four ESHs. The general limitations of ESHs that were discussed in previous sections of this study (Chapters 2, 3 and 4) add uncertainty to the calculation of habitat loss over time. In addition, uncertainty can be found in the land cover/forest cover loss data used in the calculation of each ESH over time (ESHOF, ESH2005, ESH2012, ESH2032 and ESH2062) as the species' environmental preferences used in each calculation have remained identical.

6.4.2.1 Calculation of ESHOF

The calculation of the species' ESHOF was calculated using the OFGC map, a map which combines information from the original forest cover map (UNEP-WCMC, 1998) and the land cover GlobCover (2005) map. Thus, the accuracy of the species' ESHOF depends on the accuracy of the OFGC map. If, for example, the ESHOF map overestimates forest cover in an area, the ESHOF of a species that occurs in that area will also be overestimated. Therefore the species' habitat loss between the pre human impact era and 2005 will also be overestimated. The original forest cover map (UNEP-WCMC, 1998) is the only freely available map of original forest cover at 1km resolution. As such, the species' ESHOFs could not be tested with an

alternative dataset to estimate the uncertainty of the map. While a global historical land use map (History Database of the Global Environment (HYDE) by Goldewijk *et al.* (2011) is frequently used in habitat loss studies, this was not used here as the map focuses on predicting past land use patterns (specifically cropland and pasture patterns) and not past forest cover.

Moreover, two assumptions were made when combining the original forest cover with non-forest land cover classes from GlobCover 2005 to create the OFGC map: firstly, that identical non-forest land cover classes existed in the pre-human impact period and that their extent was identical with that for 2005 (with the exception of forested areas); and secondly, that the species' habitat preference did not change during that period. These assumptions, which may not be correct, add uncertainty to the calculation of the species' ESHOF.

6.4.2.2 Calculation of ESH2005 and ESH2012

The uncertainty in using the high resolution land cover GlobCover map in the calculation of the ESH2005s can be identified through the comparison of the ESHs calculated using three different land cover datasets (GLCC, GLC2000 and GlobCover) (see details in Chapter 2, section 2.2.2.2.2). The comparison of the three datasets showed that there were small differences between the results produced by the datasets. However, GlobCover was selected as the most appropriate dataset since these data were collected more recently and at higher spatial resolution. Based on the evaluation of the ESH2005s (Chapter 2, section 2.3.3) and the validation of the ESH2005-derived species richness maps, it was concluded that the ESH2005s broadly reflect the reality of species distributions on the ground.

The ESH2005s were used as a baseline for the calculation of the ESH2012s. Forest cover loss data (GFC) were used to subtract suitable habitat, which was removed (deforested) between 2005 and 2012, from the ESH2005s. To test the level of uncertainty in using the selected forest cover loss data (GFC), the ESH2012s of species endemic to the Neotropics were also generated with deforestation data from a different monitoring system (Terra-i). Differences between the two sets of ESH2012s were expected, as the two land cover change monitoring systems have substantial differences (e.g. resolution, frequency, different forest definitions and calculation algorithms). When the two sets of ESH2012s were compared, it was found that the GFC data resulted in a greater mean reduction in the ESH2005 (0.6±0.9%) than the Terra-i data did (0.4±0.8%). This was expected as the GFC monitoring system calculated higher loss for this period than the Terra-i system, partly due to its higher resolution and, therefore, its ability to detect small-scale events. In general, GFC data reveal extensive areas with low percentage deforestation and define smaller areas with clear-cut deforestation when compared to Terra-i estimations. Even when setting the 50% deforestation threshold in the 1km resampled data, the GFC data showed 40% more loss than the Terra-i data. The lower deforestation estimations by Terra-i could also be attributed to the treatment of false positive land cover change due to drought, flooding and cloud cover (Reymondin *et al.*, 2012) but also to the inclusion of non-old-

growth forest loss in the GFC data. Nevertheless, the GFC and Terra-i systems both pick up the large-scale deforestation patterns.

Despite the differences between the two datasets, it was found that there is a high similarity (r^2=0.9) between the loss of species' habitat, and, therefore, the species' ESH2012s, for these two sets. This is due to the occurrence of many species in areas where Terra-i data and GFC data agree as 70% of the Terra-i data overlapped with the GFC data. Another reason for this high similarity is that 17% of the species did not experience any habitat loss based on either dataset. This high similarity shows that there is low uncertainty in using the GFC data in the calculation of the species' ESH2012s. It is important to note however, that this similarity would probably have been lower if a smaller deforestation threshold was selected when resampling both sets of data, because of the extensive low-level partial deforestation within the GFC data. At the moment, GFC provides the highest resolution gross forest cover loss data and the only forest cover loss data available across the globe. If the GFC monitoring system continues to provide forest cover loss data annually, the GFC data will be ideal for the calculation of the species' ESHs every five years.

Edge effects were partially accounted for by selecting a 50% deforestation threshold for the deforestation data resampled to 1 km and assuming that at this level of forest loss, the remaining forest in the pixel will be degraded due to fragmentation and edge effects. However, edge effects were not taken into consideration for the 100% deforested pixels in the calculation of the species' ESH2012s. In the ESH2012s calculation, only pixels that were marked as deforested were subtracted from the species' ESH2005s. As mentioned in the Introduction (section 7.1), plant species are affected by edge effects that can be obvious up to 1 km from the edge of the forest (Gascon *et al*., 2000). If these effects were taken into account, the species' ESH2012s would have been even smaller and the habitat loss between 2005 and 2012 would have been greater. Due to the fact that edge effects differ according to the age, physiognomy, aspect, size and shape of the forest fragment (Matlack, 1993; Murcia, 1995; Laurance *et al.*, 1998), fragmentation metrics need to be calculated before incorporating edge effects in the ESH methodology. Also, an investigation of the impact of edge effects on plant species' ranges needs to be conducted.

6.4.2.3 Calculation of ESH 2032 and 2062

The species' ESH2032s and ESH2065s were calculated by using deforestation data for the years between 2012 and 2032 and 2012 and 2062 respectively to deduct suitable habitat from the species' ESH2012s. Deforestation data for the years 2012 to 2062 were predicted by the QUICKLUC land use change model. Thus, source of uncertainty in ESH2032s and ESH2062s can be traced to this specific model and to the different decision steps made when building the future land use scenario.

The QUICKLUC model is a geographical land use change model and thus its projections are based on the proximity to recent deforested areas, agricultural suitability and accessibility of a specific area. While its projections match land use to specific geographic location, it does not take into account the interaction between supply, demand and trade. Therefore, it is not as complex as the Integrated Model to Assess the Global Environment (IMAGE) (Alcamo *et al*., 1994) which is frequently used in biodiversity studies (e.g. van Vuuren *et al*., 2006; Jetz *et al*., 2007; Alkemade *et al*., 2009; Dobrovolski *et al*., 2011; Visconti *et al*., 2011; Rondinini & Visconti, 2015; Visconti *et al.,* 2015). It is, however, a finer resolution model as it is run at 1 km resolution compared to the IMAGE model which is run at 10 km resolution. Another advantage of the QUICKLUC model is that it is included in the freely available web-based tool, Co$ting Nature, which already incorporates various remote sensing datasets that can be used in the model. For the needs of this study, QUICKLUC was ideal as it allows the development of land use scenarios based on recent rates and location of deforestation according to the GFC data, which were also used in calculating the ESH2012s. Thus, the projections of the model and therefore the species' ESH2032s and ESH2062s are compatible with the species ESH2012s. However, the key limitation of the QUICKLUC model cannot be ignored. Its reliance on historic deforestation patterns and rates to determine those in the future means that the model is unable to predict deforestation in areas where deforestation has never occurred.

The aim was to build a simple scenario that could be applied globally. A few assumptions, though, add uncertainty to the projections of the model, the first being that there is clear-cut deforestation (100% forest loss) in all 1km pixels predicted to be deforested. This may not be true in areas with small-scale deforestation events. Another assumption is that deforestation will continue at current rates. If, for example, the rate of future deforestation was set to be twice as high as the current rate, the ESH2032s and ESH2062s would have been smaller accordingly. As the model calculates current rates of deforestation regionally before aggregating them to a global scale, different rules could be set for each region based on knowledge of the future conservation efforts in the region. Moreover, the future land use scenario constrained deforestation to be outside of protected areas assuming high management effectiveness within protected areas. However, a deforestation leakage into protected areas with low management effectiveness (e.g. in Africa (Leverington *et al.*, 2008)) could be applied (e.g. 10%). This will influence the ESH2032 and ESH2062 of many species, especially threatened species, as protected areas have high species richness and high conservation interest (Pressey *et al*., 1993). Further, multiple impacts of land use change and impacts of climate change were not taken into consideration which could have resulted in the overestimation of the species' ESH2032 and ESH2062. Finally, the uncertainties of the GFC data used to project deforestation forward, which have been already discussed (e.g. associated with the chosen deforestation threshold), contribute to the uncertainty in the projections of the model.

6.4.3 ESH methodology and IUCN Red List conservation assessments

Threatened species are categorised based on five quantitative criteria (Appendix A1), any one of which needs to be met in order for a species to be classed as threatened (IUCN, 2012a). As mentioned in Chapter 2, Criterion B is the most appropriate for specimen-based assessments in the majority of cases (Willis et al., 2003). It was used to categorise more than half (59%) of species assessed for the SRLI for Plants (Brummitt & Bachman, 2010; Brummitt et al., 2015a; Brummitt et al., 2015b), as population data are not available for the majority of plant species. Under Criterion B, the species' geographical range is evaluated by calculating the EOO and AOO metrics, the values of which are compared with the quantitative thresholds for threatened categories. However, at least two out of three sub-criteria must also be met in order for a species to categorised as threatened.

One of those sub-criteria is sub-criterion b(iii), the continuing decline in the area, extent and/or quality of habitat, which until now has been qualitatively evaluated (Brummitt *et al.*, 2015a). It has been suggested by this study and others (Rondinini *et al*., 2011; Brummitt *et al*., 2015a) that the ESH metric could be incorporated into the IUCN Red List assessments by creating ESH thresholds under sub-criterion b (iii). These ESH thresholds will represent an appropriate amount of suitable habitat for each threatened category. In this study, this suggestion was made based on a stable relationship found between the size of the baseline ESH (2005) and the degree of IUCN threat. This relationship was also shown here: the size of all ESHs (ESHOF, ESH2005, ESH2012, ESH2032 and ESH2062) differed significantly between the IUCN threat categories, with the average ESH being larger in the Least Concern category and smaller in the Critically Endangered category in every case. This supports the argument that the ESH is an appropriate metric for IUCN Red List assessments.

Results also showed that ESH size and not the amount of habitat loss should be used to satisfy sub-criterion b(iii), as the species in the most threatened categories (Critically Endangered and Endangered) did not experience the greatest habitat loss over the years. However, these results could have been influenced by the low number of the most threatened species in the SRLI forest pteridophyte sample (Critically Endangered: 1 species, Endangered: 11 species). Nevertheless, the mean habitat loss of the species in the Vulnerable category was the highest one among the categories for all periods (pre-human impact era – 2005: 25.6%, 2005 – 2012: 0.8%, 2012 – 2032: 1.1% and 2032 – 2062: 3.3%), showing the exposure of these narrow range species to risk of extinction. Furthermore, it was expected that species with larger ESHs would have experienced greater habitat loss as more habitat would be available to be destroyed. Instead it was found that, on average, habitat loss was greater in species with small original EOO and small ESHOF (although as already mentioned habitat loss was not greater in the threatened species with the smallest EOO and ESHOF). Widespread species, experienced the lower mean habitat loss for all investigated periods, a result that agrees with Jetz *et al.* (2007) who estimated that habitat loss between 1985 and 2050 was minimal for bird species with large ranges. Thus, these habitat generalist species will be the least affected by land use change activities.

The advantage of the ESH metric is the ability for it to be re-calculated at regular intervals based on land cover change observations. The calculation of the species' ESH2012s, ESH2032s and ESH2062s demonstrated that by using frequently updated data from a land cover change monitoring system, ESHs can be recalculated and used in species' IUCN assessment every five years. Thus, every five years, the ESH of a species could be assessed against the suggested ESH thresholds under criterion Bb(iii). At the same time, the ESHs over different periods could be compared in order to show a decline in the extent of the species' suitable habitat and satisfy sub-criterion b(iii). Such examples were shown with the species *Tectaria keckii, Selaginella sambasensis, Asplenium lamprophyllum* and *Ctenitis aspidioides* (Figure 142). For each species, a record of its ESHs through time can be kept and updated every five years. Threatened species will have quantitative proof that their habitat is indeed declining (e.g. *Selaginella sambasensis*). Near Threatened species with EOO size less than 20 000 km² (the baseline EOO threshold for threatened categories) that were not categorised as threatened due to lack of evidence of habitat decline and therefore not fulfilling at least two of the sub-criteria, will now be able to be categorised. Moreover, predictions of the species' future ESH could be incorporated into the rationale section of the species' IUCN conservation assessment under which the reasoning behind each listing is included. Non-threatened species with predictions of high habitat loss could be prioritised in the case that not all species are assessed every five years (due to financial or logistic constraints). Further, predictions of the fate of species in the future can be used as a prioritision tool for conservation decisions on the assessed species.

The species' ESHs were not assessed against the EOO thresholds as performed by Jetz *et al* (2007). IUCN has released strict guidelines for using the EOO metric in species Red List assessments (IUCN, 2014) and therefore the two metrics were treated separately here. Replacing the EOO metric would not be realistic since that would mean all species previously assessed under Criterion B (or Criterion A) would need to be re-assessed. As the EOO does not change over time, unless a new species locality is found beyond its current range (Brummitt et al., 2015a) the conservation status of a species will remain the same even in the case where the ESH is shown to be declining. In contrast, a change in the species' AOO could be seen with the reduction of the ESH. Such an example is *Bolbitis virens*, a Least Concern species that according to its four calculated ESHs, will lose 61% of its original suitable habitat by 2062, including the majority (6 out of 8) of the species' localities. Since the AOO is measured as the sum of grid cells within the EOO where the species is actually known to occur (known localities), the AOO of a species will be reduced if these localities are considered lost. In the case of *Bolbitis virens*, 75% of its AOO will be reduced. Therefore, the species could be placed into a different Red List Category.

6.5 CONCLUSIONS

The last three objectives of this study were addressed in this chapter. The geographical ranges of the SRLI forest pteridophyte species were assessed against the degree of human impact through time using land cover information and deforestation data. Moreover, by applying a future land use scenario, change in the species' future range was also calculated. By calculating the species' ESHs at four different time points, it was found that the species' mean ESH reduced over the years as the mean habitat loss increased. Species experienced the greatest habitat loss between the pre-human impact era and 2005, reflecting the intensive forest cover loss during that period. However, significant habitat loss was also found for the other periods (2005 – 2012, 2012 – 2032 and 2032 – 2062). The species' mean habitat loss varied across the biogeographical regions, showing that species are affected differently by human impact depending on where they occur. In addition, mean habitat loss was greater in species with small ranges than in widespread species, indicating that smaller-ranged species will be more affected by land use change.

A stable relationship was also found between the size of the ESHs and the degree of IUCN threat, with the average ESH being larger in the Least Concern category and smaller in the Critically Endangered category in every case. This finding supports the argument that the ESH should be incorporated into IUCN Red List assessments by creating ESH thresholds under sub-criterion b(iii), which will represent an appropriate amount of suitable habitat for setting thresholds for each threatened category. It was suggested that species' ESHs should be re-calculated every five years using frequently updated data from a land cover change monitoring system and be assessed against the suggested ESH thresholds. It was also proposed that the ESHs of different times be compared in order to show decline in the extent of the species' suitable habitat and satisfy sub-criterion b(iii). Finally it was shown that, despite the fact that the EOO of a species may not change with the decline of ESH, the species AOO could change if species' localities are lost from the updated ESH. This change could influence the IUCN categorisation of the species. The systematic updating of the species' ESH based on the ESH methodology presented here can be the basis of an operational system that will assess and re-assess plant species' conservation status pan-tropically.

CHAPTER 7

CONCLUSIONS and FUTURE WORK

In 2010, the SRLI for Plants project provided a baseline assessment of the conservation status of plant species. Conservation assessments had been generated for globally-representative samples of species and showed that more than 1 in 5 plant species is threatened with extinction (Phase I) (Brummitt & Bachman, 2010; Brummitt *et al.*, 2015b). They now need to be re-assessed on a 5-year time frame to calculate the change in the Index and so monitor global trends in conservation status (Phase II) (Brummitt *et al*., 2015a). The aim of this PhD study, which belonged to the second phase of the SRLI project, was to provide the scientific basis for an automated procedure to assess and re-assess species' conservation status. Due to the importance of biodiversity in tropical areas and to the higher number of tropical species, this study mainly focused on the tropical parts of the world (Neotropics, Afrotropics and Indomalaya).

The first objective of this study was to improve the method for calculating species' ranges within it to better account for the impact of habitat on species distributions. This was addressed by adopting the ESH geographical range metric. While the ESH metric has been used in several studies (Rondinini *et al*., 2005; Jetz *et al*., 2007; Boitani *et al*., 2008; Buchanan *et al*., 2008; Catullo *et al*., 2008; Beresford *et al*., 2011a; Rondinini *et al*., 2011; Visconti *et al*., 2011), this was the first time that ESH has been calculated for IUCN plant species. An ESH method was built for the SRLI forest pteridophyte species (Chapter 2): species' ESHs were produced based on information of the appropriate ecology of each species (altitude range and water balance range preference) and land cover information, within the convex hull defining the species' EOO. By testing different variables and datasets, it was concluded that the ESH method should be used carefully, by selecting the most appropriate variables for each taxonomic group and by choosing the most suitable available remote-sensing datasets. Specifically, high spatial resolution datasets should be used when calculating the species' ESH in order to better detect the areas with suitable habitat for the species. In addition, it was recognised that the ESH is dependent upon the selection of the land cover classes that are assigned to the species. Therefore, a sensitivity analysis for several species is recommended to investigate the impact of differences in opinion of habitat class on the projected ESH for those species.

By validating the species' ESHs using independent data from GBIF, it was shown that the ESH is an improved measure of calculating the species' range since it reduces commission errors relative to the widely-used EOO metric, as the ESH only incorporates areas with appropriate conditions for the species. This agrees with the findings of previous studies which calculated species distribution using the ESH metric (Rondinini *et al.*, 2005; Jetz *et al.*, 2008; Beresford *et al.*, 2011a; Beresford *et al.*, 2011b; Buchanan *et al.*, 2011; Rondinini *et al.*, 2011). The species' ESHs were also evaluated indirectly, through the global species richness map generated by

stacking the species' ESHs (Chapter 3). The general patterns in the ESH-derived map of species richness agreed with previous studies showing that species' ESHs broadly reflect species distributions on the ground, at least within the boundaries of the original EOO. Differences between the ESH-derived maps and the findings of previous studies were attributed to the different pool of species and methods used in each study, but also to the geographical sampling bias found in the SRLI forest occurrence species' specimen data that were used in calculating the species' ESHs. The recognised issue of geographical sampling bias in natural history collections appears to have influenced the ESH-derived species richness map and consequently the species' ESHs. This problem will be addressed in the future by ensuring that the species' occurrence points used in the ESH calculation cover the species' full known distribution, according to published checklists. In the case that the natural history collections are not covering the species' full known distribution, fieldwork expeditions will be used to improve the SRLI database. Botanical expeditions have already been scheduled for the SRLI for Plants project, through which under-sampled areas could be targeted. Another approach to dealing with the geographical sampling bias in the SRLI data will be to test different techniques (e.g. spatial filtering, background manipulation with bias files, using pseudo-absence data) that have been suggested for correcting sampling bias in Species Distribution Modelling (Phillips *et al*., 2009; Kramer-Schadt *et al*., 2013; Syfert *et al*., 2013).

Moreover, it was obvious that differences between the ESH-derived species richness map and results of previous ecological studies and field-based assessments were also a result of an overestimation of ESH-derived species richness in the lowlands. This was confirmed by the validation of the ESH-derived species richness map with fieldwork data from a previous study (Kessler *et al*., 2011). This overestimation was partly explained by the fact that ESHs do not take into consideration all abiotic and biotic factors that could further limit a species range (Davis *et al*., 1998; Morrison *et al*., 2006), although another reason could be the overestimation of the species altitudinal range used in the ESH calculation. Despite the attempt to improve this issue, by excluding the extreme (outlying) altitude values of a species, this problem still persists and needs to be addressed in the future. An initial approach in addressing this issue will be to cross check the coordinates given to georeferenced herbarium specimens and the altitudinal ranges provided by collectors.

Additionally to the direct and indirect validation of the species' ESHs, ESHs were compared with the equivalent SDMs, fulfilling the fourth objective of this study (Chapter 4). To the author's knowledge, this was the first direct comparison of species' ESHs and SDMs. The comparison of the simple ESH method with the established and more complex SDM approach showed that the ESH metric still overestimates the species' distribution even after reducing commission errors relative to the EOO. More importantly, though, it revealed that there was a considerable level of similarity not only between the species' ESHs and SDMs but also between the ESH- and SDM-derived species richness maps. This shows that the ESH approach, despite its limitations, is not only a practical but also a relatively effective method in calculating both species ranges and identifying hotspots of species richness.

The second objective of this study was addressed by producing the first global maps of species richness and endemism derived from ESH measures for SRLI pteridophyte species. As expected, pteridophyte species richness peaked in tropical humid montane areas at mid-altitudes and with abundant water availability agreeing with Kreft *et al*. (2010). Intriguingly, areas of endemism for pteridophytes were found to have the same general spatial pattern as the tropical montane cloud forest areas, reflecting the clear habitat preference of the group. Despite the limitations of the ESH metric, the ESH-derived biodiversity maps predicted meaningful spatial patterns in comparison with previous studies and identified the expected areas in each biogeographical realm as hotspots of species richness and endemism. Interestingly, the major centres of species richness overlapped with the equivalent centres of endemism which was explained by the particular habitat preference (montane humid forests) of pteridophytes. Due to the practicality and effectiveness of the ESH-derived maps, it was suggested that these maps could be used in order to rapidly prioritise areas for conservation. Time-effective methods are needed for such prioritisation, as conservation targets are not being met in time (Butchart *et al*., 2010; Hirsch, 2010; Juffe-Bignoli *et al*., 2014), and therefore the ESH method could be proven more useful compared to the data intensive macroecological approach and time-consuming SDM approach. It was also proposed to use the ESH-derived maps for the prioritisation of areas for future botanical expeditions. This was put into practice for identifying and prioritising areas for future expeditions for the SRLI for Plants (Chapter 5). Results of the scheduled SRLI expeditions will verify if the ESH metric is useful in identifying areas for field expeditions, as Brooks & Matiku (2011) suggested, and will also validate the ESH-derived biodiversity maps confirming whether these maps generally reflect the reality on the ground.

The comparison between the ESH and EOO-derived biodiversity maps (Chapters 3 and 5) demonstrated the advantage of using the species' ESH over the species' original EOO. While the two sets of maps broadly agreed on the species richness and endemism patterns, the EOO-derived maps appeared to be homogeneous across large regions, in contrast to the ESH-derived maps which appeared to better reflect the habitat heterogeneity on the ground. Therefore, it was shown that the prioritisation of areas for both fieldwork and conservation would have been difficult based on the more general EOO-derived patterns.

The ESH method was built and tested with the SRLI pteridophyte forest species but was then applied to a different SRLI plant group, the SRLI forest angiosperm species (third objective - Chapter 5). The comparison between the ESHs of the two plant groups showed that the ESH method can be applied to other plant groups, as it produced meaningful results which reflected the overall differences of the two groups. In contrast to the habitat specificity of pteridophytes, angiosperms appeared to occur in many types of habitat, reflecting their greater ability to adapt to a wider range of ecological niches and also their known ecological dominance in the terrestrial biota. However, the application of the ESH method was restricted to the forest angiosperm species of Africa, the distribution of which is strongly dependent on water availability (Swaine, 1996; Holmgren *et al*., 2004; Maharjan *et al*., 2011). Thus, the selection of

variables in the ESH method for pteridophyte forest species was also suitable for angiosperm forest species. The next step will be to apply the ESH method to the forest species of all SRLI plant groups, globally. For each plant group, the most ecologically relevant variables will be selected, tested and eventually combined with land cover in order to standardise the group's ESH method. Furthermore, due to the fact that the ESH method was built for forest species, it will also be tested using non-forest species. The first step towards this has already been made by matching all IUCN habitat classes (IUCN, 2007) to GlobCover's land cover classes (Appendix A12). The next step will be to identify the key factor which indicates change in each environment (e.g. deforestation in forest, fire in savanah).

The last three objectives of this study were met in Chapter 6 in which ESH-derived ranges of the forest pteridophyte species were assessed against the degree of human impact through time, using land cover information and forest cover loss data. It was shown that the species' mean ESH reduced over the years as mean habitat loss increased, reflecting forest cover loss. Significant loss was found in all periods investigated (pre-human impact era – 2005, 2005 – 2012 and 2012– 2062) with the greatest loss found between the pre-human impact era and 2005. It was concluded that species are affected differently by human impact depending on where they occur and on the size of their range. Regardless, it was found that on average, the SRLI forest pteridophyte species have lost 16% of their original suitable habitat whereas an additional 3% will be lost by 2062. This result is consistent with other global biodiversity studies on different taxonomic groups which also predicted that habitat loss will continue to occur in the future and so affect species' geographical ranges (van Vuuren *et al*., 2006; Jetz *et al*, 2007; Visconti *et al*., 2011; Visconti *et al*., 2015).

Uncertainties in the calculation of habitat loss through time were identified and traced back to the general assumptions of the ESH methodology and the different data used in the calculation of the species' ESHs. The land use change model and future land use scenario defined were identified as the major sources of uncertainty in the species' ESH calculation, and therefore, future work will focus on testing different scenarios and performing sensitivity analyses. This will result in a better understanding of the likely impacts of land use change on forest cover and thus on the species' ranges. Moreover, future work should concentrate on incorporating edge effects in the calculation of species' ranges in order to better reflect the situation on the ground. Fragmantation metrics could be computed using spatial pattern analysis programmes (e.g. FRAGSTATS, BIOFRAG) and rules should be set according to the size and aspect of the forest fragments. If for example edge effects are calculated to occur between 500m and 1km from the forest fragment, the pixels next to the deforested areas will also be assigned as unavailable for forest species in the calculation of the species' ESH. Also, an investigation of the impact of edge effects on plant species' ranges needs to be conducted. This was explored during fieldwork in Costa Rica where sampling was conducted along a human impact gradient (from the middle of the pasture area to the middle of the forest patch). The aim of the fieldwork was to capture the relationship of land cover/use change and pteridophyte species loss both directly in areas deforested but also indirectly in remaining forest patches subject to edge effects. These

data will be used to understand the sensitivity of different species to fragmentation and edge effects.

Throughout this study, a relationship was found between the size of the species' ESHs and the degree of IUCN threat, with the average ESH being larger in the Least Concern category and smaller in the Critically Endangered category (Chapter 2, Chapter 5 and Chapter 6). Based on this stable relationship and on the fact that the majority of the SRLI plant species were categorised using Criterion B, a suggestion was made to incorporate the ESH measure into the IUCN Red List assessments under Criterion B sub-criterion b(iii). This suggestion was also made by Rondinini *et al.* (2011) and Brummitt *et al.* (2015). ESH thresholds for all SRLI plant species can be created under sub-criterion b(iii) which will represent an appropriate amount of suitable habitat and therefore the baseline ESH threshold for each threatened category. Chapter 6 presented the ESH methodology through which the ESHs can be re-calculated at regular intervals based on frequently updated data from a land cover change monitoring system and be assessed against ESH thresholds. The next step will be to quantify these thresholds by applying the ESH method to all SRLI plant species and using the degree of habitat loss observed in previously assessed species. Further, Chapter 6 demonstrated that by comparing the ESHs of different times a possible decline in the extent of the species' suitable habitat will be evidenced and thus sub-criterion b(iii) will be satisfied. Thus, non-threatened species that were not categorised as threatened due to lack of evidence of habitat decline, and therefore not fulfilling at least two of the sub-criteria, will now be categorised. Finally it was shown that, while the ESH will not replace the already incorporated EOO and AOO measures, as instructed by IUCN, it could influence the calculation of the species AOO if species' localities are lost based on the updated ESH.

This study created an easy ESH methodology as a practical method was needed in order for it to be easily incorporated into the IUCN Red List assessment process and applied by any assessor. The ESH methodology could be further formalised into an automated procedure by incorporating it into a powerful tool such as Co$ting Nature and GEOCAT. By first gathering information on the species' habitat preference and assigning the appropriate ranges/classes of the environmental/land cover variables to each species, the species' ESHs could be automatically calculated using the tool's input maps, constantly updated land cover change data and in-built fragmentation models. In this way the available suitable habitat will be automatically measured for each species at the time of the analysis. The available suitable habitat could then be compared with the created quantified thresholds of ESH for threatened Red List Categories under the sub-criterion Bb (iii).

Bearing in mind all the limitations mentioned above, the ESH methodology has accomplished the main aim of this study, in terms of providing an easy and practical methodology which could be the basis of an operational system that will assess and re-assess plant species' conservation status pan-tropically. In this way, more dynamic, comparable, repeatable and spatially-detailed Red List Index updates could be provided than is currently possible.

REFERENCES

ACHARD, F. 2009. *Vital Forest graphics,* Arendal, Norway, UNEP/GRID-Arendal.

ACHARD, F., EVA, H. D., STIBIG, H.-J., MAYAUX, P., GALLEGO, J., RICHARDS, T. & MALINGREAU, J.-P. 2002. Determination of deforestation rates of the world's humid tropical forests. *Science,* 297**,** 999-1002.

ADENEY, J. M., CHRISTENSEN, N. L. & PIMM, S. L. 2009. Reserves protect against deforestation fires in the Amazon. *PLos one,* 4**,** e5014.

ALCAMO, J., KREILEMAN, G., KROL, M. S. & ZUIDEMA, G. 1994. Modeling the global society-biosphere-climate system: Part 1: Model description and testing. *Image 2.0.* Springer.

ALDASORO, J., CABEZAS, F. & AEDO, C. 2004. Diversity and distribution of ferns in sub-Saharan Africa, Madagascar and some islands of the South Atlantic. *Journal of Biogeography,* 31**,** 1579-1604.

ALKEMADE, R., VAN OORSCHOT, M., MILES, L., NELLEMANN, C., BAKKENES, M. & TEN BRINK, B. 2009. GLOBIO3: a framework to investigate options for reducing global terrestrial biodiversity loss. *Ecosystems,* 12**,** 374-390.

ANDERSON, P. R., DUDÍK, M., FERRIER, S., GUISAN, A., HIJMANS, J. R., HUETTMANN, F., LEATHWICK, R. J., LEHMANN, A., LI, J. & LOHMANN, G. L. 2006. Novel methods improve prediction of species' distributions from occurrence data. *Ecography,* 29**,** 129-151.

ANDERSON, R. P., PETERSON, A. T. & GÓMEZ-LAVERDE, M. 2002. Using niche-based GIS modeling to test geographic predictions of competitive exclusion and competitive release in South American pocket mice. *Oikos,* 98**,** 3-16.

ARAÚJO, M. B. 2003. The Coincidence of People and Biodiversity in Europe. *Global Ecology and Biogeography,* 12**,** 5-12.

ARAÚJO, M. B. & LUOTO, M. 2007. The importance of biotic interactions for modelling species distributions under climate change. *Global Ecology and Biogeography,* 16**,** 743-753.

ARAÚJO, M. B., PEARSON, R. G., THUILLER, W. & ERHARD, M. 2005. Validation of species–climate impact models under climate change. *Global Change Biology,* 11**,** 1504-1513.

ARMENTERAS, D., RODRÍGUEZ, N., RETANA, J. & MORALES, M. 2011. Understanding deforestation in montane and lowland forests of the Colombian Andes. *Regional Environmental Change,* 11**,** 693-705.

AUSTIN, M. 2002. Spatial prediction of species distribution: an interface between ecological theory and statistical modelling. *Ecological modelling,* 157**,** 101-118.

BACHMAN, S., BAKER, W. J., BRUMMITT, N., DRANSFIELD, J. & MOAT, J. 2004. Elevational gradients, area and tropical island diversity: an example from the palms of New Guinea. *Ecography,* 27**,** 299-310.

BACHMAN, S., MOAT, J., HILL, A. W., DE LA TORRE, J. & SCOTT, B. 2011. Supporting Red List threat assessments with GeoCAT: geospatial conservation assessment tool. *ZooKeys,* 150.

BAI, L. 2010. *Comparison and Validation of Five Land Cover Products over the African Continent.* Lund University.

BAILLIE, J., HILTON-TAYLOR, C. & STUART, S. N. 2004. *2004 IUCN red list of threatened species: a global species assessment*, IUCN.

BAILLIE, J. E., COLLEN, B., AMIN, R., AKCAKAYA, H. R., BUTCHART, S. H., BRUMMITT, N., MEAGHER, T. R., RAM, M., HILTON-TAYLOR, C. & MACE, G. M. 2008. Toward monitoring global biodiversity. *Conservation Letters,* 1**,** 18-26.

BAKER, T. R., PHILLIPS, O. L., MALHI, Y., ALMEIDA, S., ARROYO, L., DI FIORE, A., ERWIN, T., HIGUCHI, N., KILLEEN, T. J. & LAURANCE, S. G. 2004. Increasing biomass in Amazonian forest plots. *Philosophical Transactions of the Royal Society of London. Series B: Biological Sciences,* 359**,** 353-365.

BARNOSKY, A. D., MATZKE, N., TOMIYA, S., WOGAN, G. O. U., SWARTZ, B., QUENTAL, T. B., MARSHALL, C., MCGUIRE, J. L., LINDSEY, E. L., MAGUIRE, K. C., MERSEY, B. & FERRER, E. A. 2011. Has the Earth/'s sixth mass extinction already arrived? *Nature,* 471**,** 51-57.

BARRINGTON, D. S. 1993. Ecological and historical factors in fern biogeography. *Journal of Biogeography***,** 275-279.

BARRINGTON, D. S. 2005. Helechos de los páramos de Costa Rica. *In:* KAPPELLE, M. H., S.P. (ed.) *Páramos de Costa Rica.* INBio, Santo Domingo de Heredia.

BARRY, S. & ELITH, J. 2006. Error and uncertainty in habitat models. *Journal of Applied Ecology,* 43**,** 413-423.

BARTHLOTT, W., HOSTERT, A., KIER, G., KÜPER, W., KREFT, H., MUTKE, J., RAFIQPOOR, M. D. & SOMMER, J. H. 2007. Geographic Patterns of Vascular Plant Diversity at Continental to Global Scales (Geographische Muster der Gefäßpflanzenvielfalt im kontinentalen und globalen Maßstab). *Erdkunde***,** 305-315.

BARTHLOTT, W., RAFIQPOOR, D., KIER, G. & KREFT, H. 2005. Global centers of vascular plant diversity. *Nova Acta Leopoldina NF,* 92**,** 61-83.

BARTHLOTT, W., SCHMIT-NEUERBURG, V., NIEDER, J. & ENGWALD, S. 2001. Diversity and abundance of vascular epiphytes: a comparison of secondary vegetation and primary montane rain forest in the Venezuelan Andes. *Plant Ecology,* 152**,** 145-156.

BENITEZ-MALVIDO, J. 1998. Impact of forest fragmentation on seedling abundance in a tropical rain forest. *Conservation Biology,* 12**,** 380-389.

BERESFORD, A., BUCHANAN, G., DONALD, P., BUTCHART, S., FISHPOOL, L. & RONDININI, C. 2011a. Poor overlap between the distribution of protected areas and globally threatened birds in Africa. *Animal Conservation,* 14**,** 99-107.

BERESFORD, A. E., BUCHANAN, G. M., DONALD, P. F., BUTCHART, S. H. M., FISHPOOL, L. D. C. & RONDININI, C. 2011b. Minding the protection gap: estimates of species' range sizes and holes in the Protected Area network. *Animal Conservation,* 14**,** 114-116.

BERTZKY, B., CORRIGAN, C., KEMSEY, J., KENNEY, S., RAVILIOUS, C., BESANÇON, C. & BURGESS, N. 2012. *Protected Planet Report 2012: Tracking progress towards global targets for protected areas. ,* IUCN, Gland, Switzerland and UNEP-WCMC,Cambridge, UK. .

BEYER, H. 2007. *Hawth's analysis tools for ArcGIS, version 3.27* [Online]. Available: http://www.spatialecology.com/htools

BHATTARAI, K. R., VETAAS, O. R. & GRYTNES, J. A. 2004. Fern species richness along a central Himalayan elevational gradient, Nepal. *Journal of Biogeography,* 31**,** 389-400.

BICHERON, P., DEFOURNY, P., BROCKMANN, C., SCHOUTEN, L., VANCUTSEM, C., M., H., BONTEMPS, S., LEROY, M., ACHARD, F., HEROLD, M., RANERA, F. & ARINO, O. 2008. *GlobCover 2005 – Products description and validation report, Version 2.2* [Online]. Available: http://ionia1.esrin.esa.int/ [Accessed 30 December 2012].

BICKFORD, S. A. & LAFFAN, S. W. 2006. Multi-extent analysis of the relationship between pteridophyte species richness and climate. *Global Ecology and Biogeography,* 15**,** 588-601.

BILLINGTON, C., V. KAPOS, M.S. EDWARDS, S. BLYTH & IREMONGER, S. 1996. Estimated Original Forest Cover Map—a First Attempt. *UK trade bulletin (SFIA).* WCMC, Cambridge.

BOAKES, E. H., MCGOWAN, P. J., FULLER, R. A., CHANG-QING, D., CLARK, N. E., O'CONNOR, K. & MACE, G. M. 2010. Distorted views of biodiversity: spatial and temporal bias in species occurrence data. *PLoS Biol,* 8**,** e1000385.

BOITANI, L., SINIBALDI, I., CORSI, F., DE BIASE, A., CARRANZA, I. D. I., RAVAGLI, M., REGGIANI, G., RONDININI, C. & TRAPANESE, P. 2008. Distribution of medium-to large-sized African mammals based on habitat suitability models. *Biodiversity and Conservation,* 17**,** 605-621.

BOND, P. & GOLDBLATT, P. 1984. Plants of the Cape flora.

BONTEMPS, S., DEFOURNY, P., VAN BOGAERT, E., ARINO, O., KALOGIROU, V. & PEREZ, J. R. 2011. *GlobCover 2009 – Products description and validation report Version 2.3* [Online]. Available: http://ionia1.esrin.esa.int/ [Accessed 30 December 2012].

BRAMWELL, D. & CAUJAPÉ-CASTELLS, J. 2011. *The biology of island floras*, Cambridge University Press.

BROOKS, T. & MATIKU, P. 2011. The science–policy interface for safeguarding key biodiversity areas. *Animal Conservation,* 14**,** 111-113.

BROOKS, T. M., MITTERMEIER, R. A., DA FONSECA, G. A., GERLACH, J., HOFFMANN, M., LAMOREUX, J. F., MITTERMEIER, C. G., PILGRIM, J. D. & RODRIGUES, A. S. 2006. Global biodiversity conservation priorities. *Science,* 313**,** 58-61.

BRUMMITT, N. & BACHMAN, S. 2010. Plants under pressure—a global assessment: the first report of the IUCN sampled red list index for plants. *Royal Botanic Gardens Kew, UK*.

BRUMMITT, N., BACHMAN, S. P., ALETRARI, E., CHADBURN, H., GRIFFITHS-LEE, J., LUTZ, M., MOAT, J., RIVERS, M. C., SYFERT, M. M. & NIC LUGHADHA, E. M. 2015a. The Sampled Red List Index for Plants, phase II: ground-truthing specimen-based conservation assessments. *Philosophical Transactions or the Royal Society B,* 370.

BRUMMITT, N., BACHMAN, S. P. & MOAT, J. 2008. Applications of the IUCN Red List: towards a global barometer for plant diversity. *Endangered Species Research,* 6**,** 127-135.

BRUMMITT, N. & NIC LUGHADHA, E. 2003. Biodiversity: where's hot and where's not. *Conservation Biology,* 17**,** 1442-1448.

BRUMMITT, N. A., S.P. BACHMAN, J. GRIFFITHS-LEE, M. LUTZ, J.F. MOAT, A. FARJON, J.S. DONALDSON, C. HILTON-TAYLOR, T.R. MEAGHER, S. ALBUQUERQUE, E.

ALETRARI, K. ANDREWS, G. ATCHISON, E. BALOCH, B. BARLOZZINI, A. BRUNAZZI, J. CARRETERO, M. CELESTI, H. CHADBURN, E. CIANFONI, C. COCKEL, V. COLDWELL, B. CONCETTI, S. CONTU, V. CROOK, P. DYSON, L., GARDINER, N., GHANIM, H. GREENE, A. GROOM, R. HARKER, D. HOPKINS, S. KHELA, P. LAKEMAN-FRASER, H. LINDON, H. LOCKWOOD, C. LOFTUS, D. LOMBRICI, L. LOPEZ-POVEDA, J. LYON, P. MALCOLM-TOMPKINS, K. MCGREGOR, L. MORENO, L. MURRAY, K. NAZAR, E. POWER, M. QUITON TUIJTELAARS, R. SALTER, R. SEGROTT, H. THACKER, L.J. THOMAS, S. TINGVOLL, G. WATKINSON, WOJTASZEKOVA, K. & LUGHADHA, E. M. N. 2015b. Green plants in the red: a baseline global assessment for the IUCN Sampled Red List Index for Plants. *PLoS One*.

BRUNER, A. G., GULLISON, R. E., RICE, R. E. & DA FONSECA, G. A. 2001. Effectiveness of parks in protecting tropical biodiversity. *Science,* 291**,** 125-8.

BRYANT, D. G., NIELSEN, D. & TANGLEY, L. 1997. *The last frontier forests: ecosystems & economies on the edge : what is the status of the world's remaining large, natural forest ecosystems? ,* Washington, DC, World Resources Institute, Forest Frontiers Initiative.

BUCHANAN, G. M., BUTCHART, S. H., DUTSON, G., PILGRIM, J. D., STEININGER, M. K., BISHOP, K. D. & MAYAUX, P. 2008. Using remote sensing to inform conservation status assessment: estimates of recent deforestation rates on New Britain and the impacts upon endemic birds. *Biological Conservation,* 141**,** 56-66.

BUCHANAN, G. M., DONALD, P. F. & BUTCHART, S. H. 2011. Identifying priority areas for conservation: a global assessment for forest-dependent birds. *PloS one,* 6**,** e29080.

BUCKLEY, L. B. & JETZ, W. 2008. Linking global turnover of species and environments. *Proceedings of the National Academy of Sciences,* 105**,** 17836-17841.

BURGER, W. C. 1981. Why Are There So Many Kinds of Flowering Plants? *BioScience,* 31**,** 572, 577-581.

BURGESS, N., DOGGART, N. & LOVETT, J. C. 2002. The Uluguru Mountains of eastern Tanzania: the effect of forest loss on biodiversity. *Oryx,* 36**,** 140-152.

BURGESS, N., HALES, J., UNDERWOOD, E., DINERSTEIN, E., OLSON, D., ITOUA, I., SCHIPPER, J., RICKETTS, T., NEWMAN, K. & HALES, J. 2004. *Terrestrial ecoregions of Africa and Madagascar: a conservation assessment*, Island Press.

BURGMAN, M. A. & FOX, J. C. 2003. Bias in species range estimates from minimum convex polygons: implications for conservation and options for improved planning. *Animal Conservation,* 6**,** 19-28.

BUSBY, J. R. 1991. BIOCLIM-a bioclimate analysis and prediction system. *In:* MARGULES CR, A. M. (ed.) *Nature conservation: cost effective biological surveys and data analysis.* CSIRO, Melbourne, .

BUTCHART, S., STATTERSFIELD, A., BAILLIE, J., BENNUN, L., STUART, S., AKÇAKAYA, H., HILTON-TAYLOR, C. & MACE, G. 2005. Using Red List Indices to measure progress towards the 2010 target and beyond. *Philosophical Transactions of the Royal Society B: Biological Sciences,* 360**,** 255-268.

BUTCHART, S. H., WALPOLE, M., COLLEN, B., VAN STRIEN, A., SCHARLEMANN, J. P., ALMOND, R. E., BAILLIE, J. E., BOMHARD, B., BROWN, C. & BRUNO, J. 2010. Global biodiversity: indicators of recent declines. *Science,* 328**,** 1164-1168.

CAIN, S. A. & CASTRO, G. D. O. 1960. Manual of Vegetation Analysis. *Soil Science,* 89**,** 359.

CALLMANDER, M. W., PHILLIPSON, P. B., SCHATZ, G. E., ANDRIAMBOLOLONERA, S., RABARIMANARIVO, M., RAKOTONIRINA, N., RAHARIMAMPIONONA, J., CHATELAIN, C., GAUTIER, L. & LOWRY, P. P. 2011. The endemic and non-endemic vascular flora of Madagascar updated. *Plant Ecology and Evolution,* 144**,** 121-125.

CARDILLO, M., MACDONALD, D. & RUSHTON, S. 1999. Predicting mammal species richness and distributions: testing the effectiveness of satellite-derived land cover data. *Landscape Ecology,* 14**,** 423-435.

CARDOSO, P., BORGES, P. A., TRIANTIS, K. A., FERRÁNDEZ, M. A. & MARTÍN, J. L. 2011. Adapting the IUCN Red List criteria for invertebrates. *Biological Conservation,* 144**,** 2432-2440.

CARPENTER, G., GILLISON, A. & WINTER, J. 1993. DOMAIN: a flexible modelling procedure for mapping potential distributions of plants and animals. *Biodiversity & Conservation,* 2**,** 667-680.

CATULLO, G., MASI, M., FALCUCCI, A., MAIORANO, L., RONDININI, C. & BOITANI, L. 2008. A gap analysis of Southeast Asian mammals based on habitat suitability models. *Biological Conservation,* 141**,** 2730-2744.

CAVELIER, J. & ETTER, A. 1995. Deforestation of montane forests in Colombia as a result of illegal plantations of opium (Papaver somniferum). *Biodiversity and conservation of Neotropical montane forests***,** 541-549.

CBD 2005. *Handbook of the Convention on Biological Diversity Including its Cartagena Protocol on Biosafety,* 3rd edition, Montreal, Canada.

CEBALLOS, G., EHRLICH, P. R., BARNOSKY, A. D., GARCÍA, A., PRINGLE, R. M. & PALMER, T. M. 2015. Accelerated modern human–induced species losses: Entering the sixth mass extinction. *Science Advances,* 1.

CGIAR-CSI. 2008. *Global-PET Database* [Online]. Available: (http://www.cgiar-csi.org/) [Accessed 10 October 2013].

CHAPE, S., HARRISON, J., SPALDING, M. & LYSENKO, I. 2005. *Measuring the extent and effectiveness of protected areas as an indicator for meeting global biodiversity targets*.

CIMMERY, V. 2010. *SAGA-GIS software, version 2.2* [Online]. Available: saga-gis.org [Accessed 6 April 2015].

COLLINS, N. M., J.A. SAYER & WHITMORE, T. C. 1991. The Conservation Atlas of Tropical Forests: Asia and the Pacific. International Union for the Conservation of Nature and Natural Resources.

COLWELL, R. K. & HURTT, G. C. 1994. Nonbiological Gradients in Species Richness and a Spurious Rapoport Effect. *The American Naturalist,* 144**,** 570-595.

CONNOR, E. F. & MCCOY, E. D. 1979. The statistics and biology of the species-area relationship. *American Naturalist***,** 791-833.

CONTRERAS-HERMOSILLA, A. 2000. *The underlying causes of forest decline*, Center for International Forestry Research Bogor, Indonesia.

CORSI, F., DUPRÈ, E. & BOITANI, L. 1999. A Large-Scale Model of Wolf Distribution in Italy for Conservation Planning. *Conservation Biology,* 13**,** 150-159.

COWLING, R. M. & HILTON-TAYLOR, C. 1997. Phytogeography, flora and endemism. *Vegetation of southern Africa***,** 43-61.

CUMMING, G. S. 2000. Using Habitat Models to Map Diversity: Pan-African Species Richness of Ticks (Acari: Ixodida). *Journal of Biogeography,* 27**,** 425-440.

DA FONSECA, G. A. B., BALMFORD, A., BIBBY, C., BOITANI, L., CORSI, F., BROOKS, T., GASCON, C., OLIVIERI, S., MITTERMEIER, R. A., BURGESS, N., DINERSTEIN, E., OLSON, D., HANNAH, L., LOVETT, J., MOYER, D., RAHBEK, C., STUART, S. & WILLIAMS, P. 2000. Following Africa's lead in setting priorities. *Nature,* 405**,** 393-394.

DAVIS, A. J., JENKINSON, L. S., LAWTON, J. H., SHORROCKS, B. & WOOD, S. 1998. Making mistakes when predicting shifts in species range in response to global warming. *Nature,* 391**,** 783-786.

DEFENSE MAPPING AGENCY. 1992. *Digital Chart of the World, Defense Mapping Agency*. Fairfax, Virginia.

DEFRIES, R., HANSEN, M., TOWNSHEND, J., JANETOS, A. & LOVELAND, T. 2000. A new global 1-km dataset of percentage tree cover derived from remote sensing. *Global Change Biology,* 6**,** 247-254.

DEFRIES, R. S., FOLEY, J. A. & ASNER, G. P. 2004. Land-use choices: balancing human needs and ecosystem function. *Frontiers in Ecology and the Environment,* 2**,** 249-257.

DEFRIES, R. S., HOUGHTON, R. A., HANSEN, M. C., FIELD, C. B., SKOLE, D. & TOWNSHEND, J. 2002. Carbon emissions from tropical deforestation and regrowth based on satellite observations for the 1980s and 1990s. *Proceedings of the National Academy of Sciences,* 99**,** 14256-14261.

DENGLER, J. 2009. Which function describes the species–area relationship best? A review and empirical evaluation. *Journal of Biogeography,* 36**,** 728-744.

DENNIS, R. L. H. & THOMAS, C. D. 2000. Bias in Butterfly Distribution Maps: The Influence of Hot Spots and Recorder's Home Range. *Journal of Insect Conservation,* 4**,** 73-77.

DIMICELI, C. M., M.L. CARROLL, R.A. SOHLBERG, C. HUANG, M.C. HANSEN & TOWNSHEND, J. R. G. 2010. *Annual Global Automated MODIS Vegetation Continuous Fields (MOD44B) at 250 m Spatial Resolution for Data Years Beginning Day 65, 2000 - 2010, Collection 5 Percent Tree Cover* [Online]. University of Maryland, College Park, MD, USA.

DIRZO, R. & RAVEN, P. H. 2003. Global state of biodiversity and loss. *Annual Review of Environment and Resources,* 28**,** 137-167.

DIRZO, R., YOUNG, H. S., GALETTI, M., CEBALLOS, G., ISAAC, N. J. B. & COLLEN, B. 2014. Defaunation in the Anthropocene. *Science,* 345**,** 401-406.

DOBROVOLSKI, R., DINIZ-FILHO, J. A. F., LOYOLA, R. D. & JÚNIOR, P. D. M. 2011. Agricultural expansion and the fate of global conservation priorities. *Biodiversity and Conservation,* 20**,** 2445-2459.

DUBUIS, A., POTTIER, J., RION, V., PELLISSIER, L., THEURILLAT, J.-P. & GUISAN, A. 2011. Predicting spatial patterns of plant species richness: a comparison of direct macroecological and species stacking modelling approaches. *Diversity and Distributions,* 17**,** 1122-1131.

DUPONT, L. M., JAHNS, S., MARRET, F. & NING, S. 2000. Vegetation change in equatorial West Africa: time-slices for the last 150 ka. *Palaeogeography, Palaeoclimatology, Palaeoecology,* 155**,** 95-122.

ELITH, J., BURGMAN, M. A. & REGAN, H. M. 2002. Mapping epistemic uncertainties and vague concepts in predictions of species distribution. *Ecological Modelling,* 157**,** 313-329.

ELITH, J. & GRAHAM, C. H. 2009. Do they? How do they? WHY do they differ? On finding reasons for differing performances of species distribution models. *Ecography,* 32**,** 66-77.

ELITH, J., H. GRAHAM, C., P. ANDERSON, R., DUDÍK, M., FERRIER, S., GUISAN, A., J. HIJMANS, R., HUETTMANN, F., R. LEATHWICK, J., LEHMANN, A., LI, J., G. LOHMANN, L., A. LOISELLE, B., MANION, G., MORITZ, C., NAKAMURA, M., NAKAZAWA, Y., MCC. M. OVERTON, J., TOWNSEND PETERSON, A., J. PHILLIPS, S., RICHARDSON, K., SCACHETTI-PEREIRA, R., E. SCHAPIRE, R., SOBERÓN, J., WILLIAMS, S., S. WISZ, M. & E. ZIMMERMANN, N. 2006. Novel methods improve prediction of species' distributions from occurrence data. *Ecography,* 29**,** 129-151.

ELITH, J. & LEATHWICK, J. R. 2009. Species distribution models: ecological explanation and prediction across space and time. *Annual Review of Ecology, Evolution, and Systematics,* 40**,** 677.

EMANUEL, W., SHUGART, H. & STEVENSON, M. 1985. Climatic change and the broad-scale distribution of terrestrial ecosystem complexes. *Climatic Change,* 7**,** 29-43.

ENGLER, R., GUISAN, A. & RECHSTEINER, L. 2004. An improved approach for predicting the distribution of rare and endangered species from occurrence and pseudo-absence data. *Journal of Applied Ecology,* 41**,** 263-274.

ENQUIST, C. A. F. 2002. Predicted regional impacts of climate change on the geographical distribution and diversity of tropical forests in Costa Rica. *Journal of Biogeography,* 29**,** 519-534.

ESRI. 2009. *ArcGIS, version 9.3. Environmental Systems Research Institute* [Online].

EUROPEAN COMMISSION. 2003. *Global Land Cover 2000 database* [Online]. Joint Research Centre. Available: http://bioval.jrc.ec.europa.eu/products/glc2000/glc2000.php [Accessed 20 December 2012].

EWERS, R. M. & DIDHAM, R. K. 2006. Confounding factors in the detection of species responses to habitat fragmentation. *Biological Reviews,* 81**,** 117-142.

EXELL, A. W. & WILD, H. 1973. A STATISTICAL ANALYSIS OF A SAMPLE OF THE FLORA ZAMBESIACA—II: GRAMINEAE AND PTERIDOPHYTA. *Kirkia,* 9**,** 87-93.

FAO 1993. *Forest Resources Assessment 1990: Tropical Countries, Forestry Paper No. 112,* Rome, Italy.

FAO 2001. *State of the World's Forest 2001,* Rome, Italy.

FAO 2009. How to Feed the Word in 2050. Rome, Italy.

FAO 2010. *Global Forest resources assessment 2010, FA0 Forestry Paper 163,* Rome, Italy.

FAO. 2012a. *Global Agro-Ecological Zones (GAEZ v 3.0)* [Online]. Available: http://www.fao.org/nr/gaez/en/.

FAO 2012b. State of the world's forests. Rome, Italy.

FAO. 2014. *Global Administrative Unit Layers (GAUL)* [Online]. Available: http://www.fao.org/geonetwork/srv/en/metadata.show?id=12691.

FEARNSIDE, P. M. 2000. Global warming and tropical land-use change: greenhouse gas emissions from biomass burning, decomposition and soils in forest conversion, shifting cultivation and secondary vegetation. *Climatic change,* 46**,** 115-158.

FERRAZ, G., RUSSELL, G. J., STOUFFER, P. C., BIERREGAARD, R. O., PIMM, S. L. & LOVEJOY, T. E. 2003. Rates of species loss from Amazonian forest fragments. *Proceedings of the National Academy of Sciences,* 100**,** 14069-14073.

FERREIRA, L. V. & LAURANCE, W. F. 1997. Effects of forest fragmentation on mortality and damage of selected trees in central Amazonia. *Conservation Biology,* 11**,** 797-801.

FIELD, R., O'BRIEN, E. M. & WHITTAKER, R. J. 2005. Global models for predicting woody plant richness from climate: development and evaluation. *Ecology,* 86**,** 2263-2277.

FISHER, B. 2010. African exception to drivers of deforestation. *Nature Geosci,* 3**,** 375-376.

FJELDSAÅ, J. & LOVETT, J. C. 1997. Geographical patterns of old and young species in African forest biota: the significance of specific montane areas as evolutionary centres. *Biodiversity & Conservation,* 6**,** 325-346.

FRANCIS, A. P. & CURRIE, D. J. 2003. A globally consistent richness-climate relationship for angiosperms. *The American Naturalist,* 161**,** 523-536.

FRANKLIN, J. 1998. Predicting the distribution of shrub species in southern California from climate and terrain-derived variables. *Journal of Vegetation Science***,** 733-748.

FRANKLIN, J. 2009. *Mapping Species Distributions: Spatial Inference and Prediction* Cambridge University Press, Ecology, Biodiversity and Conservation.

FRIEDMAN, J. H. 1991. Multivariate adaptive regression splines. *The annals of statistics***,** 1-67.

FRIEDMAN, J. H. 2001. Greedy function approximation: a gradient boosting machine. *Annals of statistics***,** 1189-1232.

FROST, P. 1996. The ecology of miombo woodlands. *The miombo in transition: Woodlands and welfare in Africa***,** 11-57.

GASCON, C. & LOVEJOY, T. E. 1998. Ecological impacts of forest fragmentation in central Amazonia. *Zoology-Analysis of Complex Systems,* 101**,** 273-280.

GASCON, C., LOVEJOY, T. E., BIERREGAARD JR, R. O., MALCOLM, J. R., STOUFFER, P. C., VASCONCELOS, H. L., LAURANCE, W. F., ZIMMERMAN, B., TOCHER, M. & BORGES, S. 1999. Matrix habitat and species richness in tropical forest remnants. *Biological Conservation,* 91**,** 223-229.

GASCON, C., WILLIAMSON, G. B. & DA FONSECA, G. A. 2000. Receding forest edges and vanishing reserves. *Science,* 288**,** 1356-1358.

GASTON, K. J. 1991. How large is a species' geographic range? *Oikos,* 61**,** 434-438.

GASTON, K. J. 1994. Measuring geographic range sizes. *Ecography,* 17**,** 198-205.

GASTON, K. J. 2000. Global patterns in biodiversity. *Nature,* 405**,** 220-227.

GASTON, K. J., BLACKBURN, T. M. & GOLDEWIJK, K. K. 2003a. Habitat conversion and global avian biodiversity loss. *Proceedings of the Royal Society of London. Series B: Biological Sciences,* 270**,** 1293-1300.

GASTON, K. J. & FULLER, R. A. 2009. The sizes of species' geographic ranges. *Journal of Applied Ecology,* 46**,** 1-9.

GASTON, K. J., JONES, A. G., HÄNEL, C. & CHOWN, S. L. 2003b. Rates of species introduction to a remote oceanic island. *Proceedings of the Royal Society of London. Series B: Biological Sciences,* 270**,** 1091-1098.

GEIST, H. J. & LAMBIN, E. F. 2001. What drives tropical deforestation. *LUCC Report series,* 4**,** 116.

GEIST, H. J. & LAMBIN, E. F. 2002. Proximate Causes and Underlying Driving Forces of Tropical Deforestation Tropical forests are disappearing as the result of many pressures, both local and regional, acting in various combinations in different geographical locations. *BioScience,* 52**,** 143-150.

GIBBS, H., RUESCH, A., ACHARD, F., CLAYTON, M., HOLMGREN, P., RAMANKUTTY, N. & FOLEY, J. 2010. Tropical forests were the primary sources of new agricultural land in the 1980s and 1990s. *Proceedings of the National Academy of Sciences,* 107**,** 16732-16737.

GILIBA, R. A., BOON, E. K., KAYOMBO, C. J., MUSAMBA, E. B., KASHINDYE, A. M. & SHAYO, P. F. 2011. Species composition, richness and diversity in Miombo woodland of Bereku Forest Reserve, Tanzania. *Journal of Biodiversity,* 2**,** 1-7.

GOLDBLATT, P. 1977. Systematics of Moraea (Iridaceae) in tropical Africa. *Annals of the Missouri Botanical Garden***,** 243-295.

GOLDEWIJK, K. K., BEUSEN, A., VAN DRECHT, G. & DE VOS, M. 2011. The HYDE 3.1 spatially explicit database of human-induced global land-use change over the past 12,000 years. *Global Ecology and Biogeography,* 20**,** 73-86.

GONZÁLEZ-MAYA, J. F., FINEGAN, B. G., SCHIPPER, J. & CASANOVES, F. 2008. Densidad absoluta y conservación del jaguar y sus presas en la región Talamanca, Pacífico, Costa Rica. *The Nature Conservancy, San José, Costa Rica*.

GOODMAN, S. M. & BENSTEAD, J. P. 2005. Updated estimates of biotic diversity and endemism for Madagascar. *Oryx,* 39**,** 73-77.

GOTELLI, N. J., ANDERSON, M. J., ARITA, H. T., CHAO, A., COLWELL, R. K., CONNOLLY, S. R., CURRIE, D. J., DUNN, R. R., GRAVES, G. R., GREEN, J. L., GRYTNES, J.-A., JIANG, Y.-H., JETZ, W., KATHLEEN LYONS, S., MCCAIN, C. M., MAGURRAN, A. E., RAHBEK, C., RANGEL, T. F. L. V. B., SOBERÓN, J., WEBB, C. O. & WILLIG, M. R. 2009. Patterns and causes of species richness: a general simulation model for macroecology. *Ecology Letters,* 12**,** 873-886.

GRAHAM, C. H., VANDERWAL, J., PHILLIPS, S. J., MORITZ, C. & WILLIAMS, S. E. 2010. Dynamic refugia and species persistence: tracking spatial shifts in habitat through time. *Ecography,* 33**,** 1062-1069.

GRAINGER, A. 2008. Difficulties in tracking the long-term global trend in tropical forest area. *Proceedings of the National Academy of Sciences,* 105**,** 818-823.

GREEN, G. M. & SUSSMAN, R. W. 1990. Deforestation History of the Eastern Rain Forests of Madagascar from Satellite Images. *Science,* 248**,** 212-215.

GREEN, J. M. H., LARROSA, C., BURGESS, N. D., BALMFORD, A., JOHNSTON, A., MBILINYI, B. P., PLATTS, P. J. & COAD, L. 2013. Deforestation in an African biodiversity hotspot: Extent, variation and the effectiveness of protected areas. *Biological Conservation,* 164**,** 62-72.

GRENOUILLET, G., BUISSON, L., CASAJUS, N. & LEK, S. 2011. Ensemble modelling of species distribution: the effects of geographical and environmental ranges. *Ecography,* 34**,** 9-17.

GROOMBRIDGE, B. 1992. *Global Biodiversity: State of the Earth's Living Resources,* New York, NY, Chapman and Hall.

GROOMBRIDGE, B. & JENKINS, M. 1994. *Biodiversity data sourcebook*, World Conservation Press Cambridge.

GROOMBRIDGE, B. & JENKINS, M. D. 2002. *World atlas of biodiversity*, University of California Press Berkeley, CA.

GUILHAUMON, F., GIMENEZ, O., GASTON, K. J. & MOUILLOT, D. 2008. Taxonomic and regional uncertainty in species-area relationships and the identification of richness hotspots. *Proceedings of the National Academy of Sciences,* 105**,** 15458-15463.

GUISAN, A., BROENNIMANN, O., ENGLER, R., VUST, M., YOCCOZ, N. G., LEHMANN, A. & ZIMMERMANN, N. E. 2006. Using Niche-Based Models to Improve the Sampling of Rare Species

Utilización de Modelos Basados en Nichos para Mejorar el Muestreo de Especies Raras. *Conservation Biology,* 20**,** 501-511.

GUISAN, A., THEURILLAT, J. P. & KIENAST, F. 1998. Predicting the potential distribution of plant species in an alpine environment. *Journal of Vegetation Science,* 9**,** 65-74.

GUISAN, A. & THUILLER, W. 2005. Predicting species distribution: offering more than simple habitat models. *Ecology Letters,* 8**,** 993-1009.

GUISAN, A., TINGLEY, R., BAUMGARTNER, J. B., NAUJOKAITIS-LEWIS, I., SUTCLIFFE, P. R., TULLOCH, A. I. T., REGAN, T. J., BROTONS, L., MCDONALD-MADDEN, E., MANTYKA-PRINGLE, C., MARTIN, T. G., RHODES, J. R., MAGGINI, R., SETTERFIELD, S. A., ELITH, J., SCHWARTZ, M. W., WINTLE, B. A., BROENNIMANN, O., AUSTIN, M., FERRIER, S., KEARNEY, M. R., POSSINGHAM, H. P. & BUCKLEY, Y. M. 2013. Predicting species distributions for conservation decisions. *Ecology Letters,* 16**,** 1424-1435.

GUISAN, A. & ZIMMERMANN, N. E. 2000. Predictive habitat distribution models in ecology. *Ecological modelling,* 135**,** 147-186.

HAFFER, J. 1969. Speciation in amazonian forest birds. *Science,* 165**,** 131-137.

HAGEN, A. 2006. *Comparing continuous valued raster data: A cross disciplinary literature scan,* the Netherlands, RIKS bv.

HAILA, Y. & MARGULES, C. R. 1996. Survey research in conservation biology. *Ecography,* 19**,** 323-331.

HALL, L. S., KRAUSMAN, P. R. & MORRISON, M. L. 1997. The habitat concept and a plea for standard terminology. *Wildlife Society Bulletin,* 25**,** 173-182.

HAMILTON, A. 1974. Distribution patterns of forest trees in Uganda and their historical significance. *Plant Ecology,* 29**,** 21-35.

HAMILTON, A. 1976. significance of patterns of distribution shown by forest plants and animals in tropical Africa for the reconstruction of Upper Pleistocene palaeoenvironments: a review. *Palaeoecology of Africa & of the surrounding islands & Antarctica*.

HAMILTON, L. S., JUVIK, J. O. & SCATENA, F. N. 2012. *Tropical montane cloud forests*, Springer Science & Business Media.

HAMMER, D., KRAFT, R. & WHEELER, D. 2009. Forma: Forest Monitoring for Action-Rapid Identification of Pan-Tropical Deforestation Using Moderate-Resolution Remotely Sensed Data. *Center for Global Development Working Paper*.

HANLEY, J. A. & MCNEIL, B. J. 1982. The meaning and use of the area under a receiver operating characteristic (ROC) curve. *Radiology,* 143**,** 29-36.

HANSEN, M., DEFRIES, R., TOWNSHEND, J. R. & SOHLBERG, R. 2000. Global land cover classification at 1 km spatial resolution using a classification tree approach. *International journal of remote sensing,* 21**,** 1331-1364.

HANSEN, M. C., POTAPOV, P. V., MOORE, R., HANCHER, M., TURUBANOVA, S. A., TYUKAVINA, A., THAU, D., STEHMAN, S. V., GOETZ, S. J., LOVELAND, T. R., KOMMAREDDY, A., EGOROV, A., CHINI, L., JUSTICE, C. O. & TOWNSHEND, J. R. G. 2013. High-Resolution Global Maps of 21st-Century Forest Cover Change. *Science,* 342**,** 850-853.

HANSEN, M. C., POTAPOV, P. V., MOORE, R., HANCHER, M., TURUBANOVA, S. A., TYUKAVINA, A., THAU, D., STEHMAN, S. V., GOETZ, S. J., LOVELAND, T. R., KOMMAREDDY, A., EGOROV, A., CHINI, L., JUSTICE, C. O. & TOWNSHEND, J. R. G. 2015. *Global Forest Change 2000-2014 Documentation* [Online]. Available: http://earthenginepartners.appspot.com/science-2013-global-forest [Accessed 1 August 2015].

HARPER, G. J., STEININGER, M. K., TUCKER, C. J., JUHN, D. & HAWKINS, F. 2007. Fifty years of deforestation and forest fragmentation in Madagascar. *Environmental Conservation,* 34**,** 325-333.

HARRIS, G. & PIMM, S. L. 2008. Range Size and Extinction Risk in Forest Birds

Amplitud de Rango de Distribución y Riesgo de Extinción en Aves de Bosque. *Conservation Biology,* 22**,** 163-171.

HASTENRATH, S. 1997. Annual cycle of upper air circulation and convective activity over the tropical Americas. *Journal of Geophysical Research: Atmospheres (1984–2012),* 102**,** 4267-4274.

HASTIE, T. & TIBSHIRANI, R. 1986. Generalized additive models. *Statistical science***,** 297-310.

HAVLÍK, P., SCHNEIDER, U. A., SCHMID, E., BÖTTCHER, H., FRITZ, S., SKALSKÝ, R., AOKI, K., DE CARA, S., KINDERMANN, G. & KRAXNER, F. 2011. Global land-use

implications of first and second generation biofuel targets. *Energy Policy,* 39**,** 5690-5702.

HAWKINS, B. A., FIELD, R., CORNELL, H. V., CURRIE, D. J., GUÉGAN, J.-F., KAUFMAN, D. M., KERR, J. T., MITTELBACH, G. G., OBERDORFF, T. & O'BRIEN, E. M. 2003. Energy, water, and broad-scale geographic patterns of species richness. *Ecology,* 84**,** 3105-3117.

HEISTERMANN, M., MÜLLER, C. & RONNEBERGER, K. 2006. Land in sight?: Achievements, deficits and potentials of continental to global scale land-use modeling. *Agriculture, Ecosystems & Environment,* 114**,** 141-158.

HEMP, A. 2002. Ecology of the pteridophytes on the southern slopes of Mt. Kilimanjaro – I. Altitudinal distribution. *Plant Ecology,* 159**,** 211-239.

HENGEVELD, R. 1990. *Dynamic biogeography,* Cambridge University Press, Cambridge, UK.

HIETZ, P. 2010. Fern adaptations to xeric environments. *In:* MEHLTRETER, K., WALKER, L. R. & SHARPE, J. M. (eds.) *Fern ecology.* Cambridge University Press.

HIJMANS, R. J., CAMERON, S. E., PARRA, J. L., JONES, P. G. & JARVIS, A. 2005. Very high resolution interpolated climate surfaces for global land areas. *International journal of climatology,* 25**,** 1965-1978.

HIRSCH, T. 2010. *Global biodiversity outlook 3*, UNEP/Earthprint.

HIRZEL, A. H. & LE LAY, G. 2008. Habitat suitability modelling and niche theory. *Journal of Applied Ecology,* 45**,** 1372-1381.

HOBOHM, C. 2014. *Endemism in vascular plants*, Springer.

HOEKSTRA, J. M., BOUCHER, T. M., RICKETTS, T. H. & ROBERTS, C. 2005. Confronting a biome crisis: global disparities of habitat loss and protection. *Ecology Letters,* 8**,** 23-29.

HOLDRIDGE, L. R. & GRENKE, W. 1971. Forest environments in tropical life zones: a pilot study. *Forest environments in tropical life zones: a pilot study.*

HOLMGREN, M., POORTER, L., SIEPEL, A., BONGERS, F., KOUAMÉ, F. & HAWTHORNE, W. 2004. What explains the distribution of rare and endemic West African plants? *Biodiversity of West African forests: an ecological atlas of woody plant species***,** 73-85.

HOSONUMA, N., HEROLD, M., DE SY, V., DE FRIES, R. S., BROCKHAUS, M., VERCHOT, L., ANGELSEN, A. & ROMIJN, E. 2012. An assessment of deforestation and forest degradation drivers in developing countries. *Environmental Research Letters,* 7**,** 044009.

HUTCHINGS, J. A. & REYNOLDS, J. D. 2004. Marine fish population collapses: consequences for recovery and extinction risk. *BioScience,* 54**,** 297-309.

HUTCHINSON, G. E. 1957. Population Studies - Animal Ecology and Demography - Concluding Remarks. *Cold Spring Harbor Symposia on Quantitative Biology,* 22**,** 415-427.

INPE. 2008. *Metodologia DETER* [Online]. Available: http://www.obt.inpe.br/deter/index.html [Accessed 10 August 2015].

INPE 2014. Projeto Prodes Monitoramento Da Floresta Amazonica Brazileira por Satelite [Online]. Available: www.inpe.br [Accessed 30 August 2015].

IONIA. 2009. *GlobCover land cover map* [Online]. Available: http://ionia1.esrin.esa.int [Accessed 30 December 2012].

IUCN. 2007. *IUCN Habitat Classification Scheme: version 3* [Online]. Available: http://www.iucnredlist.org/technical-documents/classification-schemes/habitats-classification-scheme-ver3.

IUCN 2012a. IUCN Red List categories and criteria: version 3.1. *Prepared by the IUCN Species Survival Commission*.

IUCN. 2012b. *The IUCN Red List of Threatened Species. Version 2012.2* [Online]. Available: http://www.iucnredlist.org [Accessed 10 December 2013].

IUCN. 2014. *Guidelines for Using the IUCN Red List Categories and Criteria. Version 11.* [Online]. The Standards and Petitions Subcommittee. Available: http://www.iucnredlist.org/documents/RedListGuidelines.pdf [Accessed 10 December 2014].

IUCN & UNEP. 2015. *The World Database on Protected Areas (WDPA)* [Online]. UNEP-WCMC, Cambridge. Available: http://www.protectedplanet.net/ [Accessed 6 June 2015].

IVERSON, L. R. & PRASAD, A. M. 1998. Predicting abundance of 80 tree species following climate change in the eastern United States. *Ecological Monographs,* 68**,** 465-485.

JARVIS, A. & MULLIGAN, M. 2011. The climate of cloud forests. *Hydrological Processes,* 25**,** 327-343.

JARVIS, A., REUTER, H. I., NELSON, A. & GUEVARA, E. 2008. Hole-filled SRTM for the globe Version 4. *available from the CGIAR-CSI SRTM 90m Database (http://srtm. csi. cgiar. org)*.

JETZ, W., MCPHERSON, J. M. & GURALNICK, R. P. 2012. Integrating biodiversity distribution knowledge: toward a global map of life. *Trends in Ecology & Evolution,* 27**,** 151-159.

JETZ, W. & RAHBEK, C. 2002. Geographic Range Size and Determinants of Avian Species Richness. *Science,* 297**,** 1548-1551.

JETZ, W., RAHBEK, C. & COLWELL, R. K. 2004. The coincidence of rarity and richness and the potential signature of history in centres of endemism. *Ecology Letters,* 7**,** 1180-1191.

JETZ, W., SEKERCIOGLU, C. H. & WATSON, J. E. 2008. Ecological correlates and conservation implications of overestimating species geographic ranges. *Conservation Biology,* 22**,** 110-119.

JETZ, W., WILCOVE, D. S. & DOBSON, A. P. 2007. Projected impacts of climate and land-use change on the global diversity of birds. *PLoS Biol,* 5**,** e157.

JIMÉNEZ-VALVERDE, A., LOBO, J. M. & HORTAL, J. 2008. Not as good as they seem: the importance of concepts in species distribution modelling. *Diversity and Distributions,* 14**,** 885-890.

JOHNS, R. 1995. Malesia-An Introduction. *Curtis's Botanical Magazine,* 12**,** 52-62.

JONES, M. M., TUOMISTO, H., CLARK, D. B. & OLIVAS, P. 2006. Effects of mesoscale environmental heterogeneity and dispersal limitation on floristic variation in rain forest ferns. *Journal of Ecology,* 94**,** 181-195.

JOPPA, L. N., BUTCHART, S. H. M., HOFFMANN, M., BACHMAN, S., AKÇAKAYA, H. R., MOAT, J., BÖHM, M., HOLLAND, R. A., NEWTON, A., POLIDORO, B. & HUGHES, A. 2015. Impact of alternative metrics on estimates of extent of occurrence for extinction risk assessment. *Conservation Biology***,** DOI: 10.1111/cobi.12591.

JOPPA, L. N., LOARIE, S. R. & PIMM, S. L. 2008. On the protection of “protected areas”. *Proceedings of the National Academy of Sciences,* 105**,** 6673-6678.

JOPPA, L. N., LOARIE, S. R. & PIMM, S. L. 2009. On population growth near protected areas. *PLoS One,* 4**,** e4279.

JOPPA, L. N. & PFAFF, A. 2010. Global protected area impacts. *Proceedings of the Royal Society of London B: Biological Sciences*.

JUFFE-BIGNOLI, D., BURGESS, N., BINGHAM, H., BELLE, E., DE LIMA, M., DEGUIGNET, M., BERTZKY, B., MILAM, A., MARTINEZ-LOPEZ, J. & LEWIS, E. 2014. Protected planet report 2014. *UNEP-WCMC: Cambridge, UK*.

KADMON, R., FARBER, O. & DANIN, A. 2004. Effect of roadside bias on the accuracy of predictive maps produced by bioclimatic models. *Ecological Applications,* 14**,** 401-413.

KALENSKY, Z. 1998. AFRICOVER land cover database and map of Africa. *Canadian journal of remote sensing,* 24**,** 292-297.

KANI, I. 2011. Rare and endemic species: why are they prone to extinction? *Turk J Bot,* 35**,** 411-417.

KAPOS, V. 1989. Effects of isolation on the water status of forest patches in the Brazilian Amazon. *Journal of tropical Ecology,* 5**,** 173-185.

KAPOS, V., WANDELLI, E., CAMARGO, J. & GANADE, G. 1997. Edge-related changes in environment and plant responses due to forest fragmentation in central Amazonia. *Tropical forest remnants: ecology, management, and conservation of fragmented communities. University of Chicago Press, Chicago,* 101**,** 33-44.

KAPPELLE, M. & GÓMEZ-PIGNATARO, L. D. 1992. Distribution and diversity of montane pteridophytes of the Chirripó National Park, Costa Rica. Distribución y diversidad de pteridófitas montanas del Parque Nacional Chirripó, Costa Rica. *Brenesia.***,** 67-77.

KAPTUÉ TCHUENTÉ, A. T., ROUJEAN, J.-L. & DE JONG, S. M. 2011. Comparison and relative quality assessment of the GLC2000, GLOBCOVER, MODIS and ECOCLIMAP land cover data sets at the African continental scale. *International Journal of Applied Earth Observation and Geoinformation,* 13**,** 207-219.

KESSLER, M. 2000. Elevational gradients in species richness and endemism of selected plant groups in the central Bolivian Andes. *Plant Ecology,* 149**,** 181-193.

KESSLER, M. 2002a. The elevational gradient of Andean plant endemism: varying influences of taxon-specific traits and topography at different taxonomic levels. *Journal of Biogeography,* 29**,** 1159-1165.

KESSLER, M. 2002b. Range size and its ecological correlates among the pteridophytes of Carrasco National Park, Bolivia. *Global Ecology and Biogeography,* 11**,** 89-102.

KESSLER, M. 2010. Biogeography of ferns. *In:* MEHLTRETER, K., L.R. WALKER & SHARPE, J. M. (eds.) *Fern ecology.* Cambridge University Press.

KESSLER, M., KLUGE, J., HEMP, A. & OHLEMÜLLER, R. 2011. A global comparative analysis of elevational species richness patterns of ferns. *Global Ecology and Biogeography,* 20**,** 868-880.

KIER, G. & BARTHLOTT, W. 2001. Measuring and mapping endemism and species richness: a new methodological approach and its application on the flora of Africa. *Biodiversity & Conservation,* 10**,** 1513-1529.

KIER, G., KREFT, H., LEE, T. M., JETZ, W., IBISCH, P. L., NOWICKI, C., MUTKE, J. & BARTHLOTT, W. 2009. A global assessment of endemism and species richness across island and mainland regions. *Proceedings of the National Academy of Sciences,* 106**,** 9322-9327.

KIER, G., MUTKE, J., DINERSTEIN, E., RICKETTS, T. H., KÜPER, W., KREFT, H. & BARTHLOTT, W. 2005. Global patterns of plant diversity and floristic knowledge. *Journal of Biogeography,* 32**,** 1107-1116.

KIM, D. H., SEXTON, J. O. & TOWNSHEND, J. R. 2015. Accelerated deforestation in the humid tropics from the 1990s to the 2000s. *Geophysical Research Letters*.

KISSINGER, G., HEROLD, M. & DE SY, V. 2012. Drivers of deforestation and forest degradation: a synthesis report for REDD+ policymakers.

KLUGE, J., KESSLER, M. & DUNN, R. R. 2006. What drives elevational patterns of diversity? A test of geometric constraints, climate and species pool effects for pteridophytes on an elevational gradient in Costa Rica. *Global Ecology and Biogeography,* 15**,** 358-371.

KNAPP, S. & MALLET, J. 2003. Refuting refugia? *Science,* 300**,** 71.

KNOLL, A. H. 1998. The Origin and Early Diversification of Land Plants: A Cladistic Study. *International Journal of Plant Sciences,* 159**,** 172-174.

KORNAS, J. 1993. The significance of historical factors and ecological preference in the distribution of African pteridophytes. *Journal of Biogeography***,** 281-286.

KRAMER-SCHADT, S., NIEDBALLA, J., PILGRIM, J. D., SCHRÖDER, B., LINDENBORN, J., REINFELDER, V., STILLFRIED, M., HECKMANN, I., SCHARF, A. K., AUGERI, D. M., CHEYNE, S. M., HEARN, A. J., ROSS, J., MACDONALD, D. W., MATHAI, J., EATON, J., MARSHALL, A. J., SEMIADI, G., RUSTAM, R., BERNARD, H., ALFRED, R., SAMEJIMA, H., DUCKWORTH, J. W., BREITENMOSER-WUERSTEN, C., BELANT, J. L., HOFER, H. & WILTING, A. 2013. The importance of correcting for sampling bias in MaxEnt species distribution models. *Diversity and Distributions,* 19**,** 1366-1379.

KREFT, H. & JETZ, W. 2007. Global patterns and determinants of vascular plant diversity. *Proceedings of the National Academy of Sciences,* 104**,** 5925-5930.

KREFT, H., JETZ, W., MUTKE, J. & BARTHLOTT, W. 2010. Contrasting environmental and regional effects on global pteridophyte and seed plant diversity. *Ecography,* 33**,** 408-419.

KRUCKEBERG, A. R. & RABINOWITZ, D. 1985. Biological aspects of endemism in higher plants. *Annual Review of Ecology and Systematics,* 16**,** 447-479.

LAMBIN, E. F., ROUNSEVELL, M. D. A. & GEIST, H. J. 2000. Are agricultural land-use models able to predict changes in land-use intensity? *Agriculture, Ecosystems & Environment,* 82**,** 321-331.

LAMOREUX, J. F., MORRISON, J. C., RICKETTS, T. H., OLSON, D. M., DINERSTEIN, E., MCKNIGHT, M. W. & SHUGART, H. H. 2006. Global tests of biodiversity concordance and the importance of endemism. *Nature,* 440**,** 212-214.

LAURANCE, W. F. 1991. Edge effects in tropical forest fragments: application of a model for the design of nature reserves. *Biological conservation,* 57**,** 205-219.

LAURANCE, W. F., CAROLINA USECHE, D., RENDEIRO, J., KALKA, M., BRADSHAW, C. J. A., SLOAN, S. P., LAURANCE, S. G., CAMPBELL, M., ABERNETHY, K., ALVAREZ, P., ARROYO-RODRIGUEZ, V., ASHTON, P., BENITEZ-MALVIDO, J., BLOM, A., BOBO, K. S., CANNON, C. H., CAO, M., CARROLL, R., CHAPMAN, C., COATES, R., CORDS, M., DANIELSEN, F., DE DIJN, B., DINERSTEIN, E., DONNELLY, M. A., EDWARDS, D., EDWARDS, F., FARWIG, N., FASHING, P., FORGET, P.-M., FOSTER, M., GALE, G., HARRIS, D., HARRISON, R., HART, J., KARPANTY, S., JOHN KRESS, W., KRISHNASWAMY, J., LOGSDON, W., LOVETT, J., MAGNUSSON, W., MAISELS, F., MARSHALL, A. R., MCCLEARN, D., MUDAPPA, D., NIELSEN, M. R., PEARSON, R., PITMAN, N., VAN DER PLOEG, J., PLUMPTRE, A., POULSEN, J., QUESADA, M., RAINEY, H., ROBINSON, D., ROETGERS, C., ROVERO, F., SCATENA, F., SCHULZE, C., SHEIL, D., STRUHSAKER, T., TERBORGH, J., THOMAS, D., TIMM, R., NICOLAS URBINA-CARDONA, J., VASUDEVAN, K., JOSEPH WRIGHT, S., CARLOS ARIAS-G, J., ARROYO, L., ASHTON, M., AUZEL, P., BABAASA, D., BABWETEERA, F., BAKER, P., BANKI, O., BASS, M., BILA-ISIA, I., BLAKE, S., BROCKELMAN, W., BROKAW, N., BRUHL, C. A., BUNYAVEJCHEWIN, S., CHAO, J.-T., CHAVE, J., CHELLAM, R., CLARK, C. J., CLAVIJO, J., CONGDON, R., CORLETT, R., DATTARAJA, H. S., DAVE, C., DAVIES, G., DE MELLO BEISIEGEL, B., DE NAZARE PAES DA SILVA, R., DI FIORE, A., DIESMOS, A., DIRZO, R., DORAN-SHEEHY, D., EATON, M., EMMONS, L., ESTRADA, A., et al. 2012. Averting biodiversity collapse in tropical forest protected areas. *Nature,* 489**,** 290-294.

LAURANCE, W. F., DELAMÔNICA, P., LAURANCE, S. G., VASCONCELOS, H. L. & LOVEJOY, T. E. 2000. Conservation: rainforest fragmentation kills big trees. *Nature,* 404**,** 836-836.

LAURANCE, W. F., FERREIRA, L. V., RANKIN-DE MERONA, J. M. & LAURANCE, S. G. 1998. Rain forest fragmentation and the dynamics of Amazonian tree communities. *Ecology,* 79**,** 2032-2040.

LAURANCE, W. F., NASCIMENTO, H. E., LAURANCE, S. G., ANDRADE, A., RIBEIRO, J. E., GIRALDO, J. P., LOVEJOY, T. E., CONDIT, R., CHAVE, J. & HARMS, K. E. 2006. Rapid decay of tree-community composition in Amazonian forest fragments. *Proceedings of the National Academy of Sciences,* 103**,** 19010-19014.

LAURANCE, W. F., PÉREZ-SALICRUP, D., DELAMÔNICA, P., FEARNSIDE, P. M., D'ANGELO, S., JEROZOLINSKI, A., POHL, L. & LOVEJOY, T. E. 2001. Rain forest fragmentation and the structure of Amazonian liana communities. *Ecology,* 82**,** 105-116.

LEAN, J. & WARRILOW, D. 1989. Simulation of the regional climatic impact of Amazon deforestation. *Nature,* 342**,** 411-413.

LEATHWICK, J. R. & AUSTIN, M. P. 2001. Competitive Interactions between Tree Species in New Zealand's Old-Growth Indigenous Forests. *Ecology,* 82**,** 2560-2573.

LEVERINGTON, F., HOCKINGS, M. & COSTA, K. L. 2008. *Management effectiveness evaluation in protected areas: a global study*, World Commission on Protected Areas.

LINDER, H. 1983. The historical phytogeography of the Disinae (Orchidaceae). *Bothalia,* 14**,** 565-570.

LINDER, H. P. 2001. Plant diversity and endemism in sub-Saharan tropical Africa. *Journal of Biogeography,* 28**,** 169-182.

LIU, C., WHITE, M. & NEWELL, G. Measuring the accuracy of species distribution models: a review. Proceedings 18th World IMACs/MODSIM Congress. Cairns, Australia, 2009. Citeseer, 4241-4247.

LOISELLE, B. A., HOWELL, C. A., GRAHAM, C. H., GOERCK, J. M., BROOKS, T., SMITH, K. G. & WILLIAMS, P. H. 2003. Avoiding pitfalls of using species distribution models in conservation planning. *Conservation biology,* 17**,** 1591-1600.

LOMOLINO, M. V. 2000. Ecology's most general, yet protean 1 pattern: the species-area relationship. *Journal of Biogeography,* 27**,** 17-26.

LÓPEZ-PUJOL, J., ZHANG, F.-M. & GE, S. 2006. Plant biodiversity in China: richly varied, endangered, and in need of conservation. *Biodiversity & Conservation,* 15**,** 3983-4026.

LOVEJOY, T. E., BIERREGAARD JR, R., RYLANDS, A., MALCOLM, J., QUINTELA, C., HARPER, L., BROWN JR, K., POWELL, A., POWELL, G. & SCHUBART, H. 1986. Edge and other effects of isolation on Amazon forest fragments.

LOVELAND, T., REED, B., BROWN, J., OHLEN, D., ZHU, Z., YANG, L. & MERCHANT, J. 2000. Development of a global land cover characteristics database and IGBP DISCover from 1 km AVHRR data. *International Journal of Remote Sensing,* 21**,** 1303-1330.

LOVETT, J. & FRIIS, I. 1996. Patterns of endemism in the woody flora of north-east and east Africa. *The biodiversity of African plants.* Springer.

LUOTO, M., VIRKKALA, R. & HEIKKINEN, R. K. 2007. The role of land cover in bioclimatic models depends on spatial resolution. *Global Ecology and Biogeography,* 16**,** 34-42.

LUOTO, M., VIRKKALA, R., HEIKKINEN, R. K. & RAINIO, K. 2004. Predicting bird species richness using remote sensing in Boreal agricultural forest mosaics. *Ecological Applications,* 14**,** 1946-1962.

MACARTHUR, R. H. & WILSON, E. O. 1967. *The theory of island biogeography,* Princeton University Press, New Jersey.

MACE, G. M., MASUNDIRE H., BAILLIE J.E.M. 2005. Biodiversity. Chapter 4 Current state and trends: Findings of the condition and trends working group. Volume 1. *Millennium ecosystem assessment.* Washington, D.C: Island Press.

MAES, D., GILBERT, M., TITEUX, N., GOFFART, P. & DENNIS, R. L. H. 2003. Prediction of butterfly diversity hotspots in Belgium: a comparison of statistically focused and land use-focused models. *Journal of Biogeography,* 30**,** 1907-1920.

MAGURA, T. 2002. Carabids and forest edge: spatial pattern and edge effect. *Forest Ecology and Management,* 157**,** 23-37.

MAHARJAN, S. K., POORTER, L., HOLMGREN, M., BONGERS, F., WIERINGA, J. J. & HAWTHORNE, W. D. 2011. Plant Functional Traits and the Distribution of West African Rain Forest Trees along the Rainfall Gradient. *Biotropica,* 43**,** 552-561.

MAIORANO, L., FALCUCCI, A., GARTON, E. O. & BOITANI, L. 2007. Contribution of the Natura 2000 network to biodiversity conservation in Italy. *Conservation Biology,* 21**,** 1433-1444.

MAJOR, R. E., CHRISTIE, F. J., GOWING, G., CASSIS, G. & REID, C. A. 2003. The effect of habitat configuration on arboreal insects in fragmented woodlands of south-eastern Australia. *Biological Conservation,* 113**,** 35-48.

MALANSON, G. P., WESTMAN, W. E. & YAN, Y.-L. 1992. Realized versus fundamental niche functions in a model of chaparral response to climatic change. *Ecological Modelling,* 64**,** 261-277.

MALCOLM, J. 1997. Biomass and diversity of small mammals in Amazonian forest fragments. *Tropical forest remnants: ecology, management, and conservation of fragmented communities. University of Chicago Press, Chicago***,** 207-221.

MALCOLM, J. R., LOWMAN, M. & NADKARNI, N. 1995. Forest structure and the abundance and diversity of neotropical small mammals. *Forest canopies.***,** 179-197.

MALHI, Y., ADU-BREDU, S., ASARE, R. A., LEWIS, S. L. & MAYAUX, P. 2013. African rainforests: past, present and future. *Philosophical Transactions of the Royal Society B: Biological Sciences,* 368**,** 20120312.

MALHI, Y. & WRIGHT, J. 2004. Spatial patterns and recent trends in the climate of tropical rainforest regions. *Philosophical Transactions of the Royal Society B: Biological Sciences,* 359**,** 311-329.

MALIMBWI, R. & MUGASHA, A. 2002. Reconnaissance Timber Inventory Report for Handeni Hill Forest Reserve in Handeni District, Tanzania for the Tanga Catchment Forest Project. FORCONSULT, Faculty of Forestry and Nature Conservation, Sokoine University of Agriculture, Morogoro, Tanzania.

MARMION, M., PARVIAINEN, M., LUOTO, M., HEIKKINEN, R. K. & THUILLER, W. 2009. Evaluation of consensus methods in predictive species distribution modelling. *Diversity and distributions,* 15**,** 59-69.

MASON, H. L. 1946. The edaphic factor in narrow endemism II. The geographic occurence of plants of highly restricted patterns of distribution. *Madrono,* 8**,** 241-257.

MATEO, R. G., CROAT, T. B., FELICÍSIMO, Á. M. & MUÑOZ, J. 2010. Profile or group discriminative techniques? Generating reliable species distribution models using pseudo-absences and target-group absences from natural history collections. *Diversity and Distributions,* 16**,** 84-94.

MATEO, R. G., FELICISIMO, A. M., POTTIER, J., GUISAN, A. & MUNOZ, J. 2012. Do stacked species distribution models reflect altitudinal diversity patterns? *PLoS One,* 7**,** e32586.

MATLACK, G. R. 1993. Microenvironment variation within and among forest edge sites in the eastern United States. *Biological conservation,* 66**,** 185-194.

MATTHEWS, E. 2001. Understanding the FRA 2000. *Oceania,* 88**,** 129.

MAVRIDIS, L., NATH, N. & MITCHELL, J. 2013. PFClust: a novel parameter free clustering algorithm. *BMC Bioinformatics,* 14.

MAY, R. M., LAWTON, J. H. & STORK, N. E. 1995. Assessing extinction rates. *Extinction rates***,** 1-24.

MAYAUX, P., EVA, H., GALLEGO, J., STRAHLER, A. H., HEROLD, M., AGRAWAL, S., NAUMOV, S., DE MIRANDA, E. E., DI BELLA, C. M. & ORDOYNE, C. 2006. Validation

of the global land cover 2000 map. *Geoscience and Remote Sensing, IEEE Transactions on,* 44**,** 1728-1739.

MAYAUX, P., GOND, V. & BARTHOLOME, E. 2000. A near-real time forest-cover map of Madagascar derived from SPOT-4 VEGETATION data. *International Journal of Remote Sensing,* 21**,** 3139-3144.

MAYAUX, P., HOLMGREN, P., ACHARD, F., EVA, H., STIBIG, H.-J. & BRANTHOMME, A. 2005. Tropical forest cover change in the 1990s and options for future monitoring. *Philosophical Transactions of the Royal Society of London B: Biological Sciences,* 360**,** 373-384.

MCCAIN, C. M. 2009. Global analysis of bird elevational diversity. *Global Ecology and Biogeography,* 18**,** 346-360.

MCCULLAGH, P. & NELDER, J. A. 1989. *Generalized linear models*, CRC press.

MCDONALD, J. H. 2009. *Handbook of biological statistics*, Sparky House Publishing Baltimore, MD.

MCLAUGHLIN, J. F., HELLMANN, J. J., BOGGS, C. L. & EHRLICH, P. R. 2002. Climate change hastens population extinctions. *Proceedings of the National Academy of Sciences,* 99**,** 6070-6074.

MCPHERSON, M. J. & JETZ, W. 2007. Effects of species' ecology on the accuracy of distribution models. *Ecography,* 30**,** 135-151.

MEDAIL, F. & QUEZEL, P. 1997. Hot-spots analysis for conservation of plant biodiversity in the Mediterranean Basin. *Annals of the Missouri Botanical Garden***,** 112-127.

MEHLTRETER, K. 1996. Species richness and geographical distribution of montane pteridophytes of Costa Rica, Central America. *Feddes Repertorium,* 106**,** 563-584.

MEROW, C., SMITH, M. J. & SILANDER, J. A. 2013. A practical guide to MaxEnt for modeling species' distributions: what it does, and why inputs and settings matter. *Ecography,* 36**,** 1058-1069.

MILLENNIUM ECOSYSTEM ASSESSMENT 2005. *Ecosystems and human well-being: biodiversity synthesis*, Island Press.

MITTERMEIER, R. A., MYERS, N., THOMSEN, J. B., DA FONSECA, G. A. & OLIVIERI, S. 1998. Biodiversity hotspots and major tropical wilderness areas: approaches to setting conservation priorities. *Conservation biology,* 12**,** 516-520.

MORAN, C. R. 2004. *A Natural Histoy of Ferns,* Timber Press, London.

MORAN, R., CHURCHILL, S., BALSLEV, H., FORERO, E. & LUTEYN, J. The importance of mountains to pteridophytes, with emphasis on Neotropical montane forests. Biodiversity and conservation of Neotropical montane forests. Proceedings of a symposium, New York Botanical Garden, 21-26 June 1993., 1995. New York Botanical Garden, 359-363.

MORRISON, M. L., B.G. MARCOT & MANNAN, R. W. 2006. *Wildlife-Habitat Relationships: Concepts and Applications.,* Third Edition, Island Press, Washington DC.

MULLIGAN, M. 2006. *Revised original forest cover based on UNEP-WCMC original forest data and GlobCover 2005 data.* [Online]. Available: http://www.policysupport.org/simterra.

MULLIGAN, M. 2009. SimTerra: A consistent global gridded database of environmental properties for spatial modelling. *King's College London, UK*.

MULLIGAN, M. 2010. Modelling the tropics-wide extent and distribution of cloud forest and cloud forest loss, with implications for conservation priority. *Tropical Montane Cloud Forests. Science for Conservation and Management,* 2010**,** 14-38.

MULLIGAN, M. 2011. *Cumulative water balance data. SimTerra : A consistent global gridded database of environmental properties for spatial modelling* [Online]. Available: http://www.policysupport.org/simterra.

MULLIGAN, M. 2014a. *Global fractional deforestation data based on GFC dataset* [Online]. Available: http://blog.policysupport.org/2014/03/what-you-see-depends-on-how-you-see.html.

MULLIGAN, M. 2014b. Global fractional deforestation data based on Terra-i dataset.

MULLIGAN, M. 2014c. *What you see depends on how you see* [Online]. Policy Support Blog. Available: http://blog.policysupport.org/2014/03/what-you-see-depends-on-how-you-see.html.

MULLIGAN, M. 2015a. Trading off agriculture with nature's other benefits, spatially. *In:* ZOLIN, C. A. & RODRIGUES, R. D. A. R. (eds.) *Impact of Climate Change on Water Resources in Agriculture.* CRC Press.

MULLIGAN, M. 2015b. *User guide to the Co$ting Nature Policy support system [version 2.2].* [Online]. Available: https://goo.gl/Grpbnb [Accessed 20 June 2015].

MULLIGAN, M. & BURKE, S. 2005. Global cloud forests and environmental change in a hydrological context. *DFID FRP Project ZF0216, Final Report, Ambiotek*.

MURCIA, C. 1995. Edge effects in fragmented forests: implications for conservation. *Trends Ecology and Evolution,* 10**,** 58-62.

MURRAY-SMITH, C., BRUMMITT, N. A., OLIVEIRA-FILHO, A. T., BACHMAN, S., MOAT, J., LUGHADHA, E. M. N. & LUCAS, E. J. 2009. Plant Diversity Hotspots in the Atlantic Coastal Forests of Brazil

Sitios de Importancia para la Conservación de la Diversidad de Plantas en los Bosques de la Costa del Atlántico de Brasil. *Conservation Biology,* 23**,** 151-163.

MYERS, N., MITTERMEIER, R. A., MITTERMEIER, C. G., DA FONSECA, G. A. & KENT, J. 2000. Biodiversity hotspots for conservation priorities. *Nature,* 403**,** 853-858.

NATHAN, R. 2006. Long-distance dispersal of plants. *Science,* 313**,** 786-8.

NELSON, B. W., FERREIRA, C. A. C., DA SILVA, M. F. & KAWASAKI, M. L. 1990. Endemism centres, refugia and botanical collection density in Brazilian Amazonia. *Nature,* 345**,** 714-716.

NEWBOLD, T. 2010. Applications and limitations of museum data for conservation and ecology, with particular attention to species distribution models. *Progress in Physical Geography,* 34**,** 3-22.

NIC LUGHADHA, E., BAILLIE, J., BARTHLOTT, W., BRUMMITT, N., CHEEK, M., FARJON, A., GOVAERTS, R., HARDWICK, K., HILTON-TAYLOR, C. & MEAGHER, T. 2005. Measuring the fate of plant diversity: towards a foundation for future monitoring and

opportunities for urgent action. *Philosophical Transactions of the Royal Society B: Biological Sciences,* 360**,** 359-372.

NICHOLSON, S. E. 1994. Recent rainfall fluctuations in Africa and their relationship to past conditions over the continent. *The Holocene,* 4**,** 121-131.

NOOTEBOOM, H. P. 1992. Point of view on the species concept. *Taxon,* 41**,** 318-320.

OBANDO-ACUÑA, V. 2002. *Biodiversidad en Costa Rica: Estado del conocimiento y gestión,* Santo Domingo de Heredia, Costa Rica, Instituto Nacional de Biodiversidad, INBio.

OBANDO-ACUÑA, V. 2007. *Biodiversidad de Costa Rica en cifras*, INBio.

ODUM, E. P. 1971. *Fundamentals of ecology,* Philadelphia, Penn., W. B.Sanders Co.

OKE, O. A. & THOMPSON, K. A. 2015. Distribution models for mountain plant species: The value of elevation. *Ecological Modelling,* 301**,** 72-77.

OLDEMAN, L., HAKKELING, R. U. & SOMBROEK, W. G. 1991. *World map of the status of human-induced soil degradation: an explanatory note*, International Soil Reference and Information Centre.

OLSON, D. M., DINERSTEIN, E., WIKRAMANAYAKE, E. D., BURGESS, N. D., POWELL, G. V., UNDERWOOD, E. C., D'AMICO, J. A., ITOUA, I., STRAND, H. E. & MORRISON, J. C. 2001. Terrestrial Ecoregions of the World: A New Map of Life on Earth A new global map of terrestrial ecoregions provides an innovative tool for conserving biodiversity. *BioScience,* 51**,** 933-938.

ORME, C. D. L., DAVIES, R. G., BURGESS, M., EIGENBROD, F., PICKUP, N., OLSON, V. A., WEBSTER, A. J., DING, T.-S., RASMUSSEN, P. C. & RIDGELY, R. S. 2005. Global hotspots of species richness are not congruent with endemism or threat. *Nature,* 436**,** 1016-1019.

ORME, C. D. L., DAVIES, R. G., OLSON, V. A., THOMAS, G. H., DING, T.-S., RASMUSSEN, P. C., RIDGELY, R. S., STATTERSFIELD, A. J., BENNETT, P. M., OWENS, I. P. F., BLACKBURN, T. M. & GASTON, K. J. 2006. Global Patterns of Geographic Range Size in Birds. *PLoS Biol,* 4**,** e208.

PACIENCIA, M. L. B. & PRADO, J. 2005. Effects of Forest Fragmentation on Pteridophyte Diversity in a Tropical Rain Forest in Brazil. *Plant Ecology,* 180**,** 87-104.

PAGE, C. N. 2002. Ecological strategies in fern evolution: a neopteridological overview. *Review of Palaeobotany and Palynology,* 119**,** 1-33.

PARMENTIER, I., MALHI, Y., SENTERRE, B., WHITTAKER, R. J., ALONSO, A., BALINGA, M. P., BAKAYOKO, A., BONGERS, F., CHATELAIN, C. & COMISKEY, J. A. 2007. The odd man out? Might climate explain the lower tree α-diversity of African rain forests relative to Amazonian rain forests? *Journal of Ecology,* 95**,** 1058-1071.

PARRIS, B. S. 1985. Ecological aspects of distribution and speciation in Old World tropical ferns. *Proceedings of the Royal Society of Edinburgh Section B: Biological Sciences,* 86**,** 341-346.

PARVIAINEN, M., MARMION, M., LUOTO, M., THUILLER, W. & HEIKKINEN, R. K. 2009. Using summed individual species models and state-of-the-art modelling techniques to identify threatened plant species hotspots. *Biological Conservation,* 142**,** 2501-2509.

PATON, A. J., BRUMMITT, N., GOVAERTS, R., HARMAN, K., HINCHCLIFFE, S., ALLKIN, B. & LUGHADHA, E. N. 2008. Towards Target 1 of the Global Strategy for Plant Conservation: a working list of all known plant species—progress and prospects. *Taxon,* 57**,** 602-611.

PAUSAS, J. G. & SÁEZ, L. 2000. Pteridophyte richness in the NE Iberian Peninsula: biogeographic patterns. *Plant Ecology,* 148**,** 195-205.

PEARSON, R. G. & DAWSON, T. P. 2003. Predicting the impacts of climate change on the distribution of species: are bioclimate envelope models useful? *Global ecology and biogeography,* 12**,** 361-371.

PEARSON, R. G., DAWSON, T. P. & LIU, C. 2004. Modelling species distributions in Britain: a hierarchical integration of climate and land-cover data. *Ecography,* 27**,** 285-298.

PEARSON, R. G., RAXWORTHY, C. J., NAKAMURA, M. & TOWNSEND PETERSON, A. 2007. Predicting species distributions from small numbers of occurrence records: a test case using cryptic geckos in Madagascar. *Journal of Biogeography,* 34**,** 102-117.

PENA, D. C. J. C., KAMINO, L. H. Y., RODRIGUES, M., MARIANO-NETO, E. & DE SIQUEIRA, M. F. 2014. Assessing the conservation status of species with limited available data and disjunct distribution. *Biological Conservation,* 170**,** 130-136.

PETERSON, A. T. 2011. *Ecological niches and geographic distributions (MPB-49)*, Princeton University Press.

PFEIFER, M., BURGESS, N. D., SWETNAM, R. D., PLATTS, P. J., WILLCOCK, S. & MARCHANT, R. 2012. Protected areas: mixed success in conserving East Africa's evergreen forests. *PLoS One,* 7**,** e39337.

PHILLIPS, O. L., MALHI, Y., HIGUCHI, N., LAURANCE, W. F., NÚNEZ, P. V., VÁSQUEZ, R. M., LAURANCE, S. G., FERREIRA, L. V., STERN, M. & BROWN, S. 1998. Changes in the carbon balance of tropical forests: evidence from long-term plots. *Science,* 282**,** 439-442.

PHILLIPS, S. J., ANDERSON, R. P. & SCHAPIRE, R. E. 2006. Maximum entropy modeling of species geographic distributions. *Ecological modelling,* 190**,** 231-259.

PHILLIPS, S. J., DUDIK, M., ELITH, J., GRAHAM, C. H., LEHMANN, A., LEATHWICK, J. & FERRIER, S. 2009. Sample selection bias and presence-only distribution models: implications for background and pseudo-absence data. *Ecological Applications,* 19**,** 181-197.

PIMENTEL, D. 2001. Agricultural invasions. *Encyclopedia of biodiversity,* 1**,** 71-83.

PIMM, S., RAVEN, P., PETERSON, A., ŞEKERCIOĞLU, Ç. H. & EHRLICH, P. R. 2006. Human impacts on the rates of recent, present, and future bird extinctions. *Proceedings of the National Academy of Sciences of the United States of America,* 103**,** 10941-10946.

PIMM, S. L., AYRES, M., BALMFORD, A., BRANCH, G., BRANDON, K., BROOKS, T., BUSTAMANTE, R., COSTANZA, R., COWLING, R., CURRAN, L. M., DOBSON, A., FARBER, S., DA FONSECA, G. A., GASCON, C., KITCHING, R., MCNEELY, J., LOVEJOY, T., MITTERMEIER, R. A., MYERS, N., PATZ, J. A., RAFFLE, B., RAPPORT, D., RAVEN, P., ROBERTS, C., RODRIGUEZ, J. P., RYLANDS, A. B., TUCKER, C.,

SAFINA, C., SAMPER, C., STIASSNY, M. L., SUPRIATNA, J., WALL, D. H. & WILCOVE, D. 2001. Environment. Can we defy nature's end? *Science,* 293**,** 2207-8.

PIMM, S. L., JENKINS, C. N., ABELL, R., BROOKS, T. M., GITTLEMAN, J. L., JOPPA, L. N., RAVEN, P. H., ROBERTS, C. M. & SEXTON, J. O. 2014. The biodiversity of species and their rates of extinction, distribution, and protection. *Science,* 344.

PIMM, S. L., RUSSELL, G. J., GITTLEMAN, J. L. & BROOKS, T. M. 1995. The future of biodiversity. *Science-AAAS-Weekly Paper Edition,* 269**,** 347-349.

POWELL, G., PALMINTERI, S. & SCHIPPER, J. 2001. Terrestrial Ecoregions-- Talamancan montane forests.

PRESSEY, R. L., HUMPHRIES, C. J., MARGULES, C. R., VANE-WRIGHT, R. I. & WILLIAMS, P. H. 1993. Beyond opportunism: Key principles for systematic reserve selection. *Trends in Ecology & Evolution,* 8**,** 124-128.

PRIMACK, R. B. 2006. *Essentials of conservation biology*, Sinauer Associates Sunderland, MA.

PRYER, K. M., SCHNEIDER, H., SMITH, A. R., CRANFILL, R., WOLF, P. G., HUNT, J. S. & SIPES, S. D. 2001. Horsetails and ferns are a monophyletic group and the closest living relatives to seed plants. *Nature,* 409**,** 618-622.

RABINOWITZ, D. 1981. Seven forms of rarity. *In:* SYNGE, H. (ed.) *The biological aspects of rare plants conservation.* Chichester.

RAES, N., ROOS, M. C., SLIK, J., VAN LOON, E. E. & STEEGE, H. T. 2009. Botanical richness and endemicity patterns of Borneo derived from species distribution models. *Ecography,* 32**,** 180-192.

RAHBEK, C. 1995. The elevational gradient of species richness: a uniform pattern? *Ecography,* 18**,** 200-205.

RAHBEK, C. 2005. The role of spatial scale and the perception of large-scale species-richness patterns. *Ecology letters,* 8**,** 224-239.

RAXWORTHY, C. J., MARTINEZ-MEYER, E., HORNING, N., NUSSBAUM, R. A., SCHNEIDER, G. E., ORTEGA-HUERTA, M. A. & PETERSON, A. T. 2003. Predicting distributions of known and unknown reptile species in Madagascar. *Nature,* 426**,** 837-841.

REDDY, S. & DÁVALOS, L. M. 2003. Geographical sampling bias and its implications for conservation priorities in Africa. *Journal of Biogeography,* 30**,** 1719-1727.

REYMONDIN, L. 2015. *pers.comm, 1 February 2015.*

REYMONDIN, L., JARVIS, A., PÉREZ-URIBE, A., TOUVAL, J., ARGOTE, K., REBETEZ, J., GUEVARA, E. & MULLIGAN, M. 2012. A methodology for near real-time monitoring of habitat change at continental scales using MODIS-NDVI and TRMM. *Submitted Remote Sensing of Environment*.

RICHARDS, J. F. 1990. Land transformation. *In:* TURNER, B. L. (ed.) *The Earth as Transformed by Human Action.* New York

Cambridge University Press.

RICHARDS, P. W. 1973. Africa, the'odd man out'. *Meggers, B, J,, Ayensu, E, S, and Duckworth, W, D ed (s). Tropical forest ecosystems in Africa and South America***,** 21-26.

RIITTERS, K., J. WICKHAM, R. O'NEILL, B. JONES & SMITH., E. 2000. Global-scale patterns of forest fragmentation. *Conservation Ecology,* 4**,** 3.

RIVERS, M. C., BACHMAN, S. P., MEAGHER, T. R., LUGHADHA, E. N. & BRUMMITT, N. A. 2010. Subpopulations, locations and fragmentation: applying IUCN red list criteria to herbarium specimen data. *Biodiversity and conservation,* 19**,** 2071-2085.

RIVERS, M. C., TAYLOR, L., BRUMMITT, N. A., MEAGHER, T. R., ROBERTS, D. L. & LUGHADHA, E. N. 2011. How many herbarium specimens are needed to detect threatened species? *Biological Conservation,* 144**,** 2541-2547.

RODGERS, W. & HOMEWOOD, K. 1982. Species richness and endemism in the Usambara mountain forests, Tanzania. *Biological Journal of the Linnean Society,* 18**,** 197-242.

RODRIGUES, A. S. L., ANDELMAN, S. J., BAKARR, M. I., BOITANI, L., BROOKS, T. M., COWLING, R. M., FISHPOOL, L. D. C., DA FONSECA, G. A. B., GASTON, K. J., HOFFMANN, M., LONG, J. S., MARQUET, P. A., PILGRIM, J. D., PRESSEY, R. L., SCHIPPER, J., SECHREST, W., STUART, S. N., UNDERHILL, L. G., WALLER, R. W., WATTS, M. E. J. & YAN, X. 2004. Effectiveness of the global protected area network in representing species diversity. *Nature,* 428**,** 640-643.

RODRÍGUEZ, J. P., BROTONS, L., BUSTAMANTE, J. & SEOANE, J. 2007. The application of predictive modelling of species distribution to biodiversity conservation. *Diversity and Distributions,* 13**,** 243-251.

RONDININI, C., DI MARCO, M., CHIOZZA, F., SANTULLI, G., BAISERO, D., VISCONTI, P., HOFFMANN, M., SCHIPPER, J., STUART, S. N. & TOGNELLI, M. F. 2011. Global habitat suitability models of terrestrial mammals. *Philosophical Transactions of the Royal Society B: Biological Sciences,* 366**,** 2633-2641.

RONDININI, C., STUART, S. & BOITANI, L. 2005. Habitat Suitability Models and the Shortfall in Conservation Planning for African Vertebrates. *Conservation Biology,* 19**,** 1488-1497.

RONDININI, C. & VISCONTI, P. 2015. Scenarios of large mammal loss in Europe for the 21st century. *Conservation Biology,* 29**,** 1028-1036.

RONDININI, C., WILSON, K. A., BOITANI, L., GRANTHAM, H. & POSSINGHAM, H. P. 2006. Tradeoffs of different types of species occurrence data for use in systematic conservation planning. *Ecology Letters,* 9**,** 1136-1145.

ROSEGRANT, M. W., PAISNER, M. S., MEIJER, S. & WITCOVER, J. 2001. *2020 global food outlook: trends, alternatives, and choices*, Intl Food Policy Res Inst.

ROSENZWEIG, L. M. 1995. *Species Diversity in Space and Time,* Cambridge University Press, Cambridge, UK.

ROSENZWEIG, M. L. & ZIV, Y. 1999. The echo pattern of species diversity: pattern and processes. *Ecography,* 22**,** 614-628.

ROTHWELL, G. 1999. Fossils and ferns in the resolution of land plant phylogeny. *The Botanical Review,* 65**,** 188-218.

RUDEL, T. K. 2013. The national determinants of deforestation in sub-Saharan Africa. *Philosophical Transactions of the Royal Society of London B: Biological Sciences,* 368.

SACHS, J. D., BAILLIE, J. E., SUTHERLAND, W. J., ARMSWORTH, P. R., ASH, N., BEDDINGTON, J., BLACKBURN, T. M., COLLEN, B., GARDINER, B. & GASTON, K. J. 2009. Biodiversity conservation and the millennium development goals. *Science,* 325**,** 1502-1503.

SADER, S. A. & JOYCE, A. T. 1988. Deforestation rates and trends in Costa Rica, 1940 to 1983. *Biotropica,* 20**,** 11-19.

SALA, O. E., STUART CHAPIN , F., III, ARMESTO, J. J., BERLOW, E., BLOOMFIELD, J., DIRZO, R., HUBER-SANWALD, E., HUENNEKE, L. F., JACKSON, R. B., KINZIG, A., LEEMANS, R., LODGE, D. M., MOONEY, H. A., OESTERHELD, M. N., POFF, N. L., SYKES, M. T., WALKER, B. H., WALKER, M. & WALL, D. H. 2000. Global Biodiversity Scenarios for the Year 2100. *Science,* 287**,** 1770-1774.

SANBI. 2015. *Red List of South African Plants* [Online]. Available: http://redlist.sanbi.org/ [Accessed June 2015].

SÁNCHEZ-AZOFEIFA, G. A., HARRISS, R. C. & SKOLE, D. L. 2001. Deforestation in Costa Rica: A quantitative analysis using remote sensing imagery1. *Biotropica,* 33**,** 378-384.

SÁNCHEZ-AZOFEIFA, G. A., QUESADA-MATEO, C., GONZALEZ-QUESADA, P., DAYANANDAN, S. & BAWA, K. S. 1999. Protected areas and conservation of biodiversity in the tropics. *Conservation Biology,* 13**,** 407-411.

SAUNDERS, D. A., HOBBS, R. J. & MARGULES, C. R. 1991. Biological consequences of ecosystem fragmentation: a review. *Conservation biology,* 5**,** 18-32.

SCHELPE, E. 1983. Aspects of the phytogeography of African Pteridophyta. *Bothalia,* 14**,** 417-419.

SCHMITT, C. B., BELOKUROV, A., BESANÇON, C., BOISROBERT, L., BURGESS, N. D., CAMPBELL, A., COAD, L., FISH, L., GLIDDON, D., HUMPHRIES, K., KAPOS, V., LOUCKS, C., LYSENKO, I., MILES, L., MILLS, C., MINNEMEYER, S., PISTORIUS, T., RAVILIOUS, C., STEININGER, M. & WINKEL, G. 2009. *Global Ecological Forest Classification and Forest Protected Area Gap Analysis. Analyses and recommendations in view of the 10% target for forest protection under the Convention on Biological Diversity (CBD),* 2nd revised edition, Freiburg University Press, Freiburg, Germany.

SCHNEIDER, H. 2013. *pers.comm, 7 March 2013.*

SCHNEIDER, H., SCHUETTPELZ, E., PRYER, K. M., CRANFILL, R., MAGALLON, S. & LUPIA, R. 2004. Ferns diversified in the shadow of angiosperms. *Nature,* 428**,** 553-557.

SCOTT, J. M., HEGLUND, P. J., MORRISON, M. L., HAUFLER, J. B., RAPHAEL, M. G., WALL, W. A. & SAMSON, F. B. 2002. *Predicting Species Occurrences: Issues of Accuracy and Scale, Part 2: Temporal and Spatial Scales,* Island Press, Washington DC.

SEGURADO, P. & ARAÚJO, M. B. 2004. An evaluation of methods for modelling species distributions. *Journal of Biogeography,* 31**,** 1555-1568.

SÉRGIO, C., FIGUEIRA, R., DRAPER, D., MENEZES, R. & SOUSA, A. J. 2007. Modelling bryophyte distribution based on ecological information for extent of occurrence assessment. *Biological Conservation,* 135**,** 341-351.

SHAW, P., MUSINA, J. & GICHUKI, P. 2003. Estimating change in the geographical range and population size of Hinde's Babbler Turdoides hindei. *Bird Conservation International,* 13**,** 1-12.

SHI, H., SINGH, A., KANT, S., ZHU, Z. & WALLER, E. 2005. Integrating habitat status, human population pressure, and protection status into biodiversity conservation priority setting. *Conservation biology,* 19**,** 1273-1285.

SINAC. 2009. *National System of Conservation Areas (Costa Rica) report* [Online]. Available: http://www.sinac.go.cr/ [Accessed 9 September 2013].

SIZER, N. C., TANNER, E. V. & FERRAZ, I. K. 2000. Edge effects on litterfall mass and nutrient concentrations in forest fragments in central Amazonia. *Journal of Tropical Ecology,* 16**,** 853-863.

SMITH, A., BARCELONA, J., TSUTSUMI, C., KATO, M., MAKGOMOL, K., SHEFFIELD, E., DE LA SOTA, E., MARTÍNEZ, O., ZENKTELER, E. & KWANA, H. 2005. Floristics in the 21st century: balancing user-needs and phylogenetic information. *Fern Gazette,* 17**,** 105.

SMITH, A. B. 2010. Caution with curves: Caveats for using the species–area relationship in conservation. *Biological Conservation,* 143**,** 555-564.

SMITH, A. R. 1972. Comparison of Fern and Flowering Plant Distributions with Some Evolutionary Interpretations for Ferns. *Biotropica,* 4**,** 4-9.

SOARES-FILHO, B. S., NEPSTAD, D. C., CURRAN, L. M., CERQUEIRA, G. C., GARCIA, R. A., RAMOS, C. A., VOLL, E., MCDONALD, A., LEFEBVRE, P. & SCHLESINGER, P. 2006. Modelling conservation in the Amazon basin. *Nature,* 440**,** 520-523.

SOARES-FILHO, B. S., RODRIGUES, H. & COSTA, W. L. 2009. *Modeling environmental dynamics with Dinamica EGO* [Online]. Available: http://csr.ufmg.br/dinamica/.

SOBERON, J. 2005. Interpretation of models of fundamental ecological niches and species' distributional areas.

SOBERÓN, J. 2007. Grinnellian and Eltonian niches and geographic distributions of species. *Ecology letters,* 10**,** 1115-1123.

SPANGENBERG, J. H., BONDEAU, A., CARTER, T. R., FRONZEK, S., JAEGER, J., JYLHÄ, K., KÜHN, I., OMANN, I., PAUL, A. & REGINSTER, I. 2012. Scenarios for investigating risks to biodiversity. *Global Ecology and Biogeography,* 21**,** 5-18.

SPRACKLEN, D. V., ARNOLD, S. R. & TAYLOR, C. M. 2012. Observations of increased tropical rainfall preceded by air passage over forests. *Nature,* 489**,** 282-285.

STANTON, J. C., PEARSON, R. G., HORNING, N., ERSTS, P. & REŞIT AKÇAKAYA, H. 2012. Combining static and dynamic variables in species distribution models under climate change. *Methods in Ecology and Evolution,* 3**,** 349-357.

STATTERSFIELD, A. J., CROSBY, M. J., LONG, A. J. & WEGE, D. C. 2005. Endemic bird areas of the world: priorities for biodiversity conservation.

STEINMEIER, C. 2013. *CORINE Land Cover 2000/2006* [Online]. Switzerland. Available: http://www.wsl.ch/dienstleistungen/publikationen/pdf/12359.pdf [Accessed 1 August 2015].

STEPHENSON, N. L. 1990. Climatic Control of Vegetation Distribution: The Role of the Water Balance. *The American Naturalist,* 135**,** 649-670.

STEPHENSON, N. L. 1998. Actual evapotranspiration and deficit: biologically meaningful correlates of vegetation distribution across spatial scales. *Journal of Biogeography,* 25**,** 855-870.

STEPHENSON, N. L. 2000. Climate, Vegetation, and Considerations for Restoration. *In:* J. E. KEELEY, M. B.-K., AND C. J. FOTHERINGHAM (ed.) *2nd Interface Between Ecology and Land Development in California. U.S. Geological Survey Open-File Report 00-62.*

STEVENS, G. C. 1992. The elevational gradient in altitudinal range: an extension of Rapoport's latitudinal rule to altitude. *American naturalist***,** 893-911.

STOMS, D. M., DAVIS, F. W. & COGAN, C. B. 1992. Sensitivity of wildlife habitat models to uncertainties in GIS data. *Photogrammetric engineering and remote sensing,* 58**,** 843-850.

STORK, N. E. 1993. How many species are there? *Biodiversity & Conservation,* 2**,** 215-232.

STRAHLER, A. H., BOSCHETTI, L., FOODY, G. M., FRIEDL, M. A., HANSEN, M. C., HEROLD, M., MAYAUX, P., MORISETTE, J. T., STEHMAN, S. V. & WOODCOCK, C. E. 2006. Global land cover validation: Recommendations for evaluation and accuracy assessment of global land cover maps. *European Communities, Luxembourg,* 51.

SWAINE, M. D. 1996. Rainfall and Soil Fertility as Factors Limiting Forest Species Distributions in Ghana. *Journal of Ecology,* 84**,** 419-428.

SYFERT, M. M., JOPPA, L., SMITH, M. J., COOMES, D. A., BACHMAN, S. P. & BRUMMITT, N. A. 2014. Using species distribution models to inform IUCN Red List assessments. *Biological Conservation,* 177**,** 174-184.

SYFERT, M. M., SMITH, M. J. & COOMES, D. A. 2013. The Effects of Sampling Bias and Model Complexity on the Predictive Performance of MaxEnt Species Distribution Models. *PLoS ONE,* 8**,** e55158.

THAPA, N. 2002. *Pteridophytes of Nepal.* , Bulletin of Department of Plant Resources, no. 19, Department of Plant Resources, Nepal.

THOMAS, C. D., CAMERON, A., GREEN, R. E., BAKKENES, M., BEAUMONT, L. J., COLLINGHAM, Y. C., ERASMUS, B. F., DE SIQUEIRA, M. F., GRAINGER, A. & HANNAH, L. 2004. Extinction risk from climate change. *Nature,* 427**,** 145-148.

THORN, J. S., NIJMAN, V., SMITH, D. & NEKARIS, K. 2009. Ecological niche modelling as a technique for assessing threats and setting conservation priorities for Asian slow lorises (Primates: Nycticebus). *Diversity and Distributions,* 15**,** 289-298.

THUILLER, W. 2004. Patterns and uncertainties of species' range shifts under climate change. *Global Change Biology,* 10**,** 2020-2027.

THUILLER, W., ALBERT, C., ARAÚJO, M. B., BERRY, P. M., CABEZA, M., GUISAN, A., HICKLER, T., MIDGLEY, G. F., PATERSON, J. & SCHURR, F. M. 2008. Predicting global change impacts on plant species' distributions: future challenges. *Perspectives in Plant Ecology, Evolution and Systematics,* 9**,** 137-152.

THUILLER, W., ARAÚJO, M. B. & LAVOREL, S. 2004. Do we need land-cover data to model species distributions in Europe? *Journal of Biogeography,* 31**,** 353-361.

TRYON, R. 1970. Development and evolution of fern floras of oceanic islands. *Biotropica***,** 76-84.

TRYON, R. 1972. Endemic areas and geographic speciation in tropical American ferns. *Biotropica***,** 121-131.

TRYON, R. 1986. The biogeography of species, with special reference to ferns. *The Botanical Review,* 52**,** 117-156.

TRYON, R. M. & CONANT, D. S. 1975. The ferns of Brazilian amazonia. *Acta Amazonica (Brazil)*.

TRYON, R. M. & TRYON, A. F. 2012. *Ferns and allied plants: with special reference to tropical America*, Springer Science & Business Media.

TUOMISTO, H., POULSEN, A. D., RUOKOLAINEN, K., MORAN, R. C., QUINTANA, C., CELI, J. & CAÑAS, G. 2003. Linking Floristic Patterns with soil heterogeneity and satellite imagery in Ecuadorian Amazonia. *Ecological Applications,* 13**,** 352-371.

UCHIDA, H. & NELSON, A. 2009. Agglomeration Index: Towards a New Measure of Urban Concentration. Background paper for the World Bank's World Development Report.

UNEP-WCMC 1997. Tropical Montane Cloud Forests: An Urgent Priority for Conservation, WCMC Biodiversity Bulletin 2.

UNEP-WCMC. 1998. *Global Generalised 'Original' Forest dataset (V 1.0)* [Online]. Available: http://www.unep-wcmc.org/resources-and-data/generalised-original-and-current-forest.

UNEP. 2002. *Strategic Plan for the Convention on Biological Diversity. COP Decision VI/26* [Online]. Available: http://www.cbd.int/decision/cop/?id=7200 [Accessed 12 December 2012].

UNEP. 2005. *Millennium Ecosystem Assessment* [Online]. Available: http://www.maweb.org [Accessed 12 December 2012].

UNEP. 2006. *Framework for monitoring implementation of the achievement of the 2010 target and integration of targets into the thematic programmes of work. COP Decision VIII/15* [Online]. Available: http://www.cbd.int/decision/cop/?id=11029 [Accessed 12 December 2012].

UNEP. 2010. *The Strategic Plan for Biodiversity 2011-2020 and the Aichi Biodiversity Targets. COP Decision X/2* [Online]. Available: http://www.cbd.int/decision/cop/?id=12268 [Accessed 12 December 2012].

USGS-EROS. 1996. *GTOPO30: Global 30-Arc-Second Elevation Data Set*. U.S. Geological Survey.

USGS-NASA. 2000. *Global Land Cover Characteristics Datasets* [Online]. Distributed Active Archive Center. Available: http://edcdaac.usgs.gov/glcc/globdoc2-0.htm [Accessed 25 December 2012].

USHER, M. B. 1986. Wildlife conservation evaluation: attributes, criteria and values. *Wildlife conservation evaluation.* Springer.

VAN GEMERDEN, B. S., OLFF, H., PARREN, M. P. E. & BONGERS, F. 2003. The pristine rain forest? Remnants of historical human impacts on current tree species composition and diversity. *Journal of Biogeography,* 30**,** 1381-1390.

VAN VUUREN, D. P., SALA, O. E. & PEREIRA, H. M. 2006. The future of vascular plant diversity under four global scenarios. *Ecology and Society,* 11**,** 25.

VANDERWAL, J., SHOO, L. P., GRAHAM, C. & WILLIAMS, S. E. 2009. Selecting pseudo-absence data for presence-only distribution modeling: How far should you stray from what you know? *Ecological Modelling,* 220**,** 589-594.

VENIER, L. A., PEARCE, J., MCKEE, J. E., MCKENNEY, D. W. & NIEMI, G. J. 2004. Climate and satellite-derived land cover for predicting breeding bird distribution in the Great Lakes Basin. *Journal of Biogeography,* 31**,** 315-331.

VERBURG, P., SCHOT, P., DIJST, M. & VELDKAMP, A. 2004. Land use change modelling: current practice and research priorities. *GeoJournal,* 61**,** 309-324.

VERBURG, P. H., NEUMANN, K. & NOL, L. 2011. Challenges in using land use and land cover data for global change studies. *Global Change Biology,* 17**,** 974-989.

VETAAS, O. R. 1993. Spatial and temporal vegetation changes along a moisture gradient in northeastern Sudan. *Biotropica***,** 164-175.

VETAAS, O. R. 2002. Realized and potential climate niches: a comparison of four Rhododendron tree species. *Journal of Biogeography,* 29**,** 545-554.

VISCONTI, P., BAKKENES, M., BAISERO, D., BROOKS, T., BUTCHART, S. H. M., JOPPA, L., ALKEMADE, R., DI MARCO, M., SANTINI, L., HOFFMANN, M., MAIORANO, L., PRESSEY, R. L., ARPONEN, A., BOITANI, L., RESIDE, A. E., VAN VUUREN, D. P. & RONDININI, C. 2015. Projecting Global Biodiversity Indicators under Future Development Scenarios. *Conservation Letters***,** http://dx.doi.org/10.1111/conl.12159.

VISCONTI, P., PRESSEY, R. L., GIORGINI, D., MAIORANO, L., BAKKENES, M., BOITANI, L., ALKEMADE, R., FALCUCCI, A., CHIOZZA, F. & RONDININI, C. 2011. Future hotspots of terrestrial mammal loss. *Philosophical Transactions of the Royal Society of London B: Biological Sciences,* 366**,** 2693-2702.

VISSER, H. & DE NIJS, T. 2006. The Map Comparison Kit *Environmental Modeling & Software,* 21**,** 346-358.

WALTHER, B. A., COTGREAVE, P., PRICE, R. D., GREGORY, R. D. & CLAYTON, D. H. 1995. Sampling effort and parasite species richness. *Parasitol Today,* 11**,** 306-10.

WALTHER, B. A. & MARTIN, J.-L. 2001. Species richness estimation of bird communities: how to control for sampling effort? *Ibis,* 143**,** 413-419.

WATKINS, J. E., CARDELÚS, C., COLWELL, R. K. & MORAN, R. C. 2006. Species richness and distribution of ferns along an elevational gradient in Costa Rica. *American Journal of Botany,* 93**,** 73-83.

WHITE, F. 1983. The vegetation of Africa, a descriptive memoir to accompany the UNESCO/AETFAT/UNSO vegetation map of Africa (3 Plates, Northwestern Africa, Northeastern Africa, and Southern Africa, 1: 5,000,000). Unesco, Paris.

WHITTAKER, R. J. & FERNÁNDEZ-PALACIOS, J. M. 2007. *Island biogeography: ecology, evolution, and conservation*, Oxford University Press.

WILLIAMS, C. B. 1943. Area and number of species. *Nature,* 152**,** 264-267.

WILLIAMS, M. 2000. Dark ages and dark areas: global deforestation in the deep past. *Journal of Historical Geography,* 26**,** 28-46.

WILLIAMS, M. 2002. *Deforesting the earth: from prehistory to global crisis*, University of Chicago Press.

WILLIAMS, P. H., MARGULES, C. R. & HILBERT, D. W. 2002. Data requirements and data sources for biodiversity priority area selection. *Journal of Biosciences,* 27**,** 327-338.

WILLIG, M. R., KAUFMAN, D. M. & STEVENS, R. D. 2003. Latitudinal gradients of biodiversity: pattern, process, scale, and synthesis. *Annual review of ecology, evolution, and systematics*, 273-309.

WILLIG, M. R. & LYONS, S. K. 1998. An analytical model of latitudinal gradients of species richness with an empirical test for marsupials and bats in the New World. *Oikos*, 93-98.

WILLIS, F., MOAT, J. & PATON, A. 2003. Defining a role for herbarium data in Red List assessments: a case study of Plectranthus from eastern and southern tropical Africa. *Biodiversity & Conservation,* 12, 1537-1552.

WILSON, K. A., MCBRIDE, M. F., BODE, M. & POSSINGHAM, H. P. 2006. Prioritizing global conservation efforts. *Nature,* 440, 337-340.

WISZ, M. S., HIJMANS, R. J., LI, J., PETERSON, A. T., GRAHAM, C. H., GUISAN, A. & GROUP, N. P. S. D. W. 2008. Effects of sample size on the performance of species distribution models. *Diversity and Distributions,* 14, 763-773.

WOODWARD, F. I. & WILLIAMS, B. G. 1987. Climate and plant distribution at global and local scales. *Vegetatio,* 69, 189-197.

WWF. 2015. *Global 200* [Online]. Available: https://www.worldwildlife.org/publications/global-200 [Accessed 20 March 2015].

YANG, W., MA, K. & KREFT, H. 2013. Geographical sampling bias in a large distributional database and its effects on species richness–environment models. *Journal of Biogeography,* 40, 1415-1426.

YATES, C. J., MCNEILL, A., ELITH, J. & MIDGLEY, G. F. 2010. Assessing the impacts of climate change and land transformation on Banksia in the South West Australian Floristic Region. *Diversity and Distributions,* 16, 187-201.

YODER, A. D. & NOWAK, M. D. 2006. Has Vicariance or Dispersal Been the Predominant Biogeographic Force in Madagascar? Only Time Will Tell. *Annual Review of Ecology, Evolution, and Systematics,* 37, 405-431.

ZADEH, L. 1965. Fuzzy sets. *Information and Control,* 8, 338-353.

APPENDIX

A1. Summary of the five criteria (A-E) used to evaluate if a taxon belongs in an IUCN Red List Threatened Category (IUCN, 2012a)

A. Population size reduction. Population reduction (measured over the longer of 10 years or 3 generations) based on any of A1 to A4

	Critically Endangered	Endangered	Vulnerable
A1	≥ 90%	≥ 70%	≥ 50%
A2, A3 & A4	≥ 80%	≥ 50%	≥ 30%

A1 Population reduction observed, estimated, inferred, or suspected in the past where the causes of the reduction are clearly reversible AND understood AND have ceased.

A2 Population reduction observed, estimated, inferred, or suspected in the past where the causes of reduction may not have ceased OR may not be understood OR may not be reversible.

A3 Population reduction projected, inferred or suspected to be met in the future (up to a maximum of 100 years) *[(a) cannot be used for A3].*

A4 An observed, estimated, inferred, projected or suspected population reduction where the time period must include both the past and the future (up to a max. of 100 years in future), and where the causes of reduction may not have ceased OR may not be understood OR may not be reversible.

based on any of the following:

(a) direct observation *[except A3]*
(b) an index of abundance appropriate to the taxon
(c) a decline in area of occupancy (AOO), extent of occurrence (EOO) and/or habitat quality
(d) actual or potential levels of exploitation
(e) effects of introduced taxa, hybridization, pathogens, pollutants, competitors or parasites.

B. Geographic range in the form of either B1 (extent of occurrence) AND/OR B2 (area of occupancy)

	Critically Endangered	Endangered	Vulnerable
B1. Extent of occurrence (EOO)	< 100 km²	< 5,000 km²	< 20,000 km²
B2. Area of occupancy (AOO)	< 10 km²	< 500 km²	< 2,000 km²
AND at least 2 of the following 3 conditions:			
(a) Severely fragmented OR Number of locations	= 1	≤ 5	≤ 10
(b) Continuing decline observed, estimated, inferred or projected in any of: (i) extent of occurrence; (ii) area of occupancy; (iii) area, extent and/or quality of habitat; (iv) number of locations or subpopulations; (v) number of mature individuals			
(c) Extreme fluctuations in any of: (i) extent of occurrence; (ii) area of occupancy; (iii) number of locations or subpopulations; (iv) number of mature individuals			

C. Small population size and decline

	Critically Endangered	Endangered	Vulnerable
Number of mature individuals	< 250	< 2,500	< 10,000
AND at least one of C1 or C2			
C1. An observed, estimated or projected continuing decline of at least (up to a max. of 100 years in future):	25% in 3 years or 1 generation (whichever is longer)	20% in 5 years or 2 generations (whichever is longer)	10% in 10 years or 3 generations (whichever is longer)
C2. An observed, estimated, projected or inferred continuing decline AND at least 1 of the following 3 conditions:			
(a) (i) Number of mature individuals in each subpopulation	≤ 50	≤ 250	≤ 1,000
(ii) % of mature individuals in one subpopulation =	90–100%	95–100%	100%
(b) Extreme fluctuations in the number of mature individuals			

D. Very small or restricted population

	Critically Endangered	Endangered	Vulnerable
D. Number of mature individuals	< 50	< 250	D1. < 1,000
D2. *Only applies to the VU category* Restricted area of occupancy or number of locations with a plausible future threat that could drive the taxon to CR or EX in a very short time.	-	-	D2. typically: AOO < 20 km² or number of locations ≤ 5

E. Quantitative Analysis

	Critically Endangered	Endangered	Vulnerable
Indicating the probability of extinction in the wild to be:	≥ 50% in 10 years or 3 generations, whichever is longer (100 years max.)	≥ 20% in 20 years or 5 generations, whichever is longer (100 years max.)	≥ 10% in 100 years

A2. Description of the nine IUCN Red List Categories (Not Evaluated, Data Deficient, Least Concern, Near Threatened, Vulnerable, Endangered, Critically Endangered, Extinct in the Wild, Extinct) (IUCN, 2012a)

IUCN Category	Description
EXTINCT (EX)	A taxon is Extinct when there is no reasonable doubt that the last individual has died. A taxon is presumed Extinct when exhaustive surveys in known and/or expected habitat, at appropriate times (diurnal, seasonal, annual), throughout its historic range have failed to record an individual. Surveys should be over a time frame appropriate to the taxon's life cycle and life form.
EXTINCT IN THE WILD (EW)	A taxon is Extinct in the Wild when it is known only to survive in cultivation, in captivity or as a naturalized population (or populations) well outside the past range. A taxon is presumed Extinct in the Wild when exhaustive surveys in known and/or expected habitat, at appropriate times (diurnal, seasonal, annual), throughout its historic range have failed to record an individual. Surveys should be over a time frame appropriate to the taxon's life cycle and life form.
CRITICALLY ENDANGERED (CR)	A taxon is Critically Endangered when the best available evidence indicates that it meets any of the criteria A to E for Critically Endangered, and it is therefore considered to be facing an extremely high risk of extinction in the wild.
ENDANGERED (EN)	A taxon is Endangered when the best available evidence indicates that it meets any of the criteria A to E for Endangered, and it is therefore considered to be facing a very high risk of extinction in the wild.
VULNERABLE (VU)	A taxon is Vulnerable when the best available evidence indicates that it meets any of the criteria A to E for Vulnerable, and it is therefore considered to be facing a high risk of extinction in the wild.
NEAR THREATENED (NT)	A taxon is Near Threatened when it has been evaluated against the criteria but does not qualify for Critically Endangered, Endangered or Vulnerable now, but is close to qualifying for or is likely to qualify for a threatened category in the near future.
LEAST CONCERN (LC)	A taxon is Least Concern when it has been evaluated against the criteria and does not qualify for Critically Endangered, Endangered, Vulnerable or Near Threatened. Widespread and abundant taxa are included in this category.
DATA DEFICIENT (DD)	A taxon is Data Deficient when there is inadequate information to make a direct, or indirect, assessment of its risk of extinction based on its distribution and/or population status. A taxon in this category may be well studied, and its biology well known, but appropriate data on abundance and/or distribution are lacking. Data Deficient is therefore not a category of threat. Listing of taxa in this category indicates that more information is required and acknowledges the possibility that future research will show that threatened classification is appropriate. It is important to make positive use of whatever data are available.
NOT EVALUATED (NE)	A taxon is Not Evaluated when it is has not yet been evaluated against the criteria.

A3. IUCN Habitat Classification Scheme Categories (version 3) (IUCN, 2007)

IUCN Habitat type Categories
1. Forest
2. Savanna
3. Shrubland
4. Grassland
5. Wetlands (inland)
6. Rocky Areas
7. Caves and Subterranean Habitats (non-aquatic)
8. Desert
9. Marine Neritic
10. Marine Oceanic
11. Marine Deep Ocean Floor
12. Marine Intertidal
13. Marine Coastal/Supratidal
14. Artificial - Terrestrial
15. Artificial - Aquatic
16. Introduced Vegetation
17.Other
18. Unknown

A4. Description of the IUCN Forest Habitat category and subcategories (IUCN, 2007)

IUCN Habitat Classification category/subcategories	Description
1. Forest	Forest consists of a continuous stand of trees and includes both forested areas (generally with a closed canopy) and wooded areas (canopy more open).
1.1 Boreal Forest	Distributed across the high latitudes of the northern hemisphere (occurring between 50 and 60° N) in a broad belt across Eurasia and North America. Trees are predominantly coniferous (pine, fir and spruce), though a few deciduous genera are nearly ubiquitous in their distribution and are locally common.
1.2 Subarctic Forest	Included for completeness sake - probably little forest occurs at these high latitudes.
1.3 Subantarctic Forest	Stunted forest on subantarctic islands.
1.4 Temperate Forest	Distributed in the temperate regions (under the influence of moist continental climates) of North and South America (primarily Chile), Europe, Asia (China/Korea/Japan) and Australia/New Zealand. Includes forest types described as coniferous, broadleaved evergreen, broadleaved deciduous, and mixed; also riverine and alluvial. The deciduous trees shed their leaves in the winter season. In the northern hemisphere, the coniferous (or needleleaf evergreen) component increases towards the north where the mixed forest transitions to Boreal Forest.
1.5 Subtropical/Tropical Dry Forest	Distributed in the subtropical/tropical regions of the Neotropics, Africa and Indo-Malesia. Typically forests that experience a dry season of several months.
1.6 Subtropical/Tropical Moist Lowland Forest	Distributed in the subtropical/tropical regions of the Neotropics, Africa and Indo-Malesia, generally below c.1,200 m (but varying with geography and topography).
1.7 Subtropical/Tropical Mangrove Forest Vegetation Above High Tide Level	Distributed in the subtropics and tropics, growing in sheltered estuaries and along coastlines in brackish or salt water

1.8 Subtropical/Tropical Swamp Forest	Distributed in the subtropics and tropics. Typically flooded for at least part of the year and dependent on this flooding for its existence.
1.9 Subtropical/Tropical Moist Montane Forest	Distributed in the subtropical/tropical regions of the Neotropics, Africa and Indo-Malesia, generally above c.1,200 m (but varying with geography and topography).

A5 Global Land Cover Characteristics (GLCC) classes (USGS-NASA, 2000)

GLCC CLASSES			
Value	**Description**	**Value**	**Description**
1	Urban	**50**	Sand Desert
2	Low Sparse Grassland	**51**	Semi Desert Shrubs
3	Coniferous Forest	**52**	Semi Desert Sage
4	Deciduous Conifer Forest	**53**	Barren Tundra
5	Deciduous Broadleaf Forest	**54**	Cool Southern Hemisphere Mixed Forests
6	Evergreen Broadleaf Forests	**55**	Cool Fields and Woods
7	Tall Grasses and Shrubs	**56**	Forest and Field
8	Bare Desert	**57**	Cool Forest and Field
9	Upland Tundra	**58**	Fields and Woody Savanna
10	Irrigated Grassland	**59**	Succulent and Thorn Scrub
11	Semi Desert	**60**	Small Leaf Mixed Woods
12	Glacier Ice	**61**	Deciduous and Mixed Boreal Forest
13	Wooded Wet Swamp	**62**	Narrow Conifers
14	Inland Water	**63**	Wooded Tundra
15	Sea Water	**64**	Heath Scrub
16	Shrub Evergreen	**65**	Coastal Wetland, NW
17	Shrub Deciduous	**66**	Coastal Wetland, NE
18	Mixed Forest and Field	**67**	Coastal Wetland, SE
19	Evergreen Forest and Fields	**68**	Coastal Wetland, SW
20	Cool Rain Forest	**69**	Polar and Alpine Desert
21	Conifer Boreal Forest	**70**	Glacier Rock
22	Cool Conifer Forest	**71**	Salt Playas
23	Cool Mixed Forest	**72**	Mangrove
24	Mixed Forest	**73**	Water and Island Fringe
25	Cool Broadleaf Forest	**74**	Land, Water, and Shore
26	Deciduous Broadleaf Forest	**75**	Land and Water, Rivers
27	Conifer Forest	**76**	Crop and Water Mixtures
28	Montane Tropical Forests	**77**	Southern Hemisphere Conifers
29	Seasonal Tropical Forest	**78**	Southern Hemisphere Mixed Forest
30	Cool Crops and Towns	**79**	Wet Sclerophylic Forest
31	Crops and Town	**80**	Coastline Fringe
32	Dry Tropical Woods	**81**	Beaches and Dunes
33	Tropical Rainforest	**82**	Sparse Dunes and Ridges
34	Tropical Degraded Forest	**83**	Bare Coastal Dunes
35	Corn and Beans Cropland	**84**	Residual Dunes and Beaches
36	Rice Paddy and Field	**85**	Compound Coastlines
37	Hot Irrigated Cropland	**86**	Rocky Cliffs and Slopes
38	Cool Irrigated Cropland	**87**	Sandy Grassland and Shrubs
39	Cold Irrigated Cropland	**88**	Bamboo
40	Cool Grasses and Shrubs	**89**	Moist Eucalyptus
41	Hot and Mild Grasses and Shrubs	**90**	Rain Green Tropical Forest
42	Cold Grassland	**91**	Woody Savanna
43	Savanna (Woods)	**92**	Broadleaf Crops
44	Mire, Bog, Fen	**93**	Grass Crops
45	Marsh Wetland	**94**	Crops, Grass, Shrubs
46	Mediterranean Scrub	**95**	Evergreen Tree Crop
47	Dry Woody Scrub	**96**	Deciduous Tree Crop
48	Dry Evergreen Woods	**99**	Interrupted Areas (Goodes Homolosine Projection)
49	Volcanic Rock	**100**	Missing Data

A6. Global Land Cover 2000 (GLC2000) classes (European Commission, 2003)

GLC2000 CLASSES	
1	Tree Cover, broadleaved, evergreen
2	Tree Cover, broadleaved, deciduous, closed
3	Tree Cover, broadleaved, deciduous, open
4	Tree Cover, needle-leaved, evergreen
5	Tree Cover, needle-leaved, deciduous
6	Tree Cover, mixed leaf type
7	Tree Cover, regularly flooded, fresh water (& brackish)
8	Tree Cover, regularly flooded, saline water
9	Mosaic: Tree cover / Other natural vegetation
10	Tree Cover, burnt
11	Shrub Cover, closed-open, evergreen
12	Shrub Cover, closed-open, deciduous
13	Herbaceous Cover, closed-open
14	Sparse Herbaceous or sparse Shrub Cover
15	Regularly flooded Shrub and/or Herbaceous Cover
16	Cultivated and managed areas
17	Mosaic: Cropland / Tree Cover / Other natural vegetation
18	Mosaic: Cropland / Shrub or Grass Cover
19	Bare Areas
20	Water Bodies (natural & artificial)
21	Snow and Ice (natural & artificial)
22	Artificial surfaces and associated areas

A7. GlobCover Land Cover classes (IONIA, 2009)

GLOBCOVER CLASSES	
11	Post-flooding or irrigated croplands (or aquatic)
14	Rainfed croplands
20	Mosaic cropland (50-70%) / vegetation (grassland/shrubland/forest) (20-50%)
30	Mosaic vegetation (grassland/shrubland/forest) (50-70%) / cropland (20-50%)
40	Closed to open (>15%) broadleaved evergreen or semi-deciduous forest (>5m)
50	Closed (>40%) broadleaved deciduous forest (>5m)
60	Open (15-40%) broadleaved deciduous forest/woodland (>5m)
70	Closed (>40%) needleleaved evergreen forest (>5m)
90	Open (15-40%) needleleaved deciduous or evergreen forest (>5m)
100	Closed to open (>15%) mixed broadleaved and needleleaved forest (>5m)
110	Mosaic forest or shrubland (50-70%) / grassland (20-50%)
120	Mosaic grassland (50-70%) / forest or shrubland (20-50%)
130	Closed to open (>15%) (broadleaved or needleleaved, evergreen or deciduous) shrubland (<5m)
140	Closed to open (>15%) herbaceous vegetation (grassland, savannas or lichens/mosses)
150	Sparse (<15%) vegetation
160	Closed to open (>15%) broadleaved forest regularly flooded (semi-permanently or temporarily) - Fresh or brackish water
170	Closed (>40%) broadleaved forest or shrubland permanently flooded - Saline or brackish water
180	Closed to open (>15%) grassland or woody vegetation on regularly flooded or waterlogged soil - Fresh, brackish or saline water
190	Artificial surfaces and associated areas (Urban areas >50%)
200	Bare areas
210	Water bodies

220	Permanent snow and ice
230	No data (burnt areas, clouds,…)

A8. GIS script written in Python Language using ArcGIS libraries (final ESH version)

```
# Import system modules
import sys, string, os, arcgisscripting, glob

# Create the Geoprocessor object
gp = arcgisscripting.create()

# Check out any necessary licenses
gp.CheckOutExtension("spatial")

# Load required toolboxes...
gp.AddToolbox("C:/Program Files (x86)/ArcGIS/ArcToolbox/Toolboxes/Spatial Analyst Tools.tbx")


# Local variables...
input_shp_files_directory = "C:\\SRLI\\Forest Pteridophytes\\EOOs\\EOOs_forESHmodel\\"
str_output_directory = "C:\\GIS\\ESH\\2005\\Globcover_w_wbminmax5_NEW\\srtm_alt\\"
alt_output_directory = "C:\\GIS\\ESH\\2005\\Globcover_w_wbminmax5_NEW\\srtm_alt\\"
gca_output_directory = "C:\\GIS\\ESH\\2005\\Globcover_w_wbminmax5_NEW\\gc\\"
gcr_output_directory = "C:\\GIS\\ESH\\2005\\Globcover_w_wbminmax5_NEW\\gc\\"
altgc_output_directory = "C:\\GIS\\ESH\\2005\\Globcover_w_wbminmax5_NEW\\gc\\"
mwb_output_directory = "C:\\GIS\\ESH\\2005\\Globcover_w_wbminmax5_NEW\\wb\\"
mwbr_output_directory = "C:\\GIS\\ESH\\2005\\Globcover_w_wbminmax5_NEW\\wb\\"
eshr_output_directory = "C:\\GIS\\ESH\\2005\\Globcover_w_wbminmax5_NEW\\esh\\"
esh_output_directory = "C:\\GIS\\ESH\\2005\\Globcover_w_wbminmax5_NEW\\esh\\"
esh_pr_output_directory = "C:\\GIS\\ESH\\2005\\Globcover_w_wbminmax5_NEW\\pr\\"
cvalue_directory = "C:\\GIS\\ESH\\2005\\Globcover_w_wbminmax5_NEW\\cv\\"
input_classification_file = "C:\\SRLI\\Forest Pteridophytes\\Alt_range_formodelFINAL.txt"
input_gc_classification_file = "C:\\SRLI\\Forest
Pteridophytes\\GlobcoverformodelFINAL_2005.txt"
input_wb_classification_file = "C:\\SRLI\\Forest Pteridophytes\\Wbminmax_formodel.txt"
input_c_value_classification_file = "C:\\SRLI\\Forest
Pteridophytes\\CvalueGCwwb_2005_wbmm.txt"
RasterSRTMv4 = "C:\\GIS\\SRTM_v4_1Km\\RasterSRTMv4"
SRTM_gtopo30 = "C:\\GIS\\GTOPO30\\srtm4_gtopo30"
GC = "C:\\GIS\\GC\\Globcover_V2.2_Global\\globcov5_1kmr"
WB = "C:\\GIS\\Water_balance\\cwatb_wcmin\\cwatb_wcmin"

os.chdir(input_shp_files_directory)
for file_to_process in glob.glob("*.shp"):

   # get file name without the extension
   file_name = file_to_process[23:][:-4]
   file_parts = file_name.partition('_')

   # get the output file name by using 3 characters from each word in the filename
   output_file_name = file_parts[0][:3] + file_parts[1] + file_parts[2][:3]
   os.mkdir(str_output_directory + file_name )

   # get all the ouput file paths
   srtm_output_path = str_output_directory + file_name + "\\SRTM_" + output_file_name
   altr_output_path = alt_output_directory + file_name + "\\ALTR_" + output_file_name
   gca_output_path = gca_output_directory + "\\gca_" + output_file_name
   gcr_output_path = gcr_output_directory + "\\gcr_" + output_file_name
```

```
    final_gc_output_path = altgc_output_directory + "\\altgc_" + output_file_name
    final_classification_output_path = eshr_output_directory + "\\eshr_" + output_file_name
    project_output_path = esh_pr_output_directory + "\\esh_" + output_file_name + "PR"
    mwb_output_path = mwb_output_directory + "\\mwb_" + output_file_name
    mwbr_output_path = mwbr_output_directory + "\\mwbr_" + output_file_name
    esh_output_path = esh_output_directory + "\\esh_" + output_file_name
    cv_classification_output_path = cvalue_directory + "\\eshcv_" + output_file_name

    try:
        print input_shp_files_directory
        print "Processing File: " + file_to_process

        # Process: Extract by Mask (1) (masking SRTM_gtopo30 using the species EOO)
        tempEnvironment0 = gp.snapRaster
        gp.snapRaster = RasterSRTMv4
        gp.ExtractByMask_sa(SRTM_gtopo30, input_shp_files_directory
                            + file_to_process, srtm_output_path)
        gp.snapRaster = tempEnvironment0
        fh = open(input_classification_file,'r')
        # find the entry for the file being processed in the input classification file, get the lower and
upper limit
        # and set a value of 1 between the lower and upper limit and value of 0 to the rest
        for line in fh:
            parts = line.partition(',')
            if parts[0] == file_name:
                lower_limit = parts[2].partition(',')[0]
                upper_limit = parts[2].partition(',')[2].partition('\n')[0]
                value = ""
                if lower_limit != "-505":
                    value ="-505 " + str(int(lower_limit) - 1) +" NODATA;"
                value = value + lower_limit+" "+ upper_limit + " 1;"
                if upper_limit != "8496":
                    value = value +str(int(upper_limit)+1)+" 8496 NODATA"
                print "Classifying with limits " + lower_limit + " " + upper_limit
                                    + " Range " + value
                # Process: Reclassify (2) (selecting the species altitudinal range)
                gp.Reclassify_sa(srtm_output_path, "VALUE", value, altr_output_path, "DATA")

        # Process: Extract by Mask (3) (selecting GlobCover 2005 within the species
        # EOO using srtm_output_path)
        print "Process(3)"
        tempEnvironment0 = gp.snapRaster
        gp.snapRaster = RasterSRTMv4
        gp.ExtractByMask_sa(GC, srtm_output_path, gca_output_path)
        gp.snapRaster = tempEnvironment0
        fh1 = open(input_gc_classification_file,'r')
        # find the entry for the file being processed in the input
        # gc classification file, get the data values
        # and for each number from 1-231 if it exists in the data values set the
        # the value to 1 eitherwise set it to 0
        for line in fh1:
            parts = line.partition('-')
            value = ""
            if parts[0] == file_name:
                data_values = parts[2].split(',')
                for num in range(1,231):
                    exists = 0
                    for data_value in data_values:
                        if num == int(data_value):
                            exists = 1
                    if exists:
                        value = value + str(num)+" 1;"
```

```
            else:
                value = value + str(num)+" NODATA;"
        print "Reclassifying gc"
        # Process: Reclassify (4) (selecting the species GlobCover suitable classes)
        gp.Reclassify_sa(gca_output_path, "VALUE", value, gcr_output_path, "DATA")
        print "Process (4)"

        # Process: Extract by Mask (5) (combining the species altitudinal range
        # with GlobCover suitable classes)
        tempEnvironment0 = gp.snapRaster
        gp.snapRaster = RasterSRTMv4
        gp.ExtractByMask_sa(altr_output_path, gcr_output_path, final_gc_output_path)
        gp.snapRaster = tempEnvironment0

    # Process: Extract by Mask (6)(selecting Water balance within the
    # species EOO using srtm_output_path)
    print "Process (6)"
    tempEnvironment0 = gp.snapRaster
    gp.snapRaster = RasterSRTMv4
    gp.ExtractByMask_sa(WB, srtm_output_path, mwb_output_path)
    gp.snapRaster = tempEnvironment0
    fh = open(input_wb_classification_file,'r')
    # find the entry for the file being processed in the input wb classification file,
    # get the lower and upper limit
    # and set a value of 1 between the lower and upper limit and value of 0 to the rest
    for line in fh:
      parts = line.partition(',')
      if parts[0] == file_name:
        lower_limit = parts[2].partition(',')[0]
        upper_limit = parts[2].partition(',')[2].partition('\n')[0]
        value = ""
        if lower_limit != "-6302":
          value ="-6302 " + str(int(lower_limit) - 1) +" NODATA;"
        value = value + lower_limit+" "+ upper_limit + " 1;"
        if upper_limit != "9130":
          value = value +str(int(upper_limit)+1)+" 9130 NODATA"
        print "Classifying with limits " + lower_limit + " " + upper_limit
                              + " Range " + value
        # Process: Reclassify (7) (selecting Water balance range appropriate for
        # the species)
        gp.Reclassify_sa(mwb_output_path, "VALUE", value, mwbr_output_path, "DATA")


    # Process: Extract by Mask (8) (combining the altitudinal range,
    # the GlobCover suitable classes and the water balance range of the species)
    print "Process (8)"
    tempEnvironment0 = gp.snapRaster
    gp.snapRaster = RasterSRTMv4
    gp.ExtractByMask_sa(final_gc_output_path, mwbr_output_path, esh_output_path)
    gp.snapRaster = tempEnvironment0
    # Process: Reclassify (9) (Assigning 1 to the ESH and 0 to No Data)
    print "Process (9)"
    gp.Reclassify_sa(esh_output_path, "VALUE", "1 1;NODATA 0",
                     final_classification_output_path, "DATA")

    # Process: Project Raster (10) (Project ESH)
    print "Process (10)"
    gp.ProjectRaster_management(final_classification_output_path, project_output_path,
"PROJCS['World_Cylindrical_Equal_Area',GEOGCS['GCS_WGS_1984',DATUM['D_WGS_1984',SPHEROI
D['WGS_1984',6378137.0,298.257223563]],PRIMEM['Greenwich',0.0],UNIT['Degree',0.017453292
5199433]],PROJECTION['Cylindrical_Equal_Area'],PARAMETER['False_Easting',0.0],PARAMETER['F
alse_Northing',0.0],PARAMETER['Central_Meridian',0.0],PARAMETER['Standard_Parallel_1',0.0],UNI
```

```
T['Meter',1.0]]", "NEAREST", "903.588525", "", "",
"GEOGCS['GCS_WGS_1984',DATUM['D_WGS_1984',SPHEROID['WGS_1984',6378137.0,298.2572235
63]],PRIMEM['Greenwich',0.0],UNIT['Degree',0.0174532925199433]]")

    # Process: Reclassify (11) (Assigning c-values to each ESH pixel)
    print "Process (11)"
    fh2 = open(input_c_value_classification_file,'r')
    # find the entry for the file being processed in the c value classification file,
    # get the value in the file
    # and replace 1 with the value
    for line in fh2:
      parts = line.split('-')
      value = ""
      if parts[0] == file_name:
        value = int(parts[1].partition('\n')[0])
        value = "0 0;1 " + str(value)
        print value
        gp.Reclassify_sa(final_classification_output_path, "VALUE", str(value),
                         cv_classification_output_path, "DATA")

  except Exception, err:
    print Exception, err
    print "Failed to proccess the file: " + file_to_process
```

A9. Transect characteristics of the 20 elevational pteridophyte transects included in Kessler *et al*. (2011) study.

No.	Name and coordinates	Elevational sampling range (m)	Upper transect limit (m)	Number and size of plots	Data source
t01	N California, Humboldt Redwoods State Park to Mt Shasta 40.68 (± 0.42) N/ 122.91 (± 0.60) W	50–2300	Timb. 2700 m	20; 400 m^2	M.K., Aug 2003
t02	Tobago 11.17 (± 0.02) N/60.39 (± 0.03) W	25–500	Island peak 594 m	10; 400 m^2	M.K., Jan 2003
t03	Costa Rica, Braulio Carrillo National Park and Cerro de la Muerte 10.13 (± 0.25) N/ 84.03 (± 0.13) W	100–3400	Timb. 3300 m	156; 400 m^2	J.K., 2001–2002 Kluge *et al.*, (2006)
t04	NW Ecuador, Felipe Carrillo Puerto to Volcán Pichincha 0.02 (± 0.02) N/78.47 (± 0.20) W	450–3600	Timb. 4200 m	22; 400 m^2	M.K. and M. Lehnert, Sep 2004
t05	SE Ecuador, Podocarpus National Park 3.67 (± 0.17) S/78.98 (± 0.15) W	1000–2800	Timb. 3300 m	32; 400 m^2	M. Lehnert, P. Salazar and MK, 2003, 2004
t06	N Bolivia, Carrasco National Park 17.02 (± 0.15) S/65.23 (± 0.29) W	200–3750	Timb. 4200 m	123; 400 m^2	Kessler (2001a)
t07	C Bolivia, Masicurí Valley 18.55 (± 0.18) S/ 63.49 (± 0.04) W	500–2450	m.p. 2853 m	47; 400 m^2	Kessler (2000)
t08	Tanzania, northern slope of Mt Kilimanjaro 2.95 (± 0.05) S/37.32 (± 0.12) E	1850–3200	Timb. 3600 m	41; 1000 m^2	A.H., 1996–2004
t09	Tanzania, south slope of Mt Kilimanjaro 3.14 (± 0.04) S/37.27 (± 0.11) E	1300–4000	Timb. 4000 m	337; 1000 m^2	A.H., 1996–2004
t10	Malaysia 3.76 (± 0.40) N/101.77 (± 0.39) E	0–1280	m.p. 1850 m	36; 400 m^2	M.K., D. Cicuzza, Sep 2007
t11	Borneo, Danum Valley and Mt Kinabalu 5.84 (± 0.36) N/116.5 (± 0.39) E	200–2650	Timb. 3600 m, m.p. 4095 m	20; 400 m^2	Kessler *et al.*, (2001)
t12	Sulawesi, Mt Rorekatimbu 1.17 (± 0.15) S/ 120.06 (± 0.21) E	50–2400	m.p. 2450 m	20; 400 m^2	M.K., Jan 2003
t13	Java, Carita, Mt Halimun, Mt Pangrango 6.40 (± 0.10) S/106.44 (± 0.44) E	250–2200	m.p. 3020 m	25; 400 m^2	M.K., Jan 2003 & 2005
t14	La Réunion 21.07 (± 0.05) S / 55.34 (± 0.05) E	100–2800	m.p. 3070 m, timb. 1800 m	18; 400 m^2	M.K., Mar 2008
t15	Harz, Germany, 51.71 (± 0.05) N/10.55 (± 0.06) E	300–1000	m.p. 1142 m	34; 400 m^2	J.K., Sept 2004
t16	New Zealand, Urewera 38.42 (± 0.01) S/ 177.06 (± 0.02) E	600–1200	m.p. 1340 m, timb. 1400 m	6; 2500 m^2	R.O., Feb–Mar 1998
t17	New Zealand, Mt Ruapehu 39.21 (± 0.01) S/175.29 (± 0.00) E	650–1450	m.p. 2797 m, timb. 1350 m	5; 2500 m^2	R.O., Feb–Mar 1998
t18	New Zealand, St. Arnaud 41.48 (± 0.00) S/ 172.36 (± 0.00) E	630–1400	m.p. 2339 m, timb. 1450 m	6; 2500 m^2	R.O., Feb–Mar 1998
t19	New Zealand, Franz Josef Glacier 43.27 (± 0.05) S/169.92 (± 0.25) E	30–800	m.p. 3754 m, timb. 1100 m	6; 2500 m^2	R.O., Feb–Mar 1998
t20	New Zealand, Haast Pass 43.97 (± 0.16) S/ 169.22 (± 0.00) E	20–800	m.p. 2423 m, timb. 1000 m	7; 2500 m^2	R.O., Feb–Mar 1998

A10. SRLI species endemic to the Neotropics (Central and South America) used to produce the ESH and SDM species richness maps.

SRLI forest species endemic to Central and South America			
Adiantopsis chlorophylla	Campyloneurum anetioides	Elaphoglossum polyblepharum	Polypodium fraternum
Adiantum decoratum	Campyloneurum tucumanense	Elaphoglossum raywaense	Polypodium fraxinifolium
Adiantum deflectens	Campyloneurum xalapense	Elaphoglossum rzedowskii	Polypodium loriceum
Adiantum feei	Ceradenia melanopus	Elaphoglossum sellowianum	Polypodium martensii
Adiantum incertum	Ceradenia pruinosa	Elaphoglossum squarrosum	Polypodium segregatum
Adiantum poeppigianum	Cnemidaria varians	Elaphoglossum velongum	Polypodium ursipes
Adiantum scabrum	Ctenitis aspidioides	Enterosora ecostata	Polystichum echinatum
Alsophila imrayana	Ctenitis chiriquiana	Eriosorus stuebelii	Polystichum montevidense
Alsophila incana	Ctenitis grisebachii	Goniopteris paucipinnata	Polystichum ordinatum
Amauropelta firma	Ctenitis refulgens	Hymenophyllum plumosum	Polystichum speciosissimum
Amauropelta funckii	Cyathea amazonica	Hymenophyllum protrusum	Polytaenium chlorosporum
Amauropelta scalaris	Cyathea dissimilis	Hymenophyllum pyramidatum	Pseudocolysis bradeorum
Amauropelta thomsonii	Cyathea ebenina	Hymenophyllum simplex	Pteris bakeri
Anemia hirsuta	Cyathea pallescens	Hymenophyllum trichomanoides	Pteris deflexa
Anemia karwinskyana	Cyathea pseudonanna	Hypolepis hostilis	Pteris gigantea
Anemia oblongifolia	Cyathea williamsii	Jamesonia boliviensis	Pteris orizabae
Anemia phyllitidis	Danaea wendlandii	Lastreopsis killipii	Scoliosorus ensiformis
Anemia tomentosa	Dicranoglossum furcatum	Lellingeria apiculata	Selaginella bombycina
Arachniodes rigidissima	Diplazium ambiguum	Lellingeria limula	Selaginella cladorrhizans
Asplenium auriculatum	Diplazium avitaguense	Lindsaea pallida	Selaginella diffusa
Asplenium blepharodes	Diplazium bicolor	Lomagramma guianensis	Selaginella flagellata
Asplenium congestum	Diplazium franconis	Lomariopsis wrightii	Selaginella humboldtiana
Asplenium dimidiatum	Diplazium grandifolium	Marattia interposita	Selaginella pallescens
Asplenium hastatum	Diplazium immensum	Melpomene allosuroides	Selaginella poeppigiana
Asplenium lamprocaulon	Diplazium mutilum	Melpomene assurgens	Selaginella radiata
Asplenium macilentum	Diplazium sanctae-rosae	Meniscium angustifolium	Selaginella revoluta
Asplenium polyphyllum	Diplazium tomentellum	Metaxya rostrata	Selaginella vernicosa
Asplenium pseudonitidum	Elaphoglossum acutifolium	Microgramma megalophylla	Stigmatopteris lechleri
Asplenium soleirolioides	Elaphoglossum albescens	Microgramma piloselloides	Tectaria pubens
Asplenium triquetrum	Elaphoglossum apodum	Microgramma tecta	Tectaria rivalis
Asplenium ulbrichtii	Elaphoglossum ciliatum	Microgramma ulei	Terpsichore alfarii
Asplenium underwoodii	Elaphoglossum delasotae	Niphidium anocarpos	Terpsichore alsophilicola
Asplenium wacketii	Elaphoglossum deltoideum	Niphidium macbridei	Terpsichore atroviridis
Astrolepis beitelii	Elaphoglossum floccosum	Odontosoria aculeata	Terpsichore longa
Athyrium arcuatum	Elaphoglossum gratum	Ormoloma imrayanum	Terpsichore pichinchense
Athyrium palmense	Elaphoglossum lasioglottis	Paesia glandulosa	Terpsichore subtilis
Blechnum asplenioides	Elaphoglossum lingua	Pecluma alfredii	Thelypteris clivalis
Blechnum corralense	Elaphoglossum lloense	Pecluma curvans	Trichomanes botryoides
Blechnum fraxineum	Elaphoglossum longicrure	Pellaea pringlei	Trichomanes micayense
Blechnum microphyllum	Elaphoglossum longifolium	Phanerophlebia nobilis	Trichomanes osmundoides
Blechnum ryanii	Elaphoglossum luridum	Plagiogyria semicordata	Trichomanes polypodioides
Blechnum schomburgkii	Elaphoglossum minutum	Pleopeltis fructuosa	Triplophyllum funestum
Blechnum spannagelii	Elaphoglossum montgomeryi	Pleopeltis polylepis	Zygophlebia sectifrons
Blotiella lindeniana	Elaphoglossum moranii	Polybotrya caudata	Zygophlebia werffii
Bolbitis aliena	Elaphoglossum nanoglossum	Polybotrya osmundacea	
Bolbitis pergamentacea	Elaphoglossum nidiformis	Polypodium alansmithii	
Bommeria pedata	Elaphoglossum pachyphyllum	Polypodium bombycinum	

A11. GIS script written in Python Language using ArcGIS libraries for the calculation of the species' four ESHs: ESHOF, ESH2005, ESH2012 and ESH2062.

```
# Check out any necessary licenses
gp.CheckOutExtension("spatial")

# Load required toolboxes...
gp.AddToolbox("C:/Program Files (x86)/ArcGIS/ArcToolbox/Toolboxes/Spatial Analyst Tools.tbx")


# Local variables...
input_shp_files_directory = "C:\\SRLI\\Forest Pteridophytes\\EOOs\\EOOs_forESHmodel\\"
str_output_directory = "C:\\GIS\\ESH\\2005\\Globcover_w_wbminmax5_NEW\\srtm_alt\\"
alt_output_directory = "C:\\GIS\\ESH\\2005\\Globcover_w_wbminmax5_NEW\\srtm_alt\\"
gca_output_directory = "C:\\GIS\\ESH\\2005\\Globcover_w_wbminmax5_NEW\\"
gcr_output_directory = "C:\\GIS\\ESH\\2005\\Globcover_w_wbminmax5_NEW\\"
altgc_output_directory = "C:\\GIS\\ESH\\2005\\Globcover_w_wbminmax5_NEW\\"
mwb_output_directory = "C:\\GIS\\ESH\\2005\\Globcover_w_wbminmax5_NEW\\wb\\"
mwbr_output_directory = "C:\\GIS\\ESH\\2005\\Globcover_w_wbminmax5_NEW\\wb\\"
eshr_output_directory = "C:\\GIS\\ESH\\2005\\Globcover_w_wbminmax5_NEW\\extra\\"
esh_output_directory = "C:\\GIS\\ESH\\2005\\Globcover_w_wbminmax5_NEW\\extra\\"
esh_pr_output_directory = "C:\\GIS\\ESH\\2005\\Globcover_w_wbminmax5_NEW\\pr\\"
cvalue_directory = "C:\\GIS\\ESH\\2005\\Globcover_w_wbminmax5_NEW\\cv\\extra\\"
gfc_directory = "C:\\GIS\\ESH\\2005\\Globcover_w_wbminmax5_NEW\\GFC\\"
scenario_directory = "C:\\GIS\\ESH\\2005\\Globcover_w_wbminmax5_NEW\\scenario\\"
input_classification_file = "C:\\SRLI\\Forest Pteridophytes\\Alt_range_formodelFINAL.txt"
input_gc_classification_file = "C:\\SRLI\\Forest
Pteridophytes\\GlobcoverformodelFINAL_2005.txt"
input_wb_classification_file = "C:\\SRLI\\Forest Pteridophytes\\Wbminmax_formodel.txt"
input_c_value_classification_file = "C:\\SRLI\\Forest
Pteridophytes\\CvalueGCwwb_2005_wbmm.txt"
RasterSRTMv4 = "C:\\GIS\\SRTM_v4_1Km\\RasterSRTMv4"
SRTM_gtopo30 = "C:\\GIS\\GTOPO30\\srtm4_gtopo30"
GC = "C:\\GIS\\GC\\Globcover_V2.2_Global\\globcov5_1kmr"
WB = "C:\\GIS\\Water_balance\\cwatb_wcmin\\cwatb_wcmin"
GFC = "C:\\Users\\Elina\\Documents\\PhD\GIS\\Hansen_def_data\\gfc50_compgc5"
Scenario = "C:\\GIS\\global_cn_scenarios\\scencompgcgfc"


os.chdir(input_shp_files_directory)
for file_to_process in glob.glob("*.shp"):

    # get file name without the extension
    file_name = file_to_process[23:][:-4]
    file_parts = file_name.partition('_')

    # get the output file name by using 3 characters from each word in the filename
    output_file_name = file_parts[0][:3] + file_parts[1] + file_parts[2][:3]
    os.mkdir(str_output_directory + file_name )

    # get all the ouput file paths
    srtm_output_path = str_output_directory + file_name + "\\SRTM_" + output_file_name
    altr_output_path = alt_output_directory + file_name + "\\ALTR_" + output_file_name
    gca_output_path = gca_output_directory + "\\gca_" + output_file_name
    gcr_output_path = gcr_output_directory + "\\gcr_" + output_file_name
    final_gc_output_path = altgc_output_directory + "\\altgc_" + output_file_name
    final_classification_output_path = eshr_output_directory + "\\eshr_" + output_file_name
    project_output_path = esh_pr_output_directory + "\\esh_" + output_file_name + "PR"
    mwb_output_path = mwb_output_directory + "\\mwb_" + output_file_name
    mwbr_output_path = mwbr_output_directory + "\\mwbr_" + output_file_name
    esh_output_path = esh_output_directory + "\\esh_" + output_file_name
    cv_classification_output_path = cvalue_directory + "\\eshcv_" + output_file_name
```

```
    gfc_output_path = gfc_directory + "\\gfc_" + final_output_file_name
    pr2_output_path = gfc_directory + "\\gfc_" + final_output_file_name + "PR"
    scenario_output_path = scenario_directory + "\\sce_" + final_output_file_name
    scenpr_output_path = scebarui_directory + "\\sce_" + final_output_file_name + "PR"



    try:
        print input_shp_files_directory
        print "Processing File: " + file_to_process

        # Process: Extract by Mask (1) (masking SRTM_gtopo30 using the species EOO)
        tempEnvironment0 = gp.snapRaster
        gp.snapRaster = RasterSRTMv4
        gp.ExtractByMask_sa(SRTM_gtopo30, input_shp_files_directory + file_to_process,
srtm_output_path)
        gp.snapRaster = tempEnvironment0
        fh = open(input_classification_file,'r')
        # find the entry for the file being processed in the input classification file,
        # get the lower and upper limit
        # and set a value of 1 between the lower and upper limit and value of 0 to the rest
        for line in fh:
            parts = line.partition(',')
            if parts[0] == file_name:
                lower_limit = parts[2].partition(',')[0]
                upper_limit = parts[2].partition(',')[2].partition('\n')[0]
                value = ""
                if lower_limit != "-505":
                    value ="-505 " + str(int(lower_limit) - 1) +" NODATA;"
                value = value + lower_limit+" "+ upper_limit + " 1;"
                if upper_limit != "8496":
                    value = value +str(int(upper_limit)+1)+" 8496 NODATA"
                print "Classifying with limits " + lower_limit + " " + upper_limit
                                    + " Range " + value
                # Process: Reclassify (2) (selecting the species altitudinal range)
                gp.Reclassify_sa(srtm_output_path, "VALUE", value, altr_output_path, "DATA")


        # Process: Extract by Mask (3) (selecting GlobCover 2005 within the species
        # EOO using srtm_output_path)
        print "Process(3)"
        tempEnvironment0 = gp.snapRaster
        gp.snapRaster = RasterSRTMv4
        gp.ExtractByMask_sa(GC, srtm_output_path, gca_output_path)
        gp.snapRaster = tempEnvironment0
        fh1 = open(input_gc_classification_file,'r')
        # find the entry for the file being processed in the input gc classification file,
        # get the data values
        # and for each number from 1-231 if it exists in the data values set the the
        # value to 1 eitherwise set it to 0
        for line in fh1:
            parts = line.partition('-')
            value = ""
            if parts[0] == file_name:
                data_values = parts[2].split(',')
                for num in range(1,231):
                    exists = 0
                    for data_value in data_values:
                        if num == int(data_value):
                            exists = 1
                    if exists:
                        value = value + str(num)+" 1;"
```

```
            else:
                value = value + str(num)+" NODATA;"
        print "Reclassifying gc"
        # Process: Reclassify (4) (selecting the species GlobCover suitable classes)
        gp.Reclassify_sa(gca_output_path, "VALUE", value, gcr_output_path, "DATA")
        print "Process (4)"

        # Process: Extract by Mask (5) (combining the species altitudinal
        # range with GlobCover suitable classes)
        tempEnvironment0 = gp.snapRaster
        gp.snapRaster = RasterSRTMv4
        gp.ExtractByMask_sa(altr_output_path, gcr_output_path, final_gc_output_path)
        gp.snapRaster = tempEnvironment0

    # Process: Extract by Mask (6)(selecting Water balance within the species
    # EOO using srtm_output_path)
    print "Process (6)"
    tempEnvironment0 = gp.snapRaster
    gp.snapRaster = RasterSRTMv4
    gp.ExtractByMask_sa(WB, srtm_output_path, mwb_output_path)
    gp.snapRaster = tempEnvironment0
    fh = open(input_wb_classification_file,'r')
    # find the entry for the file being processed in the input wb classification file,
    # get the lower and upper limit
    # and set a value of 1 between the lower and upper limit and value of 0 to the rest
    for line in fh:
      parts = line.partition(',')
      if parts[0] == file_name:
        lower_limit = parts[2].partition(',')[0]
        upper_limit = parts[2].partition(',')[2].partition('\n')[0]
        value = ""
        if lower_limit != "-6302":
          value ="-6302 " + str(int(lower_limit) - 1) +" NODATA;"
        value = value + lower_limit+" "+ upper_limit + " 1;"
        if upper_limit != "9130":
          value = value +str(int(upper_limit)+1)+" 9130 NODATA"
        print "Classifying with limits " + lower_limit + " " + upper_limit
                              + " Range " + value
        # Process: Reclassify (7) (selecting Water balance range appropriate for
        # the species)
        gp.Reclassify_sa(mwb_output_path, "VALUE", value, mwbr_output_path, "DATA")

    # Process: Extract by Mask (8) (combining the altitudinal range, the GlobCover
    # suitable classes and the water balance range of the species resulting to ESH2005)
    print "Process (8)"
    tempEnvironment0 = gp.snapRaster
    gp.snapRaster = RasterSRTMv4
    gp.ExtractByMask_sa(final_gc_output_path, mwbr_output_path, esh_output_path)
    gp.snapRaster = tempEnvironment0
    # Process: Reclassify (9) (Assigning 1 to the ESH2005 and 0 to No Data)
    print "Reclassify final (9)"
    gp.Reclassify_sa(esh_output_path, "VALUE", "1 1;NODATA 0",
                     final_classification_output_path, "DATA")

    # Process: Project Raster (10) (Project ESH2005)
    print "Process (10)"
    gp.ProjectRaster_management(final_classification_output_path, project_output_path,
"PROJCS['World_Cylindrical_Equal_Area',GEOGCS['GCS_WGS_1984',DATUM['D_WGS_1984',SPHEROI
D['WGS_1984',6378137.0,298.257223563]],PRIMEM['Greenwich',0.0],UNIT['Degree',0.017453292
5199433]],PROJECTION['Cylindrical_Equal_Area'],PARAMETER['False_Easting',0.0],PARAMETER['F
alse_Northing',0.0],PARAMETER['Central_Meridian',0.0],PARAMETER['Standard_Parallel_1',0.0],UNI
T['Meter',1.0]]", "NEAREST", "903.588525", "", "",
```

```
"GEOGCS['GCS_WGS_1984',DATUM['D_WGS_1984',SPHEROID['WGS_1984',6378137.0,298.2572235
63]],PRIMEM['Greenwich',0.0],UNIT['Degree',0.0174532925199433]]")

    # Process: Extract by Mask (11) (removing the GFC deforestation pixels from the
    # ESH2005 resulting to ESH2012)
    print "Process (11)"
    tempEnvironment0 = gp.snapRaster
    gp.snapRaster = RasterSRTMv4
    gp.ExtractByMask_sa(GFC, esh_output_path , gfc_output_path)
    gp.snapRaster = tempEnvironment0

    # Process: Define Projection (12)
    print "Process (12)"
    gp.DefineProjection_management(gfc_output_path,
"GEOGCS['GCS_WGS_1984',DATUM['D_WGS_1984',SPHEROID['WGS_1984',6378137.0,298.2572235
63]],PRIMEM['Greenwich',0.0],UNIT['Degree',0.0174532925199433]]")
    # Process: Project ESH2012
    print "Project"
    gp.ProjectRaster_management(gfc_output_path, pr2_output_path,
"PROJCS['World_Cylindrical_Equal_Area',GEOGCS['GCS_WGS_1984',DATUM['D_WGS_1984',SPHEROI
D['WGS_1984',6378137.0,298.257223563]],PRIMEM['Greenwich',0.0],UNIT['Degree',0.017453292
5199433]],PROJECTION['Cylindrical_Equal_Area'],PARAMETER['False_Easting',0.0],PARAMETER['F
alse_Northing',0.0],PARAMETER['Central_Meridian',0.0],PARAMETER['Standard_Parallel_1',0.0],UNI
T['Meter',1.0]]", "NEAREST", "903.588525", "", "",
"GEOGCS['GCS_WGS_1984',DATUM['D_WGS_1984',SPHEROID['WGS_1984',6378137.0,298.2572235
63]],PRIMEM['Greenwich',0.0],UNIT['Degree',0.0174532925199433]]")


    # Process: Extract by Mask (13) (removing the scenario deforestation pixels from
    # the ESH2012 resulting to either ESH2032 or ESH2062)
    print "Process (13)"
    tempEnvironment0 = gp.snapRaster
    gp.snapRaster = Terrai
    gp.ExtractByMask_sa(Scenario, esh_output_path , scenario_output_path)
    gp.snapRaster = tempEnvironment0

    # Process: Define Projection (14)
    print "Process (14)"
    gp.DefineProjection_management(scenario_output_path,
"GEOGCS['GCS_WGS_1984',DATUM['D_WGS_1984',SPHEROID['WGS_1984',6378137.0,298.2572235
63]],PRIMEM['Greenwich',0.0],UNIT['Degree',0.0174532925199433]]")
    # Process: Project ESH2062 (15)
    print "Process (15)"
    gp.ProjectRaster_management(scenario_output_path, scenpr_output_path,
"PROJCS['World_Cylindrical_Equal_Area',GEOGCS['GCS_WGS_1984',DATUM['D_WGS_1984',SPHEROI
D['WGS_1984',6378137.0,298.257223563]],PRIMEM['Greenwich',0.0],UNIT['Degree',0.017453292
5199433]],PROJECTION['Cylindrical_Equal_Area'],PARAMETER['False_Easting',0.0],PARAMETER['F
alse_Northing',0.0],PARAMETER['Central_Meridian',0.0],PARAMETER['Standard_Parallel_1',0.0],UNI
T['Meter',1.0]]", "NEAREST", "903.588525", "", "",
"GEOGCS['GCS_WGS_1984',DATUM['D_WGS_1984',SPHEROID['WGS_1984',6378137.0,298.2572235
63]],PRIMEM['Greenwich',0.0],UNIT['Degree',0.0174532925199433]]")


  except Exception, err:
    print Exception, err
    print "Failed to proccess the file: " + file_to_process
```

A12. Assigned GlobCover classes for each IUCN habitat category.

IUCN Habitat Classification	Globcover Classes	IUCN Habitat Classification	Globcover Classes	IUCN Habitat Classification	Globcover Classes
1 Forest		3.3 Boreal Shrubland	110,120,130	5.2 Seasonal/Intermittent/Irregular Rivers, Streams, Creeks	180,210
1.1 Boreal Forest	70, 90, 100,	3.4 Temperate Shrubland	110,120,130	5.3 Shrub Dominated Wetlands	180
1.2 Subarctic Forest	90	3.5 Subtropical/Tropical Dry Shrubland	110,120	5.4 Bogs, Marshes, Swamps, Fens, Peatlands [generally over 8 ha]	160,180
1.3 Subantarctic Forest	100	3.6 Subtropical/Tropical Moist Shrubland	110,120	5.5 Permanent Freshwater Lakes [over 8 ha]	210
1.4 Temperate Forest	50, 60,70, 90,100	3.7 Subtropical/Tropical High Altitude Shrubland	130	5.6 Seasonal/Intermittent Freshwater Lakes [over 8 ha]	210
1.5 Subtropical/Tropical Dry Forest	40,50,60,100	3.8 Mediterranean-type Shrubby Vegetation	120,130,150	5.7 Permanent Freshwater Marshes/Pools [under 8 ha]	180
1.6 Subtropical/Tropical Moist Lowland Forest	40,50,60,100	**4 Grassland**		5.8 Seasonal/Intermittent Freshwater Marshes/Pools [under 8 ha]	180
1.7 Subtropical/Tropical Mangrove Forest Vegetation Above High Tide Level	160	4.1 Tundra	140,150,220	5.9 Freshwater Springs and Oases	210
1.8 Subtropical/Tropical Swamp Forest	160,170	4.2 Subarctic Grassland	150	5.10 Tundra Wetlands [includes pools and temporary waters from snowmelt]	180
1.9 Subtropical/Tropical Moist Montane Forest	40,50,60,90,100	4.3 Subantarctic Grassland	140, 150	5.11 Alpine Wetlands [includes temporary waters from snowmelt]	160,180
2 Savanna		4.4 Temperate Grassland	110,120,140	5.12 Geothermal Wetlands	210
2.1 Dry Savanna	120,140,150	4.5 Subtropical/Tropical Dry Lowland Grassland	110,120,140,	5.13 Permanent Inland Deltas	180
2.2 Moist Savana	120,140,150	4.6 Subtropical/Tropical Seasonally Wet/Flooded Lowland Grassland	110,120,140,180	5.14 Permanent Saline, Brackish or Alkaline Lakes	170,180
3 Shrubland		4.7 Subtropical/Tropical High Altitude Grassland	140,150	5.15 Seasonal/Intermittent Saline, Brackish or Alkaline Lakes and Flats	160,180
3.1 Subarctic Shrubland	150	**5 Wetlands (inland)**		5.16 Permanent Saline, Brackish or Alkaline Marshes/Pools	170,180
3.2 Subantarctic Shrubland	130	5.1 Permanent Rivers, Streams, Creeks [includes waterfalls]	160,210	5.17 Seasonal/Intermittent Saline, Brackish or Alkaline Marshes/Pools	180

A11. Assigned GlobCover classes for each IUCN habitat category (continued)

IUCN Habitat Classification	Globcover Classes	IUCN Habitat Classification	Globcover Classes	IUCN Habitat Classification	Globcover Classes
6 Rocky Areas	150,200	12.5 Salt Marshes (Emergent Grasses)	180	14.5 Urban Areas	190
7 Caves and Subterranean Habitats		12.6 Tidepools	180	14.6 Subtropical/Tropical Heavily Degraded Former Forest	20,30
7.1 Caves	N/A	12.7 Mangrove Submerged Roots	170,180	**15 Artificial - Aquatic**	
7.2 Other Subterranean Habitats	N/A	**13 Marine Coastal/Supratidal**		15.1 Water Storage Areas [over 8 ha]	210
8 Desert		13.1 Sea Cliffs and Rocky Offshore Islands	140,150	15.2 Ponds [below 8 ha]	210
8.1 Hot	150	13.3 Coastal Sand Dunes	140,150	15.3 Aquaculture Ponds	11,190
8.2 Temperate	150	13.4 Coastal Brackish/Saline Lagoons/Marine Lakes	210	15.4 Salt Exploitation Sites	180,210
8.3 Cold	150	13.5 Coastal Freshwater Lakes	210	15.5 Excavations (open)	210
12 Marine Intertidal		**14 Artificial - Terrestrial**		15.6 Wastewater Treatment Areas	210
12.1 Rocky Shoreline	180	14.1 Arable Land	11,14	15.7 Irrigated Land [includes irrigation channels]	11
12.2 Sandy Shoreline and/or Beaches, Sand Bars, Spits	180	14.2 Pastureland	11,14	15.8 Seasonally Flooded Agricultural Land	11
12.3 Shingle and/or Pebble Shoreline and/or Beaches	180	14.3 Plantations	40	15.9 Canals and Drainage Channels, Ditches	190
12.4 Mud Shoreline and Intertidal Mud Flats	180	14.4 Rural Gardens	11,14,30		